CONTRACTOR REPORT

SAND82—7157/3 of 4
Unlimited Release
UC—63

Analysis of Concentrating PV-T Systems for the Commercial/Industrial Sector

Volume III. Technical Issues and Design Guidance

W. E. Schwinkendorf
The BDM Corporation
1801 Randolph Rd, SE
Albuquerque, NM 87106

Prepared by Sandia National Laboratories Albuquerque, New Mexico 87185 and Livermore, California 94550 for the United States Department of Energy under Contract DE-AC04-76DP00789

Printed September 1984

When printing a copy of any digitized SAND Report, you are required to update the markings to current standards.

Issued by Sandia National Laboratories, operated for the United States Department of Energy by Sandia Corporation.
NOTICE: This report was prepared as an account of work sponsored by an agency of the United States Government. Neither the United States Government nor any agency thereof, nor any of their employees, nor any of their contractors, subcontractors, or their employees, makes any warranty, express or implied, or assumes any legal liability or responsibility for the accuracy, completeness, or usefulness of any information, apparatus, product, or process disclosed, or represents that its use would not infringe privately owned rights. Reference herein to any specific commercial product, process, or service by trade name, trademark, manufacturer, or otherwise, does not necessarily constitute or imply its endorsement, recommendation, or favoring by the United States Government, any agency thereof or any of their contractors or subcontractors. The views and opinions expressed herein do not necessarily state or reflect those of the United States Government, any agency thereof or any of their contractors or subcontractors.

Printed in the United States of America
Available from
National Technical Information Service
U.S. Department of Commerce
5285 Port Royal Road
Springfield, VA 22161

NTIS price codes
Printed copy: A13
Microfiche copy: A01

SAND82–7157/3 of 4
Unlimited Release
Printed September 1984

Distribution
Category UC–63

Analysis of Concentrating PV-T Systems for the Commercial/Industrial Sector

Volume III. Technical Issues and Design Guidance

W. E. Schwinkendorf
The BDM Corporation
1801 Randolph Rd, SE
Albuquerque, NM 87106

Abstract

This report provide appropriate guidance for addressing the major technical issues associated with the design and installation of a photovoltaic-thermal (PV-T) system. Nomographs are presented for developing preliminary sizing and costing, and issues associated with specific components and the overall design of the electrical and mechanical system are discussed. SAND82–7157/2 presents a review of current PV-T technology and operating systems and a study of potential PV-T applications. Detailed PV-T system designs for three selected applications and the results of a trade-off study for these applications are presented in SAND82–7157/4. A summary of the major results of this entire study and conclusions concerning PV-T systems and applications is presented in SAND82–7157/1.

FOREWORD

This volume of technical report BDM/A-82-458-TR-R1 is submitted by The BDM Corporation, 1801 Randolph Road, S.E., Albuquerque, NM 87106. This report documents work performed for Sandia National Laboratories under contract 68-0361. This volume documents technical issues that must be dealt with when designing a PV-T system, and provides guidance in resolving those issues.

This work was performed under the guidance of Mr. Miguel Rios, the Sandia contract monitor.

TABLE OF CONTENTS

Chapter		Page
I	INTRODUCTION	I-1
II	SIZING AND LOAD MATCHING	II-1
	A. DESIGN ISSUES	II-1
	1. Objective	II-1
	2. Background - The Design Process	II-1
	3. Description of PV-T Systems	II-4
	4. Overview	II-5
	B. CONCEPT DEVELOPMENT	II-5
	1. Introduction	II-5
	2. Design Issues for Concept Development Phase	II-5
III	ELECTRICAL SYSTEM DESIGN	III-1
	A. IDENTIFICATION OF TECHNICAL ISSUES	III-1
	1. Inverters	III-1
	2. PV Array Configuration	III-10
	3. Power Conditioning	III-22
	4. System Protection	III-24
	5. Miscellaneous Electrical Components	III-27
	6. Wiring Sizes	III-33
	7. Safety Grounding	III-36
	8. Control Strategy	III-37
	9. Instrumentation Systems--General	III-39
	B. DESIGN CRITERIA	III-42
	1. Inverters	III-42
	2. Power Conditioning	III-45
	3. Miscellaneous Electrical Components	III-46
	4. Ground Fault Protection	III-47
	5. Safety Switches	III-49
	6. Utility Interface	III-51
	7. Wiring Sizes	III-51
	8. Safety Grounding	III-54
	9. Array Wiring Configuration	III-54
	10. Diodes	III-56
	11. Control Strategy	III-56
	12. Operating Modes	III-61
	13. Data Acquisition Systems	III-61

TABLE OF CONTENTS (Continued)

Chapter		Page
	C. DESIGN GUIDANCE	III-63
	1. System Design Criteria	III-63
	2. Data Acquisition Design Guidance	III-79
	3. Design Specifications	III-90
IV	THERMAL AND MECHANICAL SYSTEM DESIGN	IV-1
	A. INTRODUCTION	IV-1
	B. COOLANT FLOW RATE	IV-1
	C. HEAT EXCHANGER SIZING AND SELECTION	IV-6
	1. Introduction	IV-6
	2. Types of Heat Exchangers	IV-14
	3. Heat Transfer Relations	IV-25
	4. Selection and Sizing a Heat Exchanger	IV-39
	D. COOLING SYSTEMS	IV-57
	1. Cooling Towers	IV-58
	2. Air Coolers	IV-62
	3. An Example Tower Selection	IV-63
	E. SENSIBLE HEAT STORAGE	IV-64
	F. PUMP SELECTION AND SIZING	IV-72
	G. VALVES	IV-83
	1. Selection of Valves	IV-83
	2. Construction of Valves	IV-84
	3. Types of Valves	IV-87
	4. Automation of Valves	IV-94
	5. Location of Valves	IV-94
	6. Application of Valves	IV-96
	H. MANIFOLD PIPING	IV-97
	1. Pipe Sizing and Cost Analysis	IV-97
	2. Field Pressure Drop Calculation	IV-106
	3. Power Piping Code	IV-121
	4. Types of Pipe	IV-121

TABLE OF CONTENTS (Continued)

Chapter		Page
	I. INSULATION	IV-123
	1. Economic Thickness	IV-143
	2. Acceptable Heat Loss Thickness	IV-164
	J. AUXILIARY HEATERS	IV-166
	1. Heat Pumps	IV-169
	2. Auxiliary Heaters (Steam and Hot Water)	IV-173
	REFERENCES	IV-187
V	RELIABILITY, AVAILABILITY, AND MAINTAINABILITY	V-1
	A. INTRODUCTION	V-1
	B. CONSTRAINTS	V-2
	C. RAM THEORY	V-2
	1. Introduction	V-2
	2. Reliability	V-2
	3. Maintainability	V-14
	4. Availability	V-21
	D. RAM TRADE-OFF ANALYSIS	V-23
VI	STRUCTURES AND FOUNDATIONS TO SUPPORT PHOTOVOLTAIC-THERMAL (PV-T) SINGLE AND TWO-AXIS TRACKING SYSTEMS	VI-1
	A. INTRODUCTION	VI-1
	B. ISSUES ASSOCIATED WITH STRUCTURES AND FOUNDATIONS FOR PV-T SYSTEMS	VI-5
	1. Roof Mountings	VI-9
	2. Ground Mountings	VI-11
	C. LOADS-DETERMINATION	VI-14
	1. Wind Velocities, Forces, and Design for Winds	VI-17
	2. Examples of Wind Load Calculations on Linear Parabolic Troughs	VI-26
	3. General Comments on Wind Loadings	VI-28

TABLE OF CONTENTS (Continued)

Chapter		Page
	D. DESIGN AND CONSTRUCTION RELATED ISSUES	VI-29
	1. Optimum Cost-Effective Configuration of Structure and Foundation	VI-29
	2. Examples of Foundation Designs for PV-T Systems	VI-30
	3. Example Pier Foundation Designs for a Linear Parabolic Trough System	VI-32
	4. Example Foundation Designs for the Martin Marietta Two-Axis Tracking Pedestal-Mounted System	VI-33
	5. Example Foundation Designs for the E-System Two-Axis Tracking PV-T System	VI-33
	6. Alternative Approaches to and Solutions for the Structure and Foundation Problem	VI-39
	E. GUIDELINES AND SUGGESTIONS FOR ADDITIONAL INVESTIGATION	VI-39
VII	INSTITUTIONAL ISSUES	VII-1
	A. LEGAL ISSUES	VII-1
	1. Guaranteed Solar Access	VII-1
	2. Building Codes	VII-3
	3. Liability and Insurance	VII-6
	B. ECONOMIC ISSUES	VII-8
	1. Tax Incentives	VII-8
	2. Investment Criteria	VII-9
	3. Prototype Nature of Photovoltaic Systems	VII-10
	C. UTILITY INTERFACE	VII-11
	1. Protection	VII-12
	2. Stability	VII-12
	3. System Unbalance	VII-12
	4. Voltage Regulation	VII-12
	5. Harmonics	VII-13
	6. Employee Safety	VII-13

TABLE OF CONTENTS (Concluded)

Chapter			Page
	7.	Metering	VII-13
	8.	System Planning	VII-13
D.	HEALTH AND SAFETY		VII-13
	1.	Fire Safety	VII-14
	2.	Physical Hazards	VII-15
	3.	Component Toxicity and Disposal	VII-16
	4.	Overtemperature and Overpressure Protection	VII-17
	5.	Contamination of Product	VII-18
	6.	Vandalism	VII-21
E.	ENVIRONMENTAL		VII-21
	1.	Land Use	VII-21
	2.	Microclimate Effects	VII-21
	3.	Electro-Magnetic Interference	VII-23
	4.	Aesthetics	VII-23

LIST OF FIGURES

Figure		Page
I-1	Design Methodology	I-2
I-2	Conceptual PV-T System for Preliminary Analysis and Sizing	I-4
II-1	Design Phases for Application of PV-T Design Concepts	II-3
II-2	Yearly Average Direct Normal Irradiance During Daylight Hours	II-8
II-3	Maximum Annual Average Insolation Available to LFF and LPT Collectors	II-10
II-4	Annual Available Thermal Energy for a Linear Parabolic Trough Collector	II-11
II-5	Annual Available Electrical Energy for a Linear Parabolic Trough Collector	II-12
II-6	Annual Available Thermal Energy for a 2-Axis Tracking Line Focus Fresnel Collector	II-13
II-7	Annual Available Electrical Energy for a 2-Axis Tracking Line Focus Fresnel Collector	II-14
II-8	Nomograph for Calculating Annual Average Array Coolant Temperature	II-15
II-9	Chart for Determining the Array Area Which Will Supply a Required Load Fraction	II-20
II-10	Chart for Determining the Array Area Which Will Satisfy an Instantaneous Load for an Instantaneous Insolation	II-21
II-11	Chart for Determining Economic Feasibility	II-23
II-12	Chart for Preliminary Heat Exchanger Sizing	II-27
II-13	Cooling Tower Parasitic Power Consumption	II-30
II-14	Average Daily PV-T Array Thermal Output	II-32

LIST OF FIGURES (Continued)

Figure		Page
II-15	Average Daily PV-T Array Electrical Output for an Inlet Temperature of 34°C	II-33
II-16	Average Daily PV-T Array Electrical Output Versus Inlet Temperature and Average Daily Insolation	II-35
II-17	Array Inlet Versus Output Temperature	II-36
II-18	Calculation of the Average Array Outlet Temperature for the Dixon Meat-Packing Plant	II-39
II-19	Typical Thermal Storage Configuration for the Dixon Plant	II-40
III-1	Temperature Dependence of Concentrator Photovoltaic Cell Current - Voltage Characteristics	III-12
III-2	Percent Power Loss Versus Fluid Temperature Differential	III-18
III-3	Typical Data Line Logic Protection Circuit	III-28
III-4	Inverter Cost Versus Size Based on DECC Pricing Information	III-43
III-5	Multiple Inverter Cost and Reliability Comparison	III-44
III-6	Power Conditioning Equipment Cost	III-45
III-7	Relative Enclosure Construction Quality Versus Cost	III-47
III-8	Relative Cost of Terminal Versus Current Rating	III-48
III-9	Safety Switch Reliability Versus Cost	III-50
III-10	Wire Size Versus Cost of Copper and Aluminum Wire	III-52
III-11	Cable Size Versus Cost for Various Insulation Types	III-53
III-12	Resistance of a Typical Copper Wire Versus Temperature	III-55
III-13	Relative Cost Versus Number of Wiring Connections for Various Wire Sizes	III-57

LIST OF FIGURES (Continued)

Figure		Page
III-14	Relative Cost of Diodes Versus Rating Overdesign	III-58
III-15	Power Loss Versus Number and Type of Blocking Diodes in a System	III-59
III-16	Bypass Diode Reliability Versus Junction Temperature	III-60
III-17	Inverter Cost Versus Modes of Operation	III-61
III-18	Data Acquisition System Capability Versus Cost	III-62
III-19	PV Array Electrical Isolation	III-66
III-20	Safety Interlock Concept	III-67
III-21	Short Circuit Failure	III-69
III-22	AC Switchgear Sensing Circuit	III-71
III-23	Thermal Circuit for Example MTTF Calculation at Elevated Temperature	III-73
III-24	Mean Time to Failure Versus Junction Temperature for Example Diode	III-75
III-25	Thermal Resistance Calculation for J-Box	III-77
III-26	Monitoring a Base PV System	III-81
III-27	Pyranometer Measurement Schematic	III-83
III-28	Data Acquisition System Cost Comparison	III-85
III-29	Typical Detailed Photovoltaic System Block Diagram	III-91
III-30	AC Power One-Line Diagram	III-92
III-31	String Voltage Matrix	III-93
III-32	Simple Model of PV-T Heat Transfer Network	III-96
III-33	DC Block Wiring Diagram	III-107
III-34	Peak Power Tracking Error Examples	III-109

LIST OF FIGURES (Continued)

Figure		Page
III-35	Example of Imbalance	III-110
III-36	Major Utility Interface Components	III-113
III-37	Peak Power Tracker Oscillation	III-114
IV-1	Annual Net Electrical and Thermal Energy Available for a Line Focus Fresnel Collector for Various Numbers of 4-Module Arrays/Row	IV-7
IV-2	Annual Net Electrical and Thermal Energy Available for a Line Focus Fresnel Collector for Various Numbers of 4-Module Arrays Per Row	IV-8
IV-3	Maximum Temperature Rise Versus Flow Rate and Number of 4-Module Arrays Per Row for the Line Focus Fresnel Collector System	IV-9
IV-4	Floating Tubesheet Exchanger	IV-11
IV-5	Plate and Frame Heat Exchangers	IV-12
IV-6	Cost Comparison of Plate and Shell-and-Tube Heat Exchangers	IV-13
IV-7	Double-Pipe Heat Exchanger	IV-15
IV-8	Fixed Tube Sheet Design	IV-16
IV-9	"U" Tube Design	IV-16
IV-10	Floating Head Pull-Through Bundle Type	IV-16
IV-11	Tube Arrangements Used for Shell-and-Tube Heat Exchangers	IV-19
IV-12	Plate Heat Exchangers Flow Patterns	IV-23
IV-13	Heat Transfer Effectiveness as a Function of Number of Transfer Units and Capacity Rate Ratio; Counterflow Exchanger	IV-28
IV-14	Specific Pressure Drop Versus Channel Film Heat Transfer Coefficient	IV-36

LIST OF FIGURES (Continued)

Figure		Page
IV-15	Countercurrent ε-NTU Relations for Loop Patterns	IV-37
IV-16	Configuration for Heat Exchanger Analysis	IV-42
IV-17	Total Cost of Heat Exchanger Penalty for I = 600 W/M^2 and N = 9	IV-50
IV-18	Total Cost of Heat Exchanger Penalty for I = 600 W/M^2 and N = 18	IV-51
IV-19	Total Cost of Heat Exchanger Penalty for I = 300 W/M^2 and N = 18	IV-52
IV-20	Optimum Effectiveness and Minimum Total Penalty Cost for I = 300 W/M^2	IV-54
IV-21	Optimum Effectiveness and Minimum Total Penalty Cost for I = 600 W/M^2	IV-55
IV-22	Cooling Tower Interface Schematic	IV-63
IV-23	Cooling Tower Performance Factors	IV-65
IV-24	Typical PV-T System Without Storage	IV-70
IV-25	Typical PV-T System with Storage in Parallel with the Load	IV-70
IV-26	Series Tank with Mixing Valve	IV-72
IV-27	Impeller Design Versus Specific Speed	IV-78
IV-28	Radial Flow Pump	IV-79
IV-29	Variable Impeller Diameter Curves	IV-79
IV-30	Nomograph Relating Pumping Head, Capacity, and Speed to Determine Pump and Suction Specific Speeds for Centrifugal Pumps	IV-80
IV-31	Specific Diameter Versus Specific Speed and BEP	IV-82
IV-32	Typical Cut-away View of Valves	IV-88

LIST OF FIGURES (Continued)

Figure		Page
IV-33	Pipe Sizing Chart for 5 gpm/row	IV-100
IV-34	Pipe Sizing Chart for 6 gpm/row	IV-101
IV-35	Pipe Sizing Chart for 8 gpm/row	IV-102
IV-36	Pipe Sizing Chart for 10 gpm/row	IV-103
IV-37	Pipe Sizing Chart for 12 gpm/row	IV-104
IV-38	Specific Gravity of Aqueous Solutions of Ethylene Glycol	IV-108
IV-39	Viscosity of Aqueous Solutions of Ethylene Glycol	IV-109
IV-40	Collector Field Flow Resistance Network	IV-111
IV-41	Equivalent Series Flow Resistance	IV-112
IV-42	Series Reduced Network	IV-113
IV-43	Equivalent Parallel Flow Resistance	IV-113
IV-44	Parallel Reduced Network	IV-114
IV-45	Computational Procedure for Calculating the Pressure Drop Across an End Feed Direct Return Collector Field	IV-116
IV-46	Center Feed Collector Layout and Flow Resistance Network	IV-117
IV-47	Equivalent Flow Resistance Network	IV-119
IV-48	Calculation Procedure for Pressure Drop	IV-120
IV-49	Typical Insulated Hanger	IV-123
IV-50	Pipe Layout for Flexibility Analysis	IV-131
IV-51	Typical PV-T Pipe Layout	IV-136
IV-52	Typical PV-T System Layout and Outlet Manifold	IV-136
IV-53	Detail of Flex Hose Connection--Section G-G of Figure IV-41	IV-138

LIST OF FIGURES (Continued)

Figure		Page
IV-54	Insulation Costs and Heat Lost as a Function of Thickness	IV-140
IV-55	Optimum Thermal Resistance Per Foot of Pipe	IV-148
IV-56	Bare Pipe Heat Loss	IV-149
IV-57	Flow of 60°F Water in Schedule 40 Pipe	IV-157
IV-58	Pipe Hangers	IV-161
IV-59	Insulation With a Gap	IV-164
IV-60	Approximate Thermal Conductivities of Pipe	IV-167
IV-61	Heat-Loss Rate Versus Insulation Thickness for Various Pipe Diameters	IV-168
IV-62	PV/T System With Heat Pump	IV-170
IV-63	Typical COPs for Heat Pump	IV-174
IV-64	Typical Boiler System Showing Major Components	IV-177
IV-65	Ways of Preheating a Boiler	IV-178
IV-66	Spray Stack Economizer Boiler	IV-180
IV-67	Losses From a Typical Industrial Boiler	IV-182
IV-68	Extra Fuel Energy Use Compared to Total Use	IV-184
V-1	Symbolic Logic Block Diagram	V-5
V-2	Example Fault Tree Versus Functional Diagram	V-8
V-3	Reliability Block Diagram Versus Functional Diagram	V-11
V-4	Preventive Maintenance Intervals	V-20
VI-1	Linear Parabolic Trough Collectors	VI-2
VI-2	Four-Module Fresnel Lens Array	VI-3

LIST OF FIGURES (Concluded)

Figure		Page
VI-3	Martin Marietta Second Generation Array	VI-4
VI-4	Design of Structures and Foundation for PV-T System	VI-7
VI-5	Structures and Foundation Issues Associated with PV-T System Design Ground-Mounted System	VI-12
VI-6	Proposed Categorization of Solar Array Foundation Soils	VI-13
VI-7	Array Support Structure Wind Forces Determination	VI-15
VI-8	Characteristics of E-Systems Array	VI-18
VI-9	Model Axis System	VI-22
VI-10	Definition of Coordinate System	VI-24
VI-11	Martin Marietta System Wind Tunnel Test Results	VI-25
VI-12	Basic Equations of Rigid-Pile Theory	VI-31
VI-13	Solar Collector Drive Pylon	VI-34
VI-14	Solar Collector Interior Pylon	VI-35
VI-15	Martin Marietta Foundation Pier	VI-36
VI-16	Layout of "J" Bolts and Reinforcements	VI-37
VI-17	Linear Focus Two-Axis Tracking Foundation	VI-38
VI-18	Four-Spring Subgrade Modulus Model	VI-40
VI-19	Some Guidelines for Design of Structures and Foundations	VI-41
VI-20	Areas Deserving Additional Investigation	VI-41
VII-1	PV-T Receiver Heat-Up Curves for Two Types of Failure	VII-19
VII-2	PV-T Receiver Stagnation Temperatures	VII-20

LIST OF TABLES

Table		Page
II-1	Annual Average Daytime Ambient Temperatures for SOLMET Sites	II-9
II-2	Average Daily Insolation and Hours of Operation	II-34
III-1	Results of Temperature Differential Study	III-14
III-2	Modeling Validation	III-16
III-3	Matrix of Analysis Run Conditions	III-17
III-4	Results of PV-TAP Thermal Length Study	III-19
III-5	Diode Reliability Characteristics Versus Junction Temperature	III-76
III-6	Radiation Properties of Materials	III-78
III-7	Typical Critical Design Specifications for Inverters for Commercial and Industrial Utility-Interactive Applications	III-104
IV-1	Qualitative Comparison of Shell and Tube and Plate Heat Exchangers	IV-13
IV-2	Typical Overall Heat Transfer Coefficients for Tubular Exchangers	IV-29
IV-3	Typical Fouling Factors for Shell-and-Tube Heat Exchangers	IV-38
IV-4	Typical Fouling Factors for Plate Heat Exchangers	IV-38
IV-5	Typical Frequency and Duration of Summer Wet Bulb Temperatures	IV-59
IV-6	Cooling Tower Size Selection	IV-66
IV-7	Applicability of Various Storage Tanks	IV-73
IV-8	Suggested Pipe Support Spacing	IV-124
IV-9	Stress Range Reduction Factors	IV-127

LIST OF TABLES (Concluded)

Table		Page
IV-10	ANSI/ASME B31.1-1980 Edition Appendix B Thermal Expansion Data	IV-132
IV-11	Surface Resistance as a Function of Emittance Insulation Resistance, and Wind Velocity	IV-144
IV-12	Insulation Price Per Volume	IV-150
IV-13	Dimensions and Properties of Steel Pipe	IV-153
IV-14	Pipe Hanger Characteristics	IV-162
VI-1	Power Law Exponents for Various Terrain Types	VI-20
VI-2	Porosity Effects on Martin Marietta System	VI-23

CHAPTER I
INTRODUCTION

The selection of a PV-T system appropriate for a particular application, and the design decisions necessary to make that system function in the most efficient way requires knowledge of a vast variety of technical and design issues. This volume was written to present most of the technical issues which must be considered when selecting or designing a PV-T system.

A general design methodology is provided in figure I-1, which indicates the sequence of events in the design of a PV-T system. First, the designer must determine the characteristics of the site and the load including weather data; local energy costs, land costs, and economic data; daily and seasonal load profiles and temperature requirements; and site constraints such as land availability, shadowing by adjacent structures, and localized pollution.

When the site/application characteristics have been determined, the designer can use generalized collector and system characteristics, annual solar availability for that site, and load characteristics to develop an initial conceptual design. Although detailed performance and economic analysis would require an hour-by-hour simulation for an entire year, this generalized analysis is the first step in determining the feasibility of using a PV-T system for a particular site/applications pair. The techniques for performing this initial feasibility analysis and preliminary array sizing are described in the next section.

If the initial feasibility analysis indicates further consideration of a PV-T system is warranted, a preliminary array layout can be developed based on electrical requirements and site configuration. Tradeoffs must now be made between the optimum array size and power output, site configuration, input voltage requirements of the inverter, and penalties associated with paralleling collectors at different temperatures. Design issues and guidance associated with the electrical system are discussed in Chapter III.

DESIGN METHODOLOGY

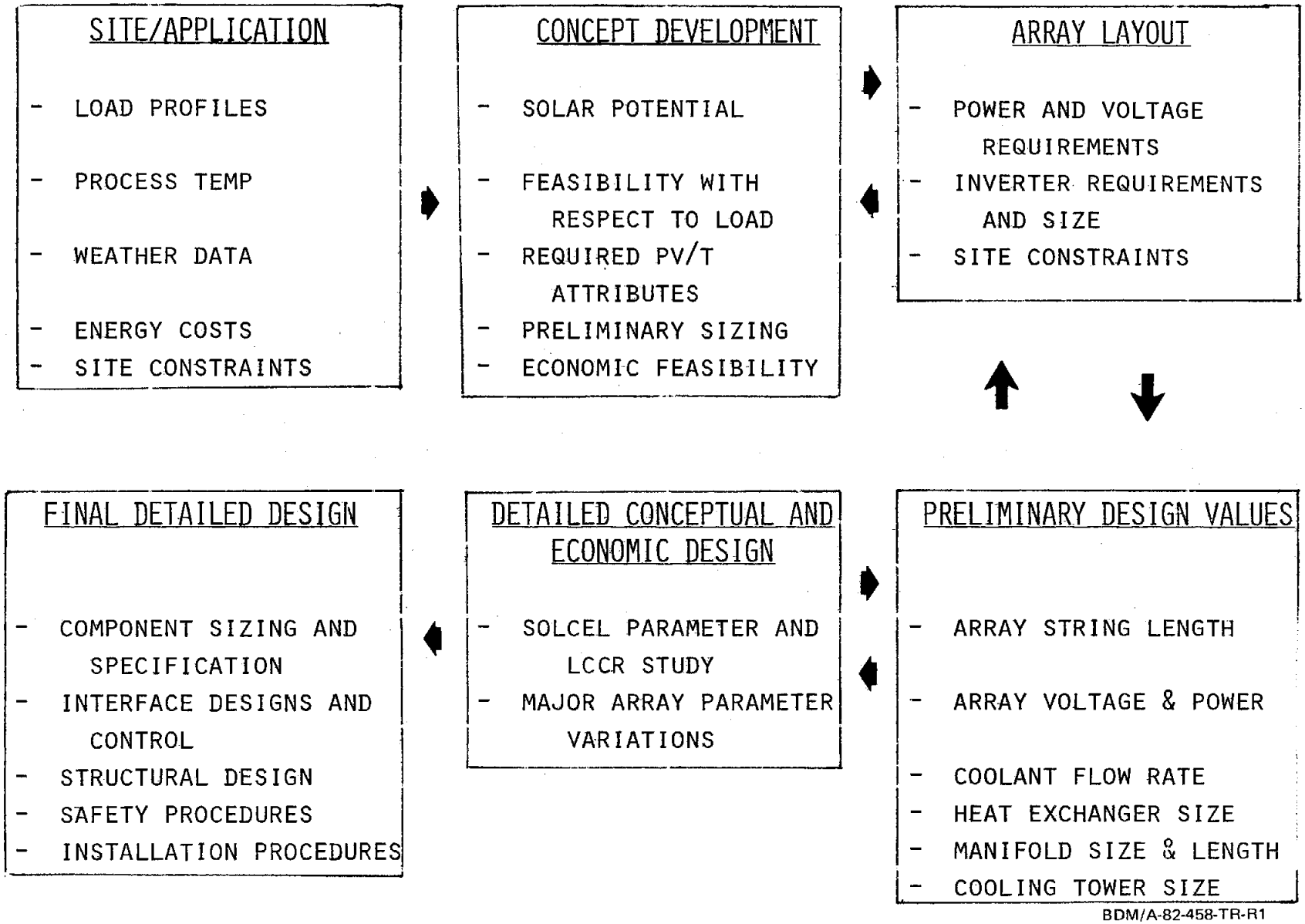

BDM/A-82-458-TR-R1

Figure I-1. Design Methodology

Issues associated with overall field layout and row spacing were discussed in Volume I, chapter I, along with the characteristics of various collector types.

Since the array electrical output depends on the average array temperature, as well as the temperature difference between paralleled collectors, iterations are required between the thermal design and electrical design to develop an optimum field layout. A typical conceptual configuration is shown in figure I-2. The major thermal design parameters which will affect the system output include the coolant flow rate through each row of collectors, row length, heat exchanger size, and cooling tower size. Preliminary sizing can be performed using techniques described in subsequent sections.

Once a preliminary array size, field layout, and component sizing has been accomplished, a performance simulation and life cycle cost study is recommended using an hour-by-hour system simulation with a computer code such as SOLCEL-II, modified to include the thermal system components. Such a simulation code can be used to vary major array parameters to size the system and components so that an optimum system is achieved in terms of minimum life cycle cost.

Finally, a detailed design may be developed that would include sizing and selecting various electrical and mechanical components such as J-Boxes, switches, wire, pumps, insulation, etc. In addition, the structural design, safety procedures, and installation procedures should be developed at this stage.

Design guidance for overall system design, as well as component selection, is provided in the following sections. Other issues which the engineer must consider include those associated with component and system reliability and maintainability, and institutional issues peculiar to PV-T systems.

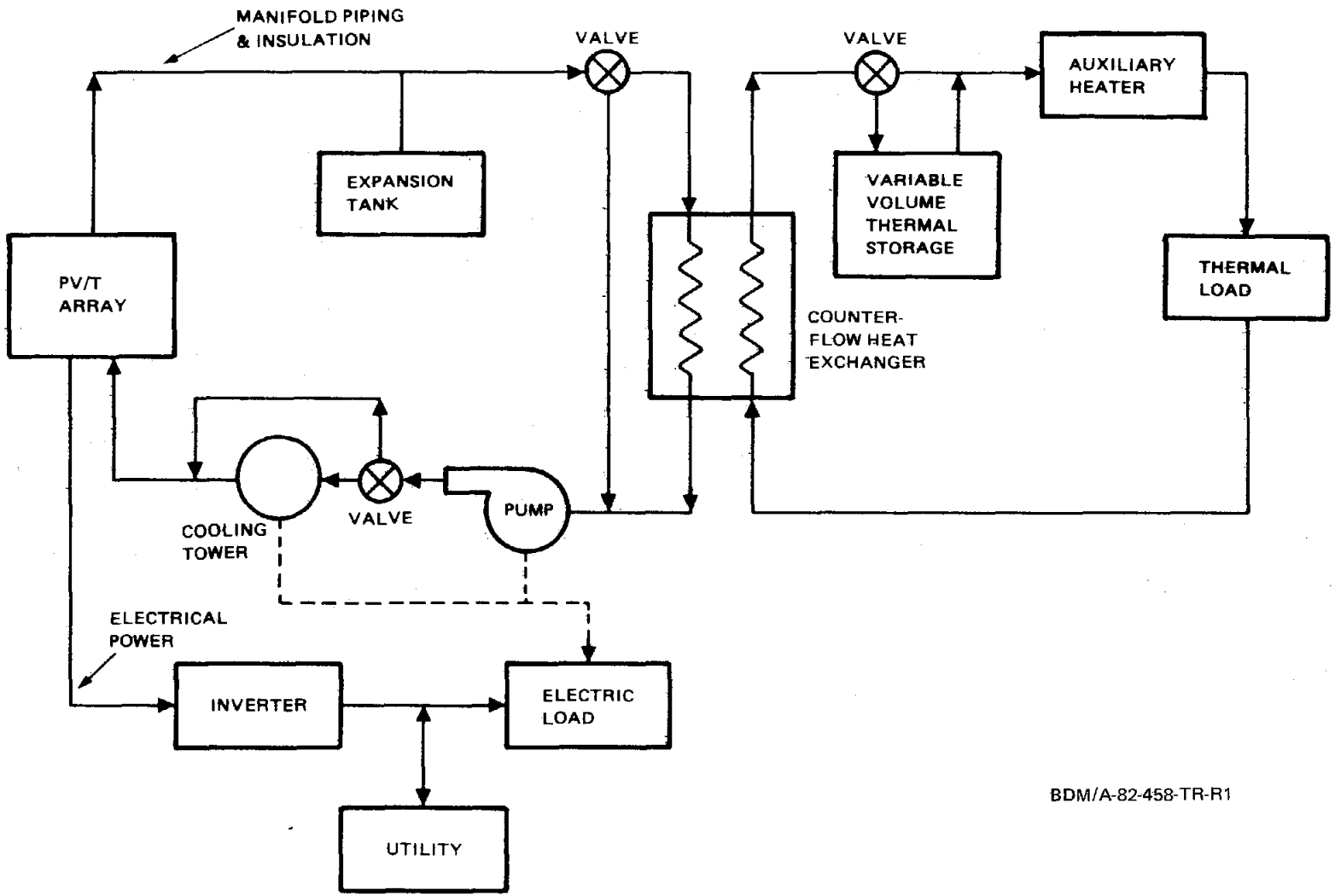

Figure I-2. Conceptual PV-T System for Preliminary Analysis and Sizing

CHAPTER II
SIZING AND LOAD MATCHING

A. DESIGN ISSUES

1. Objective

This chapter introduces the issues associated with the design of PV-T systems. These issues are presented in a manner intended to enhance and extend the designer's understanding of the PV-T design process and to provide an intuitive base for those issues unique to PV-T. Methods are also presented by which the design issues may be addressed and quantified. The next section reviews the major phases in the design process and their related design issues.

2. Background - The Design Process

To set the stage for the work presented below, let us consider the design process that this effort is meant to support. The design of a system normally evolves through four phases, with two additional phases if construction and startup are considered. During each phase a number of iterations and tradeoffs occur in the selection and sizing of components and subsystems to arrive at a suitable system configuration. Iterations may also be necessary between phases or combinations of phases as the design progresses. The basic factors that effect these tradeoffs are discussed in the next paragraph.

The characteristics of the load to be met have a great impact on the concepts to be considered. Load patterns are quite different for commercial applications, such as stores or light manufacturing plants, as compared to industrial applications, which can have wide variations in load characteristics. System ownership will affect system characteristics such as simplicity, accessibility, maintenance, reliability, longevity, safety requirements, and the initial and operating costs. The value society places on "going solar" will have a tremendous impact on the economic aspects of the system, particularly in the commercial and industrial sectors.

The utility interface has a very strong influence on the acceptability of a PV-T concept. This single interface is perhaps the most important and responsive impact that the system will have on society.

In designing a system to utilize the PV-T design concept the aforementioned factors must be addressed as the design evolves. At each stage of the design process, the designer must make decisions regarding the design parameters involved in that stage, often with little insight or guidance available regarding the effects of these decisions on later stages of the process. For reference purposes the basic phases of the engineering design process for a PV-T project are outlined in figure II-1.

As can be seen from this outline the design participants need a variety of design aids, guides, and techniques which reflect their needs and responsibilities at each stage of the process. A brief listing of specific components of a design methodology for PV-T systems is given below.

(1) Concept Development
   - (a) Guidelines for selection of the most promising PV-T technologies and configurations.
   - (b) Rule of thumb (pencil and paper) design parameter estimations based on gross load/climate characteristics should be configuration-independent.
   - (c) Guidelines for satisfaction of utility and plant or building interface requirements.
   - (d) Methodology to quickly assess the technical and economic promise of the application utilizing a given design concept.
   - (e) Guidelines for assessing the effects of conservation actions on the feasibility of using a PV-T configuration.

(2) Schematic Development
   - (a) Simple (hand calculator) techniques for determining "reasonable" design values for configurations of interest.

Concept Development

- Applications requirements
- Client needs/desires
- Compilation of supporting information
- Site resources
  - Solar
  - Microclimate
- Local building practices/costs
- Zoning
- Identification of appropriate PV-T design configurations with consideration of conservation opportunities
- Utility interface requirements
- Selection of suitable concept(s)
- Preliminary design tradeoffs on technical and economic performance

Schematic Development

- Quantify design requirements
  - Structural limitations, site, microclimate, interfaces, local practice and building codes
- Identify design criteria
  - Reliability, cost, aesthetics, maintainability
- Identify configurations that qualitatively meet requirements and criteria
- Evaluate promising configurations to identify most qualitatively desirable design solution

Design Development--Synthesis

- Iteratively develop design layout and specifications with client
- Design tradeoffs, optimization of final configuration, construction detail recommendations

Contract Documents

- Working drawings, specifications, vendor lists for bidding, obtaining permits, financial negotiations, appraisals
- Performance prediction and evaluation

Assemble operating and maintenance manuals

----------End of Design Effort----------

Construction

- Modification for cost, ease of construction
- Client requests

Post Construction

- Tuning, owner training, performance verification

BDM/A-82-458-TR-R1

Figure II-1. Design Phases for Application of PV-T Design Concepts

(b) Performance/cost estimation techniques for configuration and component selection.

(c) Criteria for cross configuration comparisons.

(3) Design Development

(a) Simple to complex (depending on magnitude of project) techniques for determining optimal design parameter values for a configuration.

(b) Final performance/cost estimation techniques.

(c) Sensitivity of design to parameters accessible for post construction tuning.

(4) Contract Documents

(a) Methodology for developing lender/financial presentation - must reflect magnitude of project construction.

(b) Methodology for making detailed engineering calculations.

(c) Techniques for onsite evaluation of modifications and changes during construction.

(5) Post Construction

(a) Performance monitoring and evaluation

(b) Identification and evaluation of final tuning procedures for optimal performance of "as built" system.

3. Description of PV-T Systems

Prior to addressing the design issues the project must be focused by defining the system(s) being addressed. For our purposes a PV-T system is a solar system that seeks to provide both thermal and electrical energy to a load with utility sellback. It is assumed that the system consists of actively cooled concentrating photovoltaic collectors, indirectly coupled to the load via a heat exchanger. Because of the relative values of electricity and heat, the system will contain a cooling tower or other heat rejection device if the thermal load is insufficient or non-existent during periods of possible operation. In some cases thermal storage on the load side may be required for proper operation.

Coupling the above description with the control system requirements for a particular collector technology and load results in a large number of possible configurations. Add to this the requirements and constraints of the load, climate, and site, and the magnitude of the designer's task becomes impressive. The remainder of this chapter will guide the designer to a successful result.

4. Overview

In this section we address the concept development phase of the design process for PV-T systems. The design issues pertinent to this phase are identified, followed by a discussion of how they may be quantified and resolved at the appropriate level of detail. The chapter concludes with a discussion of the interaction of the Concept Development phase with the remaining design phases.

B. CONCEPT DEVELOPMENT

1. Introduction

The design issues associated with the preliminary assessment of a PV-T application are identified in this section. Methods and guidelines for addressing these issues and arriving at an assessment of the feasibility of a given application are developed. The primary objectives of this phase in the design process are:

(1) Assess technical and economic feasibility.

(2) Identify most promising technologies and design configurations for a given application.

(3) Establish preliminary design values for the major design parameters.

This phase culminates in a decision, with supporting data, to continue or terminate the design exercise for a candidate application.

2. Design Issues for Concept Development Phase

The issues of concern to the PV-T system designer at this phase in the design are:

(1) Assess the site's solar potential.

(2) Evaluate feasibility of application with respect to thermal and electrical load characteristics.

(3) Identify required/desirable PV-T system attributes and relate them to technologies and configurations.

(4) Establish preliminary sizing requirements.

(5) Assess requirements for economic feasibility and relate them to design requirements.

(6) Present client with sufficient information to support a decision on the continuation of project.

To address these issues in a cost competitive manner, the designer must have access to an efficient design methodology. The methodology must be general enough to address all regions of the country and a wide range of application characteristics. At the same time it must be easy to use and sufficiently accurate to ensure confidence in its results. In the following sections each of the design issues is discussed and an appropriate method for addressing it is developed and explained.

a. Solar Potential

In prior sections we have addressed the issues and concerns used to identify a favorable site application pair. In this section we address the evaluation of the gross annual thermal and electrical energy produced by the various collector technologies.

Based on the correlations derived in references II-1 and II-2, and reproduced in equation II-1 for a two-axis tracking collector, the average annual available energy from a collector may be determined for the average insolation at a site and the threshold insolation given by equation II-2.

$$Q/F_m\eta_o = -0.041 + 15.558I - 0.311\ I^2 + (-2.264 - 30.876\ I + 20.7389\ I^2)\ X + (3.987 + 7.711\ I - 14.538\ I^2)\ X^2 \qquad \text{(Eq. II-1)}$$

$$X = \frac{U_L(T_f - T_a)}{\eta_o} \qquad \text{(Eq. II-2)}$$

At insolation levels below the threshold the collector loses more energy than it gains. The collector characteristics, U_L and η_o, have been defined in Volume I. T_f is the average coolant temperature, T_a is the annual average daytime temperature, and I is the average direct normal insolation in kW/m^2. The average annual direct normal insolation for the United States is shown in figure II-2, and the annual average temperatures for solmet sites are given in table II-1.

As shown in Volume I, line focus Fresnel (LFF) and linear parabolic trough (LPT) collectors have the highest annual efficiencies and largest output for the land area used. The maximum available energy from these systems (for X = 0) is shown in figure II-3. For convenience, major cities are shown corresponding to their annual average direct normal radiation. Figures II-4 through II-7 show the average electrical and thermal energies from LPT and LFF collectors. These curves were calculated using the collector characteristics defined in Volume I. Since LFF systems have the greatest available energy, subsequent analyses will be performed only for this type of collector.

In order to use these curves to determine solar availability, the average collector temperature must be determined. This can be found using figure II-8. This nomograph was developed using equations II-3 through II-6.

$$q_u = F_R \left[I\eta_o - U(T_{a,i} - T_a) \right] = \frac{\dot{M}_a C_p}{A_a} \quad (T_{a,o} - T_{a,i}) \qquad \text{(Eq. II-3)}$$

$$T_f = \frac{1}{2} \quad (T_{a,o} + T_{a,i}) \qquad \text{(Eq. II-4)}$$

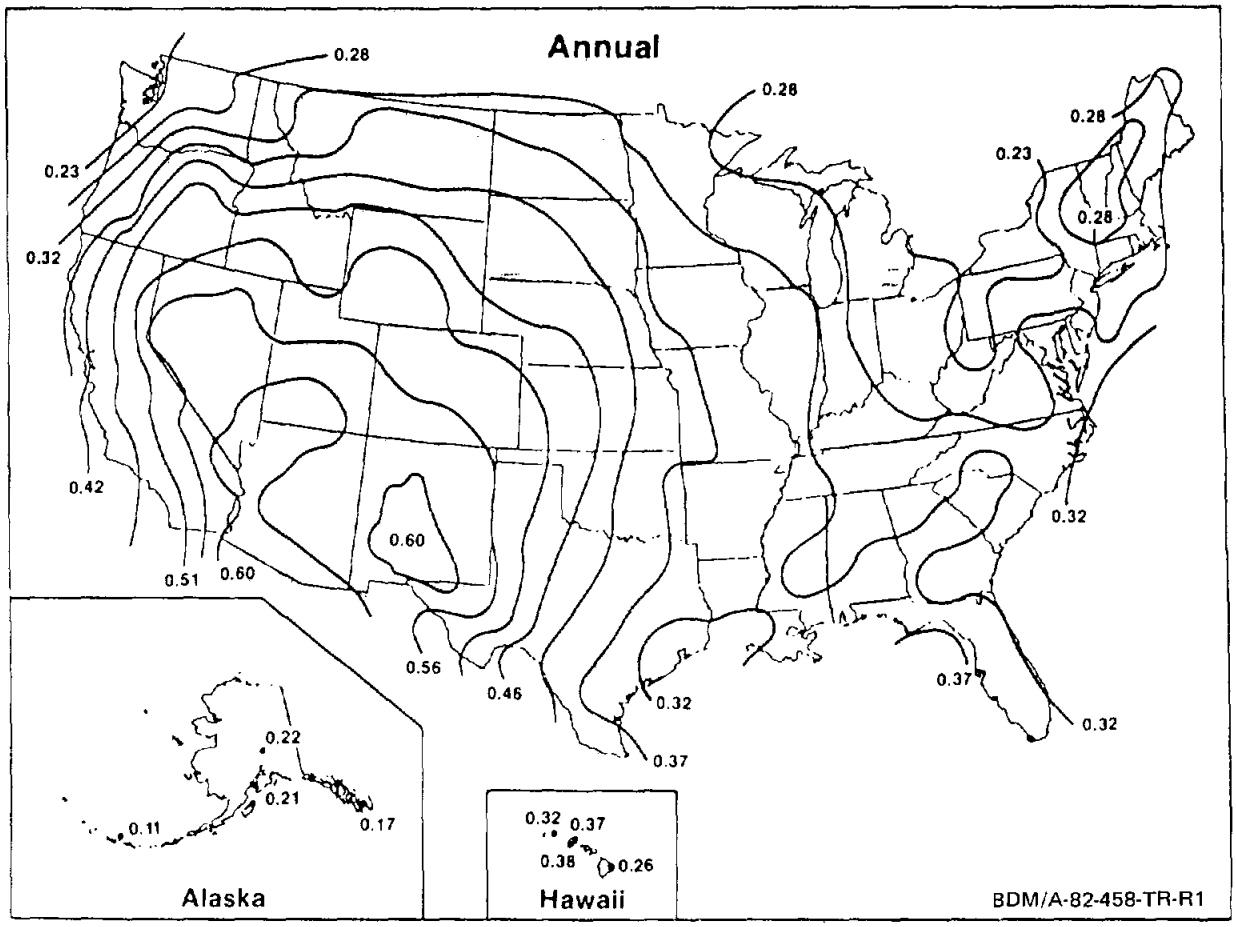

Figure II-2. Yearly Average Direct Normal Irradiance (in kW/m^2) During Daylight Hours

TABLE II-1. ANNUAL AVERAGE DAYTIME AMBIENT TEMPERATURES FOR SOLMET SITES (°C)

SOLMET SITE	LATITUDE (DEG)	APPROXIMATE ELEVATION (M)	YEARLY
FT. WORTH, TX	32.0	204.	20.9
LAKE CHARLES, LA	30.2	0.	22.1
COLUMBIA, MO	39.0	231.	15.5
APALACHICOLA, FL	29.7	0.	22.1
MIAMI, FL	25.8	0.	25.5
BROWNSVILLE, TX	25.9	10.	24.7
CHARLESTON, SC	32.9	0.	20.5
NASHVILLE, TN	36.1	100.	17.6
DODGE CITY, KS	37.8	701.	15.6
CARIBOU, ME	46.9	135.	6.9
MADISON, WI	43.1	263.	11.0
EL PASO, TX	31.0	1209.	20.9
ALBUQUERQUE, NM	35.1	1511.	16.2
ELY, NV	39.3	1959.	10.8
PHOENIX, AZ	33.4	332.	25.0
SANTA MARIA, CA	34.9	66.	15.7
BISMARCK, ND	46.8	512.	9.2
GREAT FALLS, MO	47.5	1016.	10.0
MEDFORD, OR	42.4	424.	14.5
SEATTLE, WA	47.5	30.	12.0
FRESNO, CA	36.0	90.	20.0
CAPE HATTARAS, NC	35.3	0.	10.5
WASHINGTON, DC	39.0	15.	15.4
BOSTON, MA	42.4	0.	12.6
NEW YORK, NY	40.8	0.	13.0
OMAHA, NE	41.4	317.	13.0

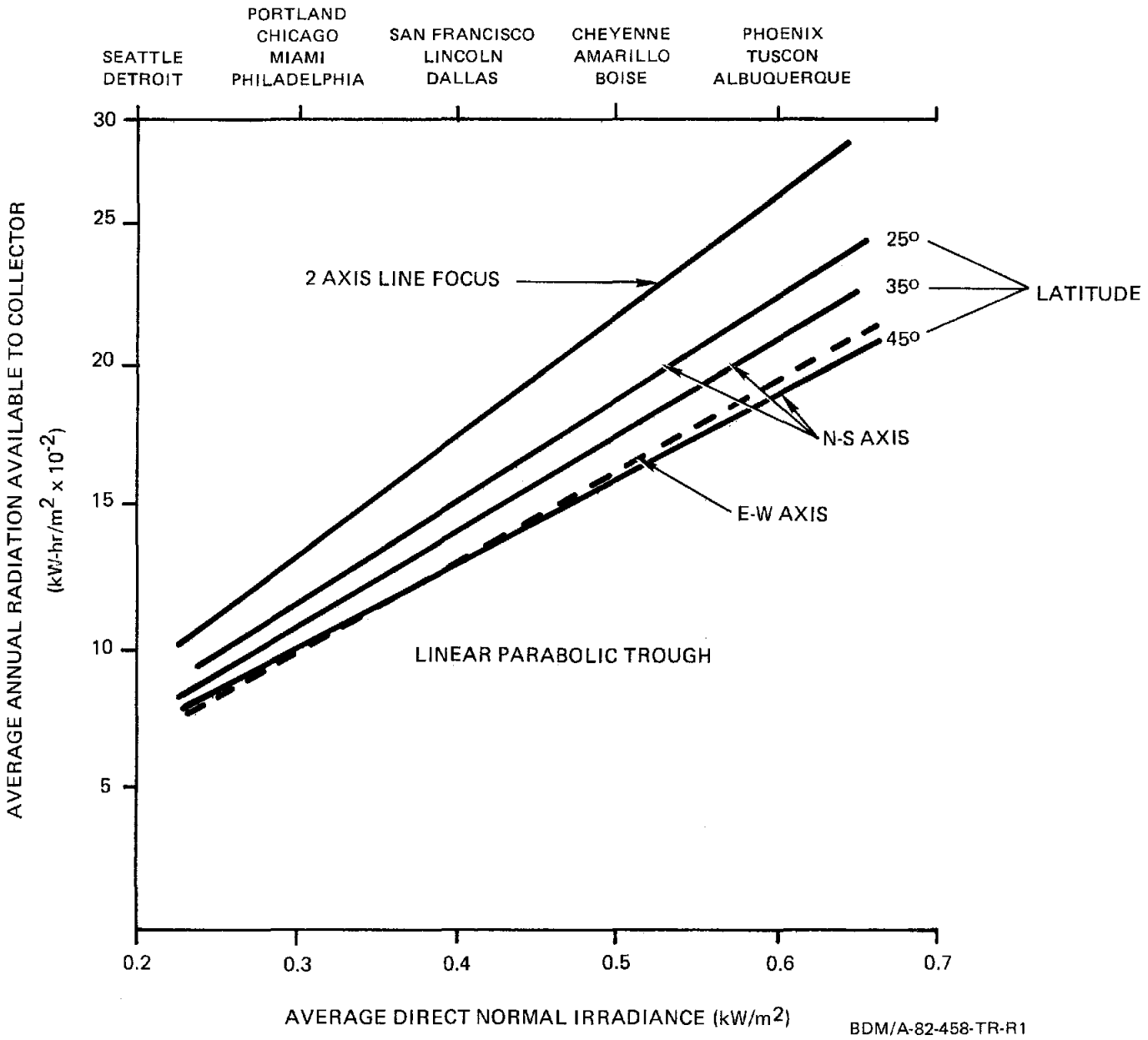

Figure II-3. Maximum Annual Average Insolation Available to LFF and LPT Collectors

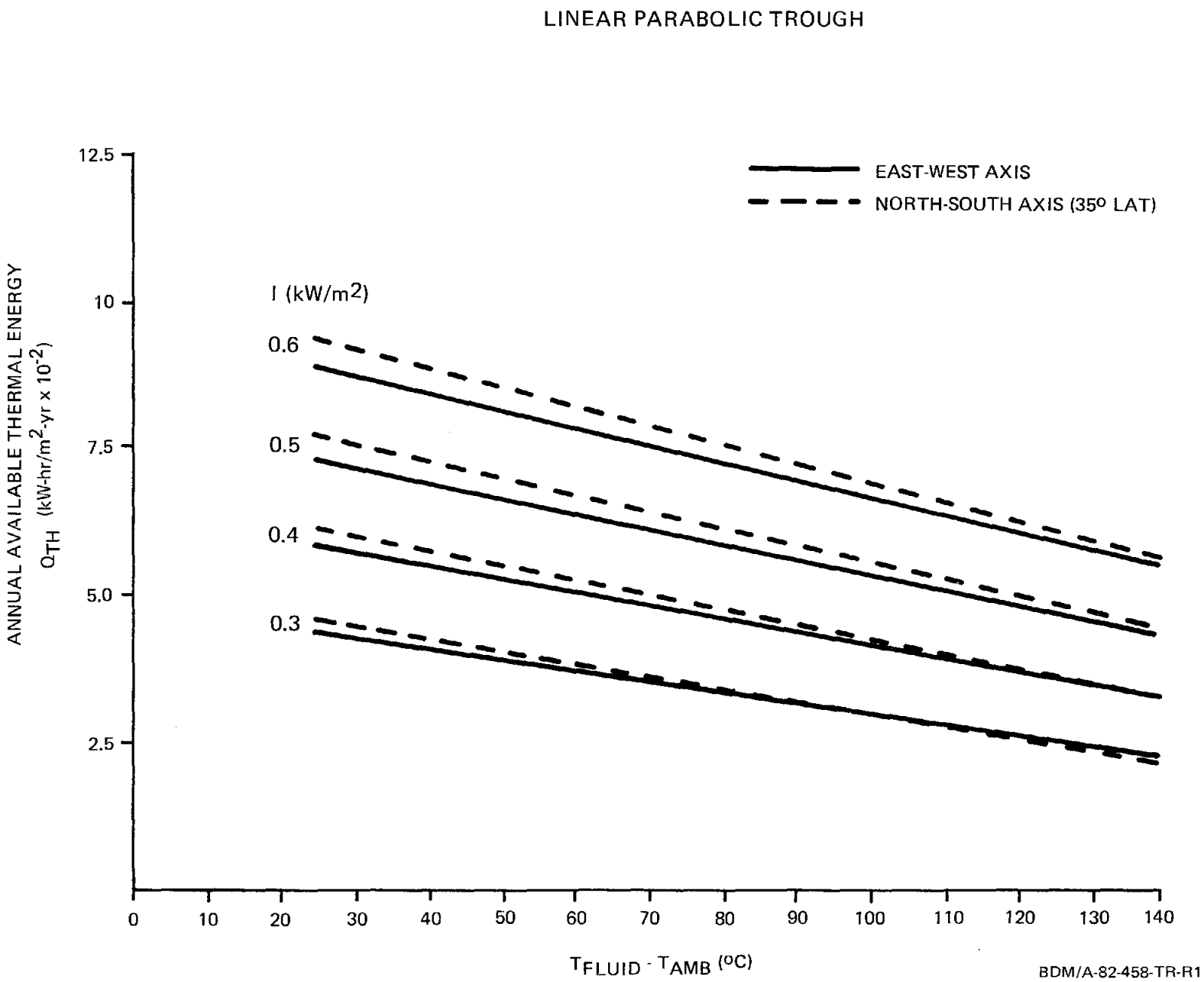

Figure II-4. Annual Available Thermal Energy for a Linear Parabolic Trough Collector

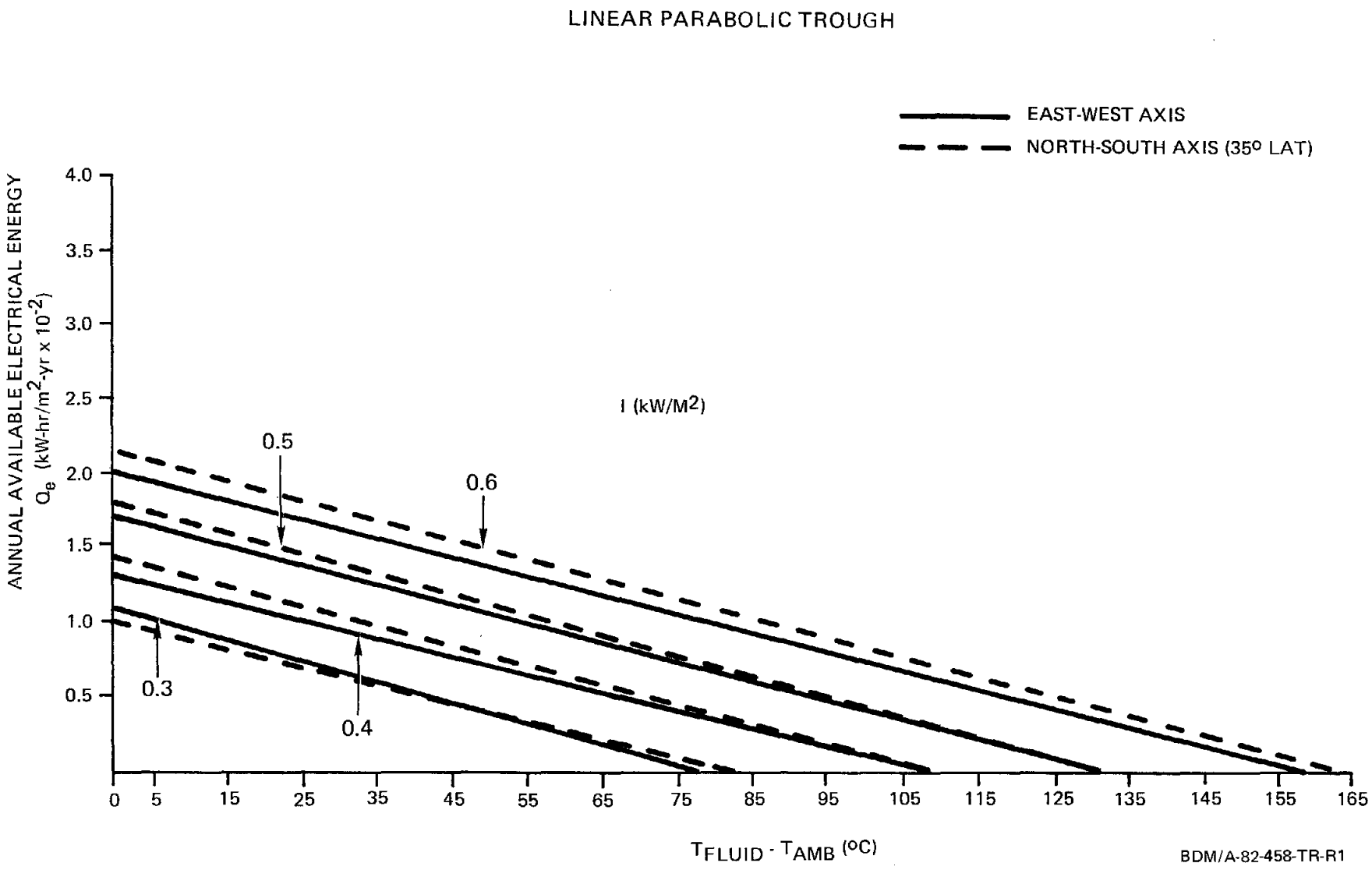

Figure II-5. Annual Available Electrical Energy for a Linear Parabolic Trough Collector

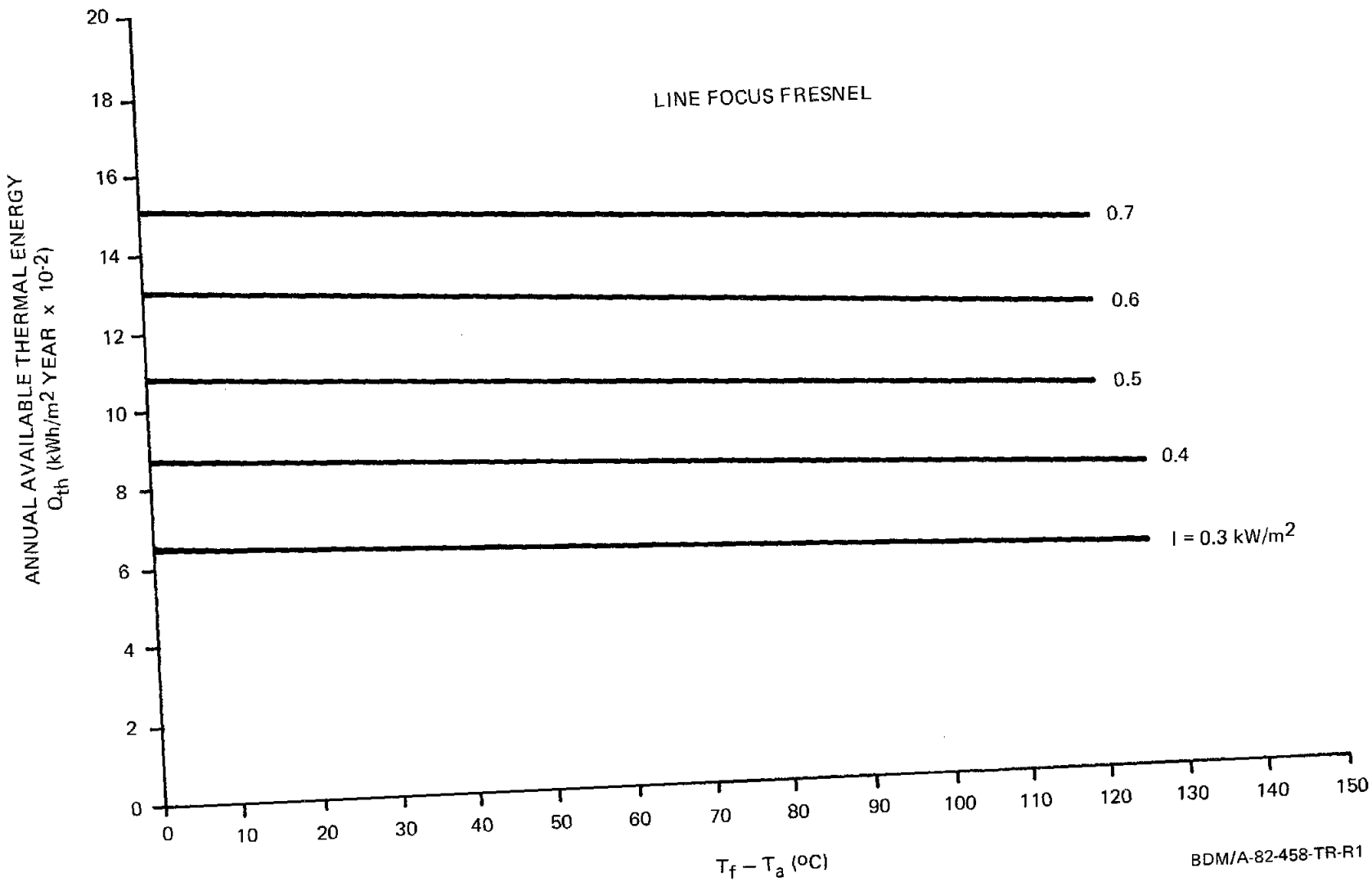

Figure II-6. Annual Available Thermal Energy for a 2-Axis Tracking Line Focus Fresnel Collector

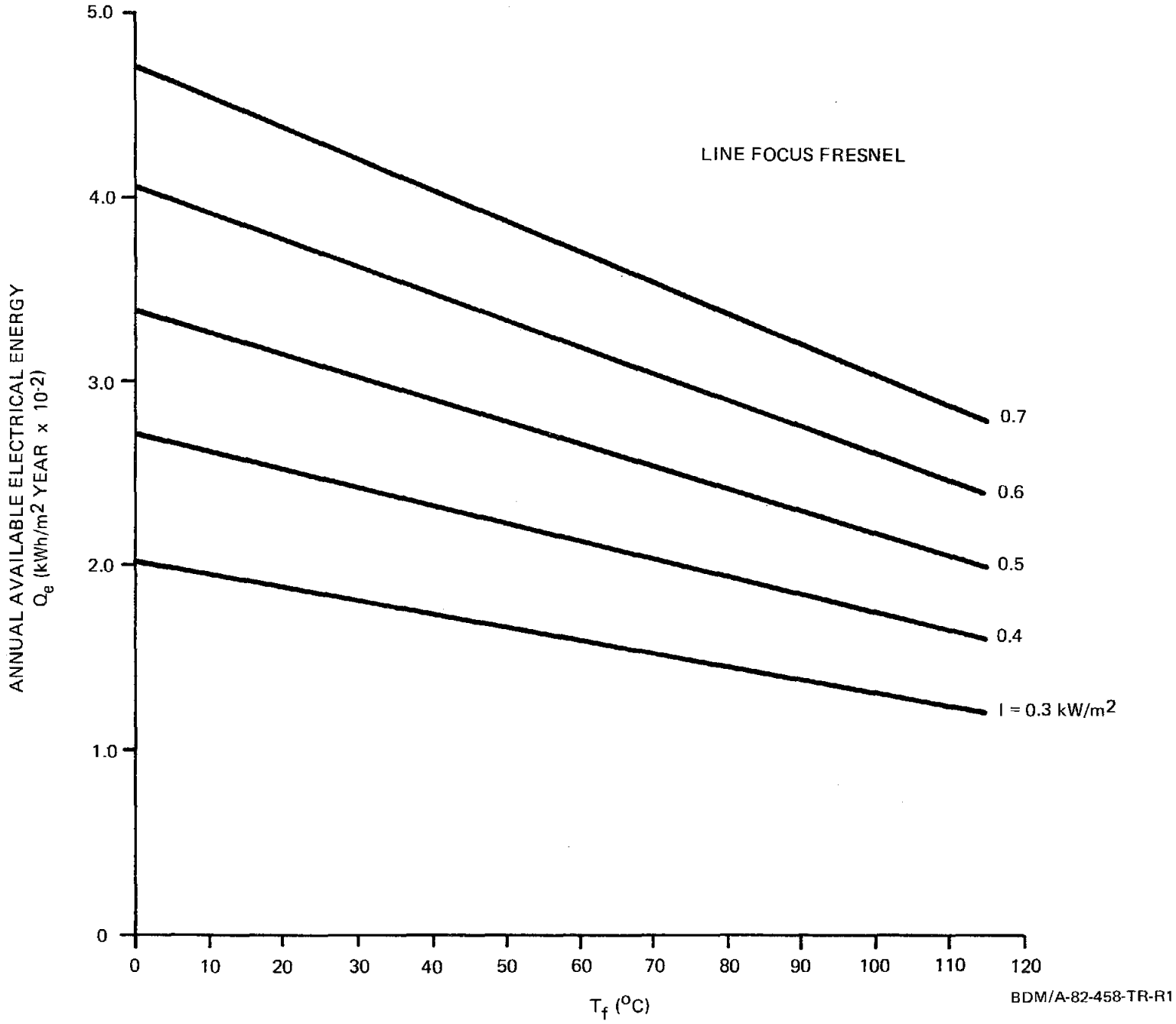

Figure II-7. Annual Available Electrical Energy for a 2-Axis Tracking Line Focus Fresnel Collector

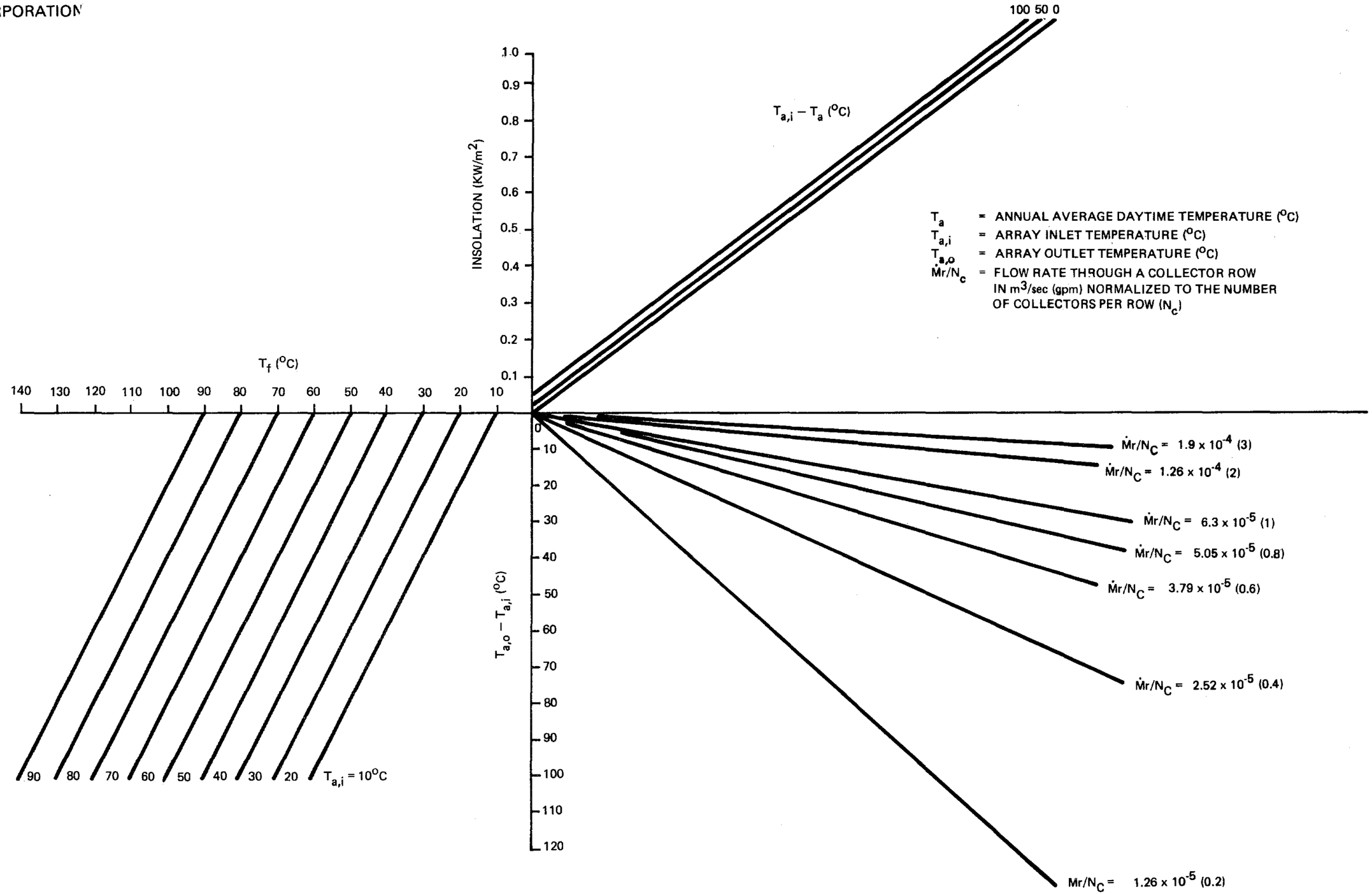

BDM/A-82-458-TR-R1

Figure II-8. Nomograph for Calculating Annual Average Array Coolant Temperature

$$F_R = \frac{\dot{M}_a C_p}{UA_a} \left[1 - \exp\left(\frac{-UA_a F_m}{\dot{M}_a C_p} \right) \right] \qquad \text{(Eq. II-5)}$$

$$A_a/\dot{M}_a = \frac{A_c N_c N}{\dot{M}_r N} = \frac{A_c}{\dot{M}_r/N_c} \qquad \text{(Eq. II-6)}$$

where F_m = heat removal factor based on the average fluid temperature and defined in Volume I.

F_R = heat removal factor based on the array inlet temperature

A_a = array area (m^2)

A_c = collector area (11.2 m^2 for LFF)

$\dot{M}_a$ = total array flow rate

$\dot{M}_r$ = flow rate through a row

N_c = number of collectors per row

N = number of rows

$\dot{q}_u$ = useful thermal energy produced by the array.

This nomograph may be used as follows:

(1) Assume an array inlet temperature. This may be the load return temperature or, if a heat exchanger is used in the system, it should be at least 5^oC to 10^oC above the load return temperature.

(2) Determine the average daytime temperature from table II-1 and calculate $T_{a,i}-T_a$.

(3) For an assumed maximum insolation of 1 kW/m^2, determine the normalized flow rate ($\dot{M}_r/N_c$) which will give the maximum allowable temperature rise across the collector. The maximum outlet temperature must be less than 100^oC.

(4) The annual average coolant temperature may now be determined for the average annual insolation (I) which is obtained from figure II-1 for the site in question. For I, inlet to ambient temperature difference, and $\dot{M}_r/N_c$ determined in step 3, the average fluid temperature can be found for the assumed inlet temperature.

In step 3, the normalized flow rate cannot be taken arbitrarily. The flow rate must be great enough to provide good heat transfer in the coolant channel. However, the flow rate and row length combination is limited by restrictions on the maximum allowable pressure which the collector system can withstand. These restrictions are generally due to limitations of fittings and flex hoses. Data generated by E-Systems for their LFF array indicated a maximum allowable pressure of 6.9×10^5 Pa (100 psi). A lower bound of 5.68×10^4 $W/m^2{}^oK$ (10,000 BTU/hr $ft^2{}^oF$) on the convective heat transfer coefficient gives a range of allowable flow rates (in m^3/sec) defined in equation II-7. Optimum flow rates vs. row length have been calculated and are presented in chapter IV.

$$1.23 \times 10^{-4} < \dot{M}_r < \frac{1.84 \times 10^{-3}}{N_c^{\ 0.56}} \qquad \text{(Eq. II-7)}$$

Upon determining the average fluid temperatures, the annual average thermal and electrical energy can be obtained from figures II-4 and II-5 for the site being analyzed. The correlations for annual availabilities assume a continuous 365 day operation; therefore, to determine the energy available to the load, the values obtained from the curves must be multiplied by the fraction of the days that the load operates. That is, if the load is a 5 day a week operation, the availability values must be multiplied by 260/365.

b. Array Area Determination

When the available energy to the load has been determined, the load must be specified in order to calculate the area required to

meet the load. Since the availability correlations assume a continuous operation, the load must be assumed to operate continuously during the daylight hours, or from 6 a.m. to 6 p.m. Hour-by-hour simulations, reported in Volume I, indicate that if an application is not feasible without thermal storage, it will not be feasible with thermal storage. Therefore, for this preliminary analysis, we will assume that the array is to be sized to meet only the daytime load.

The annual thermal and electric loads can be calculated using equation II-8, where D is the number of days per year that the load operates, L' is the averaged daytime load in kilowatts, and L is the annual thermal or electric load in kilowatt-hours.

$$L = 12\ L'\ D \qquad \text{(Eq. II-8)}$$

By dividing the annual available energy by the annual load, the array area can be found for a desired fraction of the daytime load to be supplied, from figure II-9. If a specified fraction of the thermal load is to be supplied, then an array area which will satisfy this demand can be found. The fraction of the electrical load which is supplied for this area can also be found from figure II-9.

For comparison purposes, a nomograph to determine the array area required to meet an instantaneous load was developed and is shown in figure II-10. Thus, for an average fluid temperature of 50°C, an array of 4000 m^2 will satisfy a 2000 kW thermal load when the instantaneous insolation is at its peak of 1 kW/m^2. The same array will satisfy an electric load of about 500 kW.

Once the array area has been determined, a rough estimate of the economic feasibility may be found from figure II-11. This figure was developed using equations II-9 through II-12. The lifetime cost savings (LCS) is defined as the value of the energy supplied to the load minus the cost of the solar system. The present value factors are defined in reference II-3.

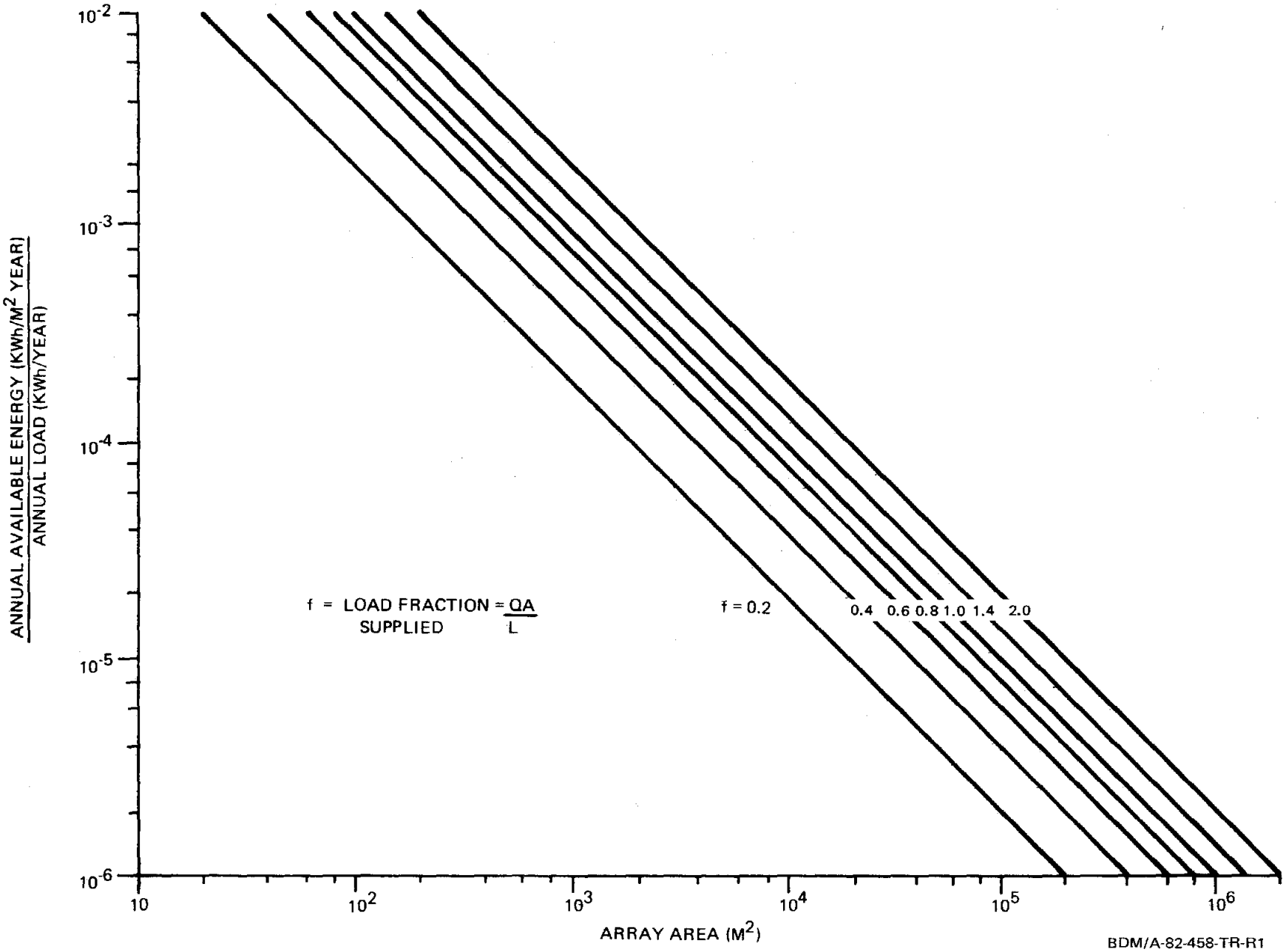

Figure II-9. Chart for Determining the Array Area Which Will Supply a Required Load Fraction

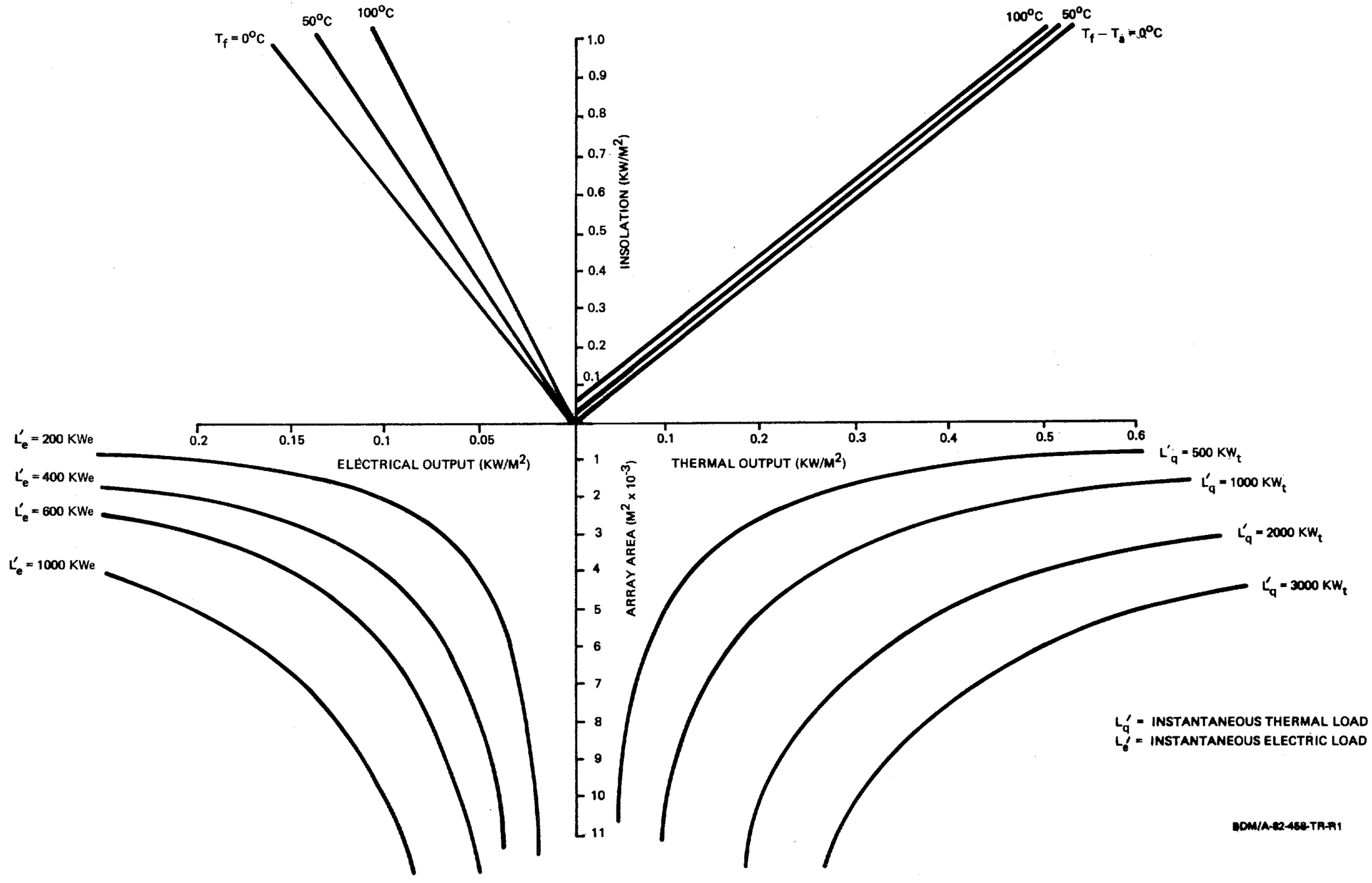

Figure II-10. Chart for Determining the Array Area Which Will Satisfy an Instantaneous Load for an Instantaneous Insolation

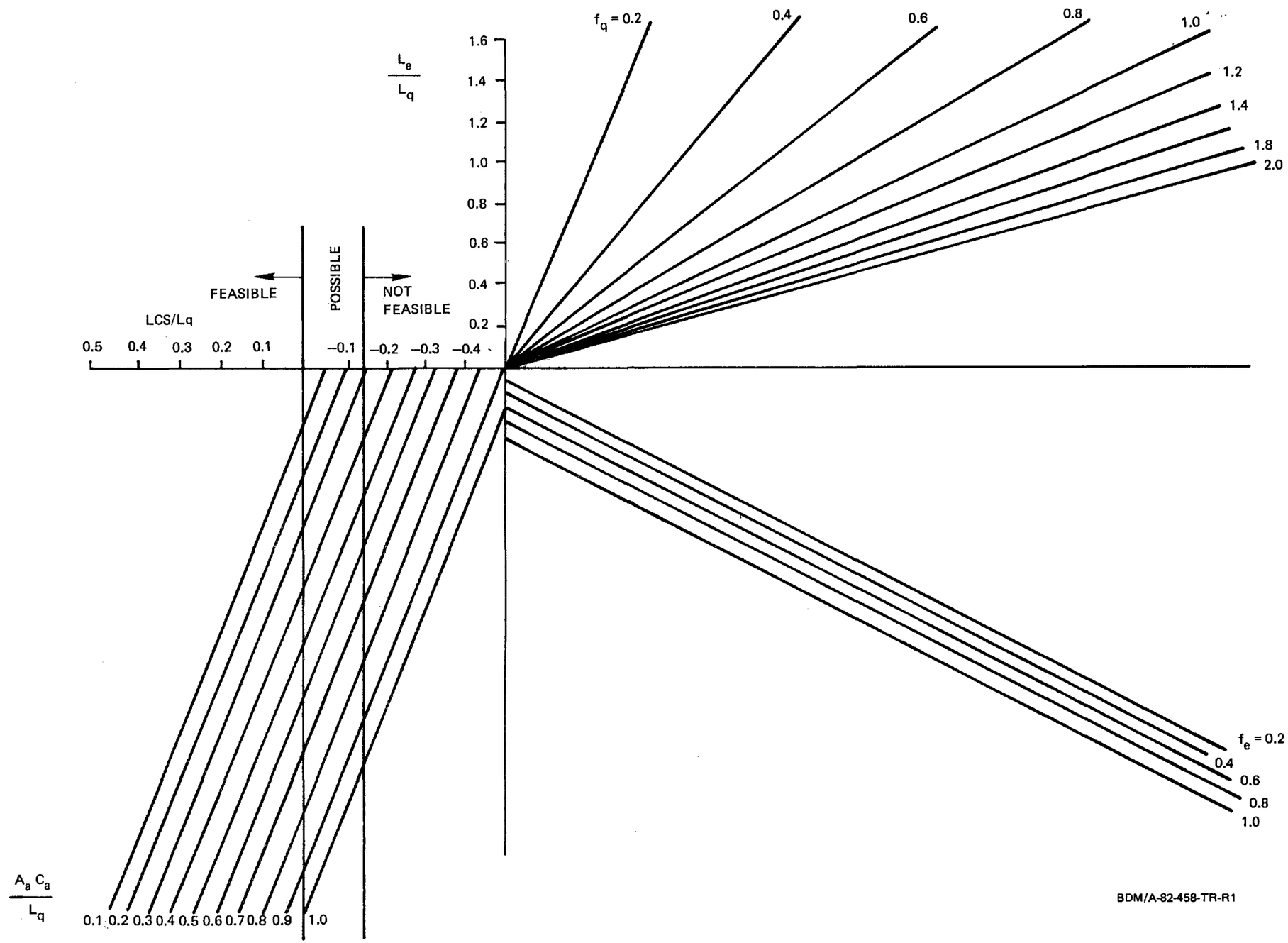

Figure II-11. Chart for Determining Economic Feasibility

$$\frac{LCS}{L_q} = \left[\frac{L_e}{L_q} K P_e \, PVF\,(d, e_e, N) + f_q P_q \, PVF\,(d, e_q, N)\right] (1-t)$$

$$- \frac{A_a C_a}{L_q}\left[1 - \frac{i}{1+d} - t\,(PVD) + (1-t)\,\eta_{om}\, PVF\,(d, g, N)\right] \quad \text{(Eq. II-9)}$$

$$K = f_e \text{ for } f_e \leq 1$$

$$K = 1 + (f_e - 1)\,\eta_s \text{ for } f_e > 1 \quad \text{(Eq. II-10)}$$

$$PVD = \frac{2\left[N_D - PVF\,(d, 0, N_D)\right]}{N_D\,(N_D + 1)\,d} \quad \text{(for SOYD depreciation)} \quad \text{(Eq. II-11)}$$

$$PVF\,(A, B, C) = \frac{1}{A - B}\left[1 - \left(\frac{1+B}{1+A}\right)^C\right] \quad \text{(Eq. II-12)}$$

where L_e, L_q = annual electric and thermal loads
f_e, f_q = fraction of electric and thermal loads supplied
A_a = array area (m^2)
C_a = Solar System Cost ($\$/m^2$)

The parameters in the present value function (Eq. II-12) are defined as

A = discount rate
B = escalation rate
C = number of years

Average economic parameters used in equation II-9 are defined as follows:

P_e = price of electricity (0.05 $/kWh)
P_q = price of natural gas (0.015 $/kWh)
e_e = escalation rate of electricity (0.1)
e_q = escalation rate of natural gas (0.12)
N = system lifetime (20 years)
N_D = depreciation period (7 years)
η_s = electricity sellback ratio (0.75)
η_{om} = operation and maintenance factor (0.015)

t = tax rate (0.5)

i = income tax credit (0.25)

d = discount rate (0.2)

g = inflation rate (0.08)

For an electric to thermal load ratio, and the fractions of thermal and electric energy supplied, the lifetime cost savings can be determined as a function of array area and cost. The LCS and total array cost are normalized to the annual thermal load. The loads, area, and load fractions were determined previously so that the total array cost will determine economic feasibility.

It should be noted that the use of these graphs for determining array size and feasibility involves gross simplifications and assumptions. Comparing this simplified analysis with the hour-by-hour simulations described in Volume I indicates that this "first-cut" approach is quite conservative. That is, site/application pairs found feasible using a detailed simulation gave a slightly negative LCS. For this reason an error band was placed on the LCS values in figure II-11.

Using this simplified technique, one can quickly determine whether an application may be feasible and warrant a more detailed design and economic analysis. An approximation of the area required to supply a given load fraction can be determined and compared to the land area available at the site.

c. Component Sizing

Once the array size has been determined, a preliminary heat exchanger and cooling tower size may be determined. Most PV-T systems require a heat exchanger to separate the array cooling fluid from the process fluid. In addition, a cooling tower is required to maintain the array at a sufficiently low temperature when the thermal load is inadequate to cool the array cooling fluid.

A preliminary heat exchanger size may be determined from figure II-12. The heat exchanger size determined from this figure is that size required to maintain an array outlet temperature at 100°C at a peak insolation of 1 kW/m^2 for a given array inlet temperature, load

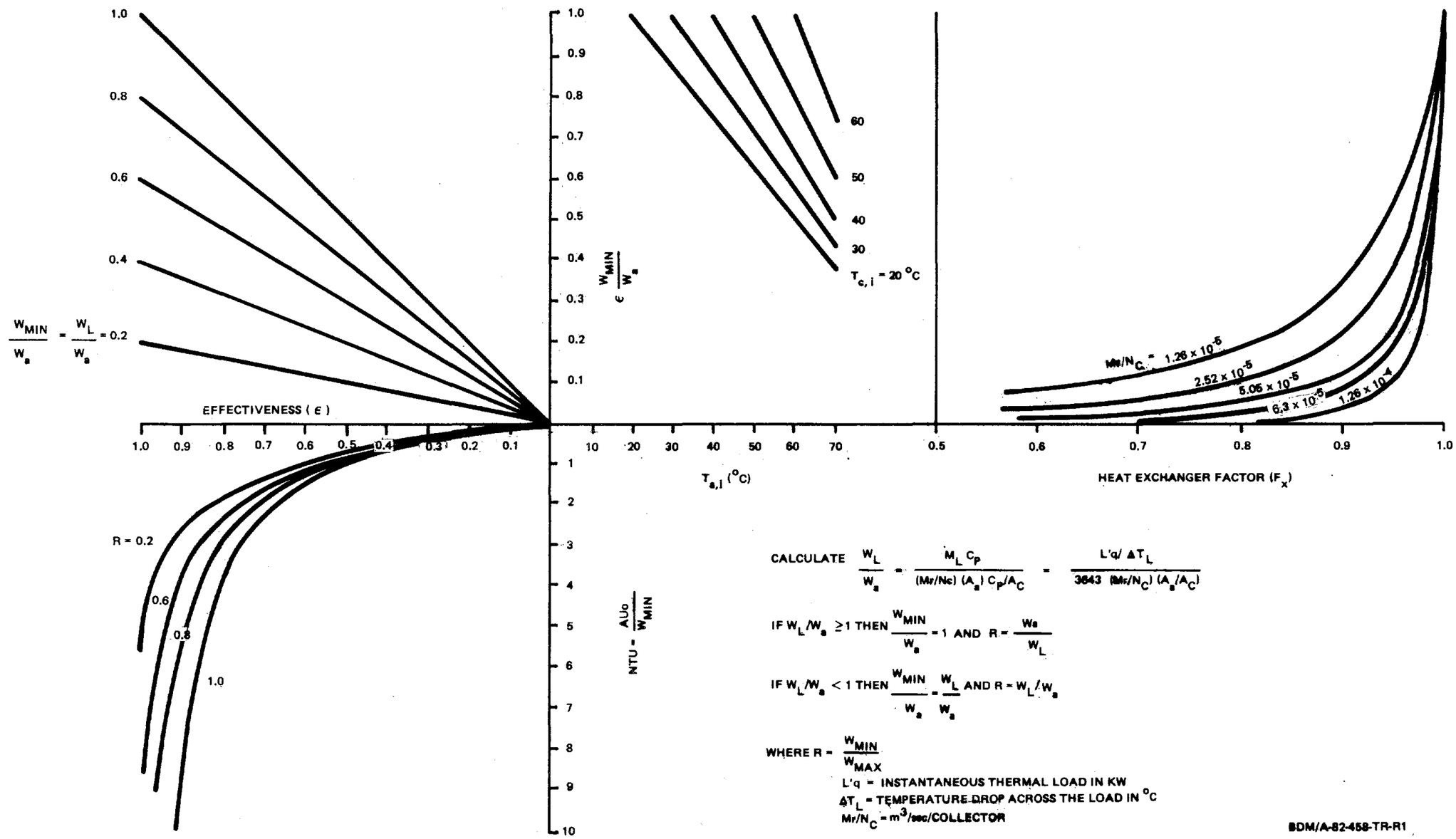

CALCULATE $\frac{W_L}{W_a} = \frac{M_L C_P}{(Mr/Nc)(A_a) C_P/A_C} = \frac{L'q/\Delta T_L}{3643\ (Mr/N_C)(A_a/A_C)}$

IF $W_L/W_a \geq 1$ THEN $\frac{W_{MIN}}{W_a} = 1$ AND $R = \frac{W_a}{W_L}$

IF $W_L/W_a < 1$ THEN $\frac{W_{MIN}}{W_a} = \frac{W_L}{W_a}$ AND $R = W_L/W_a$

WHERE $R = \frac{W_{MIN}}{W_{MAX}}$

L'q = INSTANTANEOUS THERMAL LOAD IN KW

ΔT_L = TEMPERATURE DROP ACROSS THE LOAD IN °C

Mr/N_C = m^3/sec/COLLECTOR

BDM/A-82-458-TR-R1

Figure II-12. Chart for Preliminary Heat Exchanger Sizing

return temperature ($T_{c,i}$), and capacity flow rate ratio (W_L/W_a). These curves were developed using equation II-3 and the equations in the heat exchanger section of chapter IV. Figure II-12 should be entered with the array inlet temperature ($T_{a,i}$) and the load return temperature ($T_{c,i}$). For the normalized row flow rate ($\dot{M}_r/N_c$) determined previously, the heat exchanger factor (F_x) may be determined. This factor defines the degree to which the thermal output of the combination of array plus heat exchanger is degraded with respect to the thermal output of the array alone.

To determine the heat exchanger size, the capacity rate ratios must be calculated as indicated in figure II-12. At the left section of the figure one finds the line corresponding to the calculated capacity rate ratio (W_L/W_a). If this ratio is greater than one, the line $W_L/W_a = 1$ should be used. Proceeding down from this intercept to the calculated ratio, R, the heat exchanger effectiveness (ε) can be read off the graph. By continuing to the right, the required number of transfer units (NTU) can be determined.

At this stage a judgment must be made concerning the overall heat transfer coefficient (U_o) for the heat exchanger. As indicated in chapter IV, a plate heat exchanger appears appropriate for a PV-T system. Such heat exchangers have heat transfer coefficients ranging from 2270 (400) to 5674 $W/m^2{}^oK$ (1,000 BTU/hr $ft^2{}^oF$). For a preliminary estimate a typical value of 4540 $W/m^2{}^oK$ (800 BTU/hr $ft^2{}^oF$) may be chosen.

The annual parasitic power consumption of the cooling tower may be estimated from figure II-13. This figure was developed using Baltimore aircoil industrial fluid cooler data (ref. II-4). Since, in most instances, excess electrical power may be sold back to the utility, the PV-T system will be operating even when there is no thermal load. If excess thermal energy is produced while the thermal load is operational, then the amount of energy which must be dissipated may be calculated from equation II-13. For a five day per week load for which $f_q \leq 1$, the energy which must be dissipated is given by equation II-14.

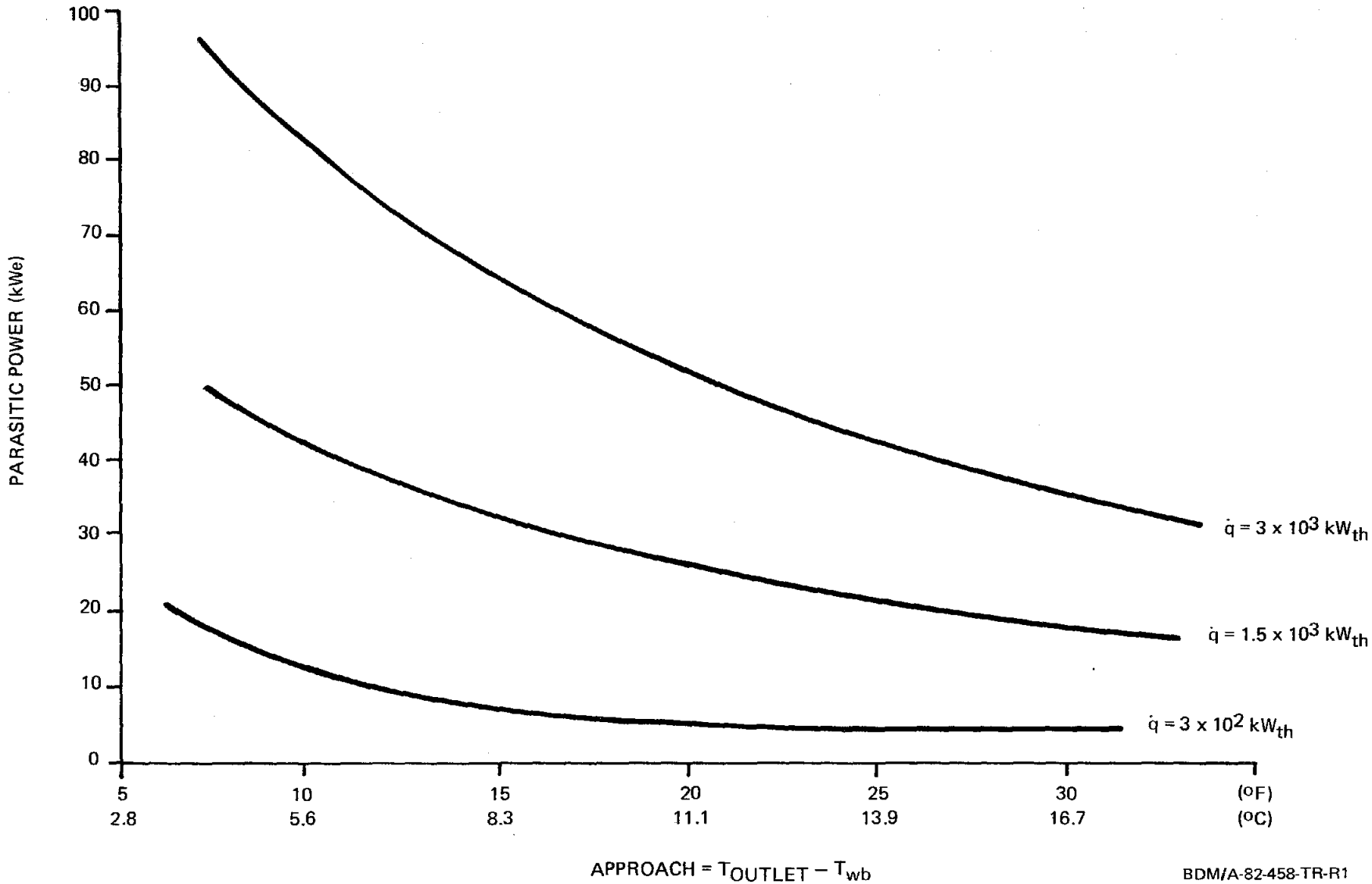

Figure II-13. Cooling Tower Parasitic Power Consumption (Fan and Pump)

$$Q_D = L_q \, (f_q - 1) \qquad \text{(Eq. II-13)}$$

$$Q_D = A_a \, Q_{th} \, \frac{105}{365} \qquad \text{(Eq. II-14)}$$

This is the thermal energy collected on weekends where Q_{th} is the annual available thermal energy from figure II-6. The time during which the cooling tower operates depends on the heat dissipation rate, $\dot{q}$, and is given in equation II-15.

$$t_c = \frac{Q_D}{\dot{q}} \qquad \text{(Eq. II-15)}$$

d. Solcel Developed Design Charts

Additional performance graphs have been developed for an LFF system to further quantify the ability of a PV-T system to displace a thermal and electric load. These graphs have been developed independent of a particular load profile since a multitude of design charts could be developed for a large variety of load requirements and still not serve the needs of all system designers. The analysis of the site/application pairs revealed that the economic feasibility is dependent on the site, the load profile, and the quality of energy required (i.e., required temperature), the load return temperature, and the economic factors. The quantity of parameters involved was prohibitive to effective development of a set of design curves applicable to a large number of applications. Therefore, design curves have been developed which define the daily average energy (electrical and thermal) available from an LFF collector system as a function of area, site, and inlet temperature.

The design curves which define the average daily thermal and electrical output of an LFF array are shown in figures II-14 and II-15, respectively. Several calculations have indicated that the

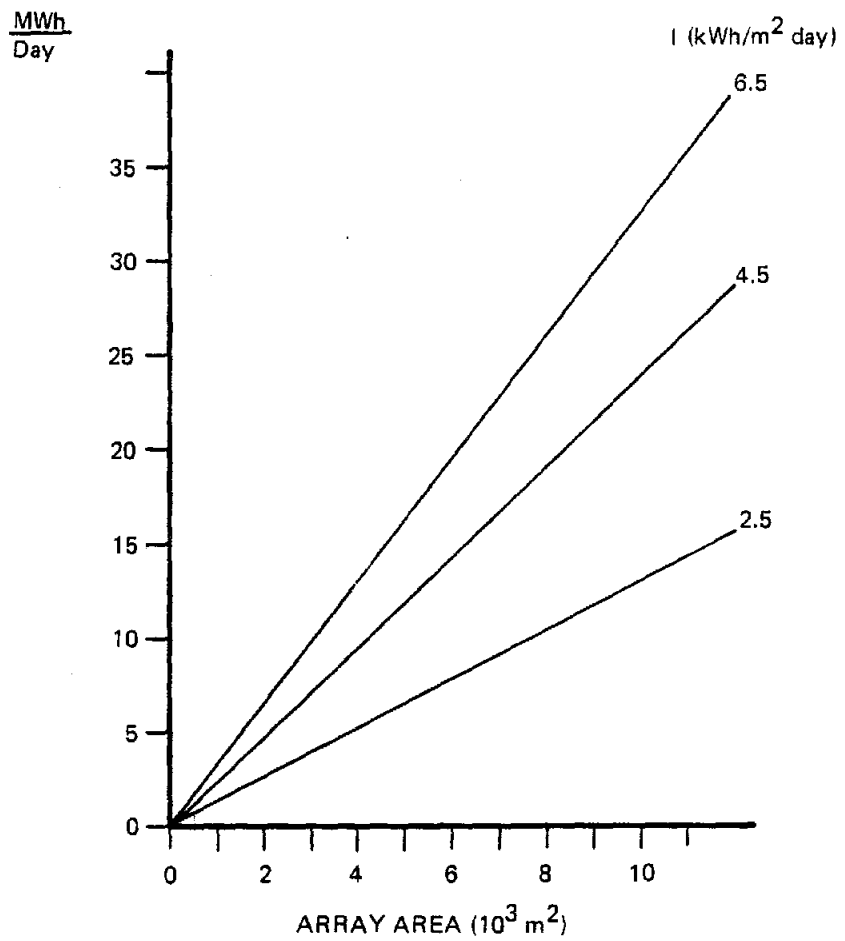

BDM/A-82-458-TR-R1

Figure II-14. Average Daily PV-T Array Thermal Output

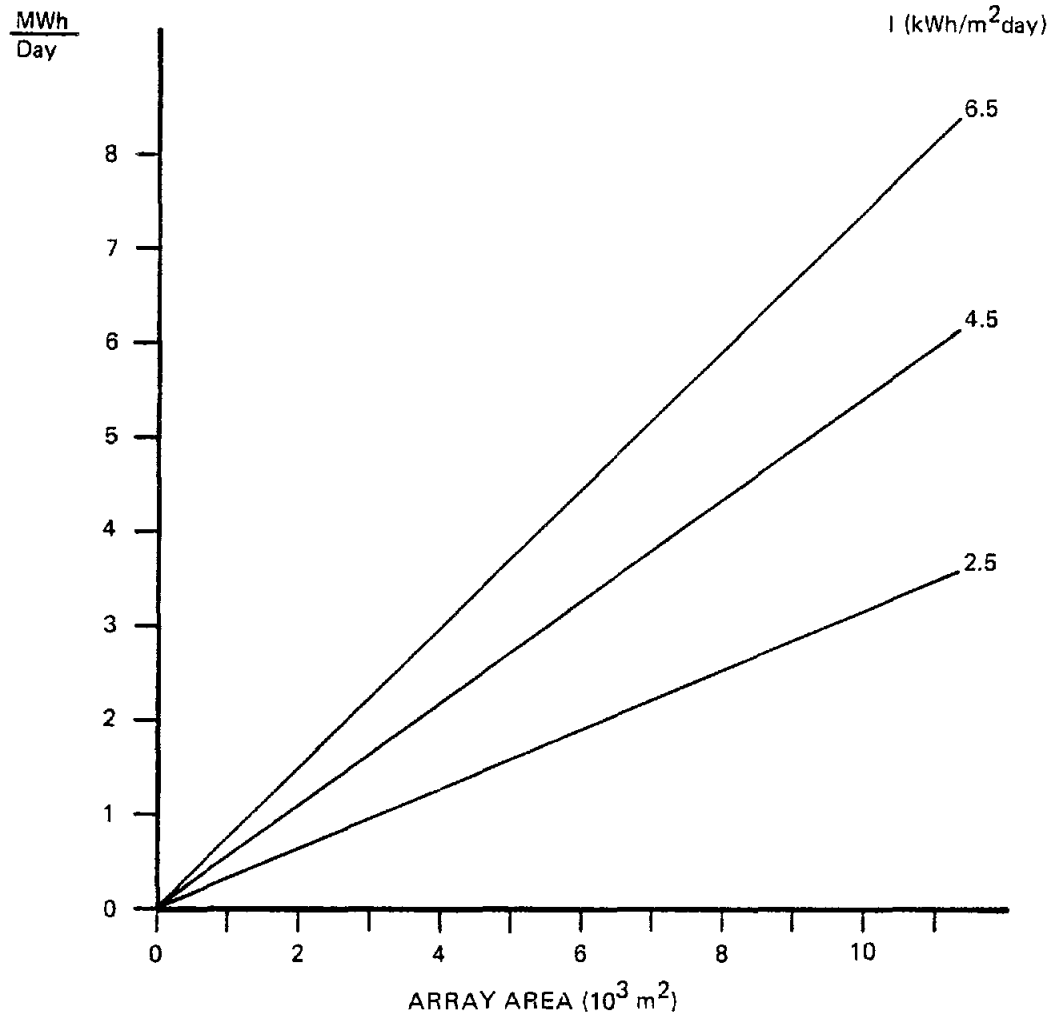

BDM/A-82-458-TR-R1

Figure II-15. Average Daily PV-T Array Electrical Output for an Inlet Temperature of 34°C (93°F)

average daily output is primarily a function of the average daily insolation available at the site (kWh/m^2 day). Thus, the curves have been developed for various average daily insolation factors which are characteristic of several sites, as shown in table II-2. These insolation values are the hourly insolation levels greater than 50 W/m^2, summed up and averaged over 365 days of the year. Due to the accuracy of the tracking system, the collectors can only operate at insolatin levels greater than 50 W/m^2. The annual average number of hours per day of operation is also shown in table II-2 for the sites considered. The thermal output is independent of array inlet temperature, and the electrical output is only slightly dependent on inlet temperature as shown in figure II-16. The average array outlet temperature versus inlet temperature and location is shown in figure II-17.

TABLE II-2. AVERAGE DAILY INSOLATIN AND HOURS OF OPERATION

SITE	INSOLATION* (kW-hr/m^2 DAY)	AVERAGE HOURS OF* OPERATION/DAY
El Paso, Texas	7.39	10.68
Albuquerque, New Mexico	6.48	10.58
Fresno, California	6.44	10.15
Phoenix, Arizona	6.30	10.19
Dodge City, Kansas	5.97	9.47
Ft. Worth, Texas	4.55	8.30
Boston, Massachusetts	3.94	8.26
Charleston, South Carolina	2.55	5.88
Seattle, Washington	2.38	5.41

*For insolation levels greater than 50W/m^2

The Dixon meat-packing plant serves as an example of how these graphs may be used. For this application, the inlet to the heat

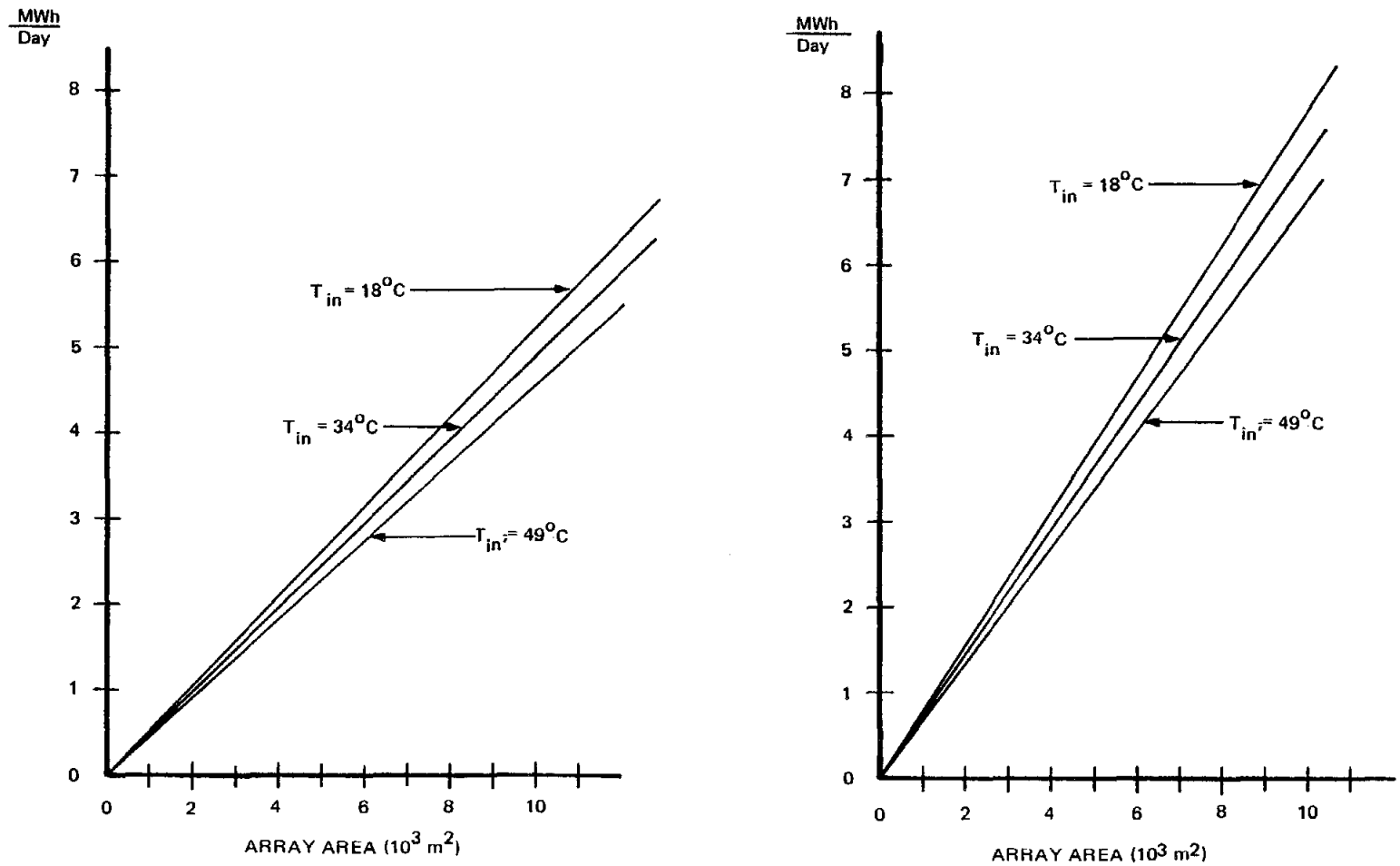

(A) AVERAGE DAILY INSOLATION OF 4.5 kWh/m^2 Day

(B) AVERAGE DAILY INSOLATION OF 6.5 kWh/m^2 Day

BDM/A-82-458-TR-R1

Figure II-16. Average Daily PV-T Array Electrical Output Versus Inlet Temperature and Average Daily Insolation

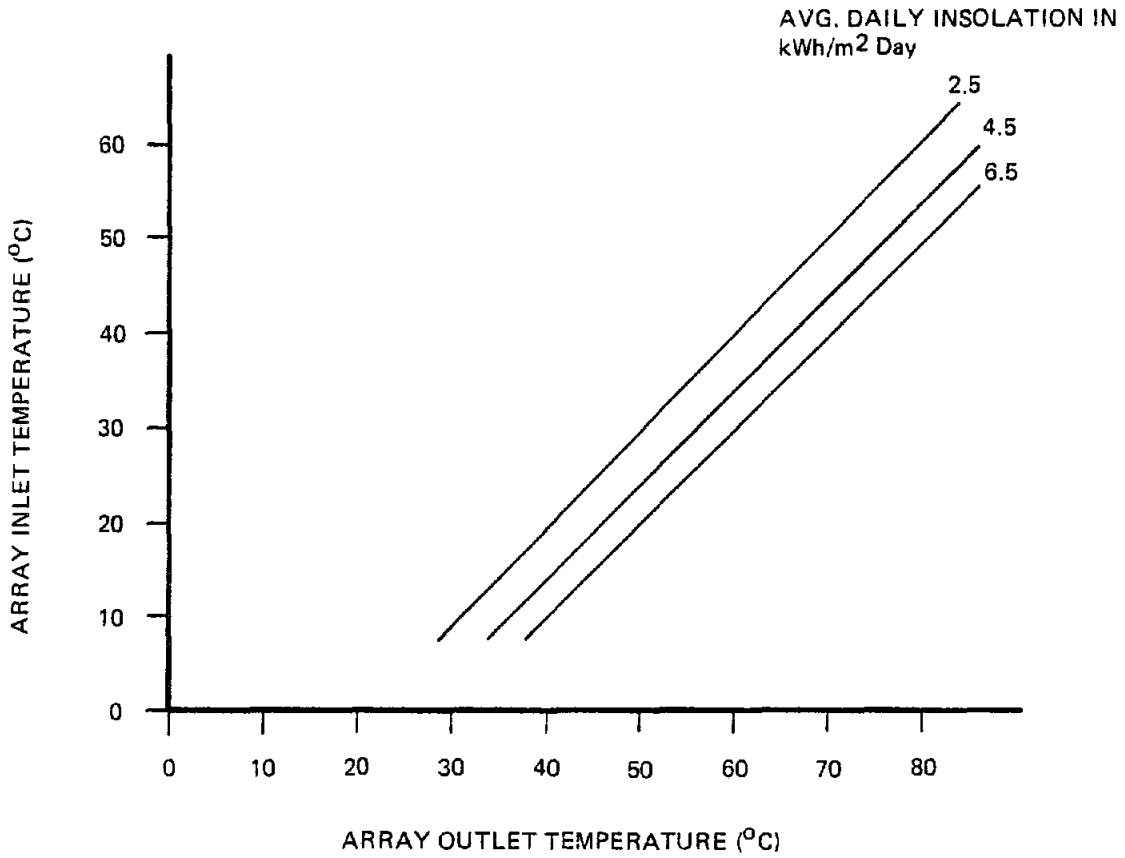

BDM/A-82-458-TR-R1

Figure II-17. Array Inlet Versus Output Temperature

exchanger is well water at 18.3°C (65°F) and the load requirement is 60°C (140°F) wash water. Based on information provided by the plant engineer, the average wash water requirement is about 0.0124 m^3/sec (197 gpm) during the day and 0.0084 m^3/sec (133 gpm) in the early morning. This gives a daytime thermal requirement of 2.17 MW (7.4 x 10^6 Btu/hr) and 1.24 MW (4.24 x 10^6 Btu/hr) at night. Assuming an average of 59 percent of the daily load is to be displaced by the PV-T system, then the average daily requirement of 60°C (140°F) water is:

$$0.59 \left[(2.17 \text{ MW})\ (18 \text{ hrs}) + (1.24 \text{ MW})\ (6 \text{ hrs})\right] = 27.4 \text{ MW hrs/day}$$

For the Dixon site the average daily insolation is about 6.44 kWh/m^2 day. Using figure II-14, the array size necessary to meet the daytime load is about 8300 m^2. Detailed calculations for the Dixon plant, described in volume III, indicate a coolant flow rate per row of 3.2 x 10^{-4} m^3/sec (5 gpm) and a row length of 10 arrays/row is about optimum. Assuming these values, the flow rate on the array side is approximately:

$$\frac{3.2 \times 10^{-4} m^3/\text{sec/row}}{10 \text{ arrays/row}} \quad \frac{1 \text{ array}}{11.2 \text{ m}^2} \; 8300 \text{m}^2 = 0.0234 \text{ m}^3/\text{sec (370 gpm)}$$

Again, detailed calculations indicate an optimum heat exchanger NTU is between 5 and 6. Assuming an NTU of 6, the heat exchanger effectiveness is:

$$\varepsilon = \frac{1 - e^{-NTU\ (1 - R)}}{1 - R\ e^{-NTU\ (1 - R)}} = 0.9588$$

$$R = \frac{W_{min}}{W_{max}} = \frac{\left(\dot{m}C_p\right)_{min}}{\left(\dot{m}C_p\right)_{max}} = \frac{(197)\ \ (1)}{(370)\ \ (1.05)\ \ (0.82)} = 0.6184$$

For a 10.15-hour operating day, the average insolation is 634 W/m^2. Using equation IV-51, the array outlet temperature can be calculated as indicated in figure II-18. Assume a variable volume storage tank in series with the array heat exchanger and the load, as shown in figure II-19.

Performing an energy balance at point A:

$$\dot{m}_1 + \dot{m}_2 = 0.0124\ m^3/sec$$

$$\dot{m}_1(69.4^oC) + \dot{m}_2(18.3^oC) = (0.0124\ m^3/sec)\ (60^oC)$$

$$\dot{m}_1 = 0.0101\ m^3/sec\ (162.4\ gpm)$$

$$\dot{m}_2 = 0.0023\ m^3/sec\ (34.6\ gpm)$$

The available storage is then:

$$Q_s = (0.0124\ m^3/sec - 0.0101\ m^3/sec)(993\ kg/m^3)(4.166\ KJ/Kg\ ^oC)(69.4 - 18.3)$$

$$Q_s = 486\ kW$$

Since this is collected over a 10.15-hour period, a total of 4.93 MW hrs are supplied to storage, on the average. This will supply the thermal load for about 2.27 hours after the array has been stowed.

The array electrical output is found from figure II-16b for an array inlet temperature of 40^oC to be 6.1 MWh/day. Assuming an 89 percent DC to AC conversion efficiency, this gives 5.43 MWh/day available to the load on the average (or an average daily power output of 535 kW). Over 365 days, this means that 1.98×10^6 kW hours are available. This can be compared to 2.08×10^6 kW hours of AC power produced by the Dixon meat-packing PV-T array as calculated with SOLCEL-II and discussed in volume III.

$$T_{a,o} = \frac{\frac{A_a F_m}{\varepsilon W_{min}} \left(I\eta_o + U_L T_a\right) + \left(1 - \frac{A_a F_m U_L}{2W_a}\right) T_{c,i}}{1 + \frac{A_a F_m U_L}{\varepsilon W_{min}} - \frac{A_a F_m U_L}{2W_a}}$$

A_a = (8300 m^2)
W_{min} = (0.0124 m^3/sec) (993 kg/m^3) (4.166 KJ/kg°C)
= 51.3 kW/°C

F_m = 0.77
η_o = 0.66
U_L = 0.32 W/m^2°C
T_a = 20°C
$T_{c,i}$ = 18.3°C
ε = 0.9588

W_a = (0.0234 m^3/sec) (993 kg/m^3) (1.05) (3.43 KJ/kg°C)
W_a = 83.7 kW/°C
I = 634 W/m^2

$$C_1 = \frac{A_a F_m}{\varepsilon W_{min}} (I\eta_o + U_L T_a) = \frac{(8300\ m^2)(0.77)}{(0.9588)(51.3\ kW/^oC)} \left[(0.634\ kW/m^2)(0.66) + (0.32\ W/m^2{}^oC)\ (20^o\ C)\right]$$

$$= \frac{(8300\ m^2)(0.77)}{(0.9588)(51.3\ kW/^oC)} \left[(0.634\ kW/m^2)(0.66) + (3.2x10^{-4} kW/m^2{}^oC)(20^oC)\right]$$

$$= 55.2^oC\ (131.4^oF)$$

$$C_2 = \left(1 - \frac{A_a F_m U_L}{2W_a}\right) T_{ci}$$

$$= \left[1 - \frac{(8300\ m^2)(0.77)(3.2x10^{-4}\ kW/m^2{}^oC)}{(2)\ (83.7\ kW/^oC)}\right] (18.3^oC)$$

$$= 18.1^oC\ (64.6^oF)$$

$$C_3 = A_a F_m U_L \left[\frac{1}{\varepsilon W_{min}} - \frac{1}{2W_a}\right]$$

$$= (8300\ m^2)(0.77)(3.2x10^{-4} kW/m^2{}^oC) \left[\frac{1}{(0.9588)(51.3\ kW/^oC)} - \frac{1}{(2)(83.7\ kW/^oC)}\right]$$

$$= 0.0294$$

$$T_{a,o} = \frac{C_1 + C_2}{1 + C_3} = \frac{55.2 + 18.1}{1.0294} = 71.2^oC\ (160.2^oF)$$

$$T_{a,i} = \left[1 - \frac{\varepsilon W_{min}}{W_a}\right] T_{a,o} + \frac{\varepsilon W_{min}}{W_a} T_{c,i}$$

$$= \left[1 - \frac{(0.9588)(51.3)}{83.7}\right] (71.2^oC) + \frac{(0.9588)(51.3)}{83.7} (18.3)$$

$$= 40.1^oC\ (104^oF)$$

$$T_{c,o} = \frac{Wa}{W_L} (T_{a,o} - T_{a,i}) + T_{c,i}$$

$$= \frac{83.7}{51.3} (71.4 - 40.1) + 18.3$$

$$= 69.4^oC\ (157^oF)$$

BDM/A-82-458-TR-R1

Figure II-18. Calculation of the Average Array Outlet Temperature for the Dixon Meat-Packing Plant

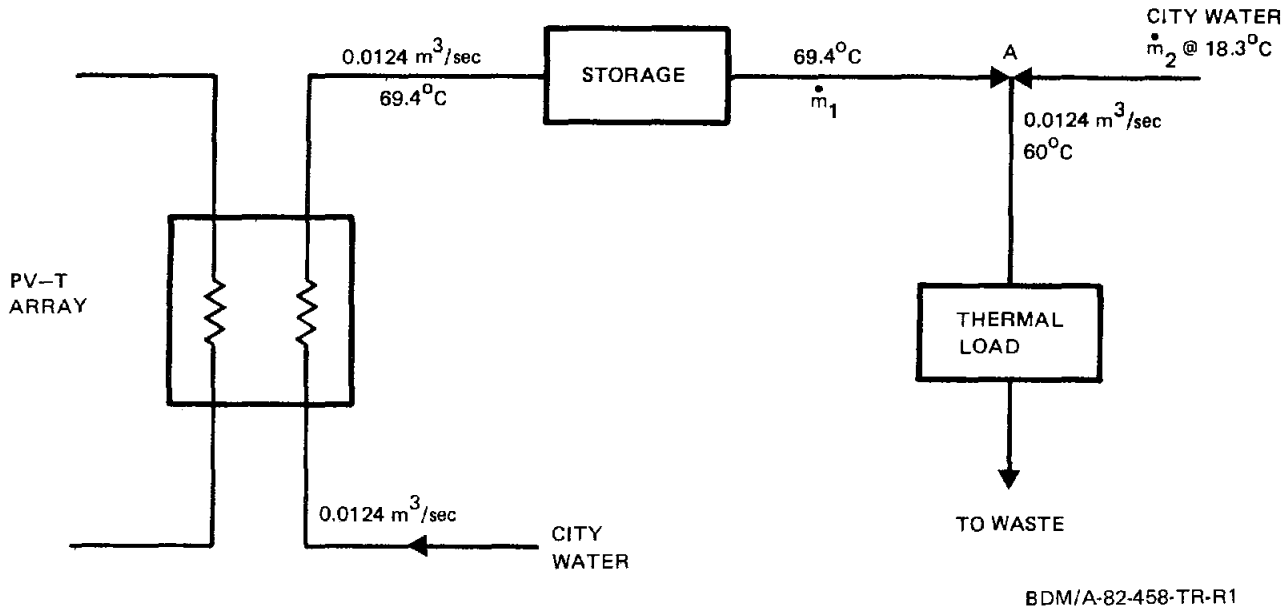

Figure II-19. Typical Thermal Storage Configuration for the Dixon Plant

e. Subsequent Design Efforts

After determination that an economically feasible array can be constructed in the available land area, a more detailed analysis should be performed to ensure economic feasibility. Such as analysis may be performed using an hour-by-hour simulation code, such as SOLCEL-II, but using a generic field layout. This initial simulation may be performed using preliminary cooling tower and heat exchanger sizes, and an inverter size determined for the instantaneous peak electrical output from figure II-10.

If this analysis indicates that the PV-T installation is economical, then additional simulations should be performed with various sizes of thermal storage in order to determine the optimum array and storage size. Once this has been determined, then detailed systems design may proceed using the techniques discussed in subsequent chapters.

REFERENCES

II-1. A. Rabl, Yearly Average Performance of the Principal Solar Collector Types, SERI/TR-631-716, Solar Energy Research Institute, Golden, Co. (Jan. 1981).

II-2. A. Rabl, "Yearly Average Performance of the Principal Solar Collector Types", Solar Energy, Vol. 27, No. 3, pp. 215-233 (1981).

II-3. A. M. Perino, A Methodology for Determining the Economic Feasibility of Residential or Commercial Solar Energy Systems, SAND 78-0931, Sandia National Laboratories, Albuquerque, N. M. (Jan 1979).

II-4. Baltimore Aircoil, VX Industrial Fluid Coolers, Bulletin S405/1-0 (July 1978).

CHAPTER III
ELECTRICAL SYSTEM DESIGN

The following sections describe the various issues which must be considered when designing the electrical portion of a PV-T system. These issues will be discussed, criteria used to resolve those issues will be presented, and finally, guidance will be provided for overall system design and component selection.

The designer of the electrical system must consider the field layout to provide the required power and voltage, the interface between the PV array and the utility, protection from lightning and other transients, safety, and component design and selection. One of the most important and costly components is the inverter, which processes the power from the array into a usable form for either the utility or the local load. The issues associated with sizing and selection of an inverter will be discussed next.

A. IDENTIFICATION OF TECHNICAL ISSUES

1. Inverters

Inverters, also referred to as power conversion systems, are used to convert the array DC to utility-compatible AC power in a PV-T system. There are several specifications associated with the selection of the optimum inverter for any given system design. Aside from these electrical specifications, there are many other considerations affecting inverter selection, such as size, weight, safety features, etc. The purpose of this section is to identify the issues associated with specifying an inverter for use in a PV-T system.

a. Sizing

The electrical sizing requirements must be addressed first, since all of the other specifications cannot be fully explored until the kW size of the basic inverter is known. To correctly size the inverter, two parameters of the system must be known: photovoltaic array

output voltage and current, and utility or alternate load voltage requirements.

The inverter output voltage is usually determined by the load requirements (for example, the utility voltage in a utility-interactive system). The output current (or power) may be determined from the load requirements if the array can be sized to satisfy the full load, or from the array power if the system size limitations prevent satisfying the full load.

The inverter input voltage range must be matched to the array voltage range under expected temperature variations. The inverter manufacturer usually specifies a nominal operating voltage range which can be shifted up or down slightly to assist in matching the array and inverter voltage ranges.

1) Photovoltaic Output

Both the array output voltage and output current must be calculated. This entails adding up the voltages and currents from each photovoltaic cell. In a series wired configuration, the voltages add, and the current is the same as for one cell. In a parallel wired configuration, the currents add, and the voltage is the same as one cell. Normally, one would use the PV cell manufacturer's voltage and current values at rated conditions ($28^{o}C$ and $1000W/m^2$ insolation). For inverter specification, however, the normal operating conditions must be known, and their maximum values must be calculated. This is accomplished by adjusting the rated condition voltage (V_{28}) by a temperature coefficient factor ($\Delta V/\Delta T$) times the number of cells connected in series (N_S) times the difference in temperature between the rated condition and the expected worst case deviation in temperature for the application locale.

$$V_T = V_{28} + N_S(\Delta V/\Delta T)(T_C - 28^{o}C) \qquad \text{(Eq. III-1)}$$

For example, if the PV array nominal output voltage at rated conditions is 200 VDC and consists of 10 modules, each containing 40 cells in series, one would calculate the worst case operating voltages as follows:

For an assumed low temperature of $0^{o}C$ and a cell temperature coefficient of $-2mV/^{o}C$,

$$V_{0^{o}C} = (200VDC) + 400(-.002)(-28^{o}C)$$
$$= (200VDC) + 22.4VDC$$
$$= 222.4VDC$$

and assuming a high temperature of $70^{o}C$,

$$V_{70^{o}C} = (200VDC) + 400(-.002)(42)$$
$$= 166.4VDC$$

Therefore, the desirable input operating range of the inverter would encompass the 165 - 225VDC range. Additionally, a worst case (highest voltage) calculation must be done for the open circuit standoff voltage of the inverter input. This entails increasing the open circuit voltage (V_{oc}) obtained at rated conditions from the cell manufacturer for the same low temperature according to the above equation. A similar calculation must be done for the output current of the array in order to specify the input power of the inverter. The temperature coefficient of the cell current ($\Delta f_I/\Delta T$) is a positive number, approximately 0.6mA/A - ^{o}C. The following equation can be used for the array current (I_T) at temperature (T_C).

$$I_T = I_{28}\left[1 + (\Delta f_I/\Delta T)(T_C - 28^{o}C)\right] \qquad \text{(Eq. III-2)}$$

For bright cloud enhancement conditions, the output current and power should be increased by 15 to 20 percent to adequately size the inverter output.

2) Inverter Output

Another important aspect of the inverter specifications is its output power rating. This can be estimated either from the load requirements or by multiplying the photovoltaic array input power by the efficiency of the inverter. Most inverters guarantee an efficiency of 90 percent or better at full load conditions. This output rating is expressed in kW and several manufacturers of inverters offer units between 1 kW and 300 kW.

3) Single vs. Multiple Units

In large PV-T designs one may consider the cost effectiveness of installing multiple inverters instead of one large inverter. For example, four 75 kW units may be used instead of one 300 kW unit. Issues which must be addressed to optimize the design for any given system include cost, physical size of the inverters, array location and partitioning, reliability, maintainability, spare parts, and the wiring and control architecture associated with multiple units. Multiple units also permit greater power availability factors since an extra unit can be purchased as a spare at only a fraction of the cost of the larger unit. However, spare parts would still be required for repair.

b. Operational Modes

1) Stand Alone/Synchronous Modes

Inverters may be designed to operate in two basic modes: stand-alone and synchronous. Combinations of these two modes are available, with manual and automatic switching capability available between the two modes in some designs. For this contract, systems will be designed for the synchronous mode because the contract requires utility-interactive systems; however, the other modes of operation will also be discussed below.

a) Stand-Alone Mode

The stand-alone mode is used when no utility tie is available or is not desirable. In this mode of operation, all of the

available photovoltaic power produced is consumed in a local load. If the load cannot consume the full power of the array output, the inverter will draw less power from the photovoltaic array. The excess power is usually fed to a battery storage unit. The stand-alone mode inverter may be designed to output power at 60 Hz either by internal timing generation or by phase locking to the utility without delivering power to the utility.

b) Synchronous (Utility-Interactive) Mode

In the synchronous mode of operation, the inverter ties directly to the utility and gets its timing signals from the 60 Hz frequency of the utility tie. Normally in this mode, all of the inverter output power is delivered to the utility and building load; however, additional parasitic loads may be placed on the output of the inverter. The utility will supply power to the loads when the array is not operating or the loads are beyond the array capability.

c) Combinations

Specifying an inverter for local plus utility loads may be useful in some applications. For example, one might configure a system with two input power sources to the inverter, a photovoltaic array and a battery system. Battery storage may be used if the utility credit price is low. During daylight hours, the PV array runs the inverter and provides power to the utility, the batteries, and the load; at night the batteries provide enough power to operate a few hundred watts of load locally. This capability to change modes of operation may be accomplished either manually or automatically.

2) Array Voltage Control

There are two methods of controlling the operating voltage of the array: peak power tracking and fixed voltage operation. Peak power tracking is accomplished by the inverter varying the load on the array, monitoring the voltage and current, and loading the array at the voltage which produces the maximum power. Fixed voltage operation is much simpler by comparison. The inverter input voltage is set at an array voltage corresponding to the average yearly temperature (or some

other nominal temperature) and nominal insolation for the locale. The loss in power during extremes of temperature can be very significant. Most applications utilize peak power tracking, as will the systems designed for this contract.

c. Performance Specifications

1) Conversion Efficiency

There is some power loss in the conversion from DC power to AC power. This loss is consumed in the components of the inverter. Aside from the actual conversion loss, there is a parasitic power loss associated with the control circuits in the inverter. Refer to the section on tare power for this discussion. Normally the power conversion efficiency is specified at full load conditions and ranges from 87 to 93 percent. At loads below this rating, efficiency drops off and may be as low as 80 percent for a 50 percent load. Although high efficiency at low power (for example, 80 to 85 percent at 25 percent load) is obtainable, it is nevertheless important not to oversize the inverter for a given application as this will lower the overall system efficiency.

2) Tare (No-load) Power

Tare power is the minimum power level at which the inverter will begin converting power to the load. The tare power is measured by circuits inside the inverter and represents the minimum power output of the DC source (PV array) required to operate the control and power conversion circuits of the inverter. This parasitic power consumption can be several hundred watts for large scale inverters. It is also used in the calculation of conversion efficiency since it is a fixed operational loss of the power conversion unit.

3) Signal Quality

There are two specifications regarding the quality of the output signal of an inverter which should be considered carefully. These include frequency range and harmonic distortion. The output frequency of the inverter is usually 60 Hz for a utility tie connection. The frequency is synchronized to the utility bus, but in most instances

this is separately monitored for frequency deviation from the nominal 60 Hz value. If an error is measured, the inverter will automatically disconnect from the utility bus until the frequency is again within tolerance. Typical inverter frequency tolerances are 60 Hz $\pm$ 3 - 5 Hz.

Distortion of the output current waveform is also specified by the inverter manufacturer. This is normally defined as total harmonic distortion (THD), which takes into account the harmonic frequencies of 60 Hz, i.e., 120 Hz, 180 Hz, etc. THD production can be affected by the method of inverter commutation. Line commutated (LC) inverters obtain commutation signals from the utility line. Self-commutated (SC) inverters, while obtaining synchronization from the utility line, generate their own commutation signals internally. THD can be held to less than 5 percent of full load current for SC inverters, but can be quite high in LC inverters. LC inverter signal quality can be corrected to improve THD but this involves additional hardware and makes the otherwise less expensive LC inverter comparable in cost to the SC inverter.

4) Power Factor

Reactive power from the inverter is normally minimized, and the utility is expected to supply this power for highly reactive loads. A power factor of 1.0 $\pm$ .05 is reasonable to expect in inverters designed for synchronous mode operation. SC inverters can control reactive power production to achieve good power factors. LC inverters, on the other hand, require additional hardware to achieve good power factors, thus compromising their cost advantage.

5) Peak Power Tracking

Another important feature to be concerned with when selecting an inverter is the accuracy and voltage range of the peak power tracking. This portion of the unit maintains optimum power output from the DC source by varying its input load on the source. Typically, tracking accuracies of better than 1 percent can be obtained. The range of input voltages over which the unit will accomplish peak power tracking must be considered. This is also discussed in section 1.a.(1).

d. Control and Protection

Included in the most advanced inverter designs are several signal monitoring and control circuits. These circuits detect errors in signal levels as well as over-temperature conditions and cause the power processing system to disconnect itself from the load, the PV array, or both. They also provide for automatic start-up and nighttime shutdown of the inverter. Output voltage, output frequency, input voltage, input current, and ground fault conditions are typical of the types of signals which are monitored. Manual disconnect capabilities are also provided in the inverter design.

1) Input Control and Protection

The input section of the inverter usually contains three important sub-assemblies: the Electro-Magnetic Interference (EMI) protection circuitry, the shorting contactors, and the array open circuit contactors.

a) EMI Protection

Electro-magnetic interference from signals which couple into the PV array and its associated wiring, must be filtered out to provide a noise-free power source for the inverter electronics. Elimination of the unwanted signals also reduces the THD figure for the output signal quality. A simple and effective filtering technique commonly used in the input stage of inverter design is the LC network. This filter essentially eliminates all of the high frequency power (EMI) present on the array power input to the inverter.

b) Input Control

Some inverter designs include a set of shorting contacts at the input stage. These contacts short the plus and minus sides of the array together and thereby reduce the voltage potential at the PV modules to zero volts. This condition does not damage the PV array components and provides a maintenance safety feature to the system. In very large systems, it is impractical to short circuit the array due to the enormous currents.

Most inverters are designed with series contacts to open circuit the PV array. This may be used by the inverter to disconnect the PV array from the power processing circuit when the DC input power to the inverter does not meet the minimum input power requirements (tare power) of the inverter, or the inverter may simply shut down the power processing under these conditions. The tare power represents the no-load losses associated with the inverter electronics which the PV system is required to supply.

c) Over-Voltage and Over-Power Protection

The inverter will also disconnect from the array via the series contacts, or limit the array output to protect internal hardware if the input voltage or power is greater than the maximum values specified by the manufacturer.

2) Output Control and Protection

a) Isolation Transformer

In SC inverters, an isolation transformer is usually included on the output to protect against DC power flow into the utility and to prevent utility feedback into the DC system. In LC inverters, a larger isolation transformer is required to carry reactive power. This transformer may be supplied as a separate item.

b) Output Control and Protection

Contacts or circuit breakers are usually provided on the output to manually disconnect the inverter from the utility. Automatic disconnection is also accomplished through these devices in the case of utility fault conditions. Output voltage and frequency are usually monitored so that the inverter can disconnect in the event of loss of utility, excessive current into utility, or utility frequency or voltage out of range.

3) Ground Fault Protection

Ground fault monitoring and protection may be performed on both the input side (DC) and the output side (AC) of the inverter. Several commonly used techniques to detect current flow in the ground leg of the system are discussed in a later section.

4) Environmental

Every piece of electronic instrumentation is designed to operate under certain environmental conditions. Normally, temperature and humidity ranges are specified for the inverters. The typical operating temperature range for most of these units is 0 to 50°C, and up to 95 percent relative humidity without condensation. The storage temperature range of the units is much wider. If ambient temperature conditions outside the specified operating range exist, the unit may shut down (internally monitored temperature). This becomes a prime consideration and may necessitate the design of a ventilation or air conditioning system.

2. PV Array Configuration

This section addresses technical issues concerned with the electrical configuration of a PV-T array. The problem of interfacing the PV array voltage and power with the inverter will be considered, as well as the impact of series and parallel wiring in a PV-T system. The use of blocking and bypass diodes will also be discussed in this section since they are an integral part of the PV array.

a. Interface of the Array with the Inverter

In a utility-interactive system, the initial concern in developing the array electrical configuration is the interface with the inverter. As previously discussed in section 1, the array voltage range under expected temperature variations must be matched to the inverter input voltage window. If the system power is determined by the load requirements, the array would be designed to satisfy these power requirements. If, however, the system is constrained by cost or available area consideration to less than the load power requirements, the array is designed to produce the highest power within these limitations.

In order to accomplish the array/inverter interface, modules are connected in series to approximate the midpoint of the inverter voltage range. The variation in array voltage with temperature extremes expected in the locale of the system application are calculated and compared with the voltage limits (voltage window) of the inverter.

If the array voltage range is skewed with respect to the inverter voltage window, the number of modules connected in series can be increased or decreased as appropriate, or the inverter voltage window can be adjusted slightly. The technique for performing this design interface will be presented in the design guidance section. If the power requirements of this system cannot be satisfied by connecting an integral number of these series strings in parallel, the array/inverter interface must be redesigned by increasing or decreasing the number of modules connected in series and adjusting the inverter voltage window accordingly.

b. Array Electrical Connections

1) Series/Parallel Tradeoffs

The most straightforward method of performing array electrical interconnections is to connect modules in series to obtain the desired voltage, and then to connect these series strings in parallel to obtain the desired power. Some advantages can be obtained with more complicated interconnection schemes, such as connecting two or more modules in parallel to provide redundant current paths in the event of shadowing or cell failure. In a PV-T system, however, the performance of the cells in a module is affected by the thermal design of the collector/receiver assembly. In order to obtain useful thermal output, a significant differential must exist between the inlet and outlet temperatures of the cooling fluid. Therefore, adjacent cells on the receiver will operate at different temperatures. A simple study was performed using PV-TAP (ref. III-1) to assess the impact of connecting cells in series and parallel along the thermal length.

Figure III-1 contains I-V curves generated by PV-TAP for a single cell operating at different temperatures. This concentrating cell is operating under 24 suns concentration. The family of curves represents temperature variations in 20°C increments from -20°C for the x's to 120°C for the 7's. A line drawn through the peak power points shows that the peak power current is nearly constant over the temperature range, while the voltage varies almost linearly with temperature. This suggests that cells operating at different

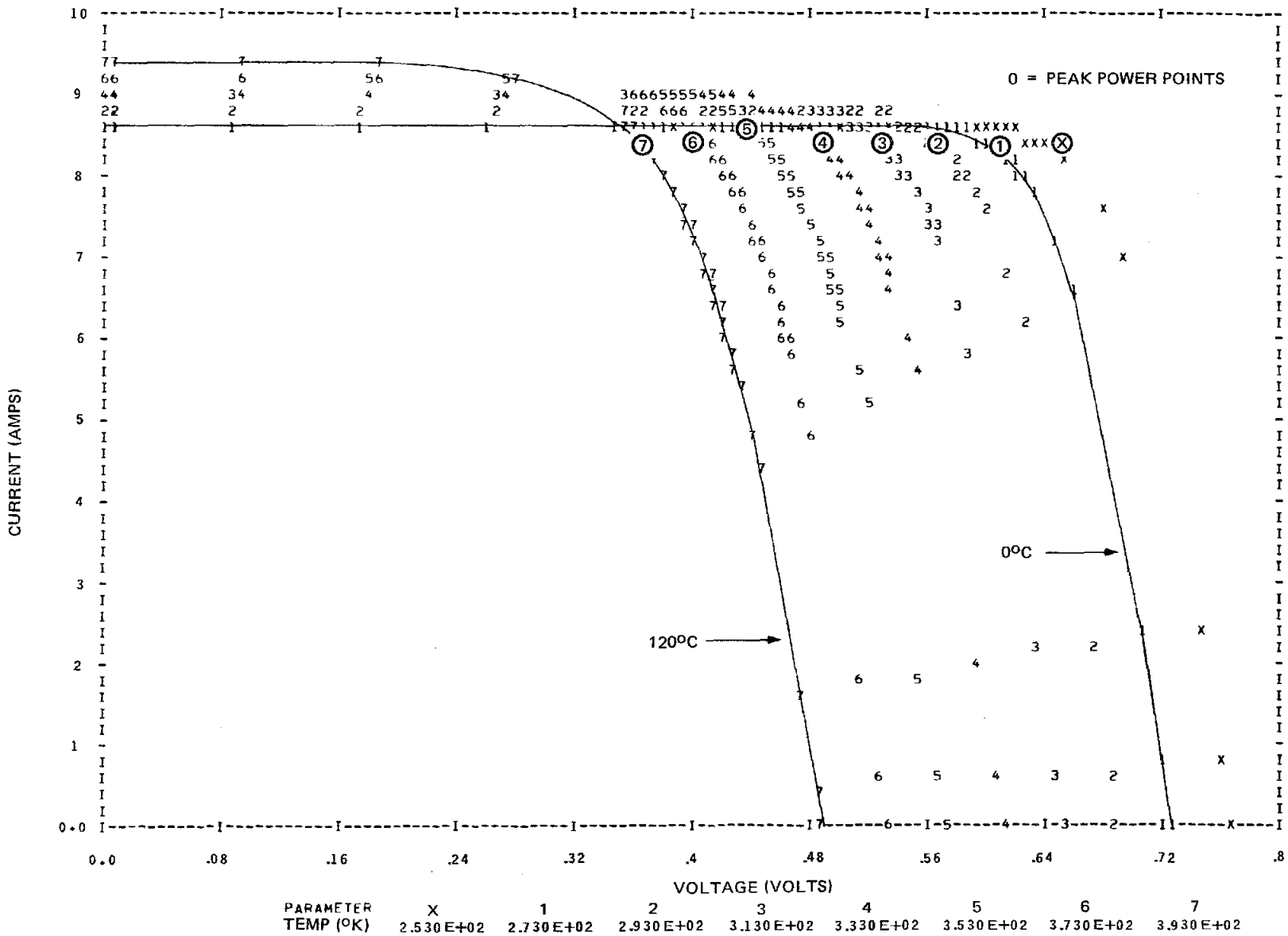

BDM/A-82-458-TR-R1

Figure III-1. Temperature Dependence of Concentrator Photovoltaic Cell Current - Voltage Characteristics

temperatures can be connected in series with little power loss since they can both operate at peak power. The same cells connected in parallel, however, will be forced to operate at the same voltage, but neither will be operating at peak power, since their peak power voltages are different.

To quantify the effect of series and parallel connection of cells at different temperatures, PV-TAP runs were made in which two cells with temperatures of $0^{o}C$ and $100^{o}C$, respectively, were connected, first in series and then in parallel. Additional runs were made in which the cells were both operated at $50^{o}C$, which was the average temperature of the two cells in the previous runs. Both series and parallel interconnection of cells at the same temperature produced identical peak powers of 1.22 watts with all cells operating at the identical peak power voltage of 0.49 volts. The results are summarized in table III-1. The cells operating at different temperatures which were connected in series produced a combined peak power of 1.21 watts, only 0.8 percent below the case with identical cell temperatures. The cells connected in parallel, however, produced only 1.01 watts, which is 17 percent below the identical temperature case.

Similar results were seen in the voltage statistics. The combined voltage of the cells at different temperatures connected in series was .99 volts, only 1.0 percent from the voltage for the identical temperature case. The voltage of the cells at different temperatures connected in parallel, however, was .43 volts, which is 12 percent from the identical temperature case. Thus, a string of series-connected cells operating at different temperatures can be adequately represented by the average temperature of the cells, while parallel connection of cells at different temperatures cannot. In addition, power loss is greater for cells connected in parallel.

This study indicates that cells should be connected in series over the thermal receiver length. Neither cells at different temperatures nor cell series strings with different average temperatures should be connected in parallel. Applying these results to a linear

TABLE III-1. RESULTS OF TEMPERATURE DIFFERENTIAL STUDY

	P_p	% Dev.	V_p	% Dev.
Series Connection (ΔT = 100°C)	1.21W	0.8	.99V	1.0
Identical Temperatures (50°C)	1.22W		.98V	
Parallel Connection (ΔT = 100°C)	1.01W	17.2	.43V	12.2
Identical Temperature (50°C)	1.22W		.49V	

parabolic trough with a V-shaped receiver tube, for example, the cells arranged along the receiver tube length should be connected in series, but the two series strings on opposite faces of the receiver tube may be connected together either in series or parallel, because the strings have the same average temperature. If, however, the thermal cooling length extends beyond a single receiver, the receiver strings should be connected together in series, not in parallel, since the strings will operate in different temperature regions. This also brings out the importance of maintaining equal coolant flow rates through each parallel connected row of collectors to ensure each row is operating at the same average temperature.

An additional study was performed using PV-TAP to assess the losses associated with paralleling modules in a typical linear focus Fresnel system produced by E-Systems. The need for the study was occasioned by the long thermal length required by this type of system.

An E-Systems array consists of four modules (or collectors) mounted together in a two-axis tracking frame. Each module produces 30.1V and 12.7A with 40X concentration of 1000 W/m^2 insolation and fluid temperature of 25^oC. The corresponding cell temperature is about 39^oC. The thermal length extends over all four modules. In addition, it is desirable to extend the thermal length over approximately 12 arrays (48 modules), since only about 36^oC fluid temperature rise is obtained over this length at a flow rate of 5×10^{-4} m^3/sec (8 gpm). Since the expected inverter voltage window is 300-450V, all 48 modules could not be connected in series. At 30V per module, it would be reasonable to connect 12 modules in series to obtain 360V. Therefore, four strings of 12 modules each, would have to be paralleled.

Based on the previous study, it was decided that if paralleling was required, it would be better to parallel modules than strings of modules since the average temperatures of the entities being paralleled would be closer. The study considered thermal lengths of 12 and 24 arrays (48 and 96 modules) with different flow rates resulting in different temperature rises from inlet to outlet. Modules were connected

in parallel first (4 modules for the 12 array case and 8 modules for the 24 array case) and then, the parallel groupings were connected in series (12 for each case). The analysis then assessed the power loss for each case with different flow rates compared to the maximum power obtainable with no temperature differential.

Two other conditions were studied for the 24 array case. In one, the four modules in an array were paralleled and 12 arrays were connected in series to form a string before the two strings were finally connected in parallel. In the second, the four modules in an array were connected in series, and three arrays were also connected in series to obtain the 360 V desired, and finally, eight series strings were paralleled. This was done to test the assumption of obtaining better performance by accomplishing all paralleling first.

In the PV-TAP Modeling, each module was represented by a single PV cell model. The cell parameters used in the previous study were factored to represent a full module rather than a cell. The 12 array system was run at 40X concentration of 1000 W/m^2 insolation with no fluid temperature rise from inlet to outlet to validate the modeling and provide a "control" run to use as a basis for comparison of power losses. The results are shown in table III-2. The 12 array system produced 18.8 kW at 365 V and 51.5A, which corresponds to 391.7W per module at 30.45 V and 12.87A. The module specifications obtained from E-Systems were 30.1 V at 12.7A for 382.3W. The voltage and current obtained are each slightly more than 1 percent above the specifications and the power is within 2.5 percent of the specification.

TABLE III-2. MODELING VALIDATION

	MODULE		
	POWER	VOLTAGE	CURRENT
CALCULATED	391.7W	30.45 V	12.87A
SPECIFIED	382.3W	30.1 V	12.7A
% DEVIATION	2.46%	1.16%	1.34%

The matrix of runs performed is shown in table III-3. The flow rates were not input to PV-TAP since only the cell temperatures are required for electrical performance. The values for fluid temperature rise from inlet to outlet were obtained from SOLCEL II analyses of the thermal loop. All cell temperatures within a given module were considered to be the same since cells in series can be represented by their average temperature. To obtain the desired temperature rise from inlet to outlet (ΔT_{FLUID}) successive modules were operated at temperatures of $\Delta T_{FLUID}/(N_M-1)$ above the previous module where N_M is the number of modules in the system. The interconnection patterns in table III-3 are read from left to right so that 4P x 12S x 2P indicates four modules in parallel in an array by 12 arrays in series by two series strings in parallel.

TABLE III-3. MATRIX OF ANALYSIS RUN CONDITIONS

CASE	ARRAY/MODULES	FLOW RATE $m^3/sec \times 10^{-4}$	FLOW RATE gpm	ΔT_{FLUID}	INTERCONNECTIONS
12-1	12/48	6.3	10 gpm	28.8°C	4Px12S
12-2		5.0	8 gpm	35.9°C	
12-3		3.8	6 gpm	47.7°C	
24-1	24/96	7.6	12 gpm	47.7°C	8Px12S
24-2		6.3	10 gpm	57.1°C	
24-3		5.0	8 gpm	71.1°C	
24-2A	24/96	6.3	10 gpm	57.1°C	4Px12Sx2P
24-2B	24/96	6.3	10 gpm	57.1°C	12Sx8P

The results of the analysis are listed in table III-4. The power per array and the percent loss from the ideal case are shown for both 12 and 24 arrays in the thermal loop. It can be seen that the power per array and the percent loss is the same for both cases which contained the 47.7°C temperature differential. By graphing the results, the curve in figure III-2 is obtained. The percentages lost exhibit a

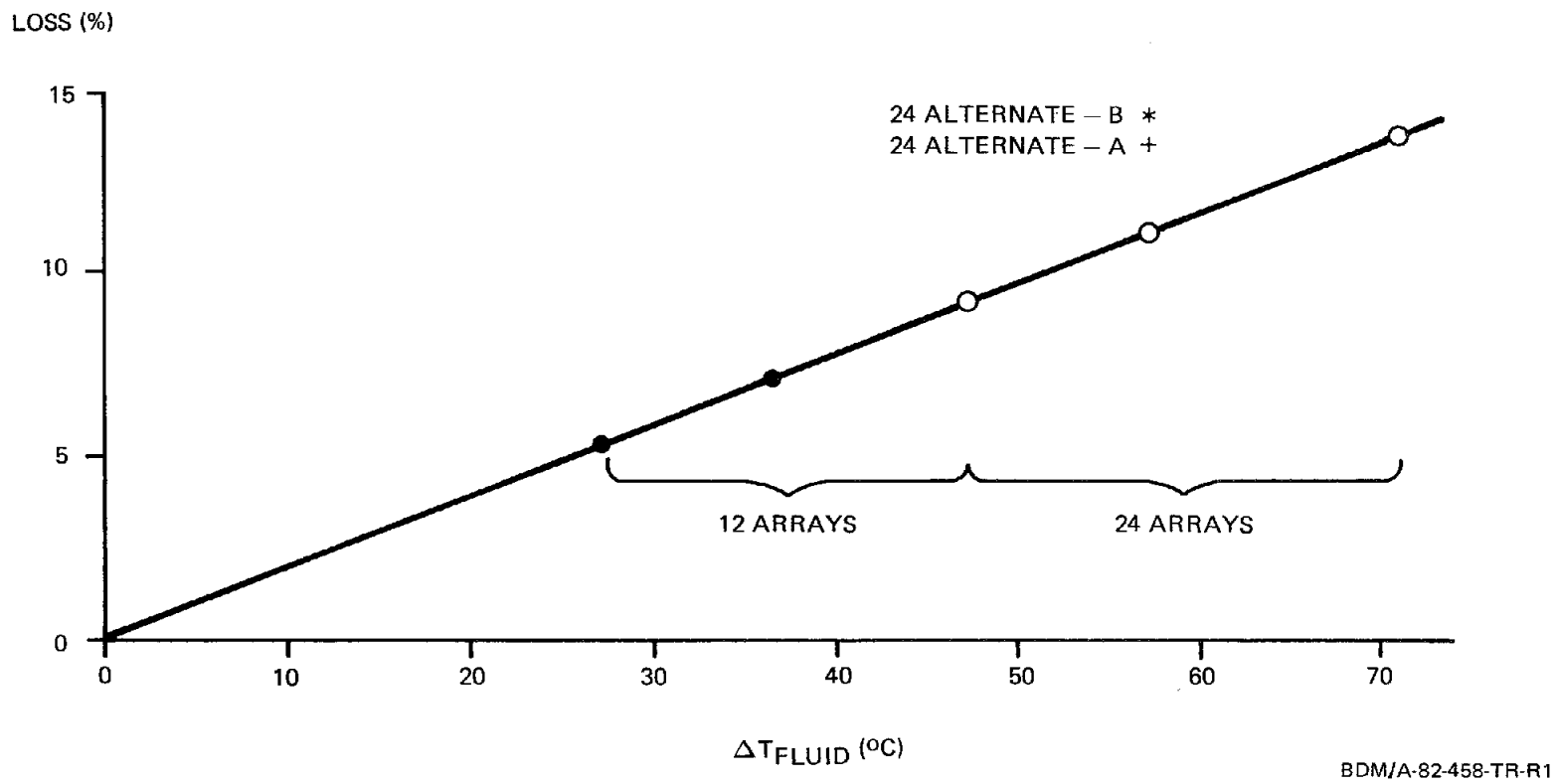

Figure III-2. Percent Power Loss Versus Fluid Temperature Differential

nearly linear relationship with ΔT_{FLUID} regardless of the number of arrays. The slope of the curve appears to be increasing only very slightly with temperature, but this deviation is within the error limits of the analysis.

TABLE III-4. RESULTS OF PV-TAP THERMAL LENGTH STUDY

ΔT_{FLUID} (°C)	12 ARRAYS POWER/ARRAY	12 ARRAYS LOSS	24 ARRAYS POWER/ARRAY	24 ARRAYS LOSS	
0	1.567 kW		1.567 kW		
28.8	1.479 kW	5.62%			
35.9	1.458 kW	6.96%			
47.7	1.421 kW	9.32%	1.421 kW	9.32%	
57.1			1.391 kW	11.23%	
71.1			1.347 kW	14.04%	
					2.43% Difference
			A-ALTERNATE 24		
57.1			1.353 kW	13.66%	
			B-ALTERNATE 24		
57.1			1.343 kW	14.29%	

The runs containing the alternate interconnection scheme exhibit definite increases in power loss. Alternate connection A had a power loss of 13.66 percent, which is 2.43 percent greater than the loss with the preferred interconnection scheme, alternative B had a loss of 14.29 percent, which is 3.06 percent greater than the loss with the preferred interconnection scheme. Therefore, the analysis supports the interconnection preference assumption.

The analysis performed represents the worst case losses obtained due to cell temperature mismatch, since each case was run at full insolation (1000 W/m^2). For a given design case, for example, 24 arrays at 6.3×10^{-4} m^3/sec (10 gpm), the actual loss will be less over the course of a year since the arrays will not receive full insolation. To assess the losses at other insolations, the loss and the ΔT can be factored by the decrease in insolation. For the 24 array-6.3×10^{-4}

m^3/sec example, full insolation loss is 11.23 percent because ΔT is 57.1°C. At half insolation, ΔT will be 28.6°C and the corresponding loss will be 5.62 percent.

2) Center Grounding

Center grounding of the array is often employed in commercial and industrial applications so that electrical equipment with lower voltage ratings can be used. This wiring technique also provides redundant current paths in the case of module failure or shadowing and results in higher outputs under these conditions. Center grounding of the array, however, results in greater danger to personnel than an ungrounded array. If someone should touch an exposed lead, a return path from ground is established through the person. With a floating array, however, no return path from ground would be established unless some part of the array had a shorting failure to the metal receiver tube. This hazard is usually considered acceptable in a commercial or industrial application where access to the array is carefully controlled and limited to trained maintenance personnel.

3) Maintenance and Other Considerations

At the current summing nodes where the blocking diodes are normally installed, the wiring system must take into account the accessibility of the different strings and possibly the accessibility of individual modules for replacement. In most cases the optimum wiring configuration will allow the maximum test flexibility and fault location in the array field. In order to do this, however, every string node must be accessible to the maintenance personnel.

c. Bypass and Blocking Diode Considerations

Both the bypass and blocking diodes perform important functions in the PV system wiring design. Correct specification of these components can lead to an optimal DC power-loss figure, and enhance system reliability.

The primary function of bypass diodes is to protect cells from excessive reverse voltage due to shadowing. Bypass diodes also improve output by passing current around a group of cells if the cells

should be shadowed or should fail open. Normally, there is at least one bypass diode mounted reverse biased on every PV module. This can also be done on a sub-module basis. The maximum number of cells which may be connected in series in a bypass group is determined either from reverse breakdown or over-heating considerations. The equations used to determine this design are presented in the design guidance chapter.

Since the bypass diode is normally reverse biased, a minimal amount of current flow can be expected through the diode. This is referred to as leakage current as specified by diode manufacturers at a given reverse voltage potential. For most silicon diodes this ranges from less than a micro amp, to as small as 10 to 20 nano amps. If a bypass group should fail to open or be shadowed, the current can flow through the bypass diode, thereby completing the circuit to other cells in the series wired string. Instead of producing power from the bypass group, the diode is actually dissipating power, in order to deliver power from the other cells below it in the series wired configuration.

Blocking diodes combine currents for series wired strings in parallel. They prevent strings that have module failures, or are shadowed, from draining current from higher voltage strings which can act as a current source for the low voltage string. Blocking diodes should be placed at one end of each array series string for uni-polar systems, and on each end for center-grounded systems.

Both the bypass and the blocking diodes must be specified for the particular PV system design. For the bypass diode, the critical parameters are the current rating, forward voltage drop, and the reverse breakdown voltage. Heating due to power dissipation in forward bias should also be considered.

The blocking diode performance parameters must also be specified in the design. These parameters include the peak reverse voltage specifications for the diode, the forward voltage drop, the maximum power dissipation allowable, and current rating of the diode. Since blocking diodes are in the series leg of the power output of each string, they consume some power, which is a parasitic DC power loss in

the system. Optimally one would choose the blocking diode with as low a forward voltage drop as possible at the current rating required. It is worth noting that blocking diodes should be over-designed in the system so the power dissipated by the diode does not cause a significant temperature rise for that component; otherwise, heat sinks will be required for each blocking diode.

3. Power Conditioning

The power conditioning in a PV-T system refers to the wiring and other system components associated with the inverter tie into the utility bus. This section will discuss circuit breakers, disconnect switches, current ratings and electrical specifications of the AC wiring, and derating of that wiring.

a. Utility Tie Components

In any PV system that uses a utility tie there are certain components which must be installed between the inverter and the utility bus. The primary purpose of these components is to serve as an electrical disconnect between the PV side of the system and the utility side of the system. In some cases, circuit breakers are used to trip over-currents on any phase of the AC circuit. In addition to the circuit breakers, safety disconnect switches are often utilized to provide an easy means of manually disconnecting the inverter from the utility bus. The characteristics of the circuit breakers and safety disconnect switches are issues in the design of the PV-T system, since there are several types of circuit breakers and disconnect switches. Careful consideration must be given to specification of these units.

b. Electrical Specifications

Besides the circuit breakers and safety disconnect switches, all the components on the AC side of the system must be specified for voltage and current. The voltage and current ratings are given in most manufacturer's catalogs for RMS values of the AC voltage or current. In addition to these components, power and energy monitoring meters may be installed to determine the power and energy flowing from the utility to the inverter or from the inverter to the utility bus. The

electrical specifications of the utility bus are also very important, because they affect the design and specifications of the inverter and indicate appropriate places for the use of transformers in step up or step down configurations. The major electrical specifications required from the utility bus prior to the design are the voltage, current, and number of phases in the wiring configuration.

c. Wiring Considerations

There are several methods of routing wiring from the inverter to the utility, or to the local load, including conduit routing and the use of cable trays. Conduit serves two purposes. The first purpose is to provide a mechanically rigid and structurally sound connection between the inverter and its load. Second, conduit provides an outer shield jacket for the conductors inside because the conduit is grounded at one or both ends of the installation and acts as a shielded cable tray to eliminate transient induced voltages in the wiring. Correct selection of the wiring size to be used for any AC application can be found in the National Electrical Code. Additionally, there are derating considerations for this wiring as a function of temperature, and special considerations for delivering power to reactive loads. Other parameters associated with wire specifications are listed as issues in the DC wiring section. They include the insulation properties, temperature coefficient of the conductors, and correct method of termination into fuses, terminal blocks, and switches.

1) Electrical Codes

Once the electrical specifications of the utility tie have been determined, the method of wiring and correct use of cabling techniques must be selected to actually interface to the utility. The National Electrical Code serves as a guide to determine wiring size and type of insulation etc.; however, based on local codes in different parts of the country and overseas, other specifications may apply. It is highly recommended that an electrical contractor familiar with the codes governing the area of installation be consulted and possibly even subcontracted to do the actual utility interface work. In some cases, the utility company may desire to perform this part of the installation.

2) Power Monitoring

Power monitoring takes into account placement of energy and power meters connecting the inverter and the utility bus. The major reason for installing power meters is to ascertain the direction and amount of power flow from the PV system to the utility, or from the utility back into the PV system. This will allow determination of the amount the user owes the utility for electricity, or the amount the utility must refund to the commercial or residential PV system owners for power provided to the utility system. In order to install (and possibly replace at a later date) the power meters, safety switches must be located on either side of the bus. This will isolate any voltage during maintenance periods or during the initial installation of meters. It may also be a convenient way of disconnecting the utility for a manually controlled combination inverter. For example, sometime during the day the owner may wish to disconnect from the utility and supply all of the PV array system power to a local load. Disconnect switches allow this to be done manually in the field.

3) Local Load Considerations

Some systems may require the local load and the utility bus to be connected to the inverter. Occasionally, the local load requirements differ from the utility bus. One example of this is a three-phase four-wire system utility, with some of the local loads for the inverter including overhead lighting for the control room, and with outlets for electric hand tools and similar items. This represents a 120-volt single-phase system, and in order to derive this from the three-phase output of the inverter, an isolation transformer must be used. Therefore, the specification and correct placement of isolation transformers in a system are very important.

4. System Protection

a. Ground Fault Protection

The importance of an adequate ground fault protection system cannot be over-emphasized. A ground fault is a significant amount of current flow in the grounding system. Ideally, no current should flow

in the ground wiring; the return circuit current should flow in dedicated return or common conductors. Although there will almost always be a few microamperes of leakage currents flowing in the ground conductors, ground fault detection circuits are usually implemented to detect appreciable current flow, and subsequently disconnect or short circuit the source of the current.

On the DC side of a PV-T system, faults can occur between either side of the array voltage and earth ground. Detecting this and short-circuiting the array provides electrical shock protection for maintenance personnel.

On the AC side of a PV-T system, faults can occur between any of the AC phases (if there are more than one) and earth ground. When they are detected (by a low impedance between the lines), the output of the inverter is disconnected.

The different methods of detecting ground currents, as well as the reliability and susceptibility to false triggering, must be investigated in any PV-T system design.

The placement of the ground fault sensing circuits is also of prime importance in the design, and a method of optimizing this location will be discussed in a later section.

b. Transients

Transients in the photovoltaic system can be generated by lightning, by the inverter switching, or by the utility. Various methods are used to block, filter, or shunt those electrical surges in order to protect the system hardware.

1) Lightning

Several studies have been performed that assess the probability of lightning striking at or near an array, estimate the magnitude and effects of the electrical transients induced, and provide methods of protecting the array and the power processing and control hardware. The results are condensed and summerized below.

For a commercial or industrial system of less than 500kW, the probability of a direct lightning strike for the worst

location in the U.S. appears to be about one strike every 6 to 12 years. For other locations, the probability may be one every 20 to 60 years. A direct lightning strike to a PV-T collector could cause severe damage to electrical hardware due to electromagnetic coupling into cables and conductors. Use of air terminals (lightning rods) is not recommended, however, because electromagnetic coupling could be equally significant from the currents induced in the rods. Grounding the large metal collectors and frames of the PV-T array should provide equivalent protection without the additional cost.

The use of a dissipation array could provide additional protection to the electrical system. This type of lightning array uses horizontal wires with numerous barbs to collect the static charge around the array and conduct it to ground, thereby reducing the probability of lightning strikes. This technique is expensive, however, and does not reduce the probability of strikes near the array. Since strikes within 100 to 200 meters of the array can still induce voltages greater than 1000 V, and up to 10,000 V, terminal protection devices will be required even with the dissipation array.

The recommended method of lightning protection is to ground the collectors and support frames or pedestals to a counterpoise system buried in the ground, and provide terminal protection devices at the ends of cable runs.

The counterpoise system consists of a network or grid of bare conductors buried 5.08 - 7.62 CM (2 - 3 in) underground which criss-cross under the array. The terminal protection devices consist of spark gaps, varistors and Zener diodes connected near the electrical equipment they are designed to protect. Standard AC surge suppression devices are available for use on AC power lines. These usually contain spark gaps. In a DC application, however, spark gaps may not extinguish, since the excursions through zero voltages experienced on AC lines are not present on DC lines. Therefore, varistors, which are voltage variable resistors, are used on DC lines. These are designed for transient protection. Zener diodes cannot handle the large power surges

associated with lightning, and are subsequently used only in combination with varistors, as shown in figure III-3, to provide additional filtering for low immunity lines such as logic inputs. The varistor conducts the major current while the resistor limits the current to the Zener diode, which clamps at about 7.5 V.

2) Other Transients

In addition to lightning, transients can also be induced by electromagnetic interference (EMI), by inverter switching, and by utility surges. Since lightning protection devices do not provide suppression of these low level transients additional protection is provided.

EMI protection is usually provided for the inverter by LC filtering in the input stage. The LC filtering also prevents transients generated in the inverter from being injected into the DC lines. An isolation transformer provides transient protection on the output of the inverter. The blocking diodes placed at the ends of the array series strings prevent reverse current flow into the strings.

c. Utility Failure Protection

Protection against anomalous utility conditions such as abnormal frequency or voltage, utility shorting, or loss of signal, is usually provided within the inverter. When monitoring circuits within the inverter sense these conditions, the inverter will disconnect from the utility and reconnect when the utility returns to normal.

Sometimes the utility company will not accept this protection, but will require external redundant protection to ensure that a down-line is not energized by the PV system. Loss of voltage or loss of power relays coupled with circuit breakers can be used to automatically break the AC lines under these conditions.

5. Miscellaneous Electrical Components

Several electrical components must be used in the electrical portion of a PV-T system design. The proper specification of these components ultimately affects reliability, safety, and cost of the system.

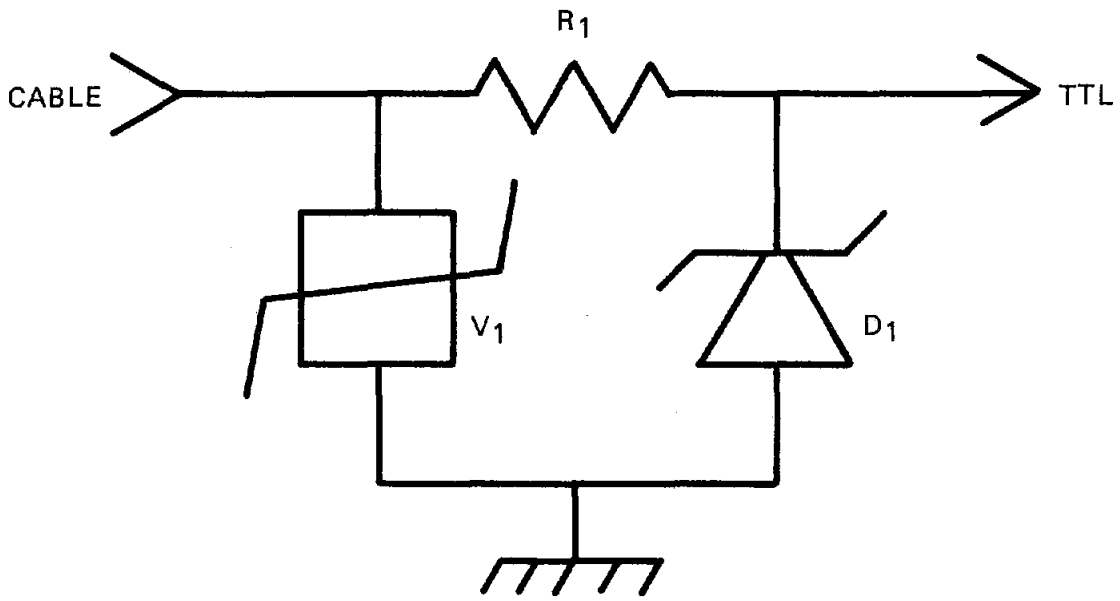

V_1 = GENERAL ELECTRIC V24ZA50 VARISTOR

D_1 = GENERAL SEMICONDUCTOR 1CTE-5

R_1 = ALLEN-BRADLEY CARBON COMPOSITION GB RESISTOR 4.7Ω ± 10% 1W

BDM/A-82-458-TR-R1

Figure III-3. Typical Data Line Logic Protection Circuit

a. Safety Switches

In all PV and PV-T system designs there are several places where safety switches are required. For example, during fuse replacement, neither side of the fuse must present an electrical shock hazard to the maintenance person. Therefore, switches are employed to open circuit the voltage source at the fuse block location. Similarly, switches are also used where operator or maintenance personnel access is required for servicing or troubleshooting.

There are three important parameters to specify when buying switch components; 1) voltage rating, 2) current rating, and 3) contact type. Additional parameters exist for circuit breakers.

1) Voltage Ratings

The voltage ratings presented by most switch manufacturer's are Underwriter's Laboratory (UL) approved and tested per UL standards. This guarantees a level of quality and a conservative rating. DC and AC ratings are different for some switches and the same for others. This can be confusing since many factors contributing to the voltage rating are not obvious to the PV-T system designer. When specifying switch voltage ratings for a given configuration, the worst case (highest) value is used; that is, the voltage between terminals and the voltage to chassis ground must be known, and the higher of these two values should be used. DC and AC voltage ratings are not interchangeable, and the exact placement in the system must be known in order to specify this parameter correctly.

2) Current Ratings

DC and AC current ratings for the switch contacts are specified by the component manufacturer similarly to the voltage figures. They take into account the size of contacts, plating used on the contacts, operation and de-activation time constants, and they affect the number of operations (useful lifetime) of the switch.

3) Contact Type

Depending on the design of the switch contact used, more or fewer operations of the switch may be expected in its useful

life. Switches can be rated from several thousand closures to several million closures, depending on the current actually flowing through the contacts and the type of contact material used. Also, the material used will be a major factor in the resistance (Ω) of the switch while in the "on" position. If the number of switch contacts in a system is high (several hundred), an appreciable amount of power loss may be expected if low quality switches are installed.

b. Circuit Breakers

Circuit breakers are used on the AC side of the PV electrical distribution system. They are available separately mounted in appropriate enclosures to suit locations, or as part of a switchboard or panelboard, depending on rating. Circuit breakers are classed in frame sizes of 50 to 4000 A, or as "molded case" and "large air", or "low-voltage power" circuit breakers.

1) Molded-Case Circuit Breakers

In this type the contacts are shutes, and operating parts are enclosed in a molded plastic body with an external operating handle protruding through the cover. They are available with magnetic-actuated elements, combination thermal-magnetic elements, and nonautomatic mechanisms. Molded-case breakers are available in frame sizes of 50 to 4000 A, with a short-circuit interrupting rating of from 5000 A to 200,000 A asymmetrical. Caution should be exercised in applying molded-case circuit breakers as they are rated for use at 120/240 (208), 277, 480, and 600V. Improper selection could cause extensive damage to property, and injury or death to unsuspecting workers.

Thermal-magnetic circuit breakers respond to overload current through a thermal bimetallic element which provides an inverse time-current relationship, and an instantaneous magnetic element that responds to short circuit current flow. The thermal element protects against overloads without nuisance tripping from momentary higher overload currents. The speed of the breakers response depends on the magnitude of the overload.

The magnetic trip element provides instantaneous protection against short circuits. These systems usually have provisions for selection of a trip setting above the harmless momentary overload level, but provide the fastest possible breaker tripping for currents above the selected tripping point. The use of such a device protects motor circuits against short circuits, with overload protection provided by the thermal element. Nonautomatic circuit breakers serve as disconnect means only, as they have no tripping devices.

A number of auxiliary attachments are available for remote tripping, for signaling that the breaker is off, on, or has tripped due to overload or short circuit. Motor-driven mechanisms are available to both open and close the breaker from a push-button or other signal. Some breakers have interchangeable trip units which can be changed to higher or lower trip values in the field; other breakers have fixed, factory-set trip elements.

2) Large Air or Low-Voltage Power Circuit Breaker

These circuit breakers are available at ratings of 225 to 4000 A with symmetrical interrupting ratings ranging from 22,000 A in the standard form, to 200,000 A with current limiting fuzes mounted on the breaker frame. They may be manually or electrically operated, and both are equipped with a manual trip button.

Some manufacturers produce these breakers with stored-energy closing mechanisms, consisting of springs which are charged either manually, or through motors, to rapidly close the breaker contacts. The motor-charged spring mechanisms may be charged manually, if necessary. Other manufacturers produce these breakers with spring-assisted closing on manual types and solenoid closing for electrically operated units.

As with molded-case circuit breakers, remote trip and signaling devices are available. The electrically operated breakers can also be easily connected to operate in pairs to transfer the power supply from one source to another, as from a utility company source to a stand-by generator.

c. Junction Boxes

In order to connect the string wires from series or parallel connected PV cells, junction boxes are required. They must be selected to fit each individual application; however, many of the parameters of the J-Boxes are common to all systems, and must be identified in order to optimize this selection process. The first of these parameters is the environmental requirement placed on the box. Standard National Electronic Manufacturers Association (NEMA) type enclosures are often used, and are available for outdoor installation applications as well as for interior mounting. The boxes must also provide for ease of PV cell/string replacement. This is usually accomplished by installing fuses or switches that allow a person to isolate the string from the rest of the PV array for safety reasons. Mounting considerations for the J-Boxes must also be taken into account, and in most cases, provisions for electrically grounding the metal enclosures must be made.

d. Terminal Strips and Jacks

To actually terminate the wires, terminal strips may be employed in the J-Box and other portions of the system wiring. The voltage rating, terminal size, and plating characteristics of the terminals should be specified. The voltage rating should be conservative (add 25 percent), and represent the highest voltage that will be present at the terminal. This rating should be considered for terminal to terminal voltage as well as for terminal to ground voltage in cases where the strips are bolted to a metal box or chassis. The terminal size can be specified by knowing the wire size used. Terminal (spade) lugs and terminal screw conections are rated by wire size (AWG), and screw size (#10-32). Various plating types are available for most termal strips.

This is a consideration especially for high humidity and salt spray areas, since the connections are more susceptible to corrosion in these environments. All of the above considerations for terminal strips also apply to test jacks and mechanical switches.

e. Fuses and Connectors

The general considerations pertaining to termal strips and jacks are also applicable to fuses and connectors. Another aspect in

specifying fuses is the delay time and over-current characteristics of the fuse. The delay time specifies how long it takes for the fuse to react to an over-current condition, and the over-current rating is the current at which the fuse will actually blow. This is a minimum current rating, and over-currents in excess of this figure will shorten the delay time.

6. Wiring Sizes

There are several issues related to wire sizes and wire types. Although the National Electrical Code may be used to determine the correct wire for any application, the guidance provided by this source relates the wire to a minimum set of standards to obtain a safe wiring configuration. PV-T systems, however, present design objectives beyond the scope of the National Electrical Code handbook.

a. Current Capacities

Current carrying capacities of wires may be rated several different ways. Some wire manufacturers give this rating as the current which may flow into a conductor just prior to melting the conductor. This obviously does not provide good design guidance, since no one except fuse designers wants the current carrying conductors to melt. Most reasonable ampacity tables give a current for each size conductor as a function of an incremental temperature rise (usually $10^{o}C$) in the conductor. This number will be different for different types of materials used, and ambient conditions. It is worth noting that the ampacity must be derated as air temperature increases, and as the number of conductors in a conduit or cable tray increases.

b. Types of Conductors

The most commonly used conductors are aluminum or copper. Wires of all common sizes (AWG) may be found in both aluminum and copper types. The two major differences between them are weight and cost. Additionally, the conductivity will be different for the two materials. Other types of wiring available but not commonly used, are silver or silver-plated, and gold-plated wires.

c. Voltage Ratings

In PV-T systems one must ensure that the correct voltage rating of the conductors is used. This entails calculating the highest potential that will exist between any two conductors, and between any single conductor and earth ground. The voltage rating required may differ throughout parts of the system, thus, different types of wire may be specified for these parts. Occasionally, it is more cost effective to use the same (highest) rated wiring for all portions of the PV-T system design for logistics and availability reasons.

d. Insulation

The insulation material and thickness for electrical conductors are many and varied. Examples of the types of materials used for insulation are rubber, thermoplastic, cotton and asbestos. The type of insulation specified affects the voltage rating of the wires, but primarily determines the environmental conditions for which the wire may be used. Temperature and humidity are prime concerns in the design and specification of insulating materials. Some insulation is oil resistant and flame retardant.

The thickness of the insulation will also determine voltage breakdown characteristics, since the ability to draw an electrical arc is directly related to the distance between the two conductors. In some cases, the insulation thickness may also affect workability of the cabling in terms of minimum bend radius and flexibility, and the ability to draw the cable through conduit. Additionally, the insulation thickness will provide a degree of protection to the conductor in areas where cabling will be walked on.

e. Temperature

All wires must be derated for temperature increases. This derating means that as the temperature rises, the ampacity of the conductor decreases. To properly determine a wire size based on current carrying capacity, one must estimate the maximum temperature of the air surrounding the conductor. This could be the ambient air condition, or it may be higher or lower than the ambient condition. Certainly, in

conduits carrying multiple conductors, the air surrounding each wire may increase due to the other wires if they carry appreciable current. Some self heating of current carrying conductors exists as currents approach the ampacity rating of these conductors. Most tables of ampacities provide a correction factor for derating of the current carrying capability of the wires as a function of temperature.

f. DC Resistance

The nominal DC resistance of different wire sizes must be taken into account for PV-T system wiring designs. There are many references which give this resistance and usually this is stated as ohms per 1000-ft. Many designs may require that the wiring specifications limit the power loss in the DC section of the wiring to as low as 1 or 2 percent of the total power from the array. Knowing the current coming from the array, this power loss in the wiring can be calculated by multiplying the square of the current times the DC resistance of the type wire per 1000-ft., times the length of wire used. In most cases, when designing for a low DC power loss, the wire size will be larger than that required by the National Electrical Code. Also, running several wires in parallel is a technique which is often used to reduce the overall resistance of a long run of cabling.

There are also resistances in the DC side of the array which are not associated exclusively with the wiring. These include the contact resistance of connectors and switches, voltage drops across fuses due to fuse resistance, and other miscellaneous parasitic losses. When the DC power loss is of prime importance in a system design, all of these parasitic losses must be taken into account. For switch contacts, connectors, and terminal lugs, typical values of 1 to 10 milliohms per connection can be used as an estimate. More detailed calculations can be performed where specifications are available from the manufacturers. In the case of fuses, the internal DC resistance of the fuse is a function of the material it is made out of, and the time in which it will react to an over-current. Some manufacturers will specify this, but in other cases it will have to be calculated.

g. AC Wiring Losses

The DC resistance of the wire can also be used to calculate losses in the AC sides of circuits; however, this must be done with the RMS value of the AC voltages and currents for that part of the system. Also, special considerations may be used in cases for reactive loads. Normally, reactive loads require derating of the conductors at high current levels.

7. Safety Grounding

There are two major reasons why a PV system should be grounded. The first is safety and the second is noise suppression. In grounding the metal framework of the modules and chassis of the enclosures housing electronic gear, the voltage potential is guaranteed to be zero volts with respect to earth ground. This eliminates any electrical shock hazard to the operators and maintenance personnel. Grounding also provides a certain degree of noise suppression for highly sensitive circuits. It not only eliminates stray electrical fields from producing transient voltages in cabling and components in systems, but it also eliminates or helps suppress radiation from portions of the systems which may be generating EMI.

a. Components Which are Grounded

Generally there are many components in a PV-T system which need to be grounded. These include the PV module frames, all mechanical components, the inverter chassis J-Boxes, any maintenance panels, and service disconnect switch chassis. Additionally, all conduits and metal cable trays should be mechanically and electrically connected to earth ground. The method of grounding these components in the system can vary, and must be associated with the counterpoise or lightning system design. In the case of the PV module frames, grounding this metallic surface prevents electrical shock hazard when replacing modules. Mechanical components and the inverter chassis need to be grounded for the same reason. The J-Boxes, maintenance panels, and conduit or cable trays, are grounded not only to prevent shock but to form an electromagnetic shield around the components inside of the enclosures. This decreases unwanted

induced voltage and current transients in the wiring and in the components in the boxes.

b. Voltage Isolation

Even though the PV array framework is grounded, there is no electrical contact between the plus or minus side of the PV modules and the metallic framework. This allows the system to be designed so the PV array can be floated with respect to earth ground. Hence, when the PV array voltage is not connected to the inverter, there is no current path between positive or negative node of the PV modules and earth ground. Therefore, operators replacing or installing modules cannot be subjected to electrical shock by touching either side of the array power and the framework on the module. Another technique is also used to reduce the voltage potential of the array to zero. This technique is designed into most input stages of inverters and allows the shorting contacts to reduce the field potential to zero volts. Depending on the system grounding configuration, either the positive or negative side of the array may be earth grounded at the inverter so a current path does exist between earth ground and one side of the array when it is started. This is not the usual configuration of the system for maintenance purposes, and the array is normally shorted only when a ground fault detection occurs. There must be isolation between the grounding system of the PV-T system and the lightning protection system design. Although both systems are earth grounded at one point or possibly at several points, the impedance to earth potential at the lightning counterpoise system must be much less than that through the normal framework grounding. This is accomplished by using smaller conductors in the framework grounding system than the conductor size which is used for the counterpoise design.

8. Control Strategy

The control strategy discussed in this portion of the report will deal with the photovoltaic array and inverter electronics of the system. Additional sections on control, dealing with the thermal aspects of the PV-T system, are found in another section.

a. Manual

The control system of most PV systems is associated with the inverter. This consolidates all the operational and control features in one room and allows easy access for shut-down of the system. On the front panel of most inverters is a main on and off switch which turns the power conditioning unit on and off. Once in the on position, however, automatic control is accomplished by the inverter's internal electronics. Several inverter designs may also have manual controls in addition to the shut-down switch. This is a common configuration when an inverter is designed to operate in more than one mode. An example of this would be a control switch on the front panel to select either utility tie or stand alone operation. Additionally, phase-locking the inverter to the utility in a stand alone mode may require another manual switch on the front of the unit. Monitoring all DC and AC electrical parameters is usually accomplished on the front of the inverter. This normally includes the DC voltage, current, power, and sometimes energy from the array, besides the AC output voltage, power and sometimes frequency, to the utility or local load.

b. Automatic Control

Present inverters have several automatic control features built into them. These control features are comprised of safety and automatic start-up and shut-down features. Among the safety features are ground fault sensing, utility line voltage and frequency sensing, and over-temperature sensing for the inverter itself. Ground fault sensing is provided at the DC input and the AC output of the inverter. AC voltage and frequency sensing is done at the utility tie output of the inverter. The temperature sensing is accomplished internally by the inverter's electronics. In the case of effective ground fault currents, both the AC and DC side of the inverter are disconnected from the array and the utility. For over-voltages or over-currents, or an error in frequency on the AC output of the inverter, the AC side is disconnected. And for an over-temperature condition in the inverter electronics, a complete shut-down occurs which isolates the inverter from both sides

(input and output). Also, in the case of ground fault currents, when the PV array is disconnected from the input side of the inverter, a shorting contact is used to reduce the field potential to zero volts. This feature, however, is not normally implemented in power conversion units of over 300 kilowatts because it is impractical to design the input contacts to these high voltage and current levels.

The automatic start-up and shut-down features of power processing units allow the inverter to stay in an idle state and consume a minimum amount of power until the array voltages and currents are sufficiently high for the inverter to turn on and begin processing the DC voltage into an AC voltage. The signals that are normally monitored in order to do this are PV array voltage, PV array current, and as additional features, PV array power, and energy are also monitored.

c. Computer Control

Many of today's systems allow easy interface with computer systems. This enables the end user to not only monitor and display certain system parameters, but in some instances, may give remote control of the system operation to the operator. One specific example of this is the emergency shut-down control that may be remotely activated from a terminal in another building. Also, for emergency shut-down capability, sometimes several switches are wired in an "or" fashion to allow the shut-down of the power processing unit from remote locations within the building itself.

9. Instrumentation Systems--General

Many PV and PV-T systems today are installed in conjunction with data systems. Several different systems are available. This section will identify general considerations necessary for choosing an instrumentation system.

a. Input Data

Since the majority of instrumentation systems deal with the collection of data from the PV array inverter and other components in the system, one of the most important considerations for selecting an instrumentation system concerns the input channels. To specify them

correctly, one must know the total number of channels to be used and the pecularities of the data which will be present on each channel. Many times, the data input to the instrumentation system is in the form of an analog voltage. In specifying analog voltage input channels, one must take into account both the accuracy and the resolution of the device used for obtaining these readings. For example, some analog outputs from the inverters are zero to 10 volts DC for a full scale reading. What this may mean for a DC current measurement on the array side of the inverter is that zero volts may represent 100 amperes, and 10 volts may represent 300 amperes. Different scaling is used and must be specified for, or by, the inverter manufacturer. Another type of data channel might be a temperature measurement for an RTD or thermister employed to obtain the temperature of various components in the system. These are usually low level signals in the range of zero to one volt. The accuracy and resolution of the measuring device (normally a DC volt meter) must be known in order to obtain an overall system measurement accuracy figure.

b. Output Data

Any instrumentation system acquiring data from the PV-T system must provide some means of outputting this data to the end user. This can be done on mag tape, disk, or in the form of printed material on electrostatic, thermal, or impact printers. The number of output devices and the types of output formatting required must be considered to specify these portions of the instrumentation system.

c. System Control

In a number of systems it may be advantageous to have control features built into the instrumentation system. This is often implemented in the form of analog output voltages or contact closures that will, in effect, reconfigure the electrical portions of the PV-T system from computer control. This may be done automatically in the software, or as a keyboard entry by the operator.

d. Transducers

There are a variety of measurements which normally need to be made in the instrumentation system. These measurements are associated

with the input data channels, and for analog signals the source of these measurements is often voltage and current transducers. Additionally, output voltages and currents from pyranometers, frequency transducers, and miscellaneous other signals may be required. When specifying the transducers that actually measure the voltage, current, temperature, and weather conditions etc., the full scale output voltage and source impedance must be known. Furthermore, the absolute accuracy of these transducers needs to be specified. In some cases, special signal conditioning and scaling of the transducer outputs may be required to ensure compatibility between the signal source and the data acquisition input cards or channels.

e. Display/Plotting

More often than not, after the data has been acquired by the instrumentation system it needs to be analyzed and further reduced. This creates a requirement for plots, graphs, permanent records, and reports also to be supplied by the instrumentation system. There are several general purpose RS 232 printers and plotters available for most instrumentation systems. In addition, specific systems such as the Hewlett Packard HPIB bus may be used. The equipment compatible with this bus architecture may be used to provide these permanent records.

f. Diagnostic Capability

In addition to using the instrumentation system for various data points in the system, it is also a useful tool to help isolate problem areas or component failures. Depending on how the software is implemented, many facts can be obtained from the instrumentation system to help troubleshoot and repair elements of the system.

g. Software

A major issue in the design and implementation of the instrumentation system is the software. This is critical due to the resources required to develop the software, and is also important from the operator's standpoint. The interactive capability of the operator to use the automated control portion of the instrumentation system cannot be overstressed. Occasionally, canned software packages may be purchased

from the manufacturer of the instrumentation system, however, more often than not, the end user will modify these programs or add to this basic software package. Therefore, when the end user of the system develops new software, it is important to remember that additions should be flexible and modular for easy integration into the canned software packages. The documentation of the new software also needs to be specified.

B. DESIGN CRITERIA

1. Inverters

The section on identification of technical issues described several parameters which must be known or calculated in order to specify the correct inverter for any PV-T system. Among these parameters are the basic size, signal quality, input protection circuitry, conversion efficiency, shut-down features, environmental operating ranges, tare power, output signal power factor, and the use of single or multiple inverters. Obviously, one cannot choose the correct inverter for a system design without knowing its input and output characteristics. This entails sizing the array and calculating its upper and lower voltage and current limits. In order to select an inverter, assuming that the selection process is being done for a single inverter design, the primary considerations in the trade study will show that the size of the inverter is directly related to its cost. This assumes that all of the miscellaneous parameters which need to be measured by the data acquisition system (if implemented) are available from the manufacturers. Other considerations such as size and weight may drive the final inverter selection, but in most cases, the cost and inverter size will be the main trade-off parameters. Figure III-4 indicates the relative costs of inverters as a function of their size. For all-practical purposes, the size of the inverter is given in terms of its AC output power rating (i.e. 10KW, 20 KW, etc.).

Certain aspects of the inverter design will increase the cost. They include the harmonic distortion specification, the number of modes of operation for which the inverter is designed, and the conversion efficiency. Also included in this cost is the minimization of tare power and the accuracy of the peak power tracker. Most systems require an inverter with a peak power tracking subsystem. What this really means is that load on the PV array is modulated in order to keep the array output power at its maximum operating point. This assumes that the load which the inverter is driving (usually the utility grid), is always demanding more power than the array can supply. Even if this is not the case, the peak power tracking network will move off the peak power point of the array to supply only the power required by the load.

For large PV systems, multiple inverters may be the optimum choice. If a tradeoff study must be done to select the optimum group of multiple inverters, price and reliability (due to added complexity) are primary considerations.

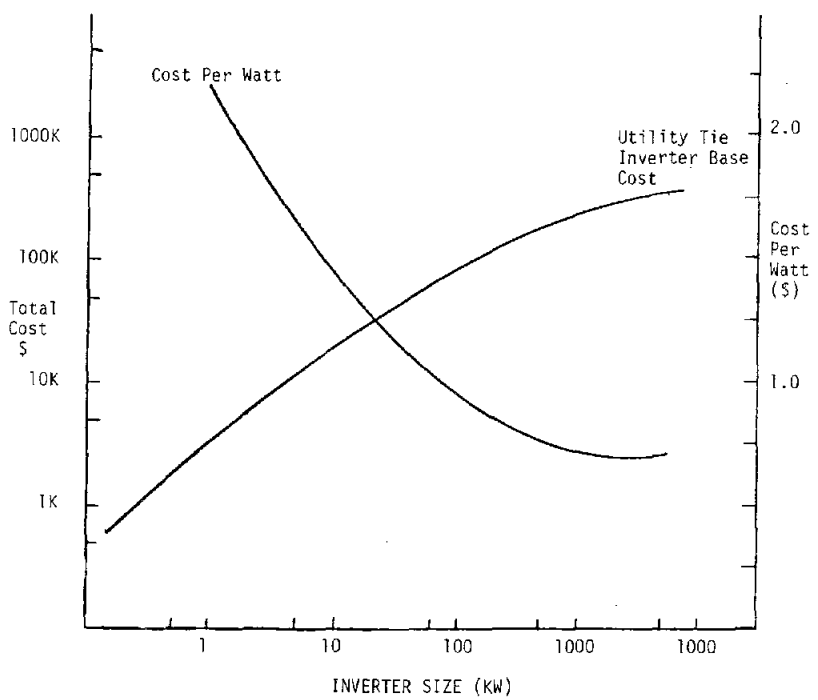

BDM/A-82-458-TR-R1

Figure III-4. Inverter Cost Versus Size Based on DECC Pricing Information

Reliability figures are very hard to obtain from the inverter manufacturers. Very few installations have been in operation long enough to obtain typical mean time between failure (MTBF) and mean time to repairs (MTTR) figures. Therefore, some general engineering guidelines must be used. For most electronic systems MTBF and MTTR numbers are inversely proportional to the number of components in a system. In fact, they are not only inversely proportional, but the function is not linear. That is, as the number of components in a system or subsystem increases, the frequency of repairs and the average time to complete such repairs is usually a "x^2" type of function. This means that for every additional component added, the reliability is decreased by $\frac{1}{X^2}$ where X^2 is the number of components in the system. When making a tradeoff study in a system using multiple inverters, the graph shown in figure III-5 will indicate that the minimum number of inverters should be selected; this is also a function of cost.

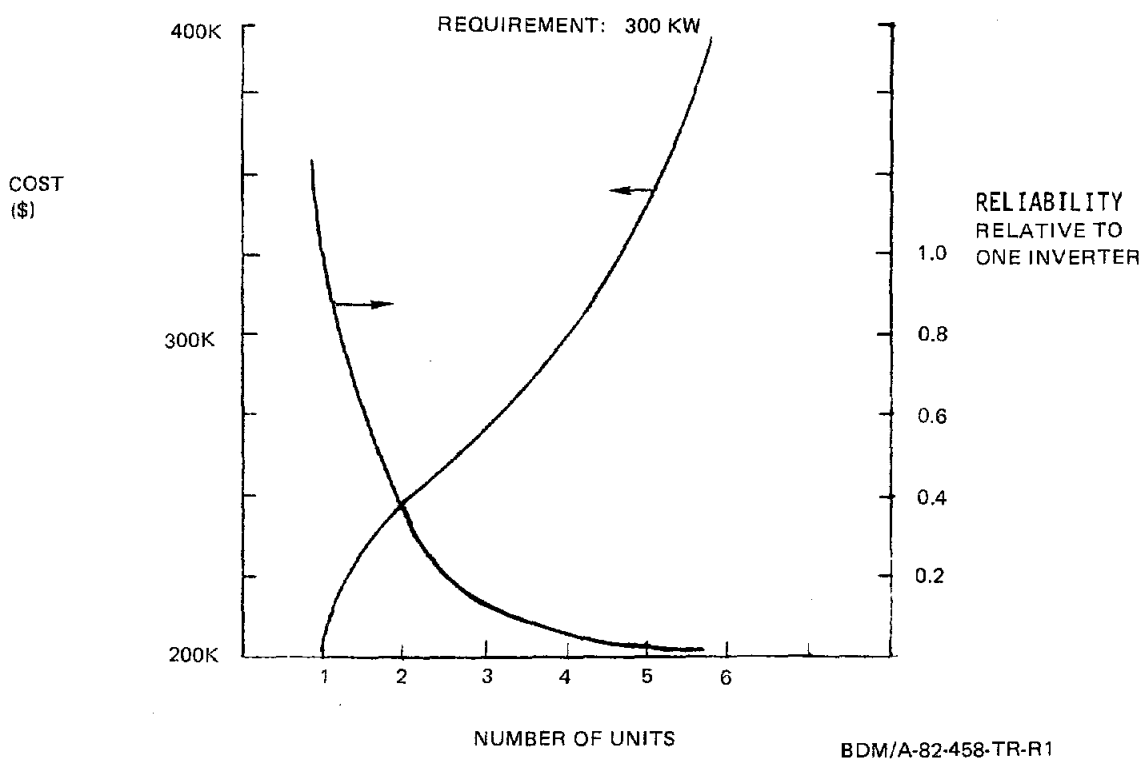

Figure III-5. Multiple Inverter Cost and Reliability Comparison

2. Power Conditioning

The power conditioning consists of all the AC wiring and utility interface components. This includes fuses, safety disconnect switches, and in some cases circuit breakers. Additionally, the wire size used and the method of routing from the inverter to the utility grid connection is of major concern. The use of cable trays or conduit for this cabling is often decided by the route the wires must take to get from the inverter to the utility tie. If an indoor wiring scheme is used, both cable trays and conduit may be specified; however, for exterior use only conduit is acceptable. Since most of the wiring sizes for the AC as well as the DC wiring in the system will be specified to obtain a certain percentage loss in power over that length of wire, this wire selection will be dealt with in the DC wiring section of the design guidelines. Therefore, driving factors for the other components on the AC side of the circuit indicate safety and reliability versus cost. Figure III-6 shows a rough approximation of the relative costs versus the design reliability.

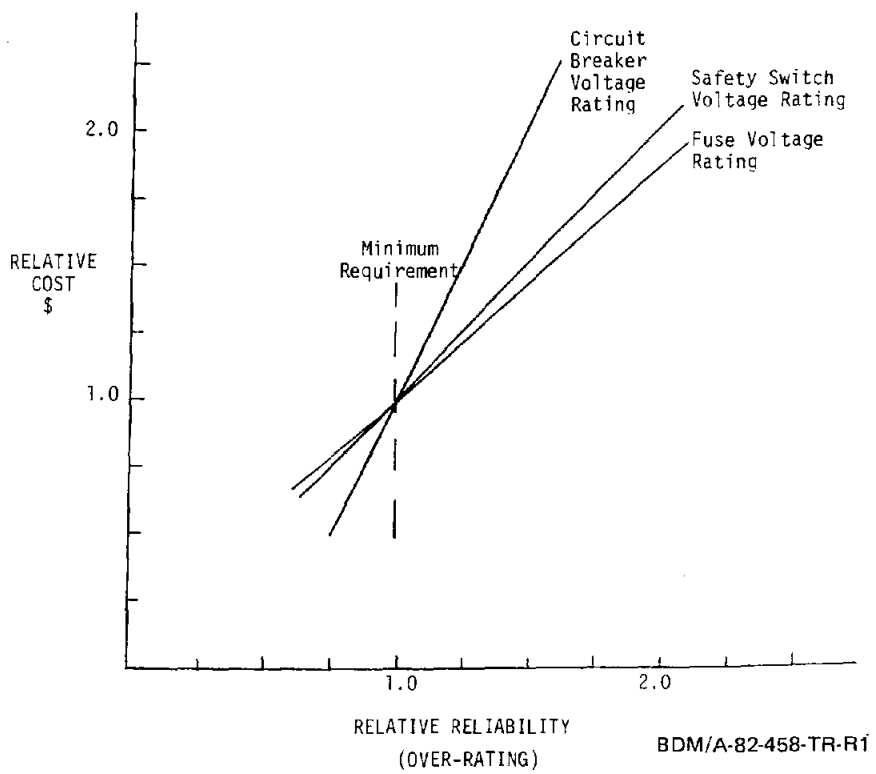

(BASED ON SQUARE-D COMPONENTS PRICING, ref. III-3)

Figure III-6. Power Conditioning Equipment Cost

Since the reliability is proportional to the design conservativeness, specifying voltages and currents in excess of what the system will actually use adds to its reliability. According to the National Electrical Code all wiring sizes should be rated 25 percent above maximum calculated current and voltage ratings measurable in the system. Going beyond this point to a more conservative design (50 percent over rating) makes for a more reliable system; however, this conservatism also increases the cost. In terms of trading off component specifications versus cost, reliability is synonymous with safety. This is true, since wires, fuses, and other components in the power conditioning section of the wiring will not only prove to be less reliable, but also less safe in extreme over-temperature conditions.

3. Miscellaneous Electrical Components

There are several electrical components in the miscellaneous category. They include junction boxes, terminal strips, test jacks, fuses and connectors. Although all of these components are specified in the National Electrical Code, they may be difficult or impossible to find due to the terminology used in that handbook. A general rule of thumb for specifying the voltage and current ratings on these items is to allow a design safety factor of at least 25 percent. That is, if a voltage or current in some portion of the system is known to be 10.0, multiplying this number by 1.25, which gives us 12.50, is an approximation for the upper limit of a reliable component design. For example, if the voltage potential going through a switch will be 100 volts maximum, the switch specified should be capable of carrying 125 volts; the same type of analogy is used for current ratings on contactors, switches, fuses, etc. Using components approved by Underwriters Laboratory generally ensures a conservative number for its voltage and current ratings. This is a reliable figure, however, and may be used as a minimum design guideline. Overspecifying components adds cost to the overall design, but in most cases, also increases its reliability and safety factor. A trade study for the miscellaneous components mentioned above, will therefore plot costs versus reliability. Again, reliability is synonymous with design

safety in terms of overstressing components in high voltage systems. The relative cost versus reliability/safety for some of these components is shown in figures III-7 and III-8.

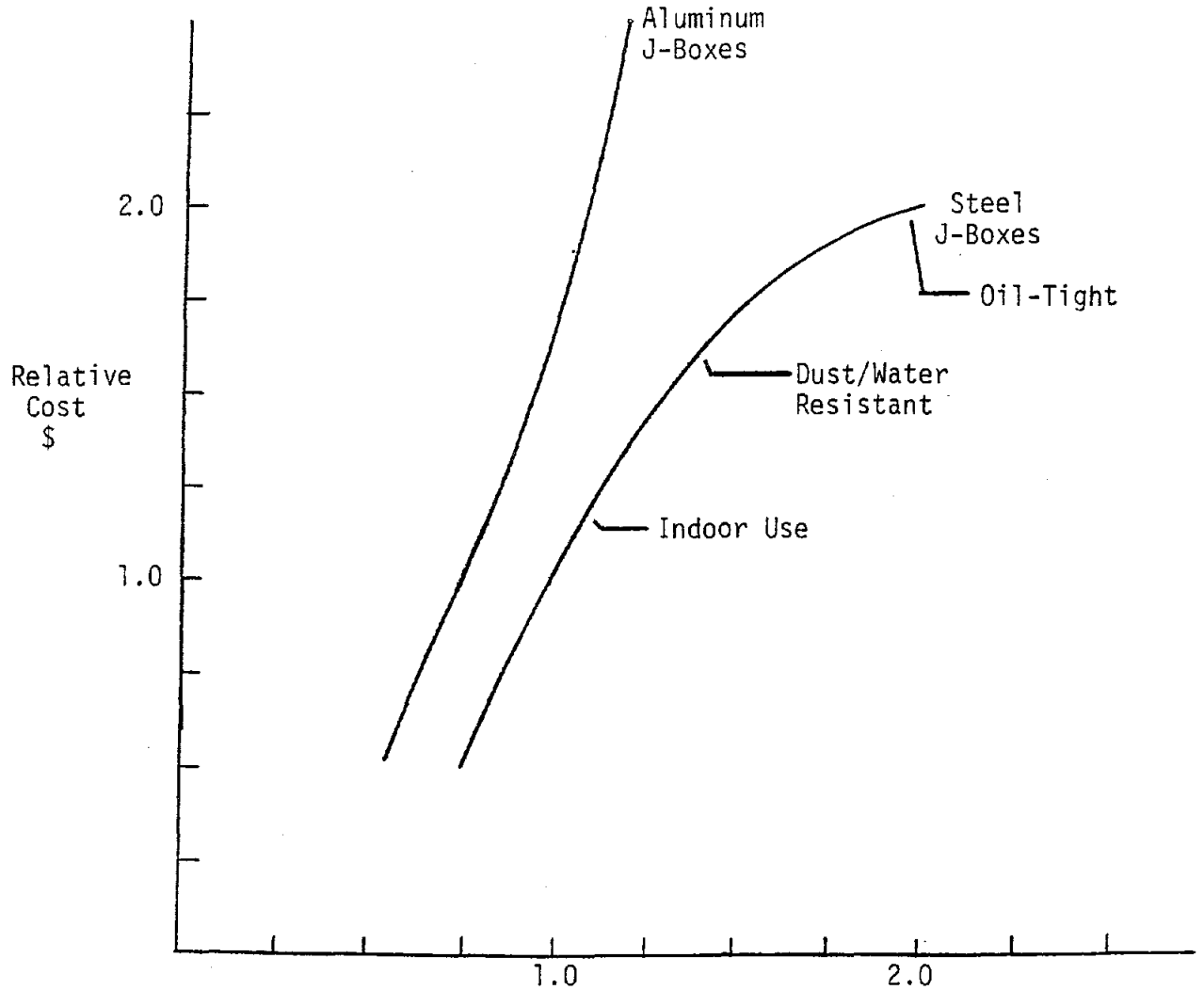

(BASED ON HOFFMAN ENCLOSURE PRICING, ref. III-3)

BDM/A-82-458-TR-R1

Figure III-7. Relative Enclosure Construction Quality Versus Cost

4. Ground Fault Protection

In most PV systems, ground fault sensing and subsequently, ground fault protection, occurs within the inverter electronics. This is

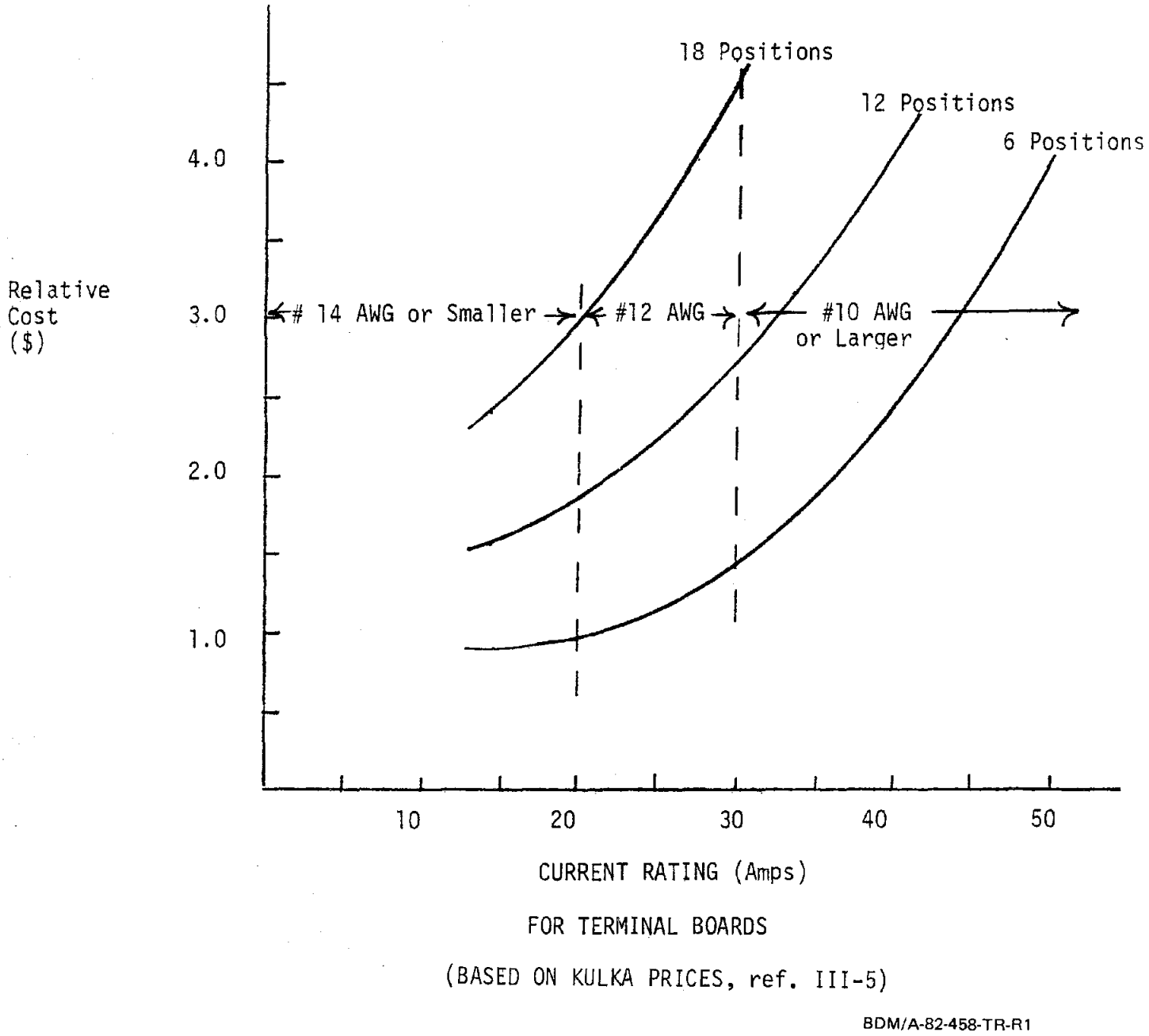

BDM/A-82-458-TR-R1

Figure III-8. Relative Cost of Terminal Versus Current Rating

not always the case, however, and in some special circumstances, one may have to specify the ground fault sensor to be implemented in a PV-T system design. The major factors of a ground fault sensing system are sensitivity, accuracy, and noise immunity. In looking at different ground fault detectors, one will have to trade off these design parameters versus cost. Ultimately, all of the design parameters affect detector reliability. Ground fault detectors for the DC side of the electrical system are generally implemented with low ohmic value resistors. Off-the-shelf units are scarce and this usually requires that the electrical designs of the PV-T system specify how the ground fault scheme is to be implemented. The reliability and noise immunity factors are, therefore, usually associated with the signal conditioning (amplification and filtering) of the voltage across this resistor. For AC applications there are many off-the-shelf units available. They are usually (but not always) designed to both sense a current in the grounding conductor, and to interrupt the source potential. This is accomplished by open-circuiting one or both sides of the AC line. Sensitivities of off-the-shelf units range from a few milliamps to hundreds of milliamps, and should be sized with an overall understanding of the ground fault conditions that may occur.

As mentioned above, the design features include sensitivity of the circuitry, noise immunity, and overall accuracy of the ground fault sensing circuit. The noise immunity may play a very important part in the ground fault sensor design, especially if it is located near the inverter or other electronic components which have a tendency to radiate electrical noise.

5. Safety Switches

The safety switches in a PV-T system design must be specified for voltage, current, and contact type. The voltage and current ratings are the same as those used for the AC components of the system. Please refer to section 2, Power Conditioning, for an explanation of the parameters of the miscellaneous components which include safety switches. Normally, safety switches are designated as the high power switching

components in a system. They are used at the input and output of the inverter, and may also be used in the array field. The idea of the safety switch is to allow the maintenance personnel or system operator to disconnect and isolate one component of the system from the rest of the system. The reliability of such components is critical. The graph in figure III-9 illustrates the reliability traded off as a function of the conservativeness of the design of the parameters for the switch. Again, these parameters are voltage, current, and contact type.

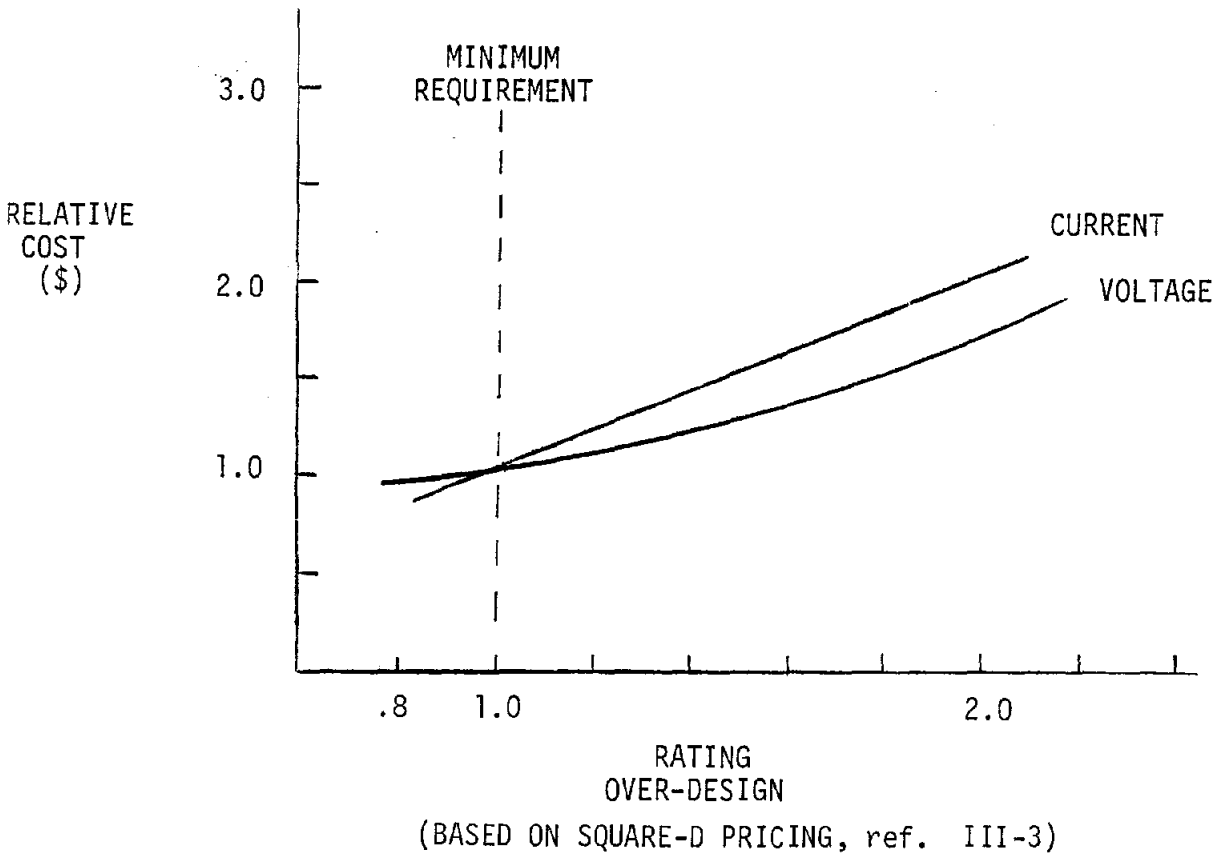

BDM/A-82-458-TR-R1

Figure III-9. Safety Switch Reliability Versus Cost

Reliability is as important as safety when considering switches and other miscellaneous electrical components of a PV-T system. The conservativeness of the design is the voltage rating and current for which the

contact or safety disconnect switch is specified. As mentioned previously, 25 percent over-design criteria may be used as a rule of thumb, although the reliability and safety of these switches is proportional to the tendency to over-design these components into the system.

6. Utility Interface

Much of the discussion in section 2, Power Conditioning, also applies to the utility interface considerations. Components not discussed in section 2 include the power and energy monitoring devices. They consist of kilowatt and kilowatt-hour meters that may be placed in various positions of the AC electrical design.

Assuming that the power meters or energy meters are specified to fit electrically into the design, the main tradeoff in choosing these instruments is a play against cost versus accuracy. Often, it is not important that the accuracy of the energy or power meter be known to within 5 or 10 percent. Naturally, this results in an inexpensive meter specification for the PV-T system design. Nonetheless, in some cases a less than 5 percent metering accuracy is desirable, and this will drive the cost up.

7. Wiring Sizes

Several factors must be known in order to specify the wiring in a system. This section deals with the DC wiring only. The following graphs assume that the minimum current rating of the wire is specified per the National Electrical Code. The first graph (figure III-10) relates the wire size versus cost for copper and aluminum wire. The characteristics of copper and aluminum wire should be understood before they are specified in a system design. The characteristics which should be known are conductivity, temperature coefficient, resistance per thousand feet, and compatibility with fuse box connectors and terminal strips to which the wires will be attached.

The plot in figure III-11 shows various types of cables and relates their cost impact as a function of their insulation. The type of insulation used will be specified depending on environmental parameters, including temperature rating and corrosive atmospheres (salt spray).

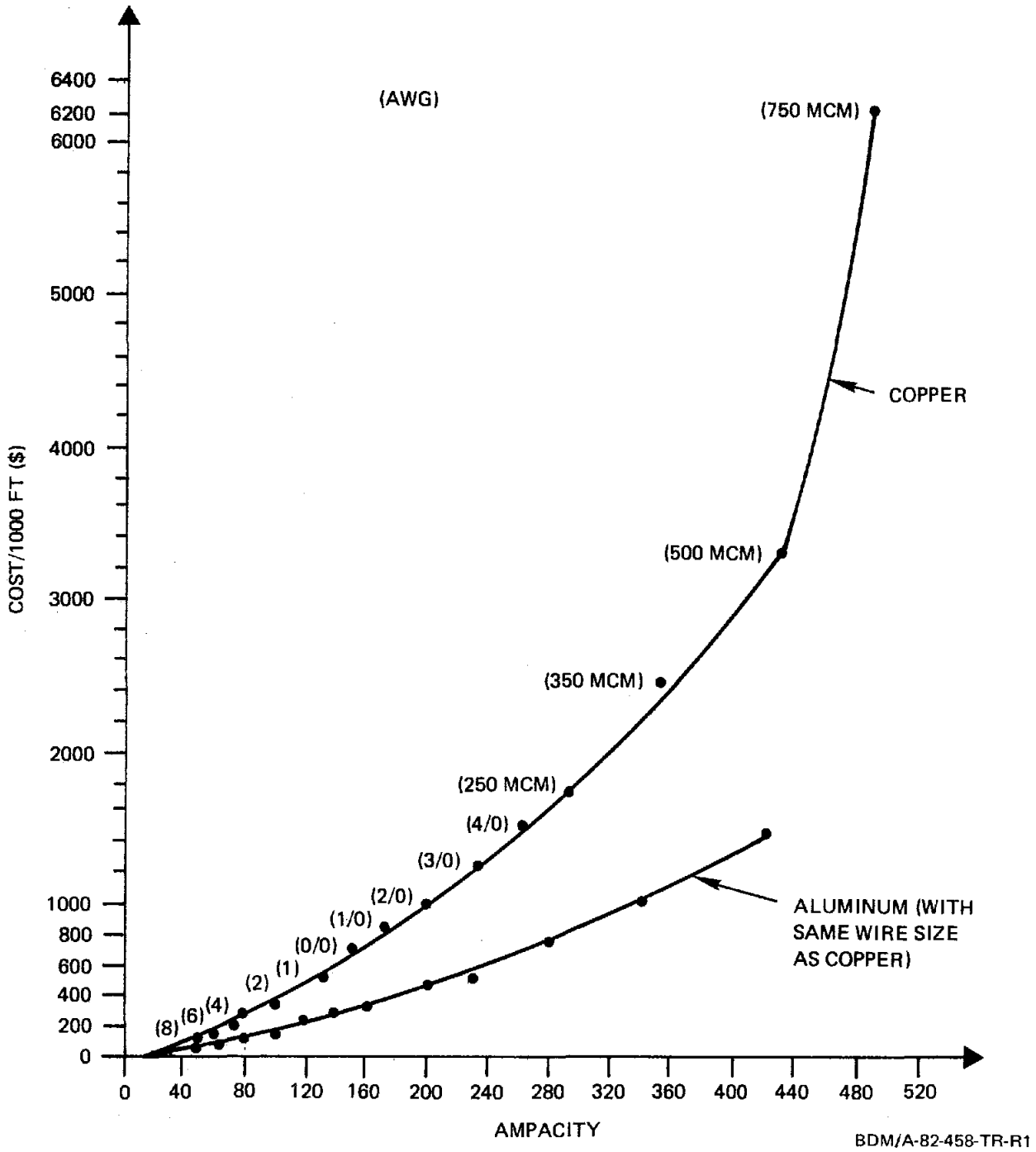

Figure III-10. Wire Size Versus Cost of Copper and Aluminum Wire

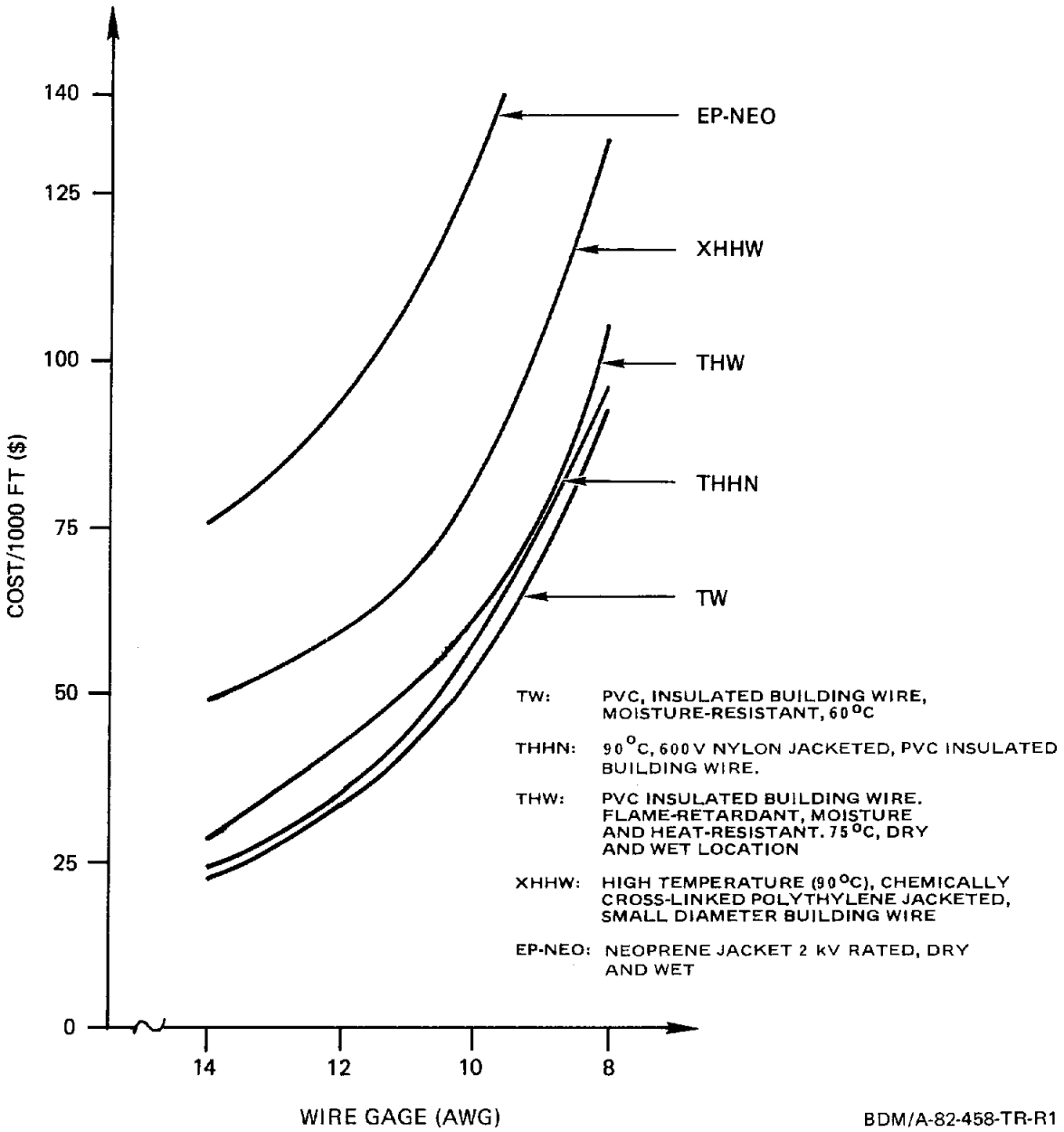

Figure III-11. Cable Size Versus Cost for Various Insulation Types

Some insulators can be used in external applications, while others are considerably more cost effective for indoor use.

Figure III-12 depicts the resistance of a typical copper conductor as a function of temperature for conductivities in the range of 90 to 100 percent of oxygen-free copper. Resistance of copper can be calculated using the equation below the plot.

8. Safety Grounding

The grounding system in all PV or PV-T systems consist of wires which are used to ground the metallic framework of the PV modules and other metallic chassis. These other chassis include J-Boxes, maintenance enclosure boxes, and the rack which comprises the inverter chassis. All design considerations pertaining to grounding the frames and chassis are particular to the wire sizes used to ground these units. Refer to section 7 on wire sizes, but keep in mind that the trade-off summaries for these wires are the same. In the National Electrical Code Handbook, grounding wire size is specified to be that size equal to the maximum current conductor in the system.

9. Array Wiring Configuration

Refer to section 7 for the different parameters which must be specified. For wiring size, insulation, and type of conductors, one other trade-off that must be accounted for in the wiring that does not have to do with the wiring size, is the terminal voltages and current produced by the array. There are practical upper limits for these voltages and currents. However, most systems are configured to meet the input specifications of a given inverter. Once this is known, trade-offs can be made to optimize the array wiring configuration. For example, if the nominal output voltage of the array is specified to be 200 to 250 volts in order to match the inverter input specifications, then several configurations of the wiring may be used. The individual module voltages and currents are needed to optimize this array configuration. Keeping in mind that series wired modules add voltage, and parallel wired modules add currents, several configurations of parallel and series combination wiring may be tried within a voltage operating range. The optimum wiring

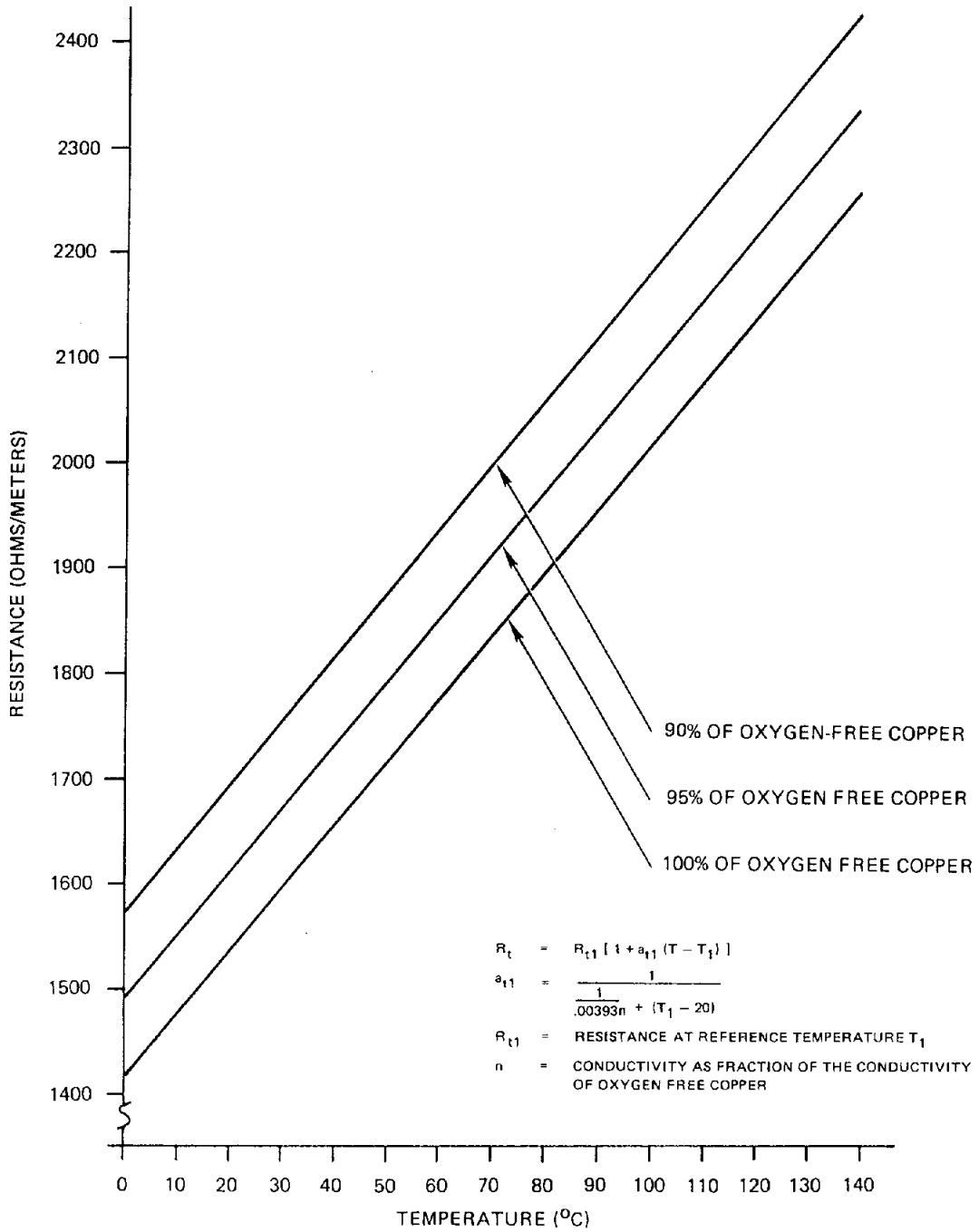

BDM/A-82-458-TR-R1

Figure III-12. Resistance of a Typical Copper Wire Versus Temperature

configuration must therefore be determined as a function of cost, due to the fact that the amount of wire used effects the cost of the configuration. This is partly a function of the actual cost of the wire but is also due to the labor cost of installation. In some cases simple wiring configurations may be specified which reduce or nearly eliminate connections except for those required at each module interface. This will have a great impact on the overall cost of the wiring. In figure III-13 the relative cost versus number of interconnects for an array wiring harness/configuration is presented for various sizes of conductors.

10. Diodes

The two types of diodes discussed in the issues section are the blocking diodes and the bypass diodes. Each performs separate functional operations within the array wiring, however, they both have the same internal characteristics. Specifying these two diodes will ultimately effect the reliability and the energy output of the PV array. Since the diode design in and of itself is not a safety feature, the number of diodes will have great impact on the cost and the power loss in the DC side of the system. Figures III-14, 15, and 16 show the relationship between the cost, power loss, and number of diodes.

Cost is proportional to the number of diodes installed in a system and the diode rating. The power loss, however, is a function only of the blocking diodes, since the bypass diodes are normally in the reverse bias region. Careful consideration must be taken to ensure the correct number of blocking diodes in any given wiring scheme.

11. Control Strategy

As mentioned in section A, there are several types of controls. Some are manual, some computer assisted, and some totally under computer control. The types and number of controls that are implemented in a system have great bearing on system safety and personnel safety. In general, the more control features implemented, the safer and more costly the system becomes.

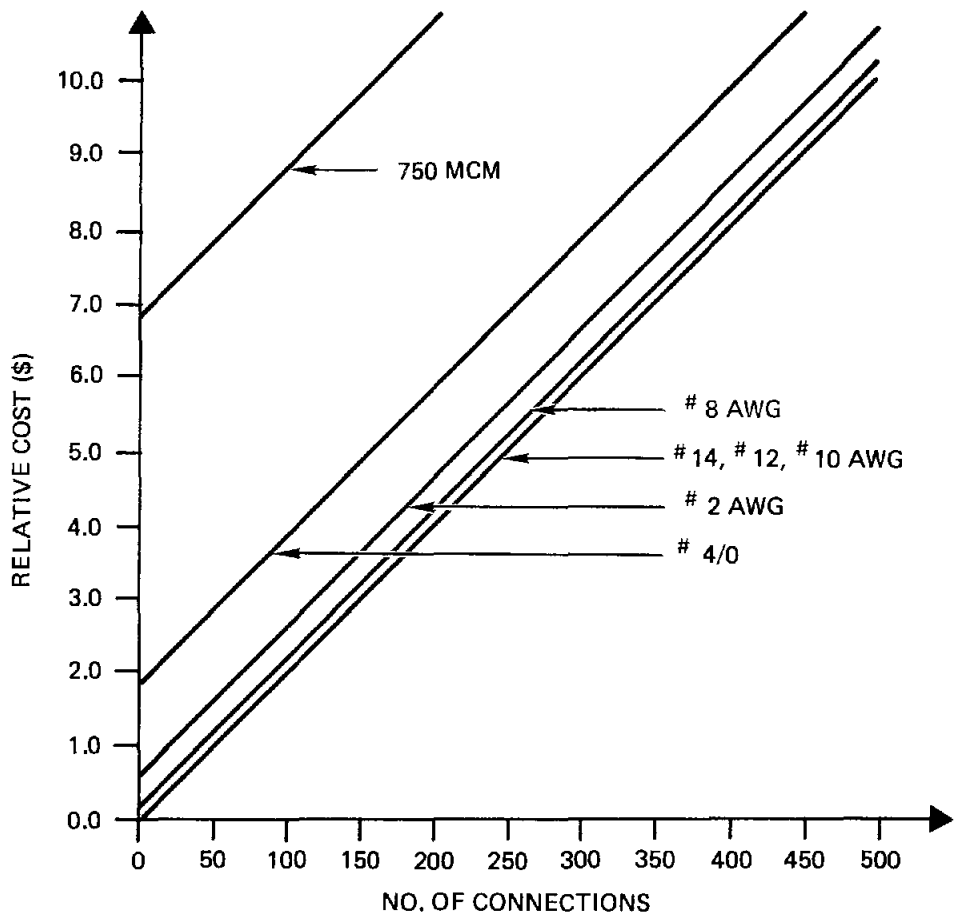

BDM/A-82-458-TR-R1

Figure III-13. Relative Cost Versus Number of Wiring Connections for Various Wire Sizes

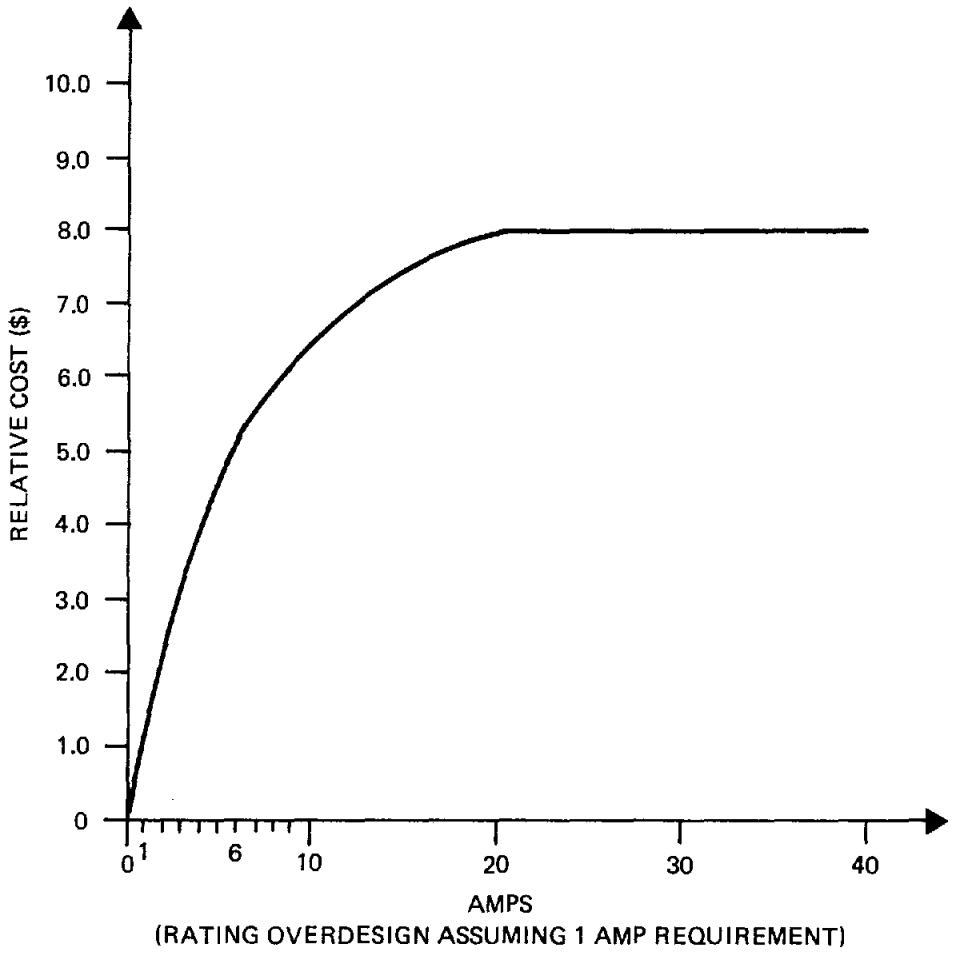

BDM/A-82-458-TR-R1

Figure III-14. Relative Cost of Diodes Versus Rating Overdesign

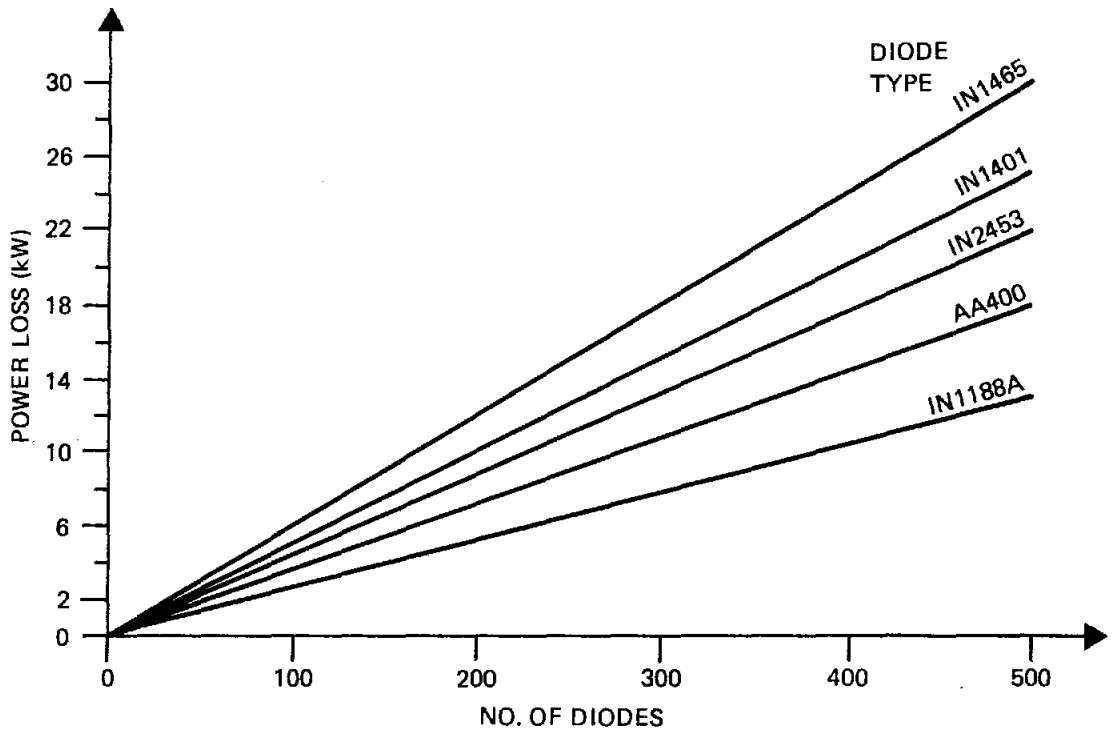

BDM/A-82-458-TR-R1

Figure III-15. Power Loss Versus Number and Type of Blocking Diodes in a System

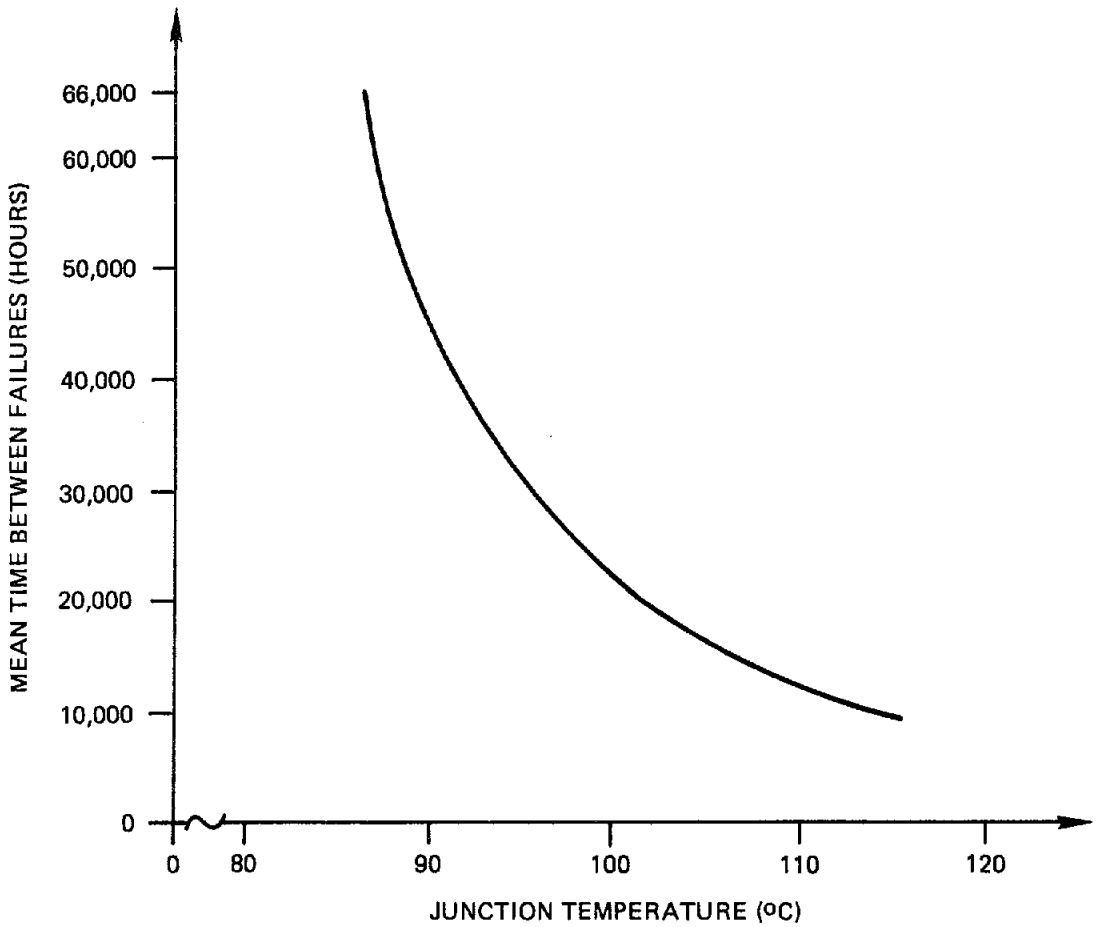

BDM/A-82-458-TR-R1

Figure III-16. Bypass Diode Reliability Versus Junction Temperature (Semiconductor Device No. 353)

12. Operating Modes

The operating modes discussed in section A of this report may not always be applicable to PV-T systems. In general, most systems will operate tied to the utility grid. This is known as the synchronous mode of operation. However, if stand-alone or combinations of stand-alone and synchronous modes are desired in the system design, the cost is greatly influenced. This is proportional to the number of modes in which the inverter is designed to operate. Shown in figure III-17 is a plot with the cost versus the number of modes of operation.

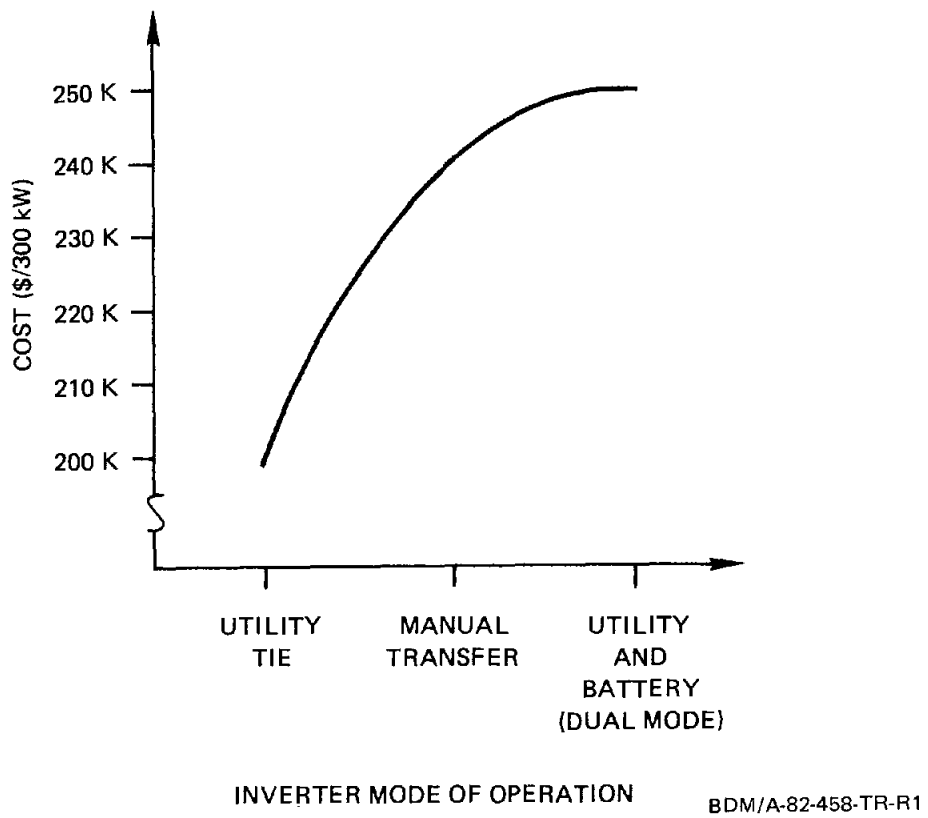

Figure III-17. Inverter Cost Versus Modes of Operation

13. Data Acquisition Systems

Data acquisition systems are commonly used in conjunction with PV or PV-T systems. Not only do they allow input data to be obtained by the operator, but they may also allow some remote control capability over

the system. The cost of such systems is directly proportional to the complexity and the amount of data required by the user. For example, a system requiring 100 data points is much more useful to the operator than one requiring 10 data points. However, this makes the data acquisition system more complicated and drives up the cost. This is a simple relationship between cost and flexibility. The graph in figure III-18 relates the data acquisition system cost to the system capability. Control features of the data acquisition system are minimal in most cases, and do not greatly effect this cost.

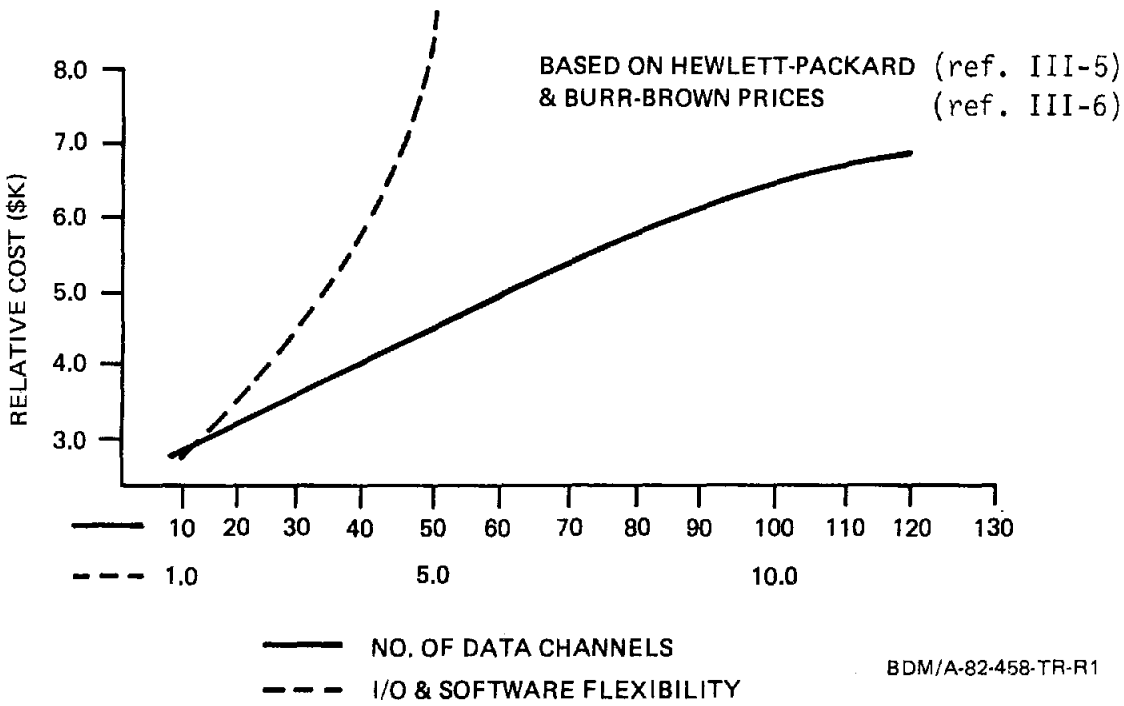

Figure III-18. Data Acquisition System Capability Versus Cost

Data acquisition systems are common in PV and PV-T systems today. A basic data acquisition cost exists which includes power supply and the processing components of the unit. Occasionally, this also includes the cost of a mass storage device or printer/plotter.

Additional channels add very little to this cost; therefore, to obtain the maximum amount of data, dozens of channels may be added once the main system is installed. The cost of additional channels is minimal, and should be taken into account when designing the system. One hidden cost of additional channels, however, is the development time and implementation of the software to manipulate the incoming data.

C. DESIGN GUIDANCE

All designs begin with an evaluation of the application requirements. The highest efficiency system is of little use if it does not satisfy the needs of the user. Thus, the prime concern is the load configuration and requirements. Next, constraints on the array sizing must be considered to determine if and how an array can be constructed to serve the load. Finally, other criteria or constraints are considered (such as safety and maintainability) which are essential to the system operation, but take the form of embellishments to the basic design (such as switches and fuses). The final design is a judicious selection and interconnection of hardware according to design specifications which satisfy all system requirements.

1. System Design Criteria

a. Load Requirements and Sizing Constraints

The basic system design considers the load requirements first, then constructs a system within the sizing constraints to satisfy this load. The four load characteristics which must be considered are:

(1) Mode of operation (stand-alone, utility-interface, UPS)

(2) Type of power (DC, AC-single phase, AC-three phase)

(3) Voltage level

(4) Power level

The load requirements are determined from the application (remote or utility-available; small power, residential, commercial, industrial or CPS). For this PV-T effort, only utility-interactive commercial and industrial applications are considered. Therefore, the first

three load characteristics are known. The PV system must produce 277/480 VAC, 3-Ø, utility-compatible power. The power level, however, may vary from tens to hundreds of kilowatts and may represent the full load demand of the application, part of it, or only the peak loading (load shaving). The power level of the PV system must take into account system sizing constraints. These limitations include allowable cost, available area, shading patterns, and strength of structural surface. These will often determine the type of system (flat plate or concentrator) and the maximum power which the array can supply. They may also determine the size of the inverter.

If the allowable cost and available area permit satisfying most or all of the specified load (full load or peak), the design begins by specifying an inverter with sufficient AC output to satisfy the load demand. Then, the array is sized to satisfy the input requirements of the inverter.

If the array can only satisfy part of the specified load, the design begins by specifying the largest array possible within size and cost constraints, then the inverter is sized to handle the maximum array power. In each case, the voltage level and type of power are dictated by the load (for example, 227/480 VAC, 3Ø).

The array voltage must be compatible with DC input requirements for the inverter. Usually, the input voltage range of off-the-shelf inverters is specified by the manufacturer. This often represents the range over which the inverter will accomplish peak power tracking. If the array peak power voltage is outside this range, the inverter will operate at its limit value, and extract less than peak power. This range can often be shifted up or down in the factory by perhaps 30 percent, but cannot be significantly spread. Thus, the number of modules of a specific voltage connected in series must be carefully determined to ensure this voltage range is not exceeded by temperature extremes expected at the application site.

The inverter must also be sized to handle the maximum power that the array will produce. Some inverters are designed to shut

down or to limit the current when the input power exceeds its nominal rated power by more than 10 to 20 percent. However, it is preferable not to force the inverter into this mode. Since the array output could exceed its nominal rated power by 15 to 25 percent on a clear, cold day, the inverter should be sized to exceed the array rated power by about 10 percent.

These considerations may be mitigated somewhat by the weather conditions in a particular location; for example, a humid climate with low seasonal variations in temperature.

b. Safety

For the electrical portions of an industrial or commercial PV-T system, safety matters can be subdivided into two distinct categories: 1) personnel safety and 2) system safety. For the purposes of this section of the design guidance, personnel safety is defined as the safety factors in the design that present harmful potentials (electric) to the installation, maintenance, and operational personnel. System safety takes into account potential electrical hazards to the equipment used in implementing the design.

1) Personnel Safety

There are many factors related to providing personnel safety. Design features and operational procedures must be specified to minimize the possibility of exposure to harmful and even fatal electrical voltages and currents. The best reference available for design purposes is the National Electrical Safety Code. This is separate from the NEC handbook, although both codes deal with grounding of equipment, etc., to prevent shock hazards to personnel. It is also a good reference for general design use for equipment safety procedures.

a) PV Cell Installation

One of the potential hazards for electrical shock to personnel occurs during the installation of the PV cells themselves. When groups of cells are placed in series, high voltages will be present unless precautions are taken to ensure otherwise. Two methods used to eliminate this voltage potential are: 1) covering the PV source

during installation, and 2) short-circuiting the PV source. The latter should not be used unless recommended by the cell manufacturer. Additionally, the cell strings should be wired to "float" from earth potential, so no current path may be established between either PV electrode and ground. This is illustrated in figure III-19.

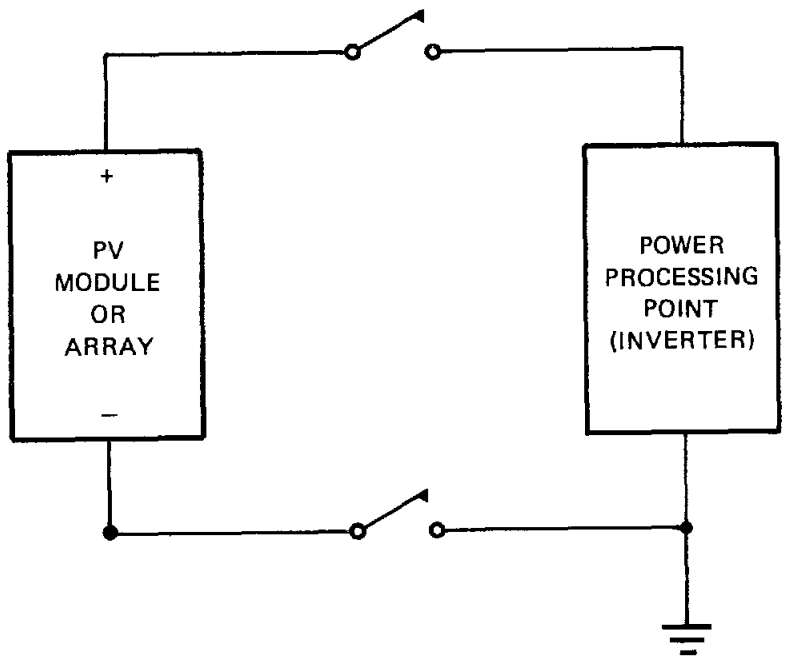

BDM/A-82-458-TR-R1

Figure III-19. PV Array Electrical Isolation

The negative side of the PV array conductor must be isolated from ground during assembly and installation of the cells. This ability to disconnect the array from earth potential is a good practice in system design as it allows cleaning and cell maintenance with no potential shock hazard to personnel.

If the PV array is electrically isolated as shown above, the only electrical shock hazard that exists is between the positive and negative conductors of the array. Normally, these are an appreciable physical distance apart; therefore, a current path is not easily established between these points.

b) Electrical Equipment

Some aspects of the design concern grounding and safety interlock controls of electrical equipment. All chassis housing such equipment must be grounded by code; however, additional safety interlocks may be added by the designer. An interlock is essentially a switch which removes all high voltage from the components in an enclosure when the door to the enclosure is opened. For installation, as well as for maintenance, safety interlocks should be designed into the high voltage switchgear enclosures of the system. The basic concept of an interlock is depicted in figure III-20.

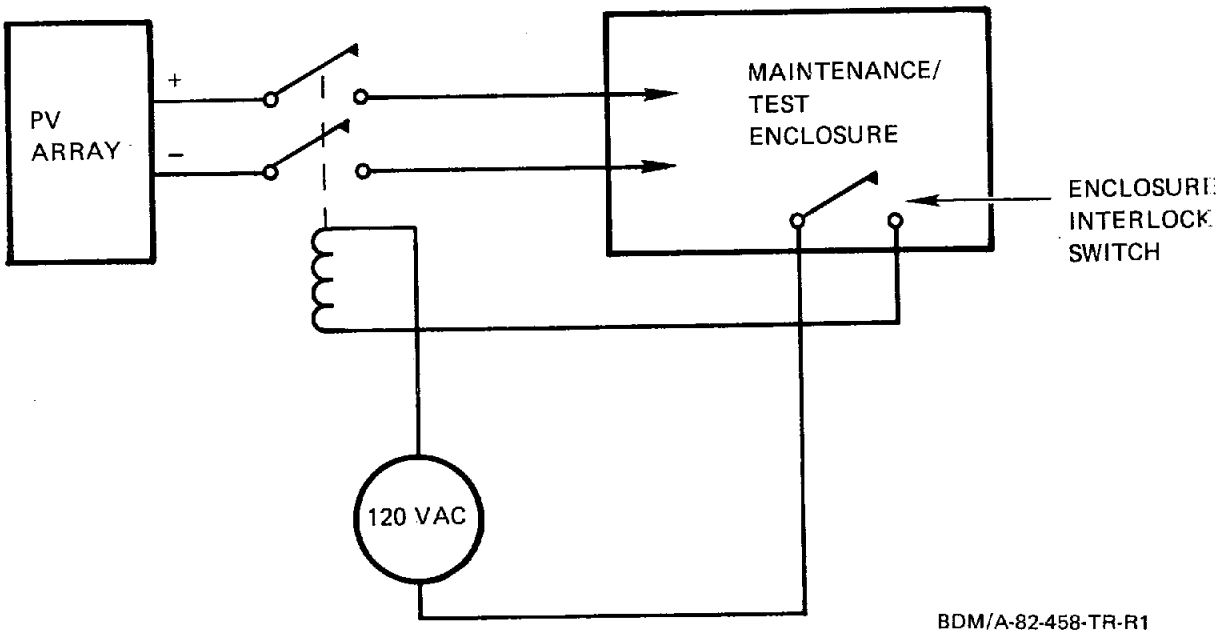

Figure III-20. Safety Interlock Concept

The switch breaks the supply voltage to a DC contactor coil that provides the PV array voltage to the maintenance/test enclosure. As soon as the enclosure door is opened, the source of high voltage in the enclosure is disconnected. This allows component replacement or maintenance with no electrical shock hazard in the enclosure.

c) Warning Labels

Labels should identify any point in the system where high voltage potentials may exist. This is common practice for AC

service disconnect boxes. This practice should be incorporated into the high voltage DC portions of the system as well.

d) Procedures

Inherent in all assembly, installation, operation, and maintenance procedures, there should be warnings for the personnel required to perform these functions. Color-coded wiring and labels that reference the wiring to the design drawings help eliminate any possible confusion as to where in the system a high voltage potential may exist.

2) System Safety

Most system safety design considerations address the fault current capabilities of the power switchgear components, the utility interface components, and the circuit breakers and fuses designed into the system. In most cases, the normal trip currents for the circuit breakers and fuses are rated at 25 percent over the maximum current that will occur at various points in the system. This does not completely satisfy system safety requirements, however, due to a fault condition prior to the clearing time of the circuit breakers and fuses. For this period of time the interrupting capacity of these components must withstand the peak short-circuit current of the system fault source. This must be calculated for each portion of the system in order to avoid melting conductors and switchgear components. For example, if a short-circuit between one of the AC Ø conductors and ground occurs at the output of the inverter, as shown in figure III-21, the switch and circuit breaker must be able to withstand the maximum short-circuit current available from the utility-connected transformer. This interrupting fault current must be calculated, and the circuit breaker rating sized to this number. Since the wiring is a small impedance in this circuit, the transformer short-circuit current may be used to determine the interrupt ampacity at the fault location. Based on the transformer design, this current may easily exceed 10,000 amperes in a 500kW, 480, 3Ø system, therefore, individual transformer ratings should be used.

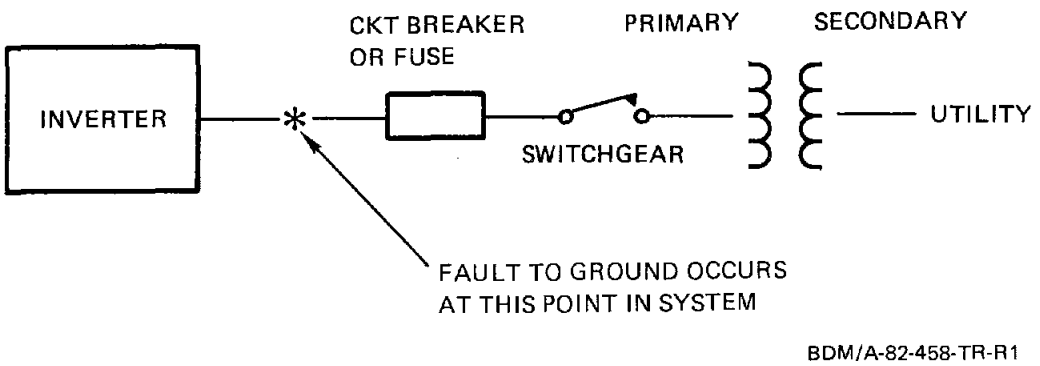

Figure III-21. Short Circuit Failure

The concept of fault-current ratings for the DC power source (PV array) is much simpler, since the array is a relatively "soft" source of power (i.e. not much difference at short-circuit). Typically, the short-circuit current available from the array is about 10 percent above its normal operating current.

c. Maintainability

1) Instrumentation

In most cases, the extent to which instrumentation is used in a PV-T system is limited to the data acquisition portion of the system. The components of the data acquisition system, therefore, must be designed for ease of maintenance, as well as for expandability, if the acquisition of additional data channels is desired. As far as the design is concerned, maintainability of the components is primarily associated with the choice of components used, and the maintainability of the software if a computerized system is implemented.

a) Choice of Components

Normally it is desirable to use "off-the-shelf" equipment whenever possible. This will eliminate the need for user-generated documentation and allows the PV-T system owner field service

support from the manufacturers and vendors of the equipment. Equipment down-time can be minimal if the manufacturer's wiring and environmental recommendations are strictly adhered to. This is especially true of line filtering specifications, and temperature and dust specifications for computerized systems employing magnetic types of data storage (tape, disc. etc.).

b) Software

One aspect of the data acquisition system which requires extensive documentation and maintenance is the software. This usually begins as a well-thought-out piece of code which is expanded, and increases in size and complexity as additional requirements are discovered. Also, due to the overall flexibility of a computerized system, changes tend to be made rapidly, and are easy to overlook when documenting the software.

c) Other Instrumentation

Aside from the data acquisition components, the transducers, amplifiers and wiring can, in a sense, be termed instrumentation. These components rarely fail; however, some calibration adjustments may be incorporated into these items. Manufacturer's recommended calibration cycles should be adhered to.

2) Control

The control portions of a PV-T power system include the fluid flow transducers, heat monitoring and bypass valve operations, inverter control electronics, and utility interface control circuits. In all of these components, switching of various voltages and currents is accomplished either manually or automatically. The automatic mode of control is often tied into the data acquisition equipment if output signals or relays are implemented as part of this computer system. Automatic timers may also be used for time-of-day operated devices; however, this method is not as reliable or as flexible in terms of overall system configuration and operation. The maintainability of the components of the control system require that standard industry proven parts be employed. They should be located for ease of replacement by the

system operation and maintenance personnel. The overall tendency to design in a part with 1.5 to 2.0 times the ratings and life cycle required is a good one, since any failure in the control portion of the system can lead to major repair expenses. A simple example of a control which may be used is the sensing of the AC switchgear by the data acquisition system to detect operational faults. The schematic for such a feedback signal is given in figure III-22.

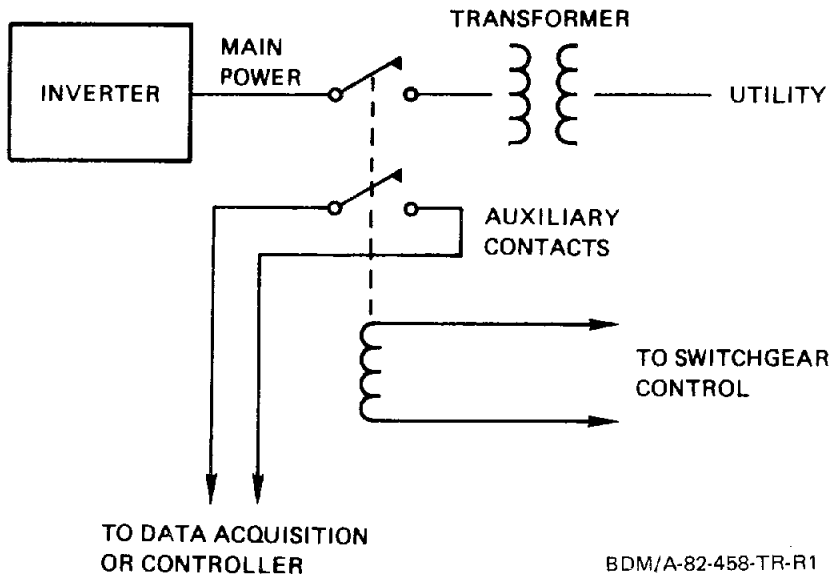

Figure III-22. AC Switchgear Sensing Circuit

In this configuration, if the main power switch does not operate when required, the controller or the DAS will supply an error condition to the operator for maintenance action to be taken.

3) Reliability

The reliability of the components used in a PV-T power system may, for the most part, be obtained from their respective manufacturers. These figures usually take the form of mean time between failure (MTBF) or mean time to fail (MTTF). Additionally, the design and implementation of these components in the system affect the MTBF and MTTF values, since these numbers are usually presented in thousands of hours of use, at rated conditions which may not be the same conditions for the parts when used in a PV-T system. The following design example was

performed to determine the MTBF of a silicon blocking diode for use in a PV system to ensure an MTBF of 12,000 hours minimum. Note that the critical parameter is the junction temperature for the diode selection and circuit implementation. The thermal circuit for this example is shown in figure III-23.

The acceleration factor (unitless) is given by:

$$AF = EXP\left[\frac{E_a}{K}\left(\frac{1}{T_1} - \frac{1}{T_2}\right)\right] \qquad \text{(Eq. III-3)}$$

with E_a = activation energy (eV)
range is ~.7 to 1.3 eV
(1.0 eV used in place of more accurate data)

$K = 8.6 \times 10^{-5}$ eV/^{o}K (Boltzmann's Constant)
T_1 = Initial temperature = 75°C
T_2 = Temperature of interest

The failure rate in percent failure per 1000 hours is given by:

$$FR = FR_{T_1} \times AF \qquad \text{(Eq. III-4)}$$

with FR_{T_1} = 0.068%/Khr (ref III-8) and the MTTF in hours given by:

$$MTTF = \frac{10^5}{FR} \qquad \text{(III-5)}$$

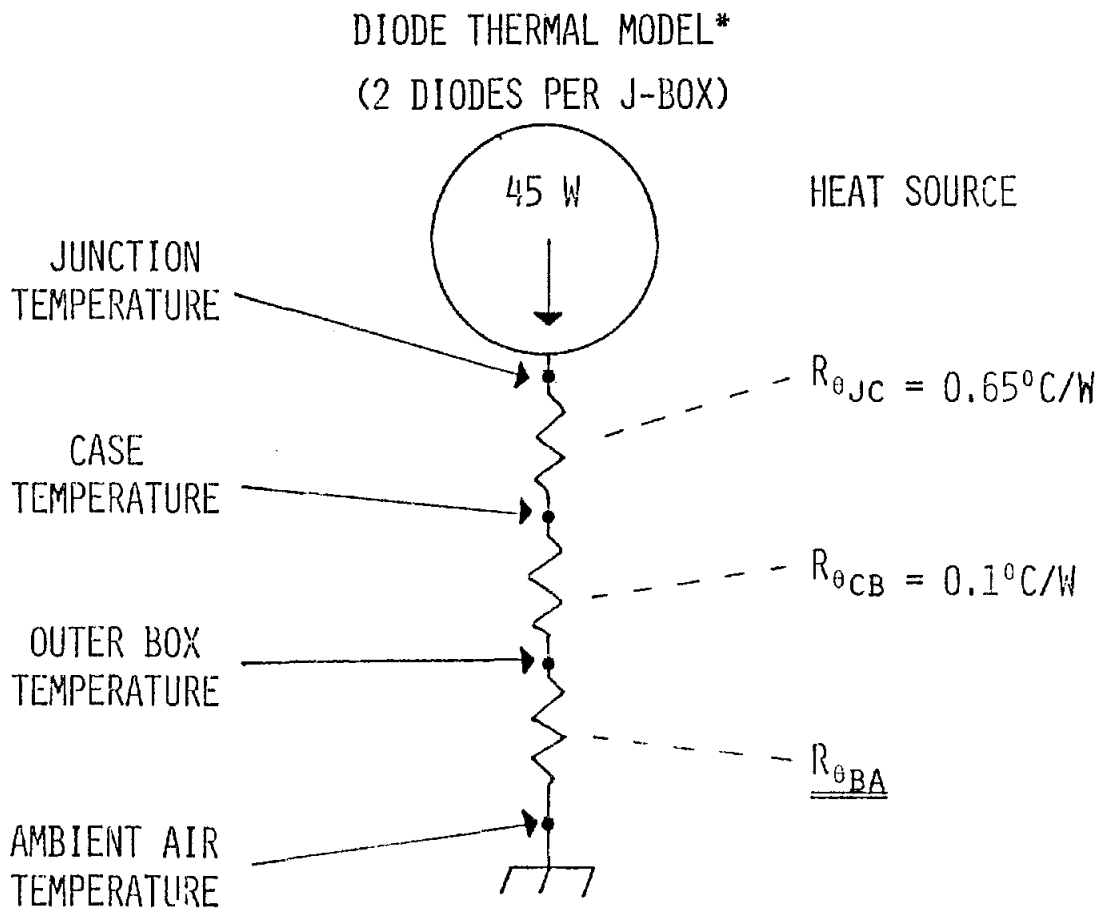

* Reference III-8

BDM/A-82-458-TR-R1

Figure III-23. Thermal Circuit for Example MTTF Calculation at Elevated Temperature

From figure III-24 or table III-5, the junction temperature must be less than 135°C if the MTTF is to be greater than 12,000 hours.

The difference between the junction temperature and ambient is given by:

$$\Delta T = RQ \qquad \text{(Eq. III-6)}$$

where Q is the power generated in the diode and R is the thermal resistance between the diode and ambient. Assuming an ambient temperature of 50°C, and a junction temperature of 135°C, the required resistance $R_{\theta BA}$ can be determined from:

$$\Delta T = 85^{o}C = 45 \left[0.65^{o}C/W + 0.1^{o}C/W + R_{\theta BA} \right] \qquad \text{(Eq. III-7)}$$

Thus, $R_{\theta BA} \leq 1.14^{o}C/W$ for the junction temperature to be less than 135°C.

The resistance is calculated as shown in figure III-25, using emissivity values in table III-6. Since the calculated resistance is less than the required resistance, the diode will survive for over 12,000 hours.

4) Replacement and Repair

It is imperative in the design of a PV-T system to keep the system modular to the greatest extent possible. If this is accomplished, the repair of system components and down-time will be minimized. Modularity is the key to quick parts replacement. This leaves the actual repair work for qualified technicians at the manufacturer's service centers. In accordance with this philosophy of maximizing the operating time of the system, spare parts should be included during the design and procurement phases of the system. A rule of thumb to use for spare expendable items is 5 to 10 percent over the calculated

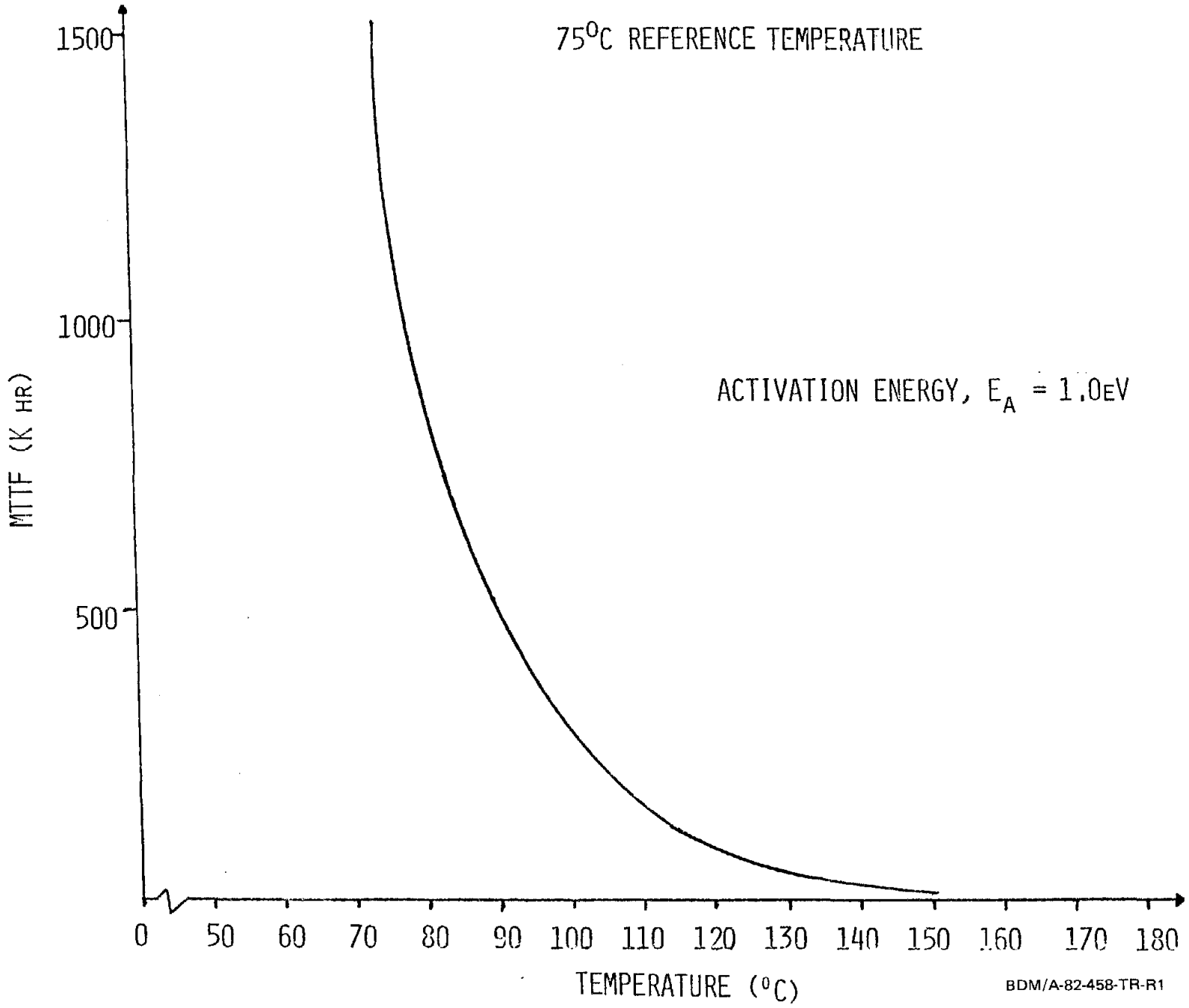

Figure III-24. Mean Time to Failure Versus Junction Temperature for Example Diode

TABLE III-5. DIODE RELIABILITY CHARACTERISTICS VERSUS JUNCTION TEMPERATURE

$T(^{o}K)/(^{o}C)$	ACCELERATION FACTOR	FAILURE RATE (%/Khr)	MTTF (Khr)
200/-73.15	1.75 x 10-11	1.19×10^{-12}	8.39×10^{13}
300/26.85	.0046	3.11×10^{-4}	3.22×10^{5}
325/51.85	.09	6.13×10^{-3}	1.63×10^{4}
348.15/75.00	.973	6.62×10^{-2}	1510.0
350/76.85	1.16	7.90×10^{-2}	1270.0
360/86.85	2.92	0.199	503.0
370/96.85	7.00	0.476	210.0
380/106.85	16.0	1.09	91.9
390/116.85	35.1	2.38	41.9
400/126.85	73.9	5.02	19.9
410/136.85	150.0	10.2	9.80
500/226.85	24700	1.68×10^{3}	59.4×10^{-2}

$$R_{\theta BA} = \frac{1}{2\ An\ (hC + hR)} \quad {}^{o}C/W$$

- hR → RADIATION TERM
- hC → CONVECTION TERM
- n → LAMINAR HEAT EFFECTIVENESS
- A → RELATED TO AREA OF BOX

$$hC = 0.546 \left[\frac{TS - TA}{A}\right]^{\frac{1}{4}} \quad W/m^{2o}C$$

$$hR = 2.28 \times 10^{-7} \quad \varepsilon \left[\frac{TS + TA}{2} + 273\right]^{3} \quad W/m^{2o}C$$

FACTORS: A (3 sides) = 0.557 m^2

hC = 3.35 $W/m^{2o}C$

<u>GRAY PAINT</u> HR = 7.47 $W/m^{2o}C$

PICK <u>n</u> FROM DESIGN HANDBOOK TO BE 0.5

$$R_{\theta BA} = \frac{1}{(2)\ (0.557m^2)\ (.5)\ \left[(3.35\ W/m^2\ {}^{o}C + (7.47\ W/m^{2o}C)\right]}$$

$$= 0.167^{o}C/W$$

BDM/A-82-458-TR-R1

Figure III-25. Thermal Resistance Calculation for J-Box (Ref. III-10)

TABLE III-6. RADIATION PROPERTIES OF MATERIALS*

PAINT	αS (Absorbtivity)	ε (Emmissivity)	$\Delta(\varepsilon-\alpha S)$
BLACK	.79 - .94	.91 - .97	.075
GRAY	.49 - .57	.84 - .91	.345
WHITE	.19 - .33	.95	.690
WHITE EPOXY	.34	.91 - .95	.590

METAL	αS	ε	$\Delta(\varepsilon-\alpha S)$
NICKEL	.33 - .45	.21	-0.18
ALUMINUM	.60	.41	-0.19
SILVER	.25	0.10	-0.15
GOLD	.30	.04 - .23	-0.16avg.

*Reference III-11

requirement. On electronic equipment, all field-replaceable printed circuit cards should be locally stocked, one each per type incorporated in the system design.

2. Data Acquisition Design Guidance

Data acquisition systems are becoming commonplace on medium to large PV and PV-T installations. They represent a small percentage of the total system cost, while supplying valuable data concerning system performance. This rationale alone should warrant the installation of a data acquisition system. Small PV systems might require a cost trade-off analysis when the installation of a data acquisition system exceeds 10 to 20 percent of the total system cost.

The following list of questions help to decide whether a data acquisition system is needed.

(1) Is the PV system a test bed for research and development?

(2) Is the end user interested in maximizing system performance and efficiency during operation, thereby requiring automated control over the PV system?

(3) Are records of system performance required?

(4) Is the design new and unproven?

(5) Will the cost of the installation be less than 10 percent of the total PV-T system cost?

(6) Are the funds available?

A yes answer to any of the above questions would certainly justify investigation, although there are no hard and fast rules governing the decision to install a data acquisition system.

a. The Data Monitoring Concept

This section investigates the application of a data acquisition system monitoring a very basic PV power system. This example will aid in the selection of the components necessary to monitor and determine the performance of the PV-T system. Various options are available to obtain temperature readings, power readings, and voltage readings. By reviewing this application, one can extract the design philosophy involving data acquisition systems for solar applications.

The block diagram shown in figure III-26 depicts a PV power system, including the solar photovoltaic array and the power processing system (inverter). The inverter converts this DC power into AC power to drive a load and/or the utility grid. This is the electrical portion of a typical PV-T system which would be implemented for an industrial or commercial environment. This does not include additional measurements and controls associated with the thermal portion of the system.

Shown on the block diagram are the various monitoring points and the minimum number of sensors required to calculate the system efficiency and performance. Starting at the upper left hand corner of figure III-26, the sensors are identified as follows:

PV Array

S1 - Solar insolation (instantaneous)

T1 - Ambient air temperature

T2 - Cell temperature

Inverter Input

V1 - DC voltage from array

P1 - DC power from array (instantaneous)

Inverter Output

V2 - AC voltage from inverter

P2 - AC power from inverter (instantaneous)

AC Load

P3 - AC power to load (if applicable)

b. Measuring Solar Energy

In order to determine the performance of the PV array the amount of available energy from the sun must be measured.

You can accurately measure solar insolation with a device called a pyranometer, shown in the upper left hand corner of figure III-26 as 'S1'. This device converts radiant energy into a voltage output similar to a PV solar cell, except the pyranometer is precisely calibrated in solar constants. One solar constant is the total

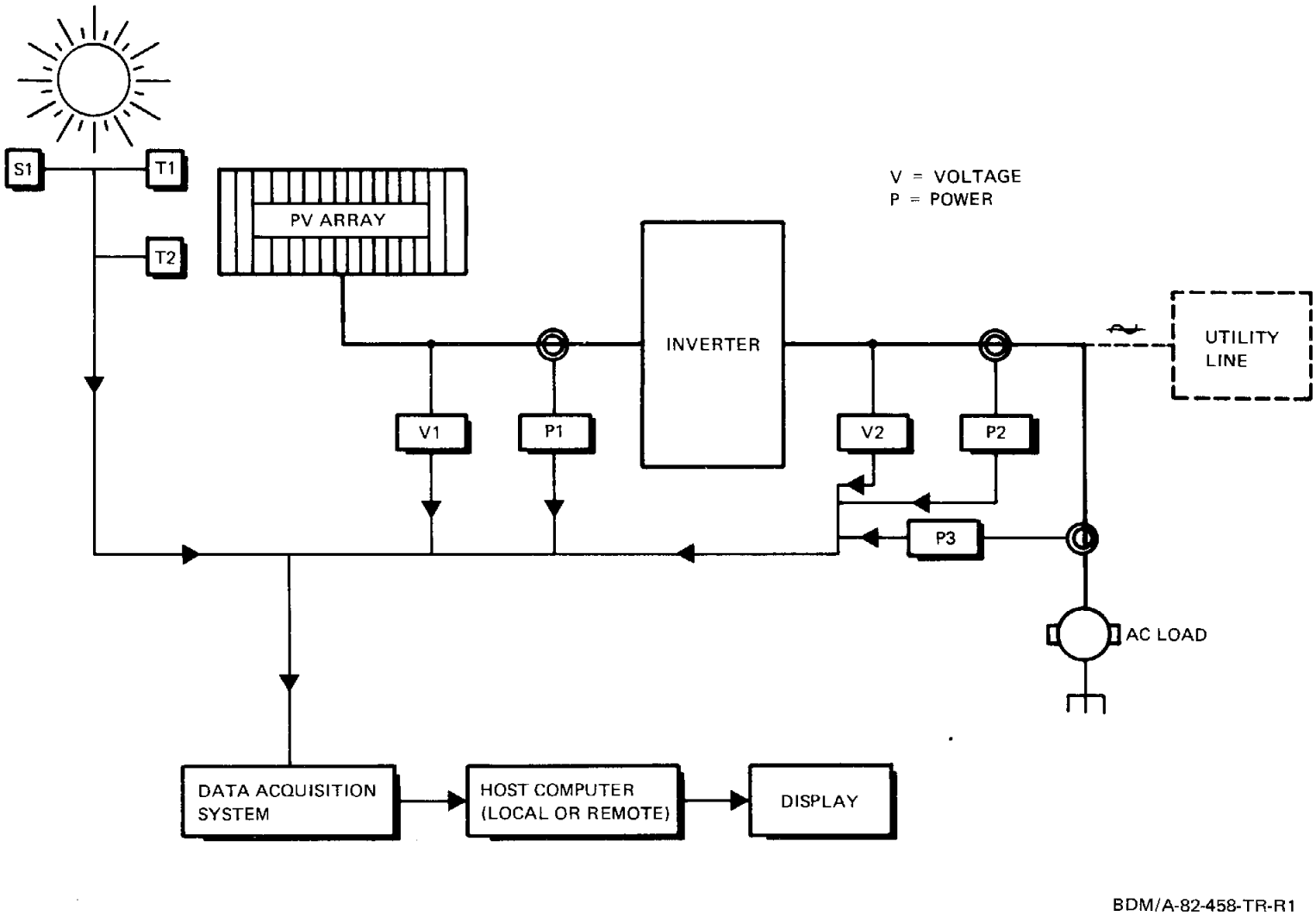

Figure III-26. Monitoring a Base PV System

energy absorbed over a known sensor area. This unit measurement is in watts per square meter. The output voltage available from these devices usually in the 0 to 20 mV range.

As an example, typical specifications for a pyronometer are given below:

Flux Range:	0 to 5 Solar Constants (one solar constant equals 0.1353 watts/cm^2).
Spectral Range:	Sensor .2 to 30 microns
Sensitivity:	5 mV/Solar Constant
Linearity:	$\pm$ 2 percent of full scale
Repeatability:	$\pm$ 0.5 percent of reading
Output Impedance:	150 to 300 ohms
Input Impedance:	Recommended min. to recorder 200K ohms
Time Constant:	Less than 500 milliseconds to 63 percent of step input
View Angle:	180°

The pyranometer is usually located some distance away from the data acquisition system and will require an amplifier to drive the line between the transducer and the input circuit of the data acquisition system. Figure III-27 is a schematic of the pyranometer measurement configuration.

Amplifiers can be selected for a 0 to 5 mV input range to convert this voltage into an accurate 4 to 20 milliamp current output. Adding a precision 250 ohm resistor at the measuring end allows accurate measurement of the voltage drop across the resistor with an analog to digital input channel of the data acquisition system. The voltage range across the resistor will now be 1 to 5 V full scale, 1 volt being zero solar insolation, 5 volts being 1.353 kW/m^2. The pyranometer's output is specified as being linear over this range by $\pm$ 2 percent.

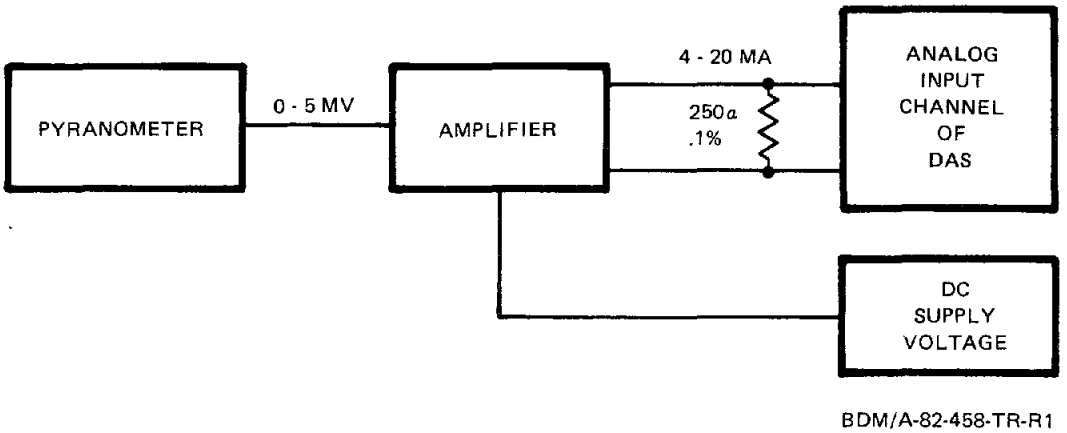

Figure III-27. Pyranometer Measurement Schematic

The amplifier requires a regulated DC voltage source that is usually available from the data acquisition system. If a DC voltage source is not available, a commercial power supply must be used, or one can be designed and fabricated.

d. Voltage and Power Measurements

Most data acquisition systems will not accept input voltages over 120 volts. The transducers used to obtain high voltage, current, and power data convert these voltages or currents into a more reasonable range for measurement. Transducer output range is usually 0 to 10 volts or 4 to 20 milliamps. Another advantage derived from using a transducer is the isolation gained from the measuring device to the input of the data acquisition system. The data acquisition system does not load down the measuring device and this isolation ensures the accuracy of the reading.

Several parameters dictate the selection of a transducer: (1) input voltage or current range, (2) output voltage or current range, and (3) accuracy.

The input requirements of an amplifier are directly related to the type of measurement needed. For example, an AC voltage amplifier will have an input range of 0 to 125 volts AC, whereas an amplifier for a pyranometer measuring solar insolation would have an input range of 0 to 5 millivolts or 0 to 10 millivolts. Sensor manufacturers usually supply or recommend an amplifier for their particular measuring device.

The output range of an amplifier is usually governed by the input requirements of the data acquisition system. Common output ranges are 0 to 1 volt, 0 to 10 volts, or ± 10 volts to 1 milliamp and 4 to 20 milliamps.

The accuracy of the transducer ranges anywhere from ± .01 percent to ± 5 percent full scale over a temperature range of 0 to 70°C.

e. Software

Writing the software is one of the most expensive and time-consuming tasks involving data acquisition systems. Software development costs today can well exceed over 100 percent of the data acquisition hardware cost. A current industry standard for programming costs is estimated at $50 per line for finished code. This kind of expenditure invites system software fixture comparison.

The chart in figure III-28, depicts a cost comparison between three different data acquisition systems. The chart represents the cost in thousands of dollars of 100 channels of temperature, analog, and digital input. All three systems have similar accuracy and temperature specifications. The basic system cost includes a CPU, power supply, RS 232 interface, and a cabinet. System B is a voltmeter type system and the basic system cost includes this feature.

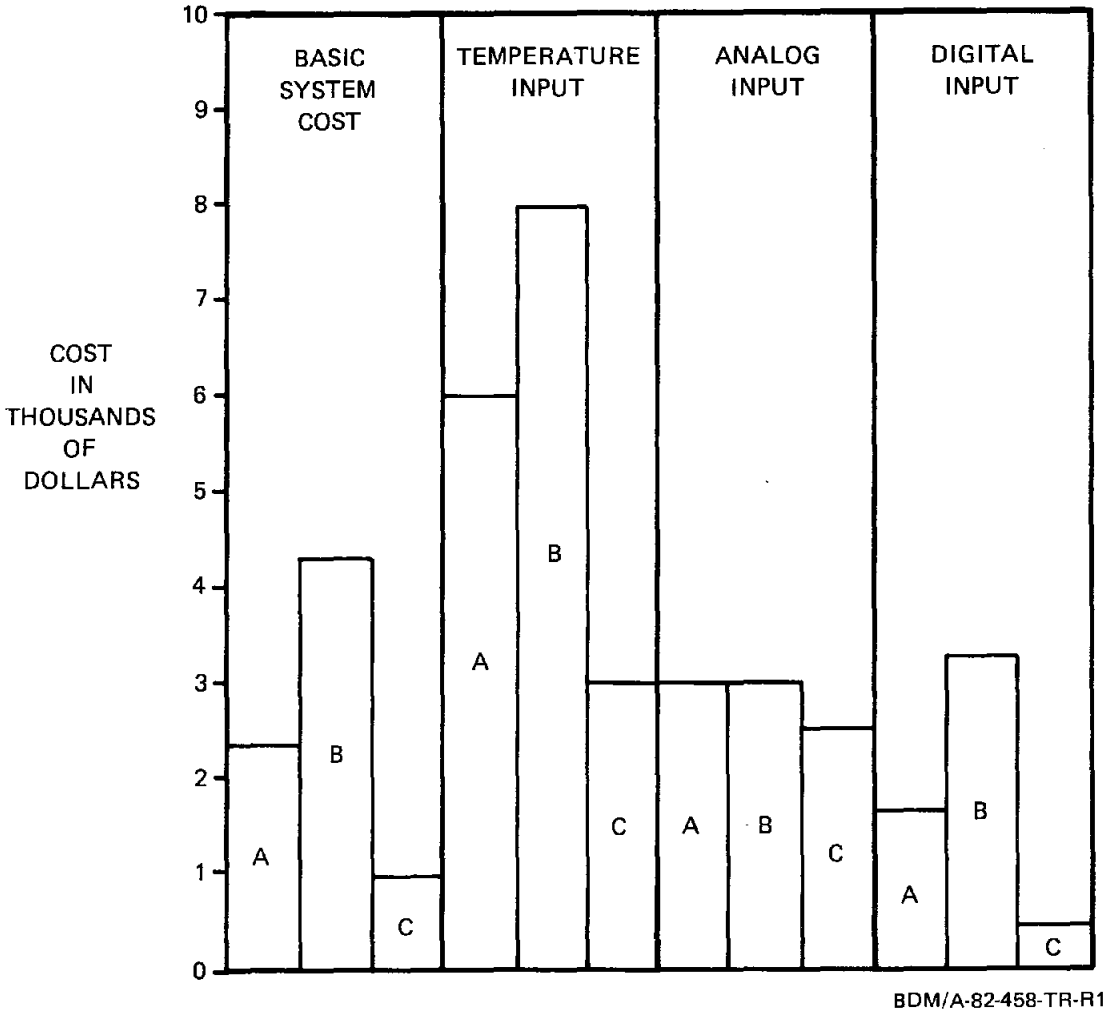

Figure III-28. Data Acquisition System Cost Comparison

If one were considering purchasing a data acquisition system based on a lower cost per channel, system C would be the obvious choice. The difference between system C and systems A and B is the lack of a software operating system. Systems A and B contain operating systems which enable a host computer or terminal to send simple basic commands to the system which configure it and cause it to scan and measure the required channels. It then transmits the raw data collected back to the host. The software overhead on this type of system is reduced to formatting and reducing the data.

On a system like C, where no software operating system is present, the software overhead is two-fold. This system requires the bare bones software to do the analog-to-digital conversions, the temporary storage of data, and the handshaking to the host, etc. The cost of developing this software could exceed the $6,000.00 cost of system A.

This is the trade-off decision on this type of system. If the time and funds are available to develop software, a system like C would be a viable choice.

f. Output Data

To incorporate automatic control functions from a data acquisition system, a method for the output of data is necessary.

The most prevalent forms of output are:

(1) Digital
(2) Digital-to-Analog
(3) Relay Closure
(4) Opto-Isolator

In the digital technique, the system outputs a digital word usually 8 bits or 16 bits wide. This digital information is then used to control external devices.

In the digital-to-analog technique, the system converts a digital word into a voltage. This voltage is then used to control external devices. The voltage output is usually limited to driving a high impedance input, usually greater than 1000 ohms.

The major drawback to either of these two techniques is the requirement of the external device accepting this type of input. These external devices are usually referred to in the industry as smart devices. Speed is the major advantage of these techniques.

The simplest form of output is the relay closure. Connection of a voltage or signal source at the common contact of a relay is required, and the external device to be controlled is connected to the normally open or normally closed contact. The data acquisition system energizes or de-energizes the coil of the relay, which in turn applies

this voltage via the contacts to the external device. The advantage of this technique is that the power of the controlling signal is limited only to the contact rating of the relay. If considerable voltage or power is required, controlling a larger relay with the data acquisition system relay is possible.

One example would be controlling a high voltage DC or AC contact. Contacts of this type usually have low voltage coils which can be energized or de-energized by a data acquisition output relay.

The opto-isolator output is similar to the relay output except that complete isolation occurs between the controlling power and the power needed to operate the data acquisition system.

This type of output controls a small current into a light-emitting diode which turns it on or off. The output of this diode is directed at the base of a photo-transistor. The output of the transistor can then be used as a solid state switch to control external devices.

The main advantage of this technique is the elimination of noise being injected back into the circuitry of the data acquisition system.

g. Input Data

A data acquisition system usually features some type of input data capability.

Two of the most frequently used techniques are:

(1) Analog to digital conversion

(2) A relay closure routing the signal to be measured into the input of a voltmeter

In the analog to digital technique, the system converts the voltage being measured to a digital value which is then read by a computer and/or displayed on an Input/Output (I/O) device.

The main advantage of this technique is speed. Well over 10,000 readings per second are possible. The resolution of this technique is determined by the number of bits in the conversion. For example, let us assume we have a system with a $\pm$ 1 volt full scale input range. The resolution of an eight bit conversion would be 2 volts/256,

which would be 7.8 mv. With a 14 bit conversion, the resolution would be 2 volts/16,384, which would be 122.0 μv.

In the voltmeter technique the system routes the voltage measured into the input of a very accurate voltmeter through a relay closure. The output of the voltmeter is then read by a computer and/or displayed on an I/O device. The voltmeter itself contains the analog to digital converter and also provides a display of the input voltage being measured.

This technique has the advantage of being very flexible if the voltmeter is programmable. Readings less than a micro-volt are possible but the speed of the measurement suffers. Readings limited to less than 300 per second are not uncommon.

The primary trade-offs of the two techniques are speed versus accuracy.

h. Display/Plotting

Data collected in its raw form is not very useful. It must usually be reduced, sorted, converted, listed, etc., to transform it into engineering units.

A multitude of devices are available to display data from a data acquisition system. One of the most valuable display devices is a CRT terminal. These are capable of displaying an enormous amount of information quickly, and can be used to generate highly detailed graphs and plots, some in full color. They are excellent tools for operator input and programming a data acquisition system.

If a hard copy is required, a printer is the logical choice. The printer could be used to generate reports, list important measurements and produce graphs, etc. Some printers can be purchased with keyboard entry similar to a typewriter, making them useful for operator input also.

When a highly detailed hard copy of a graph or plot is required a pen plotter should be used. They are available with a number of features such as multiple pens, digitizing capability, alphanumeric labeling, etc.

Other display devices can be incorporated, such as light-emitting diode (LED) displays or liquid crystal display (LCD) displays. These devices are available in alphanumeric and graphic form similar to a CRT terminal. They come configured as meter faces, bar graph displays, and in seven-segment form.

i. Diagnostic Capability

By establishing upper and lower limits of the measurements being taken, fault isolation can be performed. The system can flag the operator when a particular voltage or current is too high or too low, when a temperature reading is out of range, or when a measurement drops out completely.

A data acquisition system monitoring a PV/PV-T system is normally collecting data in order to measure system performance. The same measurements used to establish system performance can also be used for diagnostic purposes.

j. System Control

All PV/PV-T systems require some type of control. This control can be manual and/or automatic. Most automatic controls are usually overriden with a manual control in the event of a data acquisition system failure or operator error. The following list suggests some controls which are candidates for automatic control in a PV/PV-T system.

(1) Open array
(2) Short array
(3) Switch array output into inverter input
(4) Switch AC output of inverter to the load
(5) Switch fluid pumps on and off
(6) Control fluid valves
(7) Control tracking mechanisms

The number of controlling channels is only limited to the capability of the plug-in options on the data acquisition system. Most basic systems can control up to 100 channels and can be easily expanded to control up to 1000 channels.

3. Design Specifications

This section provides guidelines for the design of the electrical subsystem for PV-T systems based on existing collector/receiver configurations. It is assumed that the manufacturer will supply a basic collector and receiver assembly with PV cells interconnected as a module. The design proceeds with interconnecting modules into an array and considers all electrical aspects of delivering DC power to the inverter, converting to AC power, and interfacing with the utility and load. The equipment and interfaces described in the following sections are configured as shown in the block diagram in figures III-29 and III-30.

a. Photovoltaic Array

The photovoltaic array considers the interconnection of modules in series and parallel to form an array which will interface compatibly with the inverter. The only non-photovoltaic equipment considered are bypass diodes, since these are connected at the module or sub-module level, and blocking diodes, which protect the array from reverse power flow. Switches, varistors, etc., will be discussed under the Control, Monitoring, and Protection sections.

1) Array Operating Voltage

The array design begins by determining the optimum number of modules to be connected in series for interface with the DC-AC inverter voltage window. In the case of pedestal-mounted arrays, the manufacturer has already specified the array voltage via the pedestal design. Therefore, the interfaces are reduced to ensuring that the inverter voltage window encompasses (or can be shifted to encompass) the array voltage variations.

If, on the other hand, the collector design provides only a fraction of the nominal inverter input voltage, collectors must be connected in series to produce this voltage. A matrix of voltages versus cell temperature for typical numbers of modules can be constructed as demonstrated in figure III-31 for a passively-cooled module for residential applications. The module voltages at 28°C and at 50°C were obtained from the manufacturer's specifications and represent the rated output

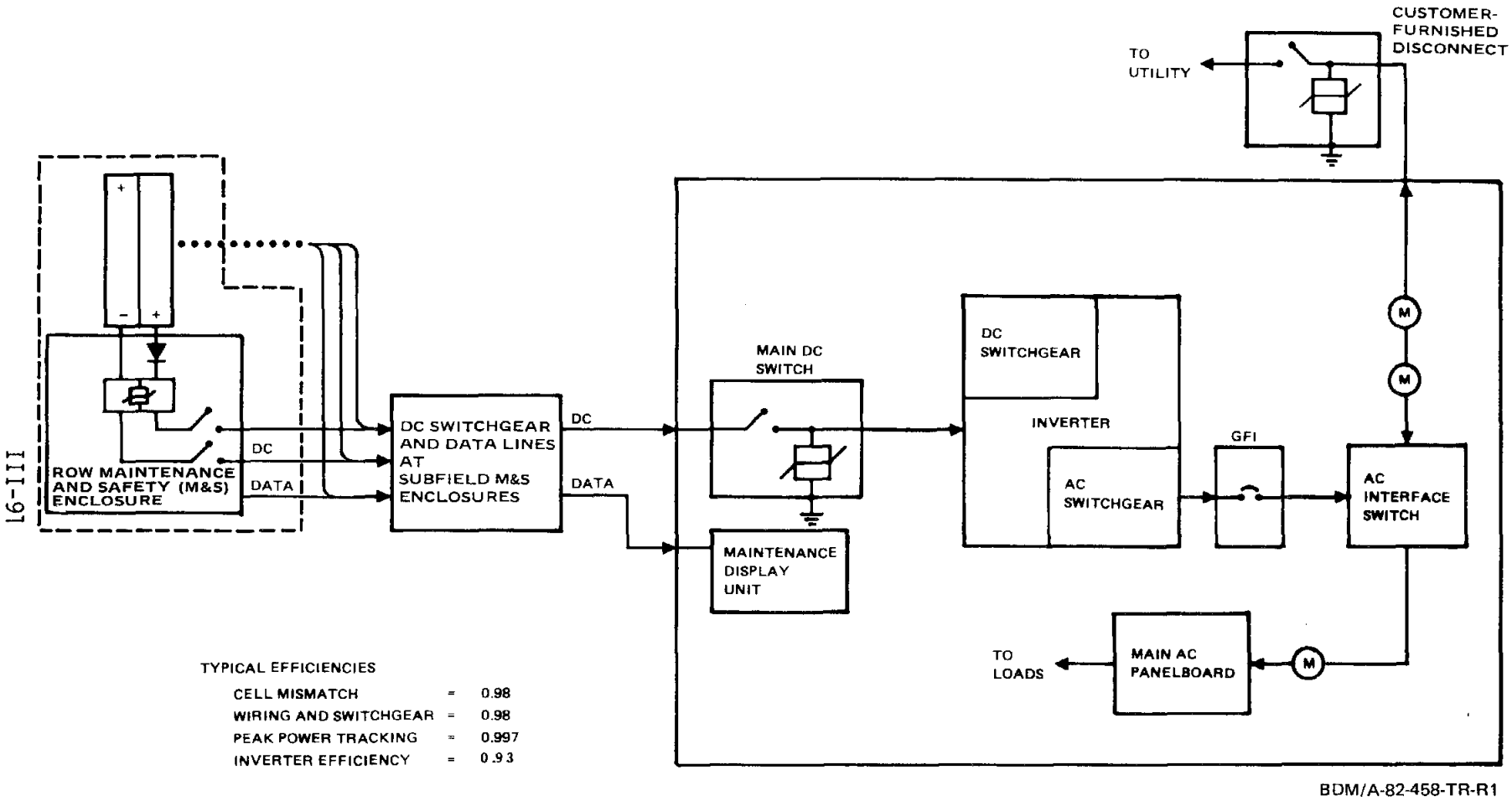

Figure III-29. Typical Detailed Photovoltaic System Block Diagram

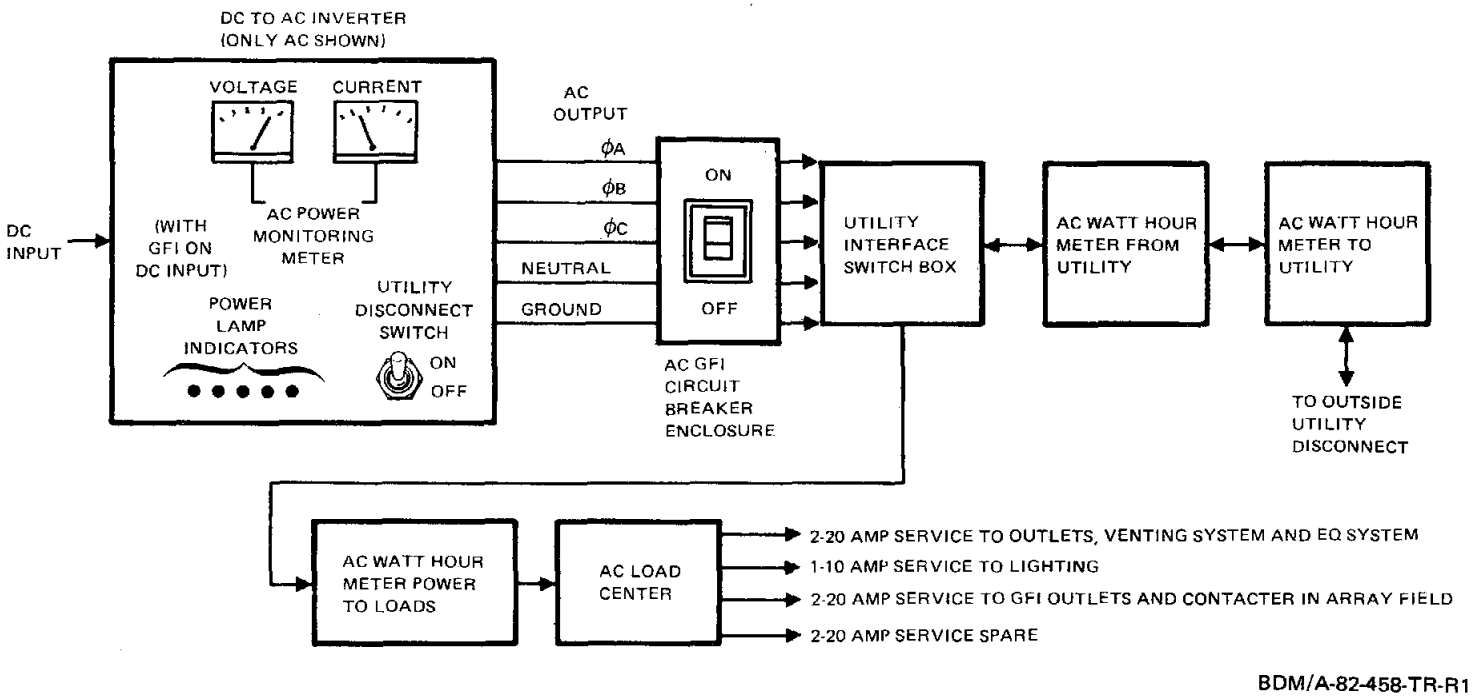

Figure III-30. AC Power One-Line Diagram

$T_{AMBIENT}$	WIND CONDITION	T_{CELL}	1-MODULE V_{MP}/V_{OC}	24-MODULE STRING V_{MP}/V_{OC}	25-MODULE STRING V_{MP}/V_{OC}	26-MODULE STRING V_{MP}/V_{OC}	27-MODULE STRING V_{MP}/V_{OC}	28-MODULE STRING V_{MP}/V_{OC}
						SANTA FE		
-20°F (-29°C)	HIGH	-14°C	9.56V/12.46V	229.4V/299.0V	239.0V/311.5V	248.6V/324.0V	258.1V/336.4V	267.7V/348.9V
							ALBUQUERQUE	
5°F (-15°C)	HIGH	0°C	8.98/11.90	215.285.6	224.5/297.5	233.5/309.4	242.5/321.3	251.4/333.2
								PHOENIX
32°F (0°C)	HIGH	15°C	8.35/11.25	200.4/270.0	208.8/281.3	217.1/292.5	225.5/303.8	233.8/315.0
–	–	28°C*	7.8V/10.7V	187.2V/256.8V	195.0V/267.5V	202.8V/278.2V	210.6V/288.9V	218.4V/299.6V
68°F (20°C)	NOM	51°C**	6.83	163.9	170.8	177.6	184.4	191.2
95°F (35°C)	NOM	66°C	6.20	148.8	155.0	161.2	167.4	173.6
105°F (40°C)	NOM	71°C	5.99	143.8	149.8	155.7	161.7	167.7
115°F (46°C)	NOM	77°C	5.74	137.8	143.5	149.2	155.0	160.7

BDM/A-82-458-TR-R1

* -- RATED CONDITION
** – NOCT (ISUN)

Figure III-31. String Voltage Matrix

cell temperature condition, and a nominal operating cell temperature (at 1 sun) condition, respectively. The first and sixth lines represent reasonable extremes for a cold environment in the West and Southwest such as Denver, Santa Fe, or Flagstaff. Lines two and seven represent the extremes for warmer climates such as Albuquerque or Las Cruces. Lines three and eight represent a hot climate such as Phoenix or Las Vegas. For the cold extremes, a worst-case condition of high winds was assumed, so that the cell temperature is close to the ambient temperature. For the hot extremes, a nominal wind speed was assumed due to convection behind a sloped array, even under still air conditions. The cell temperature is obtained by assuming a constant temperature rise above ambient (ΔT) for standard insolation and nominal wind. The open circuit voltages were only calculated for the cold extremes in order to compare them with the inverter shut-down voltage. The open circuit voltage is only a factor if the inverter is shut down and then restarted during the day under conditions of high insolation and low temperature.

The module voltage (V_T) at each cell temperature (T_C) was obtained from the following equations:

$$\Delta V/\Delta T = \frac{(V_{51}-V_{28})V}{(51-28)^{o}C} \qquad \text{(Eq. III-7)}$$

$$\Delta V/\Delta T = 0.002\ V/^{o}C$$

and

$$V_T = V_{28} + N_S(\Delta V/\Delta T)(T_C - 28) \qquad \text{(Eq. III-8)}$$

where:

$\Delta V/\Delta T$ = Rate of change of cell voltage with temperature ($V/^{o}C$)

N_S = Number of cells connected in series in the module

V_{28}, V_{51} = Voltage of module at $28^{o}C$ and $51^{o}C$, respectively (V).

In this case, the 26-module string most closely fit the specified inverter voltage window of 200 V $\pm$ 15 - 20 percent for the Santa Fe conditions, while 27 and 28 modules would be better suited to the Albuquerque and Phoenix conditions, respectively. In addition, the maximum open circuit voltages were below the inverter shut-off voltage of 330 V.

It should be noted that inverter input requirements vary from one manufacturer to the next. Some have different nominal input voltages, larger voltage windows, and lower open circuit voltage shut-down levels. For some inverters, exceeding the maximum operating voltage will result in inverter shut-down, while under-voltage results only in loss of peak power tracking. Therefore, the operating characteristics of the inverter should be carefully considered.

Sometimes an iterative design process may be required. For example, if the 26-module string cannot be arranged satisfactorily within the field size (13 is a prime number), the 24, 25, 27, or 28-module strings could be used if the manufacturer can shift the inverter range up or down.

For an actively-cooled module (PV-T), the only change required is in the determination of cell temperatures under various conditions. The cell temperature is less dependent on ambient temperature because a second reference temperature, that of the cooling fluid, is present. The following equation can be used to determine the cell temperature based on the simple model shown in figure III-32.

$$T_C = \left[\frac{T_A}{R_A} + \frac{T_R}{R_R} + I_S A_C (1 - \eta_C) \right] R_P \qquad \text{(Eq. III-9)}$$

where: T_A = Ambient temperature (^oC)
R_A = Heat transfer resistance to ambient ($^oC/W$)
T_R = Reference (cooling fluid) temperature (^oC)
R_R = Heat transfer resistance to fluid ($^oC/W$)

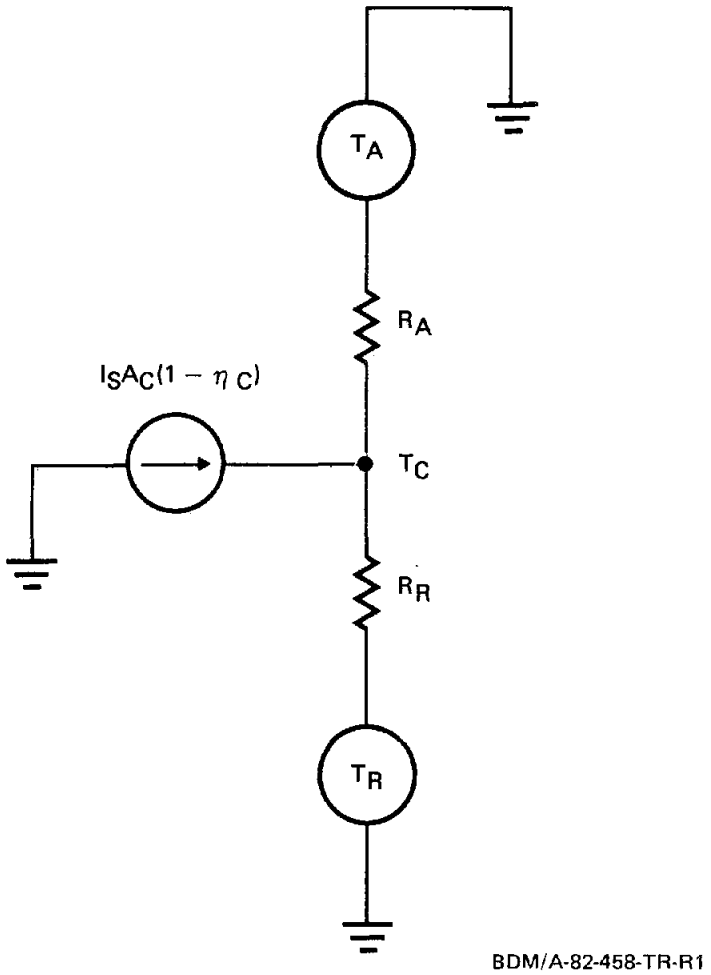

Figure III-32. Simple Model of PV-T Heat Transfer Network

I_S = Standard insolation times concentration (W/cm^2)
A_C = Cell area (cm^2)
η_C = Cell efficiency
R_P = Parallel combination of R_A and R_R ($^oC/W$)

Hence, the string voltage matrix would be based not only on variations in ambient temperature, but also on variations in cooling fluid temperature. If the cooling fluid temperature is dependent on the ambient temperature, this relationship must also be included. For the string voltage matrix, the module voltage would be measured at the design concentration.

This method assumes that the system performance can be modeled using the average temperature across the PV receiver. This assumption is valid, as discussed in the Technical Issues section, if cells are connected in series over the thermal length. Cells at different temperature (or cell series strings with different average temperatures) should not be connected in parallel. Thus, cells arranged along a receiver length should be connected in series because the cells have different temperatures, but the two series strings on opposite faces of a V-shaped receiver tube may be connected together in series or parallel, because the strings have the same average temperature. If, however, the thermal cooling length extends beyond a single receiver, the receiver strings should be connected in series, not in parallel, since the strings will operate in different temperature regions.

2) Array and System Power

The array output power should also be determined to ensure a successful inverter interface. The array power should remain between one half and full rated power of the inverter under most insolation and weather conditions. In tailoring this interface, the designer should also determine the inverter response to input power greater than rated capacity, i.e., power limiting, shut-down, continued operation at lower efficiency, etc.

The array power should be determined for the worst-case conditions used in the voltage design. For each cell temperature (T_C), the array power (P_{TA}) is obtained from the following equation:

$$P_{TA} = N_M V_T I_T = N_M V_T I_{28} \left[1 + (\Delta f_I/\Delta T)(T_C - 28)\right] \quad \text{(Eq. III-10)}$$

where: N_M = total number of modules in array
V_T = voltage of module at T_C and concentration obtained in previous section (V)
I_T = current of module at T_C and concentration (A)
I_{28} = current of module at 28°C and concentration (A)
$\Delta f_I/\Delta T$ = fractional change in current with temperature ($^oC^{-1}$)
= approximately 0.00061/°C

The AC system power (P_{AC}) may be calculated if required by the following equation:

$$P_{AC} = \eta_{CR}\ \eta_{MM}\ \eta_W\ \eta_{PC}\ \eta_I (P_{DC} - P_{PAR}) \quad \text{(Eq. III-11)}$$

where P_{DC} = Array DC power determined at rated conditions (W)
η_{CR} = Concentration efficiency (focusing, tracking)
η_{MM} = Module mismatch efficiency (manufacturing variations)
η_W = Wiring efficiency (resistance losses)
η_{PC} = Efficiency of power conditioning equipment exclusive of the inverter (switchgear, diodes, etc.)
η_I = Inverter efficiency
P_{PAR} = Parasitic power loss (pumping, tracking, etc.,) (W)

If the system specifications require a minimum power under rated conditions, equation III-11 may be reformulated to determine the number of modules required and interconnection requirements if the rated array power (P_{DC}) is written as:

$$P_{DC} = N_M P_M = N_{SS} N_G P_M \qquad \text{(Eq. III-12)}$$

where: P_M = rated power of module (W)
N_{SS} = number of modules in series string
N_G = number of groups of N_{SS} connected in parallel.

Substituting equation III-12 into equation III-11 and solving for N_M:

$$N_M = N_{SS} N_G = \frac{P_{AC} + P_{PAR}}{\eta_{CR} \eta_{MM} \eta_W \eta_{PC} \eta_I P_M} \qquad \text{(Eq. III-13)}$$

This equation can be used to determine the number of groups of N_S modules required to obtain P_{AC} system output. If N_G is not an integer, it should be raised to the next higher integer. If the resultant N_M (from N_{SS} x N_G) provides too much power for the inverter interface or the system requirements, then N_{SS} must be changed or the inverter must be resized.

3) Blocking and Bypass Diodes

Blocking diodes should be required at the end of each series string of modules. If the string is unipolar with respect to ground, only one blocking diode is required. If the string is bipolar with respect to the ground (that is, center grounded), two blocking diodes are required. They should be placed on each end of the string between the array and the isolation switch/varistor assembly. This will help to protect the blocking diodes, as well as the array, from lightning transients.

The blocking diodes should be sized to handle the maximum current from the series string with no more than about 1 V forward drop. The heating due to normal operating power dissipation should be kept within acceptable limits. The reverse breakdown voltage should be at least 20 percent greater than the string voltage. The varistor voltage must, in turn, be at least 20 percent below the blocking diode reverse breakdown voltage.

Bypass diodes should be required in all arrays to protect cells from reverse bias damage, and to improve array output under shadowing or cell failure conditions. As a rule of thumb, bypass diodes should be connected across every 6 to 12 series cells. The following equations can be used to determine the maximum bypass group size.

To prevent exceeding the reverse breakdown voltage of the shadowed cell since the probability of failure is significant in reverse breakdown:

$$V_{RMAX} = V_{BMIN} \qquad \text{(Eq. III-14)}$$

$$N_{BPB} = 1 - \frac{V_{RMAX} + V_{FD}}{V_{OC}} \qquad \text{(Eq. III-15)}$$

where:
- V_{RMAX} = Maximum allowable reverse voltage (V)
- V_{BMIN} = Lowest expected breakdown voltage (V)
- N_{BPB} = Maximum allowable seriesed cells in bypass group from breakdown considerations
- V_{FD} = Forward voltage of bypass diode (V)
- V_{OC} = Open circuit voltage of cell (V)

For example:

$$V_{BMIN} = 5\ V,\ V_{FC} = 1.0\ V,\ V_{OC} = 0.6V$$

$$N_{BPB} = 1 - \frac{-5\ V + 1.0\ V}{0.6V}$$

$$N_{BPB} = 7.7 \Longrightarrow 7 \text{ cells}$$

To prevent exceeding maximum allowable cell or encapsulant temperature:

$$V_{RMAX} = \frac{R_P(I_S A_C + \frac{T_A}{R_A} + \frac{T_R}{R_R}) - T_{CMAX}}{R_P I_{MP}} \qquad \text{(III-16)}$$

$$N_{BPT} = 1 - \frac{V_{RMAX} + V_{FD}}{V_{MP}} \qquad \text{(III-17)}$$

where:

$R_P = \frac{R_R R_A}{R_A + R_R}$ = Parallel combination of R_A and R_R ($^oC/W$)

R_A = Thermal resistance to ambient ($^oC/W$)

R_R = Thermal resistance to reference fluid ($^oC/W$)

I_S = Standard insolation ($.1W/cm^2$) times concentration ratio

A_C = Cell area (cm^2)

T_A, T_R = Ambient and fluid temperatures (^oC)

T_{CMAX} = Maximum allowable temperature (^oC)

I_{MP} = Peak power current of cell (A)

N_{BPT} = Maximum allowable seriesed cells in bypass group from temperature considerations

V_{MP} = Peak power voltage of cell (V).

For example:

$I_S = (0.1W/cm^2)(30x) = 3.0\ W/cm^2$

$A_C = 10\ cm^2$

$$T_A = 40^oC$$
$$R_A = 5.0^oC/W$$
$$T_R = 60^oC$$
$$R_R = 0.87^oC/W$$
$$T_{CMAX} = 120^oC$$
$$I_{MP} = 8.7A$$
$$V_{FD} = 1.0\ V$$
$$V_{MP} = 0.5\ V$$

$$R_P = \frac{(0.87)(5.0)}{5.0 + 0.87} = 0.741^oC/W$$

$$V_{RMAX} = \frac{0.741\ (3.0)(10) + 40/5.0 + 60/0.87 - 120}{(0.741)(8.7)}$$

$$= -6.32V$$

$$N_{BPT} = 1 - \frac{-6.32 + 1.0}{0.5}$$
$$= 11.6 \Longrightarrow 11 \text{ cells}$$

In this case, the maximum ambient temperature is used for T_A and T_R represents a maximum outlet temperature. The thermal resistances (R_A and R_R) are designed to produce a normal operation cell temperature of about 50^oC at 20^oC ambient, and 30^oC cooling fluid temperatures.

The bypass diodes should be sized to handle the maximum current of the strings they are protecting so that heating due to power dissipation is kept within acceptable limits. The reverse breakdown voltage of the bypass diode should be greater than the maximum open circuit voltage (determined at low temperature) of the strings they are protecting.

b. Inverter

This section presents guidance for the selection of the inverter for PV-T systems. Since the current effort considers only utility-interactive commercial and industrial applications, the inverter must produce 277/480 VAC, 3-Ø, 60 Hz power. The array size will be based on the minimum life cycle cost of the system. This method of sizing usually results in a PV array which supplies only a fraction of the total load requirement. Therefore, the inverter must be sized according to the array output rather than to the AC load requirement.

Additional selection consideration can be divided into three categories: 1) critical design specifications, 2) voltage window interface with array, and 3) additional desirable features. Candidate inverters should be evaluated first for compliance with the critical design specifications. Inverters that pass this test should then be evaluated for ease of interface with the array voltage variations. During this evaluation, the method of handling out-of-range voltages and the method of peak power tracking should be considered. Finally, additional desirable features should be considered for those inverters considered acceptable after tests one and two. Details of the three selection categories will now be presented.

1) Priority 1: Critical Design Specifications

A list of critical design specifications will vary somewhat with the particular application; however, a list which would apply to most commercial and industrial utility-interactive applications could be represented by the one in table III-7. The power rating of the inverter would be determined from the array output. The only critical specification concerning the input voltage is that it accept a range of voltages. This range will be considered in detail in the priority 2 considerations.

The specifications on total harmonic distortion, power factor, and other values or ranges could be specified. In actual practice, there may be small grounds for comparison of these parameters between some inverters, so other considerations are more dominant; e.g.,

TABLE III-7. TYPICAL CRITICAL DESIGN SPECIFICATIONS FOR INVERTERS FOR COMMERCIAL AND INDUSTRIAL UTILITY-INTERACTIVE APPLICATIONS

Output	
Voltage Level, Type, Frequency	277/480 VAC, 3Ø, 60 Hz
Power	Determined by application
Mode of Operation	Synchronized to utility
Current Distortion	Total Harmonic Distortion (THD) <5% of load current
Power Factor	PF > .9 (lead or lag)
Utility Isolation	Includes isolation transformer
Input	
Voltage	Must allow variable input voltages - Voltage range is a Priority 2 consideration
Mode of Operation	Automatic start-up and shut-down with peak power tracking
EMI Protection	Filtering on input
Efficiency	η > 90% from 25% to full load
Protection	
Input	Over-voltage, over-power
Output	Utility voltage or frequency out-of-range, over-current, utility loss
Environmental	
Temperature	$-10^{o}C$ to $45^{o}C$
Humidity	0 - 95%
Delivery Schedule	Based on system construction schedule

if an inverter has no isolation transformer, the absence of such a component or feature would be more important than a slight improvement in efficiency or power factor.

2) Priority 2: Voltage Window

Since the array operating voltage may vary by 15 to 20 percent above and below nominal voltage at a particular location due to weather condition extremes, those inverters having passed priority 1 considerations, and which have the widest voltage windows, would be preferred. The method of specifying the input voltage range should also be considered, however. For example, if one inverter has a 200 to 280 V input range in which peak power tracking is performed with shut-down at 500 V, this might be preferable to another inverter which has a peak power tracking range of 200 to 300 V with shut-down at 350 V. The smaller voltage window of the former may be acceptable for a particular location, but the lower shut-down voltage of the latter may not be acceptable if the system experiences intermittent operation. In such cases, attempts to restart the system on a cold day might be futile due to high open circuit voltage.

If there is doubt as to the best inverter for priority 2 considerations, the interface of each of the candidate inverters with the array should be analyzed by the methods described in section 3 to determine which would be most compatible with the array.

3) Priority 3: Additional Desirable Features

If no inverter offers a clear choice after priority 2 considerations, additional inverter features should be considered. They might include the cost of the inverter, manufacturer's field experience, meters and indicator lights on the front panel, internal voltage adjustment capability, stand-alone operation capability, ground fault interrupt circuit breakers, built-in data acquisition output terminals, etc. Note that inverter cost is considered a priority 3 consideration. The rationale behind this is that a low cost inverter which does not satisfy utility interface requirements and is therefore not acceptable to the utility company, or which experiences failures or excessive shut-downs, is not a bargain.

In some applications, however, the inverter cost (or any other of the priority 3 considerations) could be a priority 1 consideration, depending on the goals or objectives of the application. For example, an inverter used in an uninterruptible power supply (UPS) application might require more monitoring and control features.

As a final note, the issue of self-commutated inverters (SCI) versus line-commutated inverters (LCI), has not been addressed as a specific evaluation consideration. In general, LCI are less expensive and have slightly higher efficiency and simpler design. The SCI have better signal quality and power factor. These considerations would tend to favor SCI since cost is a priority 3 issue; however, power factor and harmonic distortion correction of LCI are possible at additional expense. The corrected LCI may, therefore, cost as much as the SCI. In the final analysis, the question of line- or self-commutation is not as crucial as the consideration of the operational characteristics and cost of a fully-configured inverter. The requirements for additional equipment, hardware modifications, and additional installation time should all be considered.

c. DC Wiring

The DC wiring portion of our PV or PV-T system is designed to minimize power loss from the array to the inverter. This length of wiring is sometimes several hundred feet, and the trade-off which must be performed in order to select the optimal wire size and configuration is not trivial.

In an array configuration where each sub-array or module string is nearly equidistant from the inverter location, the voltage loss (or power loss) may be easily determined using Ohms law:

$$V_{LOSS} = I_{SA} R' \frac{2\ell}{1000} \qquad \text{(Eq. III-18)}$$

where: V_{LOSS} = the DC voltage loss from the subarray to the inverter

I_{SA} = the output current of the subarray in DC Amperes

R' = the resistance of the wire to be used per 1000 ft length

ℓ = wire routing distance from the subarray output terminals to the inverter input terminals

Note the ℓ is multiplied by two, since the current flowing from the subarray returns through the second conductor length back to the negative subarray terminal. This is illustrated in figure III-33.

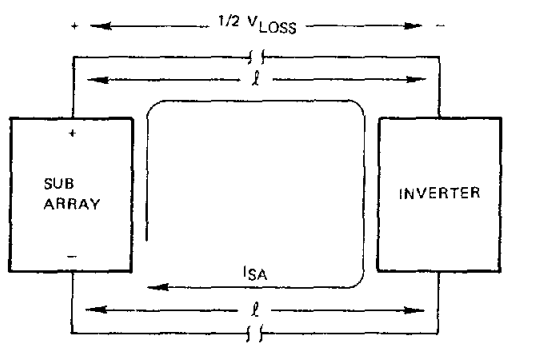

BDM/A-82-458-TR-R1

Figure III-33. DC Block Wiring Diagram

Normally one would calculate V_{LOSS} for each subarray (since ℓ varies) using several wire sizes to determine the most cost effective wiring scheme. Naturally, larger wire sizes are required at greater distances ℓ for any given V_{LOSS} figure. V_{LOSS} figures of less than 5 percent are common for system design requirement, and often less than 2 percent may be required. The wire size required to obtain an insignificant voltage level in most systems may well exceed the NEC safe ampacity rating of these conductors in some instances, although this of course, must be decided. This percent is simply calculated as:

$$\% V_{LOSS} = \frac{V_{LOSS}}{V_{SA}} \qquad \text{(Eq. III-19)}$$

where V_{SA} is the subarray output voltage.

For system design purposes, V_{SA} and I_{SA} may be chosen at any cell temperature; however, the normal operating temperature of the cells should be used, since this will reflect most accurately the average power output of the system.

As opposed to the voltage loss calculation, power loss may also be used to optimize this choice of wiring, since these two parameters are easily related.

$$P_{LOSS} = (I_{SA})^2 R' \frac{2\ell}{1000} \qquad \text{(Eq. III-20)}$$

1) Special Considerations

Since the design goal of the array wiring is to optimize the power output, balancing techniques may be used when the difference in ℓ from the nearest (to the inverter) subarray to the farthest subarray is significant. This is due to the fact that some method of peak power tracking is employed in these PV-T systems. For example, if V_{max} = 200 VDC and I_{max} = 14 Amperes for each subarray, (these are the peak power point parameters), a peak power tracking "error" occurs for two of these subarrays located at different distances from the inverter, if the same wire size is used for both. The example in figure III-34 and the calculations below illustrates this condition.

Assume:
1) V_{max} = 200 VDC and I_{max} = 14 Amperes
2) ℓ_1 = 76.2 m(250ft) (distance from subarray #1 to inverter)
3) ℓ_2 = 426.8 m(1400ft) (distance from subarray #2 to inverter)

4) Wire size is #8AWG; R' = 0.64 Ω/1000 ft

5) the average cell temperature for SA_1 and SA_2 are the same

then:

$$V_{LOSS\ (1)} = I_{SA(1)}\ R'\ \frac{2\ell_1}{1000}$$

$$= (14)(.64)\ \frac{2(250)}{1000} = 4.48\ \text{VDC}$$

$$V_{LOSS(2)} = I_{SA(2)}\ R'\ \frac{2\ell_2}{1000}$$

$$= (14)(.64)\ \frac{2(1400)}{1000} = 25.08\ \text{VDC}$$

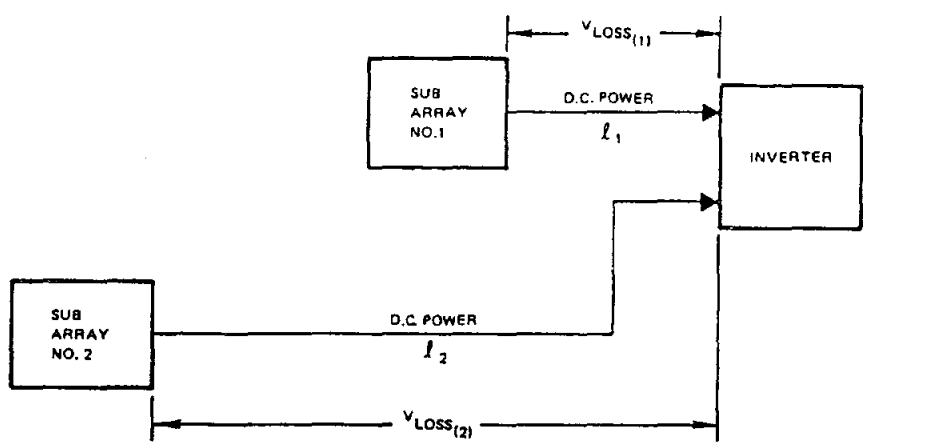

BDM/A-82-458-TR-R1

Figure III-34. Peak Power Tracking Error Examples

Since the node voltage at the input to the inverter is the same for all subarrays in the system, a peak power tracker will settle out at some subarray voltage between the nearest and farthest subarray V_{max} point. In this simple example, we can pick the midpoint of the voltage difference to illustrate the "imbalance" loss of power. The circuit model for this case is shown in figure III-35.

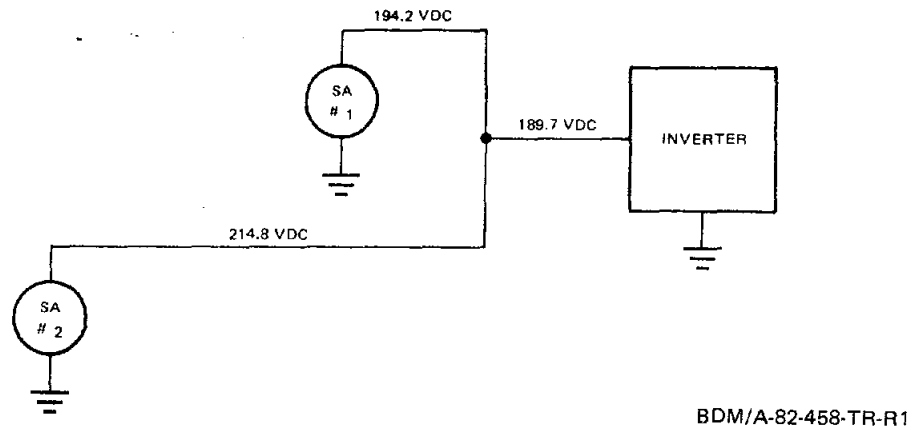

Figure III-35. Example of Imbalance

Notice that neither subarray #1 or subarray #2 are actually operating at their peak power point of 200 VDC @ 14 amperes under this condition. The actual loss of power due to this imbalance may be estimated by closely examining the cell I/V curve near V_{max}, I_{max}. For the sake of illustration, let us assume that a 1 percent voltage displacement from the V_{max} point on the I/V curve results in a 0.5 percent power output loss (V_{max} x I_{max}). Of course, the optimum output of these two subarrays, if balanced, would be:

$$P_{out(1\&2)} = 2\ (200\ \text{VDC})\ (14\ \text{amperes})$$
$$= 5600\ \text{W}$$

For the imbalance condition illustrated, this would become:

$$P_{out(1\&2)} = (194.2\ \text{VDC})\ I'_{SA1} + 214.8\ \text{VDC} \times 4\ I'_{SA2}$$

where: I'_{SA1} = the output current of SA #1 @ 194.2 V
I'_{SA2} = the output current of SA #2 @ 214.8 VDC

To obtain the currents:

$$(I'_{SA1})(194.2\ \text{VDC}) = (200\ \text{VDC})(14\ \text{amperes}) - \frac{\frac{200-194.2}{200}\ (200\ \text{VDC})(14\text{A})}{2}$$

or

$$I'_{SA1} = \frac{(200)(14) - (.029)(200)(14)/2}{194.2}$$

$$= \frac{2800 - 40.6}{194.2} = 14.2\ \text{amperes}$$

Similarly, the imbalance current of subarray #2 can be calculated:

$$I'_{SA2} = \frac{(200)(14) - \frac{214.8-200}{200}\ (200)(14)/2}{214.8}$$

$$= \frac{2800 - (0.074)(2800)/2}{214.8}$$

$$= 12.55\ \text{amperes}$$

Therefore:

$P_{out(\#2)}$ for the imbalanced condition is:

$$P_{out(\#2)} = (194.2\text{VDC})(14.21\text{A}) + (214.8\text{VDC})(12.55\text{A})$$
$$= 2760\text{W} + 2695\text{W}$$
$$= 5455\text{W}$$

This represents a percent power loss of $\frac{5600-5455}{5600}$ or 2.6 percent due to peak power tracking error.

Additionally, the I^2R losses are different, which further reduces the power which actually arrives at the inverter input. Other losses which reduce the system power output include the blocking diode forward voltage drops and parasitics associated with contact resistances and voltage drops across fuses etc.

d. Utility Interface

The design of the utility interface for each PV-T power system will vary to certain degrees, since all utility service requirements and the configuration policies of utility companies differ. Coordination with the utility engineering representatives must proceed well in advance of the actual detailed electrical design for this portion of the system. Usually the NEC handbook can be used as a general design guidance reference for all of the AC wiring size and type specifications, as well as for conduit selection. The isolation transformer between the PV power source and the utility must be specified by the utility company.

Additionally, any metering requirements associated with the utility service, may be the responsibility of either party of the contract. This must be defined early in the design phase.

Normally in the industrial and commercial PV-T power systems, the utility interface will be a 480/277VAC, 3Ø circuit and the isolation transformer will step up this voltage to a compatible utility level. The basic block diagrams in figure III-36 shows the major utility interface components which must be specified in the system design.

The control of the AC switchgear is accomplished by the utility monitoring equipment. This a protective process required for on- and off-line switching of the inverter-produced PV power. The quality of the voltage, frequency, and current provided by the PV power processing equipment is scrutinized by the utility to ensure the integrity of the signal to their customers. Although much effort is being expended by the IEEE to define a uniform set of signal quality specifications they are

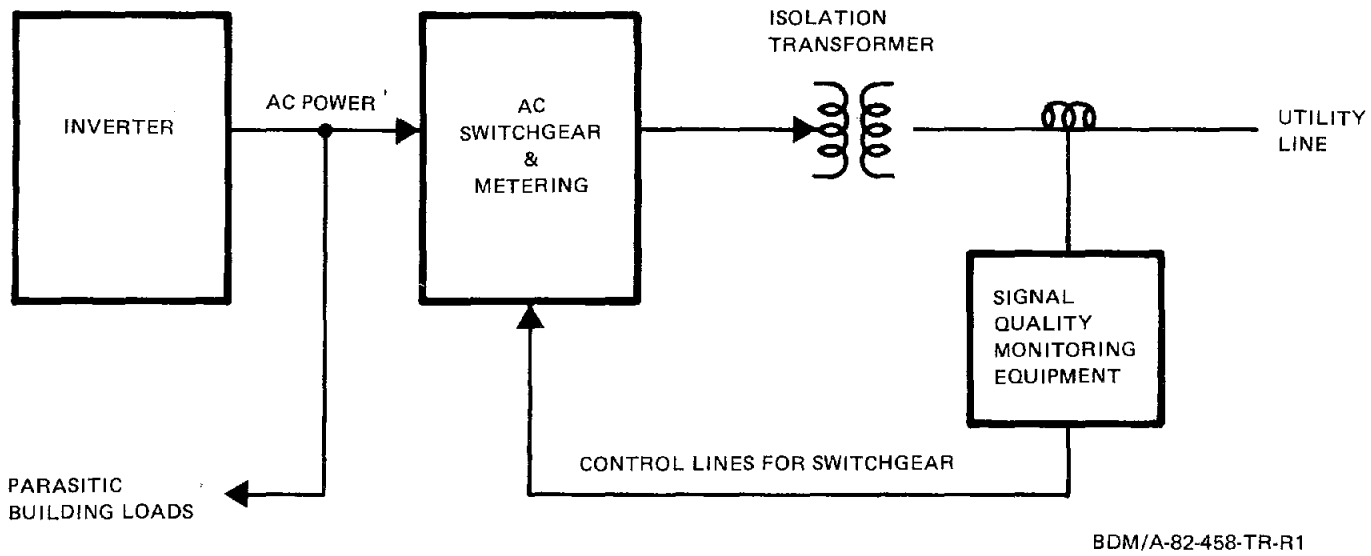

Figure III-36. Major Utility Interface Components

not yet final. The general figures for signal quality being considered for standardization of this specifications are:

Frequency	60Hz ± 5% (3Hz)
Voltage Amplitude	nominal ± 5%
Voltage Waveform Distortion	2%
Current THD	3%

e. Controls

Several types of controls are usually designed into a PV-T power system. Some are incorporated into the equipment design, and others which are used in the interfaces between pieces of equipment, will have to be designed and specified separately. Examples of built-in controls are peak power tracking and over-temperature shutdown. These two are usually a function of the inverter design (over-temperature of inverter electronics). Examples of added controls are fluid flow valves and externally actuated switchgear and HVAC equipment, if required. Although the controls themselves are simple in nature, their implementation in a system must be accomplished in such a manner that oscillatory problems do not result. A good example of a system oscillation is

the case of a poor peak power tracker design. The tracker must measure actual power from the array in order for the inverter to begin its start-up sequence. An implementation of a poor design is exemplified by a voltage-only sensing circuit. The response of this type of tracker may result in the oscillation illustrated in figure III-37:

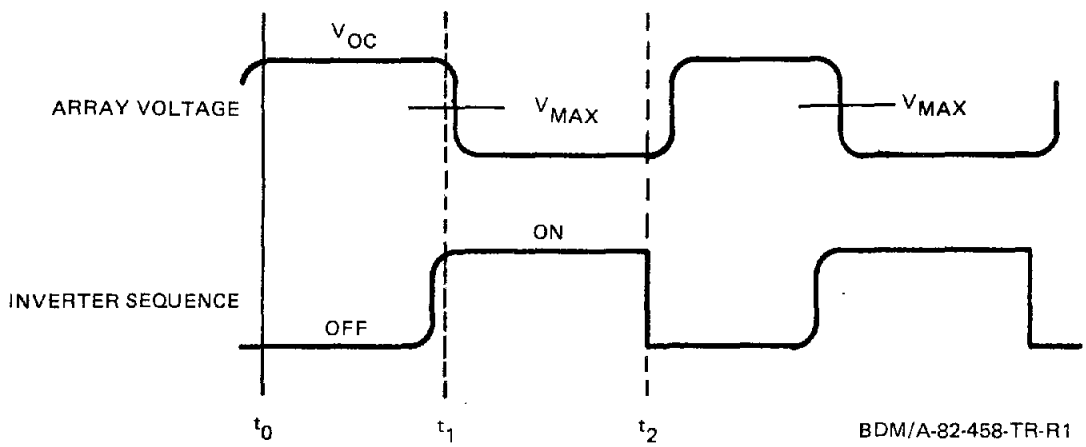

Figure III-37. Peak Power Tracker Oscillation

At time t_0, the array voltage is sensed by the inverter electronics. This is essentially V_{OC} (open-circuit voltage of the array). If the inverter does not load down the array and measure power, it will begin its start-up sequence depicted at time t_1. The array voltage collapses shortly thereafter if it cannot supply the tare power required of the inverter, and at time t_2 the inverter shuts down only to try to start up again. This condition causes erratic peak currents to be generated internal to the inverter, and if oscillation is allowed to continue, may very well damage the inverter. As a solution to this control problem, the peak power tracker must actually measure a fraction of the array power, not voltage alone.

Built-in controls in inverter designs generally include ground fault sensing, AC output parameters, and internal circuit temperatures as self-protective measures.

Controls external to the pieces of equipment in the system may be actuated manually, by computer, or both. Occasionally, it is good practice to design in redundant control circuits, especially in the case of personnel safety features such as emergency shut-down of the system and various ground fault conditions.

1) Protection

System protection devices include hardware items as well as software generated controls. Fuses, circuit breakers, and blocking diodes are prime examples of hardware protection devices, and stow and inverter shut-down commands are examples of software generated protective measures, although in "bare-bones" systems they may also be provided by limit switches and other hardware protective circuits.

In the case of fuses and circuit breakers, the designs must consider the trip or open current/voltage levels of these units, as well as the trip time. This time may vary from milliseconds up to seconds, and require specifications based on the peak interrupting fault currents available at any point in the system.

Software-generated protective commands are the result of an unfavorable system measurement such as over-temperature, high wind conditions or precipitation. They are generally closely associated with the data acquisition system computer or an individual control computer or logic.

2) Lightning Design Guidance

For a commercial industrial system of less than 500 kW, lightning rods and dissipation arrays (barbed wire which dissipates static charges to prevent lightning strikes) are not recommended. Instead, it is advisable that the collectors and support frames or pedestals be grounded to a counterpoise system buried in the ground, and that terminal protection devices be provided at the ends of cable runs.

The counterpoise system consists of a network or grid of bare conductors buried 2 to 3 inches underground. The conductors are run along the collector rows and cross-connected every 40 to 50 ft. Eight to ten-foot ground rods are sunk at each of the connection points. The collector and frame grounding wires are connected directly to the buried cables at each end of each collector assembly. Number 4 AWG bare copper wire is usually satisfactory for the counterpoise network, while #1/0 wire should be used for grounding the collectors. All disconnect switch cases and J-Boxes in the field should also be grounded.

The terminal protection devices consist of standard surge arrestors, varistors for DC lines and varistor/Zener diode circuits for data and logic lines. Standard AC surge arrestors should be used to protect all three AC power legs. They should be placed in the utility disconnect switch outside the power conditioning at the utility service entrance.

The DC varistors should be rated for at least 5000A peak surge current capacity. The varistors should be connected from the positive and negative terminals to ground at the end of each array series string. The varistor should be on the DC cable side of any blocking diodes used. The interface of the varistor voltage with the blocking diode reverse breakdown voltage is critical. If the varistor conduction voltage exceeds the diode breakdown voltage, the diode must be resized or two diodes placed in series.

Additional varistors may be placed within each array series string between collector assemblies if convenient interconnection points and J-Boxes are available. This is an added expense, and is only necessary if switchgear or monitoring circuits are located at these points.

Varistors should also be provided on ungrounded DC lines in the main DC switch at the power conditioning (PC) room. If more than one set of DC lines is brought into the PC room, the varistors may be attached after the lines are paralleled.

Varistors/Zener diode protection circuits should be provided on all data lines entering the building. If shielded cables are used, the circuit shown in figure III-3 should be sufficient to protect TTL type logic.

All equipment cases in the PC room, as well as the outside disconnect switch case, should be grounded.

REFERENCES

III-1. T. J. Lambarski, et. al., Photovoltaic Transient Analysis Program, User's Guide, SAND 7-8-7038, Sandia National Laboratories, Albuquerque, NM, October 1978.

III-2. Delta Electronics Control Corporation (DECC) Catalogue, Division of Helionetics, Inc., Irvine, CA.

III-3. Square D Company Catalogue, Palatine, Illinois, 1982.

III-4. Hoffman Engineering Company Catalogue, Division of Federal Cartridge Corporation, Anoka, Minnesota, 1979.

III-5. Kulka Electric Corporation Catalogue, Mt. Vernon, NY, 1976.

III-6. Hewlett-Packard Co. Catalogue, Los Angeles, CA, 1982.

III-7. Burr-Brown Research Corporation Catalogue, Tucson, AZ, 1982.

III-8. Reliability Analysis Center, Design Handbook No. RDH376, RADC/RBRAC, Griffis AFB, NY 1976.

III-9. Thermalloy, Inc. Catalogue, Dallas, TX, 1971.

III-10. National Semiconductor Audio Handbook.

III-11. Harper, C.A. ed., Handbook of Electronic Packaging, McGraw-Hill, NY, 1969.

CHAPTER IV
THERMAL AND MECHANICAL SYSTEM ANALYSIS

A. INTRODUCTION

After an initial feasibility analysis and concept development are performed, the PV-T designer should have a preliminary estimate of the economic array size and fraction of thermal and electric load provided. From this information, an initial field layout can be developed, based on the electrical characteristics of the collectors and inverter requirements. Preliminary values for the major thermal design parameters can now be established, including the number of collectors in thermal series in a row, coolant flow rate through a row, the number of rows, heat exchanger sizing, cooling tower sizing, and manifold sizing.

The thermal characteristics of the array, such as average operating temperatures, the temperature drop across a collector row, and the temperature difference between collectors wired in parallel, will determine the total array power output. Therefore, several iterations may be required between the electrical and thermal analysis to develop an optimum array layout in terms of the number of collectors in series and parallel.

In this chapter, guidance is provided for the initial determination of the collector coolant flow rate and for selection and sizing of various mechanical and thermal components. Once this preliminary sizing and field layout is complete, and the application of PV-T appears feasible both economically, and in terms of the load requirements, the designer should perform a more extensive analysis and economic study using a detailed system model such as SOLCEL-II.

B. COOLANT FLOW RATE

The array electrical output depends on the insolation, array temperature, and the electrical parasitic power requirements. At higher flow

rates through each collector row, the array operates cooler and therefore at a higher efficiency; however, the pumping power increases as the cube of the mass flow rate, thereby decreasing the net electrical output. The net electrical and thermal power output from an array can be determined for various flow rates and thermal string lengths using the annual collectable energy curves presented in Chapter II. In addition to these availability curves, the collector characteristics must be known, including electrical efficiencies.

Collector efficiencies may be obtained from the curves provided in Volume I of this report, or from empirical data obtained from tests. E-System's line focus Fresnel lens system has been tested extensively and efficiencies may be determined as follows:

$$\eta_e = 0.131 - \frac{0.0005}{^oC} (T_f - 25^oc) - \frac{0.00003}{W/m^2} (I-700\ W/m^2) \qquad \text{(Eq. IV-1)}$$

$$\eta_t = 0.62 - \frac{0.8W}{m^2 {}^oC} (T_f - T_a)/I \qquad \text{(Eq. IV-2)}$$

where: η_t is the total collector efficiency (thermal plus electric),

I = direct normal radiation (w/m^2)

T_f = average fluid temperature (^oc)

T_a = ambient temperature (^oc)

The efficiency curves in Volume II give relations for a typical linear parabolic trough as:

$$\eta_e = 0.119 - 0.45\ T_f/I \qquad \text{(Eq. IV-3)}$$

$$\eta_{th} = 0.79 \left[0.58 - 1.1\ \frac{(T_f - T_a)}{I}\right] \qquad \text{(Eq. IV-4)}$$

where η_{th} is the thermal efficiency, and I is the direct normal radiation (Watts/m^2).

Useful energy collected from a collector row is given by

$$\dot{q}_u = \dot{m}\ C_p\ (T_o - T_i) = I\ \eta_{th} 5\ \ A_c \qquad \text{(Eq. IV-5)}$$

where:

$\dot{q}_u$ = useful energy collected (watts)
$\dot{m}$ = fluid flow rate (kg/sec)
C_p = fluid specific heat (Joule/kg ^oC)
T_o = outlet temperature (^oC)
T_i = inlet temperature (^oC)
I = direct normal insolation (watts/m^2)
η_{th} = thermal efficiency
A_c = collector area per row

The average fluid temperature is related to the inlet and outlet temperature by:

$$T_f = \frac{1}{2}\ (T_i + T_o) \qquad \text{(Eq. IV-6)}$$

The power required to pump the fluid through a collector row is given by:

$$W_p = 0.189 \frac{\dot{m}\Delta P}{\eta_p} \qquad \text{(Eq. IV-7)}$$

where:

$\dot{m}$ = flow rate (m^3/sec)

ΔP = pressure drop (Pa)

η_p = pump and motor efficiency

W_p = pumping power (watts)

and

$$\Delta P = 0.051 \; f \frac{L}{d} \left(1 + \frac{Le}{L}\right) \rho V^2 \qquad \text{(Eq. IV-8)}$$

where:

L = row length including piping length between collectors (meters)

L_e = equivalent length of elbows, valves, etc. within the row (meters)

d = receiver section diameter (meters)

ρ = fluid density (kg/m^3)

V = fluid velocity (m/sec)

f = friction factor

For a smooth pipe, the friction factor for turbulent flow can be obtained from the relation:

$$f = (0.79 \text{ Ln Re} - 1.64)^{-2} \qquad \text{(Eq. IV-9)}$$

where:

$$Re = \frac{\rho V D}{g \mu} \qquad \text{(Eq. IV-10)}$$

and

D = receiver section diameter (meters)

μ = fluid viscosity (Pa sec)

g = 9.8 kg m/N sec^2

For a given flow rate, inlet temperature, and average insolation, the outlet temperature may be calculated from equation IV-5, and the annual average array temperature from equation IV-6. The yearly collectable energy can now be determined from the curves in Chapter II. The annual available electrical and thermal energy can be obtained from equations IV-11 and IV-12, respectively, in terms of gigajoules/m^2year.

$$Q_e = Q_{avg}\ (0) * \eta_e \qquad \text{(Eq. IV-11)}$$

$$Q_{th} = Q_{avg} * F * \eta_o \qquad \text{(Eq. IV-12)}$$

where $Q_{avg}(0)$ is the yearly collectable energy evaluated at X = 0, and F and η_o were defined in Volume II, Chapter I, for the various collector types.

The annual pumping power is obtained from equation IV-13:

$$W_p\ (\text{annual}) = \frac{W_p}{10^9} * \frac{3600 * 12 * 365}{A_r} \qquad \text{(Eq. IV-13)}$$

where 12 hours/day and 365 days/year of operation has been assumed, and A_r is the area of a collector row. The net electrical output is then obtained from equation IV-14.

$$W_{net} = Q_e - W_p\ (\text{annual}) \qquad \text{(Eq. IV-14)}$$

By adjusting various parameters, such as flow rate through each row and row length, the optimum annual energy output per unit array area can be determined. The flow rate and row length should be chosen so as not to exceed the maximum allowable temperature rise for the particular collector; therefore, the temperature rise has been calculated for the maximum insolation of 1000 watts/m^2.

Plots of annual electrical output, thermal output, and maximum temperature rise for a row of LFF collectors are shown in figures IV-1 through IV-3. These curves were determined for a 20° C inlet temperature. Higher inlet temperatures will lower the electrical and thermal output; however, the temperature rise and optimum flow rates are essentially constant with inlet temperature.

The thermal output of the collectors is essentially independent of flow rate and row length. The net electrical output has a broad maximum, with a peak flow rate of 3×10^{-4} m^3/sec (5 gpm) to 8×10^{-4} m^3/sec (12 gpm), depending on the number of collectors per row and the average annual insolation. Thus, for a given number of collectors in a row (or in a series) as determined by electrical considerations defined in the previous chapter, the maximum temperature rise and optimum flow rate can be determined. For a given inlet temperature, the maximum outlet temperature may be determined and compared to the maximum allowable outlet temperature for the array. The temperature difference can be used to determine the total power loss, due to paralleling groups of collectors at different average temperatures. If this power loss is excessive, a different field layout and collector wiring scheme may be necessary.

In the next section, the optimum flow rate and row length will be used to determine a preliminary heat exchanger size.

C. HEAT EXCHANGER SIZING AND SELECTION

1. Introduction

Many solar applications require heat exchangers because the heat transfer fluid used in the collector field cannot be utilized

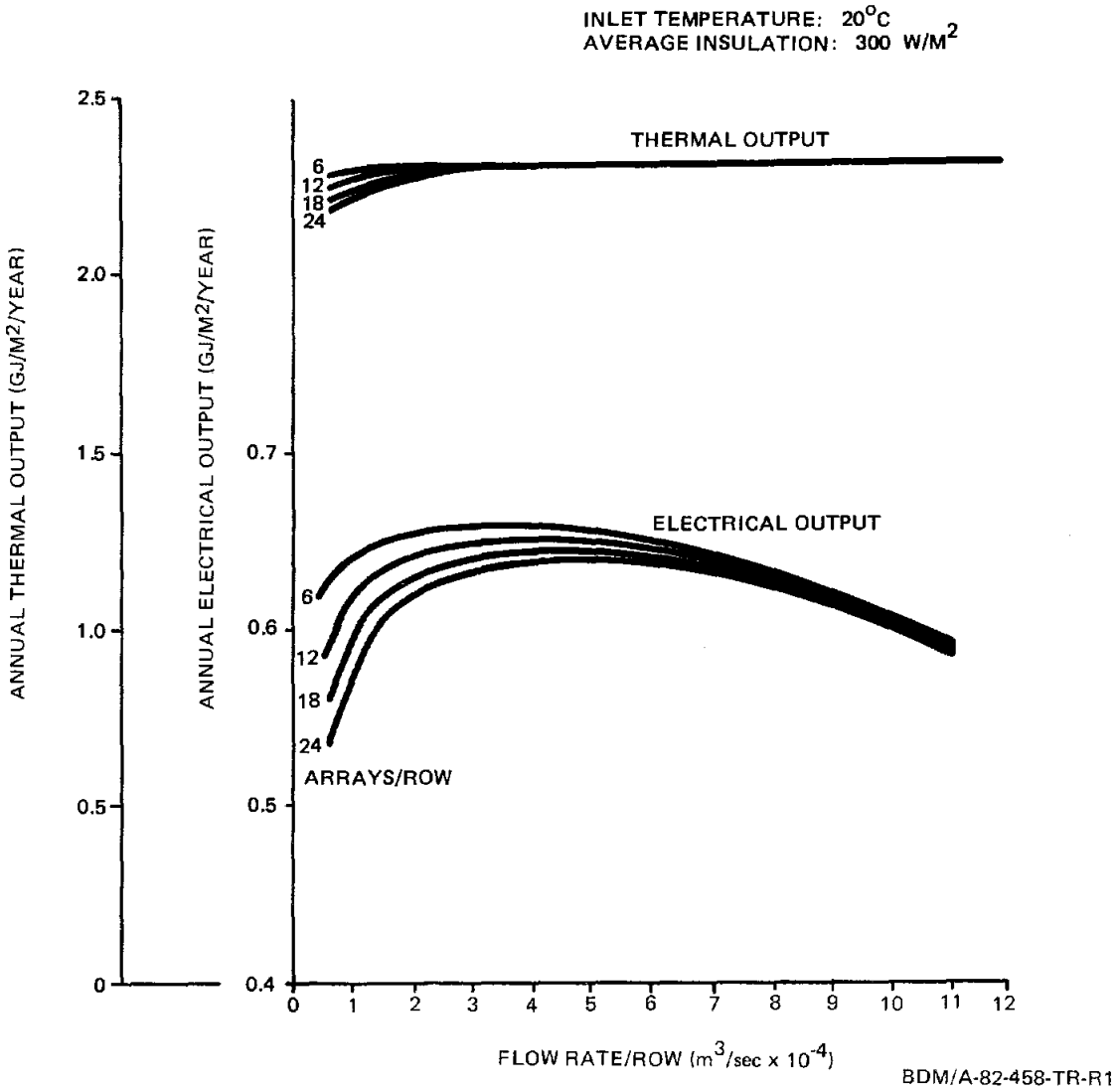

Figure IV-1. Annual Net Electrical and Thermal Energy Available for a Line Focus Fresnel Collector for Various Numbers of 4-Module Arrays/Row

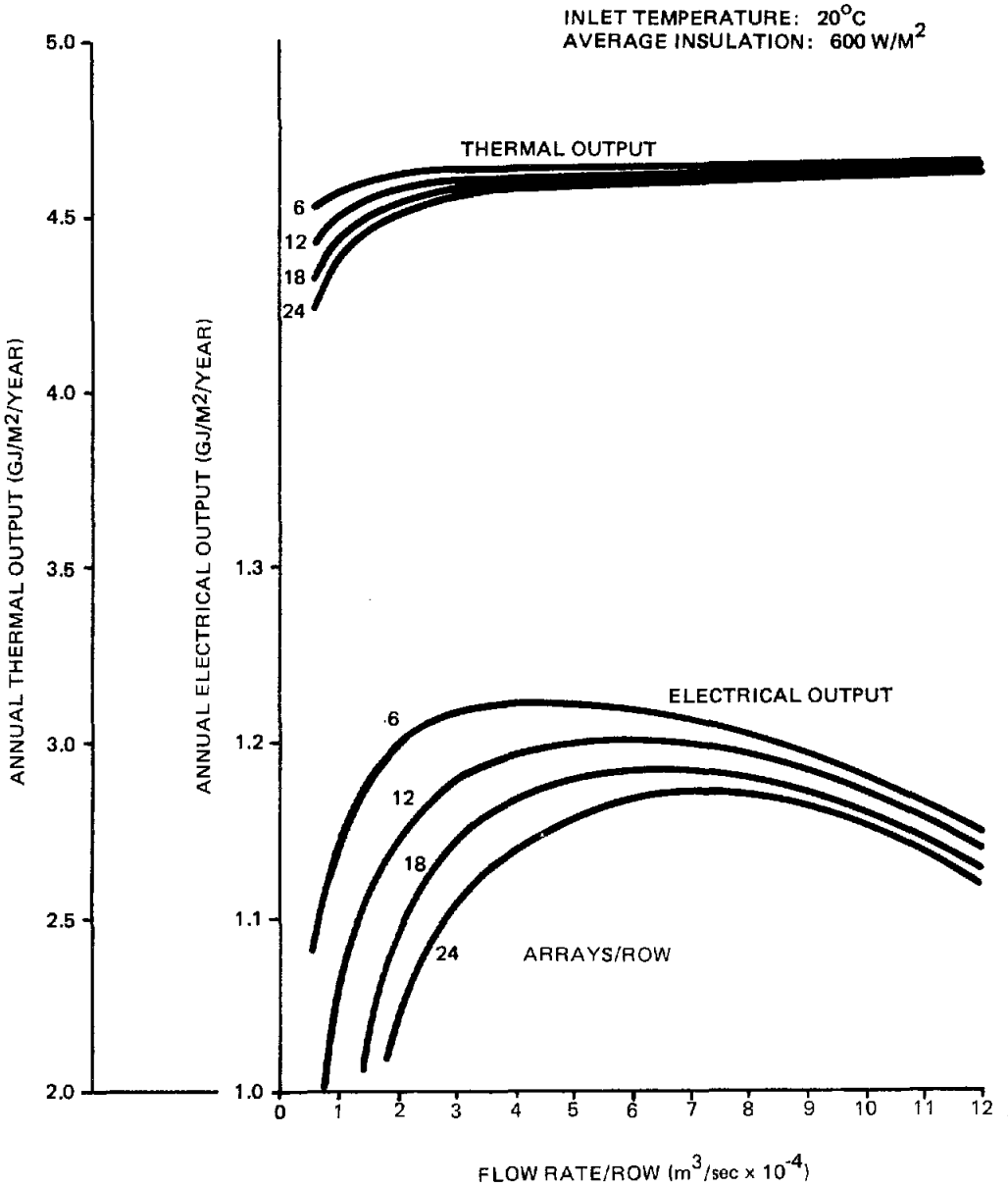

BDM/A-82-458-TR-R1

Figure IV-2. Annual Net Electrical and Thermal Energy Available for a Line Focus Fresnel Collector for Various Numbers of 4-Module Arrays Per Row

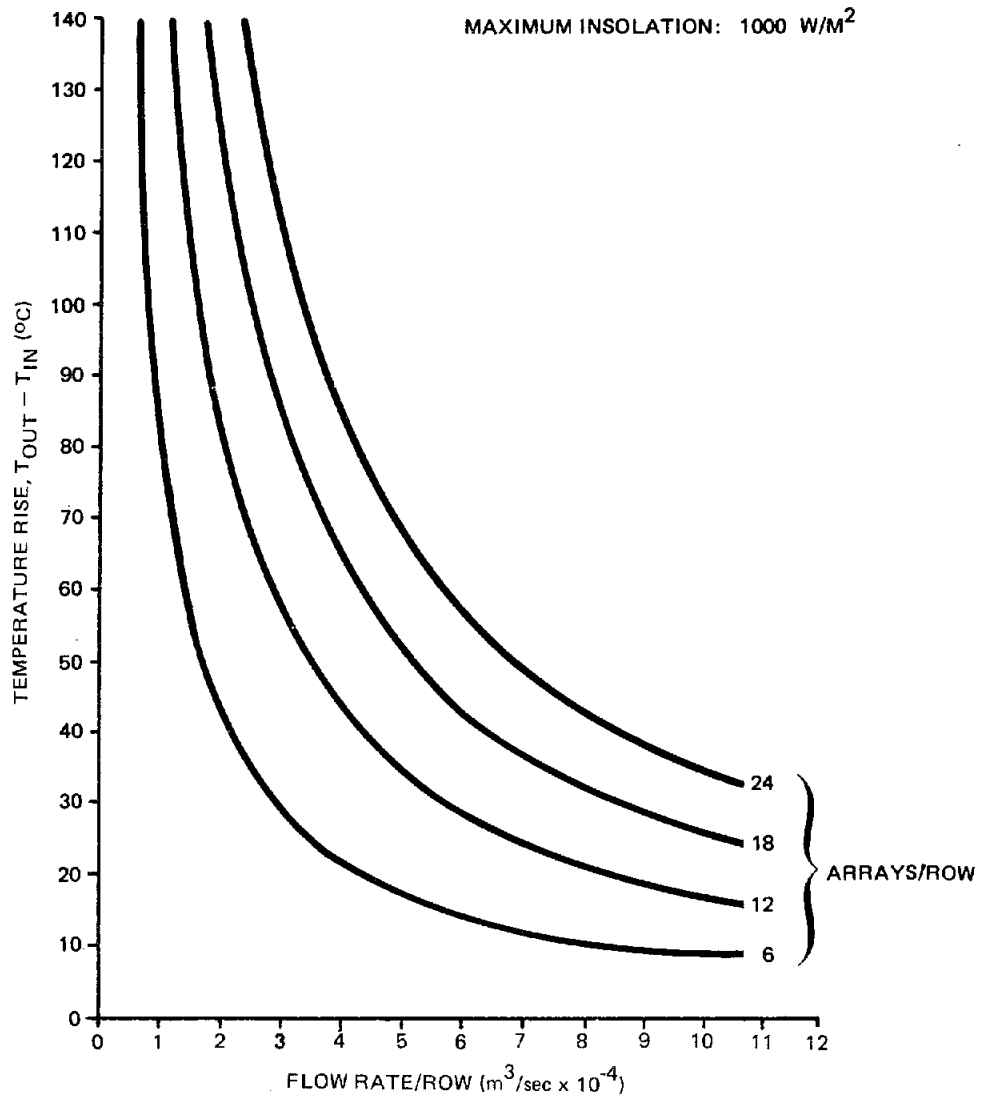

BDM/A-82-458-TR-R1

Figure IV-3. Maximum Temperature Rise Versus Flow Rate and Number of 4-Module Arrays Per Row for the Line Focus Fresnel Collector System

directly in the load process. A closed-loop solar system allows the use of collector fluids that will not freeze and are less corrosive, or less prone to scaling than the process fluid. Possible contamination of the process fluid is another factor in selecting a closed loop system. Incorporating a heat exchanger into a solar system, however, introduces cost penalties associated with the exchanger, auxiliary piping, and increased pumping power associated with the increased system pressure drop across the exchanger. An additional penalty is associated with the approach temperature: if a specified process temperature is required from the heat exchanger, the array must be operated at a higher temperature, which causes an overall decrease in array efficiency. If the array is operated at a low temperature, however, then additional auxiliary heat is necessary to attain the required process temperature. Thus, the objective in designing an exchanger for a solar application, is to select and size the exchanger to optimize overall system thermal performance, pumping power penalties, and heat exchanger capital and maintenance costs.

Two generic types of heat exchangers are available for the low pressure and temperature PV-T application--tubular and plate type heat exchangers. The shell-and-tube is the most commonly used tubular type heat exchanger. This type consists of a cylindrical shell with a bundle of tubes passing from one end to the other (figure IV-4). One stream passes through the tubes and the other through the shell, with heat transfer occuring through the tube walls.

Appreciable savings in cost, weight, and space may be gained with plate exchangers. The plate-and-frame is the most commonly used, and consists of a series of plates tightly squeezed together in a frame with gasketing to prevent external leakage and leakage between plates. In operation, the hot and cold streams flow in alternating interplate spaces, with heat transfer taking place through the plates (figure IV-5).

The two heat exchangers are compared in table IV-1, and discussed in more detail in the following sections. A general cost comparison is provided in figure IV-6 which indicates that a tubular

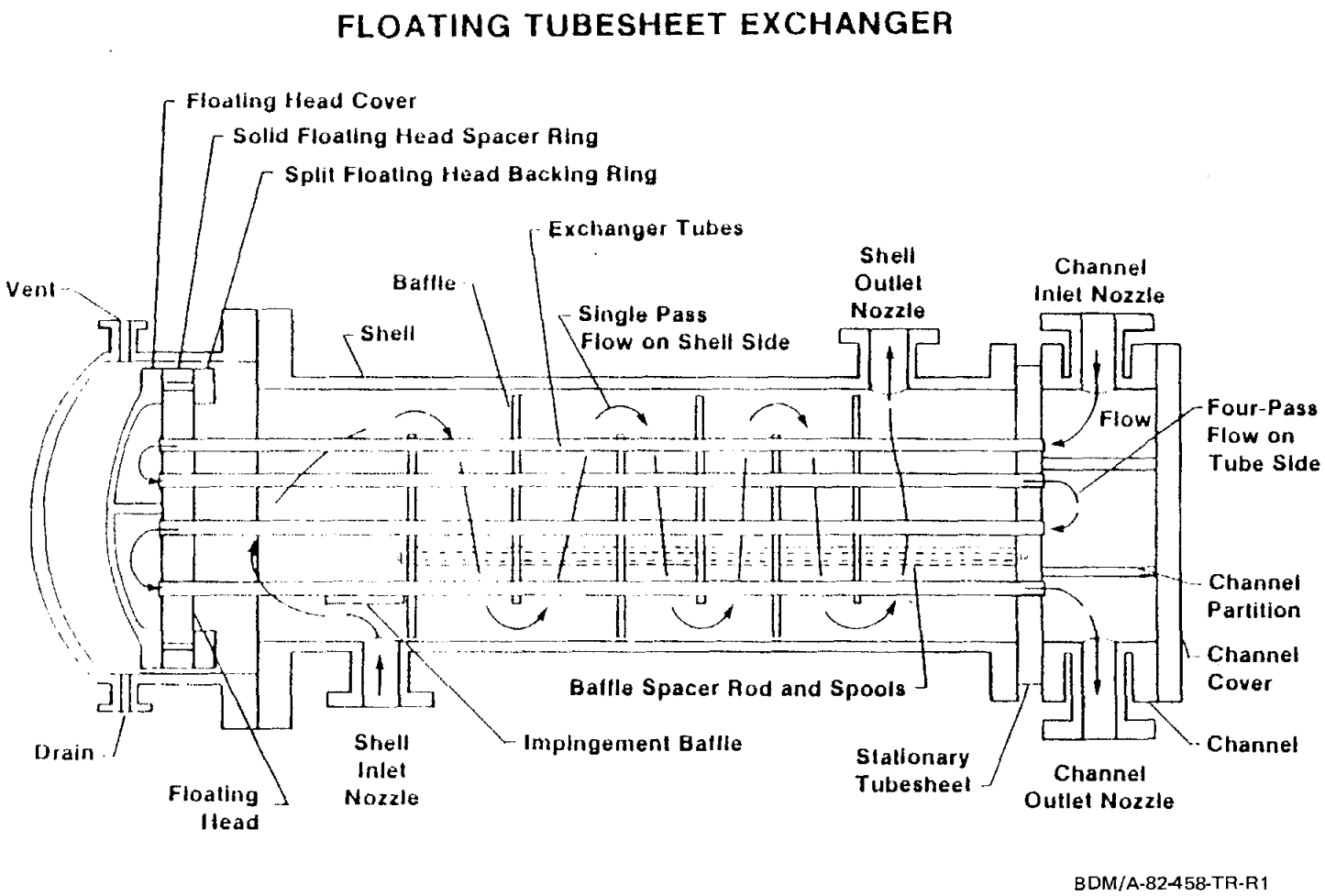

Figure IV-4. Floating Tubesheet Exchanger (ref. II-11, Volume I)

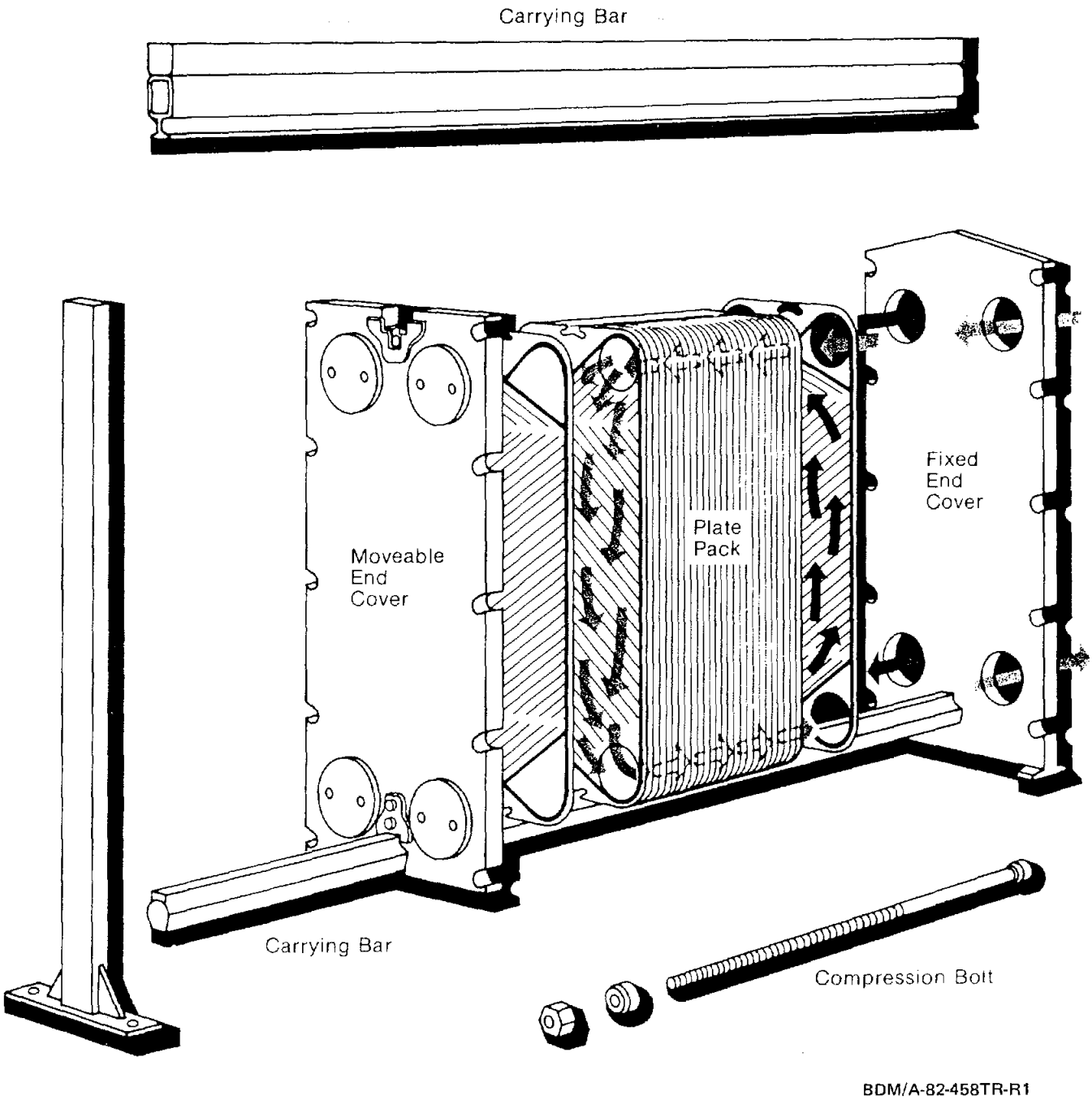

Figure IV-5. Plate and Frame Heat Exchangers (Courtesy of Alfa-Laval)

TABLE IV-1. QUALITATIVE COMPARISON OF SHELL AND TUBE AND PLATE HEAT EXCHANGERS

	P & F	S & T
PRESSURE RATING	LOW	HIGH
TEMPERATURE RATING	ANY PV-T APPLICATION	ANY PV-T APPLICATION
SPACE REQUIREMENTS		
OPERATION	SMALL	MODERATE
MAINTENANCE	SMALL	LARGE
MATERIALS OF CONSTRUCTION	ANY EXCEPT CARBON STEEL	ANY
FLUID HEAD LOSS	LOW	MODERATE
EFFICIENCY	HIGH	MODERATE TO HIGH--REQUIRES TRADE-OFF WITH HEAD LOSS
MAINTENANCE	EASY	DIFFICULT
COST	MODERATE	LOWER FOR MILD STEEL CONSTRUCTION--HIGHER FOR OTHER MATERIALS

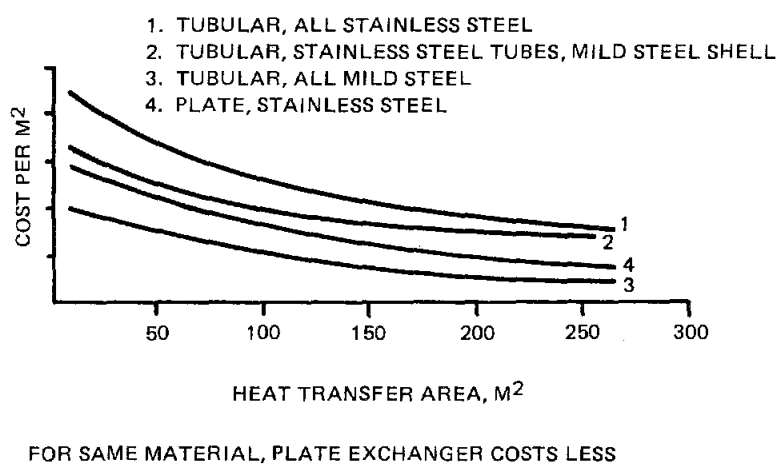

Figure IV-6. Cost Comparison of Plate and Shell-and-Tube Heat Exchangers (Excerpted by Special Permission from CHEMICAL ENGINEERING (Aug. 11, 1980) Copyright 1980, by McGraw-Hill, Inc., New York, NY, 10020).

exchanger of mild steel (or carbon steel) construction is less expensive than a plate exchanger on a cost per unit area basis. However, if the application requires corrosion resistant materials, the plate exchanger becomes more economical. Another consideration is that the required heat transfer area of a plate exchanger is usually less than that of a tubular exchanger, thereby decreasing the total exchanger cost. Before the various design and evaluation techniques are developed, a description of the heat exchangers would be useful.

2. Types of Heat Exchangers

Tubular and plate heat exchangers are the subject of this section. These exchangers are most appropriate for solar applications where the fluids are not corrosive, and liquid is on both sides of the exchanger.

a. Tubular Heat Exchangers

There are more tubular heat exchangers in use than any other type because they offer the widest variety of sizes and styles, and the technology and manufacturing capability is well established. The widespread use of tubular exchangers, their relatively low cost, their familiarity with users, and many years of satisfactory service are reasons they are chosen for most new developments.

Although tubular exchangers are designed for various duties including liquid/gas, gas/gas, condensing and boiling, the PV-T application is liquid/liquid. Hot fluid from the array, either oil or more typically, ethylene glycol and water, is on one side of the exchanger and is used to heat the process water. Both fluids are pumped through the heat exchanger, so the principal mode of heat transfer is forced convection. The high density of liquids results in very high rates of heat transfer, so there is little incentive to use fins or other devices to enhance the heat transfer.

Two types of tubular heat exchangers are appropriate for PV-T applications--double-pipe and shell-and-tube exchangers. The double pipe exchanger, shown in figure IV-7, consists of a central tube contained within a larger tube and is widely used for small capacity

systems. Typically, if the surface area falls in the range of $2m^2 \leq A \leq 50\ m^2 (\approx 20\ ft^2 \leq A \leq 500\ ft^2)$, then double pipe units should be considered. Pure counterflow can be achieved in such units, thereby providing close approach temperatures and high exchanger effectiveness. It is fairly inexpensive, easy to manufacture, and offers great flexibility since it can be made any length, and the tubes can be selected from a wide variety of sizes and materials. Such exchangers are usually operated with high temperature and pressure, and high density or corrosive fluid in the small inner tube, and the less demanding fluid (water) in the outer tube. This minimizes the requirements for thick-wall, expensive alloy materials for the larger outer tube.

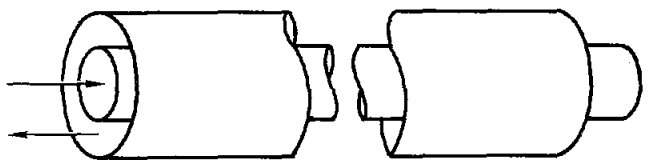

BDM/A-82-458-TR-R1

Figure IV-7. Double-Pipe Heat Exchanger

Occasionally, to increase capacity or reduce the length required, more than one internal tube is incorporated within the outer tube enclosure. The most common form of multi-tubular heat exchangers is the shell-and-tube exchanger shown in figure IV-4. These systems are typically used when areas greater than $50\ m^2$ ($\approx 500\ ft^2$) are required.

Shell-and-tube heat exchangers are available in a variety of designs, three of which are shown in figures IV-8, IV-9, and IV-10. Differences between the various types of exchangers include design or construction features which facilitate cleaning the inside or outside tube surfaces, and to accommodate differential thermal expansion. Each type of exchanger has its advantages and limitations.

The fixed tubesheet design has a low initial cost and the individual tubes are replaceable and easily cleaned; however, the unit is sensitive to temperature excursions and cycling, producing differential expansion between the tubes and shell.

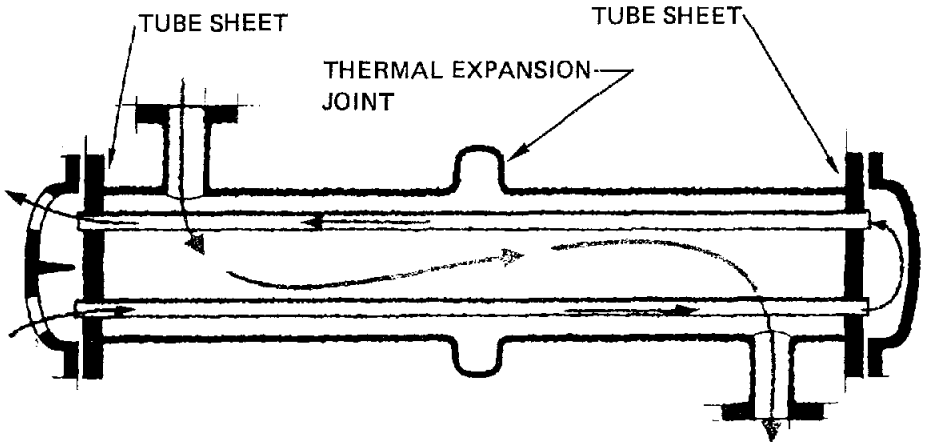

Figure IV-8. Fixed Tube Sheet Design

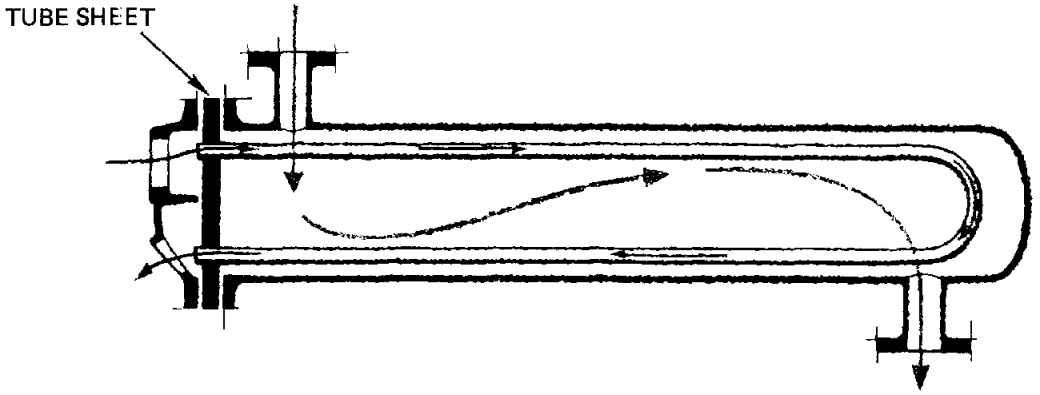

Figure IV-9. "U" Tube Design

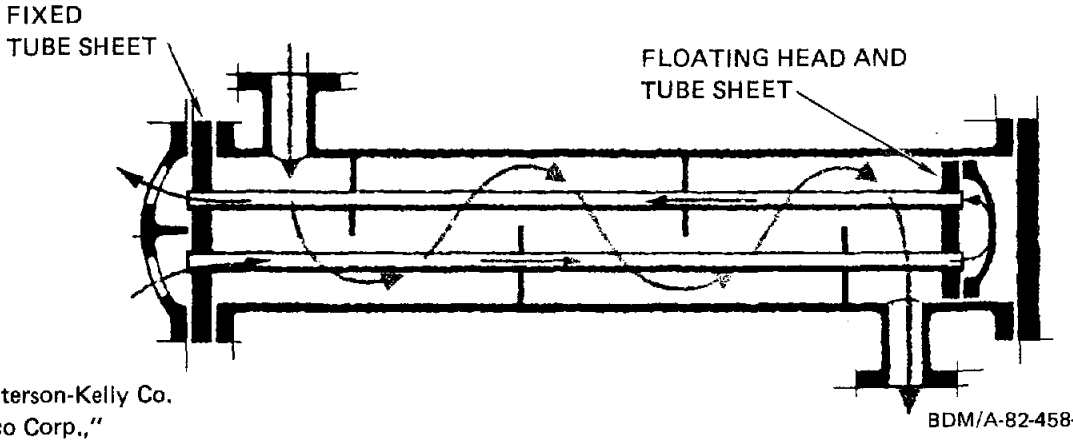

"Courtesy of Patterson-Kelly Co. Division of Harsco Corp.,"

BDM/A-82-458-TR-R1

Figure IV-10. Floating Head Pull-Through Bundle Type

The U-tube design also has a low first cost since it employs only one header and one tubesheet, and no expansion joint is required, as the tubes can expand without creating thermal stresses. This design is usually restricted to clean tubeside service due to the difficulty in cleaning.

Floating head designs are widely used for fluids that have fouling tendencies on both shellside and tubeside, since the tube bundle is removable. This exchanger can also accommodate differential tube bundle expansion; however, it is more costly than the fixed tubesheet or U-tube designs.

A great variety of shellside and tubeside flow arrangements are used in tubular exchangers. The arrangement chosen represents a compromise between the maximum temperature differentials between fluids, costs, pressure drops, fouling of heat exchanger surfaces, the desired heat exchanger effectiveness, and space limitations. Axial counterflow is the ideal configuration from thermal considerations, since in this arrangement the temperature differential between the fluids is minimal, and very high thermal effectiveness values can be achieved. In cocurrent flow, the hot fluid cannot be cooled below the cold fluid outlet temperature; thus, the ability to recover heat with cocurrent flow is limited. In either case, space limitations may prevent the use of such an exchanger, and the requirement for baffles to support the tubes will disrupt the uniform parallel shellside flow.

In addition to the single pass arrangement, various multipass flow arrangements are possible. In these exchangers there is a combination of cocurrent, countercurrent, and crossflow, resulting in a temperature difference greater than that for counterflow, but less than that for cocurrent flow. One of the most common multipass systems is the simple U-tube bundle with two tube passes and one shell pass. This provides a shorter, thicker equivalent to the single tube/single shell pass counterflow exchanger, with the advantage that all fluid connections are at one end of the exchanger. Large exchangers with as many as four tube passes and one or two shell passes are available, but greater

thermal effectivess can be achieved by combining two exchangers in series or parallel.

As indicated previously, baffles are used on the shellside for tube support as well as increasing the turbulence, and therefore, the heat transfer ability of the shellside fluid. There are many alternatives available regarding baffle arrangement and baffle type. The segmented baffle is the most common, and provides a high degree of turbulence and good heat transfer rates for the pressure drop and power consumed. Segmented baffles are simply discs with a segment removed. Baffle cuts are expressed as a percentage of total baffle diameter cut out. A 20 percent diameter cut is considered optimum because it permits the highest heat transfer for a given pressure drop. Segmented baffles are arranged so the cut edges of alternate baffles are at 180°, thereby causing the shellside fluid to flow over the tubes in crossflow as it progresses axially down the shell. Recommended maximum baffle spacing is the shell diameter, or 0.76 m (30 in), whichever is smaller. Recommended minimum spacing is one-fifth shell diameter or 5.08 cm (2-in), whichever is larger. In the majority of cases the baffle spacing ranges from 0.3 to 0.5 times the shell diameter.

Baffles have hole patterns identical to the end tube sheets to support the tubes. The tubes are generally arranged on a triangular, square, or rotated square pattern (figure IV-11). Triangular tube patterns provide better shellside heat transfer coefficients in sensible heat exchangers, and more surface area for a given shell diameter. Square-pitch tube patterns are generally used when mechanical cleaning of the outside of the tubes is necessary or expected. Square and rotated-square tube patterns, however, provide lower pressure drops, and therefore, correspondingly lower heat transfer coefficients.

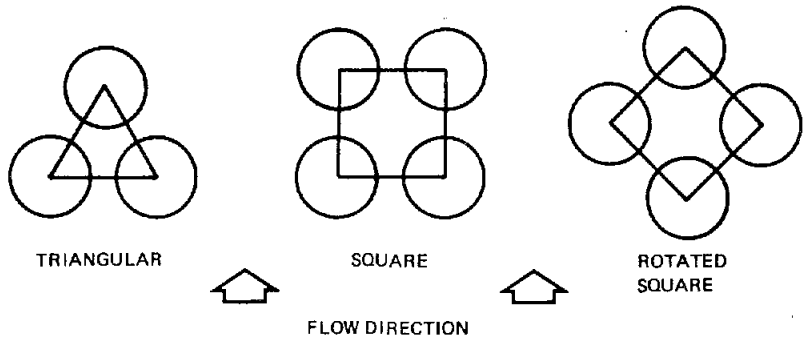

BDM/A-82-458-TR-R1

Figure IV-11. Tube Arrangements Used for Shell-and-Tube Heat Exchangers

Heat exchangers with small-diameter tubes 1.59 to 2.54 cm or (5/8-in to 1-in OD) are generally more economical than designs with larger tubes because the smaller tubes provide a more compact unit. However, the use of such small tubes may be prohibited if the allowable tubeside pressure drop is low. Under equal velocity conditions, smaller tubes increase the heat transfer coefficient as well as the pressure drop.

The selection of which fluid to pass on the shellside and which on the tubeside, involves a number of factors and is generally a compromise of conflicting requirements. Some considerations include:

(1) Pressure. The wall thickness required (and therefore, the weight and cost of the material) to contain a given pressure increases directly with the diameter. Hence, high pressure fluids should be contained in the tubes.

(2) Temperature. High temperatures reduce the permissible stress levels of materials, so a greater wall thickness is required. The effect is similar to pressure, so the high temperature fluids should be in the tubes. Moreover, if the high temperature fluid is in the shell, additional insulation may be required to conserve energy, or for safety considerations.

(3) Corrosive Fluids. Corrosive fluids require the use of special, and therefore, expensive alloys or other materials. If only one of the fluids is corrosive, passing it through the tubes

will eliminate the need for an expensive alloy shell. Both tubes and shells of corrosion resistant material will be required if the corrosive fluid is in the shell.

(4) Uncontaminated Fluids. Processes with above-average requirements for cleanliness may require the use of special materials. It will be less costly to provide special tubes, than both tubes and shell.

(5) Hazardous or Expensive Fluids. Fluid leakage is less likely from tubeside than shellside in most types of exchangers.

(6) Pressure Drop. For the same pressure drop, higher heat transfer coefficients are obtained on the tubeside. A fluid with a low allowable pressure drop should generally be placed inside the tubes.

(7) Fluid Viscosity. To maximize heat transfer, both fluids should be in turbulent flow. Fluids of high viscosity may be laminar in the tubes, but turbulent in the shell (depending on the clearance space between the tubes). If the flow is laminar in both shell and tubes, the more viscous fluid should be in the tubes, since more reliable heat transfer and flow distribution predictions can be made.

(8) Mass Flow. In general, it is better to put the fluid with the lower mass flow on the shellside. Turbulent flow is obtained at lower Reynolds numbers on the shellside. Furthermore, the complexity of multipass construction may be avoided with a consequent improvement in exchanger effectiveness.

(9) Cleaning. The shell inner surface and tube outer surface are more difficult to clean than the tube internal surface. Therefore, the cleanest fluid should be put through the shell.

b. Plate Heat Exchangers

Plate heat exchangers are used less often than tubular exchangers, but have characteristics that offer significant advantages over shell and tube exchangers for certain applications. There are several types of plate exchangers, but the plate-and-frame is the most applicable for a liquid/liquid PV-T application.

A plate exchanger consists of a frame and corrugated, or embossed metal plates. The frame includes a fixed plate, pressure plate, pressing arrangement, and connecting ports. A series of plates are clamped together so the corrugations interlock to form narrow flow channels, which produce turbulence even at low velocities. The corrugation also increases the rigidity of the thin plate, enabling it to better withstand distortion from high pressure. The numerous support points also minimize pressure deflection.

Turbulence is achieved in plate exchangers at Reynolds numbers from 10 to 500 (in smooth-pipe laminar flow, Reynolds numbers range up to 2,100) because the corrugation breaks down the stagnant insulating film at the heat transfer surface. This, combined with the thin plate and lower fouling factor, contributes to the plate exchanger's higher heat transfer coefficients than those of the shell-and-tube exchanger at the same Reynolds number flowrate. Overall heat transfer coefficients of 2270 $W/m^2\ {}^oC$ to 5674 $W/m^2\ {}^oC$ (400 to 1000 BTU/hr $ft^2\ {}^oF$) can be obtained. Temperature approaches of the plate exchanger can be as low as 1^oC, making it ideal for high recovery of energy, whereas the practical limit for the shell-and-tube exchanger is about 5^oC. The number and size of heat transfer plates chosen depends on the flowrate, temperature changes, allowable pressure drop, and physical properties of the fluids.

Gaskets allow the two fluids to be arranged in countercurrent flow, and flow volumes can be divided into a number of parallel streams. They also seal the plates at their outer edges and around the ports, which are designed so the inlet port can be at the top or bottom. Furthermore, gaskets provide a double seal between the liquid streams, making mixing impossible. The interspace between the seals is vented into the atmosphere, giving a visual indication of leakage and an escape path for the fluid. Manufacturers have evolved proprietary corrugations and embossed patterns for optimizing heat transfer and pressure drop characteristics. Plate size and thickness and frame design are, therefore, related to the particular type of corrugated or embossed pattern.

At present, there are no common plate-exchanger design standards comparable to those of the Tubular Exchanger Manufacturers Association (TEMA) for shell-and-tube exchangers. Plates can be made from material that can be cold worked, regardless of its welding characteristics. Common plate materials include stainless steel, titanium, nickel, Monel, Incoloy 825, Hastelloy C, phosphor bronze, and cupro-nickel. Titanium-stabilized materials provide greater corrosion resistance. Plate thicknesses range from 0.5 to 3 mm. Average gaps between the plates run from 1.5 to 5 mm, giving typical hydraulic diameters of 4 to 10 mm. Plate sizes vary from 0.03 to about 1.5 m^2. Total surface areas extend from 0.03 to about 1,500 m^2. The largest plate exchanger available handles flows to 2,500 m^3/hr (11,000 gpm).

Although the plate heat exchanger has operating limitations for the chemical process industry, the requirements of a PV-T application are well below these limits. The upper limit on operating pressure is determined by the end plates and gaskets and is currently about 2.4 MPa (350 psi). The gasket material limits the maximum operating temperature to about 250°C.

Some of the possible flow patterns in plate exchangers are illustrated in figure IV-12: (a) series flow, in which a continuous stream changes direction after each vertical path; (b) parallel flow, in which the stream divides and then reconverges; (c) a loop system, in which both streams flow in parallel; and (d) a combined series-parallel flow. In the latter case, one stream has a flow rate twice that of the other stream. The number of parallel passages is set by the exchanger output and the allowable pressure drop. Of course, the larger the number of parallel passages, the lower the pressure drop. The number of series passages is determined by plate efficiency and heat exchanger requirements. Pure countercurrent flow can be achieved in looped-flow when both streams have nearly the same flow rates. If the flow rates differ significantly, however, then alternative multipass arrangements may be necessary as indicated in figure IV-12(d). In such a situation, the effectiveness is decreased since the flow is now a combination of countercurrent and cocurrent flows.

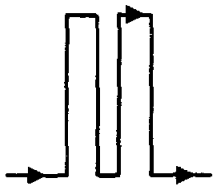

a. SERIES FLOW

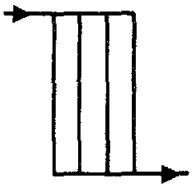

b. PARALLEL FLOW

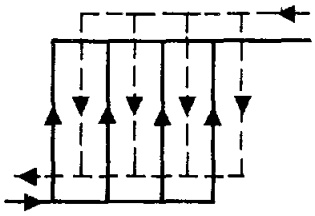

c. LOOPED FLOW
1 PASS/1 PASS
4 CHANNELS/PASS
7 THERMAL PLATES
9 PLATES TOTAL

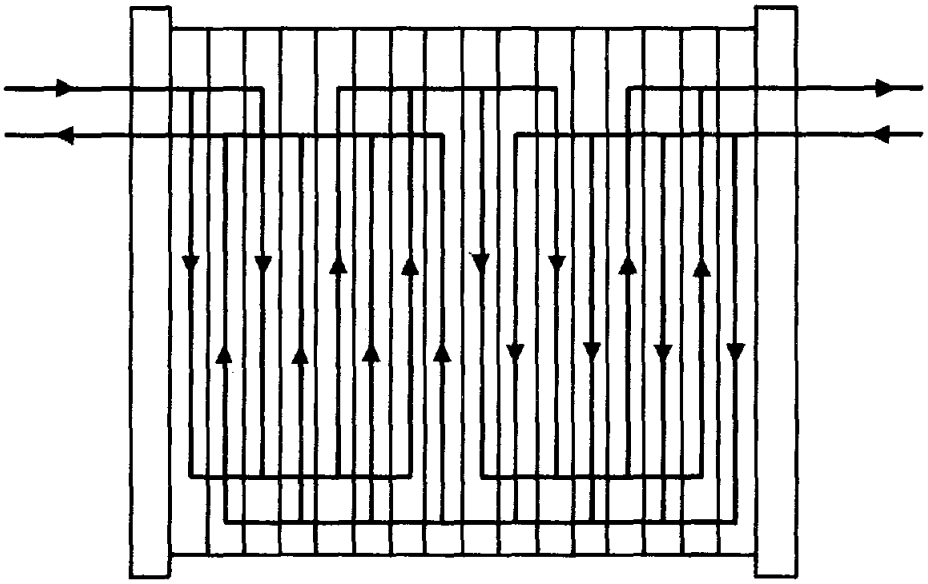

d. COMPLEX FLOW
4 PASS – 2 CHANNELS/PASS
2 PASS – 4 CHANNELS/PASS
13 THERMAL PLATES
15 PLATES

BDM/A-82-458-TR-R1

Figure IV-12. Plate Heat Exchanges Flow Patterns

Pressure drop is another important parameter; limits are normally imposed by both process and pumping cost limitations. The most economic designs are normally obtained by utilizing the maximum available pressure drop, while achieving the highest practical heat transfer coefficient. The number of passes in a heat exchanger should be kept as low as possible to make the most effective use of pressure drop as return bends increase the pressure drop without contributing to heat transfer. The advantage of modern plate exchangers in this respect is that they can be designed for most duties, such as single pass units, using variable geometry plates. The limiting flow factor for gasketed plate heat exchangers can be pressure drop losses in connections, as maximum connection sizes up to 0.4 m (16-in) are presently commercially available. It can be demonstrated that optimum economic conditions are achieved when pressure drops of 2×10^4 to 1×10^5 Pa (3 to 15 psi) per heat transfer unit are employed.

A major advantage of plate and frame heat exchangers is the accessibility of the heat exchanger surface. The movable cover may be rolled back along the frame and the plates separated for inspection and cleaning. The high turbulence in a plate exchanger also minimize fouling compared to tubular exchangers. These two factors minimize maintenance costs. Other advantages of plate and frame exchangers include:

(1) Only one-third to one-half the surface area for heat transfer is required so that savings in cost can be realized. The reduced surface area comes about due to the relatively high turbulence achieved in the corrugated flow paths between the plates, and increased exchanger effectiveness because of true countercurrent flow and because of reduced fouling (claimed to be one-tenth to one-third that of shell-and-tube exchangers) as a result of the turbulent fluid action and polished surface finish of the plates.

(2) The reduced surface areas necessary permit substantial savings in the space required for plate and frame heat exchangers. Little clearance space around the exchanger is required to

facilitate dismantling for cleaning, compared with the exchanger length required to permit withdrawing a tube bundle.

(3) The improved exchanger effectiveness from countercurrent flow, results in closer approach temperatures, a particularly significant feature in heat recovery systems.

(4) The thermal rating of the plate and frame exchanger can be readily increased or decreased by varying the number of plates. This is a most attractive feature for systems likely to involve substantial future changes in load.

(5) The internal void volume of a plate and frame heat exchanger is only 10 to 20 percent of the equivalent tube and shell exchanger. Less process media is involved so that better process control and faster response times can be achieved.

(6) The reduced surface requirement and volume of fluid contained, combine to reduce the gross mass of the plate and frame exchanger to approximately one-sixth of the equivalent shell and tube exchanger. Further savings result from lower shipping, installation, and foundation costs.

3. Heat Transfer Relations

The heat transferred across a heat exchanger, Q(watts) is given by:

$$Q = \dot{M}_a C_{pa} (T_{h,i} - T_{h,o}) = \dot{M}_l C_{pl} (T_{c,o} - T_{c,i}) \quad \text{(Eq. IV-15)}$$

where $\dot{M}_a$, $\dot{M}_l$ are mass flow rates; C_{pa}, C_{pl} are specific heats; $T_{h,i}$, $T_{c,i}$ are inlet temperatures; and $T_{h,o}$, $T_{c,o}$ are outlet temperatures on the array (hot) side, and load (cold) side, respectively. A capacity rate can be conveniently defined as:

$$W_a = \dot{M}_a C_{pa}$$

(Eq. IV-16)

$$W_l = \dot{M}_l C_{pl}$$

For a heat exchanger of infinite area, the heat transferred would be a maximum given by

$$Q_{max} = W_{min} (T_{h,i} - T_{c,i}) \qquad \text{(Eq. IV-17)}$$

where W_{min} is the minimum of the two capacity rates.

The exchanger heat transfer effectiveness is defined as the ratio of actual heat transferred across the heat exchanger, to the maximum possible heat transfer. Thus:

$$\varepsilon = \frac{Q}{Q_{max}} = \frac{W_a (T_{h,i} - T_{h,o})}{W_{min} (T_{h,i} - T_{c,i})} = \frac{W_l (T_{c,o} - T_{c,i})}{W_{min} (T_{h,i} - T_{c,i})}$$

(Eq. IV-18)

The number of heat transfer units, NTU, is a nondimensional expression of the "heat transfer size" of the exchanger and is defined as:

$$NTU = \frac{UA}{W_{min}}$$

where U is the overall average heat transfer coefficient of the heat exchanger based on the heat transfer area A. The effectiveness is related to NTU and the capacity rate ratio, as indicated in figure IV-13 and equation IV-19 for countercurrent flow conditions. This relationship depends on the particular heat exchanger geometry, and relations for a

large variety of geometries are given in reference IV-1.

$$\varepsilon = \frac{1 - e^{-NTU(1 - R)}}{1 - Re^{-NTU(1 - R)}} \qquad \text{(Eq. IV-19)}$$

where:

$$R = \frac{W_{min}}{W_{max}}$$

If the flow capacity rates on both sides of the exchanger are equal then:

$$\varepsilon = \frac{NTU}{1 + NTU} \qquad \text{(Eq. IV-20)}$$

From figure IV-13 one can see that when NTU is small, the exchanger effectiveness is low, and as NTU increases, the effectiveness approaches assymptotically the limit imposed by the flow arrangement and thermodynamics. Increasing the NTU incurs a cost, as indicated by equation IV-18. The costs may be in terms of capital costs and space as the transfer area increases, or in terms of pumping power costs as the pressure drop increases to obtain a higher overall heat transfer coefficient.

The friction factor and, therefore, the pressure drop, is related to the convective heat transfer coefficient; however, this relationship depends on the flow geometry. These relations, and methods of calculating heat transfer coefficients, will be discussed in the following sections for particular exchanger geometries.

Another technique for calculating the heat transfer between fluids is the log-mean-temperature approach where the heat transferred is given by:

$$Q = U\ A\ F\ \ \Delta T_{LM} \qquad \text{(Eq. IV-21)}$$

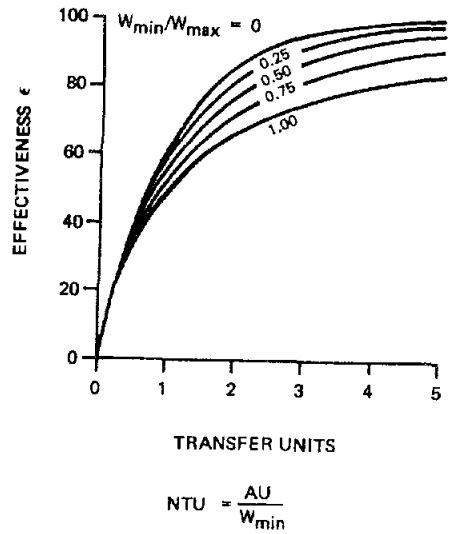

BDM/A-82-458-TR-R1

Figure IV-13. Heat Transfer Effectiveness as a Function of Number of Transfer Units and Capacity Rate Ratio; Counterflow Exchanger

where U is the overall heat transfer coefficient ($W/m^2\ {}^oC$) based on a heat transfer area A and ΔT_{LM} is the log-mean-temperature difference (LMTD) given by:

$$\Delta T_{LM} = \frac{(T_{h,i} - T_{c,o}) - (T_{h,o} - T_{c,i})}{\ln\left(\frac{T_{h,i} - T_{c,o}}{T_{h,o} - T_{c,i}}\right)} \qquad \text{(Eq. IV-22)}$$

An equivalent definition of NTU, based on the LMTD, is given in equation IV-23 where ΔT is the maximum temperature difference for either of the flow streams (i.e., the difference between the inlet and outlet of the stream with the minimum capacity rate).

$$NTU = \frac{\Delta T}{\Delta T_{LM}} \qquad \text{(Eq. IV-23)}$$

The factor F in equation IV-21 is a correction factor to account for various combinations of countercurrent, cocurrent, and cross-flow in multipass exchangers. In pure countercurrent flow, F equals unity. Graphs for determining F are given in reference IV-2 for several flow geometries for shell-and-tube exchangers. LMTD correction factors for multipass plate exchangers are given in reference IV-3.

a. Shell and Tube Exchangers

Typical values for overall heat transfer coefficients for fluids likely to be used in PV-T industrial or commercial applications are shown in table IV-2 for shell-and-tube exchangers. The overall heat transfer coefficient is based on the exterior tube surface and can be defined as:

$$\frac{1}{U_o} = \frac{D_o}{h_i D_i} + \frac{D_o}{2k} \ln \frac{D_o}{D_i} + \frac{1}{h_o} + \frac{R_{f,i} D_o}{D_i} + R_{f,o}$$

(Eq. IV-24)

where:

D_o, D_i = outside and inside tube diameters
h_o, h_i = outside and inside heat transfer coefficients
k = tube wall thermal conductivity
$R_{f,o}$, $R_{f,i}$ = outside and inside fouling factors
U_o = overall heat transfer coefficient

TABLE IV-2. TYPICAL OVERALL HEAT TRANSFER COEFFICIENTS FOR TUBULAR EXCHANGERS

TUBESIDE FLUID	SHELLSIDE FLUID	OVERALL HEAT TRANSFER COEFFICIENT $W/m^2{}^oC$	(BTU/hr $ft^2{}^oF$)
WATER	WATER	1136 - 1420	(200 - 250)
WATER	DEMINERALIZED WATER	1700 - 2840	(300 - 500)
HEAT TRANSFER OIL	WATER	284 - 710	(50 - 125)
ETHYLENE GLYCOL/ WATER MIXTURE	WATER	680 - 965	(120 - 170)

Fouling factors account for the reduced heat transfer efficiency due to scaling and will be discussed in a later section. The thermal conductivity of the tube material is readily available. Typical materials include mild steel (45 W/m ^{o}C), stainless steel (16.3 W/m ^{o}C), and brass (104 W/m ^{o}C).

The inside heat transfer coefficients can be calculated using the Dittus-Boelter equation:

$$Nu_i = \frac{h_i D_i}{k} = 0.023\ Re_i^{0.8} Pr_i^{0.33} \qquad \text{(Eq. IV-25)}$$

where Pr is the Prandtl number, and:

$$Re_i = \frac{\rho_i V_i D_i}{\mu_i} \qquad \text{(Eq. IV-26)}$$

ρ_i = density of the fluid inside the tubes
μ_i = viscosity of the fluid inside the tubes
V_i = fluid velocity

This relation assumes turbulent flow inside the tubes (Re > 2100). Turbulent flow should be a requirement for heat exchanger design since heat transfer is most efficient under turbulent conditions.

The calculation of the shellside heat transfer coefficient is more complicated and is highly dependent on the flow geometry (ref. IV-4). This outside coefficient is calculated from equation IV-27 where the factor 0.6 accounts for deviations from true crossflow due to baffle leakage and tube bypassing.

$$h_o = (0.33)(0.6)\ \frac{k}{D_o}\left(\frac{D_o G_s}{\mu}\right)^{0.6}\left(\frac{C_p \mu}{k}\right)^{0.33} \qquad \text{(Eq. IV-27)}$$

where:

k = shellside fluid thermal conductivity

D_o = tube outside diameter

μ = shellside fluid viscosity

C_p = shellside fluid specific heat

G_s = mass flow rate per unit of free area ($\dot{M}_s/a_s$)

$\dot{M}_s$ = total shellside mass flow rate

a_s = open area for crossflow

$$a_s = \frac{D_s \; C \; B}{P} \qquad \text{(Eq. IV-28)}$$

D_s = inside shell diameter

$$D_s \approx 1.75 \; D_o (nN_{pt})^{0.47} \qquad \text{(Eq. IV-29)}$$

C = minimum tube spacing

$$C = P - D_o \qquad \text{(Eq. IV-30)}$$

P = tube pitch

B = baffle spacing

n = number of tubes per pass

N_{pt} = number of tube passes per shell

For both triangular and square pitch arrangements, the tube pitch may be assumed to be 1.25 times the tube outer diameter. This is a standard pitch used in the majority of shell-and-tube heat exchangers. The shell diameter determined from equation IV-29 is for a floating head exchanger. The diameter will differ slightly for a fixed tubesheet, U-tube, or multipass shell; however, for initial calculations equation IV-29 is adequate.

The pressure drop in the exchanger is as important as the heat transfer. Increasing the flow rate on the tube or shellside, increases both the heat transfer coefficient and the pressure drop across the exchanger. Increasing the pressure drop produces an increasing parasitic power loss on the PV array output. Therefore, a trade-off must be made between the heat transferred and the parasitic pumping power in the exchanger. Empirical pressure drop relations have been developed for initial rating of heat exchangers (ref. IV-5), and are reproduced in equations IV-31, IV-32, and IV-33. These empirical relations were developed in English units since these are the usual units used by U.S. manufacturers and design engineers.

Tubeside for $2100 \leq Re \leq 10{,}000$

$$\Delta P = \left(\frac{Z_i}{S_i}\right)\left(\frac{W_i}{n}\right) \frac{N_{pt}\left[L_o/D_i + 25\right]\left[Re^{-2/3} - 125\right]}{(50.2\ D_i)^3}$$

(Eq. IV-31)

Tubeside for $Re > 10{,}000$

$$\Delta P = \frac{(Z_i)^{0.2}}{S_i}\left(\frac{W_i}{n}\right)^{1.8} \frac{N_{PT}\left[L_o/D_i + 25\right]}{(5.4\ D_i)^{3.8}}$$

(Eq. IV-32)

Shellside, crossflow

$$\Delta P = \frac{0.326}{S_o}(W_o)^2 \frac{L_o}{B^3 D_s}$$

(Eq. IV-33)

where:

S_i, S_o = specific gravity of tubeside and shellside fluids
Z_i = tubeside fluid viscosity, CP
W_i, W_o = tubeside and shellside mass flow rates, (lb/hr)/1000
D_i, D_s = inside tube and shell diameters, inches
L_o = length of shell, feet
B = baffle spacing, inches
n = number of tubes per pass
N_{pt} = number of tube passes per shell

If a U-tube exchanger is being considered, then the term $(L_o/D_i + 25)$ in equations IV-31 and IV-32 should be replaced by $(L_o/D_i + 16)$.

For preliminary heat exchanger sizing, the following values are typical for optimizing the trade-off between heat transferred and pumping power costs:

Tubeside velocity: 1.8 - 3.05 m/sec (6-10 ft/sec)
Shellside velocity: 0.3 - 0.9 m/sec (1-3 ft/sec)
Tube size: 1.59 - 2.54 cm (5/8-1 in)
Tube length: 4.9 m (16 ft)
Baffle spacing: $0.3\ D_s \leq B \leq 0.5\ D_s$

b. Plate Heat Exchangers

The modern plate heat exchanger is rapidly becoming widely used as a heat transfer device. The major deterent to the further use of plate exchangers is the general lack of design information. The complexities and variety of plate designs, and the ability to combine various corrugation patterns to obtain desired exchanger characteristics, limit the application of available information on plate exchangers. Manufacturers each have their own proprietary plate designs and analytical techniques to determine heat transfer coefficients, and pressure drops, and to develop an optimum exchanger design for a required duty.

The high degree of turbulence produced by the plate corrugations, and the small gap spacings which give small hydraulic diameters, combine to produce high overall heat transfer coefficients of 2270 $W/m^2{}^oC$

to 5674 $W/m^2 {}^oC$ (400 to 1000 BTU/hr ft^2 ^oF). A widely used correlation for estimating film coefficients for turbulent flow in plate exchangers is (ref. IV-3):

$$h = 0.2536 \frac{k}{D_e} (Re)^{0.65} (Pr)^{0.4} \qquad \text{(Eq. IV-34)}$$

where:

$$Re = \frac{\rho V D_e}{\mu} \qquad \text{(Eq. IV-35)}$$

and D_e, the hydraulic diameter, is given by:

$$D_e = \frac{4Wb}{2W + b} \qquad \text{(Eq. IV-36)}$$

where:

W = channel width

b = distance between plates

Since b is negligible in comparison with W, equation IV-36 reduces to:

$$D_e \approx 2b \qquad \text{(Eq. IV-37)}$$

For laminar flow (Re < 400) the Jackson correlation (ref. IV-3) may be used:

$$h = 0.742\ C_p\ G\ (Re)^{-0.62}\ (Pr)^{-0.667} \left(\frac{\mu_{av}}{\mu_w}\right)^{0.14} \qquad \text{(Eq. IV-38)}$$

where:

G = mass flow rate of the fluid in the channel, kg/m^2 sec

μ_{av} = fluid viscosity at the average fluid temperature

μ_w = fluid viscosity at the plate temperature
C_p = fluid specific heat, KJ/Kg ^oC

The pressure drop in a plate exchanger can be estimated by equation IV-39:

$$\Delta P = \frac{2fG^2L}{gD_e\rho} \qquad \text{(Eq. IV-39)}$$

where:

$$f = \frac{2.5}{Re^{0.3}} \qquad \text{(Eq. IV-40)}$$

L = length of the flow passage (or plate)

These equations represent highly simplified situations. Any accurate estimation of pressure drops should take into account plate geometry and pressure losses in the ports. These relations will allow an approximate sizing of a plate heat exchanger, and pressure drop determination for the analysis of a PV-T system. More detailed sizing and pressure drop optimization calculations must be performed by the exchanger manufacturers.

In assessing the performance of plate exchangers, the term "specific pressure drop" (J) is usually used. This is defined as the pressure drop per NTU.

$$J = \frac{\Delta P}{NTU} \qquad \text{(Eq. IV-41)}$$

The specific pressure drop is an empirically obtained value defined in terms of the heat transfer coefficient for a channel (h), or the overall heat transfer coefficient (U). While the values of NTU achieved per pass for various plate types varies greatly (0.15 to about 4), figure IV-14

(ref. IV-5) shows that most plates (shaded area) have a very similar J versus h (channel heat transfer coefficient) relationship. In this case, NTU is defined for the individual channel:

$$NTU_h = \frac{hA_p}{\dot{M}C_p}$$

where A_p is the plate area.

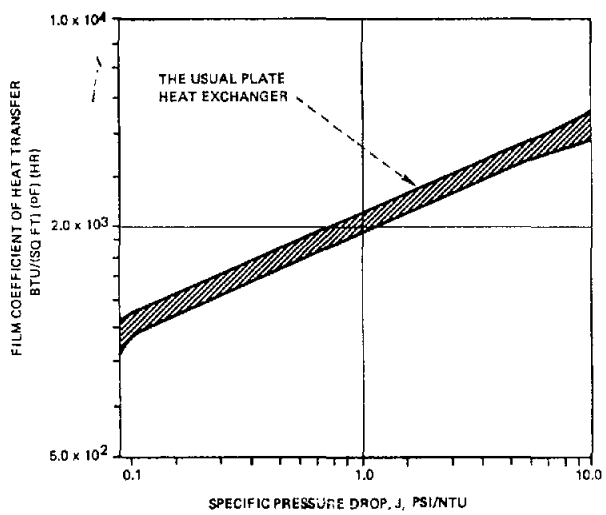

BDM/A-82-458-TR-R1

Figure IV-14. Specific Pressure Drop Versus Channel Film Heat Transfer Coefficient

Relationships between effectiveness (ε) and NTU for loop and series flow arrangements have been developed by Jackson and Troupe (ref. IV-7). The relation for countercurrent loop flow is shown in figure IV-15. As the number of channels increase, the ε-NTU curves move toward the limiting case of pure countercurrent flow. Thus, for preliminary heat exchanger sizing calculations, pure countercurrent flow may be assumed with the effectiveness calculated from equation IV-19. Typical ranges of plate exchanger parameters are as follows:

Plate thickness: 0.05 - 0.3-cm (0.02 - 0.12 in)

Channel width: 0.2 - 0.5-cm (0.08 - 0.2 in)
Effective diameter: 0.38 - 1.0-cm (0.15 - 0.4 in)
Overall heat transfer coefficient: 2270 - 5674 $W/m^2\ ^oC$
(400 - 1000 $BTU/hr\ ft^2\ ^oF$)
Pressure drop: 4.8×10^4 - 8.3×10^4 Pa (7 - 12 psi)
Flow velocities: 0.3 - 0.9 m/sec (1 - 3 ft/sec)
Plate surface area: 0.028 - 1.5 m^2 (0.3 - 16 ft^2)
Specific pressure drop: 3 x NTU - 15 x NTU

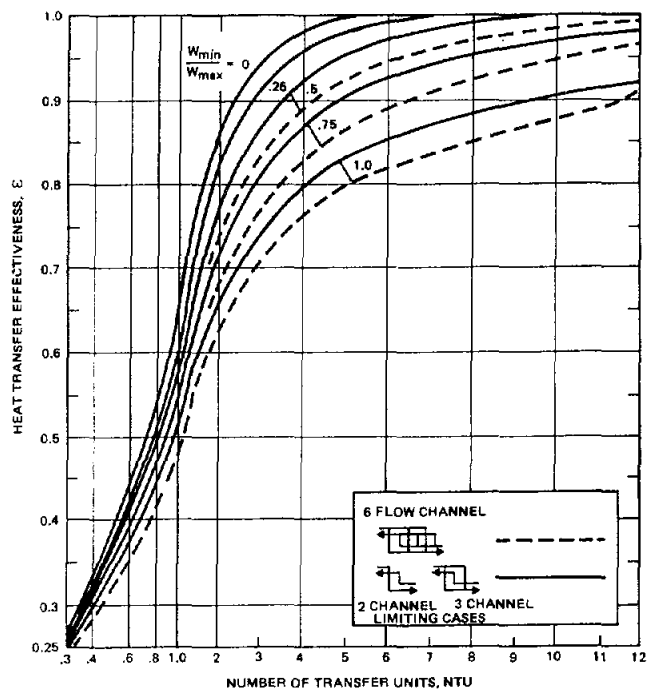

BDM/A-82-458-TR-R1

Figure IV-15. Countercurrent ε-NTU Relations for Loop Patterns

c. Fouling

In service, most heat exchangers suffer some progressive loss of heat transfer performance due to fouling. The term "fouling" refers to any deposit on a heat transfer surface which increases the thermal resistance of the surface. Generally, the fouling resistance, or

fouling factors (R_{fi} and R_{fo} in equation IV-24), are chosen based on experience. Typical fouling factors are shown in tables IV-3 and IV-4 for shell and tube and plate heat exchangers.

TABLE IV-3. TYPICAL FOULING FACTORS FOR SHELL-AND-TUBE HEAT EXCHANGERS

TYPE OF FLUID	FOULING RESISTANCE $^oCm^2/W$	FOULING RESISTANCE $^oF\ ft^2hr/BTU$
DISTILLED WATER	0.003	0.0005
TREATED BOILER FEEDWATER	0.006	0.001
CITY WATER BELOW 52°C	0.006	0.001
CITY WATER ABOVE 52°C	0.011	0.002
HEAT TRANSFER MEDIA	0.006	0.001

TABLE IV-4. TYPICAL FOULING FACTORS FOR PLATE HEAT EXCHANGERS

TYPE OF FLUID	FOULING RESISTANCE $^oCm^2/W$	FOULING RESISTANCE $^oF\ ft^2hr/BTU$
DISTILLED WATER	0.0006	0.0001
SOFT CITY WATER	0.0011	0.0002
HARD CITY WATER	0.0028	0.0005
COOLING TOWER WATER (TREATED)	0.0023	0.0004
HEAT TRANSFER OILS	0.0017	0.0003

The assumption of constant values for the fouling factors implies that a new exchanger instantaneously deteriorates to the fouled condition. There is, however, a substantial time lag before the fouling resistance approaches the design value arbitrarily selected from some experience based source. When first put into service, the clean heat exchanger will operate with reduced thermal resistance, and therefore, a surplus of heat transfer area. This excess area results in reduced flow velocities and elevated temperatures, so the exchanger deteriorates in performance at a rapid rate, thereby producing the expected fouling resistance.

There is evidence that fluid velocity is the most important parameter affecting fouling. In most cases, an increase in velocity decreases both the rate of fouling deposit formation and the ultimate fouling level attained. In addition, higher velocities increase heat transfer coefficients. However, since the pressure drop increases as the square of velocity, increased velocities inflate both capital and operating costs for pumping.

The relative propensity to fouling and the ease of cleaning are important factors in selecting the type of exchanger for a given application. Manufacturers claim the plate-and-frame and spiral plate heat exchangers are less susceptible to fouling deposits than shell-and-tube exchangers. Low fouling resistances are expected because of the typical high velocities and turbulent flows. Plate and frame heat exchangers are undoubtedly the easiest to clean, since the entire unit can be dismantled and cleaned in place without breaking any piping.

4. Selection and Sizing a Heat Exchanger

The unique characteristics of a solar system must be considered when selecting a heat exchanger. Since solar collector performance is more dependent on operating temperature than conventional heating equipment, closer approach temperatures between the hot side (collector) and cold side (process) are desirable when compared to conventional thermal processes. This would require a maximum heat exchanger efficiency. The effectiveness of the exchanger in transferring thermal energy from the collector cooling fluid to the process stream affects both the electrical and thermal performance of the PV-T array. In addition to the heat exchanger effectiveness and the array output, other considerations include trade-offs between pumping power costs, capital costs associated with heat exchanger area, the area required to house the exchanger, and maintenance costs.

Due to the complex interactions between heat transfer, array characteristics, and parasitic pumping power, the heat exchangers must be sized and selected based on an evaluation of the systems annual performance and annualized cost. In what follows, a technique is described

whereby the total cost of the heat exchanger penalty can be determined and the exchanger effectiveness (or area) found which minimizes this cost.

That the addition of heat exchangers to a system produces a penalty by decreasing the useful thermal energy available from the collector system was shown by de Winter (ref. IV-8), who derived a heat exchange factor which can be expressed in terms of the collector and heat exchanger characteristics.

$$F_x = \frac{1}{1 + \frac{F_m U_L A_c}{W_{min}} \left(\frac{1}{\varepsilon} - \frac{W_{min}}{2W_c} \right)} \qquad \text{(Eq. IV-42)}$$

where:

F_m = heat removal efficiency factor for the collector
U_L = overall collector heat loss coefficient
A_c = collector area
W_{min} = minimum capacity rate
ε = exchanger effectiveness

The useful thermal energy available is then:

$$Q_u' = F_x \, Q_u \qquad \text{(Eq. IV-43)}$$

where Q_u is the useful thermal energy available without a heat exchanger in the loop

$$Q_u = F_m \left[I\eta_o - U_L(T_f - T_a) \right] \qquad \text{(Eq. IV-44)}$$

as obtained in chapter I of Volume I. For a thermal system, the most economical heat exchanger size occurs where the heat exchange factor has

a value of about 0.95. However, this does not consider the loss of electrical power due to the collectors operating at a higher temperature.

The optimum, or most economical, heat exchanger size can be determined by minimizing the cost of the penalty incurred by using the heat exchanger. Neglecting the heat loss in the manifold, the temperature of the return fluid from the load is the inlet temperature to the array without a heat exchanger in the system. With this assumed inlet temperature, the array temperature can be calculated from:

$$T_o = T_i + \frac{IA_c\eta_{th}}{\dot{M}_a C_p} \qquad \text{(Eq. IV-45)}$$

where:

T_i = load return temperature (equals the array inlet temperature)
I = annual average insolation
A_c = array area

$$A_c = LWN \qquad \text{(Eq. IV-46)}$$

L = length of receiver section, per collector row
W = collector width
N = number of collector rows
$\dot{M}_a$ = total flow rate through the collector field

$$\dot{M}_a = N\dot{M}_r \qquad \text{(Eq. IV-47)}$$

$\dot{M}_r$ = flow rate per collector row
η_{th} = collector thermal effficiency

The average temperature can now be calculated from $T_f = .5(T_i + T_o)$, and the annual available electrical and thermal energy determined from figures II-5 and II-6.

The available energy must be determined with a heat exchanger in the system. This analysis will be performed using the configuration in figure IV-16.

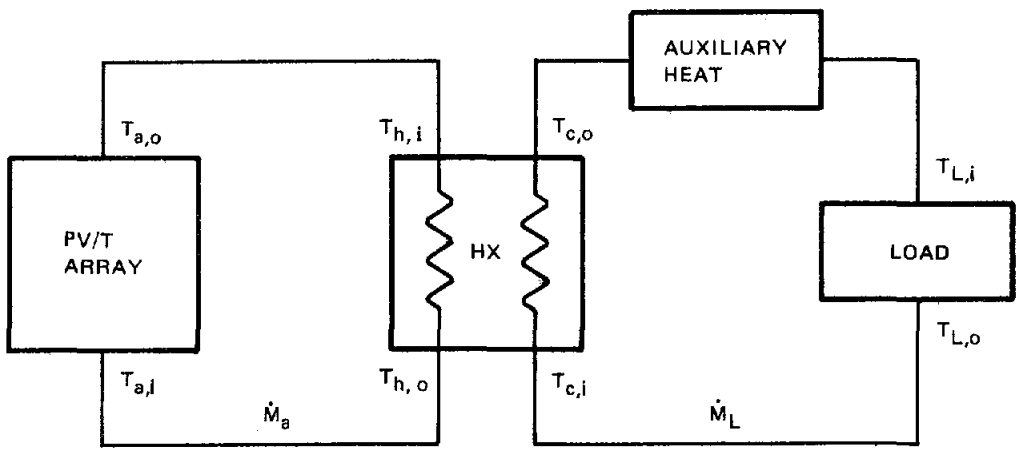

BDM/A-82-458-TR-R1

Figure IV-16. Configuration for Heat Exchanger Analysis

With the assumption of no heat loss from the manifold, the following temperature relations hold:

(1) array outlet temperature equals exchanger hot side inlet temperature ($T_{a,o} = T_{h,i}$)

(2) array inlet temperature equals exchanger hot side outlet temperature ($T_{a,i} = T_{h,o}$)

(3) Load return temperature equals exchanger cold side inlet temperature ($T_{l,o} = T_{c,i}$)

Using equation IV-18 and the above relations between temperatures, the following relations can be obtained.

$$T_{h,o} = T_{a,i} = \frac{W_a - \varepsilon W_{min}}{W_a} T_{a,o} + \frac{\varepsilon W_{min}}{W_a} T_{c,i}$$

(Eq. IV-48)

$$T_{c,o} = T_{c,i} + \frac{W_a}{W_L} (T_{a,o} - T_{a,i}) \qquad \text{(Eq. IV-49)}$$

and from equation IV-46:

$$T_{a,o} = \frac{I\ A_c \eta_{th}}{W_a} + T_{a,i} \qquad \text{(Eq. IV-50)}$$

These three equations and equation IV-49 which can be solved for the thermal efficiency, can be solved for the three unknown temperatures in terms of the load return temperature:

$$T_{a,o} = \frac{\frac{A_a\ F_m}{\varepsilon W_{min}} (I\ \eta_o + U_L\ T_a) + \left(1 - \frac{A_a\ F_m\ U_L}{2W_a}\right) T_{c,i}}{1 + \frac{A_a\ F_m\ U_L}{\varepsilon W_{min}} - \frac{A_a\ F_m\ U_L}{2W_a}}$$

Setting

$$A_a = A_r\ N_r$$

$$W_a = M_r\ C_p\ N_r$$

where: A_r = the area of a row of collectors
N_r = the number of collector rows
M_r = the flow rate per row,

the equation for the array outlet temperature becomes

$$T_{a,o} = \frac{\frac{A_r\ F_m}{\varepsilon \dot{M}_r\ C_p}\left(\frac{W_a}{W_{min}}\right)(I\ \eta_o + U_L\ T_a) + \left(1 - \frac{A_r\ F_m\ U_L}{2\dot{M}_r\ C_p}\right) T_{c,i}}{1 + \frac{A_r\ F_m\ U_L}{\varepsilon \dot{M}_r\ C_p}\left(\frac{W_a}{W_{min}}\right) - \frac{A_r\ F_m\ U_L}{2\dot{M}_r\ C_p}} \qquad \text{(Eq. IV-51)}$$

$$T_{a,i} = \left(1 - \frac{\varepsilon\ W_{min}}{W_a}\right) T_{a,o} + \frac{\varepsilon\ W_{min}}{W_a} T_{c,i} \qquad \text{(Eq. IV-52)}$$

$$T_{c,o} = \frac{W_a}{W_L} (T_{a,o} - T_{a,i}) + T_{c,i} \qquad \text{(Eq. IV-53)}$$

A new average array temperature with a heat exchanger in the system can now be determined from:

$$T_f' = \frac{1}{2} (T_{a,o} + T_{a,i}) \qquad \text{(Eq. IV-54)}$$

With this average array temperature, the annual electric and thermal energy available can again be obtained from figures II-5 and II-6.

Since the average collector temperature will be greater with a heat exchanger, the annual available electric and thermal energy to the load will be less. Thus, the cost of using a heat exchanger, in terms of decreased array output, is given by:

$$C_1 = (Q_e - Q_e')P_e + (Q_{th} - Q_{th}')P_{th} \qquad \text{(Eq. IV-55)}$$

where:

Q_e, Q_{th} = annual available electrical and thermal energy at an average collector temperature T_f (KWh/m^{2}year)

Q_e', Q_{th}' = annual available electrical and thermal energy at an average collector temperature T_f'

P_e = annualized cost of electrical energy

P_{th} = annualized cost of thermal energy

The annualized costs of energy are defined in reference IV-9 as follows:

$$P = P_p \frac{PVF(d,e,n)}{PVF(d,o,n)} (1+e)^{Y_o - Y_p} \qquad \text{(Eq. IV-56)}$$

where the function PVF is defined as:

$$PVF(A,B,C) = \frac{1}{A-B}\left[1 - \left(\frac{1+B}{1+A}\right)^C\right] \quad \text{for } A = B$$

$$= \frac{C}{1+A} \quad \text{for } A = B$$

where:

A = discount rate

B = fuel escalation rate

C = number of years of operation

Y_o = year of operation

Y_p = price year

P_p = cost of energy in the price year ($/kWh)

Since the available energy is a function of the average temperature, it is therefore a function of the local annual average insolation and flow rate ratio. The dependency on total array area and total array flow rate, can be reduced to dependency on row length (or length of receiver section, per row) and flow rate per row by using equations IV-46 and IV-57.

$$W_a = NW_r \qquad \text{(Eq. IV-57)}$$

where:

$$W_r = \dot{M}_r C_{pa}$$

The annual availabilities and heat exchanger area can be determined for various capacity rate ratios by noting the following relations:

$$\text{For } \frac{W_a}{W_L} \leq 1 \quad \text{then } \frac{W_a}{W_{min}} = 1 \quad \text{and } \frac{W_{min}}{W_{max}} = \frac{W_a}{W_L}$$

$$\text{For } \frac{W_a}{W_L} > 1 \quad \text{then } \frac{W_a}{W_{min}} = \frac{W_a}{W_L} \quad \text{and } \frac{W_{min}}{W_{max}} = \frac{W_L}{W_a}$$

The ratio of the heat exchanger area to collector area can be obtained from equation IV-58 where appropriate assumptions must be made for the overall heat transfer coefficient.

$$\frac{A_o}{A_c} = NTU \frac{W_{min}}{U_o A_c} = \frac{NTU}{U_o LW} \frac{W_{min}}{N} \qquad \text{(Eq. IV-58)}$$

where:

$$\frac{W_{min}}{N} = W_r \quad \text{for } \frac{W_a}{W_L} \leq 1$$

$$\frac{W_{min}}{N} = W_r \frac{W_L}{W_a} \quad \text{for } \frac{W_a}{W_L} > 1$$

and:

$$NTU = \frac{1}{1-R} \ln \left[\frac{1 - \varepsilon R}{1 - \varepsilon} \right] \quad \text{for} \quad R \neq 1$$

(Eq. IV-59)

$$NTU = \frac{\varepsilon}{1-\varepsilon} \quad \text{for} \quad R = 1$$

where:

$$R = \frac{W_{min}}{W_{max}}$$

Equation IV-59 is for a counterflow heat exchanger.

The annualized cost of the heat exchanger per unit collector area can now be obtained from:

$$C_2 = \frac{A_o}{A_c} P_{HX} \frac{PVF(d,g,n)}{PVF(d,o,n)} (1+g)^{Y_o - Y_p} \qquad \text{(Eq. IV-60)}$$

where:

P_{HX} = cost of the heat exchanger in $\$/m^2$

g = inflation rate

C_2 = annual cost of the heat exchanger per unit area of collector

The pumping power cost must be determined based on an assumed appropriate pressure drop in the exchanger. For a total pressure drop, ΔP, one might assume the total drop is divided between the array and load side of the exchanger as follows:

$$\Delta P_a = \Delta P \frac{\dot{M}_a^2}{\dot{M}_a^2 + \dot{M}_L^2} = \frac{\Delta P}{1 + \left(\frac{\dot{M}_L}{\dot{M}_a}\right)^2} \qquad \text{(Eq. IV-61)}$$

$$\Delta P_L = \Delta P \frac{\dot{M}_L^2}{\dot{M}_a^2 + \dot{M}_L^2} = \frac{\Delta P}{1 + \left(\frac{\dot{M}_a}{\dot{M}_L}\right)^2} \qquad \text{(Eq. IV-62)}$$

and:

$$\frac{\dot{M}_a}{\dot{M}_L} = \frac{W_a}{W_L} \frac{C_{pl}}{C_{pa}}$$

The pumping power is then:

$$W_p = M_a \left[\Delta P_a + \frac{\dot{M}_L}{\dot{M}_a} \Delta P_L \right] \qquad \text{(Eq. IV-63)}$$

and the pumping power per unit array area is:

$$\frac{W_p}{A_c} = \frac{\dot{M}_r}{LW} \left[\Delta P_a + \frac{\dot{M}_L}{\dot{M}_a} \Delta P_L \right] \qquad \text{(Eq. IV-64)}$$

The annual cost of pumping the array and load side working fluids through the heat exchanger is:

$$C_3 = \frac{W_p}{A_c} P_e \tau \qquad \text{(Eq. IV-65)}$$

where τ is the total time during the year that the pump operates.

The optimum heat exhanger effectiveness occurs when the total cost of using the heat exchanger is a minimum. The total cost is obtained by summing equations IV-55, IV-50, and IV-65.

$$C_T = C_1 + C_2 + C_3 \qquad \text{(Eq. IV-66)}$$

Unfortunately, when determining the optimum characteristics of a heat exchanger, all the information is not available. The overall heat transfer coefficient, and the pumping power required to achieve the desired heat transfer are highly dependent on the specific exchanger design, flow rates, and area. Therefore, to perform a preliminary sizing analysis, certain assumptions must be made in terms of an attainable (or typical) overall heat transfer coefficient and pressure drop.

The total cost of equation IV-66 was calculated as a function of heat exchanger effectiveness, assuming typical characteristics of a plate heat exchanger and a flow rate per row of 5×10^{-4} m^3/sec (8 gpm), based on the curves of figures IV-1 and IV-2. The following parameters were used in the calculations, and the results are shown in figures IV-17, 18, and 19.

Row Flow Rate ($\dot{M}_r$) = 5×10^{-4} m^3/sec (8 gpm)
Heat Transfer Coefficient (U_o) = 4536 w/m^2 ^oC (800 BTU/hr ft^2 ^oF)
Allowable Pressure Drop (ΔP) = 6.9×10^4 Pa/NTU (10 psi/NTU)
Heat Exchanger Cost (P_{HX}) = \$320/m^2
Cost of Electricity = \$0.05/kWh
Cost of Natural Gas = \$0.015/kWh
Electricity Escalation Rate = 0.1
Natural Gas Escalation Rate = 0.12
Inflation Rate = 10%
Discount Rate = 20%
Array = Line Focus Fresnel

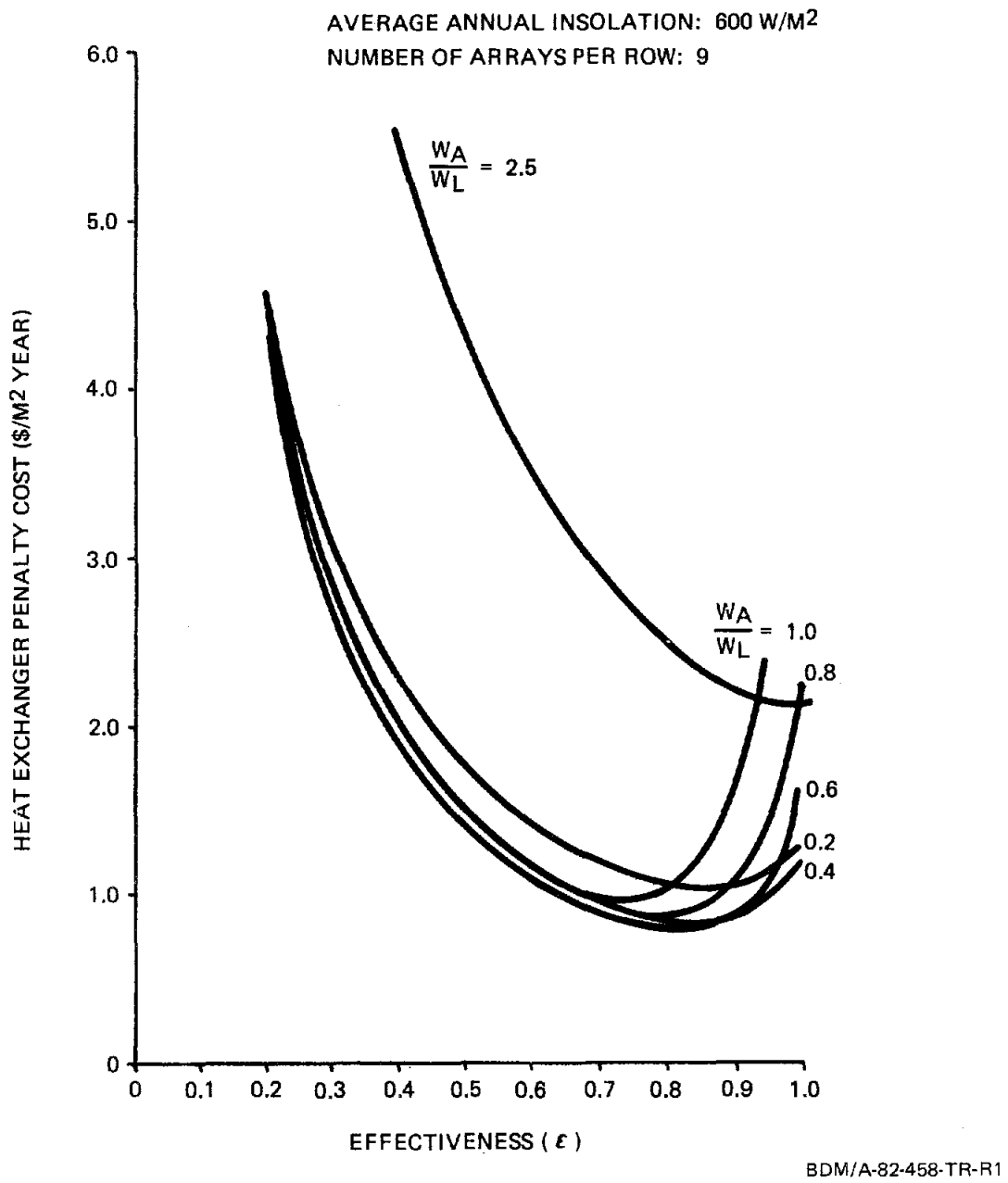

Figure IV-17. Total Cost of Heat Exchanger Penalty for I = 600 W/M^2 and N = 9.

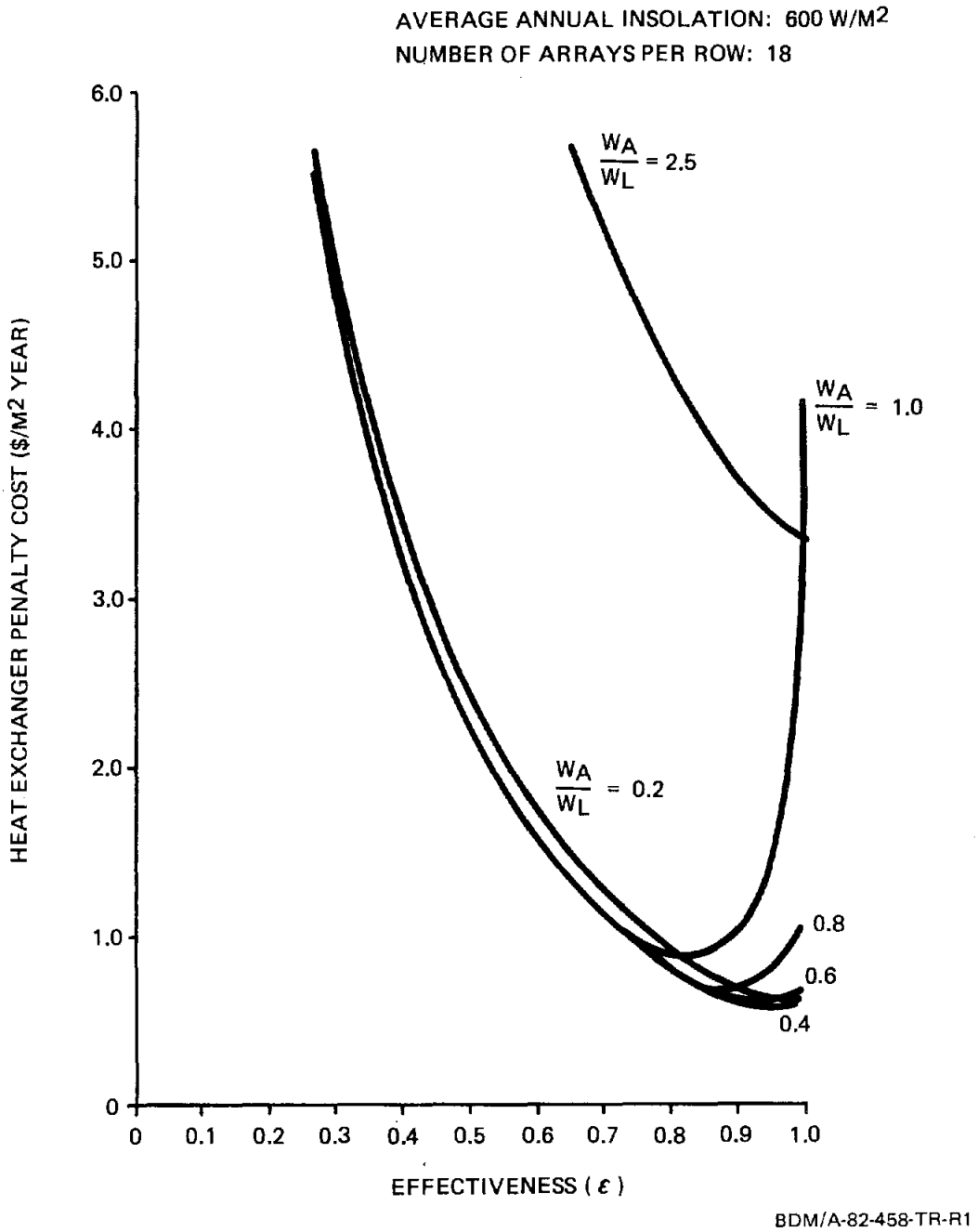

Figure IV-18. Total Cost of Heat Exchanger Penalty for I = 600 W/M^2 and N = 18

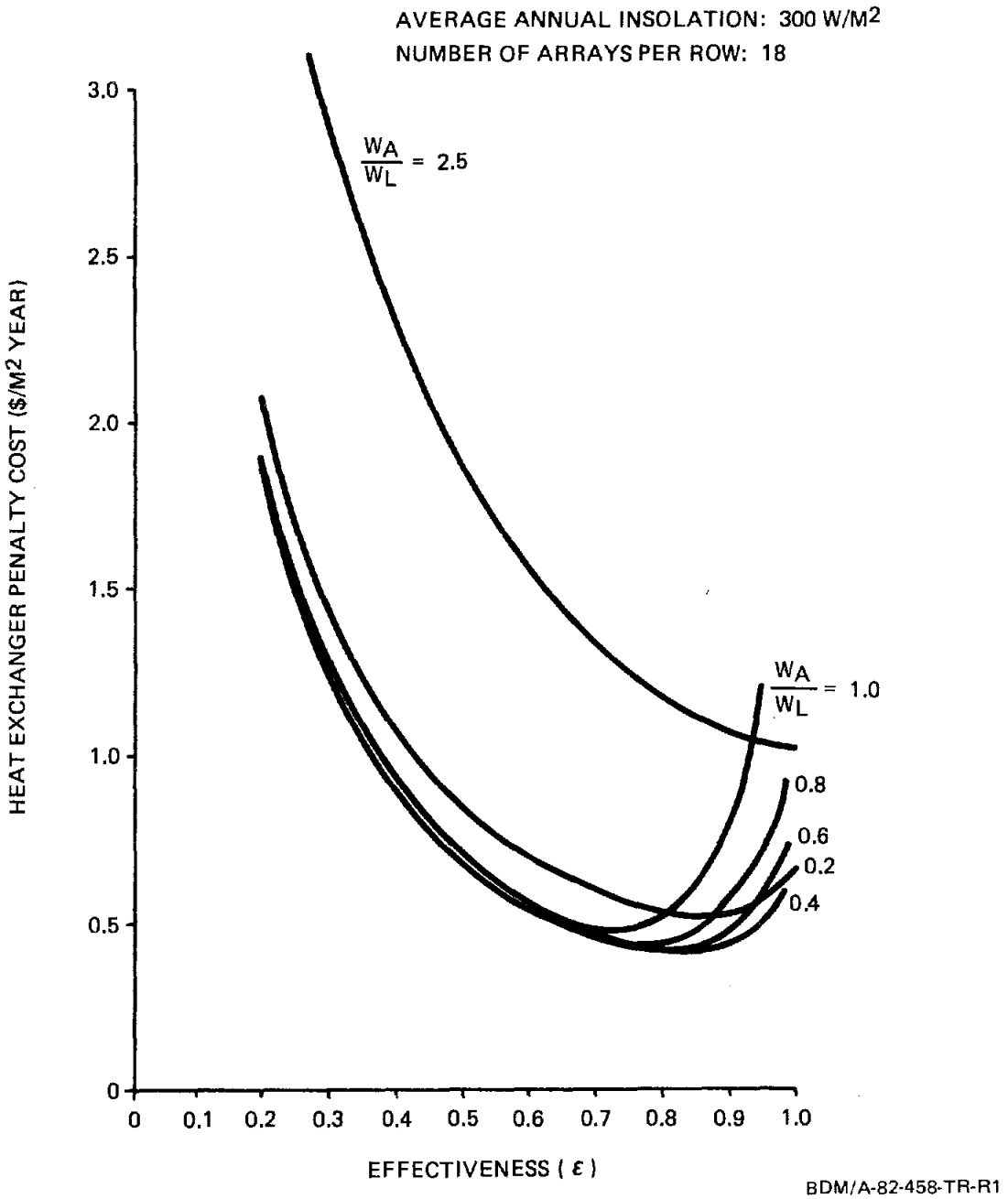

Figure IV-19. Total Cost of Heat Exchanger Penalty for I = 300 W/M^2 and N = 18

As the effectiveness (or exchanger area) increases, the exchanger transfers more heat to the load, the array runs cooler and more efficiently, and the penalty cost decreases. However, eventually the capital cost of the exchanger overtakes the improvement in system performance and the penalty cost increases.

The optimum effectiveness and minimum cost depend on the capacity rate ratios, annual average insolation, and the number of collectors per row. Increasing the number of collectors per row causes the optimum effectivness to increase and the total cost to decrease. In areas of low annual average insolation the cost increases and the optimum effectiveness decreases slightly.

A number of calculations were made to determine the optimum effectiveness and minimum cost, plotted as a function of capacity flow rate, row length, and insolation in figures IV-20 and IV-21. These curves indicate that to minimize the penalty cost of using a heat exchanger, one should design for a capacity flow rate ratio between 0.4 and 0.6, and use a large number of collectors per row. The cost curve minimum depends on the pumping power and exchanger area since only these factors vary with the capacity rate ratio for $Wa/W_L \leq 1$. As seen from equations IV-51 and IV-52, for $Wa/W_L \leq 1$ the inlet and outlet temperatures of the collector, and therefore, the average temperature, are independent of capacity rate so the electrical and thermal energy availabilities remain constant. However, as Wa/W_L increases, the outlet temperature on the load side of the exchanger ($T_{C,O}$) increases, indicating that more energy is being transferred to the load, thereby decreasing the amount of auxiliary heat required.

The number of collectors per row, the array, and the load flow rates cannot be arbitrarily chosen simply to minimize the heat exchanger cost or system cost. There may be certain restrictions placed on the row length and flow rate; for example, the maximum allowable pressure E-systems line focus Fresnel array can withstand is approximately 0.69 MPa (100 psi), due to the flexible hose and fittings used between arrays. This limitation forces a compromise between row length, flow rate through each row, and the maximum allowable fluid temperature.

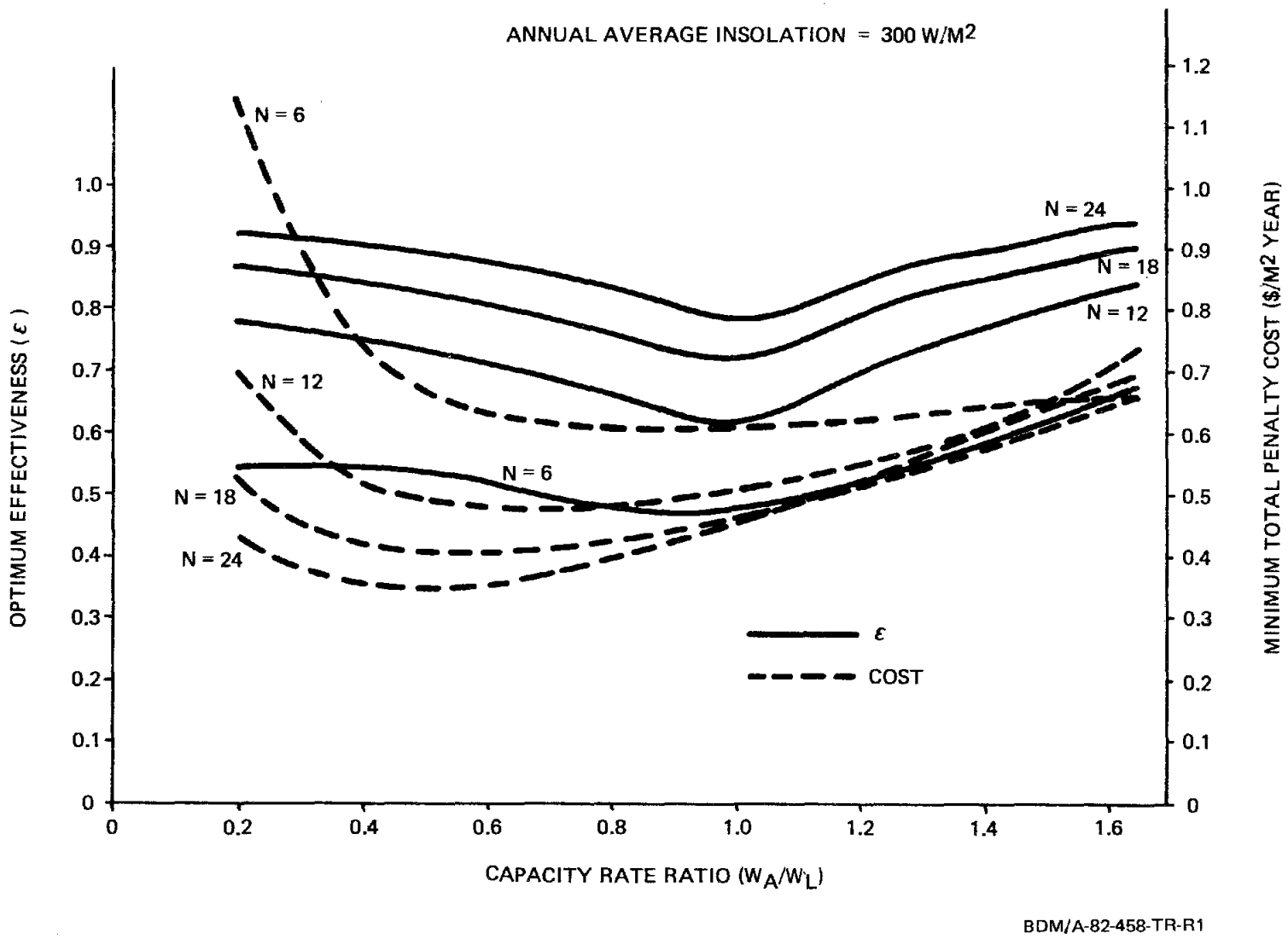

Figure IV-20. Optimum Effectiveness and Minimum Total Penalty Cost for I = 300 W/M2

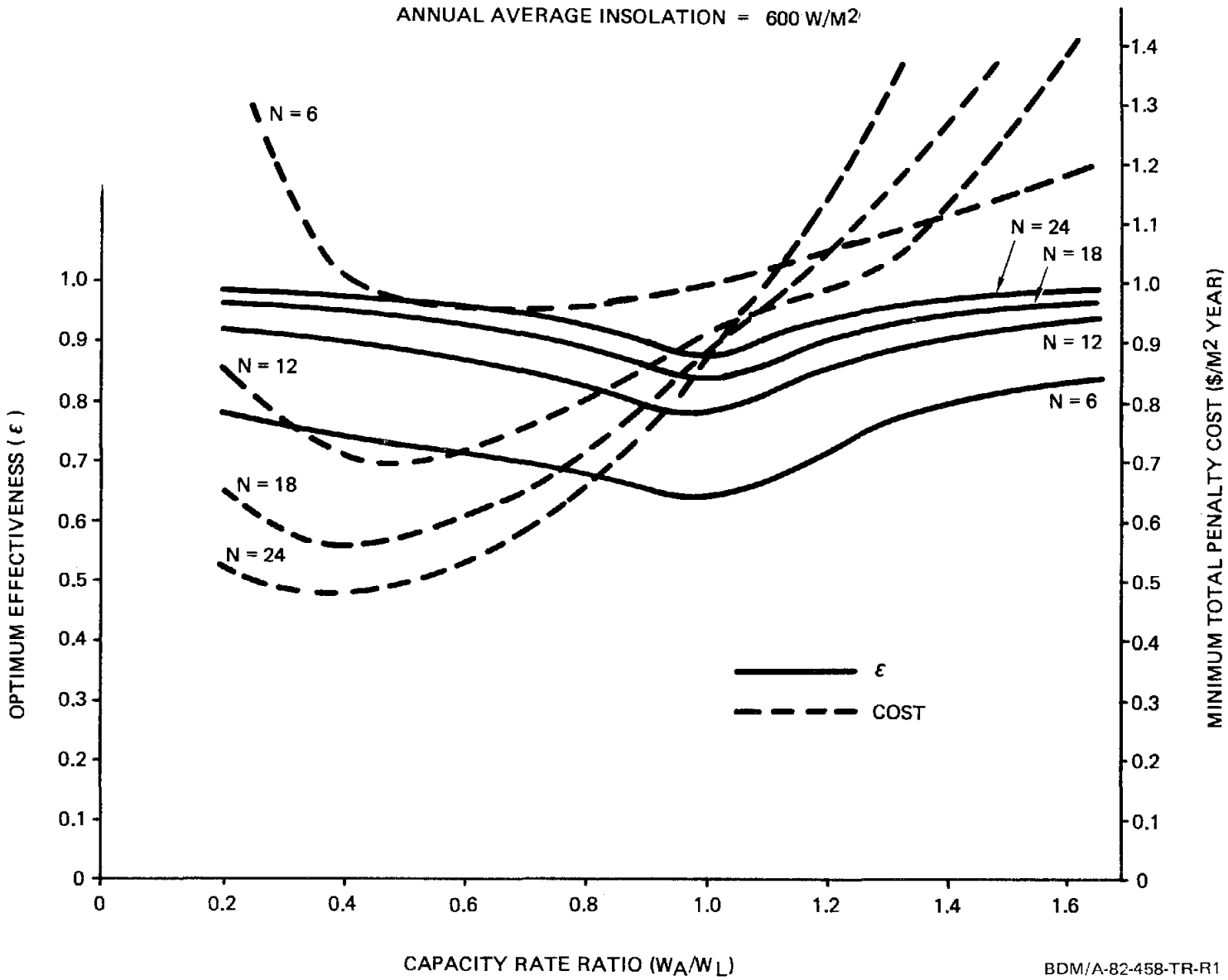

Figure IV-21. Optimum Effectiveness and Minimum Total Penalty Cost for $I = 600\ W/M^2$

For a row consisting of 10 E-system arrays, a flow rate of 3.16×10^{-4} m^3/sec (5 gpm) of 30 percent ethylene glycol and water would produce a pressure drop of 0.29 MPa (42 psi). In order to overcome the pressure losses in the manifold, heat exchanger and expansion tank, however, a higher pressure at the row inlet is required. With a flow rate of 3.16×10^{-4} m^3/sec (5 gpm), a temperature rise of about 50°C will be experienced across the collector row on a high insulation day with 1000 watts/m^2 (see figure IV-3). Therefore, to minimize operation of the cooling tower, which produces high parasitic electrical losses, the heat exchanger should be sized to produce a maximum 50°C outlet temperature to the array (assuming a maximum allowable array fluid outlet temperature of 100°C).

At this point, the size and philosophy of the thermal storage must be considered, along with the flow rate on the load side of the heat exchanger, and the load return temperature. If no storage is used, the return temperature and load flow rate are fixed, and the heat exchanger is sized to provide a 50°C coolant temperature to the array under maximum insolation conditions. If the load is intermittent, the cooling tower must be used when there is insufficient load to cool the array fluid.

The use of thermal storage allows more flexibility and minimizes cooling tower operation, but also makes heat exchanger sizing somewhat more difficult. The flow rate on the load side of the heat exchanger can now be adjusted to optimize the overall system operation. The flow rate will depend on:

(1) Size of the storage tank
(2) Rate at which fluid is extracted from storage for use in the process
(3) Optimum heat transfer through the heat exchanger
(4) Minimum operation of the cooling tower.

There are several modes of operation of the storage system which have a bearing on the sizing of the heat exchanger. The simplest system is a variable volume storage system in which the tank is filled with hot water from the heat exchanger, and water is extracted as

required by the process. In order to provide storage for evening use, the flow rate into storage must be greater than the average use rate during the day, allowing the tank to fill up. Once the tank is full, warm water may be recirculated through the heat exchanger, thereby increasing the stored energy. Once this is accomplished, the exchanger must then be sized to provide a 50°C inlet temperature to the array, with a load return temperature determined by the temperature of the storage fluid. If the storage tank temperature becomes too high, the cooling tower will be required to cool the array.

It is evident from this discussion that in order to optimize the size of a heat exchanger, a complete system analysis is required, including the characteristics and phasing of the load. One may use the previous analysis and curves to gain some insight into the factors involved in sizing a heat exchanger and to perform preliminary sizing for an inital conceptual design.

D. COOLING SYSTEMS

Two basic types of cooling systems can be used: an air heat exchanger (also called dry air cooler), or a cooling tower. Cooling towers use the evaporation of water to carry away the heat and their performance is governed by the wet bulb temperature. Air heat exchangers, on the other hand, use dry air to dissipate the heat and their performance is governed by the dry bulb temperature.

The advantages of the cooling tower are that for the same volume of air moved, a greater amount of heat can be rejected and lower temperatures can be achieved, and less sophisticated controls are needed to maintain constant temperatures. Advantages of the air heat exchanger include the fact that freeze protection of the cooling water is no longer required, scaling and corrosion due to cooling water are eliminated, plumes are eliminated, and blowdown is not required. The cooling tower's disadvantages include the need for freeze protection, and that they cannot be operated above 82.2°C (180°F) without scaling problems of the cooling water (for certain models this temperature may be lower).

1. Cooling Towers

Cooling towers are either open cooling towers, where a portion of the fluid being cooled is evaporated, or closed systems, where the fluid being cooled is piped through the tower in tubes. Open cooling towers are less complicated and more efficient, but closed systems (often called industrial fluid coolers) have the advantage of keeping the process water separate from the cooling water. This simplifies water quality problems and allows the array fluid to pass through the cooler even when glycol/water or thermal oils are used in the array.

The purpose of the cooling system is to allow the array to be used even when the load will not accept the full thermal output of the array. Operating the array at such times will be highly desirable because the electricity can still be used even if the thermal energy is not needed. Even at an array electrical-to-thermal output ratio of .2, the electrical parasitic load of the cooling system will be less than 10 percent. Therefore, the cooling system must be capable of cooling the entire array when there is no thermal load.

Cooling tower performance is determined by the characteristics of the unit, environmental conditions, and the nature of the system sending it fluid to be cooled. The thermal output of the cooling tower cannot be controlled by changing the fan power or cooling water circulating rate to a predetermined value because as these parameters change, the temperature of the fluid returning to the system changes, requiring a change in demand on the cooling tower. Control of the cooling tower must be performed by measuring temperatures of the fluid being cooled, and adjusting tower performance to produce the desired temperature. Similarly, a cooling tower cannot be sized to reject a fixed quantity of heat. The tower must be sized based on wet bulb temperature, inlet and outlet temperatures, and fluid flow rate.

Geographic variations in average summer wet bulb temperature range from 16.7^{o}C (62°F) in the West, to 27.2^{o}C (81°F) in the South. Variations in mid-summer wet bulb temperatures at one location can be as much as 23.3^{o}C (42°F). A 11.1^{o}C (20°F) change in the design wet bulb

temperature can result in a 67 percent change in the fan horsepower required to operate the cooling tower. Considering the fan as a parasitic load on the PV-T array, it is important to size it appropriately. For a particular location, the design wet bulb temperature is that temperature which is exceeded only 5 percent of the time. Table IV-5 shows that typically this reduces the design wet bulb temperature 3.9°C (7°F), whereas changing the design point 15 percent only lowers it another 1.1°C (2°F). The 5 percent design point is reasonably safe for a PV-T system because only when both the actual wet bulb temperature exceeds this design temperature and the cooling tower needs to reject the full thermal output of the array, is the cooling tower capacity inadequate. If the tower selection was made with adequate approach (difference in temperature of the fluid leaving the cooler and the wet bulb temperature), it may still be able to handle the load. If not, the array can be defocused to avoid damage to the system.

TABLE IV-5. TYPICAL FREQUENCY AND DURATION OF SUMMER WET BULB TEMPERATURES

DURATION	WET BULB TEMPERATURE	
SUMMER PEAK	23.9°C	(75°F)
1% ABOVE	21.5°C	(70.7°F)
5% ABOVE	20.2°C	(68.4°F)
15% ABOVE	19.0°C	(66.2°F)
50% ABOVE	17.3°C	(63.2°F)

In order of importance, parameters determining cooling tower performance can be ranked as follows:

(1) Approach
(2) Flow Rate
(3) Range (difference between fluid inlet and outlet temperatures)
(4) Wet Bulb Temperature

In general, some reserve capacity is desired in the cooling tower in terms of flow rate rather than approach. The idea behind this recommendation is that lowering the approach considerably reduces the performance of the cooling tower, and may result in a significant increase in size to do the same job, whereas increasing the flow rate (e.g., 10 percent) only increases the size of the tower by the same amount as the reserve capacity desired.

Suggestions for sizing cooling towers include:

(1) For a fixed flow rate, range, and wet bulb temperature, increasing the approach will reduce the size of the tower needed.

(2) For a fixed tower size, range, and wet bulb temperature, increasing the approach will allow a larger flow and the rejection of more heat.

(3) If the cold water temperature is not changed and the range is increased "at the top" (higher hot water temperature), the tower size for a fixed heat load will decrease. If the hot water temperature remains constant and the range is increased at the expense of a lower approach, the tower size will increase.

The materials chosen for tower construction must be adequate for the process involved. If chemicals are involved in the process and can get into the tower either by fluid leaks or airflow, then tower construction materials should be resistant to attack by these chemicals. Oil should not be allowed to leak into the cooling tower since as little as 30 ppm may cause significant loss of heat transfer on the surfaces and cause a 10 percent loss in cooling efficiency.

Placement of the tower must take into account wind, and location of surrounding structures. The prevailing winds should take any fumes away from the tower. Moreover, it is not desirable to let the moist fumes from the tower blow where they can cause problems; in particular, mixing with other gases to form moist corrosive air. Nearby structures should not cause the tower to intake its own exhaust.

Normally, air inlet louvers are installed facing the prevailing wind direction, but in high sand or dust areas this may not work well. In such areas, a counter flow tower is probably better than a cross flow tower. In areas with considerable sand or dust, a deep basin will allow the silt to settle. Also, the inlet for the pump can act as an overflow-weir design, which prevents sand from entering the pump.

In some areas, building codes specify wind and seismic loadings as well as materials for cooling tower construction, and whether the tower must be on the ground or on the roof.

Tower freeze protection is also required. If the tower has a closed loop for the fluid being cooled, then the fluid in this loop should have a high freeze temperature. The pan of the cooling tower can be protected by a pan heater (electric or steam), or can be drained to a remote sump where it cannot freeze. Louvers and two-speed fans help control the cooling rate and prevent freezing on the packing during operation in cold weather. If ice does form, one of the best ways to de-ice is to cover the tower with a tarpaulin, and allow the heat from the warm process fluid to melt the ice.

Water quality is very important. Salt concentration and pH (ordinarily 6.5 to 7.5) should be maintained within limits specified by the manufacturer. Operating the tower on continuous bleed (at a rate commensurate with the evaporation rate) is recommended to control the salt concentration level. The pan should not be used to mix water treatment chemicals.

Consideration should be given to altitude if the tower location is more than 305 m (1000 ft) above sea level. At higher altitudes, air will be less dense yet the fan will still move a constant volume of air, resulting in a lower mass flow. The tower fan must be increased in size to compensate for this. Also, as altitude increases, air at a given temperature is capable of holding more water vapor, tending to offset the loss in density.

Additionally, cooling towers generate noise, though improved designs have reduced noise levels. However, consideration should still

be given to noise in choosing the tower location, even though cooling towers are not as loud as dry air coolers.

2. Air Coolers

Depending on the process temperature and other factors, both evaporative and dry air cooling can be economical. Evaporative cooling works best when small approach temperatures are required. The suggested crossover point where dry cooling becomes more favorable than wet cooling towers occurs when the approach is 27.8°C (50°F), or more, above the average summer dry-bulb temperatures. Maximum summer wet-bulb temperatures are typically 11.1 to 16.7°C (20 to 30°F) lower than the maximum dry-bulb temperature. This same rule of thumb should apply to both cooling capital costs and the horsepower required to operate the cooler. Unfortunately, cooling is usually needed when the dry-bulb temperature is the highest. For a dry-bulb temperature of 40.6°C (105°F), the crossover point is about 68.3°C (155°F), thus dry air cooling becomes economical when evaporative cooling creates problems due to the high inlet temperature and subsequent scale formation.

When required, freeze protection for dry air coolers is complex and expensive. PV-T systems, however, are immune to freeze problems. In general, freezing problems in dry air coolers are due to water in the process fluid. Assuming the PV-T system is not a draindown system, the circulating fluid must be one that does not freeze (glycol/water) in order to protect the array. Ice and snow can impair the performance of a dry air cooler, and require the accumulation to be melted before normal operation. In general, the dry cooler will be needed during fair weather. Ice and snow covering the cooler can be melted by circulating the PV-T coolant through the cooler with the fan off.

Dry air coolers often require more fan horsepower and more fans to reject the same amount of heat. To reject the same amount of heat, capital cost and/or fan horsepower will go up as the approach goes down. In determining the crossover point, both operating and capital costs should be considered. Since most of the time the full output of the cooler won't be needed, there should be some way of turning down the

cooler. Dry air coolers are available with variable speed or variable pitch fans, as well as more than one fan per bay. This does increase capital cost, but reduces the electricity consumed to run the cooler.

3. An Example Tower Selection

Consider an array with a thermal output of approximately 2.93 MW (10 MBtu/hr), and cooled by 0.044 m^3/sec (700 gpm) H_2O entering at 82.2°C (180°F) and leaving at 98.9°C (210°F). Since temperatures are so high that the cooling tower might scale, it is necessary to set up a mixing flow system, as shown in figure IV-22. This drawing is for an industrial cooler or closed loop tower. If an open loop tower is to be used, the system must have a heat exchanger instead of fluid mixing. Such a system was considered for this application, but was found to require no less horsepower to operate, while requiring an extra heat exchanger. Flow rates on figure IV-22 were calculated starting with the 0.044 m^3/sec (700 gpm) to give the temperatures shown on the figure. Wet bulb was assumed and the range was chosen to give a large approach; flow through the cooler was the same as through the array, and temperatures in the cooler were low enough to prevent scaling.

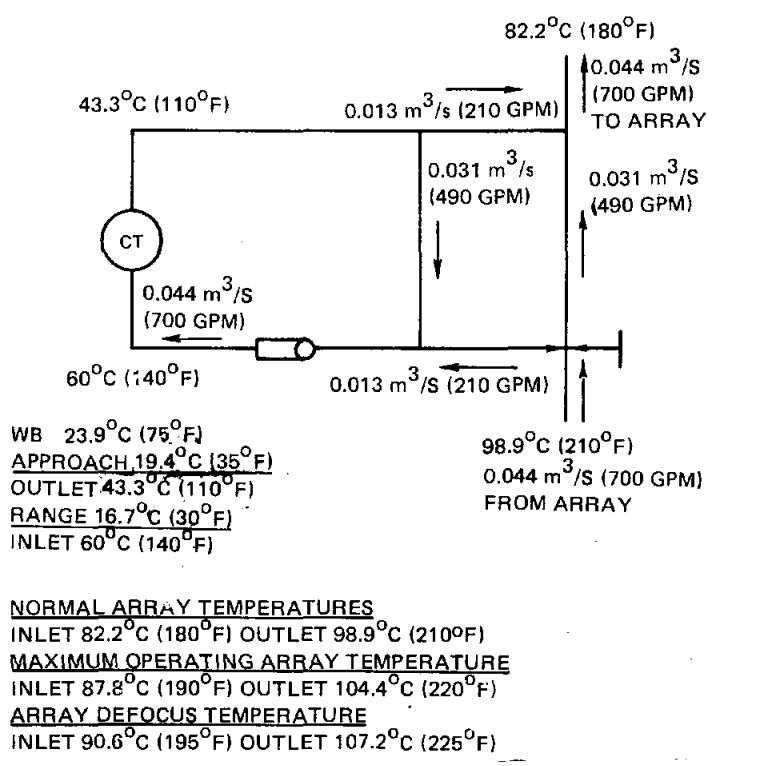

Figure IV-22. Cooling Tower Interface Schematic

From figure IV-23 the performance factor required is 5.5+. In table IV-6, the Baltimore Aircoil multi-stage axial fan large enough to handle 0.044 m^3/sec (700 gpm) at this performance factor is a VXMI-105-3. This unit has a 11.14 kW (15 hp) fan, a 3.73 kW (5 hp) cooling water circulation pump, and requires 6.7 kW (9 hp) to move the glycol/water through the cooler. Assuming an E/T ratio of .2, these pumps use only 3.5 percent of the electrical output of the array. Alternatives to this unit include a unit one size larger, which would cost more, but use 4.5 kW (6 hp) less, or a unit with a centrifugal fan. The latter unit would cost a little less and have more control over the air flow for operation at low loads, but would use an extra 11.2 kW (15 horsepower).

Control strategy might include a temperature sensor on the upstream side to sense high temperatures (over 82.2^{o}C or 180°F) and turn the unit on. This sensor should have a several minute delay before turning off, and would turn the glycol/water bypass circulating pump on, power up the cooling tower, and activate the bypass valve. The bypass valve would open gradually until, at 98.9^{o}C (210°F) upstream, it would be fully open. An orifice in the bypass line would limit the flow in this direction to 0.013 m^3/sec (210 gpm). A thermal sensor in the outlet of the cooling tower turns the tower fan on at low speed if the outlet temperature is over 46.1^{o}C (115°F). If the temperature rises above 48.9^{o}C (120°F), the remainder of the cooler is turned on in stages. This sensor should also have appropriate delays built-in to prevent the cooler from cycling on and off too frequently.

E. SENSIBLE HEAT STORAGE

Storage in a PV-T system can perform three functions: (1) reserve energy for later use, (2) filter fluctuations in PV-T output, and (3) help interface the PV-T array to the auxiliary heater. Clouds can cause significant changes in the PV-T output over a few minutes. These fluctuations will be transmitted to the load, or require the auxiliary heater to cycle rapidly to make up for these changes in PV-T array output.

Definitions
Range (°F) = Entering Fluid Temperature – Leaving Fluid Temperature
Approach (°F) = Leaving Fluid Temperature – Design Wet Bulb Temperature

To select Performance Factor, enter at Design Wet Bulb Temperature. Read down to Approach Line. Read right horizontally to Range Line. Select Performance Factor at Design Range Line.

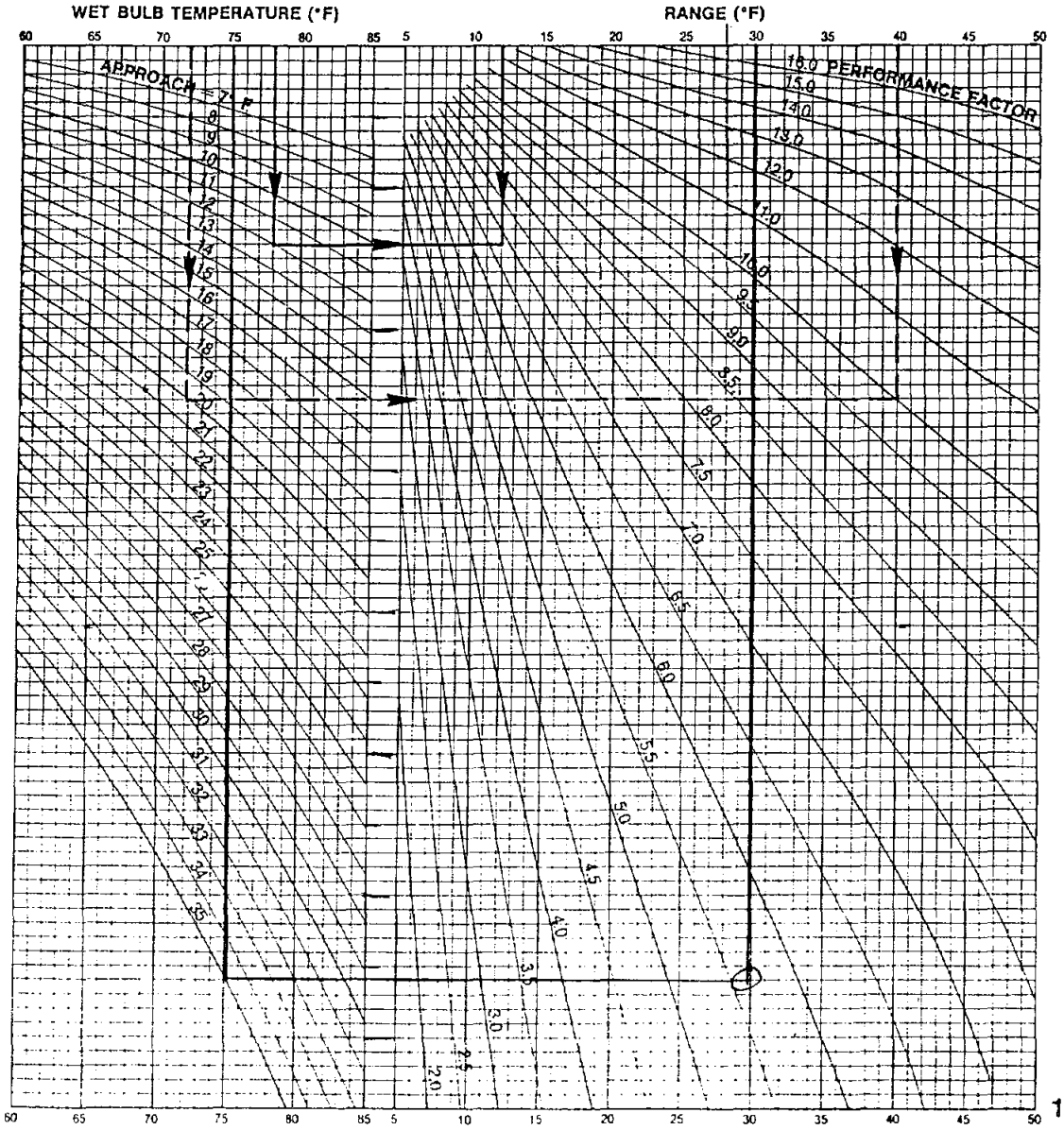

13

BDM/A-82-458-TR-R1

Figure IV-23. Cooling Tower Performance Factors (Reproduced Under Permission of the Copyright Owner © 1978, Baltimore Aircoil Company, Inc.)

TABLE IV-6. COOLING TOWER SIZE SELECTION (ref. IV-10)

UNIT SIZE	MAX. GPM	PERFORMANCE FACTORS														
		2.0	3.0	4.0	5.0	6.0	7.0	8.0	9.0	10.0	11.0	12.0	13.0	14.0	15.0	16.0
9-1	330	125	75	50	35	—	—	—	—	—	—	—	—	—	—	—
9-2	330	142	85	57	42	33	—	—	—	—	—	—	—	—	—	—
9-3	330	170	104	70	51	39	31	—	—	—	—	—	—	—	—	—
18-0	405	260	150	96	68	50	37	30	—	—	—	—	—	—	—	—
18-1	405	300	180	118	83	63	48	38	30	—	—	—	—	—	—	—
18-2	405	340	207	136	99	75	58	47	37	33	—	—	—	—	—	—
18-3	405	405	236	175	125	97	75	63	50	44	34	31	—	—	—	—
27-1	405	460*	280	185	130	—	—	—	—	—	—	—	—	—	—	—
27-2	405	520*	322	210	150	114	87	69	54	47	36	—	—	—	—	—
27-3	405	—	405	280	200	155	120	96	76	66	52	46	37	32	28	—
36-2	405	—	465*	330	243	185	142	114	88	75	58	51	40	34	29	—
36-3	405	—	—	405	308	237	185	150	120	102	80	71	58	50	44	37
50-1	585	—	585	430	—	—	—	—	—	—	—	—	—	—	—	—
50-2	585	—	685*	490	360	276	210	165	130	110	87	75	60	50	43	35
50-3	585	—	720*	525	390	300	235	185	148	125	98	84	69	58	50	42
70-1	810	1020*	706	525	372	276	205	160	124	102	—	—	—	—	—	—
70-2	810	—	935*	660	490	370	285	222	180	150	120	103	—	—	—	—
70-3	810	—	1020*	735	535	410	320	252	200	170	137	120	—	—	—	—
105-1	810	—	—	930*	670	520	400	320	255	215	173	143	112	—	—	—
105-2	810	—	—	—	780	610	480	390	310	260	213	180	146	123	104	—
105-3	810	—	—	—	810	660	530	420	342	295	245	210	172	146	125	100
120-1	1290	—	1225	890	630	470	360	270	217	170	140	117	100	—	—	—
120-2	1290	—	1260	1013	730	550	425	332	265	217	175	145	125	104	—	—
120-3	1290	—	1500*	1100	800	615	480	380	305	250	205	172	145	121	102	—
140-1	1620	2040*	1412	1050	—	—	—	—	—	—	—	—	—	—	—	—
140-2	1620	—	1870*	1320	980	740	570	444	360	300	—	—	—	—	—	—
140-3	1620	—	2040*	1470	1070	820	640	504	400	340	274	240	190	164	138	114
180-1	1290	—	—	1260	1060	815	615	480	390	313	253	215	175	143	110	88
180-2	1290	—	—	1480*	1200	950	750	600	485	400	325	270	230	190	153	125
180-3	1290	—	—	—	1260	1050	820	665	540	448	368	315	265	225	185	158
210-1	1620	—	—	1860*	1340	1040	800	640	510	430	346	286	224	180	146	110
210-2	1620	—	—	—	1560	1220	960	780	620	520	426	360	292	246	208	168
210-3	1620	—	—	—	1620	1320	1060	840	684	590	490	420	344	292	250	200
240-1	2580	—	2520	1780	—	—	—	—	—	—	—	—	—	—	—	—
240-2	2580	—	—	2026	1460	1100	850	—	—	—	—	—	—	—	—	—
240-3	2580	—	3000*	2200	1600	1230	960	760	610	500	410	344	290	242	204	175
360-1	2580	—	—	2520	2120	1630	1250	960	780	625	505	430	350	286	220	176
360-2	2580	—	—	2960*	2400	1900	1500	1200	970	800	650	540	460	380	306	250
360-3	2580	—	—	—	2520	2100	1640	1330	1080	896	736	630	530	450	370	315

BDM/A-82-458-TR-R1

Reproduced Under Permission of the Copyright Owner.
© 1978 Baltimore Aircoil Company, Inc.

Sufficient storage (15 minutes of load) to filter momentary fluctuations in PV-T array output due to clouds will make it easier to control the system and the auxiliary heater.

Auxiliary heaters cannot operate efficiently below a certain turndown rate (fraction of full load). For average demands less than the turndown rate, the auxiliary heater must cycle on and off. To prevent these cycles from being transmitted to the load, there must be some heat storage in the system. Pipes and fluid throughout the system have thermal capacity and help filter fluctuations, but are not entirely sufficient. The heat capacity of the auxiliary heater itself helps to filter out most of the fluctuations, but additional storage may be needed.

For systems where the PV-T array supplies only a fraction of the load (PV-T array output less than load), storage of energy would not ordinarily be warranted. The general rule is that if the PV-T array supplies only part of the load, the fraction of the load not supplied by the PV-T array should be greater than the output of the auxiliary heater at its greater turndown rate, i.e., the auxiliary heater load should be high enough so the auxiliary heater does not have to cycle. Another generalization states that if the PV-T array supplies only a fraction of the load, then the heat should be used immediately, rather than be stored. An exception is when the collectors might otherwise not be used for significant periods such as weekends, when the plant is not used.

As the portion of the load supplied by the PV-T array becomes large enough so that the average demand on the auxiliary heater is less than the turndown, then storage becomes important. If the output of the PV-T array is larger than the load during the day and there is an evening load, then storage is required to allow heat collected in the day to be used at night.

Cost-effective storage must be less expensive than the replacement value of the heat. That is, if storage costs more than throwing away the heat and replacing it with heat from the auxiliary boiler, then clearly it does not make sense to store. Using the same time value of money and

cost of energy as in the insulation section, the replacement value of the heat stored (RVHS) as determined by the energy replacement cost (using the auxiliary heater instead) is:

$$\begin{aligned} RVHS &= (6.14) \times (\$0.0034/kW\ hr) \times (4.166\ kJ/kg^{o}C) \\ &\quad (1\ hr/3600\ sec) \times (\Delta T) \\ &\quad \times (993\ kg/m^3) \times (V) \times (Y) \qquad \text{(Eq. IV-67)} \\ &= (\$2.4 \times 10^{-2}/m^3\,^{o}C) \times (\Delta T) \times (V) \times (Y) \end{aligned}$$

where ΔT is the temperature increase when storage is full of heat (in ^{o}C), V is the volume of the storage (in m^3), and Y is the number of times per year the heat is removed from storage. The cost of energy is based on the cost of fuel oil, and 6.14 is the present value factor. The cost of storage is (ref. IV-11):

$$\text{Storage Cost} = 1.65 \times \$2206 \times \left(V(m^3)\right)^{0.515} + \text{cost of fluid.} \qquad \text{(Eq. IV-68)}$$

where 1.65 is the maintenance factor (see section IV-I)

As an example, consider a storage tank with 6 hours of storage for a 3MW (10M Btu/hr) system. Such a tank would be appropriate for a 16 hour load of 3MW if the sun was shining an effective 10 hours per day. If the temperature difference between the load and the make-up or return water is $50^{o}C$ ($90^{o}F$), then the 6 hours of water used by the load has a volume of:

$$\frac{(300\ kW) \times (6\ hrs) \times (3600\ sec/hr)}{(4.166\ kJ/kg^{o}C) \times (50^{o}C) \times (993\ kg/m^3)}$$

$$= 313\ m^3$$

If the storage tank is the same size, the fluid supplied to the load during the 6 hours will exactly displace the fluid in the tank, and the capital cost or purchase price of the tank will be:

$$2206(313)^{.515}$$

$$= \$42 \text{ K}$$

This is about three-quarters of one percent of the cost of E-Systems array required to supply the heat. Thus, for our example, the storage cost is not a major issue. More important will be how storage affects the overall performance of the system.

The amount of heat that can be delivered to the load depends upon whether the tank operates in a draindown or mixing mode. For a draindown tank 100 percent of the energy stored in the tank can be delivered to the load. For a mixing tank, the temperature of the tank, as a function of time (t) when the array is not operating, is given by:

$$T_S = T_I + (T_{SO} - T_I) \exp(-Vt/V_T) \qquad \text{(Eq. IV-69)}$$

where T_S is the temperature of the mixed fluid in the tank, T_I is the make-up or return water temperature, T_{SO} is temperature in the storage tank when it started supplying the load, V is the flow rate through the tank, and V_T is the volume of the tank. For our example $Vt = V_T$, and if we assume the initial tank temperature is the same as the temperatures required by the load, only 63 percent of the energy stored in the tank can be delivered to the load, and only 63 percent of the load requirement is met. As the tank size increases, the temperature change of the tank is less, so a smaller fraction of the energy stored is delivered to the load, but more of the load requirement can be met because the tank is oversized. For example, if the tank holds three times the water demanded by the load, only 28 percent of the energy in the tank is used, but 85

percent of the load demand is met. This illustrates a primary problem with mixing tanks: a finite size mixing tank (unless it stores at a higher temperature than the load demands) cannot satisfy 100 percent of the load demand when the array is not operating.

Another problem of mixing tanks concerns how they effect the system when they are being charged with heat. Storage tanks are either in series or parallel. When in parallel, hot or warm water is released from the bottom of the tank and attempts to warm up the array inlet temperature. To prevent the array from running hotter, either the cooling tower will have to be turned on or flow will have to be increased through the load side of the heat exchanger. Figure IV-24 shows the assumed system without the storage tank and figure IV-25 with the storage tank. The example numbers show that by increasing the heat exchanger flow (using the assumed flow through the storage tank equal to the flow through the load), it is possible to keep the array inlet temperature from increasing. Figure IV-25 illustrates how the heat leaving the outlet of the parallel flow mixing tank recycles into the storage tank and the load.

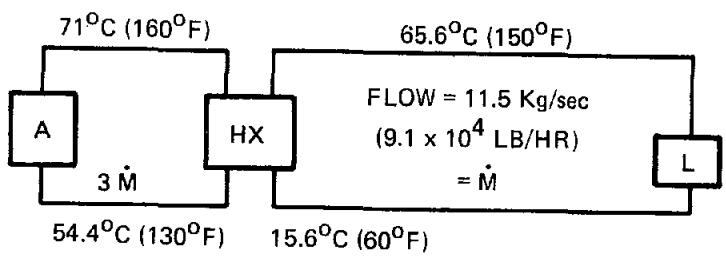

Figure IV-24. Typical PV-T System Without Storage

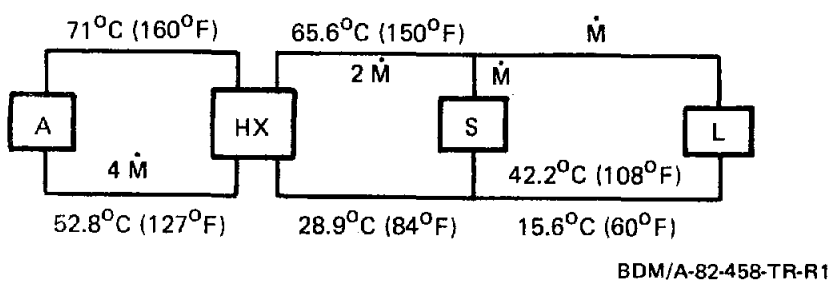

Figure IV-25. Typical PV-T System with Storage in Parallel with the Load

It is possible then, to configure the system to provide a parallel flow mixing tank that does not have a gross impact on array performance although, of course, the heat exchanger must be larger than if warm water were not leaving the storage tank outlet. Parallel flow mixing tanks can only satisfy part of the evening load and must be oversized (the heat stored in the tank must exceed the heat delivered).

Moreover, series connected storage tanks cannot always be used. As a mixing tank, they are the least complicated method of filtering out short term fluctuations that occur when the array is shaded by clouds. They are not appropriate for energy storage when the array is not above the load temperature. If the array operates at its maximum temperature in order to meet the load requirement, the only way the PV-T system can generate more heat than used by the load (heat that is to be stored and saved for evening use), is by having a flow rate higher than needed by the load. If the flow rate is higher than needed by the load, the extra flow must bypass the load, hence, the tank is not truly in series with the load, but is multipley connected--both series and parallel.

If the array can operate at a temperature beyond the load requirement, then an important mixing valve series tank option exists that should be considered (see figure IV-26). When there is extra heat, the temperature is above that required by the load, and enough fluid is diverted through the tank to keep the load temperature at the proper level. This stores heat in the tank. The return to the heat exchanger array is at normal temperature, so using the cooling tower is not required.

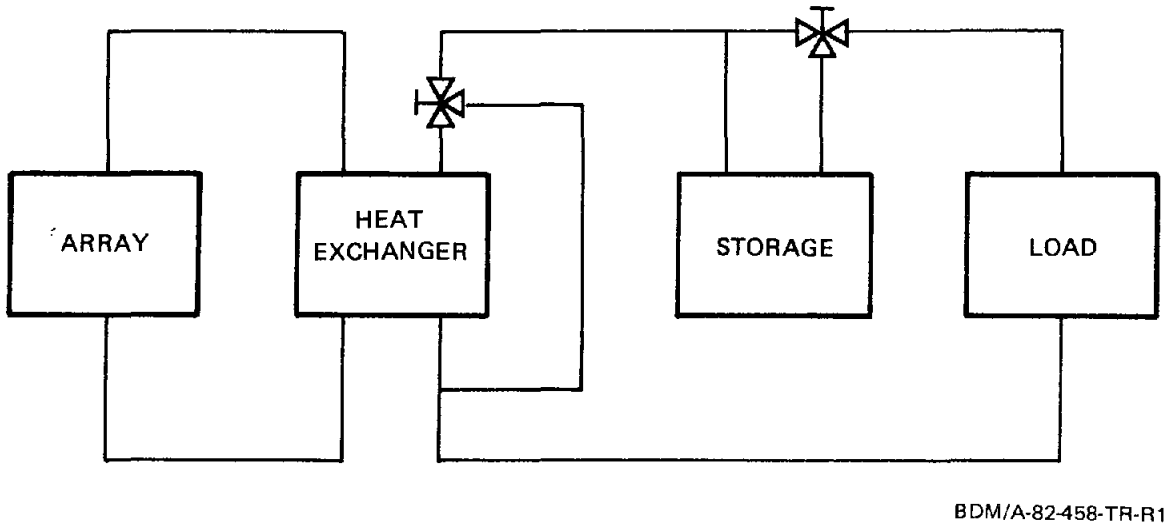

Figure IV-26. Series Tank with Mixing Valve

It can readily be shown that it is more efficient to store extra heat, even if it means operating the array at hotter than normal load requirements, than it is to use the cooling tower. That is, the penalty for lost heat and parasitic electrical power associated with using the cooling tower exceeds the penalty of poorer performance of the array when operating at higher temperatures.

Table IV-7 shows the conditions under which various types of storage tanks can be used. Variable volume storage is thermodynamically superior. Such a storage system requires level controls or a level monitoring system. It also requires an extra pump. Where more than one storage tank type is appropriate, the choice of storage system should be based on total system performance.

F. PUMP SELECTION AND SIZING

After selection of the heat transfer fluid (HTF) and the general field layout, an HTF circulation pump can be selected and sized to the PV-T system. Because manufacturers data and design curves are presented in English units and developed pressure in feet of head, the discussion in this section will use these conventional units.

TABLE IV-7. APPLICABILITY OF VARIOUS STORAGE TANKS

	ARRAY SIZE			
	OUTPUT<< DAYTIME LOAD	OUTPUT~ DAYTIME LOAD	OUTPUT> DAYTIME LOAD <<NIGHTTIME LOAD	OUTPUT ~ LOAD
ARRAY TEMPERATURE	ONLY NEED SMALL STORAGE TANK IN SERIES TO FILTER FLUXUA-TIONS IN ARRAY OUTPUT	NEED STORAGE TANK TO INTERFACE AUXILIARY HEATER TURNDOWN	NEED STORAGE TANK TO SUPPLY HEAT FOR NIGHT-TIME	NEED VARIABLE VOLUME STORAGE TANK
TA > TL		o SERIES o PARALLEL o VARIABLE VOLUME		
$T_A \leq T_L$		o PARALLEL o VARIABLE VOLUME		

The two methods of controlling a PV-T system are: (1) constant temperature (variable flow), and (2) constant flow (variable temperature). For the constant temperature system, there are two ways to vary the flow: (1) variable speed (change the rpm of the pump), or (2) variable head (change the system head by throttling with a valve). Both systems require additional system hardware capital costs such as a motor controller or a modulating control valve which have to be recovered in operational savings. The variable head system has the added disadvantage of always requiring the same pump power that the variable speed pump requires at its peak speed, so it has been dismissed as an option for PV-T systems. The variable speed system will use less pump power when the solar insolation is at off-peak conditions. However, since it is a constant temperature system like the variable head system, it has a higher collector annual average temperature than the constant flow system, and therefore has a lower collector annual efficiency. The monetary impact of operating a constant temperature/variable speed system with a lower collector efficiency is dependent on the temperature rise in a delta-T loop and the characteristics of the collector, which may vary for each system. In addition, as the flow rate through each deta-T string varies, thereby changing the manifold flow rate, the flow distribution through the collector rows will change. Thus, a valve, adjustable as the flow rate varies, is required on each row in order to maintain a balanced flow.

Constant flow systems are operated at constant pump speeds and allow the collector temperature to vary during the day as the insolation varies. This type of system is less complex, more reliable, and less costly than the constant temperature system described previously. It also has a lower collector average temperature than the constant temperature system, and therefore has a higher collector annual efficiency. Since the flow rate remains constant, flow balancing is required only at system start-up.

Before a pump is chosen for the PV-T system, certain preliminary information is required:

(1) The tentative system piping layout should be designed.

(2) The required pump capacity, Q, should be determined. This capacity is a function of the energy collected by the collector field, the field inlet and desired outlet temperatures, and the fluid specific heat, density, and maximum temperature limit.

(3) The system head loss, H, to be made up by the pump must be calculated. The head loss depends on the pipe sizes used in the system layout, consequently, pump sizing may be an iterative procedure.

(4) The net positive suction head available (NPSHA) to the pump must be determined. This is the energy in feet of liquid pumped that must exist at the pump inlet over and above the vapor pressure of the liquid at operation temperature. The available NPSHA is:

$$\text{NPSHA} = \frac{p_1 - p_v}{\rho} + (S - h_f) \qquad \text{(Eq. IV-70)}$$

where:

NPSHA = available net positive suction head during operation, meters (feet) of fluid

p_1 = pressure on surface of liquid in suction vessel, Pa (psf) absolute

p_v = vapor pressure at liquid temperature, Pa (pounds per square foot) absolute

ρ = fluid density, kg/m^3 (lb per cubic foot)

S = vertical distance from pump center line to level of liquid in suction vessel, meters (feet), positive if level is above pump, negative if below

h_f = friction losses in suction piping, meters (feet) of fluid

The NPSHA of the system must be 0.915 m (3-ft) greater than the net positive suction head required (NPSHR) by the pump in order to prevent fluid cavitation which lowers the pump efficiency, makes noise, and damages the pump. NPSHR is determined from tests conducted by the pump manufacturers, and is dependent on the pump design and flow rate.

There are generally two categories of pumps, positive displacement (PD), and centrifugal. The PD pumps are basically "constant volumetric rate" pumps when operated at a constant rpm. They include rotary (gear, screw, lobe, etc.), and reciprocating (piston, plunger, etc.) pumps. PD pumps are usually used when a metered volume of pumped fluid is to be added to a process, when pumping high viscosity fluids (oil-field mud pumps, slurry pipelines, etc.), or when high pressures are required (boiler feedwater pumps). Since the clearances are minimal between rotating parts in PD pumps, they often exhibit wear when pumping fluids that are not clean. For this reason, and the fact that PD pumps are more costly than centrifugal pumps, it is recommended that centrifugal pumps be used on the PV-T system.

Single-stage centrifugal pumps are usually used in high flow rate systems and are capable of passing larger fluid contaminates than PD pumps, thereby reducing maintenance repairs. For any given pump (PD or centrifugal), the relationship between a pump with a given diameter at two different speeds, N_1 and N_2, are described by the "affinity laws" as follows:

$$\frac{H_1}{H_2} = \left(\frac{N_1}{N_2}\right)^2 \qquad \text{(Eq. IV-71)}$$

$$\frac{Q_1}{Q_2} = \frac{N_1}{N_2} \qquad \text{(Eq. IV-72)}$$

$$\frac{BHP_1}{BHP_2} = \left(\frac{N_1}{N_2}\right)^3 \qquad \text{(Eq. IV-73)}$$

where:

N = pump speed, rpm

H = total head, meters (feet) of fluid

Q = flow rate, m^3/sec (gpm)

BHP = kilowatts (brake horsepower),

$$BHP = \frac{(Q)(H)(\text{specific gravity})}{3960\ (\text{pump efficiency})} \text{ (English units)}$$

(Eq. IV-74)

$$kW = \frac{(Q)(H)(\text{specific gravity})}{(1000)\ (\text{pump efficiency})} \text{ (SI units)}$$

Specific speed (N_s) is a non-dimensional design index used to classify pump impellers as to their type and proportions. It is defined as the speed in revolutions per minute at which a geometrically similar impeller would operate if it were of such a size as to deliver one gallon per minute against one foot head. The understanding of this definition is of design engineering significance only, however, and specific speed should be thought of as an index used to predict certain pump characteristics. The following formula is used to determine specific speed:

$$N_s = \frac{N\sqrt{Q}}{H^{3/4}} \qquad \text{(Eq. IV-75)}$$

where:

N = pump speed in rpm

Q = capacity in gpm at the best efficiency point (BEP)

H = total head per stage in feet at the best efficiency point. For double suction impellers, the total flow should be divided by two when calculating the specific speed.

The specific speed determines the general shape or class of the impeller as shown in figure IV-27. As the specific speed increases, the ratio of the impeller outlet diameter, D_2, to the inlet or eye diameter, D_1, decreases. This ratio becomes 1.0 for a true axial flow impeller.

High Head
Low Flow

Low Head
High Flow

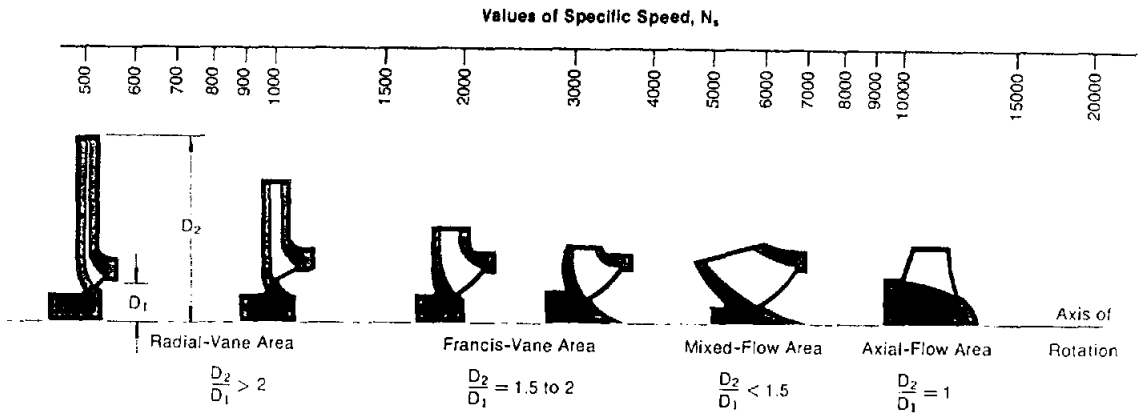

BDM/A-82-458-TR-R1

Figure IV-27. Impeller Design Versus Specific Speed

Radial flow impellers develop head principally through centrifugal force. Pumps of higher specific speeds develop head partly by centrifugal force and partly by axial force. A higher specific speed indicates a pump design with head generation more by axial forces and less by centrifugal forces. An axial flow or propeller pump with a specific speed of 10,000 or greater, generates its head exclusively through axial forces. Radial impellers are generally low flow/high head designs whereas axial flow impellers are high flow/low head designs.

Most of the pumps selected for a PV-T system will have flow rates between 0.00631 and 0.01893 m^3/sec (100 and 300 gpm), heads between 15.2 and 61 m (50 and 200-ft), and pump speeds of either 3,500, 1,750 or

1,150 rpm. This means that generally the specific speeds will be between 200 and 3,000. As indicated in figure IV-27, this type of pump will either have a Radial or Francis vane area design and will have a pump curve characteristic as shown in figure IV-28.

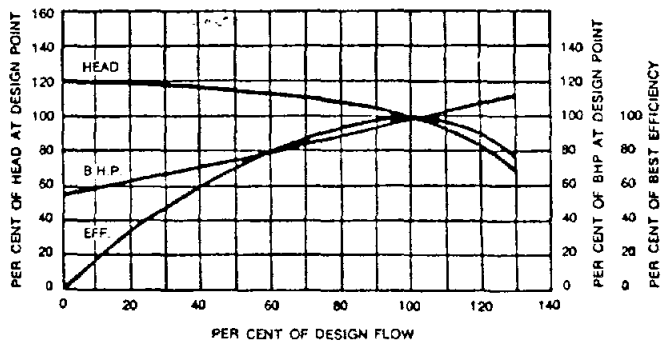

BDM/A-82-458-TR-R1

Figure IV-28. Radial Flow Pump

Figure IV-29 shows the general effect of reducing the impeller diameter for a centrifugal pump with a given casing size and rpm.

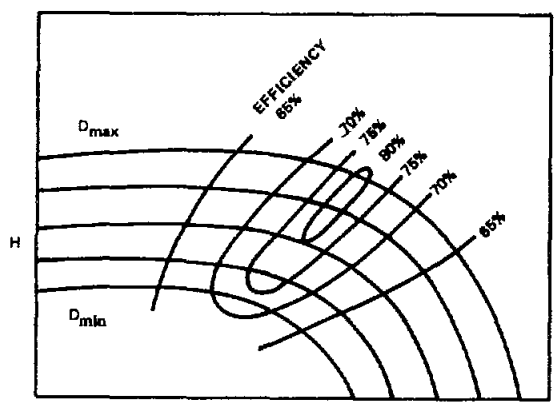

BDM/A-82-458-TR-R1

Figure IV-29. Variable Impeller Diameter Curves

After calculating the system flow rate (Q), system pressure drop (H), and system NPSHA, the optimum pump size and corresponding efficiency can be calculated. As an example, use Q = 0.0158 m^3/sec (250 gpm), H =

45.7 m (150-ft), NPSHA = 6.1 m (20-ft), and pump speed of 3500 rpm. Use the nomograph of figure IV-30 to calculate pump specific speed (N_S) by entering the graph at 250 gpm and following up to pump speed of 3500 rpm, across to the system head loss of 150-ft, and then up to read N_S = 1300.

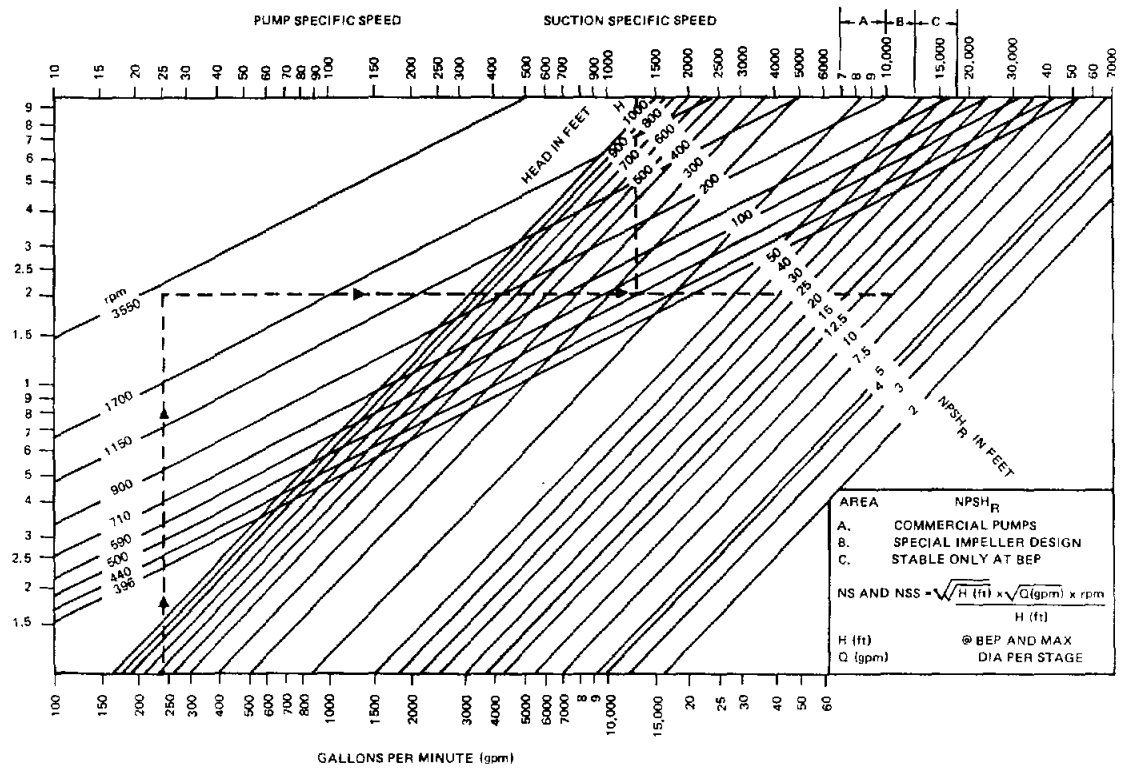

BDM/A-82-458-TR-R1

Figure IV-30. Nomograph Relating Pumping Head, Capacity, and Speed to Determine Pump and Suction Specific Speeds for Centrifugal Pumps (V. Lobanoff, "Specific Speed is a Usefull Index for Pump Design and Selection," Power, June 1979) (Reproduced with permission of Author)

Another important consideration is the suction specific speed (N_{SS}) which is calculated similarly to the pump specific speed (N_S), except that the NPSHR of the pump is used instead of the system head.

$$N_{ss} = \frac{N\sqrt{Q}}{(NPSHR)^{3/4}} \qquad \text{(Eq. IV-76)}$$

The N_{ss} of the pump cannot be calculated yet because we have not chosen the pump, and therefore do not know its NPSHR. However, most commercially available pumps operate within a N_{ss} range from 7000 to 10,000, and this range can be checked now against the operating conditions as shown with the dotted line in figure IV-30. Reading the range of NPSHR for the range of N_{ss} between 7000 to 10,000 we find that: 3.35 m < NPSHR < 4.57 m (11-ft < NPSHR < 15-ft). Since the system NPSHA is 6.1 m (20-ft), then the NPSHA exceeds the highest possible NPSHR by 1.52 m (5-ft) which is greater than the 0.91 m (3-ft) recommended, and is therefore sufficient. If this had not been the case, a lower pump speed would have been required.

Since the system's NPSHA is sufficient for almost any commercially available pump, the pump casing size and efficiency can now be calculated. Entering figure IV-31 with the N_s of 1300 calculated from figure IV-30, proceed until the maximum best efficiency point (BEP) of 77 percent is found, then read across for D_s = 1.25. This is the "specific diameter" and allows the optimum pump diameter to be calculated from:

$$D = \frac{D_s\sqrt{Q}}{H^{1/4}} \qquad \text{(Eq. IV-77)}$$

For the example:

$$D = \frac{1.25\ \sqrt{250}}{(150)^{1/4}} = 5.6\text{-in (14.2 cm)}$$

In summary, it has been shown that a constant flow rate system has a lower annual average temperature and is, therefore, more efficient than a constant temperature system. The advantages of centrifugal pumps over PD

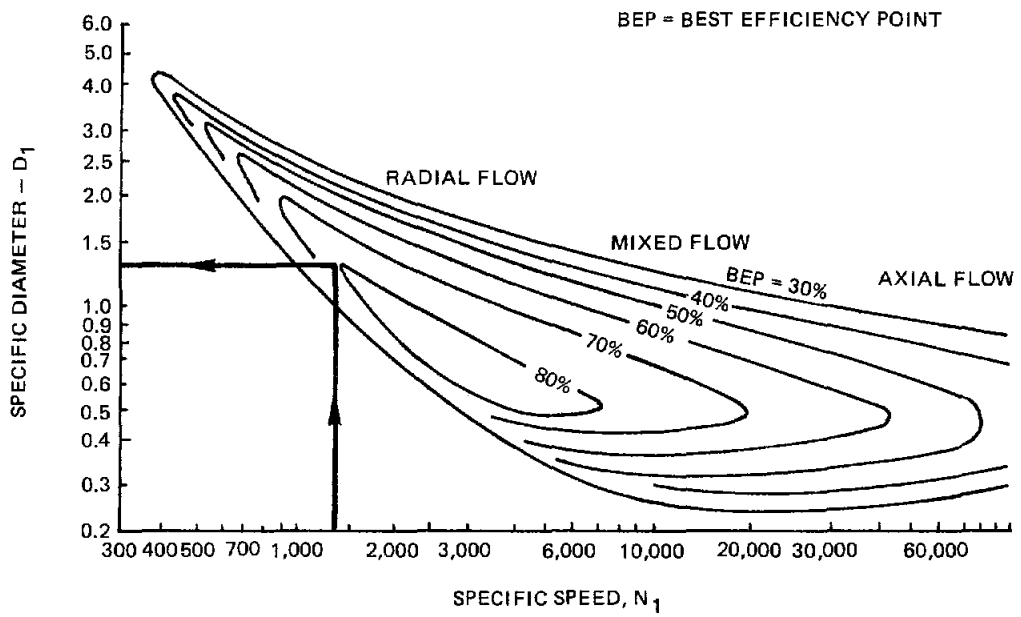

$$N_1 = \frac{N\sqrt{Q}}{H^{3/4}} \qquad D_1 = \frac{D\ H^{1/4}}{\sqrt{Q}}$$

N = REV/MIN
Q = FLOW, U.S. GPM
H = HEAD, FT
D = DIAMETER, IN.

BDM/A-82-458-TR-R1

Figure IV-31. Specific Diameter Versus Specific Speed and BEP (Excerpted by Special Permission from CHEMICAL ENGINEERING (April 3, 1978), Copyright 1978, by McGraw-Hill, Inc., New York, NY, 10020

pumps was presented and the general behavior of centrifugal pumps and their design was explained. Knowing the system's design flow rate (Q) and head (H), the optimum best efficiency point (BEP) and pump size were chosen using the specific speed (N_s) parameter. After selection of the optimum pump size, the designer can now search through pump manufacturer's catalogs and choose the appropriate pump.

G. VALVES

Valves are installed in a mechanical system to regulate flow and temperature, and to isolate flow for maintenance. The number and characteristics of valves chosen for a solar system should be selected carefully because valves add to system cost and are sources of pressure drop and heat loss during operation and overnight cool-down. PV-T systems operate at low temperatures (<103.4^{o}C) which allows flexibility in valve choice. In addition, PV-T systems generally do not operate at high pressures and are often closed systems. Sealing pressures are not high and absolute shutoff is generally not necessary. Isolation valves would most often be closed when the system is down and some degree of leakage can be accepted. Automatic valves may be used in systems that use an expensive heat transfer fluid (HTF) in order to prevent loss of the costly fluid when a leak is detected by the system.

1. Selection of Valves

Before the proper valve can be selected for an application in the PV-T system, certain design parameters must be known about the system:

(1) System pipe material and size
(2) System temperature
(3) System pressure
(4) System HTF
(5) Maintenance schedule for valve

After determining these factors, the proper valve can be chosen for a specific application in the PV-T system.

2. Construction of Valves

The materials used to construct a valve and the type of connector are important aspects of choosing a valve, and must be compatible with the rest of the system.

a. Materials

1) Valve Body

It pays to know the range of materials from which valves, fittings, and pipe are usually made, and to understand the pressure, temperature and structural limitations of each material. It may be highly unsafe to use certain materials for services beyond their recommended maximum. Piping equipment commonly used in industry falls into the four basic material groups shown below. There are also one or more variants in each of these groups, and each variant has individual service characteristics.

a) Bronze

Bronze is widely used in valves and fittings for temperatures up to 232.2^{o}C (450°F). It is an alloy of copper, tin, lead, and zinc.

b) Cast Iron

Cast Iron is regularly made in three grades--cast iron, ferrosteel, and high tensile iron. It should not be used for temperatures exceeding 232.2^{o}C (450°F). Cast iron is commonly used for small valves and fittings having light metal sections. Ferrosteel is stronger than cast iron, and used for valves and fittings having medium metal thicknesses. High tensile is a high strength alloy cast iron principally used for casting large valves.

c) Malleable Iron

Malleable iron is particularly suited for use in screwed fittings, unions, etc., and also is used to some extent for valves and flanges. It is characterized by pressure tightness, stiffness, and toughness and is especially valuable for piping materials subject to expansion and contraction stresses and shock.

d) Steel

Steel is recommended for high pressures and temperatures and for services where working conditions, either internal or external, may be too severe for bronze or iron. Its superior strength and toughness, and resistance to piping strains, vibration, shock, low temperature, and damage by fire afford reliable protection when safety and utility are desired. Many different types of steel are necessary and available because of the broad application of steel valves and fittings.

2) Valve Seal

For the temperature and pressure ranges of a PV-T system, elastomers or impregnated asbestos are used for valve seals. Five such seal materials are listed below.

a) Buna N

A general purpose elastomer suitable for handling water, chemicals, and non-aromatic oils. Features high tensile strength, excellent resiliency properties, and long-time effectiveness in addition to a temperature range of -11.1^{o} to $+82.2^{o}C$ (-20° to $180^{o}F$).

b) (Ethylene-Propylene-Terpolymer) EPT

Increasingly popular in commercial and institutional piping installations. Handles water, gases, and many chemicals. Not suitable for oils. Temperature range of -11.1^{o} to $+135^{o}C$ (-20° to $275^{o}F$).

c) Hypalon

Exceptional resistance to chemicals as well as oils and solvents. Temperature range of -11.1^{o} to $+107.2^{o}C$ (-20° to $225^{o}F$).

d) Viton

Offers top resistance against corrosives, particularly at higher temperatures. Also suitable for handling oil, gasoline, and hydrocarbons. Temperature range of -11.1^{o} to $+107.2^{o}C$ (-20° to $225^{o}F$).

e) TFE

Basic ingredients are asbestos impregnated with 30 to 35 percent TFE (tetrafluoroethylene) for use up to $192.9^{o}C$ ($375^{o}F$).

A suitable binder is used to provide stability of molded parts. In addition, packings used with ferritic steel stems contain a corrosion inhibitor to avoid pitting of the stem. This seal has good service with petroleum oil products.

b. Connections

Just as a chain is only as strong as its weakest link, a piping system is no better than its connecting links. Specifying the right end connection on valves and fittings is, therefore, crucial.

Descriptions of the types of end connections most commonly used on valves and fittings follow, although not all piping materials are available in all types of end connections. Each type has one or more variants, with steel flange joints having the greatest variety.

1) Threaded

Screwed end valves and fittings are by far the most widely used. This type of end connection is found in brass, iron, steel, and alloy piping materials. They are suited for all pressures, but are usually confined to smaller pipe sizes. The larger the pipe size, the more difficult it is to make up the screwed joint.

2) Welded

Welding ends, available in steel valves and fittings only, are used mainly for higher pressure-temperature services. They are recommended for lines not requiring frequent dismantling. There are two types of welding end materials: butt- and socket-welding. Butt-welding valves and fittings come in all sizes; socket-welding ends are usually limited to smaller sizes, (less than 5.08 cm or 2-in).

a) Butt-Welded

Butt-welded joints are designed to combine serviceability with ease of installation. Butt-welding consists of beveling the two ends, lining up the two openings, and then making the circumferential butt-welds.

b) Socket-Welded

Socket-welding simplifies the welder's task. Socket-welding fittings have deep sockets with ample "come and go," hence pipe need not be cut to precise lengths.

The socket type weld has advantages over the butt weld that render it more suitable for smaller size piping (less than 5.08 cm or 2-in). Pipe does not have to be cut accurately unless it must be butted against a fitting shoulder. Since the pipe end slips into and is supported by the socket, the joint is self-aligning. Tack welding, special clamps to line up and hold the joint, and backing rings are unnecessary. Pipe used in socket-welding does not require beveling, and "icicles" and weld spatter cannot enter the pipe.

3) Brazed

Brazed end connections are available on brass materials. The ends of such materials are specially designed to use brazing alloys to make the joint. When the equipment and brazing material are heated with a welding torch to the temperature required by the alloy, a tight seal is formed between the pipe and valve or fitting. Despite similar construction, a brazed joint will withstand higher temperatures than a soldered joint due to the brazing materials used.

4) Solder

Solder-joint valves and fittings are used with copper tubing for plumbing and heating lines and for many low pressure industrial services. The joint is soldered by applying heat. Due to narrow clearance between the tubing and the socket of the fitting or valve, the solder flows into the joint by capillary attraction. The use of soldered joints under temperature is limited because of the low melting-point of the solder.

5) Flared

Flared end connections are commonly used on valves and fittings for metal and plastic tubing up to 5.08 cm (2-in) diameter. The end of the tubing is skirted or flared, and a ring nut is used to make a union-type joint.

3. Types of Valves

Several types of valves are typically used in systems to perform specific functions of isolation, throttling, check (back flow prevention), and pressure relief. These valves are shown in figure IV-32 and are described below.

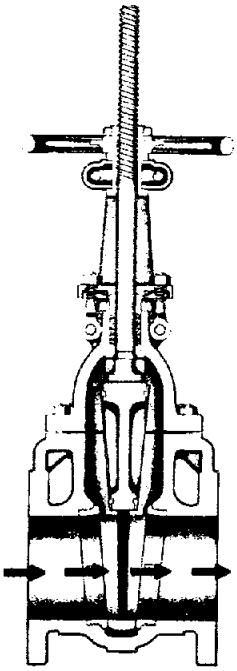

GATE VALVE

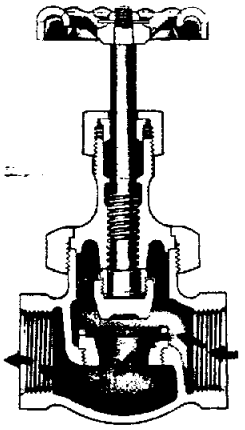

GLOBE VALVE

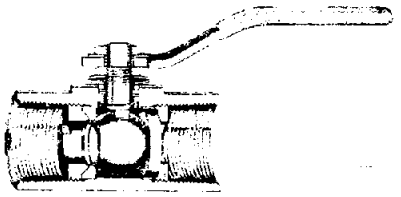

BALL VALVE

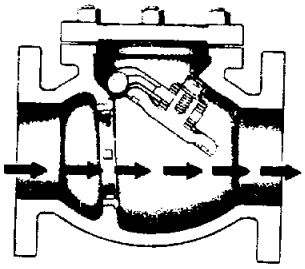

SWING CHECK

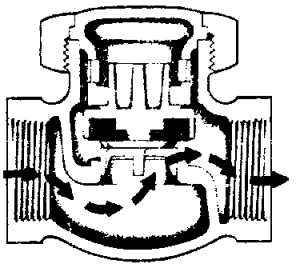

LIFT CHECK

"Courtesy of Crane Co."

BDM/A-82-458-TR-R1

Figure IV-32. Typical Cut-away View of Valves

a. Isolation Valves

Valves that are used for "on/off" or "fully open/fully closed" type of operation are called isolation valves. Types of isolation valves are quarter-turn, multi-turn, and piston/plunger which will now be described.

1) Quarter-Turn

Valves of the "quarter turn" family are so designated because a 90° turn of their operator fully opens or closes the valve. Two major categories are "butterfly" and "ball" valves. Both exhibit low pressure drop when fully open.

a) Butterfly Valves

Butterfly valves utilize elastomer seats and seals and their popularity can be attributed to the advancements made in elastomer materials and their low cost. They are used in the wide-open or fully closed position and are generally lighter in weight than conventional valves. The position of the lever indicates whether they are wide open, partially open, or fully closed. They are widely used in paper mills and cement mills, chemical and food processing plants, water filtration plants, petroleum product lines, air conditioning and water control, and similar applications. The valves are rated up to $64.4^{\circ}C$ ($180^{\circ}F$) and are bubble-tight at pressures up to 1.4 MPa (200 psi) for 5.08 cm to 30.48 cm (2 to 12 inch) sizes. Their Buna N seat is dimensioned to give maximum resiliency under the seating band of the disc. This permits optimum disc impingement for greater seat tightness without overstressing the liner. Seat materials other than Buna N are available. Butterfly valves are compact and space-saving, and easily installed in new piping or readily used as replacements in existing piping. They are easily adapted to lever, manual gear, or motor operation. They exhibit a small pressure drop due to the flow design.

Butterfly valves are available in large diameters but generally not in sizes less than 5.08 cm (2 inches) and should not be used when absolute shutoff is required.

b) Ball Valves

The advantages of quarter-turn ball valves are straight-through flow, minimum turbulence, low torque, tight closure, and compactness. Reliable operation, easy maintenance and long-life economy justify their extensive application. Industrial, chemical, petrochemical, refinery, pulp and paper, gas transmissions, water works and sewage, and power plants are utilizing ball valves where other types of valves have proven inadequate. Ball valves feature a top-entry capsule design providing easy "in-line" maintenance, if ever required. The two-piece capsule encasing the ball can be replaced with only a screwdriver or small wrench without removing the valve from the line. This inexpensive bronze valve (also carbon steel) is available in small sizes with screwed or solder-joint ends. Ball valves feature a synthetic elastomer capsule compounded especially for water service and hot oil. The elastomers, EPT and TFE, retain their resiliency and stability over a broad temperature range. All sizes have a bonnet gasket and packing box. Ball valves are an ideal choice for almost any water application within their pressure-temperature range. They are particularly suitable in water services subject to temperature fluctuations. TFE seals are recommended for a petroleum type HTF. Because of this construction, ball valves have a small drop and a small heat loss during operation.

2) Multi-Turn

A gate valve usually requires more turns to open it fully than do globe valves. Also, unlike many globe valves, the volume of flow through the valve is not in direct relation to the number of turns of the handwheel. Gate valves are by far the most widely used in industrial piping because most valves are needed as stop valves, to turn off or fully turn on flow--the only job for which gate valves are recommended. Gate valves are inherently suited for wide-open service. Flow moves in a straight line, and practically without resistance when the disc is fully raised. Seating is perpendicular or at right angles to the line of flow and meets it head on. That is one reason why gate valves are impractical for throttling service and for too frequent operation.

For instance, a 7.62 cm (3-in) gate valve holding fluid at 0.69 MPa (100 psi), puts a load of almost 454 Kg (1000 pounds) on one side of the disc, if there is only atmospheric pressure on the other. While seated tight, there is no wear or undue strain on disc or seats. But each time the valve is "cracked open," there is a threat of wire drawing and erosion of seating surfaces by the high-velocity flow. Repeated movement of the disc near point of closure under high-velocity flow, may create a drag on seating surfaces and cause galling or scoring on the downstream side. A slightly opened disc may cause turbulent flow with vibration and chattering of the disc. Since most gate valves have wedge discs with matching tapered seats, refacing or repairing of the seating surfaces is not a simple operation. Gate valves, like butterfly and ball valves, exhibit low pressure drop when fully open. They come in all sizes and are rated for the temperature and pressures of PV-T systems.

3) Piston/Plunger

Solenoid valves are similar in flow design to globe valves, but are electrically controlled to operate in either a fully open or fully closed manner. Depending on whether the valve is a normally open (N.O.) or normally closed (N.C.) valve, a piston or plunger that holds the valve disc moves on or off the disc seat to close and open the valve. Solenoid valves only work in one flow direction with the high pressure above the disc. They are mostly made of bronze and have a maximum pressure differential that they can operate against. Valve sizes are up to 7.62 cm (3-in) and they typically require 50 to 75 watts to energize. Temperatures up to 113.4^{o}C (300°F) and pressures up to 1.4 MPa (200 psi) are common.

b. Throttling Valves

Valves used to regulate or restrict flow are called throttling valves. The most common type of throttling valve is a globe valve. Unlike the perpendicular seating in gate valves, globe valve seating is parallel to the line of flow. All contact between seat and disc ends when flow begins. This is an advantage for more efficient throttling of flow, with minimum wire drawing and seal erosion. The

directly proportional relation of size of seat opening to number of turns of handwheel, a distinctive feature of plug-type globe valves, permits close flow regulation. An operator can gauge the rate of flow by the number of turns of the wheel. Shorter disc travel with fewer turns required to operate globe valves saves considerable time and work, besides wear on valve parts. Whatever wear occurs as the result of frequent or severe operation presents less of a maintenance problem than in gate valves. Seats and discs in most globe valves can be repaired without removing the valve from the pipe line. Globe valves come in all sizes and are rated for the temperatures and pressures of PV-T systems.

c. Check Valves

To prevent back flow in a pipeline, a check valve is used. Check valves allow flow in only one direction, come in all sizes, and are rated for temperatures and pressures of PV-T systems. Although all check valves fall into two basic categories, swing and lift, each has many variants. Swing checks, for example, are available in straight-way and "Y" patterns. Some have regrindable metallic discs, others, non-metallic disc facings. Outside lever and weight may be attached when necessary to increase sensitivity to flow. Lift checks are made in horizontal globe and angle patterns.

1) Lift Check Valves

Flow through a lift check follows a turning course through a horizontal bridge wall on which the disc is seated. The disc is equipped with a short guide, usually above and below, which moves vertically in integral guides in the cap and bridge wall. The disc is seated by backflow, or by gravity when there is no flow, and is free to rise and fall, depending on the pressure under it. Lift checks are recommended for steam, air, gas, water, and general vapor services.

2) Swing Check Valves

Since fluid movement through the valve body approximates straight line flow, swing check valves offer less resistance to flow than lift checks. Swing checks are, therefore, widely used for all pressure services, and especially on liquid lines. The disc, which is

hinged at the top, seats against a machined seat in the tilted bridge wall opening. The disc swings freely in an arc from fully closed position to one providing unobstructed flow. The valve is kept open by flow, with the size of opening varying with the volume of flow. Gravity and reversal of flow seat the disc, thereby preventing backflow.

d. Pressure Relief Valves

Pressure relief valves (PRV) are installed in a system in order to relieve over-pressures in the system, should they occur. Normally the discharge of the PRV is vented to the atmosphere (open discharge). The set pressure of the PRV is to be less than the smallest allowable pressure of any component of the system which is being relieved. ANSI-B31.1 Power Piping Code (1980) states:

122.6 Pressure Relief Piping

Pressure relief piping within the scope of this code shall be supported to sustain reaction forces, and shall conform to the following requirements.

122.6.1 Piping to Pressure-Relieving Safety Devices. There shall be no intervening stop valves between piping being protected and its protective device or devices.

122.6.2 Discharge Piping from Pressure-Relieving Safety Devices.

(A) There shall be no intervening stop valve between the protective device or devices and the point of discharge.

(B) When discharging directly to the atmosphere, discharge shall not impinge on other piping or equipment and shall be directed away from platforms and other areas used by personnel.

(C) It is recommended that individual discharge lines be used, but if two or more reliefs are combined, the discharge piping shall be designed with sufficient flow area to prevent blowout of steam or other fluids.

Sectional areas of a discharge pipe shall not be less than the full area of the valve outlets discharging thereinto and the discharge pipe shall be as short and straight as possible and so arranged as to avoid undue stresses on the valve or valves.

(D) Discharge lines from pressure-relieving safety devices within the scope of this Code shall be designed to facilitate drainage.

(E) When the umbrella or drip pan type of connection is used, the discharge piping shall be so designed as to prevent binding due to expansion movements.

(F) Drainage shall be provided to remove water collected above the safety valves seat.

4. Automation of Valves

If the HTF of a PV-T system is a combustible or expensive fluid, the designer may want to use automatic control valves to isolate system leaks when they are detected. Common methods of actuation are with electric or pneumatic controls. Even though a compressed air supply is often available at an industrial plant, it may not be available at a commercial building, therefore, electric controls are recommended for PV-T systems. These electric actuators may be specified for hazardous locations (NEMA 7) when used with a combustible HTF. The actuators can interface with all the valves mentioned thus far, except check and relief valves. Control of the actuators comes from temperature, pressure, and flow sensors.

5. Location of Valves

Valves work best when standing upright, with the stem pointing straight up. Any stem position from straight up to horizontal is satisfactory, but still represents a compromise. Normally, installing a valve with its stem down is not good practice. With a valve in this inverted position, the bonnet acts as a trap for sediment which may cut and damage the stem. An upside down position for valves on liquid lines subjected to freezing temperatures is bad because liquid trapped in the bonnet may freeze and rupture it. However, in solar systems, valves are usually installed with stems down so that if they leak the coolant will not saturate the insulation and produce greater heat loss. If the HTF is combustible, this acts as a safety feature, preventing wicking of oil throughout the insulation and causing a subsequent fire hazard.

On lines where continuous flow is desired, it is safer to have pressure below the disc than above it. For example, a disc may become separated from its stem and automatically shut off flow if pressure is above the disc. If this is dangerous for certain installations, then the pressure should be below the disc. In general, however, unless pressure under the disc is definitely required, a globe will give more satisfactory service when installed with pressure above the disc. An exception is a valve with a renewable composition disc which, preferably, should have pressure below the disc to assure longer disc life.

Considerable caution should be exercised when installing any check valve, whether swing or lift check type, to ensure that flow enters at the proper end, i.e., that the disc opens with flow. If the marking on the body of the valve is followed, the valve will be properly installed and the disc will be properly seated by backflow, or by gravity when there is no flow.

Spring loaded relief valves should be installed with the stem vertical. For air or gas service, these valves should preferably be installed inverted, to allow moisture to collect and seal the seating surfaces. No chips, scale, pipe dope, or other foreign matter should be left in the inlet of the valve or in the adjacent connections. Whenever piping is installed in the inlet or outlet of these valves, it must be at least as large as the valve connections. Under no circumstances should it be reduced. This piping should be adequately supported to prevent line strains from causing the valve to leak at the seat.

Valves should be located for ease of operation and maintenance. The following should be considered when locating valves:

(1) Valves should be placed in lines from headers in horizontal rather than vertical runs, so that lines can drain when valves are closed.

(2) Valves should be mounted directly to flanged equipment to avoid spooling unnecessary lengths of pipe.

(3) Adequate clearance should be provided between flanges and supports, etc., for ease of installation.

(4) Avoid, whenever possible, locating valves on pipe racks.

(5) Locate main isolation valves where they can be operated in an emergency.

(6) Manually-operated valves should be located at the plant perimeter.

(7) Protect automatic operators from the possible effects of fire.

(8) Locate valves, whenever possible, so that supports will not be on removable spools.

(9) Locate valves so that valve stems do not project into walkways, ladder space, etc.

(10) Valves in the heat transfer fluid system should be positioned with the stem downward in order to prevent insulation saturation and therefore reduce fire hazards and heat loss.

6. Application of Valves

It is generally preferable to weld steel valves in place for a solar system, particularly when operating under high pressure or using synthetic heat transfer oils. Compared to flanges and screwed fittings, welds are less massive, leak-free, have lower friction losses, and are more easily insulated. The disadvantages of welding, in addition to possibly higher initial cost, is the lack of flexibility in the piping system. For instance, the line cannot be broken for cleaning. Great care must also be taken not to gall the seat of valves welded-in-place due to replacement difficulty.

Isolation valves should be placed at the inlet and outlet of pumps. Butterfly valves should be used for temperatures less than 135°C (275°F), if possible. Storage tanks and other vessels should be isolated with valves.

Gate and globe valves are considerably more massive than butterfly or ball valves. Their stems provide a considerable surface for heat loss. Gate valves should only be used in the fully open or fully closed position. In the partially open position, the gate is subject to rapid wear and positive sealing will be lost. When fully open, a gate valve causes minimal pressure drop. A globe valve always results in

considerable pressure drop. Flow through the valve is almost proportional to the number of screw turns that the valve is open. Due to the large pressure drop across globe valves, ball valves are recommended for minor throttling.

Ball valves should be used for vents and drains, as well as to isolate instruments such as pressure and flow indicators, and for minor throttling. If piping is correctly sloped with as few changes in slope as possible, vent and drain valves can be located to serve large lengths of line, thus minimizing the number of such valves.

H. MANIFOLD PIPING

Piping in the U.S. has its diameter specified in terms of inches and pump curves are drawn in terms of gallons per minute of flow rate and feet of head of developed pressure. So that the concepts developed in this section can be applied more easily to manufacturers' data, relationships in this section will be developed in English units.

Manifold piping is required to send and return the heat transfer fluid to and from the collector field. This thermal transport system is one of the main components of a distributed, actively cooled, collector field. In designing the collector field piping, one must consider the effects of the layout on collector performance, thermal losses within the field, electrical energy for pumping, and the capital and installation costs of the piping network and insulation. In addition, the piping network must be designed for safety in accordance with the ANSI B31.1 Power Piping Code. In this section, the factors to be considered in a safe structural design, as well as the factors associated with minimizing the total piping costs will be discussed.

1. Pipe Sizing and Cost Analysis

As the diameter of the manifold pipe is increased, the electrical parasitic losses associated with pumping power decrease; however, the thermal losses and capital costs of pipe, fittings and insulation increases. As the manifold piping extends into the collector field, the

volume of fluid is reduced, so smaller pipe sizes with less heat loss and lower capital cost may be used; however, care must be taken that installation costs are not unduly increased due to the increased number of reducing flanges and associated welding.

An analysis of the economically optimized pipe size was performed in reference IV-12, which indicated greater pressure drops in the manifold than is typical for process piping systems. These larger manifold pressure drops are nearly equal to the pressure drop in the collector string, potentially causing flow regulation problems and excessive temperature differentials between the collector rows.

A study was performed in reference IV-13 in which a constraint is placed on the manifold pipe sizes such that only 20 to 30 percent of the pressure drop in the collector row is to be dropped in the manifold piping. Using this constraint, a practical way to size and telescope the manifold was developed and is summarized here.

After determining the pressure drop in a collector row (see equation IV-8) the allowable telescoping-manifold pressure drop can be determined. Only the pressure drop in the manifold piping between collector rows is included in the allowable pressure drop, because pressure drops in the supply and return lines affect all drive strings equally, and do not produce different collector flow rates. Once the telescoping-manifold pressure drop is set (typically 20 to 30 percent of the collector row pressure drop), the allowable pressure drop per foot of manifold pipe can be established. The length of the telescoping-manifold piping is divided into the total allowable pressure drop yielding the allowable average pressure drop per unit length of pipe.

The length of the manifold depends on the distance between collector rows. The optimal distance between collector rows should trade off the effects of power losses due to collector shading, capital costs, field parasitics in terms of pumping power and electrical wire losses, and land costs. Collector shading and packing factors (collector aperture area/land area) were discussed in chapter I of Volume 1 for various collector types. The other factors depend on the specific application and collector field layout.

The allowable pressure drop per unit of manifold length determines the manifold sizes. It is assumed that the average pressure drop per pipe unit is the same for all pipe sizes. This assumption prevents pipe sizing that allows large pressure drops in only one pipe size. The manifold piping may be sized using the pressure drops for the applicable unit flow given in figures IV-33 through IV-37. A flow unit is the flow rate (in gpm) through each collector row; the number of flow units is the number of rows.

For an edge feed array, the manifold length (distance between first and last collector) is given in equation IV-78. The manifold length for a center fed array is given in equation IV-79.

$$L_m = \text{row spacing} * (\text{Number of rows-1}) * 2 \qquad \text{(Eq. IV-78)}$$

$$L_m = \text{row spacing} * (\text{Number of rows} - 1.5) * 2 \qquad \text{(Eq. IV-79)}$$

For a center feed array, it is not necessary for the hot return line to extend to the end of the field.

To size the manifold, first obtain the allowable pressure drop per foot of manifold length from equation IV-80.

$$\Delta P_a = \frac{F \Delta P_r}{L_m} \qquad \text{(Eq. IV-80)}$$

where:

ΔP_r = row pressure drop
F = 20 to 30 percent

Referring to figures IV-33 through IV-37, locate the intersection of ΔP_a and the maximum number of flow units, or collector rows, on the appropriate figure for the row flow rate. Pressure curves under this intersection are for pipes that are too large, with the proper size being the one directly above the intersection. To determine the number of rows fed

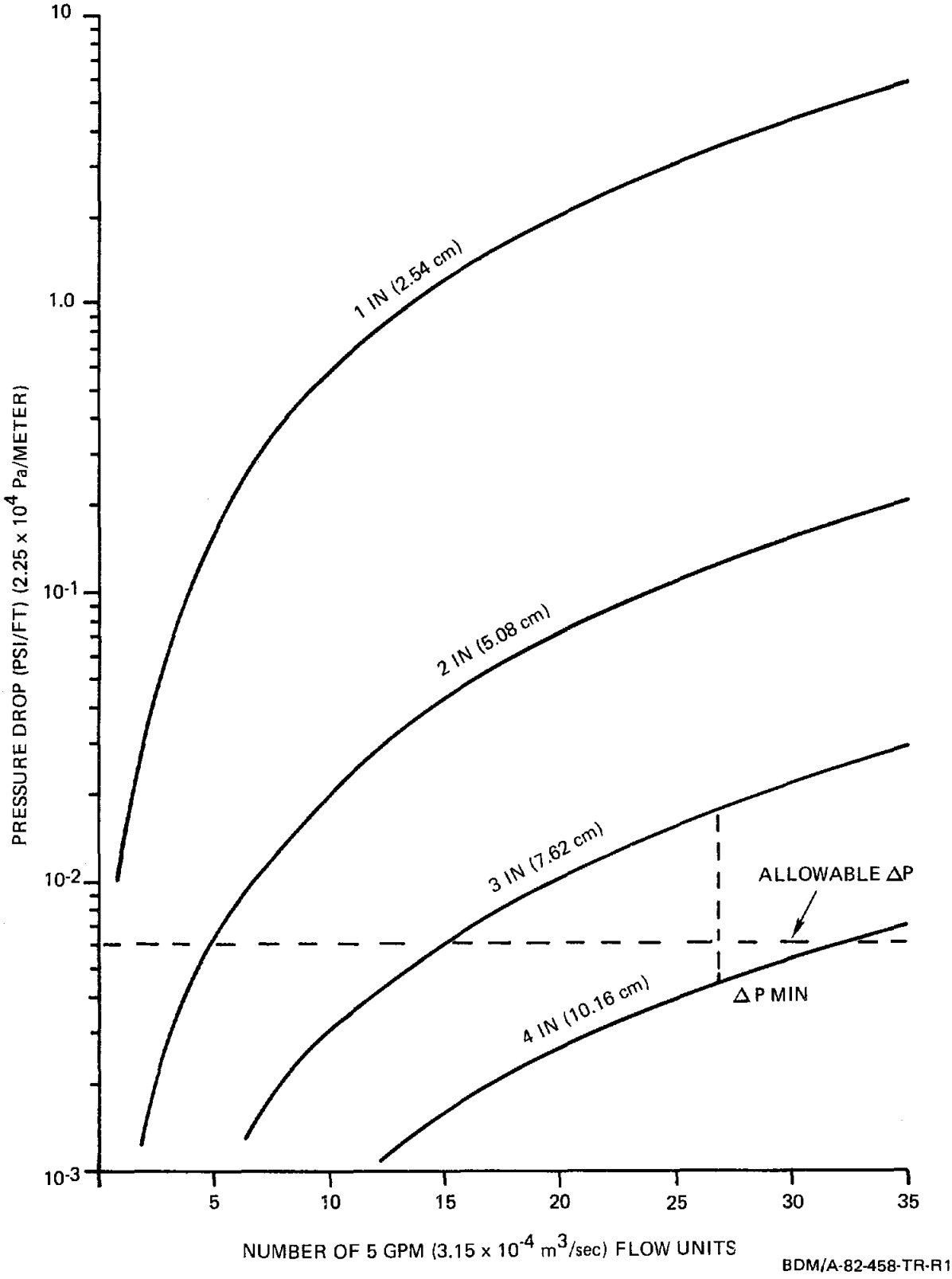

Figure IV-33. Pipe Sizing Chart for 5 gpm/row (3.15×10^{-4} m^3/sec/row)

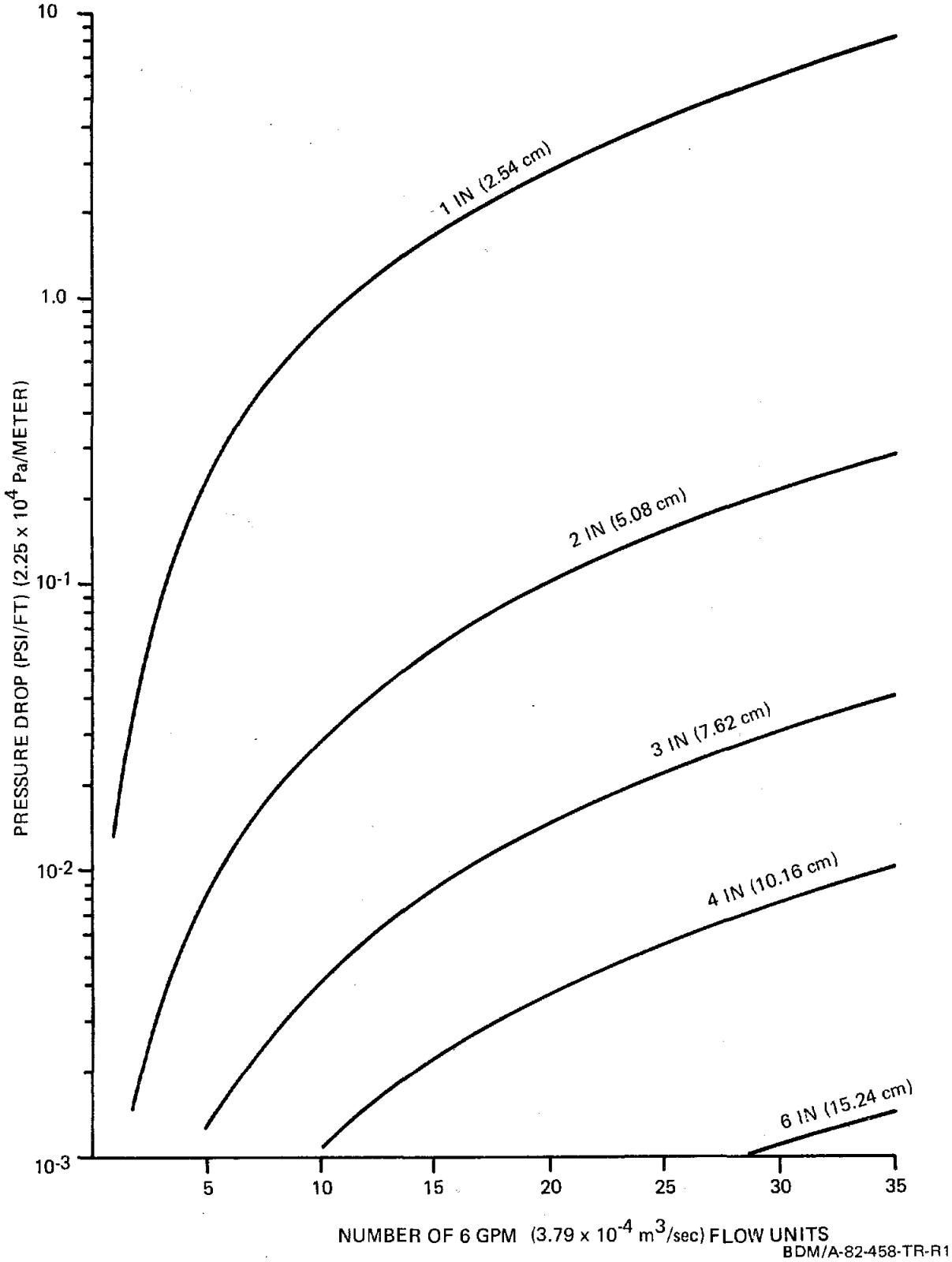

Figure IV-34. Pipe Sizing Chart for 6 gpm/row (3.79×10^{-4} m^3/sec/row)

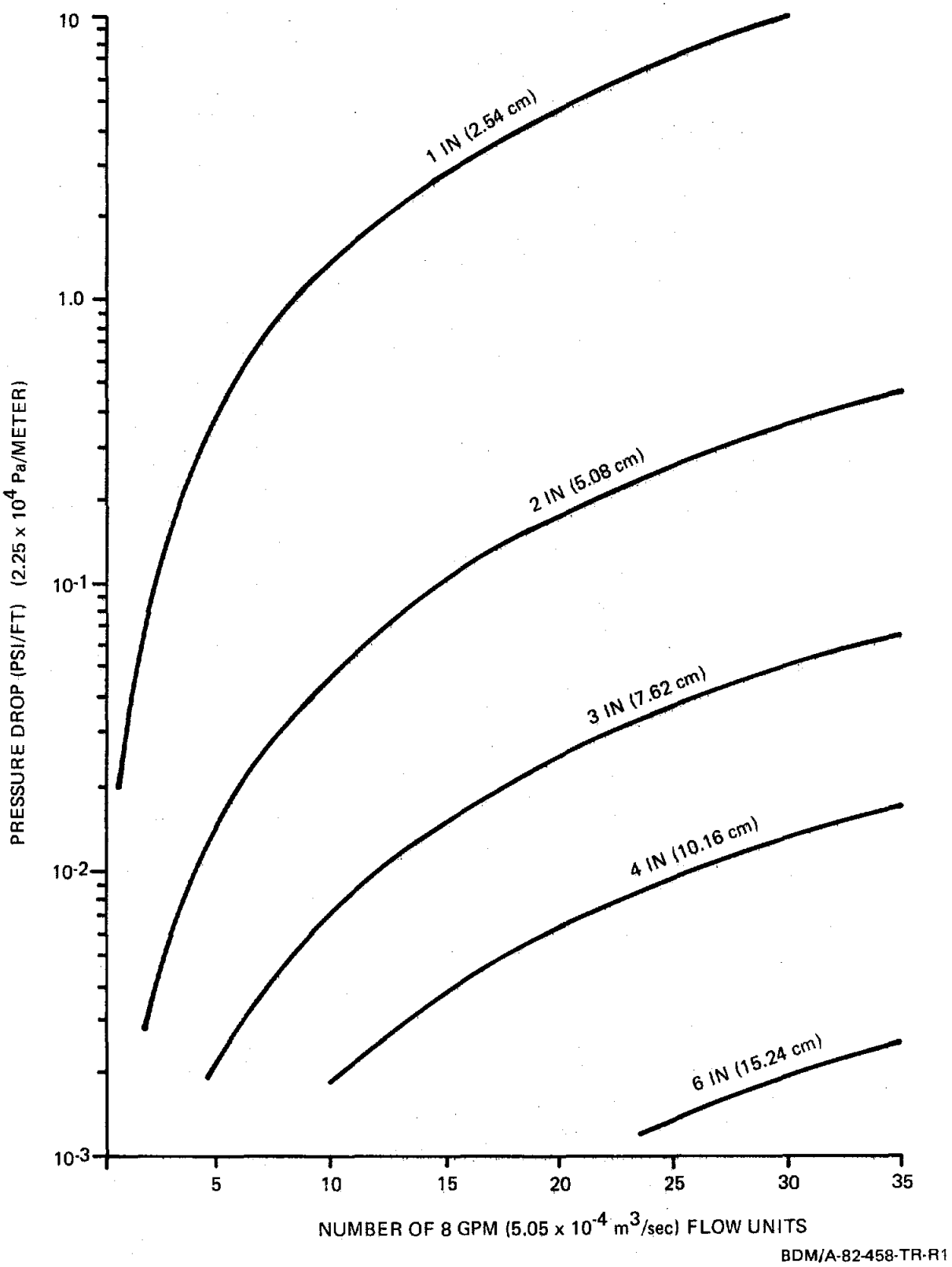

Figure IV-35. Pipe Sizing Chart for 8 gpm/row (5.05×10^{-4} m^3/sec/row)

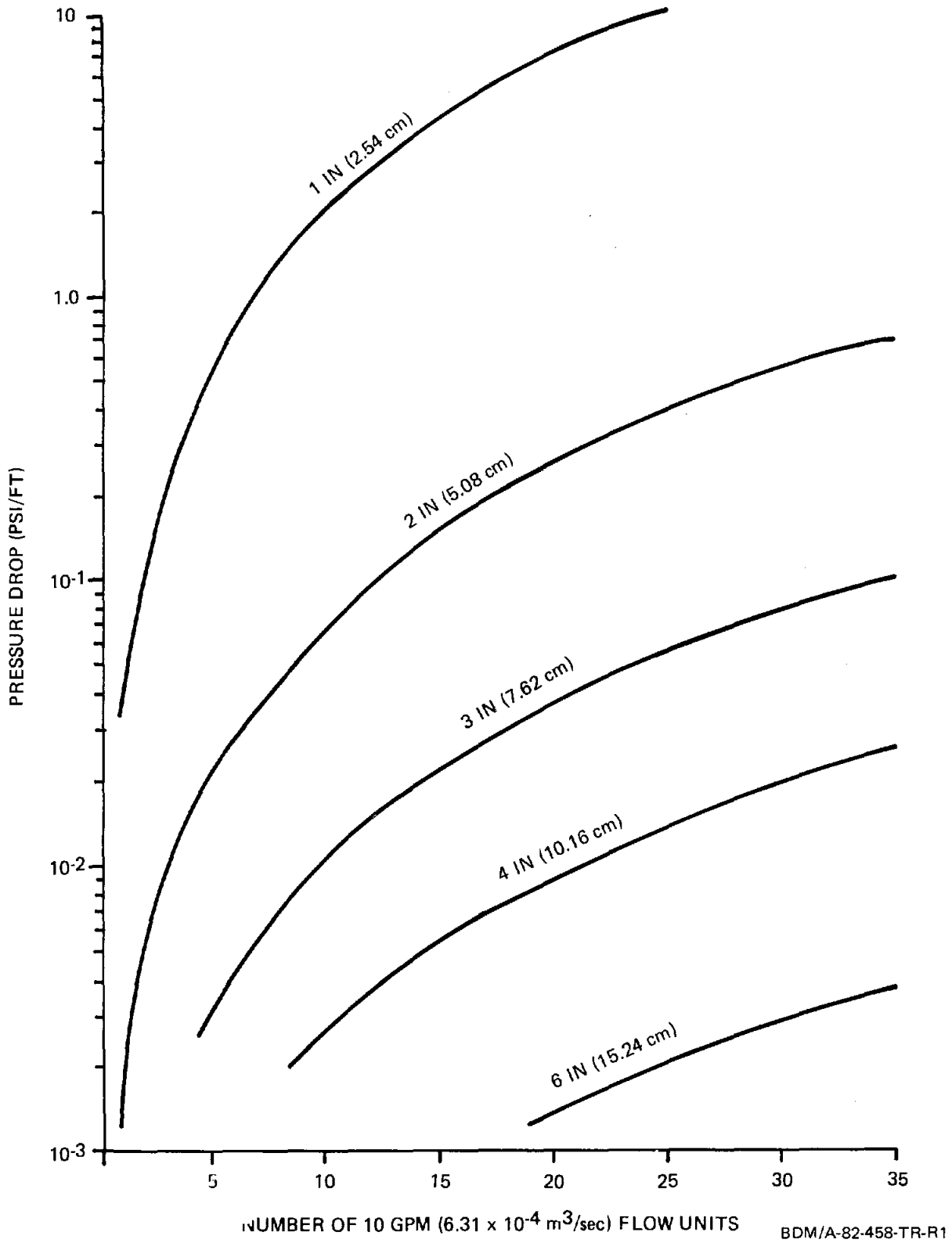

Figure IV-36. Pipe Sizing Chart for 10 gpm/row (6.31×10^{-4} m^3/sec/row)

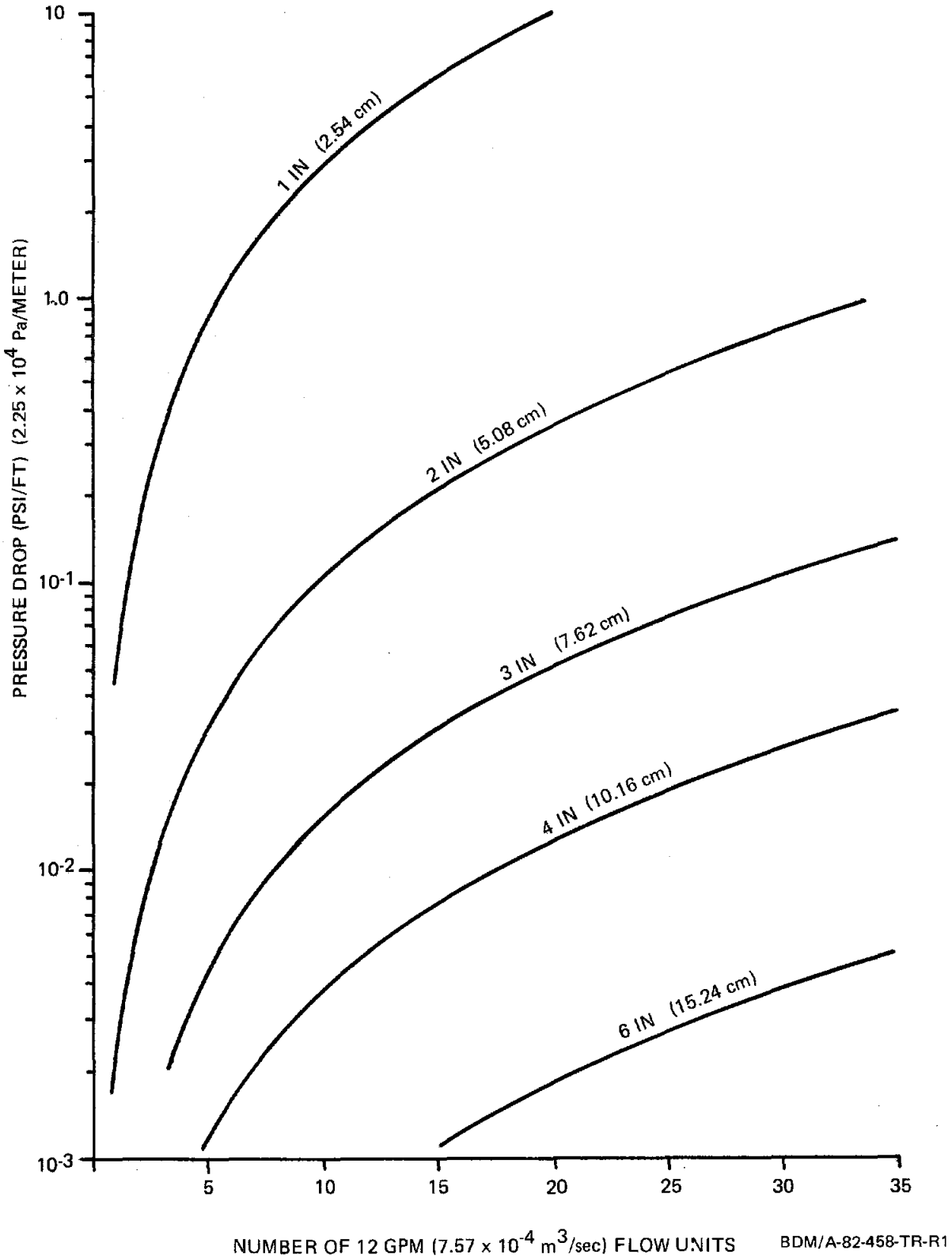

Figure IV-37. Pipe Sizing Chart for 12 gpm/row (7.57×10^{-4} m^3/sec/row)

by this pipe, the flow units are decreased until the average pressure drop in the pipe equals the allowable pressure drop. That is, when:

$$\Delta P_a = \Delta P_{avg} = \frac{1}{2} (\Delta P_{max} + \Delta P_{min}) \qquad \text{(Eq. IV-81)}$$

where ΔP_{max} is the pressure drop per foot at the maximum number of rows, and ΔP_{min} is the pressure drop that makes $\Delta P_{avg} = \Delta P_a$.

The next pipe size is chosen in the same manner by locating the pressure drop curve directly above the intersection of the allowable pressure drop and the current number of flow units. The number of rows fed by this pipe size is similarly determined by reducing the flow units until the average pressure drop in the pipe is equal to the allowable pressure drop. An example design for the telescoping manifold is given below.

Consider a collector field consisting of 36 ΔT strings of line focus Fresnel collectors, with 10 collector arrays per string. The flow rate per ΔT string is 5 gpm (0.0003155 m^3/sec) and the pressure drop per string is 41 psi (2.83×10^5 Pa). A center feed array is assumed with a row spacing of 20-ft (6.1 m). From equation IV-79, L_m = 1380-ft (421 m). From equation IV-80 with F = 0.2, the allowable pressure drop per foot of manifold length is 0.0061 psi/ft (137.3 Pa/m). Using this value in figure IV-33 locate the intersection with the number of rows. The pipe size immediately above this point is a 4-in (10.16 cm) pipe. Move down along this pressure drop curve until the average pressure drop for this pipe size equals the targeted allowable pressure drop; that is when:

$$\Delta P_{min} = 2\ \Delta P_a - \Delta P_{max} = (2)(0.0061) - 0.00765$$

$$\Delta P_{min} = 0.0045 \text{ psi/ft } (101.3 \text{ Pa/m})$$

The difference between the current flow unit and the total number of rows determines the number of rows fed by this size pipe (i.e., 9 rows are fed by the 4-in or 10.16 cm pipe).

Now locate the new pipe size (3-in or 7.62 cm) immediately above the allowable pressure drop and the current number of flow units. The maximum pressure drop per foot of the 3-in (7.62 cm) pipe is 0.0175 psi/ft (394 Pa/m) so that this pipe will feed the remainder of the array.

2. Field Pressure Drop Calculation

In order to size the circulation pump for the collector field coolant, the system head curve must be calculated. The total system head is the total discharge head (h_d) minus the total suction head (h_s). Thus:

$$H = h_d - h_s \qquad \text{(Eq. IV-82)}$$

The total discharge head is the sum of: 1) static discharge head; 2) all piping and friction losses on the discharge side of the pump including straight runs of pipe, losses at all valves, fittings, strainers, heat exchangers, and cooling towers; 3) pressure in a discharge chamber or expansion tank (if a closed vessel); and 4) losses at sudden enlargements such as vessel entrances.

Suction head exists when the liquid supply level is above the pump centerline or impeller eye. The total suction head is equal to the static height in feet that the liquid supply level is above the pump centerline less all suction line losses between the liquid supply and the pump entrance. If the supply is in an enclosed vessel, the gage pressure on the supply liquid is added.

In this section general relations are developed which can be used to calculate pressure drops through two types of collector fields.

The pressure drop through the field is combined with the pressure drop through the rest of the piping network to obtain the total discharge head for the pump.

a. Pressure Calculations

A general relation for calculating the pressure drop through a length of pipe is:

$$\Delta P = \frac{(G)^{1.8} \quad \mu^{0.2} \quad \rho^{0.8} \quad L}{4.7 \times 10^4 \quad D^{4.8}} \qquad \text{(Eq. IV-83)}$$

Where:

ΔP = pressure drop, psi (Pa)
G = flow rate, gpm (m^3/sec)
μ = viscosity, Cp (Pa·s)
L = equivalent length of pipe, ft (m)
D = pipe diameter, in (m)
ρ = fluid density, lbm/ft^3 (kg/m^3)

If SI units are used in equation IV-83, the constant in the denominator will change to 6.

As indicated previously, a data point from E-Systems for 150°F (65.6°C), 30 percent ethylene glycol at 5.85 gpm ($3.7 \times 10^{-4} m^3/s$) through nine arrays resulted in a pressure drop of 50.3 psid (3.46×10^5 Pa). The pressure drop through the collectors may be assumed to follow the above relation, and the equivalent length of an array determined. Using figures IV-38 and IV-39 to determine the density and viscosity, the equivalent length can be found from:

$$\frac{L_e}{D^{4.8}} = \frac{4.7 \times 10^4 \quad \Delta P}{G^{1.8} \quad \mu^{0.2} \quad \rho^{0.8} \quad N_c} = 403.4$$

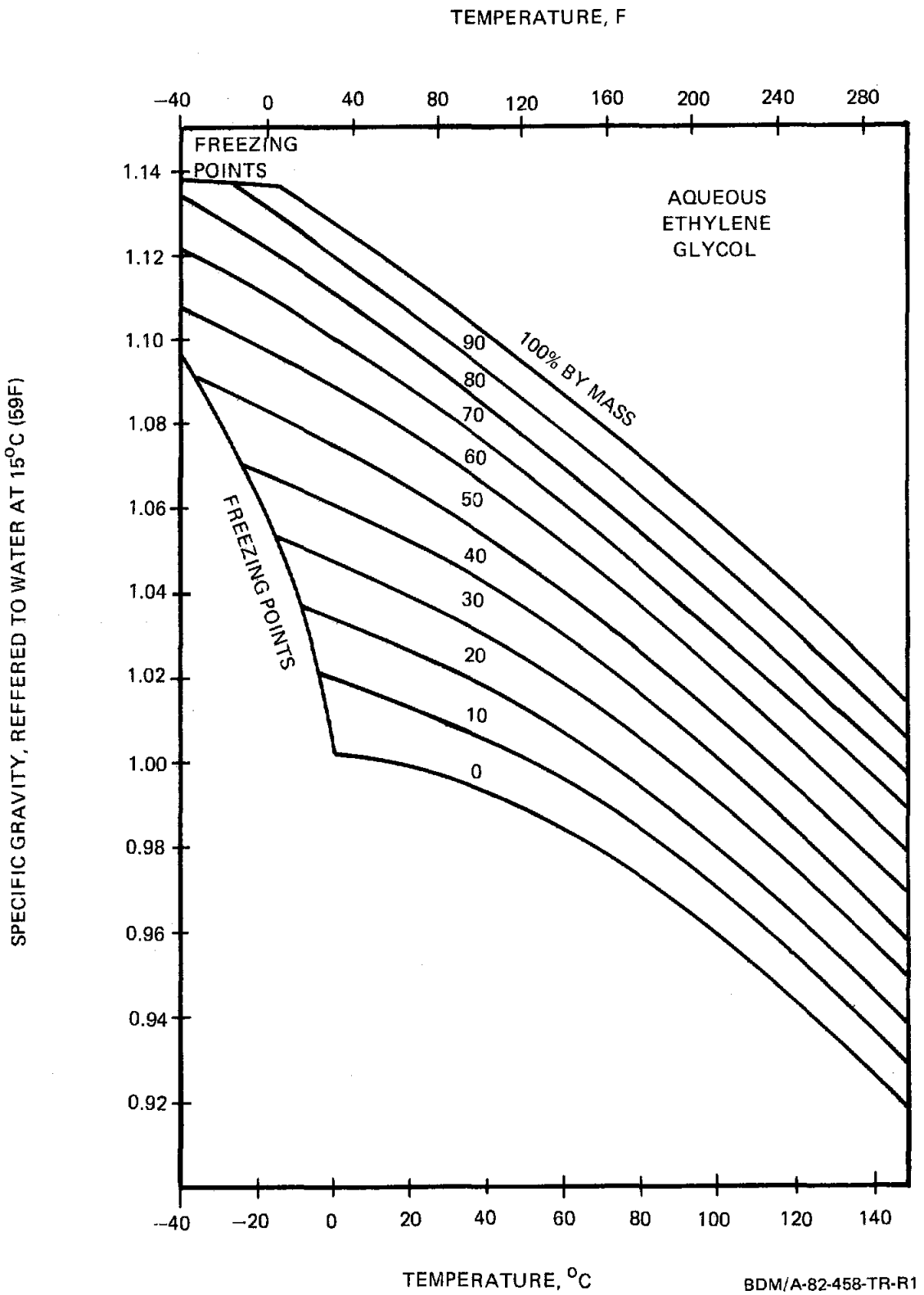

Figure IV-38. Specific Gravity of Aqueous Solutions of Ethylene Glycol

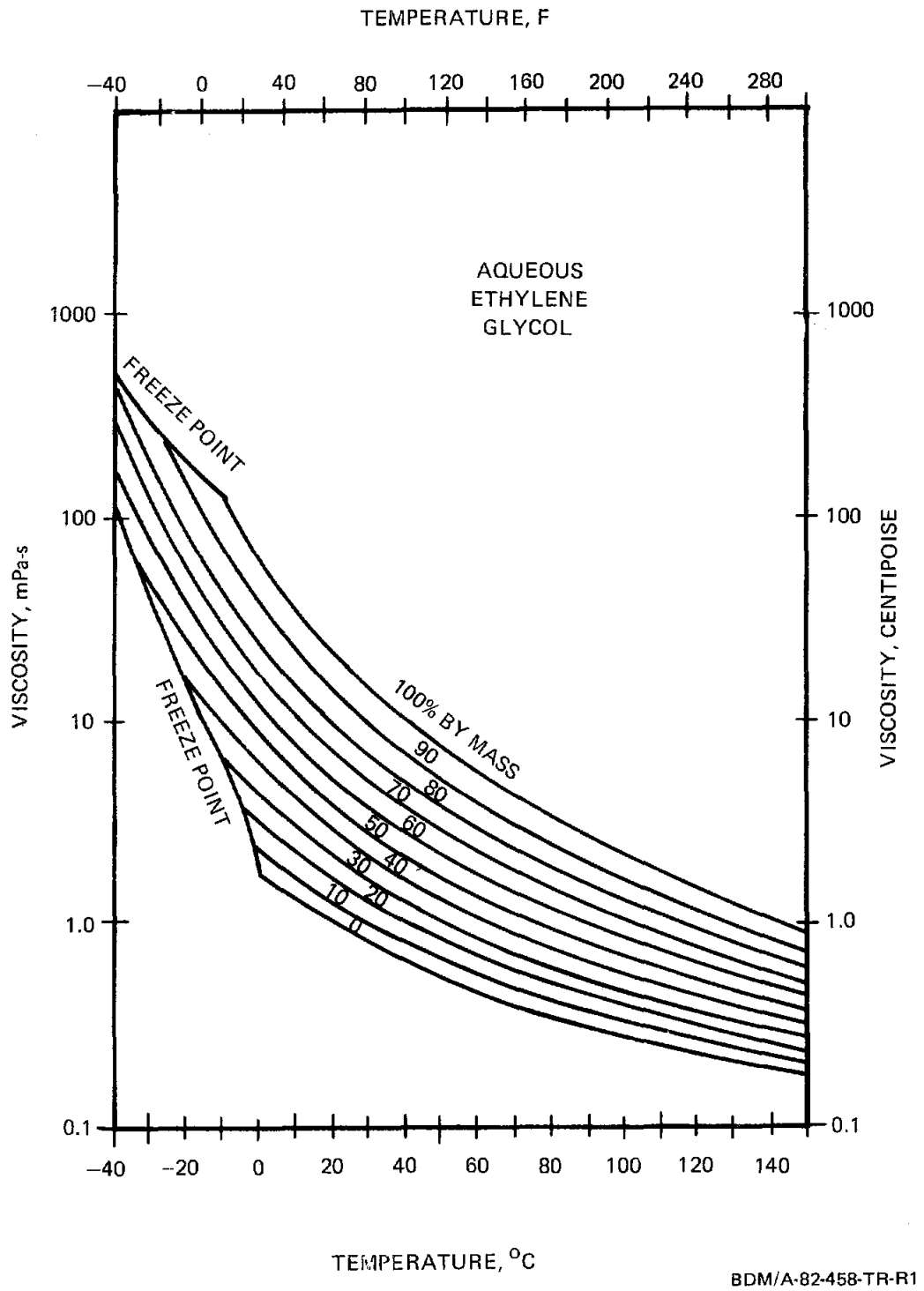

Figure IV-39. Viscosity of Aqueous Solutions of Ethylene Glycol

where N_c is the number of collectors. Then, the pressure drop in psi (or Pa) through a string of E-Systems arrays is given by:

$$\Delta P = 8.58 \times 10^{-3} \; G^{1.8} \; \mu^{0.2} \; \rho^{0.8} \; N_c \qquad \text{(Eq. IV-84)}$$

$$= 2.35 \; G^{1.8} \; \mu^{0.2} \; \rho^{0.8} \; N_c \text{ (SI units)}$$

These relations can be used to determine the head required to produce a given flow rate through the collector field. In order to determine the pressure drop in the field, an electrical analogy for the field flow resistance is used with the following relations:

$$\Delta P = R \; G^{1.8} \qquad \text{(Eq. IV-85)}$$

$$R = \frac{\Delta P}{G^{1.8}} \qquad \text{(Eq. IV-86)}$$

$$\mathring{P} = \frac{G \; \Delta P}{1714\eta} = \frac{R \; G^{2.8}}{1714\eta} \qquad \text{(Eq. IV-87)}$$

$$= \frac{G \; \Delta P}{\eta} = \frac{R \; G^{2.8}}{\eta} \text{ (SI units)}$$

where:

R = fluid flow resistance--psid/(gpm)$^{1.8}$ (Pa/(m^3/sec)$^{1.8}$)
ΔP = pressure drop--psid (Pa)
G = flow rate, gpm (m^3/sec)
$\mathring{P}$ = pumping power, hp (w)
η = pump efficiency

In the following sections, a technique will be derived for calculating the pressure drop across two types of collector field layouts, end feed with direct return, and center feed.

b. End Feed Direct Return

Consider a collector field with N rows of collectors with equal flow (G_r) through each row and with row spacing L (figure IV-40). The collector rows have supply and return manifolds on each end. The flow resistances of each row and each mainfold section are subscripted by R_{rn} and R_{mn} respectively.

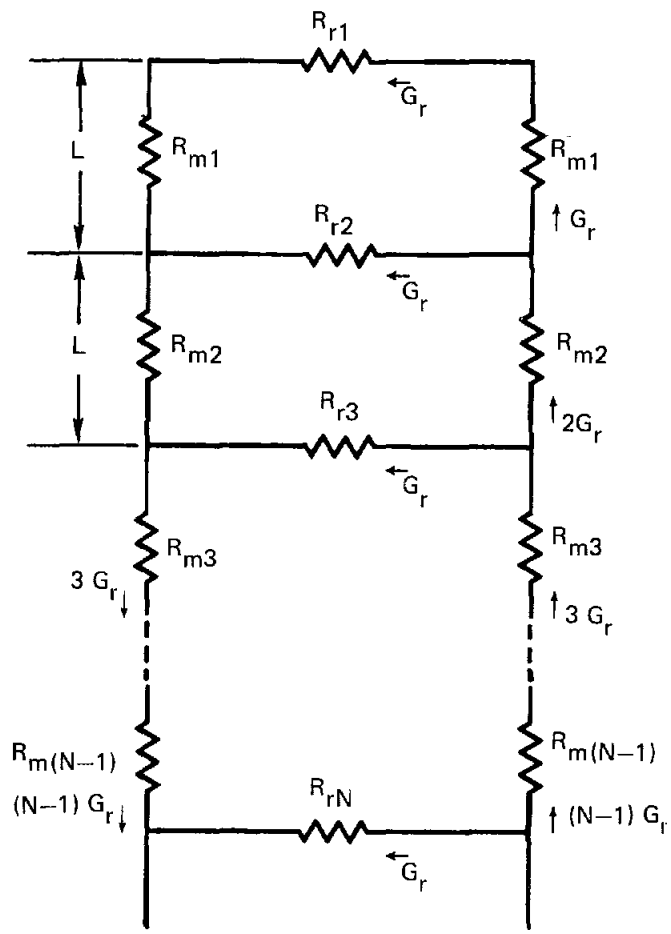

BDM/A-82-458-TR-R1

Figure IV-40. Collector Field Flow Resistance Network

This flow resistance network can be reduced to a single equivalent resistance by combining the resistances into successive

equivalent series and parallel resistances. First consider the series resistance of collector row 1 (R_{r1}) and the corresponding supply and return manifold resistances (R_{m1}). Referring to figure IV-41, the pressure drop of the equivalent resistance must equal the combined pressure drop of the manifold supply, collectors, and the manifold return.

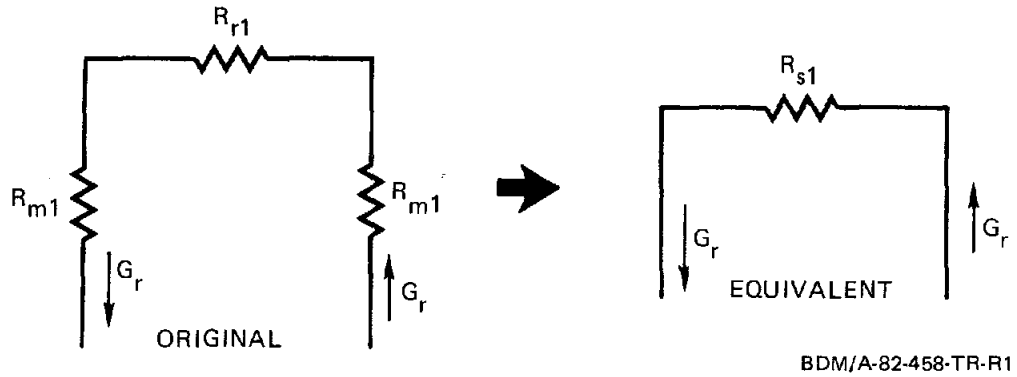

Figure IV-41. Equivalent Series Flow Resistance

Using equations IV-88 and IV-85, the equivalent series resistance is given by equation IV-90.

$$\Delta P_{m1} + \Delta P_{r1} + \Delta P_{m1} = \Delta P_{s1} \qquad \text{(Eq. IV-88)}$$

$$R_{m1}\ G_r^{1.8} = R_{r1}\ G_r^{1.8} + R_{m1}\ G_r^{1.8} = R_{s1}\ G_r^{1.8} \qquad \text{(Eq. IV-89)}$$

$$R_{s1} = 2R_{m1} + R_{r1} \qquad \text{(Eq. IV-90)}$$

The equivalent series resistance for collector row 1 reduces the network of figure IV-40 to that of figure IV-42. Now the parallel resistances of R_{s1} and R_{r2} are to be combined into an equivalent resistance (see figure IV-43). The pressure drop from node "a" to node "b" is equal through R_{s1} and R_{r2} and must be equal to the pressure drop through R_{p1}. Therefore:

$$\Delta P_{ab} = \Delta P_{s1} = \Delta P_{r2} = \Delta P_{p1} \qquad \text{(Eq. IV-91)}$$

using equation IV-85.

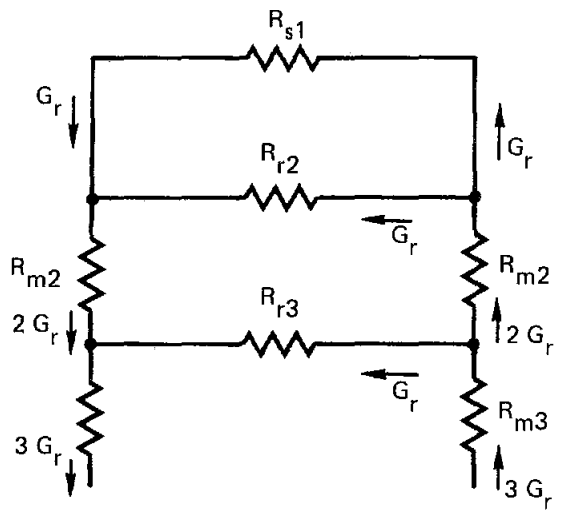

Figure IV-42. Series Reduced Network

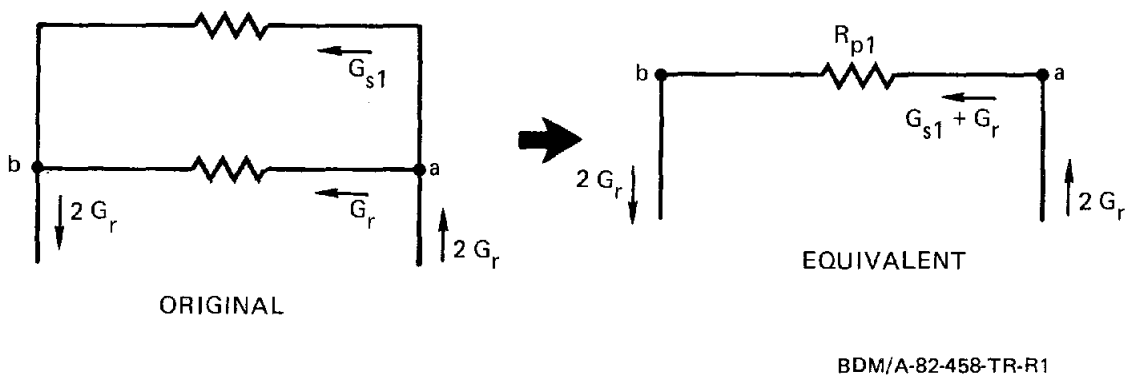

Figure IV-43. Equivalent Parallel Flow Resistance

$$R_{s1}\ G_{s1}^{1.8} = R_{r2}\ G_r^{1.8} = R_{p1}\ (G_{s1} + G_r)^{1.8} \qquad \text{(Eq. IV-92)}$$

or

$$R_{p1} = R_{s1} \left(\frac{G_{s1}}{G_{s1} + G_r} \right)^{1.8} \qquad \text{(Eq. IV-93)}$$

Equation (IV-93) gives the equivalent fluid resistance for R_{s1} and R_{r2} in parallel with flow rates of G_{s1} and G_r, respectively. Equation (IV-93) can be generalized to:

$$R_{pi} = R_{si} \left(\frac{G_{si}}{G_{si} + G_r} \right)^{1.8} = R_{si} \left(\frac{i\ G_r}{i\ G_r + G_r} \right)^{1.8}$$

$$= R_{si} \left(\frac{i}{i + 1} \right)^{1.8} \qquad \text{(Eq. IV-94)}$$

where "i" is the row number starting at the end of the collector field.

The equivalent parallel resistance for collector rows 1 and 2 reduces the network of figure IV-40 to that of figure IV-44.

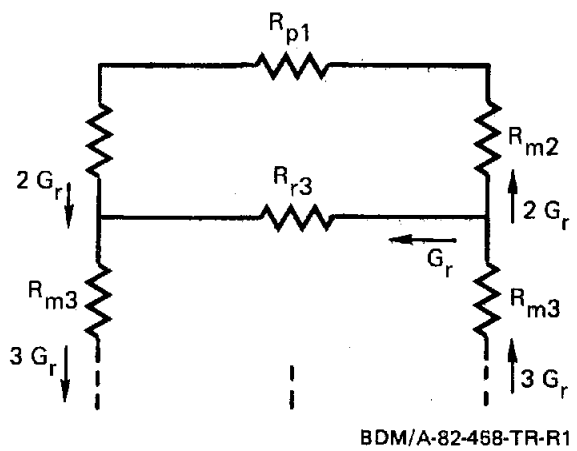

Figure IV-44. Parallel Reduced Network

Comparing figure IV-44 with figure IV-40 indicates that they have the same network configuration and that R_{r2}, R_{r1}, R_{m1} of figure IV-40 have been resolved into R_{p1}, of figure IV-44. Substituting R_{p1} for R_{r1} in equation IV-90 gives R_{s2} which is used in equation IV-94 to give R_{p2}. Thus, the general relation for the series resistance is:

$$R_{si} = 2R_{mi} + R_{pi} \qquad \text{(Eq. IV-95)}$$

with

$$R_{p1} = R_{r1}$$

Combining equations IV-83, IV-84 and IV-85, one obtains:

$$R_{r1} = 8.58 \times 10^{-3} \mu^{0.2} \rho^{0.8} N_c \qquad \text{(Eq. IV-96)}$$

$$R_{mi} = \frac{\mu^{0.2} \rho^{0.8} L_i}{4.7 \times 10^4 D_i^{4.8}} \qquad \text{(Eq. IV-97)}$$

where L_i and D_i are the length and diameter of the manifolds between rows i and i + 1.

The procedure of resolving the flow resistances into parallel and series equivalents is repeated until the network is reduced to only a single equivalent resistance. Then the pressure drop is found from:

$$\Delta P_{field} = R_{eq} (N G_r)^{1.8} \qquad \text{(Eq. IV-98)}$$

For an array with a single length between rows and a single diameter manifold, a simple computer program can be written to calculate the pressure drop across the collector field. This is shown in figure IV-45.

- o Calculate R_{r1} from equation IV-96
- o Calculate R_m from equation IV-97
- o $R_{s1} = R_{r1} + 2\ R_m$
- o For i = 1 to N - 1
- o $R_{pi} = R_{si}\ (i/(i + 1))^{1.8}$
- o $R_{s(i+1)} = R_{pi} + 2\ R_m$
- o NEXT I
- o $R_{eq} = R_{SN}$
- o $\Delta P = R_{SN}\ (N\ G_r)^{1.8}$

BDM/A-82-458-TR-R1

Figure IV-45. Computational Procedure for Calculating the Pressure Drop Across an End Feed Direct Return Collector Field

c. Center Feed

This type of collector field is shown in figure IV-46 along with its resistive network. The complete flow resistance network may be simplified by letting:

$$R_r = 2R_c + R \qquad \text{(Eq. IV-99)}$$

where R_c is the resistance of the collectors in a string, R is the resistance of the piping between two collector strings, and R_r is the total resistance of a single collector loop.

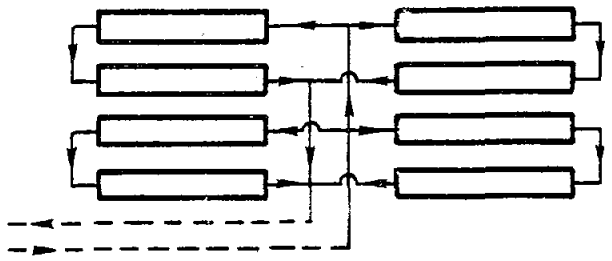

A. COLLECTOR LAYOUT

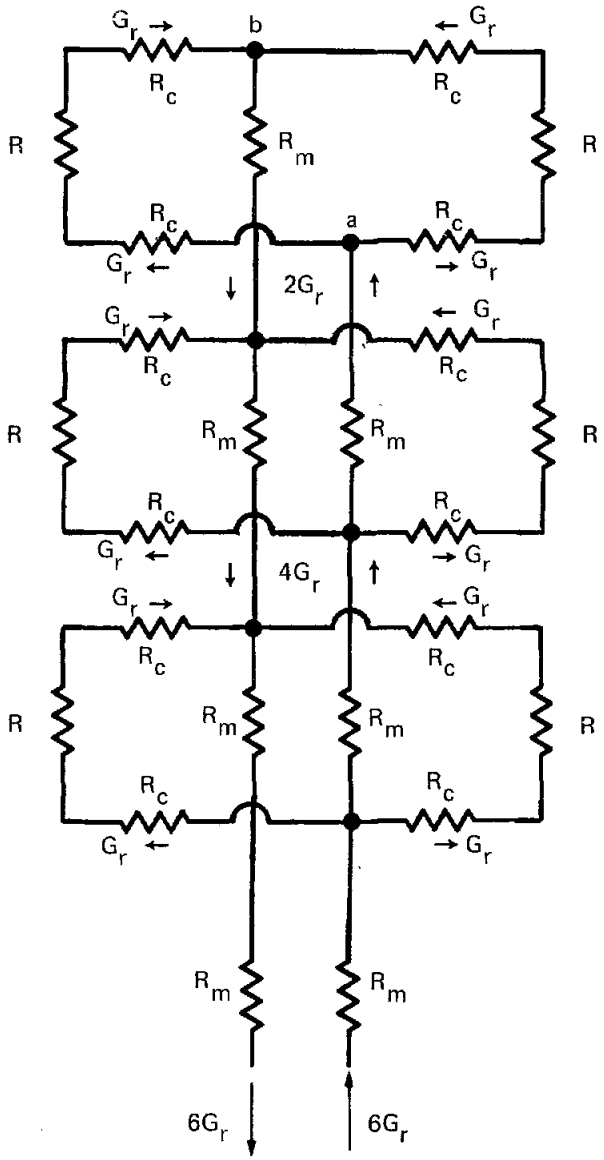

B. FLOW RESISTANCE NETWORK

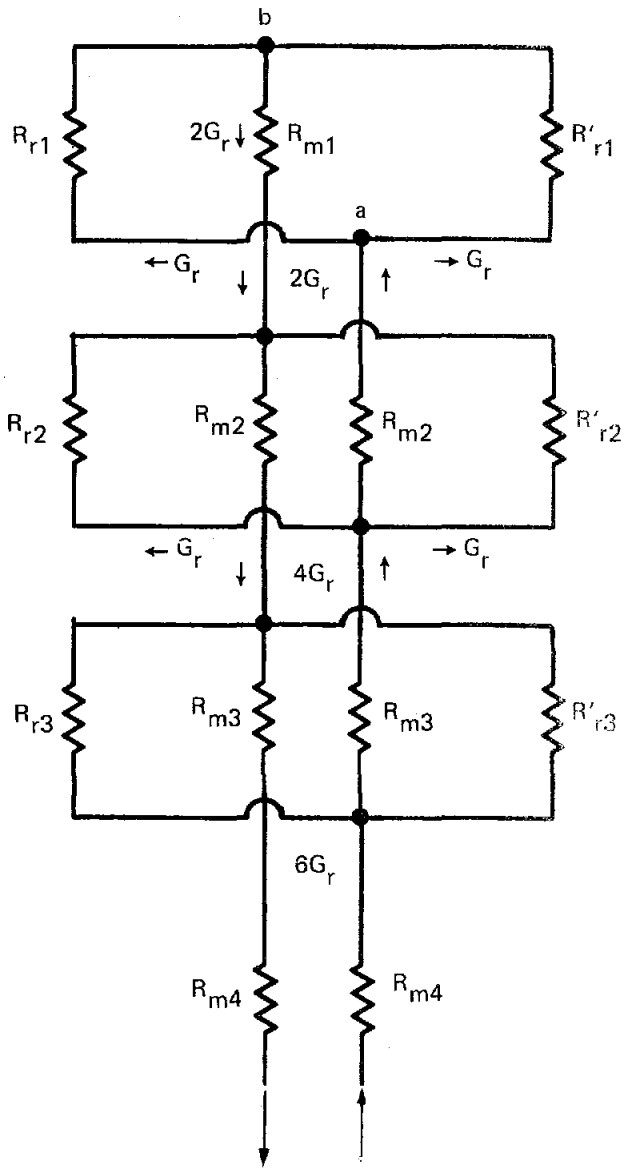

C. SIMPLIFIED RESISTANCE NETOWRK

BDM/A-82-458-TR-R1

Figure IV-46. Center Feed Collector Layout and Flow Resistance Network

Using the same arguments in the preceding section to obtain a single equivalent resistance, the pressure drop between nodes "a" and "b" is:

$$\Delta P_{ab} = \Delta P_{rl} = \Delta P_{ri} = \Delta P_{pl} \qquad \text{(Eq. IV-100)}$$

where P_{pl} is the pressure drop across and equivalent parallel resistance between nodes "a" and "b". Using equation IV-85:

$$R_{rl}\, G_r^{1.8} = R'_{rl}\, G_r^{1.8} = R_{pl}\, (2G_r)^{1.8} \qquad \text{(Eq. IV-101)}$$

$$R_{pl} = R_{rl} \left(\frac{1}{2}\right)^{1.8}$$

The equivalent network and subsequent equivalent series network is shown in figure IV-47 where:

$$R_{sl} = R_{pl} + R_{ml} \qquad \text{(Eq. IV-102)}$$

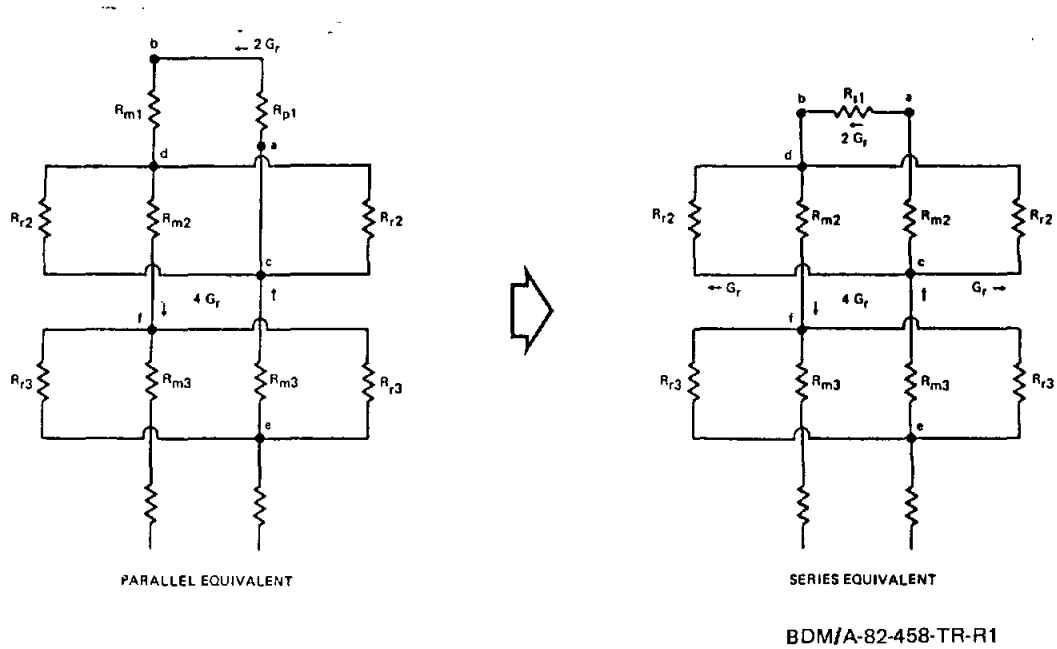

Figure IV-47. Equivalent Flow Resistance Networks

The pressure drop between nodes "c" and "d" is given by:

$$\Delta P_{cd} = \Delta P_{r2} = \Delta P_{r2'} = \Delta P_{p2} \qquad \text{(Eq. IV-103)}$$

$$R_{r2}\ G_r^{1.8} = R'_{r2}\ G_r^{1.8} = R_{p2}(4\ G_r)^{1.8} \qquad \text{(Eq. IV-104)}$$

$$R_{p2} = R_{r2}\left(\frac{1}{4}\right)^{1.8} \qquad \text{(Eq. IV-105)}$$

By analogy with the derivation of R_s, one finds:

$$R_{s2} = R_{p2} + R_{m2} \qquad \text{(Eq. IV-106)}$$

Again, a general relation for the equivalent parallel and series resistances can be deduced.

$$R_{pi} = R_r \left(\frac{1}{2i}\right)^{1.8}$$

$$R_{si} = R_{pi} + R_m$$

The collector resistance (R_c) is given by equation IV-96, and the resistance of the piping between collectors (R) is given by equation IV-97 where L_i is the sum of the length of pipe between collector strings and the equivalent length of two 90° elbows. The manifold resistance (R_m) is also given by equation IV-97 with L_i the distance between collector strings.

The total pressure drop across the field is given by equation IV-98. An equivalent resistance can be found using the procedure in figure IV-48 where N is the number of parallel loops in the field (six loops are shown in the example).

- o $R_r = 2\ R_c + R$ from equations IV-96 and IV-97
- o Calculate R_m from equation IV-97
- o For i = 1 to N/2
- o $R_{pi} = R_r\ (1/2i)^{1.8}$
- o $R_{si} = R_{pi} + R_m$
- o NEXT i
- o $R_{eq} = R_{SN}$
- o $\Delta P = R_{eq}\ (N\ G_r)^{1.8}$

BDM/A-82-458-TR-R1

Figure IV-48. Calculation Procedure for Pressure Drop

3. Power Piping Code

It is recommended that the pipe in a PV-T system be designed to comply with ANSI B31.1 Power Piping Code (ref. IV-14). This code is more conservative than some other piping codes, reflecting the need for long service life (> 10 years) and maximum reliability in solar system installations. An attempt to present the intent of the code as it applies to PV-T systems follows in this section. However, the code should be referred to in order to assure code compliance in a detailed design and even then, sound engineering judgement should be used, as indicated in the code's foreword:

> There are many instances where the code serves to warn a designer, fabricator, or erector against possible pitfalls; but the code is not a handbook, and cannot substitute for education, experience, and sound engineering judgement.
>
> The code never intentionally puts a ceiling limit on conservatism. A designer is free to specify more rigid requirements as he feels they may be justified. Conversely, a designer who is capable of a more rigorous analysis than is specified in the code may justify a less conservative design, and still satisfy the basic intent of the code.

4. Types of Pipe

a. Materials

For a typical PV-T system ($T < 250^{o}F$ ($121.1^{o}C$), $P < 100$ psi psi (0.69 MPa)), standard wall thickness pipe is sufficient to transport the HTF. Mild carbon steel (CS) is recommended as the pipe material because of its availability, cost, and weldability. In some instances, however, when there is considerable welding, it may be more cost effective to use a soldered copper system than a welded CS system. Plastic pipe is not recommended due to its susceptibility to ultraviolet and age hardening.

For CS systems, Class 150 is sufficient for the pipe and line component specification. The recommended material for pipe is

ASTM-A106 seamless Grade B for pipe less than 2-in (5.08 cm) in diameter and ASTM-A53 ERW Grade B for pipe 2-in (5.08 cm) in diameter or greater.

If small tubing (< 1-in or 2.54 cm) is required, 304 stainless steel ASTM-A268 is recommended to be used with compression fittings.

b. Connections

Several methods for making joints in CS piping systems are available including welds, flanges, and threads. Welding is the recommended method for CS systems, especially when using a highly flammable or expensive HTF. A welded system will reduce the number of hazardous or costly leaks. Socket welds (SW) are recommended for pipe sizes 2-in (5.08 cm) and smaller in diameter, while butt welds (BW) are recommended for pipe larger than 2-in (5.08 cm) in diameter. Hardware that requires high maintenance (e.g., valves, pumps, etc.) should be flanged in order to allow easy removal from the system.

c. Pipe Support

The three generic types of pipe supports are: hangers, guides, and anchors.

1) Hangers

Pipe hangers are used to support only the weight of the pipe along with the carried fluid and insulation. The pipe rests on the hanger and is free to move due to thermal expansion or other forces in the system. It is recommended that these hangers be designed with a rigid structural insulation at the point of support on the pipe (e.g., calcium silicate, foam glass, or Johns-Manville Marinite) which is capable of supporting the pipe, yet preventing excessive heat loss that would occur if the pipe directly contacted the hanger assembly (see figure IV-49).

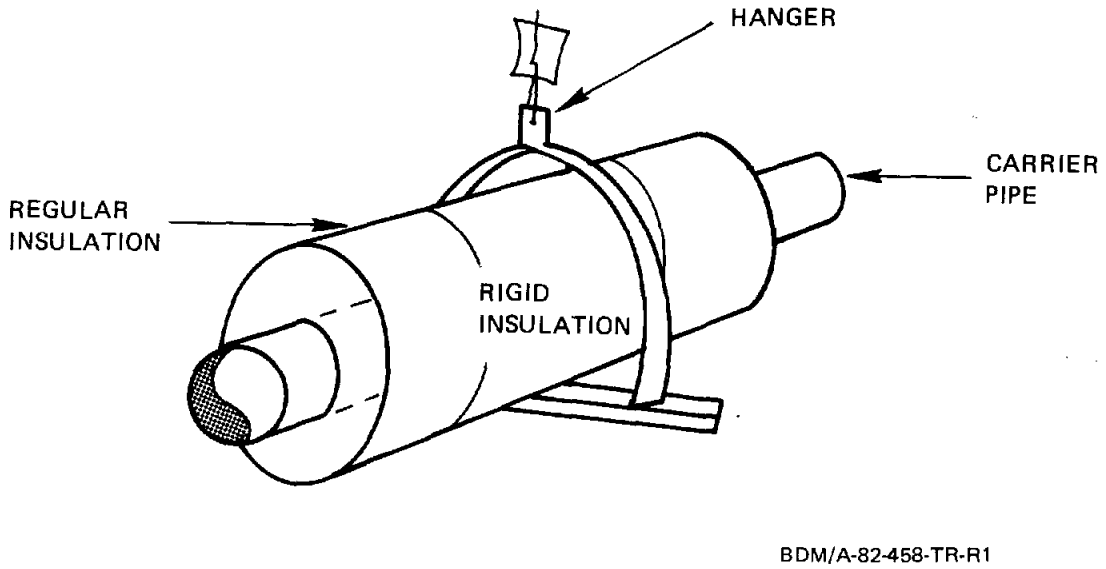

Figure IV-49. Typical Insulated Hanger

Supports for piping with the longitudinal axis in approximately a horizontal position should be spaced to prevent excessive sag, bending, and shear stresses in the piping, with special consideration given where components, such as flanges and valves, impose concentrated loads. Where calculations are not made, suggested maximum spacing of supports for standard and heavier pipe are given in table IV-8. Vertical supports should be spaced to prevent the pipe from being overstressed from the combination of all loading effects.

2) Anchors and Guides

Supports that are used to restrain movements are either anchors or guides. Anchors restrain movements in all directions, and guides restrain movement in one direction (usually transversely). These types of supports should be designed per ANSI B31.1 recommendations:

TABLE IV-8. SUGGESTED PIPE SUPPORT SPACING

NOMINAL PIPE SIZE, (IN)	(CM)	SUGGESTED MAXIMUM SPAN WATER, STEAM, GAS, OR AIR SERVICE (FT)	(M)	(FT)	(M)
1	2.54	7	2.13	9	2.74
2	5.08	10	3.05	13	3.96
3	7.62	12	3.66	15	4.57
4	10.16	14	4.27	17	5.18
5	15.24	17	5.18	21	6.40
6	20.32	19	5.79	24	7.31

NOTES:

(1) Suggested maximum spacing between pipe support for horizontal straight runs of standard and heavier pipe at maximum operating temperature of 750°F (399°C).

(2) Does not apply where span calculations are made or where there are concentrated loads between supports, such as flanges, valves, specialties, etc.

(3) The spacing is based on a fixed beam support with a bending stress not exceeding 2300 psi (15.9 MPa) and insulated pipe filled with water or the equivalent weight of steel pipe for steam, gas, or air service, and the pitch of the line is such that a sag or 0.1-in (0.254 cm) between supports is permissible.

(1) Anchors, guides, pivots, and restraints should be designed to secure the desired points of piping in relatively fixed positions. They should permit the piping to expand and contract freely in directions away from the anchored or guided point, and should be structurally suitable to withstand the thrusts, moments, and other loads imposed.

(2) Rolling or sliding supports should permit free movement of the piping, or the piping should be designed to include the imposed load and frictional resistance of these types of supports, and dimensions should provide for the expected movement of the supported piping. Materials and lubricants used in sliding

supports should be suitable for the metal temperature at the point of sliding contact.

(3) Where corrugated or slip-type expansion joints, or flexible metal hose assemblies are used, anchors and guides should be provided where necessary, to direct the expansion into the joint or hose assembly. Such anchors should be designed to withstand the force specified by the manufacturer for the design conditions at which the joint or hose assembly is to be used. If this force is otherwise unknown, it should be taken as the sum of the product of the maximum internal area times the design pressure, plus the force required to deflect the joint or hose assembly. Where expansion joints or flexible metal hose assemblies are subjected to a combination of longitudinal and transverse movements, both movements should be considered in the design and application of the joint or hose assembly.

Flexible metal hose assemblies should be supported in such a manner as to be free from any effects due to torsion and undue strain as recommended by the manufacturer.

c. Stresses in Pipe

1) Load Analyses

To comply with ANSI B31.1 Code, a piping system must be analyzed between anchors for the effects of thermal expansion, weight, other sustained loads, and other occasional loads. Each component in the system must meet the limits in this section. It should be noted that the pressure term in equations IV-107 and IV-108 may not apply for bellows and expansion joints. When evaluating stress in the vicinity of expansion joints, consideration must be given to actual cross-sectional areas that exist at the expansion joint.

a) Sustained Loads

The effects of pressure, weight, and other sustained mechanical loads must meet the requirements of equation IV-107.

$$\frac{PD_o}{4t_n} + \frac{0.75\ iM_A}{Z} \leq 1.0S_h \qquad \text{(Eq. IV-107)}$$

where:

P = internal design pressure, psig

D_o = outside diameter of pipe, in

t_n = nominal wall thickness of component, in

M_A = resultant moment loading on cross section due to weight and other sustained loads, in-lb

Z = section modulus, in^3

i = stress intensification factor. The product 0.75i shall never be taken as less than 1.0.

S_h = basic material allowable stress at maximum temperature from Allowable Stress Tables of the Code, psi

b) Additive Stresses

The requirements of either equation IV-108 or equation IV-110 must be met depending on the load. If only thermal expansion stresses are acting, then the pipe stress is given by:

$$S_E = \frac{iM_C}{Z} \leq S_A \qquad \text{(Eq. IV-108)}$$

The terms in this equation are the same as above except:

M_C = range of resultant moments due to thermal expansion.

S_A = allowable stress range for expansion stresses:

$$S_A = f(1.25S_c + 0.25S_h) \qquad \text{(Eq. IV-109)}$$

where:

S_c = basic material allowable stress at minimum (cold) temperature from the Allowable Stress Tables

S_h = basic material allowable stress at maximum (hot) temperature from the Allowable Stress Tables

f = stress range reduction factor for cyclic conditions for total number N of full temperature cycles over total number of years during which system is expected to be in operation, from table IV-9

TABLE IV-9. STRESS RANGE REDUCTION FACTORS

NUMBER OF EQUIVALENT FULL TEMPERATURE CYCLES N	f
7,000 AND LESS	1.0
7,000 - 14,000	0.9
14,000 - 22,000	0.8
22,000 - 45,000	0.7
45,000 - 100,000	0.6
100,000 AND OVER	0.5

If sustained loads are acting in addition to thermal stresses then the effects of pressure, weight, other sustained loads, and thermal expansion must meet the requirements of equation IV-110.

$$\frac{PD_o}{4t_n} + \frac{0.75iM_A}{Z} + \frac{iM_c}{Z} \leq (S_h + S_A) \qquad \text{(Eq. IV-110)}$$

2) Flexibility Design

a) General

In addition to the design requirements for pressure, weight, and other loadings, PV-T systems subject to thermal

expansion or contraction, or to similar movements imposed by other sources should be designed in accordance with the requirements for the evaluation and analysis of flexibility and stresses specified in this section.

Stresses caused by thermal expansion, when of sufficient initial magnitude, relax in the hot condition as a result of local yielding or creep. A stress reduction takes place and usually appears as a stress of reversed sign when the component returns to the cold condition. This phenomenon is designated as self-springing of the line and is similar in effect to cold springing. The extent of self-springing depends on the material, the magnitude of the initial expansion and fabrication stress, the hot service temperature and the elapsed time. While the expansion stress in the hot condition tends to diminish with time, the sum of the expansion strains for the hot and cold conditions during any one cycle remains substantially constant. This sum is referred to as the strain range; however, to permit convenient association with allowable stress, stress range is selected as the criterion for the thermal design of piping. The allowable stress range should be determined in accordance with equation IV-109.

PV-T systems should be designed to have sufficient flexibility to prevent pipe movements from causing failure from overstress of the pipe material or anchors, leakage at joints, or detrimental distortion of connected equipment resulting from excessive thrusts and moments. Flexibility should be provided by changes of direction in the piping through the use of bends, loops, or offsets; or provisions should be made to absorb thermal movements by utilizing expansion, swivel, or ball joints, corrugated pipe, or flexible metal hose assemblies.

Expansion, swivel, or ball joints, and flexible hose assemblies may be used where experience or tests have demonstrated that they are suitable for expected conditions of pressure, temperature, service, and cyclic life. Restraints and supports should be provided, as required, to limit movements to those directions and magnitudes permitted

for the specific joint or hose assembly selected. Joints of the corrugated bellows, slip, sleeve, ball, or swivel types and flexible metal hose assemblies may be used if their materials conform to the code, their structural and working parts are of ample proportions, and their design prevents the complete disengagement of working parts while in service. However, flexible metal hose assemblies, and expansion joints of the corrugated bellows, slip, or sleeve type should not be used in any piping system connecting the boiler and the first stop valve in that system.

b) Analysis

All piping should meet the following requirements with respect to thermal expansion and flexibility and it is the designer's responsibility to perform an analysis unless the system meets one of the following criteria:

(1) The piping system duplicates a successfully operating installation or replaces a system with a satisfactory service record.

(2) The piping system can be adjudged adequate by comparison with previously analyzed systems.

(3) The piping system is of uniform size, has not more than two anchors and no intermediate restraints, is designed for essentially non-cyclic service (less than 7000 total cycles), and satisfies the following approximate criterion:

$$\frac{DY}{(L - U)^2} \leq 0.03 \qquad \text{(Eq. IV-111)}$$

where:

D = nominal pipe size, in

Y = resultant of movements to be absorbed by pipe lines, in

L = developed length of line axis, ft

U = anchor distance (length of straight line joining anchors), ft

Systems that do not meet the above criteria, or cause reasonable doubt as to adequate flexibility, should be analyzed by

simplified, approximate, or comprehensive methods of analysis that are appropriate for the specific case. Approximate or simplified methods may be applied only if they are used for the range of configurations for which their adequate accuracy has been demonstrated. Acceptable comprehensive methods of analysis include analytical techniques, and model tests and chart methods which provide an evaluation of the forces, moments and stresses caused by bending and torsion from the simultaneous consideration of terminal and intermediate restraints to thermal expansion of the entire piping system under consideration, and including all external moments transmitted to the piping by its terminal and intermediate attachments. Correction factors must be applied for the stress intensification of curved pipe and branch connections, as provided by the details of the code, and may be applied for the increased flexibility of such component parts.

The flexibility equation IV-111 is valid for ferrous pipe and for 7000 total cycles. Since PV-T systems may have a life of 15 to 20 years and may thermally cycle more than once a day due to cloud cover, the piping system should be designed to survive on the order of 10,000 cycles. To provide for this, the flexibility equation should be modified using the f factor of table IV-9 as follows:

$$\frac{DY}{(L - U)^2} \leq 0.03\ f \qquad \text{(Eq. IV-112)}$$

where f = 0.9 for 7,000 < N < 14,000 cycles or:

$$\frac{DY}{(L - U)^2} \leq 0.027 \qquad \text{(Eq. IV-113)}$$

An example using equation IV-113 and the pipe layout of figure IV-50 is given as follows:

Pipe = 3-in (7.62 cm), schedule 40, Carbon Steel

Design Temperature = 300°F (148.9°C)

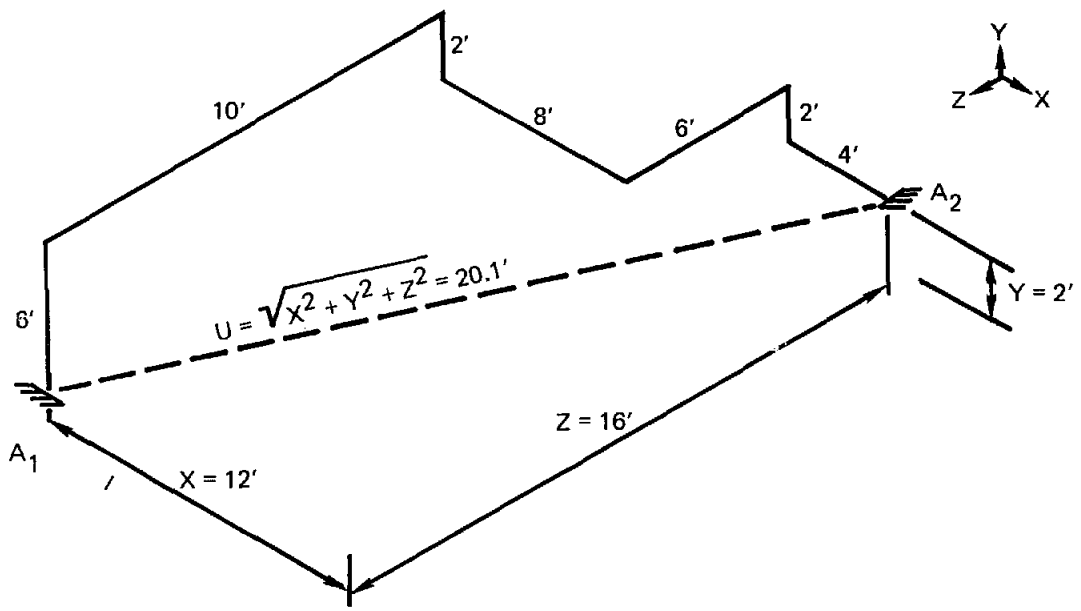

BDM/A-82-458-TR-R1

Figure IV-50. Pipe Layout for Flexibility Analysis

Step 1: Establish the distance between anchors in plan and elevation, in feet.

Y = Vertical elevation difference = 6-ft - 4-ft = 2-ft (0.61 m)

(Difference in elevation between A_1 and A_2).

X = Total line length away from A_2 = 8-ft + 4-ft = 12-ft (3.66 m)

Z = Total line length away from A_1 = 10-ft + 6-ft = 16-ft (4.88 m)

Step 2: Determine length U, the straight length in feet between points A_1 and A_2.

$$U = \sqrt{x^2 + y^2 + z^2} \qquad \text{(Eq. IV-114)}$$

$$= \sqrt{12^2 + 2^2 + 16^2}$$

$$= \sqrt{404}$$

$$= 20.1\text{-ft } (6.13 \text{ m})$$

Step 3: Determine Y in equation (IV-113)

Y = resultant of movements in inches to be absorbed by pipe lines = UB

where B = linear thermal expansion coefficient at the design temperature (in/100-ft) as given in table IV-10.

TABLE IV-10. ANSI/ASME B31.1-1980 EDITION APPENDIX B THERMAL EXPANSION DATA

Mean Coefficient of Thermal Expansion = $\frac{A}{10^6}$ (in./in./^{o}F)

Linear Thermal Expansion = B (in./100 ft)

in Going From 70°F to Indicated Temperature

Material	Coef-ficient	Temp. Range 70°F to -325	-150	-50	70	200	300	400	500	600	700	800	900	1000
Carbon Steel; Carbon-Moly Steel	A	5.00	5.50	5.80	6.07	6.38	6.60	6.82	7.02	7.23	7.44	7.65	7.84	7.97
Low-Chrome Steels (through 3Cr)	B	2.37	1.45	0.84	0	0.99	1.82	2.70	3.62	4.60	5.63	6.70	7.81	8.89

$$\text{then } Y = 20.1\text{-ft } \frac{1.82\text{-in}}{100\text{-ft}} = 0.37\text{-in } (0.94 \text{ cm})$$

Step 4: Determine value of L, the total length of line.

$$L = 6 + 10 + 2 + 8 + 6 + 2 + 4 = 38\text{-ft } (11.6 \text{ m})$$

Step 5: Solve the formula which must be equal to or less than 0.027 or full stress analysis is required.

$$\frac{DY}{(L - U)^2} \leq 0.027$$

$$\frac{3(0.37)}{(38 - 20.1)^2} = 0.003$$

then $0.003 \leq 0.027$ and, therefore, no formal stress analysis is required.

When a nonferrous (e.g., copper) material is used as the piping system, the ANSI-B31 Mechanical Design Committee Report Draft of 1976 recommends the use of the following equation with the listed restrictions to determine whether a formal stress analysis is required.

$$\frac{DY}{(L - U)^2} \leq \frac{30\ (S_A)}{E_c} \qquad \text{(Eq. IV-115)}$$

where:

- D = nominal pipe size, (in)
- Y = resultant of movements to be absorbed by pipe line, (in)
- U = anchor distance (length of straight line joining anchors), (ft)
- L = developed length of line axis, (ft)
- S_A = allowable stress range, (psi) (include stress range reduction factor "f" where more than 7000 cycles of movement are anticipated during life of installation)
- E_c = modulus of elasticity of the piping material in the cold condition, (psi)

The formula given reflects the maximum stress computed in L-, Z-, U-, and expansion U-bends of a length-to-anchor-distance ratio L/U up to a maximum of three, using a square-corner analysis, i.e., an approximate analysis in which both the increased flexibility and stress intensification associated with elbows or bends are ignored; however, in the derivation of the criterion, a stress intensification factor of 1.3 has been taken as applicable to the controlling location, wherever it occurs. Of the shapes investigated, the U-bend was found to have the highest stress by this method and, because the anchored ends controlled, the applied factor of 1.3 is more than adequate; for the balanced expansion U-bend, for which the four elbows control and a higher

stress intensification might be required depending on size, thickness and bend radius, the computed stress was only a fraction of that for the U-bend on which the criterion formula is based. This tendency for the product of basic stress and stress intensification factor to balance out explains why the adequacy of the criterion (in the form of equation (IV-111) using a constant value of 0.03 on the right side) has been found confirmed by many checks against rigorous calculations on actual systems using ferrous materials. The slightly more complex and conservative form of equation (IV-115) serves to extend it to nonferrous materials and to cyclic applications. Since no general proof can be offered to ensure that the formula will never err on the unconservative side, users are advised to use caution in applying it to abnormal configurations (unequal-leg U-bends with L/U in excess of 2.5, or near-straight sawtooth configurations), to large-diameter thin-wall pipe (stress intensification factors of the order of five or more), or to conditions where extraneous motions, other than in the direction connecting the anchor points, constitute a large proportion of the expansion duty. The criterion is applicable to multi-plane systems and can be extended to multi-branch systems by introducing a fictitious anchor at the branch point and subjecting all branches to the criterion.

d. Pipe Layout

1) General

The PV-T designer should carefully investigate structural conditions, equipment locations and orientation, equipment connections, horizontal and vertical controls and any other conditions affecting the piping work and should plan his work accordingly.

All piping should be designed as follows:

- The heat transfer fluid system should be welded, other systems should have removable flanged spools provided at pumps and other equipment that will have to be removed for maintenance and inspection.
- To avoid pocketing, piping should be arranged so that lines drain back into equipment or into lines that can be drained.

- Vents should be provided at all high points and drains should be provided at all low points in each piping system. Vents on heat transfer fluid piping should be provided with discharge piping, routed so that fluid will be directed away from the piping insulation.
- Piping should be routed to obtain adequate clearance for maintaining and removing equipment.
- Equipment, valves, etc., should be positioned with adequate clearance for operation and maintenance.
- Valves should be provided at the inlet and outlet of each ΔT string to isolate a system for either hydrostatic or pneumatic testing and maintenance.

2) Specific

a) Identifying Significant Thermal Expansions

A typical PV-T system pipe layout will be similar to figure IV-51. A manifold of length "L_m" feeds the collector field with HTF which returns to the manifold to be pumped to the heat exchanger. Typical distances between collector rows "L_R" are 15 to 30-ft (4.57 to 9.15 m). Manifold lengths may vary from 200 to 1000-ft (61 to 305 m) depending on the field size and configuration. Typical drive unit connector lengths "L_{DU}" are from 5 to 15-ft (1.52 to 4.57 m). Since the lengths and diameters for L_R or L_{DU} are small and usually have elbows on each end, there is usually little concern about the amount of expansion and the level of stress in these connectors. The thermal expansion of the manifold can, however, present problems for the PV-T system designer.

Take, for example, the PV-T system shown with the collector outlet manifold in figure IV-52. The PV-T system must have anchors as indicated at points F and B to protect the collectors and heat exchanger from undue stresses resulting from thermal expansion. A guide is located at point E to allow longitudinal expansion and prevent thermal stresses. To find the amount of thermal expansion in the manifold due to a temperature rise to 200°F (93.3°C) (130°F (72.2°C) above a typical ambient temperature of 70°F (21.1°C)), table IV-10 is used as follows:

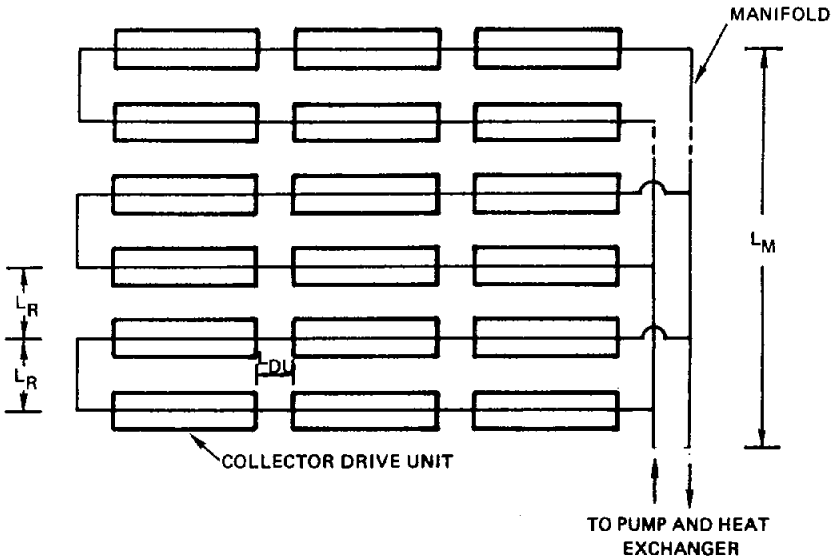

Figure IV-51. Typical PV-T Pipe Layout

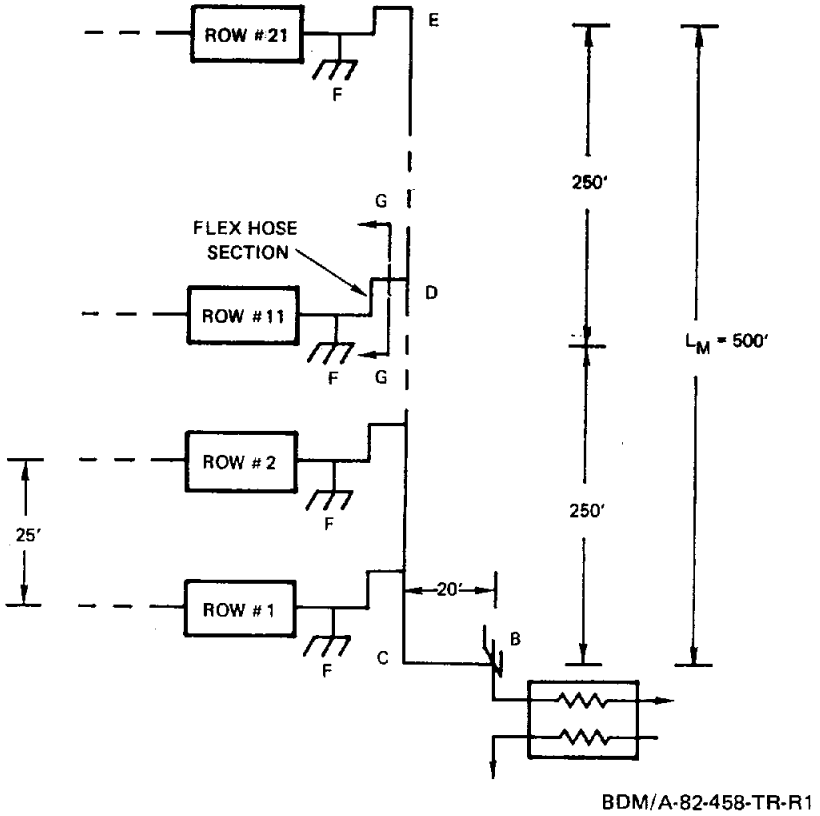

Figure IV-52. Typical PV-T System Layout and Outlet Manifold

Carbon steel pipe
6-in (15.24 cm) O.D.
Operation temperature 200°F (93.3°C)

from C to E: $\Delta L_m = L_m B = 500\text{-ft} \dfrac{0.99\text{-in}}{100\text{-ft}} = 4.95\text{-in (12.57 cm)}$

from B to C: $\Delta L_{HX} = L_{HX} B = 20\text{-ft} \dfrac{0.99\text{-in}}{100\text{-ft}} = 0.20\text{-in (0.508 cm)}$

The thermal expansion of L_{HX} is minimal but the expansion for L_m is quite significant (5-in) and must be accounted for.

b) Remedying Significant Thermal Expansions

The recommended method for compensating the movement in the manifold is to use flexible hose between the manifold and the collectors. There are three fundamental points to remember in designing corrugated flexible hose assemblies:

- Hose should not be bent below the minimum recommended bend radius.
- Install hose without twists that would develop torsional strain that is harmful to hose.
- Install so that flexing takes place in one plane.

One method of accomplishing this is to install the flex hose at each row as shown in the typical section of G-G in figure IV-52, which is shown in greater detail in figure IV-53.

If the piping system of figure IV-52 is anchored only at the points B and F, then the greatest amount of movement (5 in or 12.6 cm) will occur at point E. Flex hose manufacturers have developed relationships that describe the length of flex hose that is required to compensate for this movement. In this example of short horizontal travel, the relationships are as follows:

$$\text{Overall Length} = \text{OAL} = B + 1.57\ (A + T) \qquad \text{(Eq. IV-116)}$$

$$C = \frac{1.57\ T + B + A}{2} \qquad \text{(Eq. IV-117)}$$

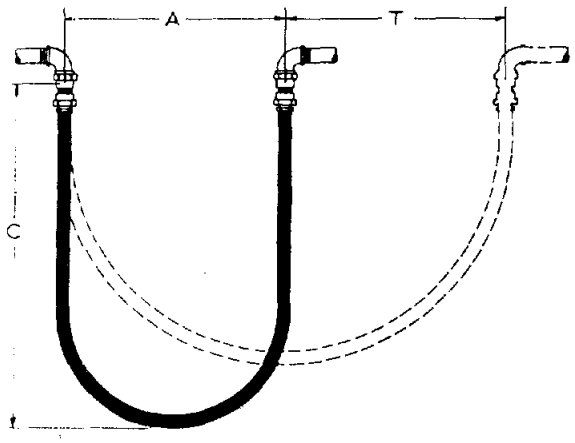

BDM/A-82-458-TR-R1

Figure IV-53. Detail of Flex Hose Connection--
Section G-G of Figure IV-41

where:

A = Bend Diameter ("Minimum Centerline Radius for Constant Flexure" x 2).

B = Factor including the length of fittings and an allowance for straight sections of flexible tubing beyond each fitting.

I.D. of Hose	1/4"	3/8"	1/2"	3/4"	1"	1-1/4"	1-1/2"	2"
B	9	11	12	14	16	18	20	22

T = Travel

C = Relaxed height as shown in figure IV-53.

For the case under consideration and for typical values of flex hose:

T = 5-in

1-in diameter flex hose with minimum centerline bend radius for constant flexure of 8.5-in (from manufacturer's catalog)

A = 8.5 x 2 = 17-in

B = 16 for 1-in diameter

then:

$$OAL = B + 1.57(A + T) = 16 + 1.57(17 + 5) = 51\text{-in } (1.3 \text{ m})$$

$$C = \frac{1.57 + B + A}{2} + \frac{1.57(5) + 16 + 17}{2} = 20\text{-in } (0.508 \text{ m})$$

The flex hoses "isolate" the thermal movements of the manifold from the collectors and therefore accomplish the task of reducing the stress on the piping between points B and F.

This method of anchoring has definite advantages over other methods, for example, consider anchoring at points B, F, and D in figure IV-52. While this second method may cut the thermal movement of point E in half, it only changes the OAL of the flex hose to 47-in (1.19 m), and it also requires a formal stress analysis for the pipe segment D-C-B since:

$$D = 6.0$$
$$U = \sqrt{(250)^2 + (20)^2} = 250.8$$
$$L = 250 + 20 = 270$$
$$Y = UB = 250.8 \ \frac{0.99 \text{ in}}{100 \text{ ft}} = 2.48$$

so that:

$$\frac{DY}{(L - U)^2} = \frac{6.0(2.48)}{(270 - 250.8)^2} = .040 > .027$$

I. INSULATION

Proper specification of insulation includes determining insulation type, insulation thickness, insulation weather-barrier, and pipe hangers. Changing pipe size changes the optimum thickness of the insulation; thus, the optimum thickness must be determined for each pipe size. As the insulation thickness increases, cost of the insulation increases (see

figure IV-54) whereas the amount of the heat loss decreases. At some insulation thicknesses the incremental cost of the insulation equals the incremental decrease in the value of heat loss, resulting in a minimum system cost.

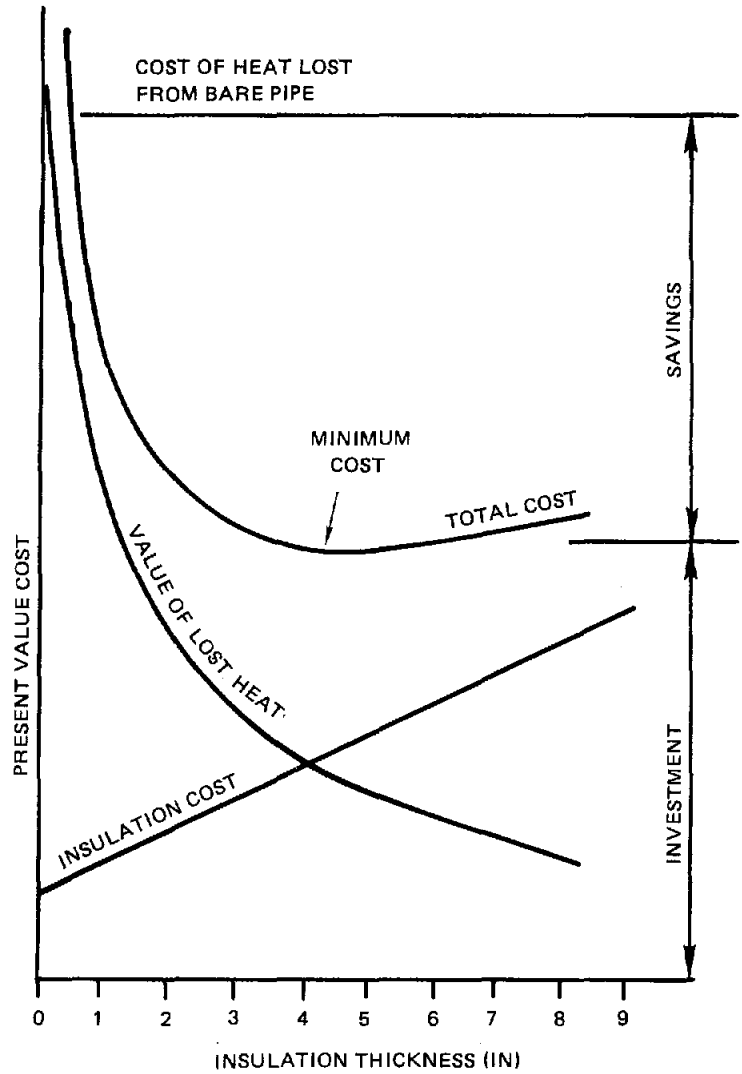

BDM/A-82-458-TR-R1

Figure IV-54. Insulation Costs and Heat Lost as a Function of Thickness

This concept of economic thickness has been extensively discussed in the power and process industries and has been analyzed in technical literature over many years. There are now lengthy books and manuals available that show the plant or design engineer how to calculate this economic thickness using tables, graphs, or computers.

Around 1973, programs called ECON-1 (tables, charts, worked examples), ECON-II (marketing manual), and R-ECON (retrofitting) became available. However, some users felt these programs had averaged too many variables to nominal values and, in addition, the minimum insulation depreciation (amortization) period was too long. This last objection showed that plant owners were not prepared to regard insulation as a long term investment--an attitude common today.

Insulation, if properly maintained, can have a very long lifetime (30 years or more), longer than the predicted life of a solar system. However, these programs were developed for the power and process industries in which the pipework may be part of a plant which rapidly becomes obsolete. Since, in many cases, insulation is scrapped rather than recovered, it makes no sense to amortize it over a longer period of time.

Accordingly, around 1976, a refinement of these tables was produced by York Research Corporation for the Federal Energy Administration and called ETI (Economic Thickness for Industrial Insulation). It consisted of 10 sections covering fuel costs, insulation costs, condensation control, and retrofitting. All the information was given in tabular, graphical, or nomograph form and also in a mathematical appendix.

However, this apparently was not suitable for all needs, and from 1976 to 1980 numerous suggestions were made to make the ETI program more useful. A recent revision has been made incorporating these suggestions, as a joint venture between the Thermal Insulation Manufacturers Association (TIMA), National Insulation Contractors Association (NICA) and Louisiana Technical University; the resulting manuals being called ETIH (Economic Thickness of Insulation for Hot Surfaces) and ETIC (Cold Surfaces).

A full analysis of insulation economics requires that at least 20 input-data variables be assigned. These can be grouped under four headings for the case of pipe insulation.

(1) Insulation factors

(a) Cost of installed insulation, of thickness t, per unit length $C_{I(t)}$

(b) Thermal conductivity of insulation, k_I

(c) Thermal resistance of insulation surface, R_S

(d) Pipe diameter (nominal), d_1

(e) Ambient temperature, T_a

(f) Ambient wind speed

(g) Pipe temperature, T_p

(h) Amortization period of insulation, n

(i) Pipe-complexity factor

(j) Maintenance and insurance costs

(2) Fuel factors

(a) Type of fuel and cost, C_F

(b) Expected annual price rise of fuel expressed as a decimal, f

(3) Heat-producing-plant factors

(a) Efficiency of conversion of fuel to heat, E

(b) Number of hours of operation per year, N

(c) Capital investment in heat-producing plant

(d) Amortization period of heat-producing plant

(4) Economic factors

(a) Cost of money, i.e., return on investment in insulation required, i

(b) Tax rate

(c) Cost of money to finance heat-producing plant

(d) Economic model used for determining the economic thickness of insulation

Recent articles and reports (refs. IV-15 and IV-16) provide techniques for optimizing insulation thicknesses for solar system piping and storage tanks. The overall heat transfer coefficient-area product per unit length of pipe (UA/L) has been calculated for various combinations of pipe diameter, insulation thickness, and insulation conductivity. The UA/L value is used to calculate the energy lost from the pipe. A sensitivity analysis showed that deviations in UA/L for outdoor pipe was only +3 percent to -8 percent, whereas deviations for indoor pipe ranged from +13 percent to -21 percent. The outdoor values of UA/L are sensitive only to wind speed while indoor pipe UA/L values are

sensitive to insulation (or jacketing material) surface emissivity, followed by fluid temperature and then ambient temperature; fluid velocity had no effect.

Thus, it appears that the inevitable uncertainties associated with thermal data can be controlled to a reasonable extent. However, it is more difficult to control the uncertainties associated with the economic data inputs to the analysis of an economic thickness of insulation.

In the following sections two types of analyses are presented for calculating the thickness of insulation. First, a very simplified economic analysis is presented. For a more detailed economic analysis, refer to references III-15 or III-16, or to the ETIH manual. The second technique completely ignores economic factors under the assumption that they cannot be known accurately and therefore one cannot make a decision on the appropriate economic thickness. Instead, economic thickness is determined by heat-loss considerations alone; the results being an "acceptable heat-loss" thickness of insulation.

1. Economic Thickness

For a pipe the heat lost per unit foot of length is given by:

$$Q_\ell = \frac{2\pi\Delta T}{\frac{\ell n(r_s/r)}{k} + R_s/r_s} \qquad \text{(Eq. IV-118)}$$

where:

Q_ℓ has the units of watts/m

ΔT is temperature difference between the pipe and ambient air (^oC)

r_s is the outside radius of the insulation (cm)

r is the inside radius of the insulation (cm)

k is the insulation thermal conductivity (W/m^oC)

R_s is the film resistance to heat transfer ($m^{2o}C/W$)

Table IV-11 shows that in general, R_s contributes only about 10 percent to the total insulation resistance. The surface resistance is a

TABLE IV-11. SURFACE RESISTANCE AS A FUNCTION OF EMITTANCE INSULATION RESISTANCE, AND WIND VELOCITY (Ref. IV-17)

			ε = 0.8 EMITTANCE	ε = 0.3 EMMITANCE
WIND VELOCITY (m/sec)	INSULATION RESISTANCE ($m^2 {}^oC/W$) MIN.	MAX.	R_s* ($m^2 {}^oC/W$)	R_s* ($m^2 {}^oC/W$)
0 (NATURAL CONVECTION)	0.176	0.882	0.125	0.178
	0.882	1.76	0.138	0.206
	1.76	2.65	0.145	0.22
	2.65	3.53	0.153	0.231
1.79	0.176	0.882	0.079	0.099
	0.882	1.76	0.092	0.115
	1.76	2.65	0.10	0.127
	2.65	3.53	0.107	0.136

* FOR PIPE FLUID TEMPERATURE 93.3°C (200°F)

WEATHER-BARRIER OR SURFACE FINISH	ε @ 37.8°C (100°F)
ALUMINUM	0.03 to 0.12
ALUMINUM PAINT	0.20 to 0.70
PAINTS - WHITE	0.55 to 0.70
- BLACK	0.90 to 0.95
PVA MASTICS	CLOSE TO PAINT COLOR

function of surface temperature and hence cannot be determined independent of the insulation thickness. In determining the optimum insulation thickness, it is appropriate to ignore R_s and consider it an added benefit. Ignoring R_s causes an error in the optimum thickness calculated that is less than 1.27 cm (1/2 in) or is less than the step size for insulation. In the example to follow including R_s would change the optimum insulation thickness from 7.62 cm (3-in) to 7.37 cm (2.9 in). When choosing the actual discrete insulation size to use, the general rule of thumb is to round down to the nearest 1.27 cm (1/2 in) size. Figure IV-54 shows that rounding up raises total system cost in a manner that results in the last increment insulation cost producing a negative incremental return on investment. Rounding down and ignoring R_s are effects that tend to cancel.

The surface resistance is important in determining the surface temperature of the insulation. This temperature should be kept low enough to prevent a hazard. The surface temperature can be calculated according to:

$$T_S = T_A + \frac{R_s \Delta T}{\frac{r_s \ \ell n(r_s/r)}{k} + R_s} \qquad \text{(Eq. IV-119)}$$

where T_S is the surface temperature (^oC) and T_A is the ambient temperature (^oC). For personnel safety, this surface temperature should not exceed 45^oC (113^oF) for a metal jacket, to prevent skin burns.

Heat is lost from the pipe both during operation, and at night, when the PV-T system is not being operated. As part of an example it will be shown later that insulation is not effective in preventing evening heat losses. If the decrease of evening heat loss with insulation thickness were plotted on figure IV-54, it would be a fairly horizontal line that does not effect the position of the minimum when compared to the daytime loss. Ignoring the benefit of insulating against such losses when

calculating the optimum thickness greatly simplifies the equations and is like ignoring R_s. The actual benefit that will be derived from the optimum thickness will thus be slightly more than calculated due to reduced nighttime losses.

The value of the heat lost (C_{HL}) can be expressed as:

$$C_{HL} = C_H(P)F(8760\ hr)Q_\ell$$

$$= \frac{A\ 2\pi k}{\ell n(r_s/r)} \qquad \text{(Eq. IV-120)}$$

where:

C_H is the cost of heat ($/kw hr)
F is the fraction of the time the system is being used
P is the present value factor, and
A is $C_H(P)F(8760hr)\ \Delta\ T$

Assuming that the cost of insulation is a function of volume, it can be expressed as:

$$C_I = M\left[C_{I/V}\pi\ (r_s^2 - r^2) + C_{I-F}\right] \qquad \text{(Eq. IV-121)}$$

where:

M is a maintenance factor
$C_{I/V}$ is the cost of insulation per volume ($/cm^{2}m)
C_{I-F} is the fixed insulation cost; installation, etc. (cost for zero thickness of figure IV-54).

The optimum thermal resistance per meter is the solution to:

$$\frac{d}{dr_s}\ (C_{HL} + C_I) = 0 \qquad \text{(Eq. IV-122)}$$

which can be determined using figure IV-55 by reading the value of (r_s/r) that corresponds to A/Br^2 where:

$$B = (MC_{I/V})/k \qquad \text{(Eq. IV-123)}$$

As an example, consider 10.16 cm (4-in) diameter pipe insulated with fiberglass ($k = 0.0415$ W/m^{o}C or 0.024 Btu/hr.-^{o}F-ft) operating at a temperature 66.7^{o}C (120°F) above ambient. Figure IV-56 shows that if the pipe is bare it will lose 946 W/m^2 (300 Btu/hr ft^2). For our 10.16 cm (4-in) O.D. diameter pipe this will result in a heat loss of 302 W/m (314 BTU/hr ft). Using the replacement price of heat based on oil ($0.03/kW or $8.61/mBtu) and a usage factor F of 8 hours per day, 5 days per week, 50 weeks per year ($F = 8 \times 5 \times 50/8760 = .228$) this results in a yearly loss of:

$0.03/kW hr x 0.302 kW/m x 0.228 x 8760 hr/yr = $18.10/m-yr

Obviously, considerable savings can result from insulation.

For our example, we shall assume the insulation is to pay for itself in 10 years and that future dollars are to be discounted at 10 percent. In this case our present value factor becomes:

$$P = \frac{(1+i)^n - 1}{i(1+i)^n} = 6.14 \qquad \text{(Eq. IV-124)}$$

In the actual determination of optimum insulation thickness for a system, this present value factor can be changed to whatever factor is appropriate for the system being designed (the same is of course true for C_H, F, ΔT, M, $C_{I/V}$, C_{I-F}, as well as P). With this factor:

$$\begin{aligned} A &= C_H(P)F(8760 \text{ hr.})\ \Delta T \\ &= \$0.03/\text{kW hr} \times 6.14 \times .228 \times 8760 \text{ hr.} \times 66.7^oC \\ &= \$24.54^oC/\text{watt} \end{aligned}$$

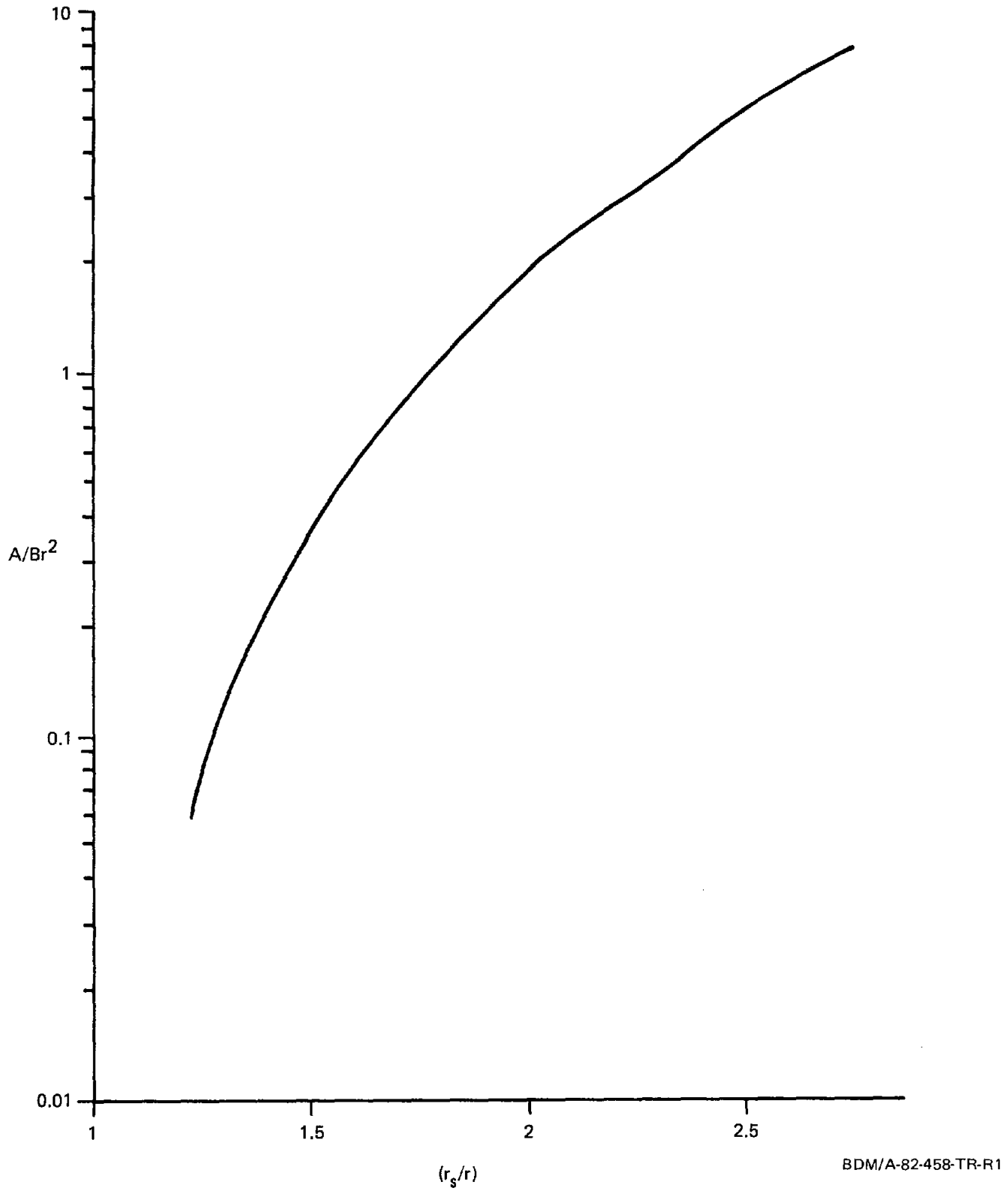

Figure IV-55. Optimum Thermal Resistance Per Foot of Pipe

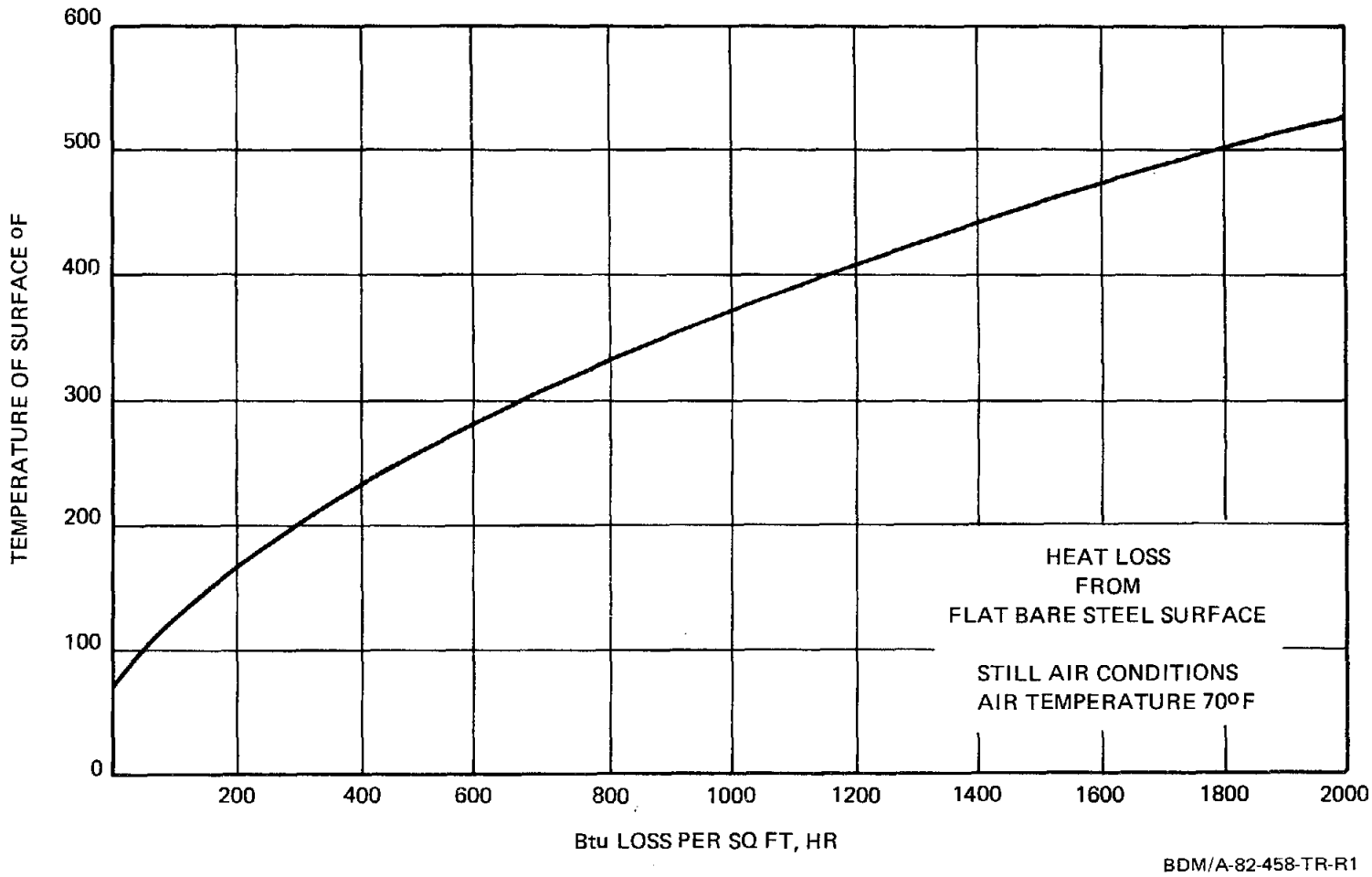

Figure IV-56. Bare Pipe Heat Loss

For the maintenance factor, we shall assume the standard 10 percent per year, and use the same 10 year period and 10 percent discount factor with the result that:

$$M = 1 + .1(6.14)$$
$$= 1.61$$

Using the cost per volume for fiberglass in table IV-12 we get:

$$B = (M\ C_{I/V})/k$$
$$= 1.61 \times (0.077/cm^2\text{-}m)/(0.042\ W/m^oC)$$
$$= \$2.95^oC/W\text{-}cm^2$$

TABLE IV-12. INSULATION PRICE PER VOLUME

MATERIAL	CONDUCTIVITY $\frac{WATT}{m^oC}$	PRICE PER VOLUME $\$/cm^2\text{-}m$
FOAM GLASS	0.066	0.065
FIBERGLASS	0.042	0.077
URETHANE	0.022	0.099
CALCIUM SILICATE	0.057	0.089
MINERALPOWDER	0.109	0.033

The factor needed for figure IV-55 is thus:

$$A/Br^2$$
$$= 24.54^oC/watt/\left[2.95^oC/Wcm^2\ (5.08\ cm)^2\right]$$
$$= 0.322$$

From figure IV-55 we see that the corresponding optimum insulation is when $r_s/r = 1.44$. The outer radius of the insulation should thus be:

$$r_s = 5.08\ cm \times 1.44$$
$$= 7.32\ cm\ (2.88\text{-}in)$$

The insulation should thus be 2.54 cm (1-in) thick. Adding this insulation will reduce the heat lost to:

$$C_H = A2\pi k/\ln(r_s/r)$$

$$= (\$24.54^{o}C/w) \times 2\pi \times (0.042\ W/m^{o}C)/\ln(3/2)$$

$$= \$15.97/m$$

Which compares to the present value of the potential bare pipe heat loss of:

6.14 yr. x \$18.10/m-yr = \$111.13/m

resulting in a savings of \$95.16/m over the 10 year period.

So far, we have seen how figure IV-55 can be used to determine the optimum thickness insulation for a given insulation type and pipe diameter. We must still determine which insulation results in the lowest system cost on figure IV-54, and verify that this insulation really does result in an acceptable return on investment. Optimum thickness is achieved when the incremental increase in insulation cost equals the incremental savings in heat lost. If, for some reason, C_{F-I} (the fixed insulation cost) was very high the economics of insulating may not be favorable. The fixed charge should not be ignored and may be the deciding factor in choosing which insulation is best.

To determine which insulation is best, one should use figure IV-55 to determine optimum thickness for the candidate insulations. Bids should then be sought to determine actual costs. In this analysis, the assumption has been made that insulation costs are proportional to volume--a reasonable assumption--but some authors assume it is proportional to radius, others that it is proportional to the flattened out area (outer circumference times thickness). Due to variations in manufacturing processes, insulation conductivities are not necessarily

constant, and insulation costs do not necessarily obey a strict proportionality. Bids that establish actual costs and give insulation conductivities at average operating temperature are therefore important. Consideration should be given to obtaining bids for varying thicknesses to verify that the optimum thickness was determined correctly.

If our 10.16 cm (4-in) O.D pipe is schedule 40 steel nominal size 8.89 cm (3-1/2-in) then the inside diameter is 9.012 cm (3.548-in) (see table IV-13). At a standard flow rate of 1.52 m/sec (5-ft/sec) and 16.7°C (30°F) temperature rise in the PV-T array the useful heat transported will be:

$$Q/\text{sec} = 4.166\text{KJ/Kg}^{\circ}\text{C} \times 16.7^{\circ}\text{C} \times 1.52\ \text{m/sec} \times \frac{\pi}{4} \times (9.012\text{x}10^{-2}\text{m})^2$$

$$\times \quad 993\ \text{Kg/m}^3 = 670\ \text{kW}$$

With the insulation the heat lost from the surface of the pipe per foot will be:

$$Q_{\ell} = \frac{2\pi \times 66.7^{\circ}\text{C} \times 0.042\ \text{w/m}^{\circ}\text{C}}{\ln(3/2)}$$

$$= 43.4\ \text{w/m}$$

For 304.9 m (1,000-ft) of piping this would result in a loss of about 2 percent of the energy delivered.

The heat left in the pipe will be (assuming the fluid is water--see data table IV-13):

$$QN = (4.166\ \frac{\text{kJ}}{\text{kg}}\ ^{\circ}\text{C}) \times (66.7^{\circ}\text{C}) \times \frac{\pi}{4} \times (0.09012\ \text{m})^2 \times (993\ \text{kg/m}^3)$$

$$+ (0.446\ \text{kJ/kg}^{\circ}\text{C}) \times (66.7^{\circ}\text{C}) \times (145.9\ \text{kg/m}^3) \times (1.73 \times 10^{-3}\text{m}^2)$$

$$= 1768\ \text{kW sec/m day} = 0.5\ \text{kw hr/m day}$$

TABLE IV-13. DIMENSIONS AND PROPERTIES OF STEEL PIPE

Nominal Size	ASTM Schedule	Diameter OD In.	Diameter ID In.	Surface Area Sq Ft/Lin Ft OD	Volume Gal/Lin Ft	Weight (plain end) Lb/Lin Ft
1/2	40 (s)	0.840	0.622	0.220	0.0158	0.850
	80 (x)	0.840	0.546	0.220	0.0122	1.09
	XX	0.840	0.252	0.220	0.00259	1.71
3/4	40 (s)	1.050	0.824	0.275	0.0277	1.13
	80 (x)	1.050	0.724	0.275	0.0225	1.47
	XX	1.050	0.434	0.275	0.00768	2.44
1	40 (s)	1.315	1.049	0.344	0.0449	1.68
	80 (x)	1.315	0.957	0.344	0.0374	2.17
	XX	1.315	0.599	0.344	0.0146	3.66
1-1/4	40 (s)	1.660	1.380	0.435	0.0777	2.27
	80 (x)	1.660	1.278	0.435	0.0666	3.00
	XX	1.660	0.896	0.435	0.0348	5.21
1-1/2	40 (s)	1.900	1.610	0.497	0.1058	2.72
	80 (x)	1.900	1.500	0.497	0.0918	3.65
	XX	1.900	1.100	0.497	0.0494	6.41
2	40 (s)	2.375	2.067	0.622	0.174	3.65
	80 (x)	2.375	1.939	0.622	0.153	5.02
	XX	2.375	1.503	0.622	0.0922	9.03
2-1/2	40 (s)	2.875	2.469	0.753	0.249	5.79
	80 (x)	2.875	2.323	0.753	0.220	7.66
	XX	2.875	1.771	0.753	0.128	13.7
3	40 (s)	3.500	3.068	0.916	0.384	7.57
	80 (x)	3.500	2.900	0.916	0.343	10.3
	XX	3.500	2.300	0.916	0.216	18.5
3-1/2	40 (s)	4.000	3.548	1.05	0.514	9.11
	80 (x)	4.000	3.364	1.05	0.462	12.5
	XX	4.000	2.728	1.05	0.304	22.9
4	40 (s)	4.500	4.026	1.18	0.661	10.8
	80 (x)	4.500	3.826	1.18	0.597	14.9
	XX	4.500	3.152	1.18	0.405	27.5

TABLE IV-13. DIMENSIONS AND PROPERTIES OF STEEL PIPE (Concluded)

Nominal Size	ASTM Schedule	Diameter OD In.	Diameter ID In.	Surface Area Sq Ft/Lin Ft OD	Volume Gal/Lin Ft	Weight (plain end) Lb/Lin Ft
5	40 (s)	5.563	5.047	1.46	1.04	14.6
	80 (x)	5.563	4.813	1.46	0.945	20.8
	XX	5.563	4.063	1.46	0.673	38.6
6	40 (s)	6.625	6.065	1.73	1.50	18.0
	80 (x)	6.625	5.761	1.73	1.35	28.6
	XX	6.625	4.897	1.73	0.978	53.1

which does have a significant annual value of:

0.5 kW hr/m-day x \$0.03/kw hr x (50 wks/yr x 5 days/wk)
= \$3.75/m-yr

The heat lost overnight is given by equation IV-125

$$Q_{Lost} = \left[1-\exp(-\Delta t/\tau)\right] MC_p \ (T_i - T_a) \qquad \text{(Eq. IV-125)}$$

where M = Mass of the fluid, pipe and insulation
C_p = Component specific heat
T_i = Initial temperature
τ = Time constant of the pipe given by MC_p/UA

Substituting the values for water, 8.83 cm (3-1/2 in) schedule 40 steel pipe, and fiberglass insulation one obtains a heat loss of 0.32 kW hr/m over a 12 hour period. If the insulation thickness is doubled to 5.08 cm (2 in), the heat loss is reduced to 0.226 kW hr/m. The present value of the savings in heat loss is:

(0.322 kW hr/m - 0.226 kW hr/m) (\$0.03/kW hr) (50 wks x 5 days/wk) x (6.14) = \$4.33/m

However, the resulting increase in insulation costs would be:

1.61 x (\$0.077/cm^2-m) π (10.16^2 - 7.62^2) cm^2
= \$17.60/m

Detailed analysis of the overnight heat loss is required to determine the value of the heat lost vs. cost of added insulation. However, it seems that annual costs cannot be reduced through adding insulation to reduce overnight heat loss.

The overnight heat loss can be minimized by reducing the size of the pipe. Pipe using a standard 1.52 m/sec (5-ft/sec) velocity delivers

0.01 m^3/sec (154 gallons per minute). This same flowrate can be delivered with a 7.62 cm (3-in) schedule 40 pipe (O.D. 8.89 cm or 3-1/2-in, ID 7.79 cm or 3.068-in) using a velocity of 2.04 m/sec (6.68-ft/sec). This would increase the pumping cost but would decrease the pipe capital cost, the overnight heat loss, the insulation cost, and the heat lost during operational hours.

The pump power required is:

$$HP = \frac{(F) \times (P)}{0.70} \qquad \text{(Eq. IV-126)}$$

where:

F is the flowrate in m^3/sec

P is the pressure in Pa, and

0.7 is the efficiency of the pump.

Figure III-57 shows the pressure drop for 1-foot of 3 1/2-in schedule 40 pipe is 77.9 Pa (0.0113 psi). Thus:

$$\text{Power} = \frac{0.01 \times 77.9}{0.70} \times 3.28 \text{ ft/m} = 3.65 \text{ W/m}$$

At 8¢/Kwh and a motor efficiency of 0.8, the yearly cost per foot to pump the fluid is:

$$3.65 \text{ W/m} \times .228 \times 8760 \text{ hr./yr.} \times (.8)^{-1} \times \$0.08/\text{Kwhr.}$$
$$= \$0.73/\text{yr-m}$$

This is less than overnight heat loss ($2.40/m-yr), or the daytime heat loss ($15.97/m ÷ 6.14 = $2.60/m-yr), and suggests that the pipe size should be decreased.

Reducing the pipe size reduces the pipe capital cost, and increases the pumping energy cost (it may also increase the flow control and balancing problems). The trade-off considering only capital cost and

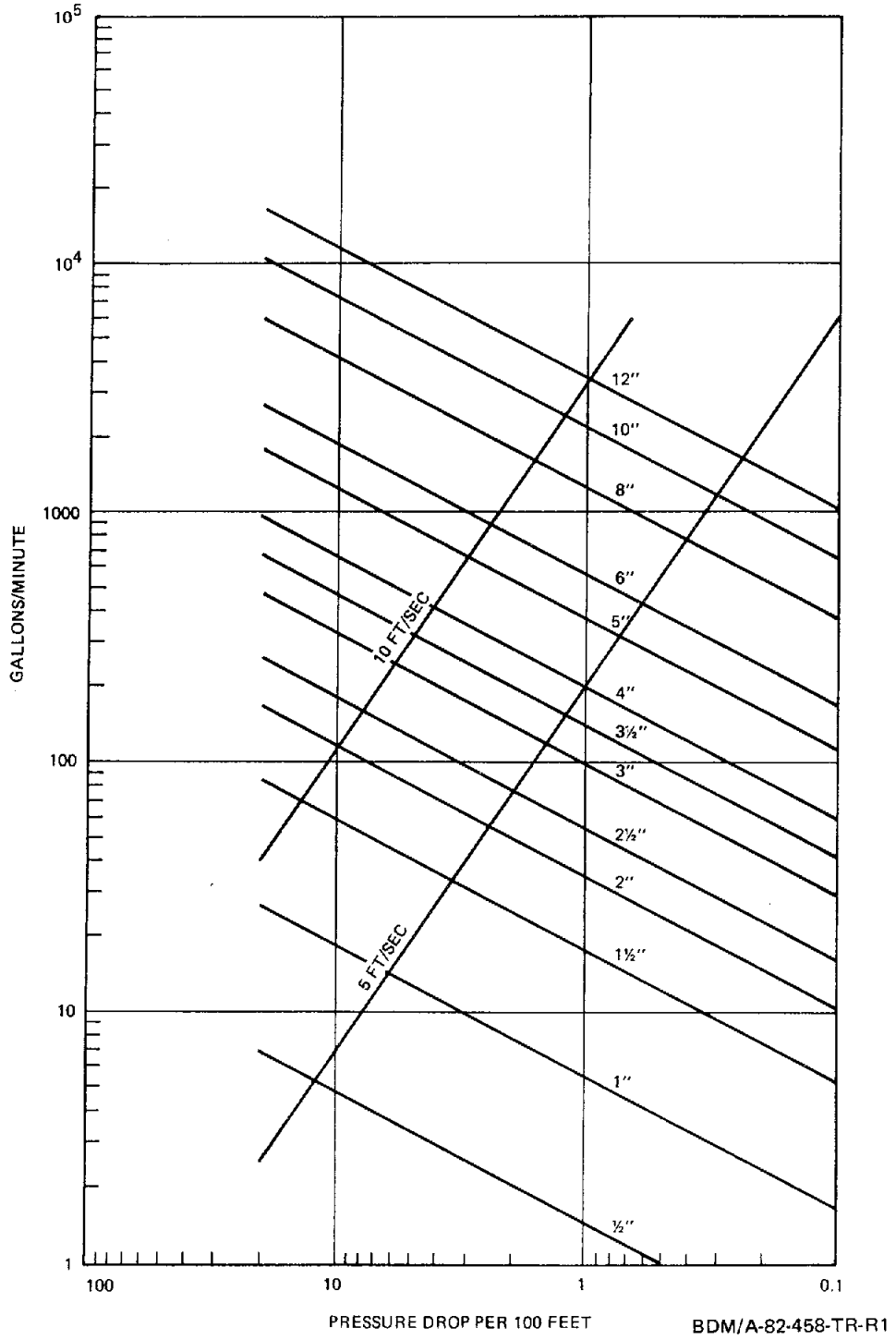

Figure IV-57. Flow of 60°F Water in Schedule 40 Pipe

pumping cost is; pipe capital costs for installed schedule 40 pipe can be calculated from:

$$C_p = 2.4S \text{ in } \$/\text{ft for S in inches}$$
$$C_p = 3.1S \text{ in } \$/\text{m for S in centimeters} \qquad \text{(Eq. IV-127)}$$

where S is the pipe size. Changing the pipe size from 8.89 cm to 7.62 cm (3-1/2 to 3-in) would result in a $3.94 reduction in pipe capital costs per meter. Pump capital cost installed can be calculated from:

$$C_{PH} = 790\ HP^{1/2} + 51\ HP \text{ for pump power in horsepower}$$
$$= 914.7\ Kw^{1/2} + 68.4\ kW \text{ for pump power in kilowatts} \qquad \text{(Eq. IV-128)}$$

Clearly, the power for one meter cannot be used to determine capital costs. In fact the power for 305 m (1000-ft) is only 1.1 kW (1.5 hp) which is also too small. Much of the system pressure loss will be in fittings, valves, heat exchangers, receiver tubes, etc. A reasonable system pump size may be 7.46 kW (10 Hp). Figure IV-57 shows that reducing the pipe size to 7.62 cm (3-in) while keeping the same total flow (0.01 m^3/sec or 154 gallons per minute) will increase pressure loss to 542.8 Pa/m (0.024 psi/ft) and increase the flow rate to 2.04 m/sec (6.68 ft/sec). This 2.12-fold increase in pressure loss will result in a 79¢/yr-m increase in electricity consumed. The change in pump capital cost will be $0.95/m. Using the same time-value-of-money factors as before the net change considering only pipe, pump, and pumping power will be:

$$\Delta C = 1.61\ (-\$3.94/m + \$0.95/m) + 6.14\ yr.\ (\$0.79/yr\text{-}m)$$
$$= \$0.037/m$$

Thus, if we only consider pipe costs, pumping power costs, and pump costs (no heat loss or insulation) reducing the pipe size to 7.62 cm (3-in) does not significantly change system cost and hence the 0.762 cm (3-in) pipe does not appear better than the 8.89 cm (3-1/2-in) pipe.

For a PV-T system it is appropriate to include the heat lost and insulation costs in the calculation of optimum pipe radius. Changing the pipe size to 7.62 cm (3-in) schedule 40 (ID = 7.79 cm or 3.068-in) changes the value of A/Br^2 that must be used to determine the new optimum insulation thickness. The new value for A/Br^2 is 0.409 which results in an optimum value of $r_s/r = 1.51$ for fiberglass according to figure IV-55. The new outer radius for the insulation should be:

$$r_s = 4.445\ cm \times 1.51$$
$$= 6.71\ cm$$

Choosing to round the insulation thickness up to 2.54 cm (1-in) (r_s = 6.99 cm or 2.75 in), this results in the following changes in insulation economics:

Δ(Cost of daytime heat lost) = -\$0.33/yr.-m
Δ(Cost of nighttime heat lost) = -\$0.43/yr.-m
Δ(Cost of insulation) = -\$0.79/m

Combining these savings with the pipe calculations above:

$$\Delta C = 1.61\ (-\$3.94 + \$0.95 - \$0.79)/m$$
$$+ 6.14\ yr\ (\$0.79 - \$0.43 - \$0.33)/m\text{-}yr.$$
$$= -\$5.90/m$$

This is a very significant savings, since it is done at a net decrease in capital costs.

If the pipe size is decreased further, the fluid velocity and pressure loss per foot will increase. Figure IV-57 shows that the cost of

pumping will increase rapidly as the pipe diameter is reduced, while the savings will increase more slowly. The optimum velocity appears to be somewhere between 2.13 and 3.05 m/sec (7 and 10 ft/sec). This analysis indicated that heat loss and insulation costs can be significantly reduced by decreasing the pipe size. However, a high design velocity makes it critical to properly evaluate pipe, valves, fittings, heat exchangers, friction factors etc.; otherwise there is a risk that pumping costs could be much higher than considered in the design. In addition, high manifold fluid velocities and high manifold pressure drops result in poor flow distribution through the collector rows and difficulty in controlling the flow. These calculations must be done in full consideration of the fluid properties (ethylene glycol if appropriate) at operating temperatures.

Pipe hangers, valves, flanges, etc. will result in a significant heat loss if they are not insulated. Once the optimum thickness for pipe insulation has been determined, the proper insulation thickness for valves, etc. can be determined by scaling thickness according to cost. The proper thickness of insulation on valves would be the same thickness unless there was a significant difference in cost. For example, if the cost for insulating a valve is twice as much per unit surface area, then the valve should only be insulated with one-half the thickness of that on the pipe. All parts of valves, flanges, etc. should be covered with insulation unless they must be exposed for operation.

Figure IV-58 shows the three basic methods of pipe support. For type "a" the pipe is fully insulated and rests in the tray. For this type of pipe hanger to be used, the insulation must be strong enough to support the pipe (including weight of fluid and insulation) without being crushed. For type "b" the insulation is cut away and the pipe rests directly on the hanger. The disadvantage of this type is, of course, the heat loss. Based on the assumption that the heat loss can be calculated by an equivalent bare pipe 5.08 cm (2-in) wide (probably conservative because of edge effects), the heat loss is:

Pages 161-162 are not in original document.

$$\frac{(7.62 \times 0.635)\text{cm}^2}{10^4\text{cm}^2/\text{m}^2} \times (43.3\ \text{W/m}^\circ\text{K}) \times \frac{66.7^\circ\text{F}}{(0.0508\text{m})}$$

$$= 27.5 \text{ watts}$$

almost twice as much as pipe hanger "b". In addition, if this pipe hanger is not insulated, there will be fin heat losses. As with pipe hanger "b", the biggest problem of pipe hanger "c" is probably not the heat loss, but the fact that it interrupts the vapor barrier. Mastic should be used with sealant that will form a water tight bond to the metal. If urethane is suitable, a board could be placed under pipe hanger "c" and the whole unit sprayed with urethane. This should reduce the heat loss by a factor of ten.

Gaps in insulation are also a problem. Inspection of typical low temperature insulation systems using preformed insulation indicate gaps of 0.635 cm (1/4-in) are common (see figure IV-59). For 8.89 cm (3-1/2-in) pipe size, such gaps expose 2 percent of the pipe area. Edge effects (heat taking a short cut through the insulation) may cause losses two or three times larger than the gap itself. If we take the total effect to be 6 percent, then for our example, the gap would reduce the present value of the heat saved through insulation ($93.32/m) by $5.61/m. This is significant compared to the $12.53/m variable insulation cost, and suggests gaps significantly effect the optimization of insulation. Six percent may not seem like much, but when added to 2 percent normal loss through the insulation, 3 percent overnight losses, and 2 percent pipe hanger loss, we see that losses can add up to be significant (13 percent). Since we have already used the optimum thickness, it is not cost-effective to reduce daytime losses more. Moreover, nighttime losses cannot be cost-effectively reduced by insulation. However, the gap should be eliminated by proper insulation sizing and installation without any additional cost. Most likely, the cause of the gap is incorrect insulation selection (mixing pipe and tubing sizes). If there is a

gap, since heat rises, placing it on the bottom should minimize the effect. Obviously, a concern over the existence of a gap is that the weather barrier is unsupported at this point.

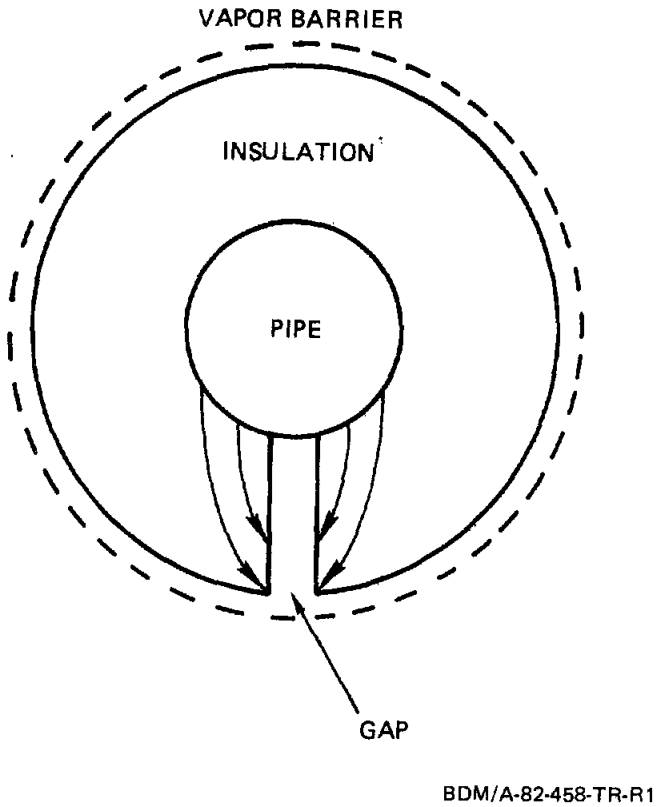

Figure IV-59. Insulation With a Gap

2. Acceptable Heat Loss Thickness

The analysis presented in this section is based on that of reference IV-18. Here, the heat loss from an insulated pipe will be limited to a fraction of the loss from a bare pipe. Equation IV-118 can be rewritten as:

$$\frac{Q_\ell}{A_I} = \frac{T_p - T_a}{\frac{r_s}{k} \ln (r_s/r_p) + R_s} \qquad \text{(Eq. IV-129)}$$

where:

$Q\ell$ = rate of heat loss from insulated pipe
A_I = external surface area of insulation
T_p = pipe wall temperature
T_a = ambient temperature
r_s = outside radius of insulation
r_p = pipe radius
R_s = thermal resistance of insulation surface
k = thermal conductivity of the insulation

The heat loss per unit area from a bare pipe can be written as:

$$Q_o/A_p = \frac{T_p - T_a}{R_p} \qquad \text{(Eq. IV-130)}$$

where

A_p = external surface area of bare pipe
R_p = thermal resistance of bare pipe surface

If the heat loss from an insulated pipe is limited to some fraction, F, of the heat loss from a bare pipe, then:

$$Q_\ell/A_I = F\,\frac{Q_o}{A_p} \qquad \text{(Eq. IV-131)}$$

Substituting equations IV-129 and IV-130 into equation IV-131 gives:

$$\frac{r_s}{r_p} \ln \left(\frac{r_s}{r_p}\right) = \frac{kR_p}{F} - kR_s$$

In most cases R_s is much smaller than R_p/F so that:

$$\frac{r_s}{r_p} \ln \left(\frac{r_s}{r_p}\right) = \frac{kR_p}{F} \qquad \text{(Eq. IV-132)}$$

and the insulation thickness is:

$$t = r_s - r_p \qquad \text{(Eq. IV-133)}$$

The bare pipe thermal resistance is given in hr $ft^{2o}F/BTU$ by equation IV-134, and the thermal conductivity of the insulation can be obtained from figure IV-60 at the average insulation temperature:

$$\frac{1}{R_p} = 0.27 \left[\frac{T_p - T_a}{2\ r_p}\right]^{0.25} + 1.54 \times 10^{-9} \times \left[(T_p + 460) + (T_a + 460)\right] \left[(T_p + 460)^2 + (T_a + 460)^2\right] \qquad \text{(Eq. IV-134)}$$

The fraction of bare pipe heat loss has been plotted versus insulation thickness and pipe diameter in figure IV-61 for average conditions in Albuquerque, New Mexico. As indicated, a heat-loss rate below 3 percent dramatically diminishes the returns of adding insulation. Thus, it is recommended that F be limited to about 3 percent.

J. AUXILIARY HEATERS

Two types of auxiliary heaters are available to augment the thermal energy gained by the PV-T system; heat pumps and fossil-fueled auxiliary heaters.

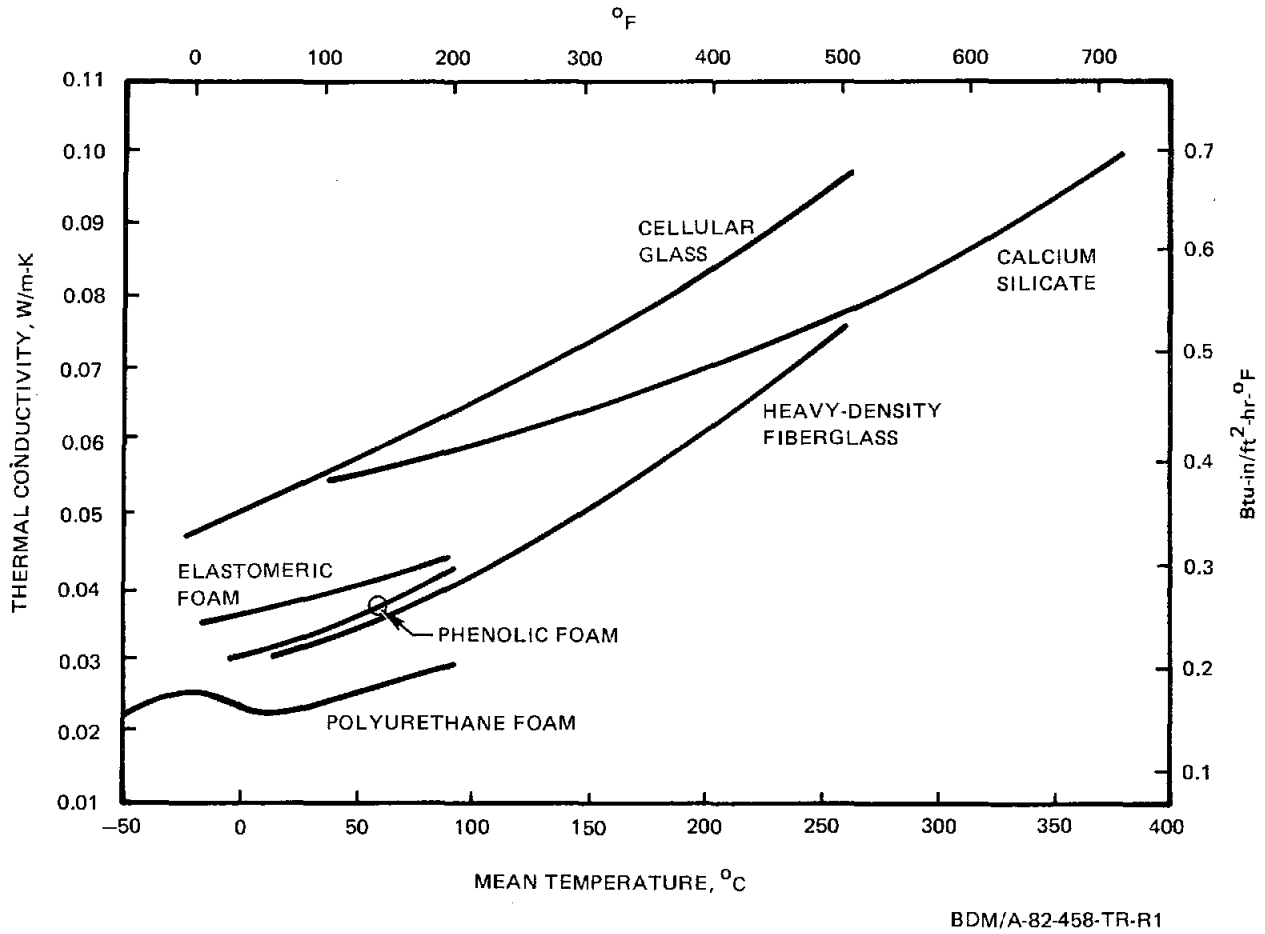

Figure IV-60. Approximate Thermal Conductivities of Pipe

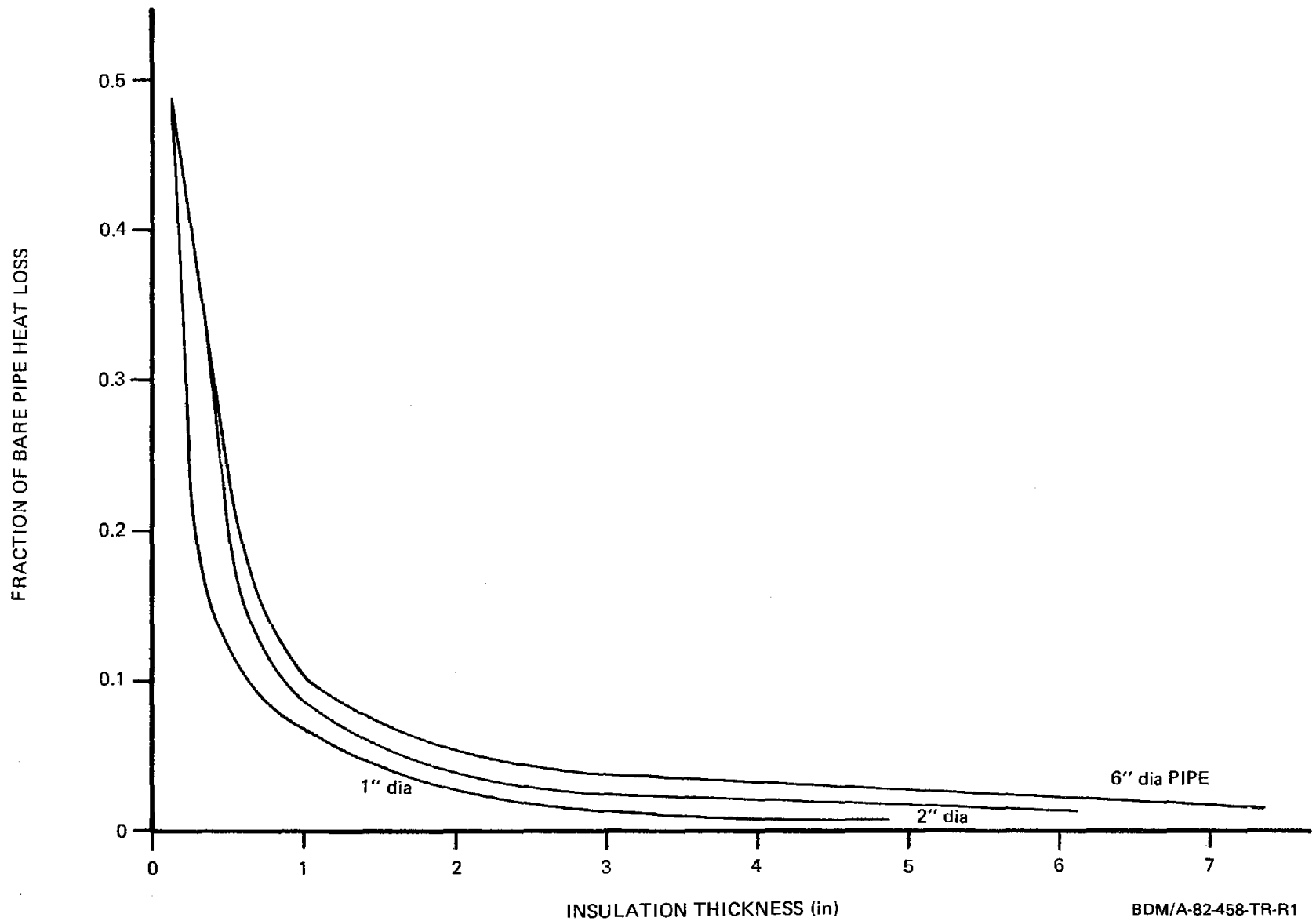

Figure IV-61. Heat-Loss Rate Versus Insulation Thickness for Various Pipe Diameters

1. Heat Pumps

To determine if a heat pump is an important option to be included in a PV-T system, two things should be considered in addition to the traditional comparison of the cost of electricity used by the heat pump to the cost of oil. First, can the PV-T system provide the electricity for the heat pump and second, could the PV-T system be redesigned to meet the load without the heat pump?

The usual analysis of energy costs for a heat pump is:

$$\text{Oil} \quad \frac{\$251/m^3}{10683 \text{ kW hr}/m^3 \times .80 \text{ overall eff}} = \$0.03/\text{kW hr}$$

$$\text{Heat Pump} \quad \frac{\$.067/\text{kwh}}{4 \text{ COP}} = \$0.017/\text{kW hr}$$

For a COP of 4 using a power generation efficiency of .343 and an electrical transmission and distribution efficiency of .9, only 237 kW of primary fuel are required to deliver 293 kW Btu's of heat whereas 366 kW of heater fuel will be required at a heater efficiency of .8.

The assumption that goes into the usual analysis of the cost of operating a heat pump is based on the idea that the heat source is waste heat. In a PV-T system the heat is not waste. Figure IV-62 shows a PV-T system with a heat pump. Consideration of the figure shows that the function of the heat pump is to change the quality of the energy reaching the load, not to change the quantity. The thermal energy becomes higher in temperature and more in quantity by the amount of the compressor electricity consumption, but the electrical energy delivered to the load is reduced by the energy consumed by the compressor; the net result is the same total energy delivered to the load. The question is then "is the change in energy quality produced by inclusion of the heat pump in the system cost effective?"

The maximum electrical energy available to the heat pump compressor is the full electrical output of the PV-T array. If more than

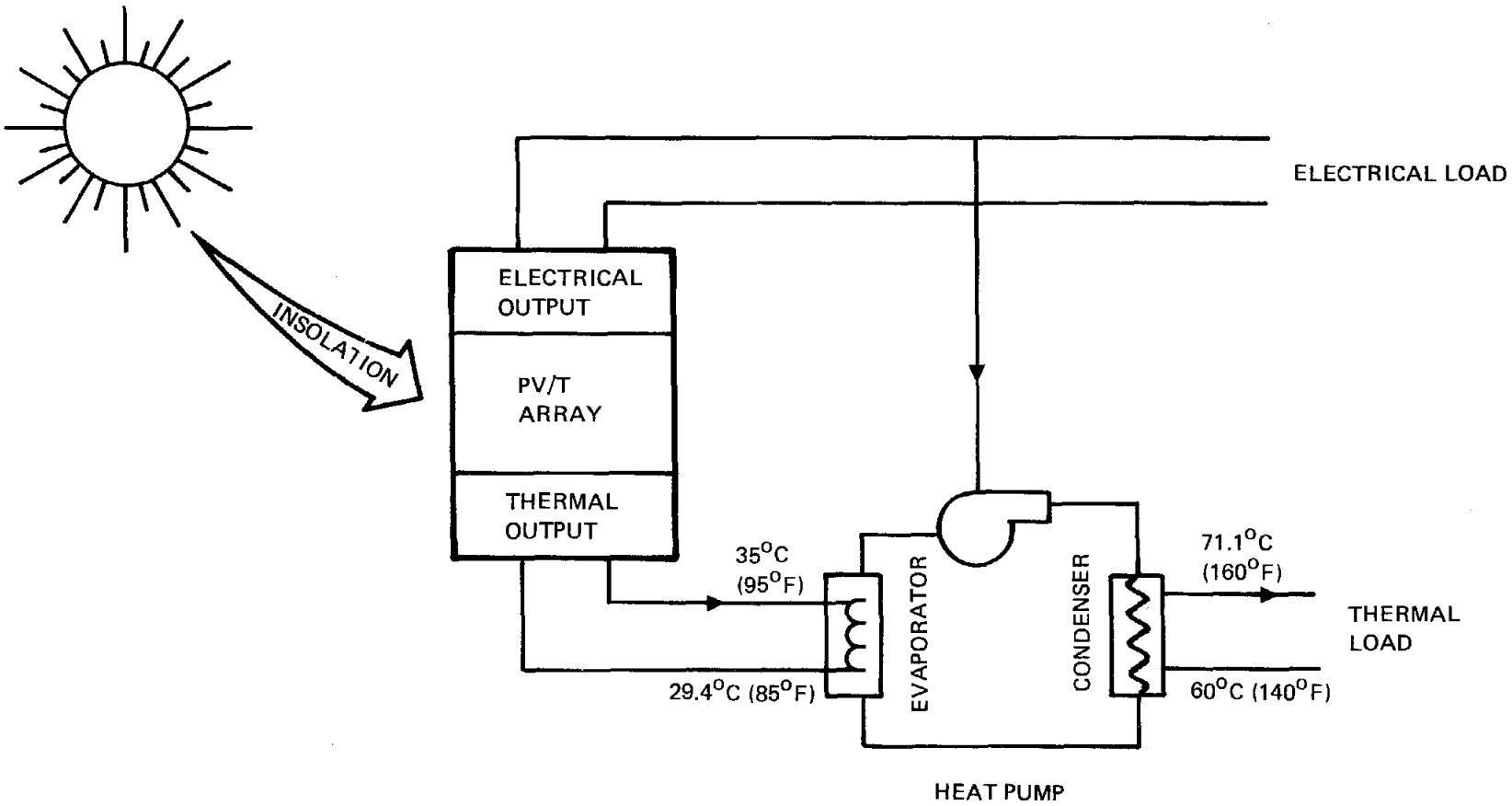

BDM/A-82-458-TR-R1

Figure IV-62. PV/T System With Heat Pump

this is required, it would make more sense to replace the whole system with a solar thermal system. At 125°C, the efficiency of a solar thermal system is as high as the total efficiency of a corresponding PV-T system. If the electrical output of the array limits the heat pump compressor electricity consumption then:

$$\frac{Q_L}{COP} < E_{PV-T} \qquad \text{(Eq. IV-135)}$$

where Q_L is the heat delivered to the load, E_{PV-T} is the electrical output of the PV-T array, and COP is the coefficient of performance of the heat pump. Since Q_L is equal to the thermal output of the array (Q_{PV-T}) plus the compressor electrical consumption $Q_{PV-T}/(COP-1)$, the above expression becomes:

$$COP > 1 + (E_{PV-T}/Q_{PV-T})^{-1} \qquad \text{(Eq. IV-136)}$$

Using the E-Systems PV-T system as representative, the electrical to thermal output ratio at 100°C is .24 implying the COP for the heat pump must be greater than 5.2. An examination of figure IV-63 shows that such a COP requires that the condenser outlet temperature be no more than 30.5°C (55°F) higher than the evaporator outlet temperature. About 8.3°C (15°F) of this difference occurs in the heat exchanger, so that only 22.2°C (40°F) improvement in temperature is possible with a COP of 5.2. Since the limit on commercial heat pumps is about 104.4°C (220°F) and the temperature limit of a PV-T array is about 121°C (250°F), little improvement is possible over the temperature that can be obtained by operating the PV-T array at maximum temperature. We thus conclude, that if the electrical consumption of the heat pump compressor is kept to a minimum so as not to consume the entire electrical output of PV-T array, then the COP of the heat pump must be high and, therefore, the temperature enhancement is small (22.2°C).

To determine if a heat pump is viable, consider two systems: one, a low temperature system that uses a heat pump to raise the temperature, and second, a PV-T-only system operating at the higher temperature. The benefit of the higher temperature system can be expressed as:

$$B_{HT} = V_E \, \eta_E \, (T_H) \, I + V_Q \eta_Q (T_H) \, I \qquad \text{(Eq. IV-137)}$$

where:

I is the insolation,
V_E is the value of the electricity ($/kwh),
V_Q is the value of the heat ($/kwh),
η_E is the electrical efficiency of the array at T_H,
η_Q is the thermal efficiency of the array at T_H,
T_H is the operating temperature of the high temperature array.

For the other system the benefit is:

$$B_{LT} = V_E \left[\eta_E (T_L) I - E_{HP} \right] + V_Q \, (COP) E_{HP} \qquad \text{(Eq. IV-138)}$$

where

E_{HP} is the energy consumed by the heat pump,
COP is the coefficient of performance of the heat pump,
T_L is the operating temperature of the low temperature array.

Requiring that $B_{LT} > B_{HT}$ implies that:

$$\frac{1 - V_Q/V_E}{COP - 1} < \frac{\eta_E(T_H) - \eta_E(T_L) + V_E \left[\eta_Q(T_H) - \eta_Q(T_L) \right] / V_Q}{\eta_Q(T_L)} \qquad \text{(Eq. IV-139)}$$

Using the E-Systems PV-T system performance data, $T_L = 75^oC$, $T_H = 100^oC$, and calculating V_Q/V_E using the above oil and electricity prices this expression reduces to:

$$COP > 13.4 \qquad \text{(Eq. IV-140)}$$

This means that for a heat pump system that boosts the temperature of an array operating at 75^oC to the load temperature of 100^oC to produce more benefit (ignoring the additional cost outlay for the heat pump) than a PV-T system operating at 100^oC, the COP of the heat pump would have to be more than 13.4. For these temperatures, figure IV-63 implies actual heat pump coefficients of performance are about 5.5.

In conclusion, the COP of heat pumps are not large enough for them to produce a significant increase in temperature without consuming the entire output of the array, and the same temperature increases can be produced more cost effectively by operating the PV-T array at a higher temperature. These conclusions are, in part, dependent upon the E-Systems PV-T efficiencies assumed but the COPs calculated to support both conclusions could be reduced by a factor of two without changing the conclusion. This analysis does not imply heat pumps are not useful when there is waste heat to be recovered, but that using them with a PV-T array is like using a heat pump to boost the temperature of the output of a heater.

2. Auxiliary Heaters (Steam and Hot Water)

An auxiliary heater is required in a PV-T system as a back-up to the solar collectors, and to supply additional heat when the collectors cannot meet the full load. To satisfy the back-up requirement, the auxiliary heater must be sized to deliver the full load when the solar system is off, and when the storage tank (if there is one) is not supplying warm water. In a PV-T system, performance is optimized for the combined thermal and electrical output. Thus, the temperature may not be high enough to meet load requirements. Interfacing requirements of the PV-T array and the auxiliary heaters are not the same as for a solar thermal system.

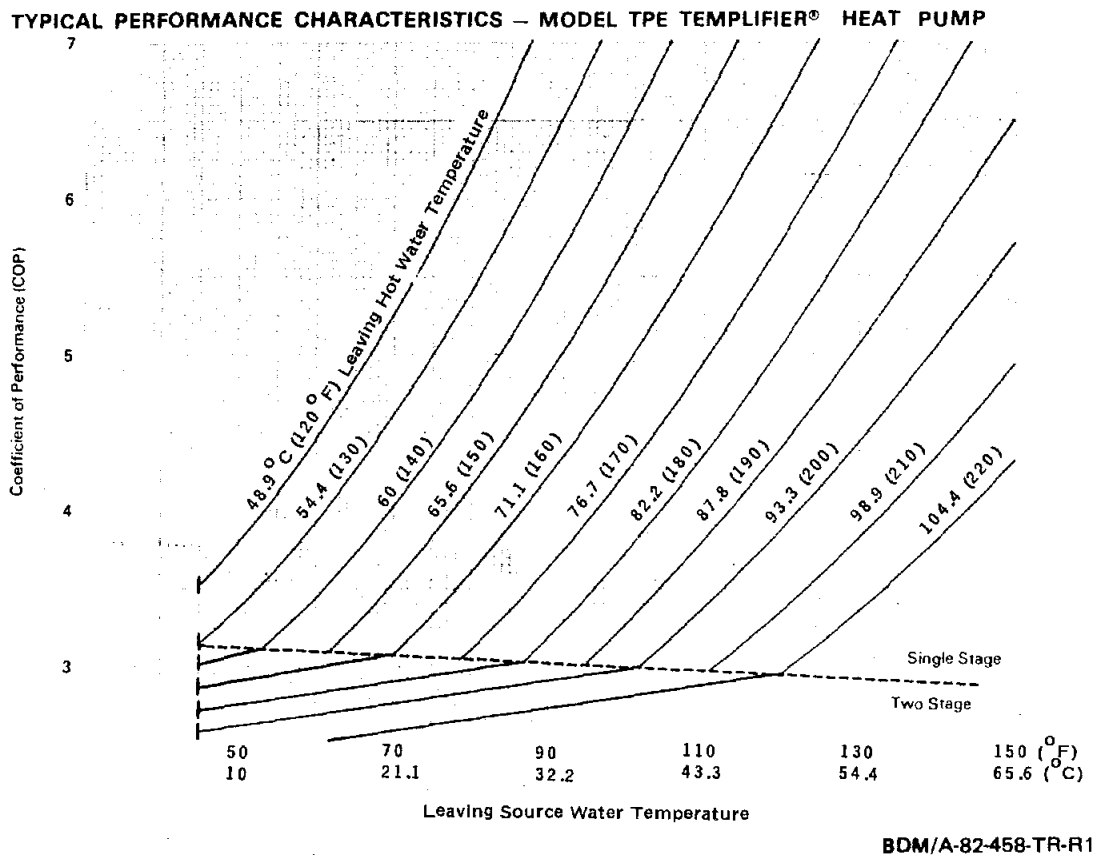

Figure IV-63. Typical COPs for Heat Pump (Source McQuay-Perfex Inc., Descriptive Bulletin TP-1). Reproduced With the Permission of McQuay-Perfex, Inc.

The PV-T array and the auxiliary heat boiler can be interfaced in series or parallel. Connecting the PV-T array and auxiliary heater in parallel can either increase or decrease the auxiliary heater's performance, depending upon whether the efficiency of the heater goes up or down with turndown. Usually, changes in heater efficiency with turndown are less than 2 percent; however, for some heaters the change may be as much as 8 percent. If the array and heater are connected in parallel, then the heater can be cycled on and off operating only at full load. For a heater which decreases in efficiency with turndown, the heater will be most efficient when connected in parallel. The array will be most efficient when the inlet temperature is as low as possible; this occurs when the heater and array are in series. Depending on the specific auxiliary heater, the array characteristics, and operating conditions, maximum system performance can be obtained either through series or parallel interfacing, but in general maximizing array efficiency through series interfacing will lead to the best system performance for many applications. For a PV-T system, if the maximum array outlet temperature is not high enough to meet the load requirement then the system must be connected in series.

Three ways the heater and array can be interfaced in series are:

(1) With the PV-T system preheating process water entering the auxiliary heater.

(2) Using heat from the PV-T system to heat the combustion air.

(3) Using heat from the PV-T system to heat the auxiliary heater fuel.

A steam or electric fuel heater is sometimes required to heat heavy fuel oils to lower their viscosity for proper atomization in the auxiliary heater burner. Fuel temperatures of up to 74.6°C (200°F) may be required. When appropriate, fuel heating can produce a savings of up to one-half of one percent. However, there are disadvantages of additional control system requirements, possible fire hazards (especially with natural gas), and problems in maintaining a constant fuel quality

when the PV-T system output varies. If fuel heating is considered, the design should be checked with the heater manufacturer and careful consideration should be given to maintaining proper fuel quality. Compared to other methods of using the PV-T system heat, fuel heating is not recommended.

Combustion air heating may require the existing air supply and burner equipment be modified to operate at higher temperatures. For a typical auxiliary heater every 37.8°C (100°F) rise in temperature of the combustion air will increase the efficiency by 3 percent. Advantages of combustion air heating are that it can be very effective, low temperatures can be used, and that interfacing the PV-T system and auxiliary heater is simple, provided heater equipment can handle higher temperatures. Disadvantages are that modifications of heater equipment may be necessary and the heater equipment may need to operate under a varying air inlet temperature as the PV-T system performance changes. Before a combustion air heating system is designed, the heater manufacturer should be consulted.

Feedwater heating is a standard practice for both hot water heaters and steam generators, and the use of the PV-T system to preheat an auxiliary heater does not introduce any unique solar design considerations. If the heater is a boiler and has a deaerator, it is important to determine if feedwater heating will raise the temperature too high for the deaerator to function properly. If this is the case, the feedwater heating rate will have to be changed or the deaerator will have to be replaced with a high temperature deaerator.

Figure IV-64 shows a typical boiler system. Not all boilers have air heaters, economizers, and deaerators. Figure IV-65 shows the two basic ways to feedwater heat the boiler in figure IV-64. Configuration "a" favors heat extraction from the blowdown water at the expense of higher inlet temperatures to the PV-T array. Configuration "b" favors increased PV-T array efficiency at the expense of waste heat in blowdown water. Typical blowdown water rates are 20 percent of the makeup water. Typical temperatures for blowdown water and makeup water are shown on configuration "a" of figure IV-65. Configuration "a" results in 19.3

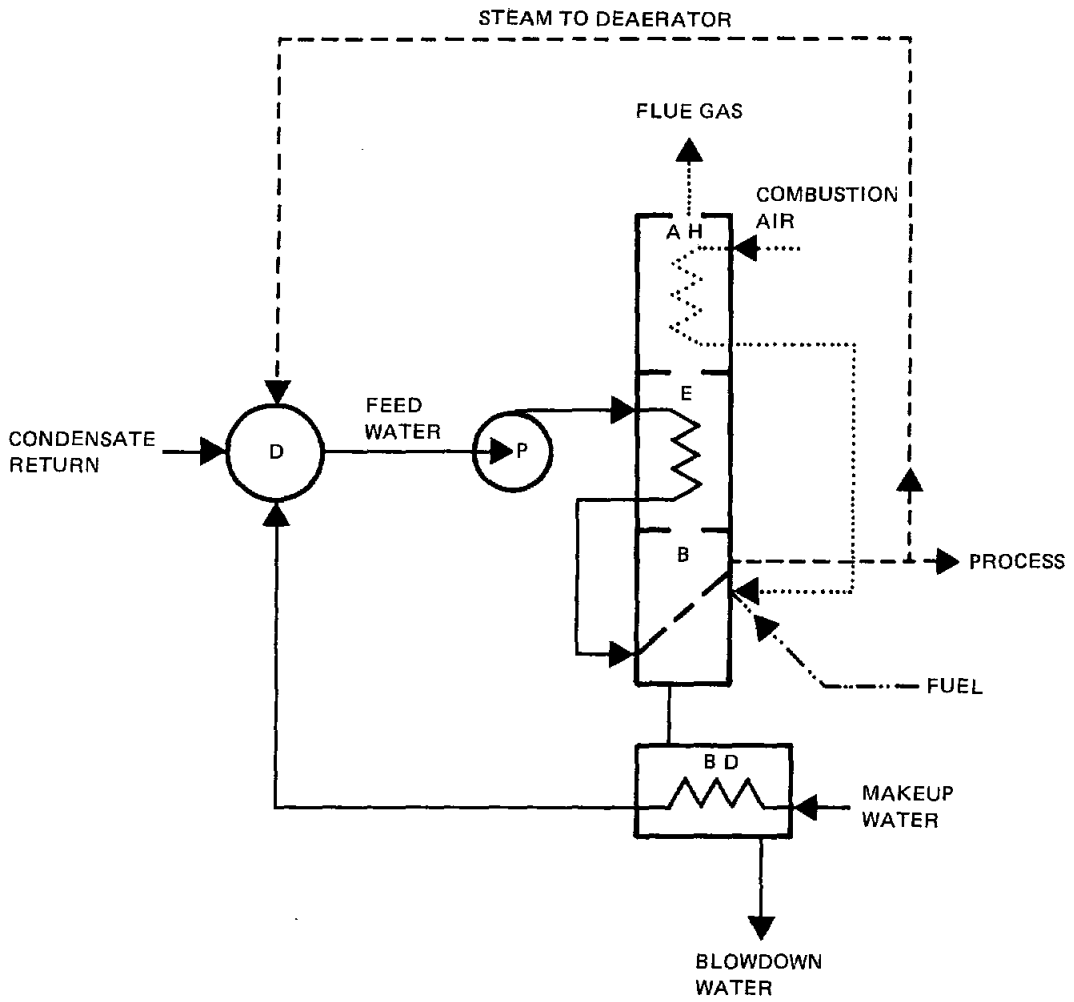

A H	AIR HEATER
B	BOILER
B D	BLOWDOWN HEAT EXCHANGER
D	DEAERATOR
E	ECONOMIZER
P	FEED PUMP

WATER
STEAM
FLUE GAS OF COMBUSTION AIR
FUEL

BDM/A-82-458-TR-R1

Figure IV-64. Typical Boiler System Showing Major Components

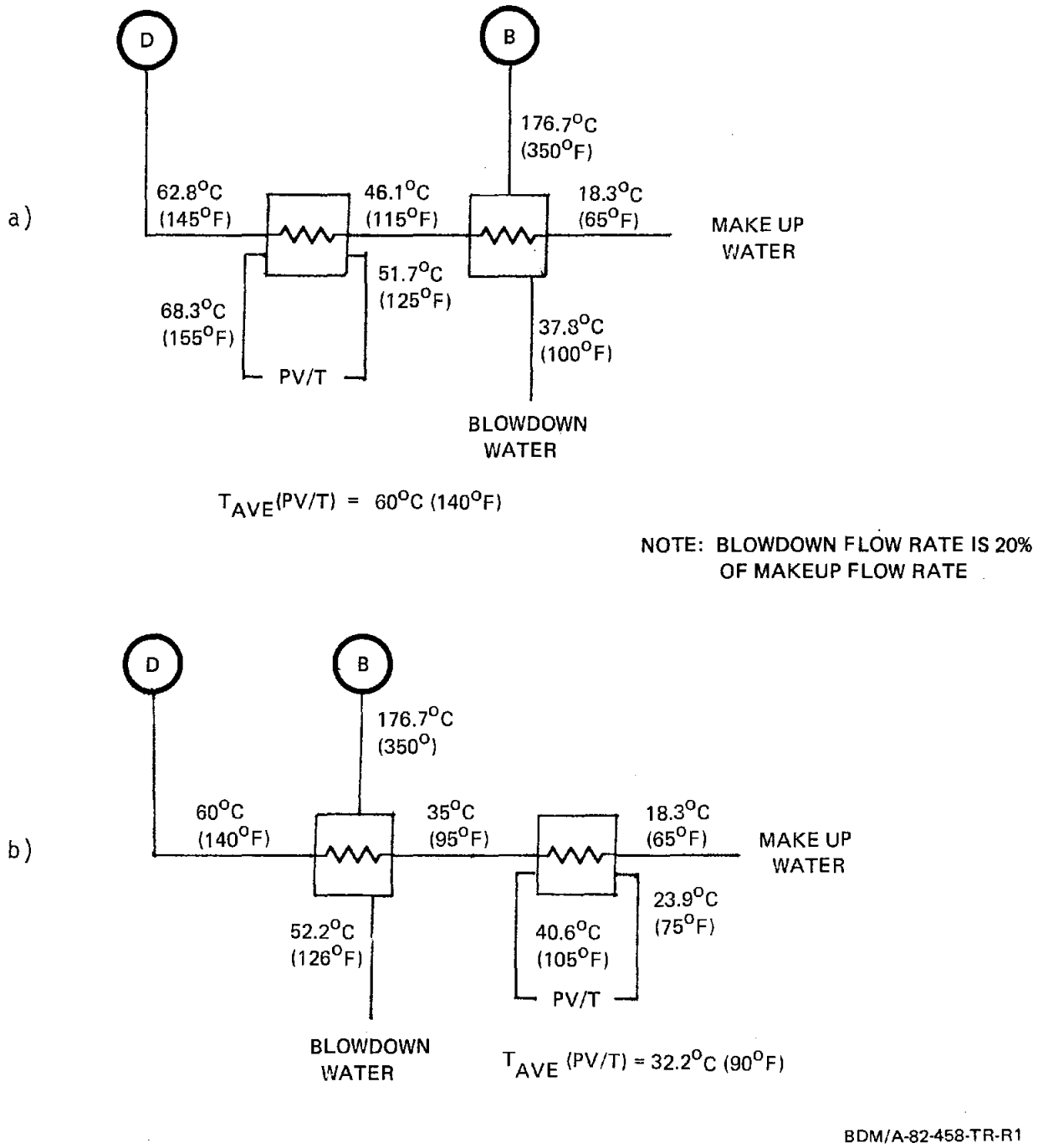

BDM/A-82-458-TR-R1

Figure IV-65. Ways of Preheating a Boiler

watt hrs/kg (30 Btu/lb) of makeup water more than without the PV-T system, whereas configuration "b" only results in 16.1 watt hrs/kg (25 Btu/lb) of makeup water. This benefit of configuration "b" is 17 percent less. For configuration "b" the average temperature in the array is 27.8^{o}C (50°F) less than configuration "a". This should result in a 7 percent increase in array performance, which is considerably less than the 20 percent poorer heating of makeup water. From the example numbers on figure IV-65 we thus expect that configuration "a" is better.

Figure IV-66 shows a heater with a spray stack economizer. The PV-T array can be interfaced to such a heater before or after the stack. Again, there will be a heater-PV-T system trade-off depending upon where the interface is.

If the boiler supplies steam and the PV-T array only delivers a temperature below boiling, enthalpy considerations (heat of vaporization vs. specific heat) imply the PV-T array can only supply a few percent of the load. Boiler efficiencies vary from a standard 80 percent up to 96 percent. Since this difference is considerably more than the 2 percent savings a PV-T array can supply, it is obvious one must not let boiler efficiency be degraded by the interface to the PV-T system. For existing boilers, one must clearly work around constraints imposed by the boiler configuration. When a new boiler is to be used, one must be careful boiler efficiency is not sacrificed to make interfacing with the PV-T system simpler or more efficient.

For a hot water heater, the contribution of the PV-T array to heat load is not limited. In this case, the system should be designed to maximize PV-T array efficiency rather auxiliary heater efficiency.

Auxiliary heaters have a range over which the burner can be turned down and still provide reliable operation with complete combustion. The typical load range is 25 to 100 percent of full rated load (a four to one turndown). Some heaters with specialized controls and burners have a ten to one turn-down. Below the turndown rate the burner no longer functions and must be turned off. Thus, if less heat is required than the turndown, the burner must be cycled.

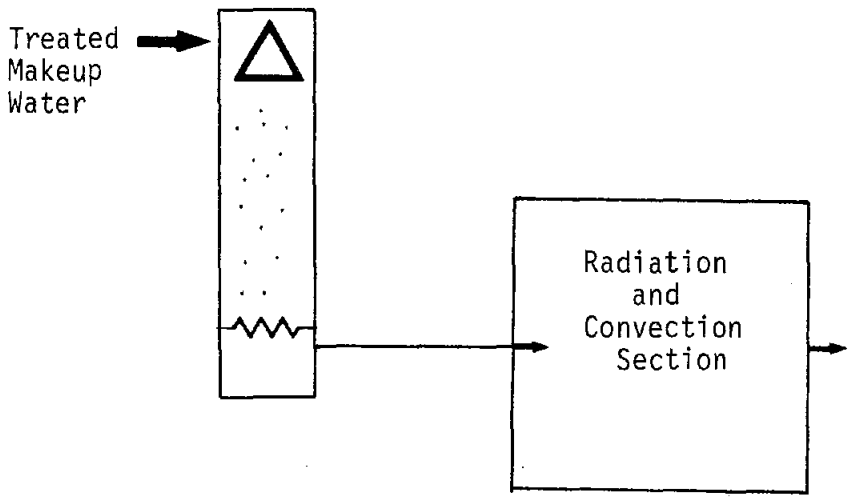

BDM/A-82-458-TR-R1

Figure IV-66. Spray Stack Economizer Boiler

During cold start-up, a low firing rate must be maintained to avoid rapid thermal expansions and, of necessity, combustion efficiency is poor, leaving some unburned fuel. Most furnace explosions occur during start-up and low operation. Operational strategy should minimize cold start-ups, i.e., the use of a storage tank to equalize the load and allow the heater to be fired up only once a day--at night--to make up any heat needed. A brief drop in load (one hour) may not cause burner problems, but the manufacturer should always be consulted about the operational strategy, i.e., turndown, cycling, and cold startup.

Heaters have a recommended safe load change rate. A change in load that is too quick is likely to cause the burner to shut off, a safety valve to lift venting pressure, a drop in pressure, or poor efficiency. Therefore, the system should be designed so the heater does not have to compensate for rapid changes in the load or rapid changes in PV-T array output.

Concern is often expressed that the use of a solar system to preheat feedwater, will cause the auxiliary heater efficiency to fall off. Figure IV-67 shows the efficiency of a heater as a function of the fuel firing rate. It should be noted that the high rise in losses for low firing rates is below manufacturer's maximum recommended turndown and thus represents using the heater in a cyclic mode. This representation of heater efficiency at low average firing rates, while not totally accurate, is adequate for present analysis. The heater losses (as shown on figure IV-67) are made up of two components:

(1) A skin loss, which depends primarily on the temperature of the heater shell, and so is essentially a constant for all firing rates, when the heater is warm.

(2) A stack loss, which is essentially a fixed precentage of the energy delivered by the heater over the entire range of firing.

Typically, these losses are 1.5 percent of the energy delivered at full load for the skin loss, and 25 percent of the energy being delivered at the actual firing rate for stack losses. The efficiency of the auxiliary heater at a given firing rate F can be approximately expressed as:

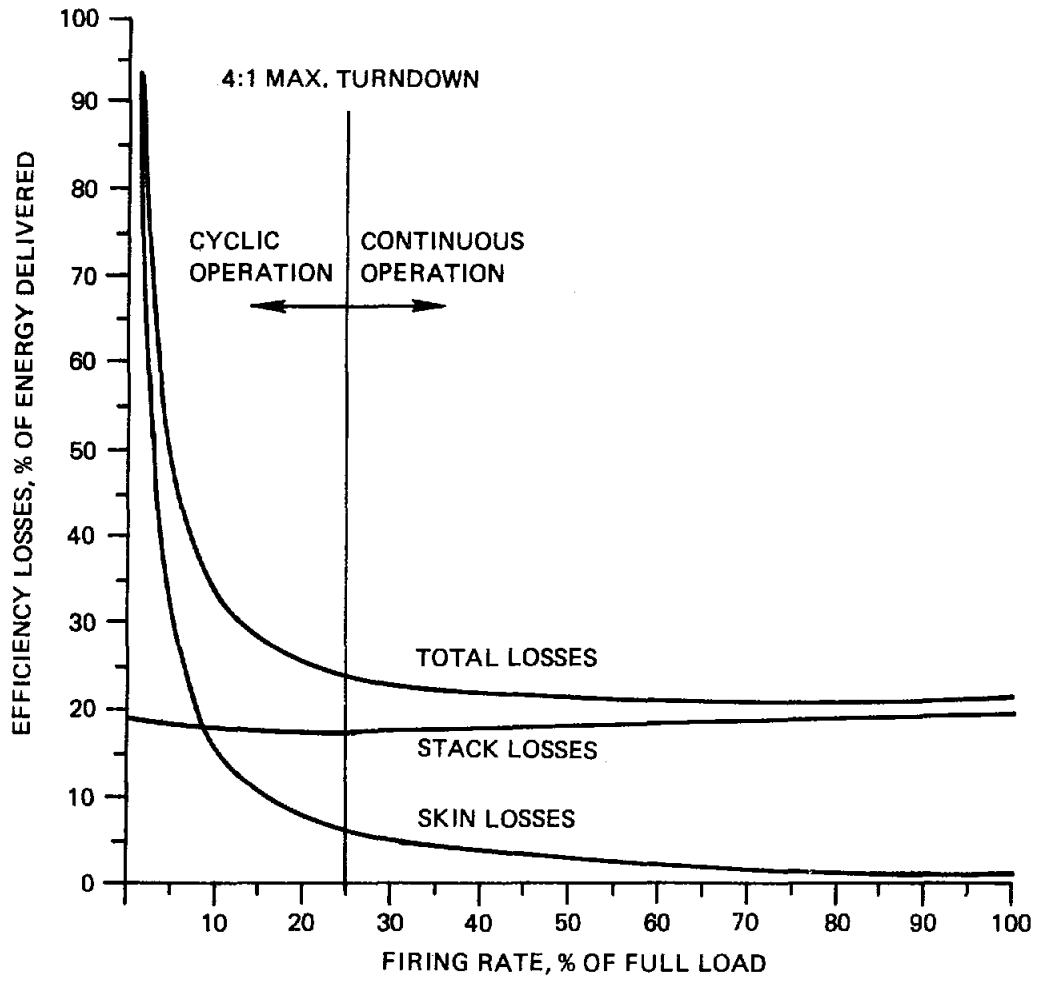

BDM/A-82-458-TR-R1

Figure IV-67. Losses From a Typical Industrial Boiler

$$\eta = (1 + B(F) + \sigma/F)^{-1} \qquad \text{(Eq. IV-141)}$$

where B(F) is stack loss fraction energy delivered at firing rate F, and σ is the skin loss constant fraction of full load. Figure IV-67 shows that at low firing rates (10 percent or less), the losses in the heater become high; hence the concern when using a PV-T system as a preheater for an auxiliary heater.

The primary evaluation of effectiveness of a PV-T system as a preheater for an auxiliary heater is not the efficiency of the heater at the firing rate being used, but the cost effectiveness of the entire system.

Figure IV-68 shows for low firing rates, a high loss fraction of the actual fuel being used, not a high fraction of the fuel that would have been used if the PV-T system were not preheating the auxiliary heater. The extra fuel used by the heater because of lower efficiency at low firing rates:

$$Q_{EXTRA} = \left\{\sigma\ (1 - F) - F\left[B(1) - B(F)\right]\right\} Q_{FULL-LOAD} \qquad \text{(Eq. IV-142)}$$

is compared to the fuel saved:

$$Q_{SAVED} = \left\{(1 - F)\left[1 + B(1)\right] + F\left[B(1)\right] - \left[B(F)\right]\right\} Q_{FULL-LOAD} \qquad \text{(Eq. IV-143)}$$

in figure IV-68. In plotting figure IV-68, it has been assumed that the variation in B, as a function of firing rate, is not more than 8 percent. The figure shows that the fuel wasted due to firing including cycling the heater at low efficiency is always a small fraction (1.2 percent) of the fuel saved for all firing rates. The reason for this is that the times when figure IV-67 shows high losses (firing rate less than 10 percent),

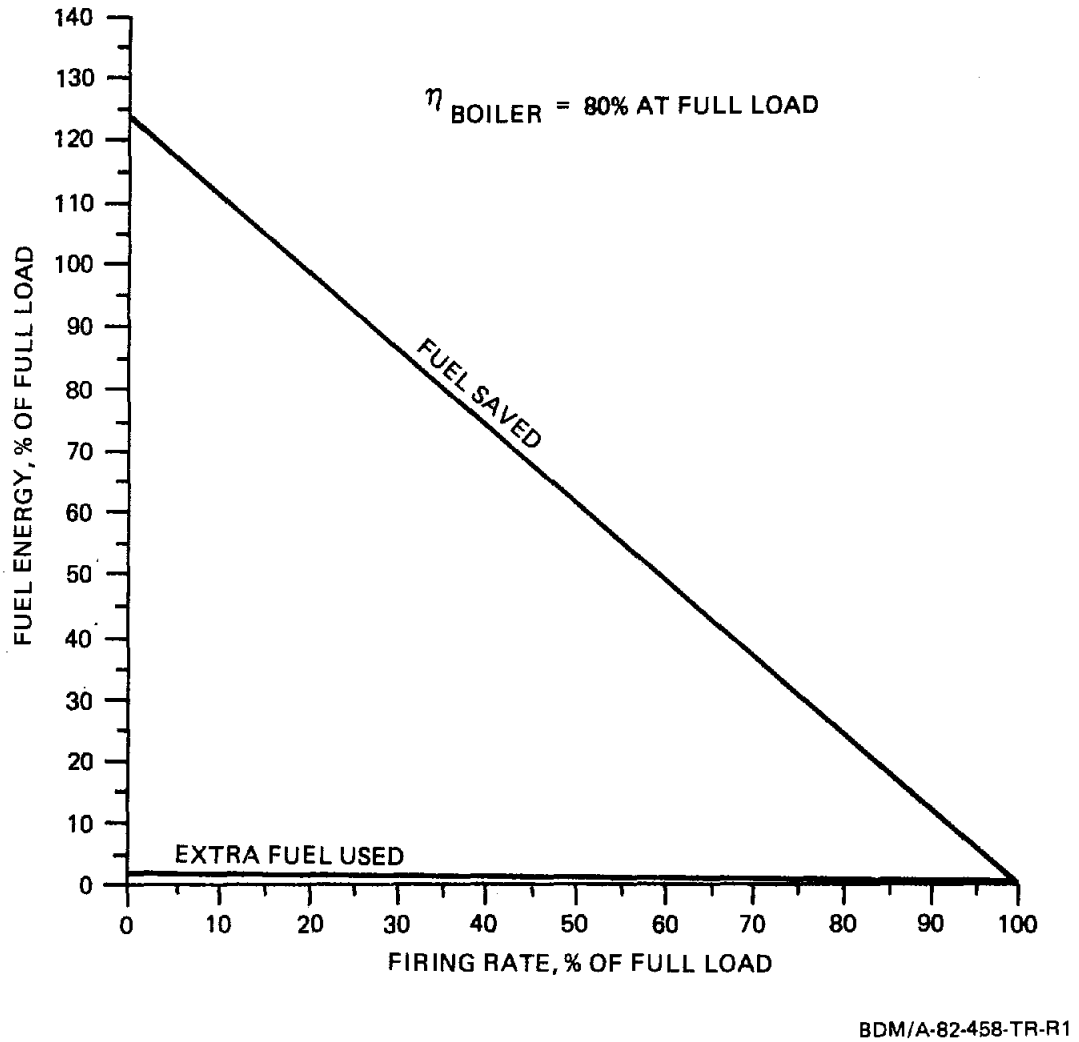

Figure IV-68. Extra Fuel Energy Use Compared to Total Use

occurs when the PV-T system has resulted in a larger fuel savings. Figure IV-67 shows that once the heater has been modified to interface with the PV-T array, the system should be operated so as to minimize heater usage, and that low average firing rates are not an efficiency problem (excepting perhaps cold start-up). The figure does not address the issue of whether it is cost effective to modify the heater to interface with the array. The answer to that question depends on the cost of using the particular heater in a conventional manner and the characteristics and costs of the PV-T array auxiliary heater system.

It can be concluded then, that the use of a PV-T system to preheat a heater will not have the adverse effect of lowering the auxiliary heater efficiency. The heater, however, may have an adverse effect on the performance of the PV-T array. In general, the PV-T system will perform best, and result in the maximum fuel savings, when the average inlet temperature of the array is low. This means the auxiliary heater should be placed in the system, and operated so as to produce as low an array inlet temperature as possible. In general, this means the auxiliary heater should be in series rather than parallel with the array, and that the heater be fired at as low a rate as possible while still satisfying the load demand. A heater should not be fired at a turn down rate less than it is designed for. The turndown rate, if possible, should be low enough that the storage can be exhausted overnight (or by the end of the week if energy is to be collected during the weekend, for use during the week); otherwise the morning array inlet temperature will be higher than necessary.

Boilers must meet all ASME codes: Boiler and Pressure Vessel Code Section IV for Heating Boilers (low pressure heaters), and Section I for Power Boilers (medium and high pressure heaters). Boilers are classified based on working pressure and temperature, fuel used, and output (steam or water). Heater performance is rated according to the Hydronics Institute, American Gas Association, or American Boiler Association. Boiler sizing is based on gross output. The gross output must, however, be sufficiently larger than the load requirement to allow for pickup and

piping loss. Pickup is the extra heat that must be added to warm up the system, and pipe loss is the heat leaving the heater that is lost in transit to the load. Further information on the use and maintenance of heaters can be found in the ASHRAE guide books.

K. REFERENCES

IV-1. Kays, W. and A. L. London, Compact Heat Exchangers, McGraw Hill Book Co., New York, NY, 1964.

IV-2. Anon. Standards of the Tubular Exchanger Manufacturers Association, TEMA, New York, NY, 1978.

IV-3. Rajee, K. S. N. and Jagdish Chand, " Consider the Plate Heat Exchanger," Chemical Engineering, August 11, 1980, pp. 133-144.

IV-4. Frank, O. "Simplified Design Procedures for Tubular Heat Exchangers," in Practical Aspects of Heat Transfer, American Institute of Chemical Engineers, New York, NY, 1978.

IV-5. Lord, R. C., et. at., "Design of Heat Exchangers" in Process Heat Exchange edited by V. Cavaseno, McGraw Hill Publishing Co., 1979.

IV-6. Marriott, J., "Where and How to Use Plate Heat Exchangers," Chemical Engineering, April 5, 1971, pp 127-134.

IV-7. Jackson, B. W., and R. A. Troupe, "Plate Heat Exchangers Designed by The NTU Method," Chemical Eng. Progress Symposium Series, Vol. 62, No. 64, pp 185-190.

IV-8. DeWinter, Francis, "Heat Exchanger Penalities in Double-Loop Solar Water Heating Systems", Solar Energy, Vol 17, No. 6, pp 335-337.

IV-9. Perino, A. M., A Methodology for Determining the Economic Feasibility of Residential or Commercial Solar Energy Systems, (SAND 78-00931), Sandia National Laboratories, Albuquerque, NM, Jan. 1979.

IV-10. Baltimore Aircoil Co., Industrial Fluid Coolers, BAC Bulletin S405/1-0, July 1978.

IV-11. Commercial Applications of Solar Total Energy Systems, Second Quarterly Progress Report, August 1, 1976, October 31, 1976 Report No. AI-ERDA-13200 (Canoga Park, CA: Rockwell, International, Atomics International Division, April 1977).

IV-12. Sharp, John K., "Design of Collector Subsystem Piping Layout II", Proceedings of the Line-Focus Solar Thermal Energy Technolgy Development Seminar, Sandia National Laboratories, NM, Sept 1980.

IV-13. Sharp, John K., Designing the Manifold Piping for Parabolic Trough Collector Fields, SAND 81-1780, Sandia National Laboratories, NM, April 1982.

IV-14. ASME Code for Pressure Piping, B31, ANSI/ASME B31.1, The American Society of Mechanical Engineers, New York (1981).

IV-15. Jones, G. F. and N. Lior, "Optimal Insulation of Solar Heating System Pipes and Tanks", Energy, Vol. 4, pp 593-621.

IV-16. Kutscher, C. F. et. al., Design Approaches for Solar Industrial Process Heat Systems, (SERI/TR-253-1356), Solar Energy Research Institute, Golden, Co., August 1982.

IV-17. Turner, W. C. and Malloy, J. F., Thermal Insulation Handbook, McGraw Hill Book Co., 1981.

IV-18. McChesney, M. and P. McChesney, "Insulation Without Economics", Chemical Engineering, May 3, 1982, pp 70-78.

CHAPTER V
RELIABILITY, AVAILABILITY, AND MAINTAINABILITY

A. INTRODUCTION

The purpose of this discussion is to present a practical technique for developing reliability, availability, and maintainability (RAM) guidelines for solar photovoltaic-thermal (PV-T) systems design. The objective is to present the methodology, highlight the issues, and provide useable quantitative information for prediction purposes.

The methodology will be applicable to any PV-T system and reflects the performance expected of state-of-the-art technology. It is sufficiently flexible to evolve with time and be applicable to anticipated technological developments of the near future.

RAM factors are significant in the design of PV-T systems because they influence both system life cycle cost and system effectiveness. Reliability and maintainability combine to affect the frequency and duration of maintenance on the system hardware availability, which has a direct impact on the system effectiveness or lifetime power output. This chapter provides information on the elements of RAM that encompasses both quantitative and qualitative features.

RAM theory is discussed to the extent necessary to analyze PV-T systems, then the system components are identified, and a generic PV-T system is described. The description is sufficiently generic to be manageable, with enough detail to represent all components. This also allows substitution where desired. The next step presents failure data for components, and is presented in tabular form for ease of use. This generic data can be expected to change as a system design matures, and should be used with this in mind. Sources of information for additional data and more refined theory are also indicated to aid prospective PV-T designers. The final section of the chapter presents an example trade-off analysis to illustrate how RAM considerations enter into the formulation of a system design.

B. CONSTRAINTS

There are some basic constraints to this analysis that should be remembered throughout the discussion.

The design of PV-T systems is, in relation to current energy systems in use, very new and somewhat immature. Component design is evolutionary and RAM data has yet to be developed and proven. Critical uncertainties still remain in the technology. The very definition of "failure" for certain PV components is not well understood and is subject to wide interpretation. This discussion evaluates current state-of-the-art technology, and uses expected value modeling analysis based on the exponential distribution and sensitivity analysis to determine RAM data and provide a methodology for future extrapolation.

To be of any value, this treatment must be consistent. The methodology has focused on basic issues such as operating time, failure modes, and possible failure consequence.

C. RAM THEORY

1. Introduction

There is significant interaction between reliability, maintainability, and availability. For convenience of presentation, each of these elements will be discussed separately in the following paragraphs. However, links between these disciplines will be identified at appropriate points in the discussion.

2. Reliability

a. General

Reliability has become a major field of study during the past twenty-five years, and a vast body of literature exists on the subject. Topics within reliability include failure mode effects and criticality analysis (FMECA), failure predictions, reliability testing and demonstration, reliability allocation, failure physics, and reliability design. In addition, the discipline is closely related to

quality assurance, system effectiveness analysis, life cycle cost, and logistics analysis. The topics of concern in this chapter will be FMECA and failure rate prediction.

For the purpose of this discussion, reliability is defined as the probability that a system will perform in a satisfactory manner for a given period of time when used under stated conditions. The term "satisfactory performance" is used deliberately to indicate that the judgment of the system operator is often the means by which failures are identified. The definition is sufficiently flexible to include out-of-tolerance failures (graceful degradation) as well as catastrophic events. Tolerance failures arise when the measurable characteristics of a part change gradually until an unacceptable performance level is reached. In catastrophic failures characteristics change abruptly, usually resulting in complete inoperability. Both types of failures are relevant in solar system design and their impact must be considered in a failure rate prediction. For predesign failure analyses it should be noted that certain historical failure data banks do not include tolerance failures, while other sources do contain such failures. The designer must ensure that tolerance failures have been included in the data base and resulting predictions, or that appropriate adjustments are performed to include them. The data in appendix A includes both types of failures.

It is also necessary to consider two other categories of failures. They are termed logistics failures and critical hardware failures. Both tolerance and catastrophic failures will be found in each of these categories. Logistics failures include all failures of the system that require eventual restoration and imply the need for maintenance personnel, and usually (but not always) spare items. Repair of logisitics failures may often be deferred to periods of low insolation or poor weather. Logistics failures will be measured in terms of mean-time-between-maintenance (MTBM), to include preventive maintenance actions (e.g., array cleaning), as well as unscheduled actions (e.g., pump failure). Logistics failures are the appropriate category to consider in resource projection studies.

Critical hardware failures include only those failures that result in unavoidable system downtime (a downing event) during periods of sufficient solar availability. Thus, critical hardware failures result in loss of system output, and are the appropriate measure for use in hardware availability analysis. These failures will be measured in terms of mean-time-between-critical-failure (MTBCF). The distinction between logistics and critical hardware failures is essential, since logistics failures are often two or three times more abundant than critical failures (and even factors of ten are not uncommon). Secondly, certain reliability design techniques, such as use of redundant components, will affect these measures differently. Redundancy will usually result in improved critical hardware reliability, but at the same time will decrease system logistics reliability (since added hardware means there are more items that will fail and require eventual repair).

b. Failure Modes, Effects and Critically Analysis (FMECA)

The FMECA is the systematic identification of failure modes, their resultant effect on system performance, and the criticality of these effects. There are two levels of a FMECA. A Phase I analysis will result in identification of the component failure modes that result in an unacceptable impact on the system, i.e., unavoidable downtime. These failure modes then become candidates for corrective design actions. A Phase II analysis is generally performed concurrent with release of detail drawings and results in the quantification of failure mode criticality. A Phase I analysis is considered to be of sufficient depth for this report. The "Development Guide for Reliability - Part Two" AMCP 706-196, contains further details on the conduct of Phase II analysis.

A Phase I analysis consists of the following three steps:

(1) Construct a Symbolic Logic Block Diagram. This diagram is a hierarchical structure that indicates the functional relationships between elements of the system. Figure V-1 is a representative example of such a diagram.

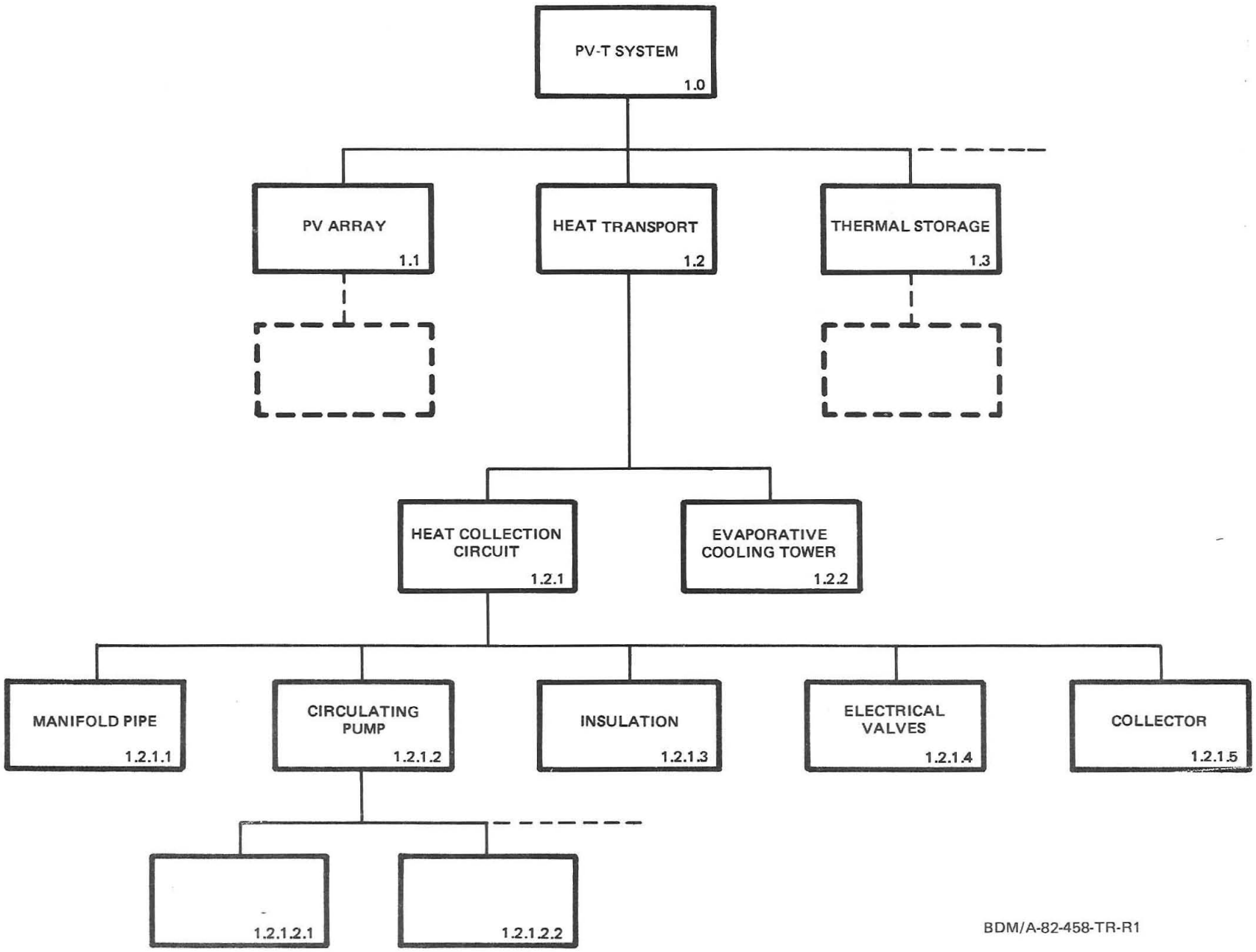

Figure V-1. Symbolic Logic Block Diagram

(2) Conduct failure effects analysis. This step identifies the failure mode of each item at the lowest level of the logic diagram, and indicates the effect of this failure mode on the next higher level. Typical failure modes include open circuits, short circuits, parameter drift, component wear, etc. This process is continued until all branches of the diagram have been exhausted.

(3) Prepare list of critical items. This list is a tabulation of lowest level items whose failure results in possible loss, probable loss, or certain loss of the next higher level item(s) of the diagram. In this context "loss" means that the next higher level item is rendered inoperable or out-of-tolerance. The lowest level items that result in system loss are identified for further assessment.

Once the critical item list has been compiled, design alternatives are generated to reduce or eliminate the problems. For example, these alterations may include use of redundant parts, or parts with different failure characteristics.

Appendix A presents a compilation of failure modes and effects for typical components in PV-T systems. It should be noted that failure effects and their criticality depend upon the system architecture, i.e., arrangement of components, as well as the component hardware characteristics. The Appendix A information should, therefore, be considered as general guidance; that is, to be modified for a particular application. These failure modes reflect current technology items, and are subject to change as new manufacturing processes are employed in fabrication of these PV-T components.

The FMECA is a "bottom up" procedure that begins with the hardware components and works upward through the block diagram to identify the effect of a failure in a hardware component (or two components simultaneously, etc.) on system level performance. A similar procedure called a fault tree starts at the system level and then identifies the next lower level subsytem that can cause the system failure.

Only subsystems (and lower level items) that can cause system failure are included in the diagram. References V-1, V-2, and V-3 provide details of the fault tree approach. Certain conventions have been developed to guide the preparation of a tree. These conventions apply to the identification of the modes or gates in the process. A simple example of a fault tree is shown in figure V-2. The figure shows a functional diagram for a three element system and the corresponding fault tree. In this case if any one of the three elements is failed, then the entire system fails (or-gate logic).

Either the FMECA or fault tre. approach (or both) may be applied in a given PV-T design. The primary value gained through application of either of these graphical/analytical aids is that potential reliability problem areas are systematically identified for designer attention. Subsystems with high failure rates, or severe impacts on the system performance, become candidates for redesign or use of redundant components, etc.

c. Failure Rate Prediction

Quantitative predictions of PV-T system failure rates are required for cost estimating studies and availability assessment. The basic steps in the estimation of logistics failure rates and critical failure rates are similar and the procedure outlined is applicable to either problem. The unique aspects of each are identified at the appropriate points in the narrative.

A seven step procedure is applied to develop failure rate predictions. This procedure has been adopted from reference V-4.

(1) The first step consists of the definition of the system for which the prediction is to be accomplished. This requires the specification of boundaries between items in the system. This step is necessary to ensure that no duplication is possible and that the complete system is considered. It has been found that errors of omission and duplication are frequently the largest sources of inaccuracies in prediction of failure rates.

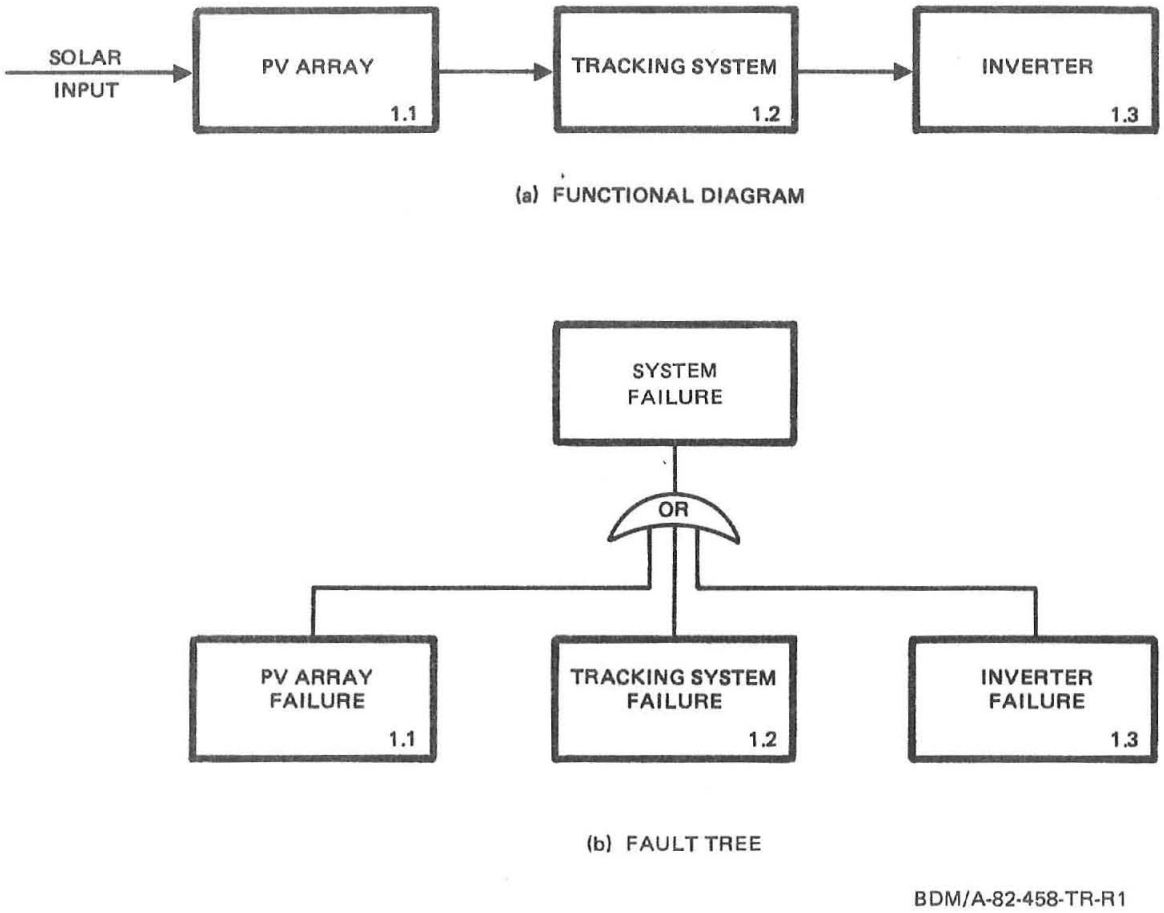

Figure V-2. Example Fault Tree Versus Functional Diagram

(2) Once the system is defined, the definition of failure is specified. Since the definition of failure may include distinctly different criteria, i.e., catastrophic failure versus graceful degradation, two separate analyses may be required. In either case, failures are defined in terms of limits for performance parameter values. For example, a resistor is failed if its resistance value is outside specified limits either due to drift or an open. Additionally, a selection must be made between logistics failure and critical hardware failure.

(3) Define Operating and Maintenance Conditions - Operating conditions include the time that the system is operating versus the time it is dormant. For PV-T systems this definition can be rather complex since certain components (such as a thermal storage unit) may be operating continuously, while the array will be operating approximately ten hours per day depending upon geographic location, time of year, weather, etc.

The environment is also defined in this step. This definition includes both induced and natural factors external to the system such as temperature range, humidity, dust levels, vibration levels, etc. These factors should be recorded even though the prediction methodology may not be fully sensitive to each factor.

Maintenance conditions include the maintenance concept (repair on equipment vs. remove/replace failed items), the preventive maintenance schedule, and similar issues. These maintenance conditions can have an impact on reliability, especially with regard to maintenance induced failures, though the effect may not be readily quantifiable.

(4) Develop Reliabilty Block Diagram - The reliability block diagram indicates the relationship between system components as they affect reliability. Those components for which a failure results in system failure, are shown in series, while redundant

items (whose failure causes system failure only when another component has also failed) are shown in parallel. One assumption inherent in the block diagram is that each block is independent of the others, or that no common cause for failure exists. If common cause failures are an issue, one approach is to consider a single block to represent the commonly effected items. Figure V-3 illustrates the differences between a functional diagram and a reliability block diagram in a simple case. The reliability block diagram is designed to represent the arrangement of subsystems from a reliability viewpoint. This fosters the development of relationships to predict system failure rates (or MTBCF). Thus, the purpose is different from indicating signal flows, or material flows as depicted in functional diagrams.

Separate block diagrams may be required for logistics failure and for critical hardware failure prediction. In general, the logistics failure diagram will consider each component in series, while the critical hardware failure diagram considers redundancy of components as it affects mission success.

The question of how detailed to make the block diagram can be difficult to answer and depends on the specific case. In general, the level of detail should agree with that in the source of failure rate data. Published sources most often report at the pump, motor, valve, etc., level for mechanical items, and IC, diode, capacitor, resistor, etc., for electronic components. Also, each block should be restricted to items with the same work cycle, if possible.

(5) Develop Reliability Formula - The reliability formula is an algebraic expression of the relationship between components shown in the block diagram. Since system failure rates are of interest the formula for a serial arrangement consists of the addition of failure rates as shown below.

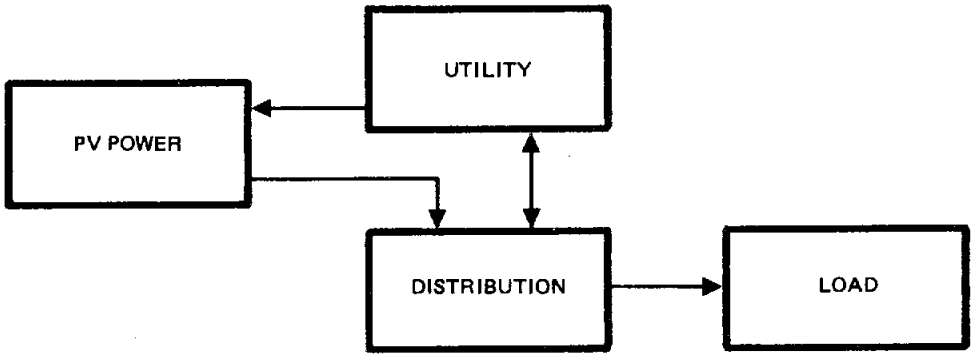

(a) FUNCTIONAL DIAGRAM

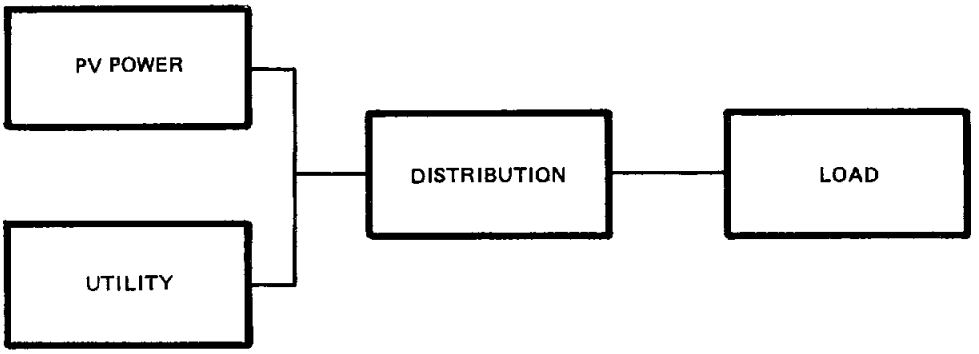

(b) RELIABILITY BLOCK DIAGRAM

BDM/A-82-458-TR-R1

Figure V-3. Reliability Block Diagram Versus Functional Diagram

$$\lambda = \sum_{i=1}^{m} \lambda_i \qquad \text{(Eq. V-1)}$$

where λ_i is the failure rate of the ith element in series (λ_i = 1/MTBCF$_i$ or1/MTBM$_i$ as appropriate). This formula assumes that all failures follow an exponential distribution which is an accepted procedure. This assumption further means that the failure rates are considered to be constant over time. This assumption has been found to be a reasonable approximation for most items, especially electronics. The above equation is especially applicable in the calculation of the logistics failure rate at the system level.

If the parallel/series arrangement of components is important, as in critical failure analyses, the failure rates of serial items are additive. Items in parallel are considered as a block with an aggregate failure rate as in equation V-2:

$$\text{Block failure rate} = \frac{1}{\sum_{i=1}^{m} \frac{1}{\lambda_i}} \qquad \text{(Eq. V-2)}$$

where λ_i is the failure rate of the ith component and there are m components in parallel. The block failure rate is then inserted into the equation that adds all serial rates together.

(6) Estimate Component Failure Rates - This step consists of estimating the failure rates for each block in the reliability diagram. Generic failure rates are provided in appendix A for a variety of items applied in PV-T systems. For logistics reliability estimates the operating and non-operating rates are combined in equation V-3:

$$\lambda = \frac{\lambda_{op}\ t_{op} + \lambda_{no}\ t_{no}}{t_{op} + t_{op}} \qquad \text{(Eq. V-3)}$$

where:

t_{op} = operating time in hours

λ_{no} = non-operating failure rate in failures per hour

t_{no} = non-operating time in hours

λ_{op} = operating failure rate in failures per hour

The non-operating time is the elapsed time in hours during which a component or equipment is connected to the system in its normal configuration, but is not experiencing the electrical, mechanical or thermal stresses inherent in the designed operation of that component or equipment. It is often an engineering judgment whether a given system is operating or not, expecially when a portion of the equipment is engaged.

The failure rates in Appendix A have been normalized to reflect standard operating environments. For example, the CRT, processor, and plotter rates assume temperature controlled environment, while PV cell, piping, tracking systems, etc. rates assume stationary external environment (dust, humidity, temperature cycling).

For ease of presentation, only point estimates of generic failure rates are contained in appendix A. Actually, failure rates are subject to wide variation depending upon manufacturer, component size, etc. Variations in failure rates by a factor of two or three above the mean, (i.e., $1/3\lambda$ to 3λ) are not uncommon. Several compilations of failure rates provide high and low values as well as the mean.

In the case where a component is not included in appendix A, the component may be similar to one tabulated in the appendix and the data for the analogous system may be used.

A second possibility is to consult published data sources such as: Military Handbook 217C (for electronics components); The Nonelectric Reliability Notebook (AD/A-005-657) and updates; The Mechanical Design and Systems Handbook (Chapter 18); or the Failure Rate Data (FARADA), published by the Government-Industry Data Exchange Program (GIDEP). Extreme care should be taken in using the data from these sources. The type of failures included in the data (tolerance or catastrophic) should be determined, as well as the time base (operating hours or operating plus non-operating) for the calculations. Environmental adjustments, usage factors and modifications for failure definition may be required to make these data useful for PV-T predictions.

(7) Calculate System Reliability - The final step consists of the calculation of system-level reliability based on the reliability function and the input failure rate data. The basic failure data are input to the equations, the model is exercised, and the system level estimate thereby obtained.

3. Maintainability

a. General

Maintainability is defined as the probability that a failed system is restored to an operable condition within a specified period of time.

As with reliability, maintainability has qualitative and quantitative aspects. The qualitative aspect concerns the design of the system for such things as safety, ease of access to failed items, and minimization of requirements for special tools and test equipment. The quantitative elements include estimates of elapsed times to accomplish repairs and inspections, maintenance crew sizes, preventive maintenance intervals, materials/component condemnation rates, and repair parts requirements.

Maintenance can also be divided into preventive maintenance, consisting of those actions necessary to retain an operating

item in an operating condition, and corrective maintenance, actions necesssary to restore a non-operating item to an operating condition.

The unique operating profile of a PV-T system affects maintainability in the same manner as discussed previously as a factor of logistical reliability. That is, the cyclic operating mode wherein many critical components do not operate when there is no solar flux (e.g., nighttime). Thus periodic preventive maintenance can often be scheduled so that it does not adversely affect availability.

The following paragraphs discuss these issues in greater detail.

b. Qualitative Maintainability

Systems design includes safety, simplicity, modularity, and ease of access. For example, improper design is the major cause of master control subsystem problems due primarily to the fact that solar heating and cooling control systems are more complex than conventional HVAC control systems. This complexity is required because the operating modes depend on variable insolation rates, intermittent demands from collectors, thermal storage and utility interface, control decisions based on changing temperature differentials, and requirements to integrate auxiliary equipment into the system operation. Major design related problems are: (1) control system enters an improper operating mode (e.g., auxilliary and solar heating systems operate simultaneously), (2) poor control sensor location, and (3) defective components. The latter item is dependent on quality of materials as well as design. The immaturity of PV-T technology means that much needs to be learned about environmental degradation of sensors, heat transport subsystems joint design and other PV-T components.

A number of guidelines and techniques have been developed to promote qualitative maintenance. It has proven difficult to evaluate the impact of incorporating these guidelines in terms of reduced support cost or improved availability. Nevertheless, these guidelines should be borne in mind during system design and followed to the extent practicable. A checklist of qualitative maintainability factors is furnished

below. The factors considered in the list are representative, but by no means exhaustive.

(1) Reduce Maintenance Complexity

(a) Complexity is reduced through provision of sufficient accessibility, work space and work clearance.

(b) Complexity is reduced by use of interchangeable parts, materials, components.

(c) Complexity is reduced by limiting the number of tools, accessories, and test equipment.

(2) Reduce the Need for Design Dictated Maintenance Activities.

(a) Incorporation of corrosion prevention/control techniques.

(b) Use of components requiring minimal preventive maintenance and calibration.

(3) Reduce Maintenance Downtime

(a) Provision of test points for positive fault detection and isolation.

(b) Provision of features to permit positive verification of repairs.

(c) Modularity to permit easy removal and replacement of failed items.

(d) Provision of features for system inspection and lubrication.

(4) Reduce Possibilties for Maintenance Errors

(a) Design to eliminate the possibility of incorrect connection, assembly, or installation, e.g., electrical leads that could be reversed, fittings that could be attached to the wrong connection.

(b) Design to reduce awkward or tedious job elements.

(c) Design to reduce ambiguity in maintenance procedures and data.

(5) Limit Maintenance Skill Requirements

(a) Clearly identify parts, test points, etc.

(b) Incorporate easy handling and transportability features (e.g., handles, weight).

(c) Minimize requirements for soldering.

(6) Reduce Maintenance Hazards

(a) Eliminate sharp edges.

(b) Eliminate blind spots.

(c) Reduce use of hazardous materials (fluids).

(d) Eliminate exposed electrical contacts.

(e) Clearly identify areas of high voltages and temperatures.

(7) Consider Effects of Climatic Extremes

(a) Eliminate requirements for extreme dexterity (unprotected hands) in cold environments.

The check list above provides an initial indication of maintainability issues to be cognizant of during PV-T system design. More extended treatments of these issues and potential design techniques to address the issues can be found in: The Army Material Command Pamphlet, "Maintainability Guide for Design", AMCP 706-134; The Air Force Systems Command Design Manual "Maintainability"; the text Maintainability Principles and Practices by B. S. Blanchard and E. E. Lowery; or the text Applied Maintainability by D. Cunningham and W. Cox.

c. Quantitative Maintainability

Quantitative factors tend to focus on people and procedures. For example, the second largest cause of control problems is inadequate sensor calibration. This problem arises because of the relatively small temperature differences that have to be detected for precise control. Unless sensors are properly calibrated, appropriate control decisions cannot be made. Similarly, a common deficiency in heat transport subsystems is fluid loss through improper interconnection of tubes and pipes. The consequences include leaking fluid damage to adjoining materials, destruction of insulation, and dissipation of collected energy.

Prediction of maintainability parameters are a useful aid in the design of PV-T systems. These predictions may be used to identify system components that cause excessive downtime due to difficult, time consuming, or frequent repair actions. This downtime will adversely affect system availability, and consequently system performance, and will also result in increased system life cycle costs. The quantitative maintainability measures of primary importance are mean-time-to-repair (MTTR), mean-manhours-to-repair (MMTR), and mean-time-between-preventive-maintenance (MTBPM).

(1) Mean-Time-To-Repair (MTTR)

MTTR is defined as the mean elapsed time (in hours) to restore the system or component to an operable condition. This measure includes the times to locate the faulty item, remove and replace that item, and to verify system operation. For this discussion, MTTR will refer to only the direct on-equipment repair hours. Excluded from this measure are hours expended in repair of the failed item at a vendor or in a shop facility. If the maintenance concept calls for replacement of failed items such as a pump or valve with a serviceable unit from an on-site supply system, MTTR will be relatively short. Alternatively, if the maintenance concept calls for repair of the component (e.g., pump) on the equipment (e.g., replacement of seals, bearings, etc.), MTTR will tend to be long. The system maintenance concept is, therefore, an important issue to be addressed during design studies, as both system cost and availability can be significantly effected.

The MTTR measure is determined only for critical failures (those resulting in downtime during periods of useable insolation). MTTR is calculated at the same level as the individual blocks of the critical hardware reliability block diagram, with additional estimates for preventive maintenance/actions that must be performed during periods of otherwise useful insolation. MTTR is the appropriate measure for input to hardware availability analyses as discussed later in this chapter. It includes only the direct hours for restoration and excludes time spent in travel, time spent awaiting a spare component, or time spent waiting for a piece of test equipment.

MTTR is a function of the system architecture and location of the components. Appendix A provides estimates of MTTR for typical components in PV-T systems. These data assume that the components are readily accessible for remove/replace actions, that skilled personnel perform the repair, and that troubleshooting requirements are minimal. As a consequence, that data should be regarded as initial guidelines to be supplemented with better data as the design matures. Further information on techniques for estimating MTTR can be found in MIL-HDBK-472, "Maintainability Prediction." Four separate estimating techniques are described in that source. These techniques are applicable at different points in the design process depending on the level of detail available. If the MIL HDBK is not readily available, the data in Appendix A may be used as a basis for estimating by analogy, supplemented with engineering judgment and familiarity with the system design.

(2) Mean-Manhours-To-Repair (MMTR)

MMTR is the second quantitative maintainability parameter of interest. This includes the crew size required for each repair, as well as the elapsed time. As with MTTR, MMTR is based on direct manhours and excludes time for travel, or awaiting spares. MMTR is calculated for all maintenance actions (not just those critical failures/actions) and is the appropriate measure for input to life cycle cost analyses. Estimates of MMTR are generated for each block in the logistics reliability block diagram, and for any preventive maintenance event not included in the reliability analysis (e.g., washing the array, lubrication of mechanical elements, inspection of hoses, etc.). MMTR is also a very strong function of the system maintenance concept. In fact, the maintenance concept has a stronger influence on MMTR than the usual design features that promote easy access, quick disconnects, or rapid verification of system operation. Appendix A provides MMTR values for typical PV-T components for use in initial design analyses. These data should be revised as a system design matures.

(3) Mean-Time-Between-Preventive-Maintenance (MTBPM)

MTBPM measures the interval of time (in elapsed hours or days) between preventive maintenance actions. Figure V-4 presents MTBPM

- Daily
  - Before Operation/Daily

Electrical	- Fuses/Breakers Operation
Thermal	- Coolant Present/Levels
Mechanical	- Lubrication
Other	- Visual Inspection
	- Hydraulic/Pneumatic System
	- Flexible Hoses

  - During Operation - No Leakage - Tracking - Proper Temperatures
  - After Operation - Proper Stowage - No Leakage of Coolant, Hydraulic Fluid, Oil/Grease
- Weekly

  Test for Automatic Stow

  Lubrication
- Monthly
  - Cleaning of Reflection/Receiver Surfaces (may be more often depending on local conditions such as recent wind or precipitation, and local pollution. Also would depend on nearby surface such as dusty ground, array placement or installation on a tar covered roof that may outgas and condense on collector surfaces while in the stowed position).
  - Concentration of Ethylene Glycol-Water Mixture
- Semi-Annual
  - General Clean Up of Nearby Area
  - Visual Check of Ground Connections for Corrosion Evidence
- Annual
  - Ground Connection Electrical continuity Test
- Beyond
  - Every 2 Years - Replacement of Ethylene Glycol Heat Transfer Fluid

BDM/A-82-458-TR-R1

Figure V-4. Preventive Maintenance Intervals

data that is representative of current PV system operations. The estimates of MTBPM are combined with projected values of MMTR for the corresponding action for input to life cycle cost analyses and assessments of manpower requirements.

4. Availability

Availability is defined as the probability that at any point in time the system is operating satisfactorily or is ready to be placed in operation on demand under stated conditions.

In this report the terms "availability" and "operational readiness" are assumed to be equivalent. The measure of availability may be stated in terms of inherent availability or operational availability. Inherent availability results from including only the elapsed time to restore the system in the estimate of downtime. This measure excludes the effects of travel delays, lack of spare parts, and start-up time. As a consequence, inherent availability overstates true system availability to a considerable extent and is therefore not a useful measure for trade-off studies that include estimates of the cost of downtime. Operational availability (which includes logistic delays) is a more reasonable measure for use in design studies that incorporate a dollar cost penalty for downtime. Operational availability will be the parameter of interest in the remainder of this chapter.

Availability is an aggregated measure that combines reliability and maintainability with logistics supportability and administrative factors. This is most readily seen from the mathematical expression for operational availability, A_o:

$$A_o = \frac{MTBCF}{MTBCF + (MDT)\ (R)} \qquad \text{(Eq. V-4)}$$

MTBCF is defined as the mean-time-between critical failure and is equal to $1/\lambda_c$, where λ_c is the critical failure rate.

MDT is defined to be equal to the sum of MTTR and any delays associated with travel, awaiting parts, tools, etc., and bringing the

system back on-line after repair has been accomplished. R is equal to the ratio of the time during which the solar source is available to total time. It accounts for darkness, etc., when maintenance can be performed without affecting system output. This is a first order approximation and OR1. The value lies between .3 and .6 depending upon geographic location, and similar factors, and represents a long-term average value.

Availability is a function of critical hardware failures only, and, therefore, excludes the impact of failures for which maintenance may be deferred. The MTTR portion of mean downtime is estimated for critical failures only. The other contributors to MDT (e.g., travel delays) are a function of the location of the system, the maintenance concept (e.g., vendor repair versus on-site repair crews, repair-in place versus remove/replace of failed items, etc.), and a number of related concerns.

The procedure for determining availability is similar to that used in reliability predictions. The first step is to construct an availability block diagram for the system. This diagram is the direct analog of the system reliability diagram, which can often be used with no modification. The guidelines described for the reliability diagram are applicable for the availability diagram (level of detail, same duty cycle for all items in a given block, etc.). The next step is the formulation of the system availability function that expressed the effect of system level availability due to components availabilities. For a system of n components in series, the formula becomes:

$$A = \prod_{i=1}^{n} A_i \qquad \text{(Eq. V-5)}$$

where:

$$A_i = \frac{MTBCF_i}{MTBCF_i + (R)\ MDT_i} \qquad \text{(Eq. V-6)}$$

is the availability of component i. For n items in a parallel arrangement, so that all items must be simultaneously unavailable for the system to be unavailable, the formula is:

$$A = 1 - \prod_{i=1}^{n} (1-A_i) \qquad \text{(Eq. V-7)}$$

where A_i is as before. These relationships assume independence between system component availabilities, which is reasonable in most applications. In cases where there are common cause failures between components a more complicated approach would be required, based on Markov chain models or fault tree analysis (ref. V-1, V-3).

The next step in the availability projection is to estimate the component availabilities from equation V-6. The values for $MTBCF_i$ and MDT_i are based on the reliability and maintainability assessments discussed earlier in this chapter. The maintainability parameter, $MTTR_i$, estimates must be supplemented with delay estimates to arrive at MDT_i. The primary delay times are travel times for repair crews, and the time to bring the system to operating status after repair. Engineering analyses and estimates are the primary means for generating these delay times.

The component availabilities are finally combined through the system availability function to produce the system level availability estimate.

D. RAM TRADE-OFF ANALYSIS

To illustrate the manner in which RAM considerations enter the PV-T design process, an example trade-off analysis is described. This trade study examines the payoffs and costs associated with adding a redundant pump to a heat transport system. For the sake of illustration, a number of simplifications will be made. The costs will include only the incremental outlays associated with addition of the pump. The pump system

will be assumed to operate 24 hours per day, and both pumps in the redundant configuration will be operated simultaneously. If one pump fails, the other is assumed capable of immediately maintaining system requirements. It will be further assumed that the failure rate for each pump is the same for both normal and stressed operation. The question to be addressed is whether the redundant pump improves availability (and therefore total output) to a sufficient extent to compensate for the added costs to the system.

A system lifetime of 20 years will be assumed. Taxes will be assumed to be zero and the analysis will consider undiscounted costs only. Inflation will be assumed to be zero. The maintenance concept will assume an on-site repair/sparing capability to minimize system downtime.

Pump System Data:

Installed unit cost = $1000

Cost per repair action = $400 (includes shop repair of failed components, and both labor and materials costs)

MTTR = 2 hours (Appendix A)

MDT = 10 hours (=MTTR plus start-up, travel, and delays)

System availability (excluding the pump(s)) = .95

Pump failure rate = 150 failures per million hours

= 6667 hour MTBCF = MTBM (Appendix A)

Yearly operations cost for pump = $100 (utilities, inspection, lubrication, etc.). Utilities are a function of use rates, pump horsepower, and pump efficiency that must be estimated for the system.

R = 1.0 (no free time for repair of a pump)

The first step is to calculate the improvement in availability for the redundant pump system.

$$\text{Single pump system availability} = .95 \times \frac{\text{MTBCF}}{\text{MTBCF} + (R)(\text{MDT})} \qquad \text{(Eq. V-8)}$$

$$= (.95)\,\frac{6667}{6667 + 10} = (.95)(.9985) = .9486$$

Redundant pump system availability:

$$(.95)(1 - (1 - A_1)(1 - A_2)) = (.95)(1 - (1 - .9985)(1 - .9985))$$

$$= .95(1 - (.0015)(.0015)) \quad .95(1) = .95$$

The improvement in availability is .95 - .9586 = <u>.0014</u> (Eq. V-9)

.0014 x 8760 hours/year = 12 hours/year or
240 hours in the system lifetime. (Eq. V-10)

The second step requires the estimation of the added costs for the redundant pump over the system life. This cost is the sum of the installed cost, the total unscheduled maintenance costs, utilities, and scheduled maintenance costs.

Installed cost = $1000

$$\text{Unscheduled Maintenance Costs} = \frac{\text{20 years x 8760 hours per year}}{\text{6667 hours between maintenance}}$$

x $400/action = $10,500

Utilities/Scheduled Maintenance = 20 years x $100/year = $2000
Total cost is thus $1000 + $10,500 + $2000 = $13,500

Thus, it is seen that the addition of a redundant pump will improve availability by 240 hours over the system life for a cost of $13,500. The redundant pump is beneficial if the cost per lost hour is greater than approximately $56 (= $\frac{1350}{240}$)

The cost per lost hour is a function of the product or output of the PV-T system, or rather, the process it is designed to support. This cost will be different for each PV-T system and will depend on the price of alternate energy sources prevailing at the location in question.

REFERENCES

V-1. Development Guide for Reliability Part Two Design for Reliability, Headquarters, U.S. Army Material Command, AMCP 706-196, January 1976.

V-2. Stenlier, L. H. "Reliability Considerations in the Design of Solar Photovoltaic Power Systems," Solar Cells Vol. 3, 1981, pp. 269-295.

V-3. Stenlier, L. H., W. R. Huss, and M. S. Bridgman, "Development of Reliability - Economics Assessment Models for Photovoltaic Power Systems: Vol. I." Draft Final Report, Battelle Columbus Division, 1982.

V-4. Von Alven, W. H. (ed), Reliability Engineering, Prentice Hall, Inc. 1964.

APPENDIX A

This appendix contains reliability and maintainability data for use in initial system design studies. The data are presented in tabular form, and arranged in terms of generic PV-T subsystems such as system control, thermal storage, etc. Because of the considerable variation in PV-T designs the data correspond to an equipment level and, in certain cases, an even finer level of detail. This approach is intended to increase the utility of the data, since the subsystem level is too aggregated to be sensitive to design alternatives.

Failure rate data are summarized in terms of failures per million hours for both operating and non-operating conditions. These data have been taken from a variety of sources (listed at the end of this section) and adjusted to preserve consistency. The data reflect an operational environment typical of the southwestern United States. The data also assume the equipment have been fabricated according to good commercial quality. These data include both catastrophic and out-of-tolerance failures as discussed in section C. Modifications to the data would be necessary to reflect more extreme environmental conditions (e.g. arctic) or use of military specification parts. Electronics parts data assumes a .5 stress ratio and ambient temperatures of 25°C.

The maintainability data (MTTR) represent elapsed time (in hours) to perform on-equipment repair tasks only. The data exclude travel times, and time awaiting tools, spares, or system start-up. These factors are typically very significant and highly site-specific. The data assume that the components are readily accessible, and that maintenance is performed by skilled personnel. MMTR estimates include both on and off-equipment repair manhours, but do not include travel times, and delays.

The reliability data include only the times between unscheduled tasks. Preventive maintenance frequency data are exhibited in figure V-4.

Notes are provided in the last column when the data are variable (between sources), or when special caveats appear warranted. In certain

cases the distinction between operating and non-operating failure could not be accomplished. In these cases, the data are presented in terms of clock hours, and assume a nominal operating cycle.

Failure modes refer to the primary mode(s) by which an item may fail. Failure effects are highly design specific. Consequently, less data can be provided in a generic description. The effects outlined in the table assume that the component is in a serial architecture. The effect describes the resultant impact on system performance. For initial assessments it is often assumed that the failure of an item (at any level of indenture) results in system failure.

This assumption results in an understatement of reliability (or availability), but may be useful in early design analysis. As the design matures, the actual architecture of the system should be incorporated into the assessment.

Sources of reliability data included:

1. Handbook of Electronic Systems Design, Charles Harper (ed). McGraw-Hill.
2. Mechanical Design and Systems Handbook, H. Rathbart (ed). McGraw-Hill.
3. Computer System Reliability, Ray Longbettom, John wiley and Sons.
4. Factors, Formulas and Structures for Life Cycle Costing, M.E. Earles. Eddins-Earles.
5. Development of Reliability-Economics Assessment Models for Photovoltaic Power Systems, Vol. I, II (Draft), L.E. Stember, et.al.
6. Missile Materiel Reliability Prediction Handbooks, Parts Current Prediction, D.F. Malik, et al., AD-A026-104
7. Dormant Operating and Storage Effects on Electronic Equipment and Part Reliability, D. F. Cottrell, et al.
8. Effects of Dormancy on Nonelectronic Components and Materials, D.F. Cottrell, et al.
9. Handbook of Electronic Systems Design, Charles Harper, (ed.), McGraw-Hill.
10. Mechanical Design and Systems Handbook, Harold Rothbart, McGraw-Hill, 1964.
11. Computer System Reliability, Ray Longbottom, John Wiley and Sons, 1980.
12. Factors, Formulas, and Structures for Life Cycle costing, Mary Eddis Earles, Eddis-Earles Publishing, 1981.
13. Stember, Lawrence E. et. al., "Development of Reliability-Economics Assessment Models for Photovoltaic Power Systems," Vol. I, Vol. II (Draft), Battelle Columbus Laboratories, 1982.
14. "Missile Materiel Reliability Prediction Handbook," U.S. Army MIRADCOM, Redstone Arsenal, AL, Report LC-78-1, February 1978.
15. Cottrell, D.F., "Dormant Operating and Storage Effects on Electronic Equipment and Part Reliability" Martin-Marietta, Orlando, Florida, Tech. Report No. RAUC-TR-67-307, July 1967.

16. "Effects of Dormancy of Non-electronic Components and Materials," Martin-Marietta Aerospace, RADC-TR-74-269, Rome Air Development Center, 1974.

Sources of maintainability data included:

1. Factors, Formulas, and Structures for Life Cycle Costing, M.E. Earles.
2. Military Handbook 472. Maintainability Prediction.
3. BDM Corporate files.

ITEM NAME	FAILURE MODE	FAILURE EFFECT	FAILURE RATE $\lambda op/\lambda no$ in FAILURES PER 10^6 HOURS	MTTR/MMTR IN HOURS	NOTES
1.0 System Control					
Digital Interface		no control or incorrect control	.5/.017	1/4	Assumes Controlled Environment
Real Time Clock		no control or incorrect control	.3/.01	1/4	
Relay Multiplexer		no control or incorrect control	.2/.007	1/4	
Processor	Many	no control or incorrect control	50/1.67	1/6	Based on HP 85
Storage (disc)	Many	no control or incorrect control	120/4.0	1/6	Floppy disc system assumed
CRT	Many		15/.3	1/4	
Printer	Many		54/1.8	1/6	
Plotter	Many		20/.67	1/6	
A/D Converter	Many	no control or incorrect control	.02/.0007	1/4	Components in the data acquisition system
Voltmeter	Many	no control or incorrect control	.5/.01	1/4	Components in the data acquisition system
Counter		no control or incorrect control	.6/.02	1/4	Components in the data acquisition system
Thermocouple		no control or incorrect control	6.2/1.2	1/3	Components in the data acquisition system
Relay	Contact failure open coil	no control or incorrect control	.17/.03	1/3	Components in the data acquisition system
Position Sensor		no control or incorrect control	.1/.01	1/3	Components in the data acquisition system
*Pyrometer		no control or incorrect control	124/41	1/4	Components in the data acquisition system
*Current Source		no control or incorrect control	.2/.003	1/4	Components in the data acquisition system
*Voltage Source		no control or incorrect control	.2/.003	1/4	Components in the data acquisition system
2.0 Thermal Storage					
Storage Tank	Leaks		1.5/.10	2/5	
Heat Exchanger	Leak, systems		150/1.5	2/5	
Hose	Material deterioration		20/2	.5/.5	
	Fitting failure corrosion, systems				
Pump (electric)	Mechanical failure		150/3	2/5	
Valve	Valve seat				
General	Detrioration		6.6/.017	1/4	
Check	Poppets sticking open or closed		3/.06	1/4	
Shut-off			14.2/.28	1/4	
Solenoid	Leaks		2.4/.05	1/4	
Hydraulic			2.3/.05	1/4	
Insulation	Degradation		.5/.01	3/6	MMTR assumes discard of degraded materials
3.0 Receiver Tube					
3.01 Tube	Corrosion, rupture, deterioration		20/1	1/2	
3.02 Flexhose	Deterioration, wear, mechanical failure		40/2	.5/2	
3.03 Thermal Exp. Bellows			20/.01	1/2	

ITEM NAME	FAILURE MODE	FAILURE EFFECT	FAILURE RATE $\lambda op/\lambda no$ in FAILURES PER 10^6 HOURS	MTTR/MMTR IN HOURS	NOTES
4.0 Power Conversion					
4.01 Wiring/ switching (each assembly)	Break, corrosion				λop - based on clock hours from reference 5 of reliability sources
4.02 Inverter	Failure, degrade		114	2/5	λop - based on clock hours from reference 5
4.021 Thyristor	Open		.35/.01	2/2	Component data are given for build up of an inverter
4.022 Inductor	Open, short		.02/.0007	2/2	
4.023 Capacitor (fixed film)	Open, degrade Short circuit		.01/.0003	2/2 2/2	Failure rate due to uncertainty of present data
4.024 Fuse	Open		.1/.003	2/2	
4.025 Diode	Short, open intermittent		.35/.01	2/2	Maintenance concept assumes discard of components upon failure
4.026 Resistor (fixed composition)	Change of value, open		.13/.004	2/2	Resistor failure rates are highly variable depending on type and quality, and environment
4.027 Pulse Width Modulator	degrade, failure		.3/.001	2/2	
4.028 Power Transistor	Open terminals, Collector/lease leakage		.6/.002	2/2	MMTR assumes discard of failed item, so manhours refer to remove/replace only
3 Pin Regulator	Degrade, failure		.1/.003	2/2	MMTR assumes discard of failed item, so manhours refer to remove/replace only
Power Supply	Degrade, failure		.02/.0007	2/2	MMTR assumes discard of failed item, so manhours refer to remove/replace only
IC, Multiplier	Failure		.1/.003	2/2	MMTR assumes discard of failed item, so manhours refer to remove/replace only
IC, Comparator	Failure		.1/.003	2/2	MMTR assumes discard of failed item, so manhours refer to remove/replace only
IC, Digital Gate	Failure		.1/.003	2/2	MMTR assumes discard of failed item, so manhours refer to remove/replace only
Signal Transistor	Open Terminals High Collector/ Lease Leakage Current		.6/.002	2/2 2/2 2/2	MMTR assumes discard of failed item, so manhours refer to remove/replace only
5.0 Distribution System			.1/.003	1/1	
Power Switch			.7/.023	1/2	MMTR data assumes remove/ replace of item, and discard of failed unit
Fuse	Open		2.1/.07	1/2	
Circuit Breaker	Mechanical Failure of Tripping Device, Open		1.3/.01	1/2	

ITEM NAME	FAILURE MODE	FAILURE EFFECT	FAILURE RATE $\lambda op/\lambda no$ in FAILURES PER 10^6 HOURS	MTTR/MMTR IN HOURS	NOTES
6.0 Array					
Cell	Degrade, Fail	Degradation of output	.1/.003	1/1	Degradation of output assumes use of blocking divider to prevent reverse bias
Zener Diode	Short Circuit, Open Circuit, Intermittent		2/.006	1/1	
Silicon Diode	Short Circuit, Open Circuit, Intermittent		2/.006	1/1	MMTR is based on discard of failed items
Thyristor			.4/.013	1/1	
7.0 Heat Transport					
Fan			2/.006	2/4	
Valves (see Thermal Storage)			--	--	
Heat Exchanger (see Thermal Storage)	Leak, Rupture		--	--	
Fittings	Mechanical Failure, Leaks		1/.002	1/2	
Piping	Corrosion, Rupture		0.4/.02	1/2	
Seals	Material Deterioration		7/.014	1/2	
8.0 Concentrator					
Lens			17	1/3	λop based on clock hours from ref 5 of reliability sources
Tracking Unit	Poor Tracking, No Tracking		17	2/6	λop based on clock hours from ref 5 of reliability sources
Servoactuator			20/.4		
Motor (electric)	Winding Failure, Bearing Failure		2/.04 -3/.06	1/4 1/4	
Structure (section)	Failure		1/1	1/2	
Actuator (hydraulic)	Failure		50/1	1/4	
9.0 Miscellaneous					
Temp Sensor			33/1.1	1/3	
Gears			12/.0024	2/4	
Counterweight (small)			.1/.01	1/2	
Brackets			.1/.005	1/2	
Regulator			21/.41	1/2	
General Item (each)			__/05	1/2	

CHAPTER VI

STRUCTURES AND FOUNDATIONS TO SUPPORT PHOTOVOLTAIC-THERMAL (PV-T) SINGLE AND TWO-AXIS TRACKING SYSTEMS

A. INTRODUCTION

PV-T systems are available in several different configurations, three of which are shown in figures VI-1, 2 and 3. The linear parabolic trough (figure VI-1) is part of a single axis tracking system which has been installed at ground level and on rooftops at various sites. The linear parabolic troughs (LPT) in use on the roof of the BDM building in Albuquerque, New Mexico, were produced by SKI Systems and have a 2.13 m (7-foot) aperture and are 6.1 m (20-ft) in length. The Accurex troughs installed at the Wilcox Hospital in Hawaii are 1.83 x 3.05 m (6 x 10-ft). Both companies are considering a variety of sites. Figure VI-2 shows the two-axis tracking linear focus Fresnel (LFF) system developed by E-Systems of Dallas-Fort Worth, Texas. One of their systems will soon be installed in a test field at Sandia National Laboratories (SNL) in Albuquerque, New Mexico. The Martin-Marietta two-axis tracking system, which uses point focus Fresnel (PFF) lens, is shown in figure VI-3. One of Martin-Marietta's PV-T configurations (first generation) is installed in a test field at SNL. All of these systems (i.e., the LPT, the LFF, and the PFF), whether single or two-axis tracking, typically require a large number of supporting pylons, and either foundation or roof support elements of simple repetitive configurations. A significant part, approximately 10 percent, of the cost of any PV-T installation goes into these pylons and roof supports or foundations (ref. VI-4).

The LPT, the LFF, and the PFF systems are all subjected to gravity (dead loads), wind, and potentially earthquake, snow, rain, hail, and ice loads, which must all be evaluated to assure the adequate design of structural supports. Usually the loading cases controlling design are combinations involving wind and dead loads (ref. VI-5). Primary emphasis in this discussion will be on the determination of wind loads by use of applicable theory and the results of wind tunnel tests.

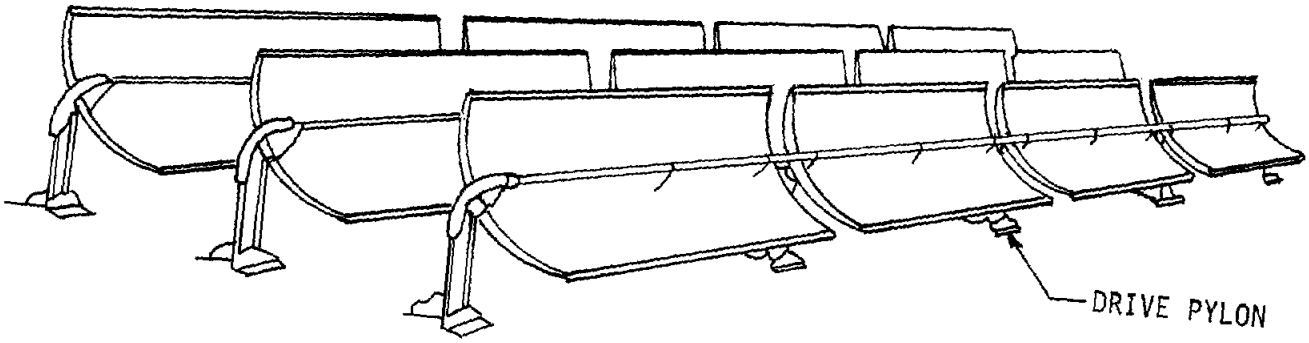

BDM/A-82-468-TR-R1

Figure VI-1. Linear Parabolic Trough Collectors (from Reed, Reference VI-1)

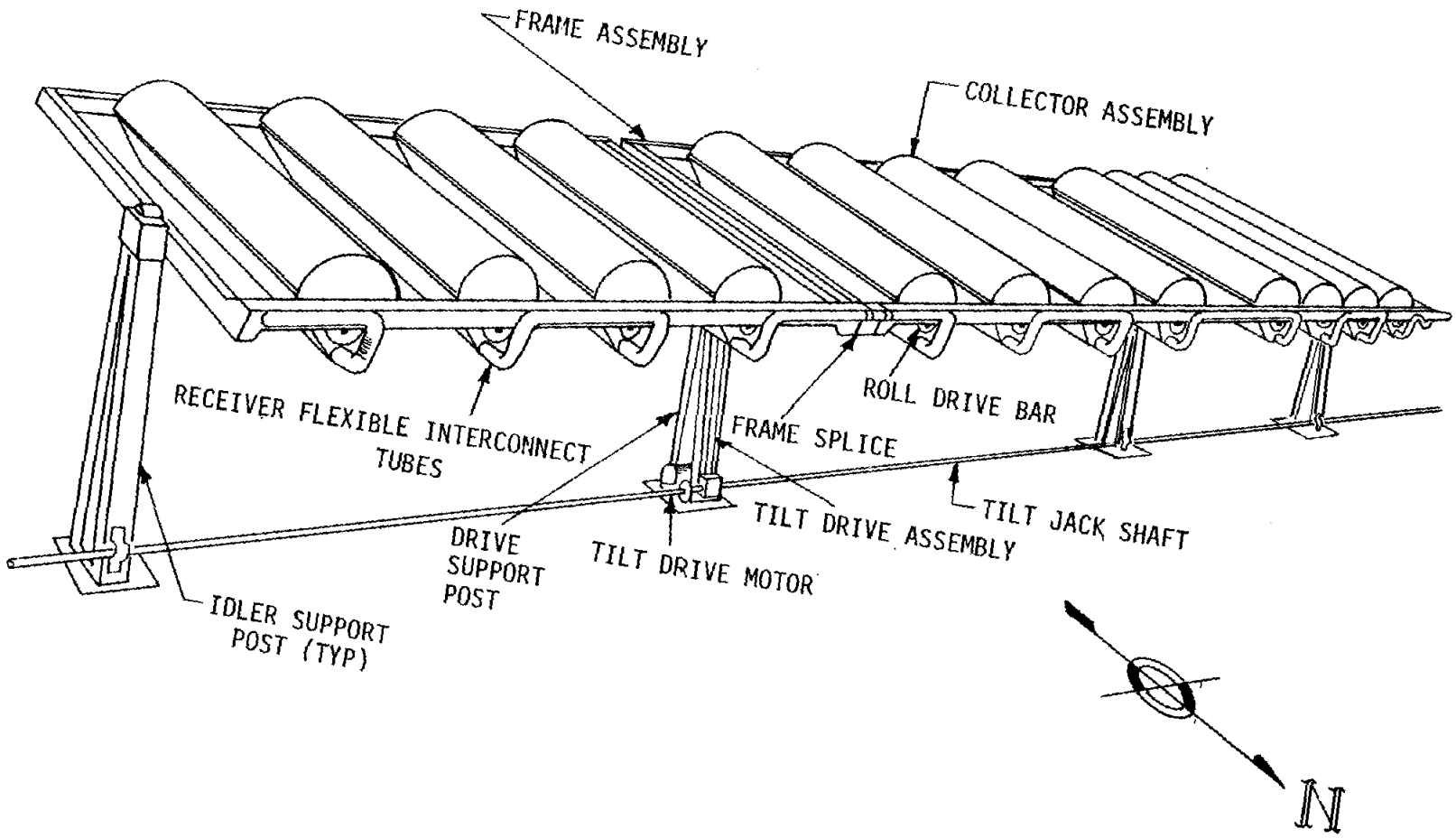

Figure VI-2. Four-Module Fresnel Lens Array (from O'Neill, Reference VI-2)

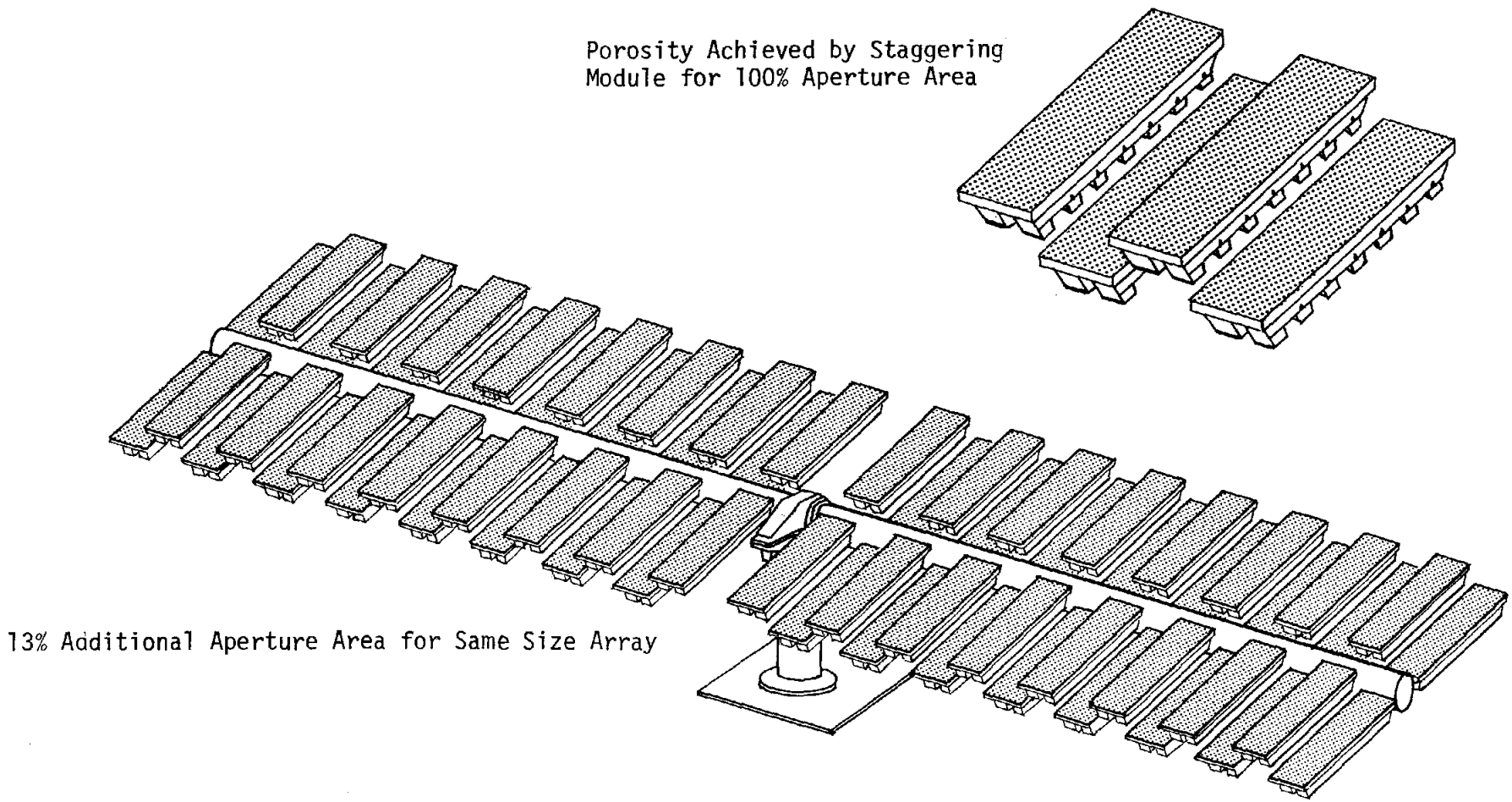

BDM/A-82-458-TR-R1

Figure VI-3. Martin Marietta Second Generation Array
(from Broadbent, Reference VI-3)

The earthquake, snow, rain, hail, and ice loads must be considered also, but they will usually be less significant in design than wind and gravity loadings. In such designs, the relevant provisions of local and national codes must be considered (e.g., ANSI A58.1-1972, ref. VI-6 and its upcoming revision (1982), ref. VI-7). When applied, these codes should take into account applicable wind tunnel data and avoid unnecessary conservatism which can lead to overdesign and unwarranted cost penalties.

Wind loadings must be accounted for and funds budgeted for the foundations and structures required to supply the needed strength, stiffness, and reliability for system performance. Structural and foundation requirements must enter into solar energy system requirements determination at the beginning of concept definition if a technically and economically viable PV-T design is to be assured. Definition of structural and foundation requirements calls for expertise in a number of disciplines such as aerodynamics, structural mechanics and structural dynamics, and geotechnical engineering. The experienced project manager will seek the required expertise from these disciplines to reach a balanced approach to PV-T systems design.

B. ISSUES ASSOCIATED WITH STRUCTURES AND FOUNDATIONS FOR PV-T SYSTEMS

As was previously mentioned, a PV-T system may be mounted either on the ground or on the roof of a structure. The industry has had experience with both types of mountings.

Figure VI-4 illustrates the method of determining whether to use a ground-mounted or a roof-mounted system. Early in concept definition (see the left block of figure VI-4), the decision will be made as to which of the systems illustrated in figures VI-1, 2, and 3 will be used. If the system illustrated in figure VI-3 (i.e., the PFF) is used, it would probably be advisable to place the system on the ground because the relatively high base bending moments will require considerable stiffness and strong roof structure. The systems in figures VI-1 and VI-2 (i.e.,

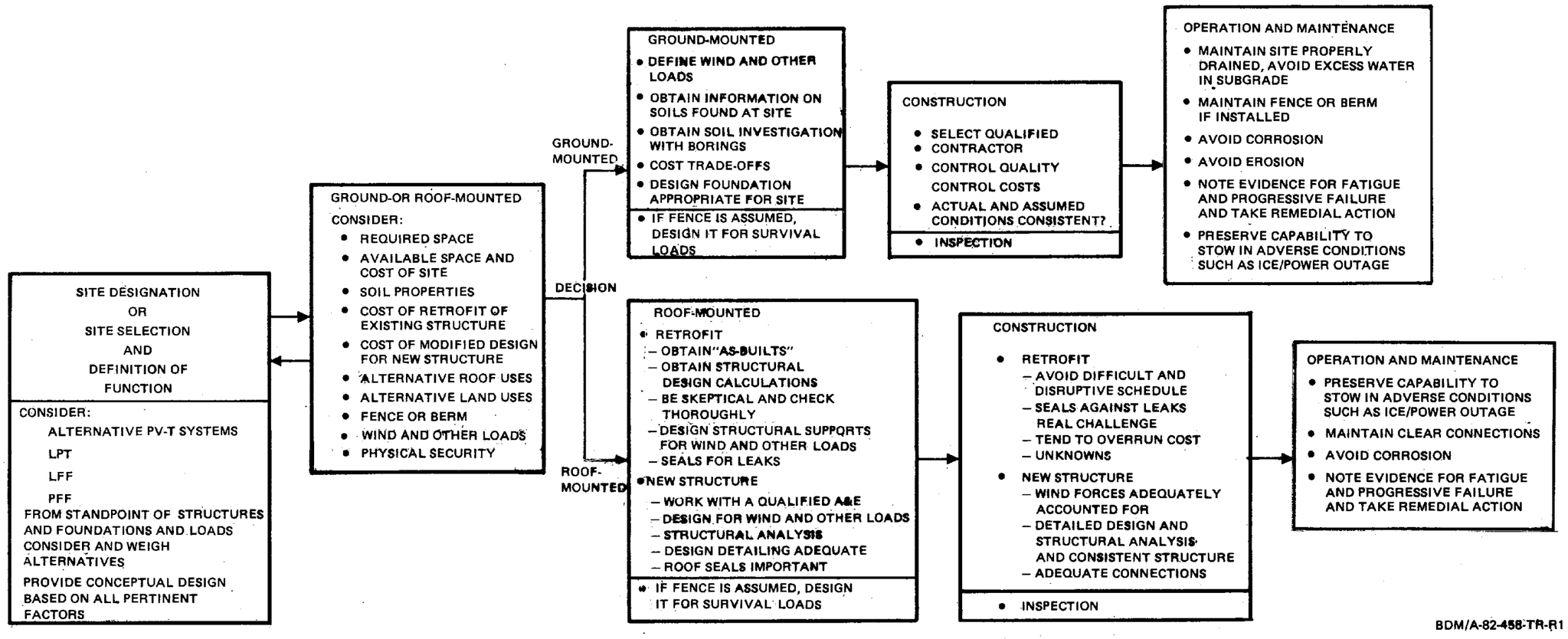

FLOW CHART — DESIGN OF STRUCTURES AND FOUNDATION FOR PV-T SYSTEM

Figure VI-4. Design of Structures and Foundation for PV-T System

the LPT and the LFF) could be more easily adapted to either roof or ground mounting because of the lower magnitudes of concentrated base bending moments carried by the roof structure. Tradeoff studies will supply the data to determine where to mount a specific installation. Considerations involved (figure VI-4) include:

- Type of system (LPT, LFF, or PFF).
- Required space for the array, compared to available roof space and vacant land.
- Soil conditions and roof conditions, current or projected.
- Relative costs of building retrofit, land use, and foundation costs.
- Roof-top wind loads versus wind loads at ground level and effects of wind fences or berms and other shielding.
- Aesthetics.

The upper (ground-mounted) path of figure VI-4 carries the ground-mounted installation through the design, construction, and operation and maintenance phase. The lower path of that figure illustrates the parallel approach to the design, construction, and operation and maintenance of a roof-mounted system.

1. Roof Mountings

Such mountings may be on new structures or retrofit to old structures. As the PV-T systems become more extensive and require a greater surface area for installation, the trend is toward ground-mounted systems.

Several examples of roof mountings of various types (not just PV-T) can be cited. (Randall, SNL, personal communication, March 29, 1982):

- Campbell Soup Plant in Sacramento, California. Some problems with roof leakage and some cost growth noted (hybrid flat plate and parabolic trough installation).
- Gilroy Foods, Gilroy, California, onion drying plant product storage building. Roof required additional reinforcing after initial completion (evacuated tube with V-shape back surface).

- Lumber drying kiln in Mississippi--roof reinforced for flat plate array.
- West Point Pepperill Textile Plant. Old building ready for re-roofing. Parabolic trough collector array for steam generation mounted on roof concurrent with re-roofing. Roof leakage problems after completion persisted and caused concern. System finally removed for various reasons.
- York Building Products--Harrisburg, Pennsylvania. Roof designed with collector array in mind. Good performance.
- Lone Star Brewery. A solar array of 930 m^2 (10,000 ft^2) was placed on a warehouse roof after the roof truss work was strengthened. The installation furnishes 1 MPa (150 psi) steam. No significant problems have been encountered.
- Ore-ida Foods, Ontario, Oregon. The initial design called for placement of a 930 m^2 (10,000 ft^2) parabolic trough installation on a roof. Further investigation before construction revealed that roof vent fans were a source of vapors containing grease which would foul the reflective trough surfaces. The installation was, therefore, changed to ground mounting.

Installation on an existing or to-be-constructed building requires the special care and attention to detail illustrated in figure IV-4. As-built drawings must be carefully reviewed for accuracy. Check the condition of the existing roof structure carefully. This can be a difficult task because structural members are often well concealed. Detailed analysis will be required to ascertain the load carrying capacity of the old structure and the loading to be put on that structure by a proposed PV-T array. Wind loading on the PV-T array must be transferred into a structure which has adequate strength, stiffness, and fatigue resistance. Roof reinforcements and assurance of a leak-proof final product are nontrivial tasks facing the retrofit project manager. Each retrofit is a different challenge. Some new buildings supposedly designed for mounting of PV-T arrays may prove, in fact, to be retrofits if the PV-T array wind loadings have not been adequately taken into

account (e.g., the new BDM building PV-T linear parabolic trough array in Albuquerque, New Mexico required additional steel to take the wind-induced support pylon moments which were calculated to be beyond the capability of precast concrete T-beams which support the roof). As is shown for ground mounted systems, the moments and horizontal forces at the base of a support pylon can be substantial, and must be taken into account along with the vertical forces. The loads on a roof structure will be somewhat different than those identified for ground-mounted systems and appropriate calculations must be made for each case encountered.

2. Ground Mountings

Figure VI-5 portrays in four categories the issues related to structures and foundations for ground-mounted PV-T systems.

Soils and geotechnical engineering issues comprise the first category on the left in figure VI-5. Soils are highly variable from site to site and frequently within a site. Material property variations can occur laterally, with respect to depth, and with time. One of the recently constructed solar arrays was placed on an expansive clay soil. Such clays display a seasonal cycle of swelling and shrinkage which would prove damaging for an array. Each site selected requires an appropriate soil survey with borings to ascertain soil properties. The expansive clays were encountered at the Johnson and Johnson Plant in Sherman, Texas where a 10,000 square foot parabolic trough installation serves a 150 psi steam generation plant. The solution to the foundation problem was to employ grade beams for the foundations at a higher cost than conventional piers. If conventional piers had been used, severe maintenance problems might have developed.

At many sites soil properties noted may fall into one of the categories in figure VI-6, where soils are rated as good, average, or poor, depending on results of standard penetration tests, allowable bearing pressures, and pullout tests. Figure VI-6 presents just one of several available attempts to categorize soils. Each of these categorizations has some range of benefit, but should not lull the project

SOILS — RELATED ISSUES GROUND-MOUNTED SYSTEM

- SOIL TYPES AND VARIABILITY LATERALLY AND WITH DEPTH
- VARIABILITY OF SOILS WITH RESPECT TO TIME
  - — SEASONAL-FREEZE, THAW, WATER SWELLING
  - — MAN-MADE VARIATIONS (E.G., DEWATERING AND NEARBY LATER CONSTRUCTION)
- EXTENT OF SOIL INVESTIGATION REQUIRED
- CONSIDERATIONS WITH RESPECT TO "GENERAL" SOIL TYPES
  - — BEWARE OF SUBJECTIVE/UNOFFICIAL DETERMINATIONS OF SOIL TYPES
  - — SAND AND GRAVEL
  - — EXPANSIVE SOILS
  - — COHESIVE SOIL
  - — SILT
  - — ROCK AND BOULDERS
  - — PEAT
- BEARING CAPACITY AND SETTLEMENT
- ELASTIC AND INELASTIC DEFORMATIONS
  - — DURING OPERATIONS
  - — AS A RESULT OF WIND
- DRILLED REINFORCED CONCRETE PIERS
  - — COST EFFECTIVE
  - — ANALYSIS AND DESIGN
  - — RELEVENCE
- REQUIREMENT FOR ATTENTION TO DETAIL AT SPECIFIC SITE

LOADS — DETERMINATION RELATED ISSUES FOR GROUND-MOUNTED SYSTEM

- PRESENCE OR ABSENCE OF FENCE OR BERM
  - — AESTHETIC
  - — ADEQUATE?
  - — COST EFFECTIVE
- LOCAL TOPOGRAPHY AND CURRENT OR PROJECTED NEARBY STRUCTURES
- OPERATIONAL WINDS VS STOWED (SURVIVAL) WINDS
  - — TIME TO STOW VS WIND VELOCITY RISE
- SELECT DESIGN WIND (STEADY STATE)
  - — RECURRENCE INTERVAL AND WIND SPEED
  - — 25 YEAR 80 MPH AT 10 METERS (SURVIVAL)?
  - — APPROPRIATE FOR LOCALITY?
  - — ADJUST FOR COLLECTOR ELEVATION WITH APPROPRIATE N VALUE DEPENDING ON TERRAIN
- EFFECTIVE PRESSURES
- DETERMINE LIFT, DRAG, AND MOMENT COEFFICIENTS
  - — BUILDING CODES CONSERVATIVE
  - — JUSTIFY USAGE OF WIND TUNNEL TEST APPROPRIATE TO PROBLEM
- USE APPROPRIATE GEOMETRY
  - — ASPECT RATIO?
  - — FLOW UNDER AND OVER?
- CONSIDER GUST LOADS AND TAKE INTO ACCOUNT
  - — DATA AVAILABLE RELEVANT?
  - — ADJUST SAFETY FACTOR OR DO DYNAMIC ANALYSIS
- LOAD FACTORS OR SAFETY FACTORS
  - — 2 OR 3
  - — JUSTIFY
- GRAVITY LOADS, EARTHQUAKES, SNOW LOADS, ICE, HAIL, RAIN

DESIGN AND CONSTRUCTION RELATED ISSUES

- ARCHITECT-ENGINEER PERFORMANCE
  - — PREVIOUS EXPERIENCE?
  - — KNOWLEDGE OF WIND LOADS AND EXPERIENCE?
  - — TEXTBOOK/STANDARD CODE APPROACH OR REAL ANALYSIS AND DESIGN?
  - — APPROPRIATE SAFETY FACTORS?
  - — COST ANALYSES AND COST TRADE-OFFS APPROPRIATE?
  - — RISK ANALYSIS AND RISK REDUCTION?
  - — DESIGN DETAILS AND CONNECTIONS
- CONTRACTOR PERFORMANCE
  - — QUALITY WORK BY REPUTATION?
  - — COST CONSCIOUS AND EFFICIENT? COST OVERRUN EXPERIENCE
  - — CONSTRUCTION MONITORING VALIDATE SOILS ASSUMPTIONS ENSURE QUALITY OF CONSTRUCTION TRACK COSTS
  - — FINAL INSPECTION — PRODUCT CONSISTENT WITH DESIGN?

OPTIMUM COST — EFFECTIVE CONFIGURATION OF STRUCTURE AND FOUNDATION

- VARIES WITH SITE CONDITIONS
- VARIES WITH ANTICIPATED LOADS
- VARIES WITH LOCAL CONSTRUCTION CAPABILITY, AVAILABLE EXPERIENCED WORKFORCE, AND MATERIAL AND EQUIPMENT COSTS
- DRILLED RIGID PIERS CAN BE JUSTIFIED FOR SOME LOCATIONS BUT DON'T MISUSE
  - — AULD/MERKLE APPROACH
  - — LLNL/EPRI CODE
- DESIGNER NEEDS A VARIETY OF OPTIONS AND CALCULATIONAL TOOLS. AVOID TUNNEL VISION

BDM/A-82-458-TR-R1

Figure VI-5. Structures and Foundation Issues Associated with PV-T System Design Ground-Mounted System

A PROPOSED CATEGORIZATION OF SOLAR ARRAY FOUNDATION SOILS[1]

SOIL TYPE	DESCRIPTION		STANDARD PENETRATION*	ALLOWABLE BEARING PRESSURE	STANDARD PULLOUT, LB**	
	GRANULAR	COHESIVE			GRANULAR	COHESIVE
A. GOOD	DENSE SAND/ GRAVEL	HARD CLAY	35 BLOW/FT	4000 PSF	1500	2000
B. AVERAGE	MEDIUM DENSE SAND/GRAVEL	VERY STIFF CLAY	25 BLOW/FT	2500 PSF	750	1000
C. POOR	MEDIUM SAND/ GRAVEL	CLAYEY SILT	20 BLOW/FT	1500 PSF	500	650

*STANDARD PENETRATION RESISTANCE TEST — ASTM D 1586 — 2-INCH SPLIT-BARREL SYSTEM DRIVEN BY 140-LB DROP, 30-INCH FALL.
**STANDARD PULL OUT — OUTDOOR ADVERTISING ASSOCIATION — UTILITY FOUNDATION ENGR. — 1½-INCH STANDARD TEST AUGER.

1. Modified from Graham Alexander et.al., Battelle, February 1982

BDM/A-82-458-TR-R1

Figure VI-6. Proposed Categorization of Solar Array Foundation Soils (from Alexander, Reference VI-8)

manager into a false sense of confidence whereby he cuts costs by using standard pier designs and omits soil surveys and consultation with a qualified geotechnical engineer. The good, average, and poor categories are arbitrary and were developed with the idea of providing a standardized design for favorable sites. Whether a specific site is favorable or not must be determined by a geotechnical investigation including the standard penetration test, the pullout test, soil sampling, mechanical analysis, Atterberg limit determinations, and other appropriate tests.

C. LOADS-DETERMINATION

Issues related to loads determination for PV-T systems are illustrated in the second column of figure VI-5. Particular aspects related to wind loads determinations are highlighted in figure VI-7.

Wind tunnel tests performed at Colorado State University have shown (ref. VI-9, 10, and 11) the value of wind fences or berms around LPT systems in reducing the applicable design loads. Randall (ref. VI-10) notes that mean wind loadings on parabolic trough solar collectors "experience an interference effect which provides a significant reduction (50 to 65 percent) of the peak lateral and lift forces originating with the wind" and that "appropriate fence or berm configurations can provide reduction of lateral and lift forces in perimeter rows equivalent to the interference effect within collector arrays". For the LPT systems Randall suggests a fence or berm approximately three-fourths of maximum collector height, with a porosity of 30 to 40 percent. A fence around a ground-mounted array may provide not only load reduction but also security and aesthetic appeal.

In both figure VI-5, column 2, and figure VI-7, there is emphasis on the need to consider site and locality specific issues in wind loads determinations. There is obviously a need to develop data for the specific system under consideration also, as illustrated previously in figures VI-1, 2, and 3. Considerable amounts of wind tunnel data have

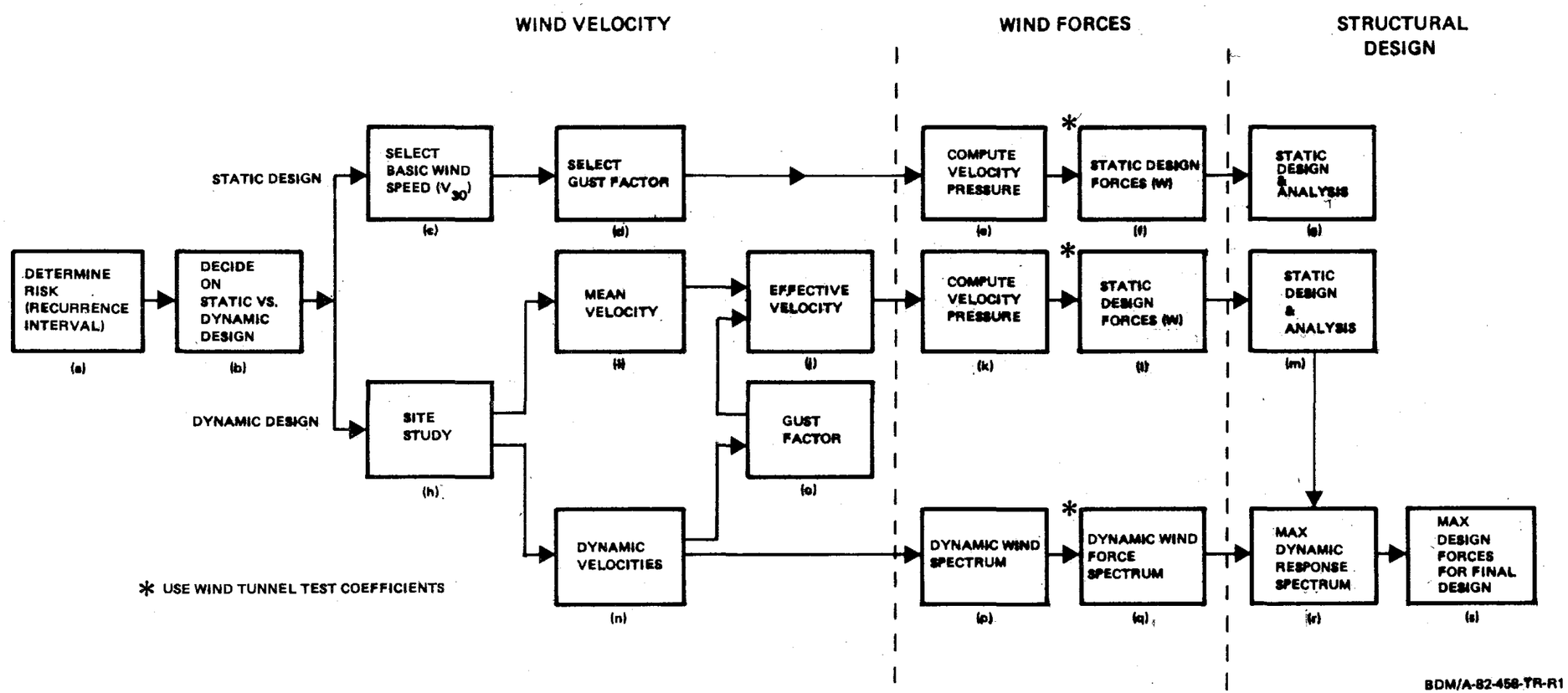

ARRAY SUPPORT STRUCTURE WIND FORCES DETERMINATION
MODIFIED FROM BECHTEL (REF. VI-5)

Figure VI-7. Array Support Structure Wind Forces Determination

been collected and interpreted for the LPT systems of figure VI-1 (see ref. VI-11) and for the Martin-Marietta system of figure VI-3 (see ref. VI-12). For the LFF (figure VI-2) wind tunnel tests have yet to be performed and the drag coefficient has been estimated by relating to some existing flat plate data as is noted in figure VI-8.

1. Wind Velocities, Forces, and Design for Winds

Recently several authors, e.g., Murphy (ref. VI-14), Bechtel (ref. VI-5), and Randall (ref. VI-9), have discussed in detail the issues relating to wind loading and design for wind of solar collectors. The ANSI A58.1-1972 building code provides a point of departure for each of these articles. The ANSI procedure involves several steps:

- Determine a recurrence interval; i.e., 25, 50, 100 years based on risks
- Determine a basic wind speed (from iso-plots, site investigations, etc.)
- Determine effective pressures related to that wind speed (take into account wind gusts)
- Ascertain pressure coefficients and then design pressures
- Apply load factors

Problems with the application of the ANSI code are several (ref. VI-13)

- The code is not particularly relevant to structures of unusual shape.
- The code is quite conservative--for example there is no provision for taking into account boundary layer effects that reduce wind velocities below 10 m.
- Load reductions by shielding of adjacent structures are not taken into account.
- Coefficients in the code were obtained from smooth flow wind tunnels rather than boundary layer tunnels.

The current best approach to design of solar collector's structural supports for wind loadings uses information and guidance from ANSI supplemented with wind tunnel data appropriate to the case being considered (Murphy, ref. VI-14).

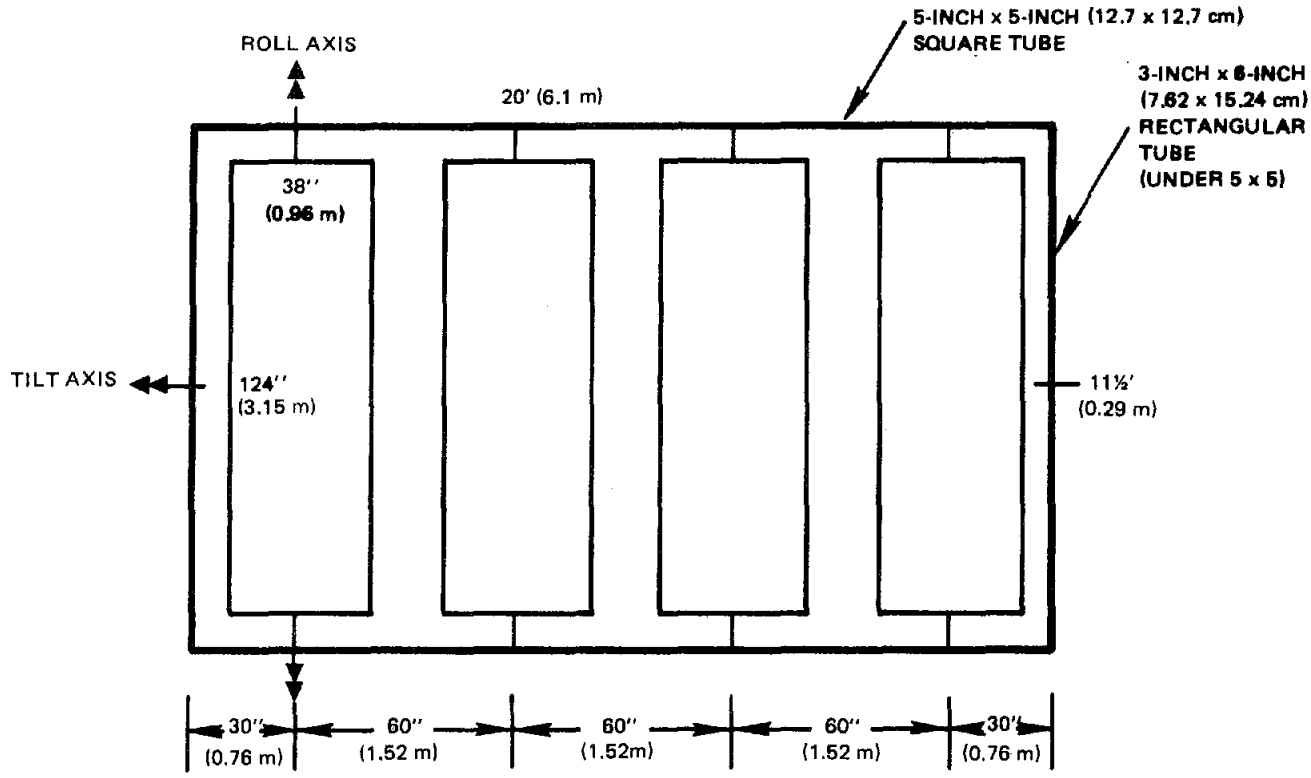

PLAN FORM OF E-SYSTEMS
(FOUR MODULES IN-A-FRAME)

NOTES (FROM VERN GOLDBERG, E-SYSTEMS, PERSONAL COMMUNICATION, APRIL 6, 1982)

- WIND
  - START TO STOW AT 30 MPH (13.4 m/sec)
  - COMPLETES STOW BY 50 MPH (22.4 m/sec)
  - SURVIVES 90-MPH (40.2 m/sec) WIND STOWED (STOW IS FRAME HORIZONTAL AND LFF MODULES FACE DOWN)
- DRAG COEFFICIENT 1.0 ESTIMATED WORST CASE WITH FRAME AT 65° TO HORIZONTAL; 145 SQUARE FEET AREA (13.5 m^2) EXPOSED INCLUDING MODULES AND FRAME. LES CONSERVATIVE DRAG COEFFICIENT 0.75 ESTIMATED
- DEADWEIGHT OF FRAME AND MODULES ON TILT AXIS IS 1000 POUNDS (454 Kg) WHICH EXCEEDS MAXIMUM LIFT
- DEADWEIGHT OF EACH PYLON AND ACCESSORIES IS APPROXIMATELY 150 POUNDS (68 Kg)
- DISTANCE FROM TILT AXIS TO TOP OF PIER IS 82 INCHES (2.08 m)
- MODULES ARE APPROXIMATELY 30 INCHES (0.76 m) DEEP

BDM/A-82-458-TR-R1

Figure VI-8. Characteristics of E-Systems Array (from Goldberg Reference VI-13)

Randall (ref. VI-9) suggests that ground mounted solar collector arrays could be designed for a mean recurrence interval of 25 years because:

- o They do not constitute a substantial risk to life and property under high winds,
- o Have an economic life less than that of the multistory buildings of the ANSI code,
- o Would not be relied upon for emergency energy after a storm.

For roof-mounted installations a 50 year recurrence interval is suggested because of the greater risk.

For a 10-m elevation and a 25-year recurrence interval most of the contiguous United States has a highest wind speed not exceeding 80 miles per hour. There are some narrow belts where this wind speed is exceeded. For the 50-year interval the wind speed would be 90 miles per hour. Allowances should be made for local conditions and gusts when considering the use of these values.

For ground-mounted collector arrays the 10-m velocity can be scaled downward to account for diminished near surface velocities resulting from boundary layer effects.

The formula used (Randall, ref. VI-9) is:

$$\frac{V}{V_{ref}} = \left(\frac{Z}{Z_{ref}}\right)^n \qquad \text{(Eq. VI-1)}$$

Here: V = velocity of height Z above ground

V_{ref} = velocity at a defined reference elevation Z_{ref}

n = exponent for power law relation

The following table (Randall, ref. VI-9) provides values of n for four types of surfaces from three different sources:

TABLE VI-1. POWER LAW EXPONENTS FOR VARIOUS TERRAIN TYPES

Type of Terrain	n	
	upper bound	lower bound
very smooth (sea, ice, snow mudflats)	0.099	0.099
open flat (rural grassland and crops)	0.161	1/7
rough (houses and woods)	0.28	1/4.5
very rough (urban city centers)	0.40	0.32

Given the velocity profiles appropriate for the terrain, it is possible to then calculate dynamic pressure profiles using the equation:

$$q = \frac{1}{2} pv^2 \qquad \text{(Eq. VI-2)}$$

Here q is the dynamic pressure, p is mass density of the air stream and v is the wind velocity. Randall (ref. VI-9) suggests a dynamic pressure design value of around 480 Pa (10 pounds per square foot) for both suburban roof-top installations and ground mounted systems where the terrain is open and flat. The lift and drag forces and the moments on the collector are determined using the equations:

$$\text{FORCE} = C_{\text{FORCE}}\, qA$$

$$\text{MOMENT} = C_{\text{MOMENT}}\, qA\ell \qquad \text{(Eq. VI-3)}$$

A is the appropriate area for the coefficients being used and ℓ is a moment arm. The values of the coefficients C_{FORCE} and C_{MOMENT} are derived from wind tunnel measurement on scale models.

a. Wind Forces on Linear Parabolic Troughs

Randall (personal communication) suggests that for ground-mounted LPT systems (figures VI-1 and VI-9) properly fenced or bermed the coefficients which can be used for design (upper bounds) are as follows:

C_{lift} = $\pm$ 0.5 (see Randall, ref. VI-10)

$C_{drag\ (lateral\ force)}$ = 0.5 (Randall, ref. VI-9)

$C_{pitching\ moment}$ = $\pm$ 0.1 (Randall, personal communication, March (1982)

Aspect ratios associated with these values are approximately 3.

These values assume at least 6 percent gaps between individual troughs of the LPT array to nullify the considerable influence that long-row aspect ratios would have. If aspect ratios of individual troughs approach 5 to 10, the coefficients should be re-evaluated. The value of $C_{pitching\ moment}$ = $\pm$ 0.1 is in accord with some recent detailed investigations by Randall, and is lower than the previously reported $\pm$ 0.35 from Randall (ref. VI-9).

The linear parabolic trough (LPT) systems commonly start to stow automatically when wind velocities reach 15.6 m/sec (35 mph) and they are in a stow position by the time the wind velocity is 22.4 m/sec (50 mph). In the stow position they are intended to survive an 35.8 to 44.7 m/sec (80 to 100 mph) wind. The coefficients given above may be used with these survival winds to calculate design forces for the structure and foundation. Obviously, for these values to be used it is assumed that the adverse conditions such as a power outage or icing conditions do not prevent movement to the stow position.

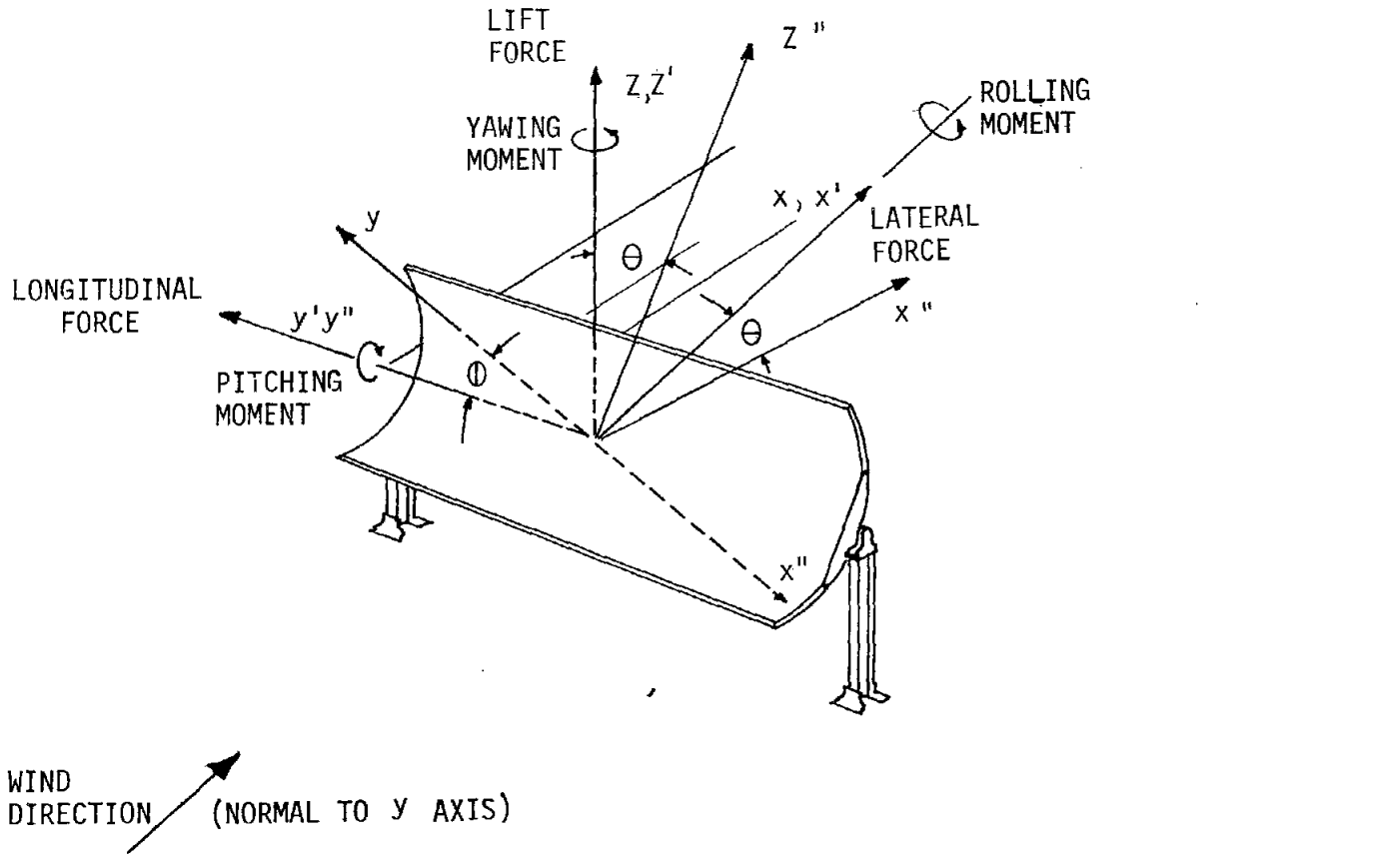

WIND AXES - UNPRIMED
FOUNDATION AXES - PRIMED
BODY AXES - DOUBLY-PRIMED

Figure VI-9. Model Axis System (from Randall, Reference VI-10)

b.. Wind Forces on the Martin Marietta Two-Axis Point Focus Fresnel (PFF) System

Wind tunnel tests at Colorado State University (CSU) (ref. VI-12) have disclosed that the wind loads on the configuration in figures VI-3 and VI-10 are quite sensitive to the "porosity" of the paddles or wings. The original first generation design of this system had a porosity of 13 percent with only 87 percent of the area effective. By going to 100 percent aperture area and by staggering the PFF modules it has been possible to increase the efficiency of the system and reduce wind loads for a given exposed area.

The results of the tests at CSU are portrayed in the table below (ref. VI-3).

TABLE VI-2. POROSITY EFFECTS ON MARTIN MARIETTA SYSTEM

	POROSITY 0	POROSITY 1	POROSITY 5
AZIMUTH TORQUE FACTOR	6.8	2.63	1.0
ELEVATION TORQUE FACTOR	1.69	1.62	1.0
BASE BENDING MOMENT FACTOR	1.31	1.16	1.0

Figure VI-11 shows the azimuth torque, elevation torque, and base bending moment for the Martin Marietta second generation array for various array angles, wind directions, and for both porosity 4 and porosity 5. Maish (ref. VI-15) points out that "introducing porosity by staggering adjacent modules front to back can reduce maximum azimuth torques by a factor of (nearly) 7 and maximum elevation torques by a factor of 1.7 over a solid array while maintaining 100 percent array aperture area utilization".

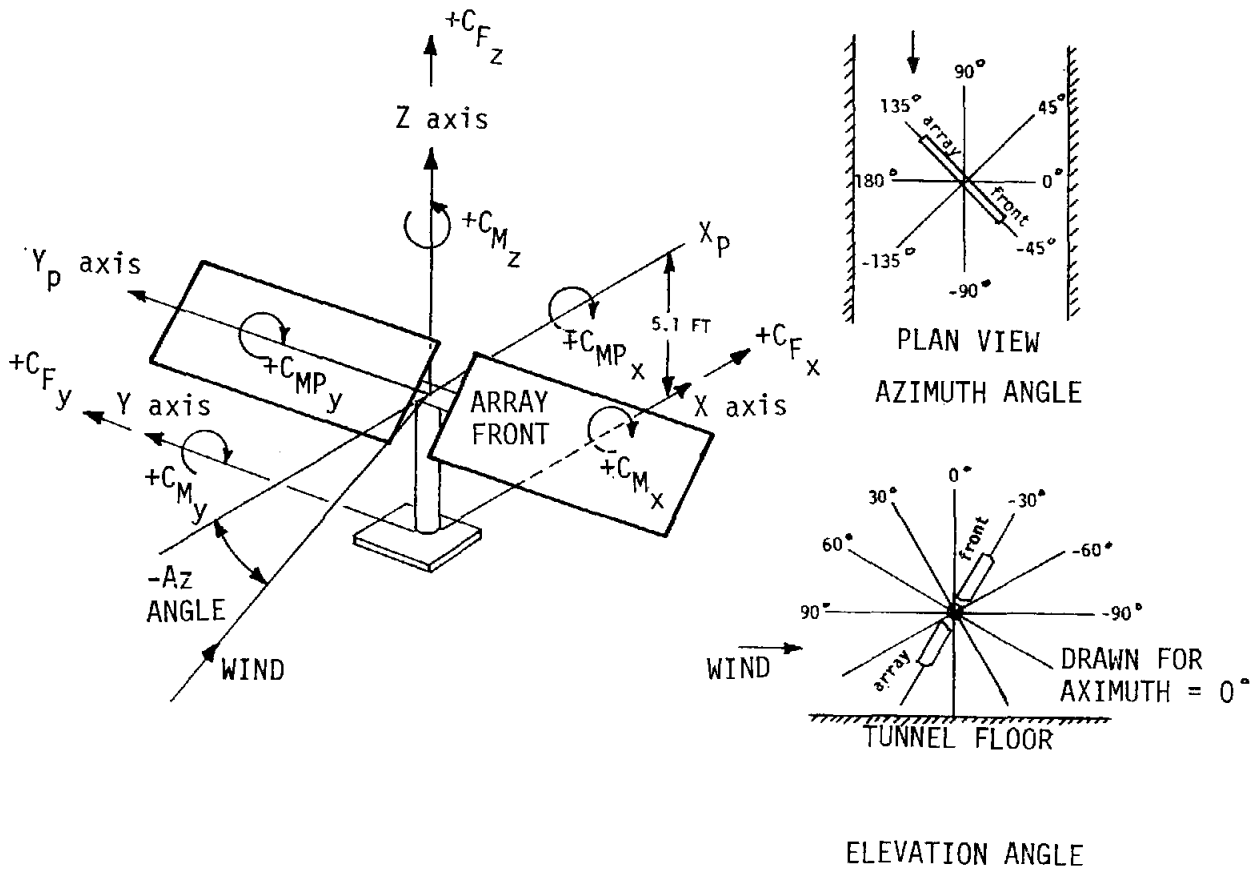

Figure VI-10. Definition of Coordinate System (from Peterka, Lou, and Cermak, Reference VI-12)

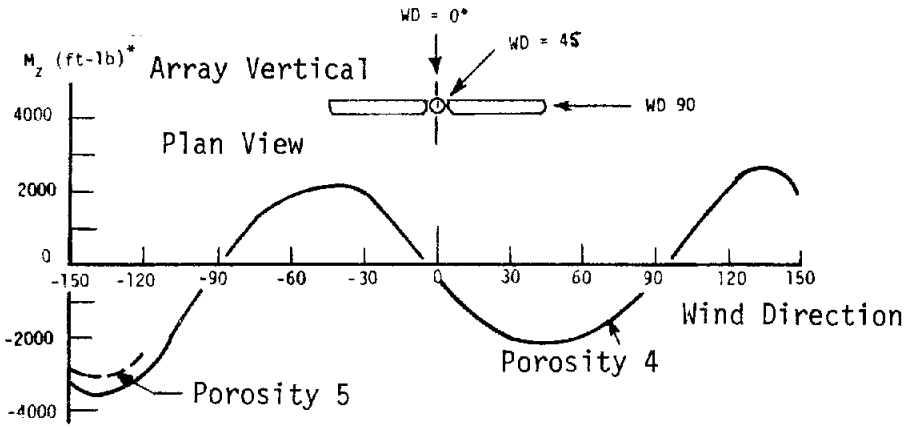

Azimuth Torque (Mz) Versus Wind Direction

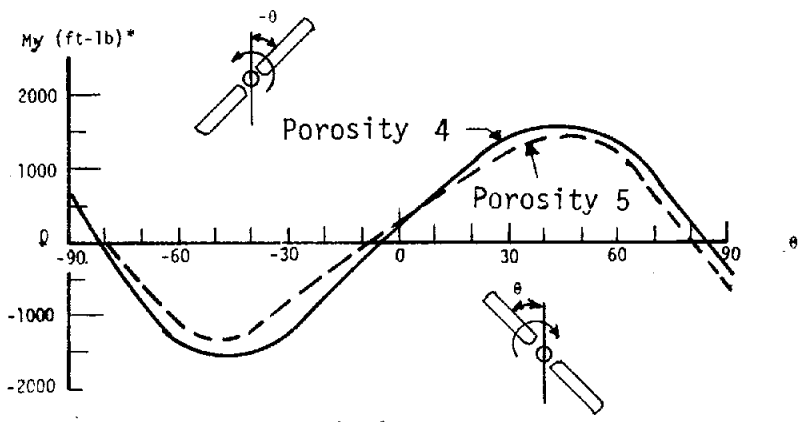

Elevation Torque (My) Versus Array Angle (θ)

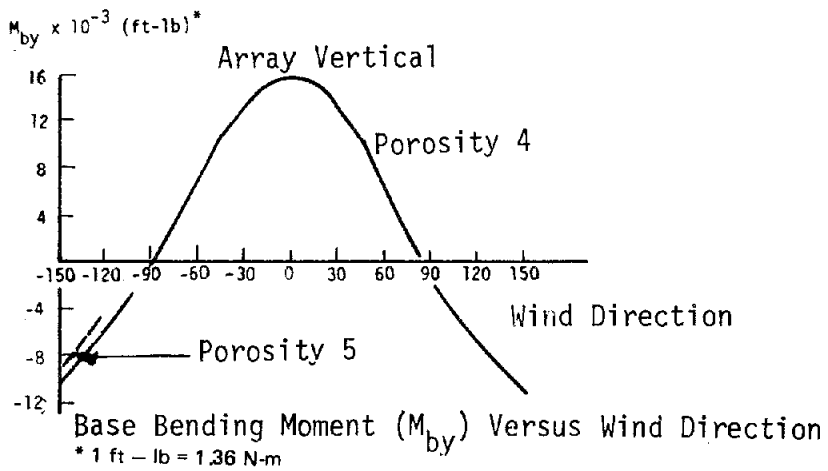

Base Bending Moment (M_{by}) Versus Wind Direction

* 1 ft – lb = 1.36 N-m

BDM/A-82-458-TR-R1

Figure VI-11. Martin Marietta System Wind Tunnel Test Results (from Broadbent, Reference VI-3)

The Martin system will start to drive to stow at 11.6-13.4 m/sec (26-30 mph) winds and will survive a 13.4 m/sec (50 mph) wind during stow. The system is intended to survive a 100 mile per hour wind in the stow position. Stow is at a 10° inclination (elevation angle) to the horizontal.

The Martin Marietta two-axis tracking single-pedestal system displays some pronounced tendencies when winds act on a number of units in a field. For units on the edge of an array, unbalanced shielding can raise the azimuth moment (doubled in one example) and flow channeling in the center of an array (ref. VI-12) can produce a "one-sided" loading on a unit.

c. Wind Forces on E-Systems Two-Axis Tracking System

Figures VI-2 and VI-8 show this system as currently designed. Figure VI-8 provides detailed data currently available (Goldberg, ref. VI-13). Stow and survival winds are indicated in figure 8 as well as the currently estimated worst case drag coefficient of 1.0 with the frame at 65° to the horizontal. Lift and moment coefficients have not been provided but can be estimated by reference to wind tunnel tests on plates.

2. Examples of Wind Load Calculations on Linear Parabolic Troughs

Randall (ref. VI-9) provides two examples of calculations of wind loads on LPT. These calculations are reproduced here to illustrate an approach to design which could be modified and applied to other PV-T systems.

a. Ground Mounted Array - Sample Calculation:

Given a ground-mounted LPT array of 2 m X 6 m (6.56 ft X 19.69 ft) collector modules installed in open flat terrain. Modules are installed with trough center line 1.5 m (4.92 ft) above ground.

Reference Area (A_R) = 2 X 6 = 12 m^2 (129.2 ft^2).

Reference Length (L_R) = 2 m (6.56 ft).

Basic Design Wind Speed* = 35.76 m/sec (80 mph or 117.3 ft/sec)

* (at 10-m elevation, 25-year recurrence).

$$\text{Velocity at Collector Center Line} = 35.76 \left(\frac{1.5}{10}\right)^{1/7} = 27.3 \text{ m/sec } (89.5 \text{ ft/sec}).$$

$$q_{10_{open}} = 0.5\ (1.226\ \text{kg/m}^3)\ (35.76)^2 = 783.9 \text{ Pa } (16.35\ \text{lbs/ft}^2).$$

$$q \text{ at Collector Center Line} = 0.5\ (1.226\ \text{kg/m}^3)\ (27.3)^2 = 456.4 \text{ Pa } (9.5\ \text{lb/f}^2).$$

Note: The boundary layer extends to approximately 275 m elevation over open country and at 275 m:

$$\text{Geostropic Wind speed} = 35.76 \left(\frac{275}{10}\right)^{1/7} = 57.3 \text{ m/sec } (188\text{-ft/sec or } 128 \text{ mph})$$

Assuming, for parabolic trough collector modules in an array protected with a wind screen fence, lateral and lift force, and pitching moment coefficients equal respectively to 0.5, $\pm$ 0.5, $\pm$ 0.35 these respective loads are:

Lateral Force F_X = 0.5 (455 Pa) (12 m^2) = 2370 Newtons (614 lbs).
Lift Force F_Z = $\pm$ 0.5 (455 Pa) (12 m^2) = $\pm$ 2730 Newtons (614 lbs).
Pitching Moment M_θ = $\pm$ 0.35 (455 Pa) (12 m^2) (2 m) = + 3822 N-m (2818-ft lbs).

We could use the $\pm$ 0.1 referred to earlier in calculating M_θ.

Note: The loads calculated here do not include a gust factor to account for the cyclical nature of the wind about the fastest mile mean value.

b. Roof Mounted Array - Sample Calculation

Given the same collector array mounted on a building roof in a suburban area representative of rough terrain. The collector centerline is 10 m (32.8-ft) above ground.

Basic Design Wind Speed* = 40.2 m/sec (132 ft/sec or 90 mph) (at 10-m elevation, 50-year recurrence).

Geostrophic Wind Speed @ 275 m = 40.2 m/sec $\left(\frac{275}{10}\right)^{1/7}$ = 64.6 m/sec (212 ft/sec or 144.5 mph).

This geostrophic wind speed exists at 400 m over rough terrain.

Velocity at Collector Center Line = 64.6 $\left(\frac{10}{400}\right)^{1/4.5}$ = 28.5 m/sec (93.4 ft/sec).

q at Collector Center Line = 0.5 (1.226 kg/m^3) (28.5)^2 = 498 Pa (10.4 lb/ft^2).

Thus, a rooftop installation at 10 m height in suburban-type terrain, experiences a dynamic pressure only 9.5 percent greater than a ground-mounted installation at 1.5 m in open terrain and proportionately higher load levels.

3. General Comments on Wind Loadings

Figure VI-7 illustrates a step-by-step approach to wind load determination for support structure and foundation designs for solar arrays. The static design force determination has been illustrated in the previous example. Lack of sufficient data or enough time for

*The 10-m elevation basic wind speed data is based upon National Weather Service anemometer stations which, largely, are located at airfields. Thus, this data base, in general, has been accumulated for velocity profiles representative of open flat terrain.

analysis frequently precludes doing the dynamic design. There is much more to force determinations and design than the above examples show. Allowance must be made for gust loads, and the dynamic response of the structure needs to be evaluated to avoid excessive vibration amplitude build-up owing to excitation at or near resonance frequencies in the absence of adequate damping. Localized extreme wind conditions not taken into account can nullify an otherwise sound approach to wind load determinations. The site study noted in figure VI-7 (see h) is important. Column 2 of figure VI-5 raises many issues, some of which deserve more treatment than has been possible in this brief survey.

D. DESIGN AND CONSTRUCTION RELATED ISSUES

Column 3 of figure VI-5 provides a summary of some of the issues related to architect engineer and contractor performance in designing and building structural supports and foundations for PV-T systems.

Many firms lack experience with PV-T technology and learning can be expensive, as has been noted in previously cited examples where oversights in design or lack of attention to detail in construction led to costly after-the-fact structural reinforcing or to leaky roofs. Figure VI-4 suggests some points to consider in the construction phase of PV-T installation. Lack of attention to detail in structural and foundation construction and inspection will exacerbate problems subsequently encountered (figure VI-4) in the operation and maintenance of structural and foundation components. The goal throughout the process is to achieve a system with low initial and life cycle costs.

1. Optimum Cost-Effective Configuration of Structure and Foundation

This category of issues from figure VI-5 relates to the quality of the end-product from this entire discussion of structures and foundations, to support PV-T systems. The optimum cost-effective solution will vary, depending on all the factors listed in column 4 of figure VI-5. Site conditions and loads have been previously discussed. Local

construction capability for structures and foundations must be taken into account in design and costing of foundations (ref. VI-16).

2. Examples of Foundation Designs for PV-T Systems

Drilled reinforced concrete piers have been noted to be a cost-effective solution to the problem of providing a suitable foundation for ground-mounted PV-T systems (ref. VI-16). These authors extended their earlier study to consider what economies could be realized in design of LPT array foundations where shielding effects of multiple rows and perimeter fences were taken into account (ref. VI-17). They concluded that appropriately reduced wind loadings can result in cost savings that are significant and that favorable sites (good soil conditions) should be sought to help keep costs of foundations down. They suggested the use of rectangular footings for PV-T systems only when site conditions preclude the use of an auger to drill the holes for the piers.

For piers Auld (ref. VI-18) used the basic equations of rigid pile theory (figure VI-12):

In the interaction equation of figure VI-12:

$P_{\mu\theta}$ = a factor of safety X magnitude of inclined load (P_θ)
θ = the angle of inclination of P_θ which is measured from the vertical axis
Q_{uv} = the gross ultimate vertical resistance ($\theta = 0$)
Q_{uh} = the gross ultimate lateral resistance ($\theta = 90^o$)

In order to calculate the vertical uplift capacity of the pier the weight and surface resistance are taken into account:

$$Q_{uv} = RA_s + W \qquad \text{(Eq. VI-4)}$$

Here, R is the average resistance per unit area to uplift over the embedded area A_s, and W is the weight of the pier. Calculation of R requires knowledge of the appropriate uplift coefficients, the cohesiveness and frictional characteristics of the soil and pier face, and the unit weight of the soil.

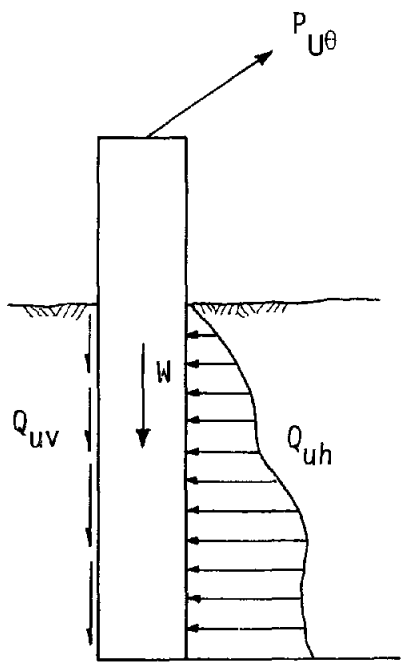

- $\frac{P_{U\theta}\cos\theta}{Q_{uv}} + \left(\frac{P_{U\theta}\sin\theta}{Q_{uh}}\right)^2 \leq 1$
- $Q_{uv} = R\ A_s + W$
- $R = f\ (c,\ \Phi,\ \gamma,\ \&\ \delta)$
- $Q_{uh} = f$ (c, Φ, γ, L, e, D, & Soil Reaction Distribution)
- Statics Utilized to Derive Equations for Q_{uh}

BDM/A-82-458-TR-R1

Figure VI-12. Basic Equations of Rigid-Pile Theory (from Auld, Reference VI-18)

Q_{uh}, the gross ultimate lateral resistance of the pier, is a function of the cohesiveness of the angle of internal friction, and the unit weight of the soil, as well as the length of embedment, the eccentricity of load, the diameter of the pier and the soil reaction distribution. A knowledge of soil and pier properties and equations of statics can be used to derive equations for Q_{uh}.

3. Example Pier Foundation Designs for a Linear Parabolic Trough System

Merkle (ref. VI-4) did testing which continued and extended the work of Auld and Lodde. He applied their pier design theory as illustrated in figure VI-12 (see ref. VI-16, appendix B) and used results of wind tunnel tests (ref. VI-9) to obtain designs for drive and interior pylon foundation piers for a shielded array of parabolic troughs. The troughs were of 2-m aperture and 6-m length. The coefficients used (lift, drag, and moment) were $C_1 = \pm 0.5$, $C_d = 0.5$, and $C_\theta = \pm 0.35$ as were cited above from Randall. Merkle used wind velocities of 16.76 m/sec (37.5 mph) operational and 40.2 m/sec (90 mph) survival. In the previously cited example, Randall used 35.8 m/sec (80 mph) survival winds. Merkle's (ref. VI-4) collector wind loads at the trough axis are:

lift force	3321 Newtons (746.6 pounds)
drag force	3321 Newtons (746.6 pounds)
pitching moment	18,600 N-m (164.6 inch-kips)

He took into account dead loads (222.6 Pa (4.65 lbs/ft^2) of aperture) and determined the following loads at the level of the top of the foundation piers:

		Wind	
		(16.8 m/sec) 37.5 MPH	(40.2 m/sec) 90 MPH
Drive Pier	- Vertical Force	(2090 N) 470 lb down	(667 N) 150 lb up
	Horizontal Force	(578 N) 130 lb	(3340 N) 750 lb
	Moment	(3955 N-m) 35 in-kips	(22600 N-m) 200 in-kips

Interior Pier -	Vertical Force	(2090 N) 470 lb down	(667 N) 150 lb up
	Horizontal Force	(578 N) 130 lb	(3340 N) 750 lb
	Moment	(791 N-m) 7 in-kips	(4520 N-m) 40 in-kips

Auld and West (ref. VI-19) designed the piers to sustain these loads. Figures VI-13 and VI-14 show the drive pylon pier design and the interior pylon pier design respectively, as designed for the soils found at the Sandia National Laboratories Albuquerque test area, where the soils are nonplastic silty sands and are well-characterized by a geotechnical investigation (ref. VI-1, appendix B). Piers for drive pylons were embedded 1.8 m (6-ft), and interior pylon piers were embedded 2.3 m (7-ft 8-in) for these tests. Vertical and lateral load carrying capability of these piers exceeded predicted capacity. Failures noted related to attachments at the tops of the piers, which were inadequate to develop full lateral bearing capacity of the piers.

4. Example Foundation Designs for the Martin Marietta Two-Axis Tracking Pedestal-Mounted System

Previously in this discussion (see figure VI-11), the results of wind tunnel tests were interpreted to bound the wind forces acting on the Martin Marietta system. This type of loading and other forces, including the gravity loads, have been taken into account along with appropriate safety factors, to develop the pier design shown in figures VI-15 and 16. Note that pier embedment lengths are to be determined based on soil analysis data. This design should be adjusted consistent with local conditions.

5. Example Foundation Designs for the E-System Two-Axis Tracking PV-T System

This system is shown in figures VI-2, 8, and 17. Figure VI-2 presents a perspective view. Figure VI-8 shows the system dimensions and the available information on dead loads and wind forces. Based on information available to him, Vernon Goldberg of E-Systems has prepared the

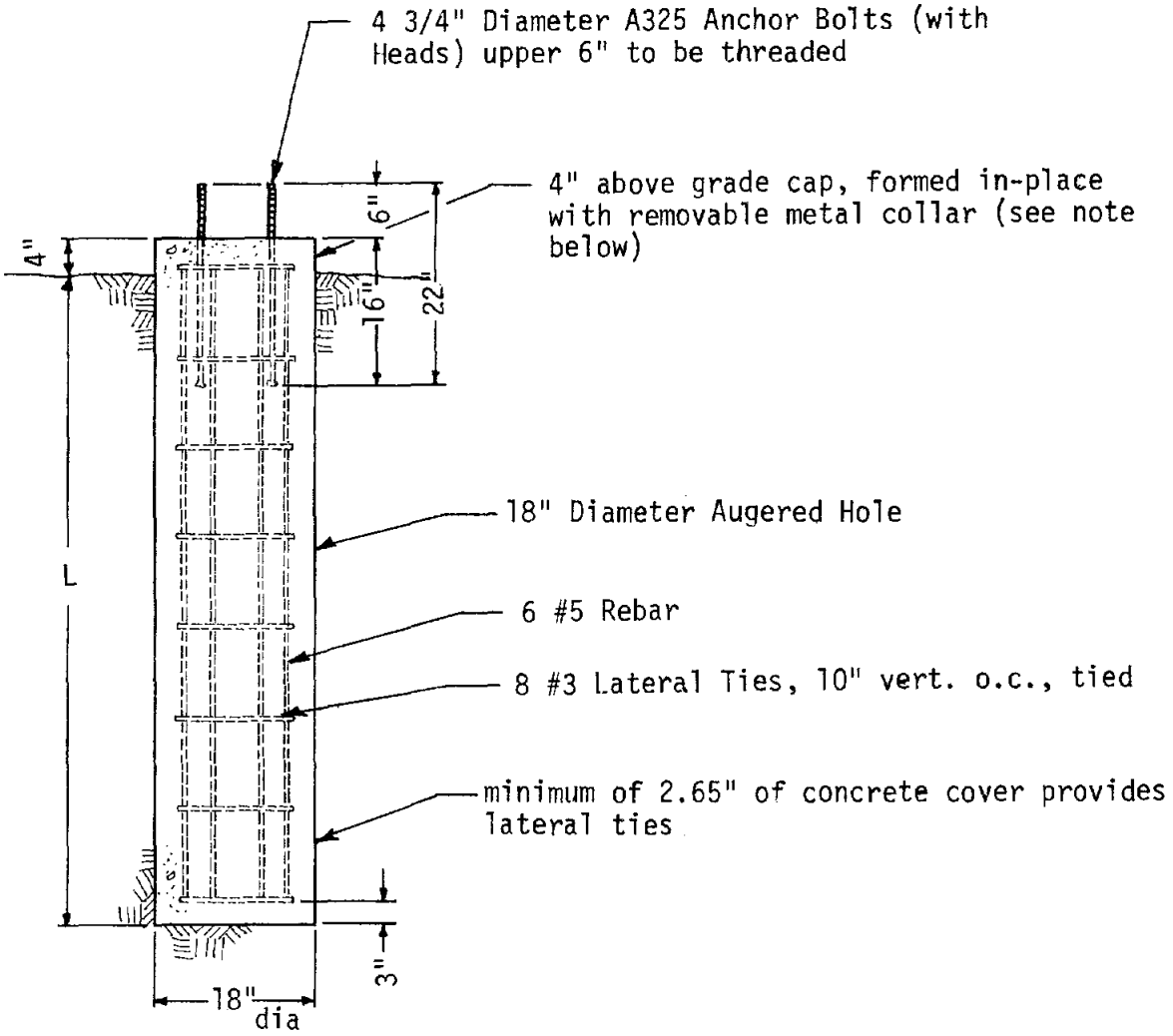

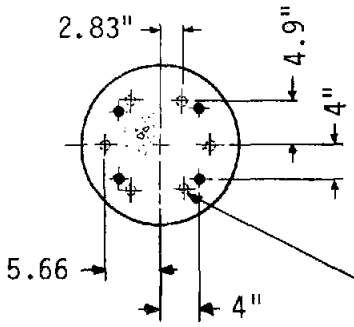

Notes: 1. Placement of cap-forming ring and anchor bolts to be set by construction jig

2. Materials:

concrete: 3,000 psi
steel: 50,000 psi
bolts: 3/4" A325

reinforcement bars set at 60° intervals on 5.66" radius

Figure VI-13. Solar Collector Drive Pylon (from Merkle, Reference VI-4)

BDM/A-82-458-TR-R1

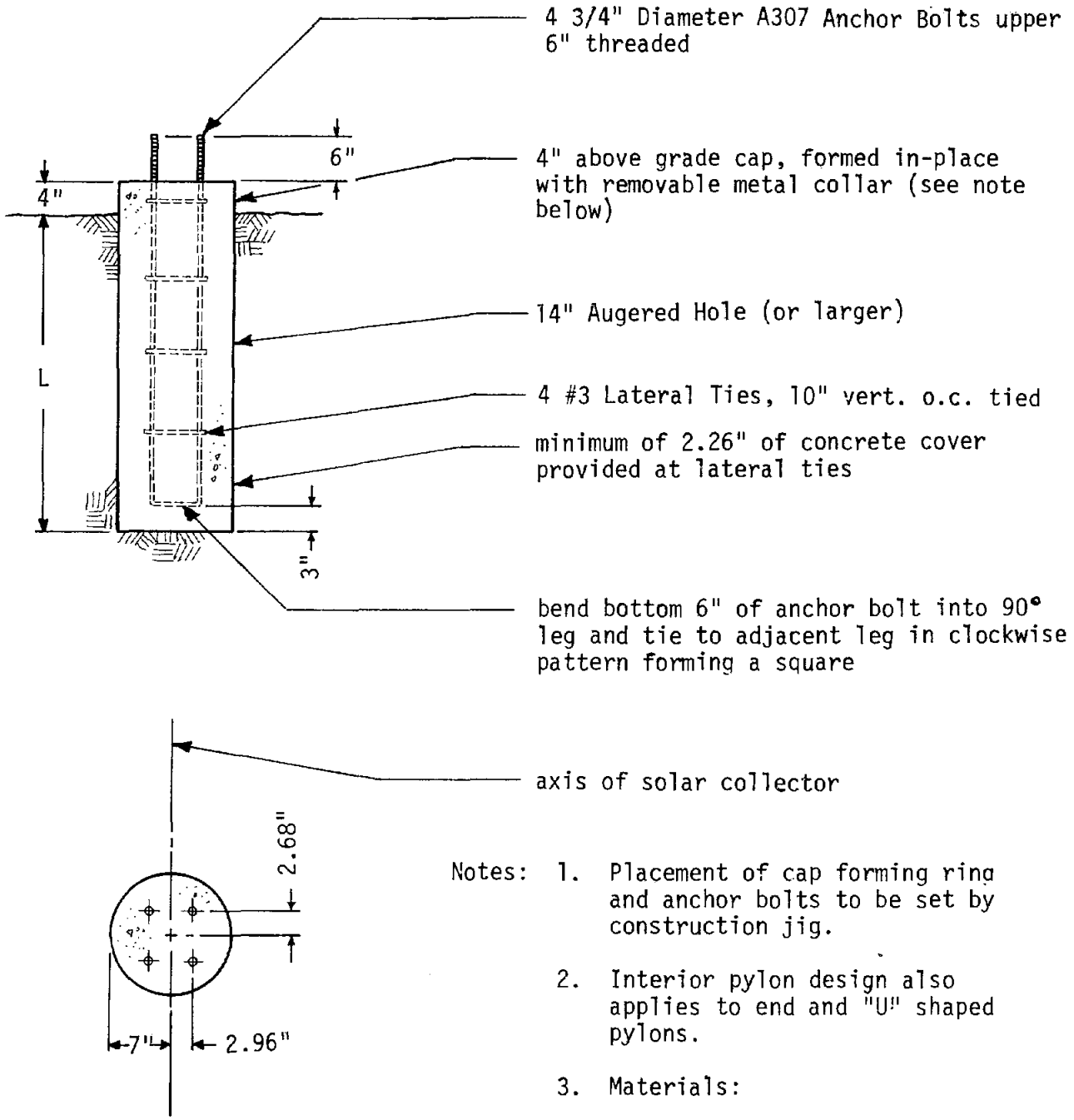

Notes:

1. Placement of cap forming ring and anchor bolts to be set by construction jig.
2. Interior pylon design also applies to end and "U" shaped pylons.
3. Materials:

   concrete: 3,000 psi
   steel: 50,000 psi
   bolts: A307

BDM/A-82-458-TR-R1

Figure VI-14. Solar Collector Interior Pylon (from Merkle, Reference VI-4)

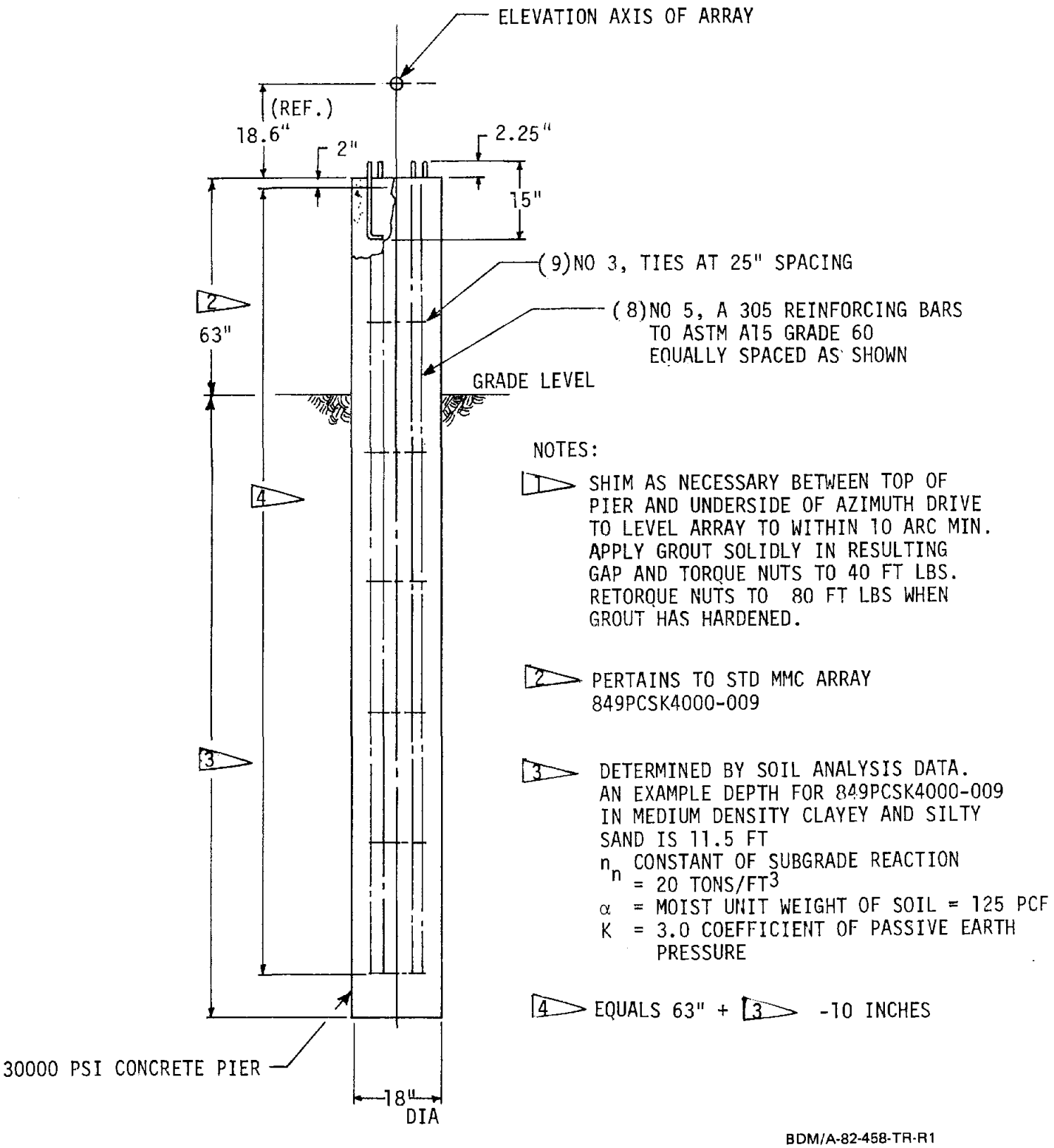

Figure VI-15. Martin Marietta Foundation Pier

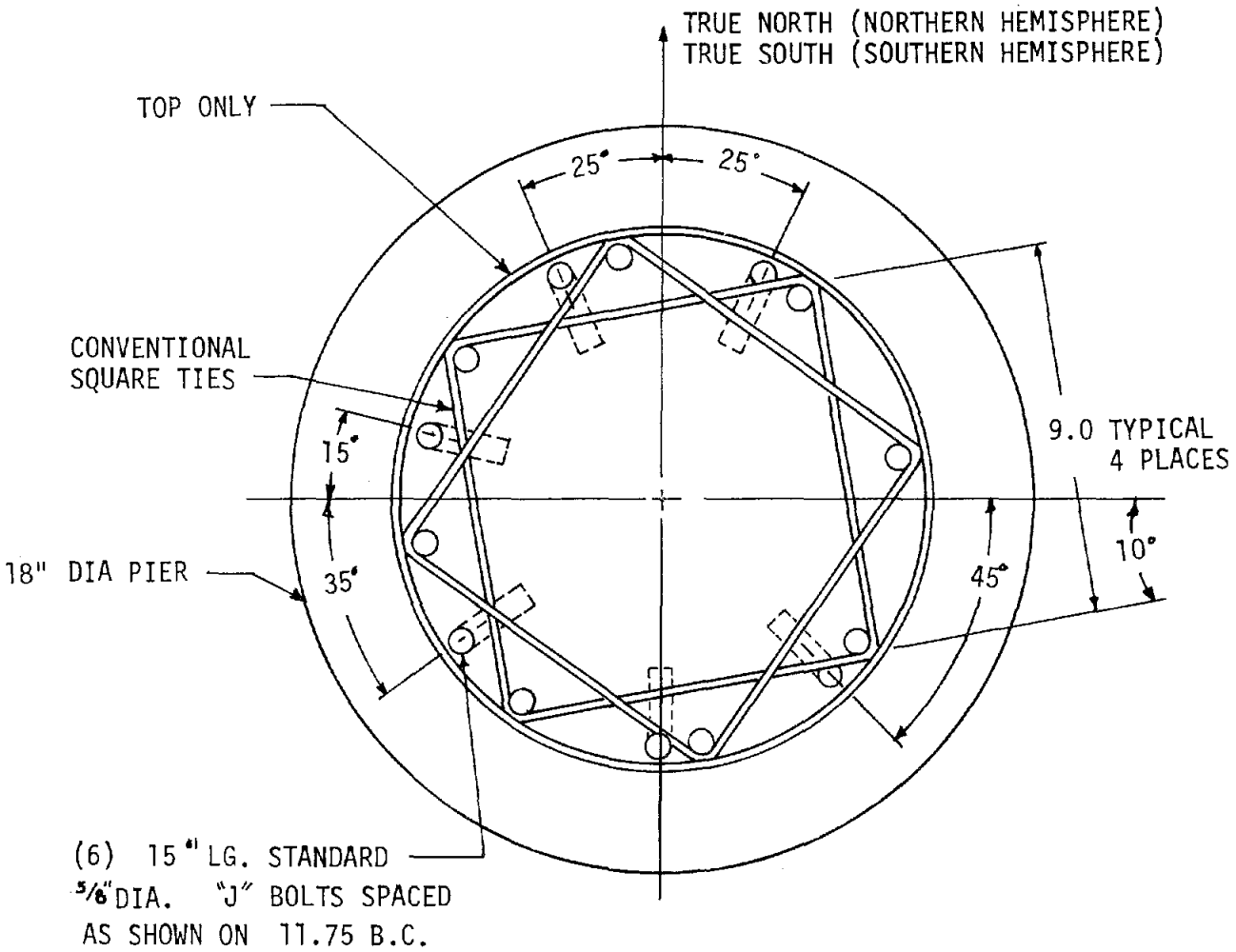

BDM/A-82-458-TR-R1

Figure VI-16. Layout of "J" Bolts and Reinforcements

LINEAR FOCUS TWO AXIS TRACKING
SOME TYPICAL E-SYSTEMS FOUNDATIONS*
(ADJUST TO SOIL TYPE LOCALLY)

SOIL STATUS	BEARING CAPACITY (PSF)	LATERAL PASSIVE (PSF)	TOTAL PIER LENGTH (1) (INCLUDES CAP)
GOOD	4000	200	6-1/2 Feet (1.98 m)
AVERAGE	2500	150	7-1/2 Feet (2.3 m)
POOR	1500	100	8-1/2 Feet (2.6 m)

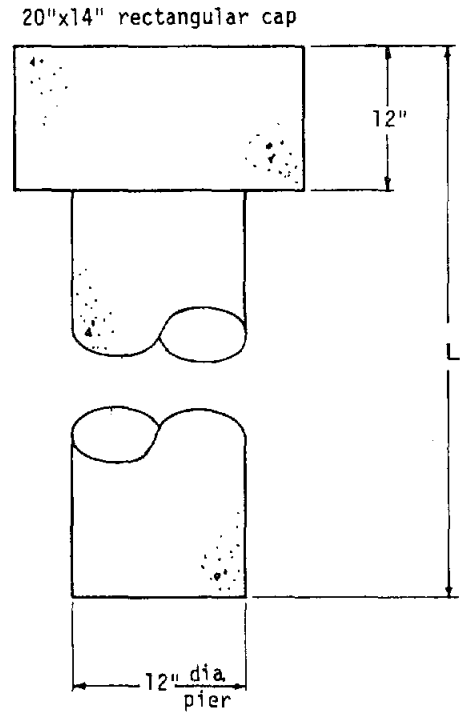

4 J Bolts for studs 7". into cap approx.

reinforcing steel 4 vertical #4 bars on 3" radius about center of pier
ties #3 12" apart

FROM VERNON GOLDBERG E-SYSTEMS STRUCTURAL GROUP

PERSONAL COMMUNICATION (APRIL,6 1982)

BDM/A-82-458-TR-R1

Figure VI-17. Linear Focus Two-Axis Tracking Foundation

sample foundation designs shown in figure VI-17. The soil status indicated apparently relates to soil types previously shown in figure VI-6. The rectangular cap shown is to be poured monolithically with the rest of the pier.

Goldberg indicates that a cost tradeoff study is desirable to show whether the cap is better than using a greater diameter pier and maintaining a continuous cross-section to avoid the hand labor of excavating for the oversize rectangular cap.

6. Alternative Approaches to and Solutions for the Structure and Foundation Problem

Figure VI-5 (last column on the right) cautions against misapplication of piers. Certainly, caution is indicated under circumstances where expansive soils may be encountered (e.g., reference the earlier discussion of Johnson and Johnson, Sherman, Texas installation).

Pier design codes have been developed and may prove to be an aid to foundation design (ref. VI-20). Dunder (ref. VI-21 and VI-22) specifically points out the advantages of the Pier Analysis and Design for Lateral Loads (PADLL) code for piers employed with second generation heliostat systems. The PADLL code is based on the subgrade modulus model shown in figure VI-18. This figure VI-18 is taken from Volume 1 of the GAI study for the Electronic Power Research Institute (EPRI) and the Sandia National Laboratories (Livermore). The model is for multilayered soils and takes into account the highly nonlinear load-deflection relationship for laterally loaded drilled piers.

The designer of structures and foundations for PV-T systems has a variety of options and calculational tools to apply in arriving at reliable and cost effective solutions.

E. GUIDELINES AND SUGGESTIONS FOR ADDITIONAL INVESTIGATION

This section now concludes with design guidelines of structures and foundations for PV-T systems (figure VI-19), and an enumeration of areas deserving additional investigation (figure VI-20). Figure VI-19 provides

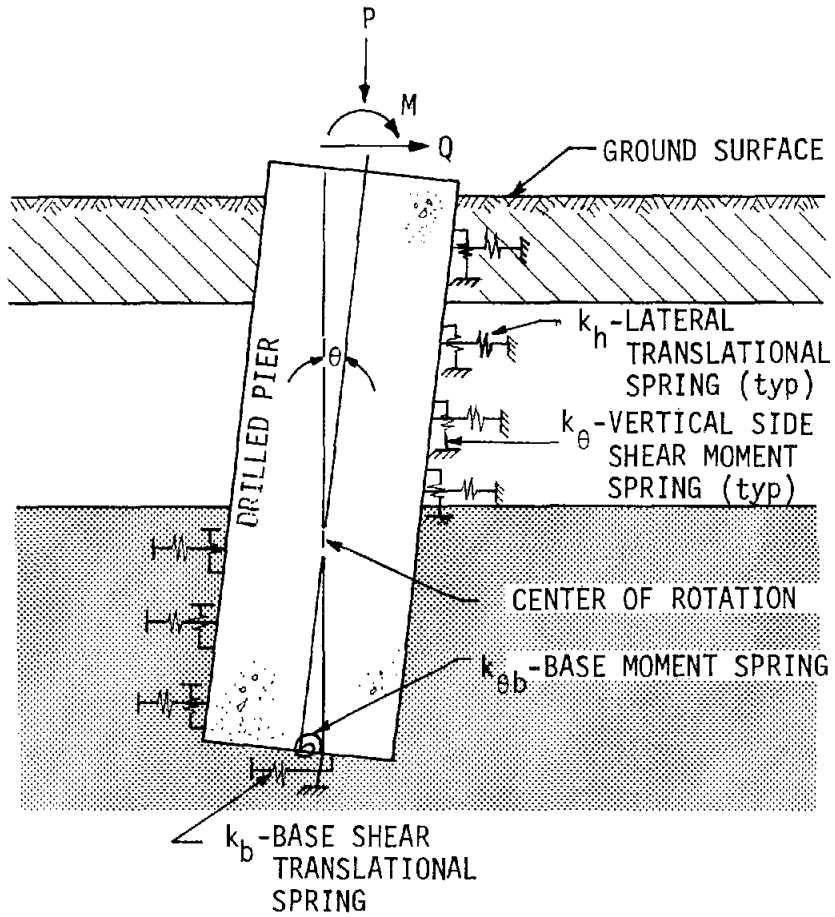

BDM/A-82-458-TR-R1

Figure VI-18. Four-Spring Subgrade Modulus Model (from GAI, Reference VI-18)

SOME GUIDELINES FOR DESIGN OF STRUCTURES AND FOUNDATIONS

- TAKE INTO ACCOUNT STRUCTURES' AND FOUNDATIONS' ASPECTS "UPFRONT" IN CONCEPTUAL DESIGN OF SYSTEM
- PERFORM AN ADEQUATE SOIL SURVEY AND NOTE EXPERIENCE WITH NEARBY FOUNDATIONS AND STRUCTURES. IF DISTRESS IS NOTED, ASCERTAIN WHY
- INVESTIGATE APPLICABILITY OF A BERM OR FENCE TO REDUCE COST OF STANDARDIZED DESIGN AND TO PROVIDE SECURITY
- PROVIDE A CLEAR AUDIT TRAIL FOR ALL WIND LOAD CALCULATIONS
  - — CLEAR ASSUMPTIONS CLEARLY STATED AND JUSTIFIED. EXAMPLES: NO HAZARD TO PERSONNEL — GROUND-MOUNTED 25-YEAR RECURRENCE 80-MPH WIND AT 10-METERS ELEVATION. SCALED TO ELEVATION OF INTEREST BY 1/7 POWER RULE
  - — WIND LOAD CALCULATIONS CLEARLY NOTED AND DEFENDED FOR LOCAL SITE CONDITIONS. IF BOULDER, COLORADO, IS SITE, PROPERLY ADJUST WIND VELOCITIES
  - — QUESTION AND REVALIDATE THE "OBVIOUS". EXAMPLE: LOCAL CONDITIONS MAY CAUSE WIND LOADING (AS BY VORTEX SHEDDING) MORE SEVERE INTERNAL-TO-ARRAY THAN EXTERNAL
  - — RELATE LIFT, DRAG, AND MOMENT COEFFICIENTS

    I.E. $C_l = 0.5$ (LIFT)
    $C_d = 0.5$ (DRAG)
    $C_\theta = 0.1$ (MOMENT)

    TO THE SPECIFIC CONDITIONS, FOR EXAMPLE
    - PARABOLIC TROUGHS (GIVE ASPECT RATIO)
    - 1.5-METERS ELEVATION
    - NO GUST FACTOR
    - PROTECTED BY WIND SCREEN
    - BASED ON CSU TESTS AND INTERPRETATION
- EVALUATE A VARIETY OF FOUNDATIONS APPROPRIATE TO LOCAL CONDITIONS OF SOIL AND LOCAL CONSTRUCTION CAPABILITIES AND COSTS AND ESTIMATED ELASTIC AND INELASTIC DEFORMATIONS
  - — PIERS IN SAND, GRAVEL, AND CLAY; DRILLED, RIGID, PROPERLY REINFORCED
  - — PIERS INAPPROPRIATE OR AT LEAST QUESTIONED FOR EXPANSIVE CLAYS, PEAT, ROCK, AND BOULDERS
  - — NEED GOOD LOAD TRANSMISSION FROM PIER TO PYLON! TESTS SHOW WEAKNESSES IN STANDARD CONNECTION DESIGN
- RELATE TO LOCAL AND NATIONAL CODES/ ORDINANCES AND EXPERIENCE AND APPROPRIATELY JUSTIFY DEVIATIONS
- MONITOR CONSTRUCTION TO GET WHAT THE DESIGN SPECIFIED

BDM/A-82-458-TR-R1

Figure VI-19. Some Guidelines for Design of Structures and Foundations

AREAS DESERVING ADDITIONAL INVESTIGATION

- WIND GUSTS AND DYNAMIC DESIGN OF FOUNDATIONS AND STRUCTURES
  - — RELEVANCE OF EXISTING DATA
  - — GAPS AND CRITICALITY OF GAPS
  - — PROCESS TO FILL GAPS
  - — DYNAMIC DESIGN OF COMPONENTS AND SYSTEMS
- STRUCTURAL AND FOUNDATION SYSTEMS DESIGN LIFE AND DEGRADATION
  - — VIBRATION CYCLES
  - — FATIGUE
  - — CORROSION AND CORROSION PREVENTION
  - — MONITORING AND MAINTENANCE
- COST TRADE-OFFS AND LIFE CYCLE COSTS OF STRUCTURES AND FOUNDATIONS
  - — INITIAL VERSUS LIFE CYCLE SAVINGS
  - — COST DRIVERS
  - — COST REDUCTION
- OBSERVATION/INSTRUMENTATION OF FOUNDATIONS AND STRUCTURES OF EXISTING SYSTEMS TO DETERMINE
  - — OVERDESIGNED AND UNDERDESIGNED COMPONENTS AND SYSTEMS
  - — DESIGN ADEQUACY
  - — RISK FACTORS AND POTENTIAL FOR RISK REDUCTION IN FUTURE EFFORTS
  - — RESPONSE CHANGES WITH RESPECT TO TIME
  - — RECURRING COSTS ASSOCIATED WITH "AS-CONSTRUCTED" FOUNDATION AND STRUCTURE
- FOUNDATION AND STRUCTURAL COSTS VERSUS TYPE OF PV-T SYSTEM
  - — SINGLE-AXIS TRACKING LINEAR PARABOLIC TROUGH
  - — TWO-AXIS TRACKING
    - LINEAR FOCUS FRESNEL
    - POINT FOCUS FRESNEL

BDM/A-82-458-TR-R1

Figure VI-20. Areas Deserving Additional Investigation

a quick reference for the designer of future PV-T systems. Consider structural and foundation problems early in the conceptual design process, in addition to establishing soil conditions. Know the assumptions behind the wind loadings being used. Do not use lift, draft, and moment coefficients without checking their origin and range of applicability (audit trail). Are they applicable to the situation under study? Don't ignore building codes. Inspect and monitor construction to ensure quality.

Figure VI-20 reveals some knowledge gaps that may cause the designer difficulty. The subject of wind gusts and dynamic design of wind-loaded structures needs additional investigation to provide a rational basis for design. Fatigue and corrosion of wind loaded structures can shorten their useful lives and cause maintenance problems. Costs must be controlled, and in order to control costs on future PV-T structures and foundation systems, it is necessary to document and learn from previous mistakes. And finally, the cost relationships for foundations and structures of the various PV-T alternatives must be carefully considered.

REFERENCES

VI-1. Reed, Theodore H., "Phylons," pages 255-264 in Proceedings of the Line Focus Thermal Energy Technology Development Seminar, Sandia National Laboratories, Albuquerque, September 9-11, 1980. Project Integration Meeting, SAND82-0239, Sandia National Laboratories, Albuquerque, NM, January 27-28, 1982.

VI-3. Broadbent, Sidney, "Second Generation Photovoltaic Array by Martin Marietta Corporation, pages 125-134 in Proceedings of the Photovoltaic Concentrator Technology Eighth Project Integration Meeting, SAND82-0239, Sandia National Laboratories, Albuquerque, NM, January 27-28, 1982.

VI-4. Merkle, Douglas H., Full Scale Load Tests of Experimental Solar Collector Foundations, Sandia National Laboratories SAND80-7076, June 1981, 109 pages.

VI-5. Bechtel National, Inc. (N. F. Somes), Wind Design of Flat Panel Photovoltaic Array Structures, Sandia National Laboratories SAND 79-7057, Albuquerque, June 1980.

VI-6. American National Standards Institute, Building Code Requirements for Minimum Design Loads in Buildings and Other Structures, ANSI A58.1-1972, New York, ANS Institute, 1972.

VI-7. American National Standards Institute, Minimum Design Loads for Buildings and Other Structures, ANSI ANSI draft A58.1-1981, New York, ANS Institute, July 1981.

VI-8. Alexander, Graham, Gerry Noel and Don Carmichael, of Battelles Columbus Laboratories, "Photovoltaic Concentrator Array Field Optimiztion and Modularity Study," presentation at Photovoltaic Systems and Applications Project Integration Meeting, Albuquerque, February 9-11, 1982.

VI-9. Randall, Duane, E., "Wind Load Definition for Line-Focus Concentrating Solar Collectors, pp.231-246, in Proceedings of the Line-Focus Solar Thermal Energy Technology Development, Sandia National Laboratories, Albuquerque, September 1980.

VI-10. Randall, D. E., D. D. McBride, and R. E. Tate, "Mean Wind Loading on Parabolic Trough Solar collectors," Journal of Solar Energy Engineering, Vol. 103, November 1981, pp. 313-322.

VI-11. Peterka, J. A., J. M. Sinou, and J. E. Cermak, Mean Wind Forces on Parabolic - Trough Solar Collectors, Sandia National Laboratories SAND80-7023, Albuquerque, May 1980, 109 pages.

VI-12. Peterka, J. A., J. J. Lou, and J. E. Cermak, Wind Tunnel Test of a Photovoltaic Concentrator Array, by Colorado State University for Martin Marietta, CER78-79 JAP-JJL-JEC62, June 1979, 34 pages.

VI-13. Goldberg, Vern E., E-Systems, Dallas-fort Worth, Personal Communication, April 6, 1982.

VI-14. Murphy, L. M., An Assessment of Existing Studies of Wind Loading on Solar Collectors, Solar Energy Research Institute (SERI) TR-632-812, Golden, Colorado, February 1981, 36 pages.

VI-15. Maish, Alexander, "Concentrator Array Development Status," pages 174-179 in Proceedings of the Photovoltaic Concentrator Technology Eighth Project Integration Meeting, SAND82-0239, Sandia National Laboratories, Albuquerque, NM, January 27-28, 1982.

VI-16. Auld, H. E., and P. F. Lodde, Study of Low-Cost Foundations/Anchor Designs for Single-Axis-Tracking Solar Collector Systems, Sandia National Laboratories, SAND 78-7048, Albuquerque, January 1979.

VI-17. Auld, H. E., and P. F. Lodde, Study of Foundation Designs for Single-Axis-Tracking Solar Collector Systems Under Reduced Loading Conditions, Sandia National Laboratories, SAND 79-7016, Albuquerque, May 1979, 21 pages.

VI-18. Auld, Harry E., "Foundations for Line Focusing Solar Colelctors," pages 247-254 in Proceedings of the Line - Focus Thermal Energy Technology Development Seminar, Sandia National Laboratories, Albuquerque, September 9-11, 1980.

VI-19. Auld, H. E. and J. B. West, Solar Collector Foundation Designs, Sandia National Laboratories, SAND80-7070, Albuquerque, September 1980, 32 pages.

VI-20. GAI Consultants (H. L. Davidson), Laterally Loaded Drilled Pier Research (Volume 1 - Design Methodology and Volume 2, Research Documentation), Electric Power Research Institute EPRI EL-2197 Palo Alto, January 1982.

VI-21. Dunder, V. D., "Analysis and Design Modification of Second Generation Heliostat Foundations Using Program PADLL (Pier Analysis and Design for Lateral Loads), Memorandum, Sandia National Laboratories, Livermore, California, March 11, 1982.

VI-23. American Concrete Institute (ACI), "Suggested Design and Construction Procedures for Pier Foundations (ACI335.3 R-72),

from ACI Manual of Concrete Practice, Part 4, published by ACI, Detroit, 1980.

VI-24. Cattaneo, Luis, J. R. Harris, T. A. Reinhold, E. Simiu, and C. W. C. Yancey, Wind, Earthquake, Snow, and Hail Loads on Solar Collectors, NBSIR81-2199, National Bureau of Standards, Washington, D.C., 1981.

VI-25. Edwards, Brian, "Collector Deflections Due to Wind Gusts and Control Scheme Design," Journal of Solar Energy, Vol. 25, pp. 231-234, Pergamon Press, 1980.

VI-26. Franklin, H. A., Bechtel Group Inc., Letter to David Hughes, Martin Marietta regarding Foundation Designs in "Integrated Structure Designs of Photovoltaic Arrays," Sandia Contract No. 62-9877, March 2, 1982.

VI-27. Miller, Ronald D., and Donald K. Zimmerman, Wind Loads on Flat Plate Photovoltaic Array Fields (Nonsteady Winds), Phase IV Final Report, DOE/JPL 954833-81/4 for Jet Propulsion Laboratory by Boeing Engineering and Construction Company, Pasadena, CA, August 1981.

VI-28. Miller, Ronald, and Donald Zimmerman, Wind Loads on Flat Plate Photovoltaic Array Fields, Phase II Final Report DOE/JPL 954833-79/2 for Jet Propulsion Laboratory by Boeing Engineering and Construction Company, Pasadena, CA, September 1979.

VI-29. Miller, Ronald D., and Zimmerman, Donald K., Wind Loads on Flat Plate Photovoltaic Array Fields, Phase III Final Report, DOE/JPL 954833-81/3 for Jet Propulsion Laboratory by the Boeing Engineering and Construction Company, Pasadena, CA, April 1981.

VI-30. Monument Solar Corporation, "A High Temperature Process Steam Application at the Southern Union Refining Company, Hobbs, NM (Solar Energy in the Oil Patch), Final Report Contract # EM-78-C-03-2223, Dallas, TX.

VI-31. Peck, Ralph B., W. E. Hanson, and T. H. Thornburn, Foundation Engineering, Second Edition, John Wiley, New York, 1974.

VI-32. Poreh, M., J. A. Peterka, and J. E. Cermak, Wind-Tunnel Study of Wind Loads on Photovoltaic Structures - Phase II (Draft) by Colorado State University for Bechtel National, Inc., Fort Collins, Colrado, 1981, 47 pages.

VI-33. Tieleman, H. W., R. E. Akins, and P. R. Sparks, An Investigation of Wind Loads on Solar Collectors, by Virginia Polytechnic Institute and State University for U.S. Department of Commerce, Blacksburg, VA, January 1980, 155 pages.

VI-34. Tschebotarioff, Gregory P., Fondations, Retaining, and Earth Structures, Second Edition, McGraw-Hill, New York, 1973.

VI-35. Wang, C. and Charles G. Salmon, Reinforced concrete Design, Third Edition, Harper and Row, New York, 1979.

CHAPTER VII
INSTITUTIONAL ISSUES

In the previous chapters, we have discussed various technical issues associated with designing and installing a PV-T system. In addition to the technical components, the engineer must be aware of other aspects of a solar system that may have a bearing on the system design and economics. Considerations include the legal, environmental, and economic issues associated with utility interfacing and sellback of excess electrical energy. Safety is a technical issue which also must be considered in the system design. Various aspects of electrical and mechanical safety were discussed in previous chapters; however, there are certain specific safety problems associated with concentrating solar collectors which will be addressed. These solar related issues are discussed in the following sections.

A. LEGAL ISSUES

1. Guaranteed Solar Access

Solar collectors need sunlight to function. There is presently no right to sunlight in the United States when the needed light passes across property owned by others before reaching the user. Very little empirical evidence exists as to whether structure shadows on collectors will be a major problem to a developing solar industry. Two rather limited studies (ref. VII-1 and VII-2) using aerial photographs, indicated that shadowing may not be a problem in suburban areas, and that the issue of solar rights may have been over-emphasized. Commercial and industrial buildings, however, are generally located in urban areas where new structures are constantly being erected and others torn down. In a more crowded and less static environment, a guaranteed access to sunlight for the life of a proposed solar system may be an essential element to its realistic economic evaluation.

Guaranteed solar access can be obtained through a number of legal means including prescriptive easements, nuisance laws, express easements, transferable development rights, restrictive covenants (equitable servitudes), zoning and land use planning.

A recent review of these methods (ref. VII-3) indicated that, for a solar retrofit, an express easement would provide the most security. Easements are limited rights to use the land owned by another. In an "express" easement, two parties (in this case, one owning the land and the other wishing sunlight to flow unhindered across the land) voluntarily and intentionally bargain for the right. Express easements for receiving light are recognized by the courts and are available in most states. Unless otherwise stated in the original contract, an easement binds all subsequent owners of either property. The limitations of an express easement are its voluntary creation and its possible cost. An owner of "burdened" who never intended to build an interfering structure may ask for an exorbitant price not to build.

The benefits are creation without government action, application to established areas, and permanence not found in easily changed zoning laws. Industries located on presently rural sites may use express easements to protect their collectors from future developments. This protection might include restriction of corrosive or clinging emmissions by a future neighbor industry as well as guaranteed solar access.

Restrictive covenants, promises involving land usually found in deeds, can protect solar access in new industrial parks. These cost nothing, and do not require an individual property owner to draw up legal documents since they are only applicable to new developments.

Several legal experts feel that zoning is the most practical method of guaranteeing solar access (ref. VII-4). Zoning can be exercised at the local or state level, can apply to new or existing structures, and is relatively inexpensive. Compensation is awarded to a party who loses property as a result of zoning ordinances, but the public usually provides the money. Zoning boards, however, are notoriously influenced by local politics, and zoning ordinances can be changed by

local authorities if there are no restrictions in the enabling legislation. Zoning may be most effectively used to protect the solar access of a publicly-owned building, such as a school or community hospital. Zoning does not necessarily provide the permanence of express easements and restrictive covenants.

Industries and commercial establishments located on rented property or in rented buildings must depend upon their landlord to guarantee their solar access. Neither express easements nor restrictive covenants directly involved tenants. The landowner makes the bargain or signs the deed. Zoning ordinances affect rental property and may be the only method of protection available to the longterm leaseholder with an uninterested or uncooperative landlord. Leasing agreements can be written to cover solar access. Obstruction of light can be grounds for releasing the tenant or can lead to payment of damages if these were specified in the contract.

Several state and local governments have recently enacted solar rights laws in various forms. The effectiveness of these laws remains to be tested. A controversial example is the New Mexico Solar Rights Act of 1977. This legislation establishes as a property right, the right to an unobstructed line-of-sight path from a solar collector to the sun. Any disputes are to be resolved by applying the concepts of "beneficial use" and "prior appropriation." The values of varying benefical uses are not defined, allowing "first in time" to establish the priority of use. Legislation of this type may not protect an industrial application if the value of benefical use is quantified and used to establish priority at a later date.

2. Building Codes

Building codes may be a barrier to the construction of a photovoltaic-thermal system. There are three widely adopted model building codes:

(1) The Basic Building Code of the Building Officials and Code Administrators, International (BOCA), found mainly in the East and Midwest.

(2) The Uniform Building Code of the International Conference of Building Officials (ICBO), found mainly in the West.

(3) The Standard Building Code of the Southern Building Codes Conference (SBCC), found mostly in the South.

Local governments usually base their building codes on one of these models but may modify the code to meet local conditions. None of the codes currently deals with solar collectors. The model code organizations have teamed together and drafted a model code on solar heating and cooling of buildings (ref. VII-5) which is in the review process. Several states have added solar provisions to their building codes. These provisions usually require building orientations favorable to solar heating and cooling but do not supply specification or performance standards for solar systems.

Once the electricity is generated and the thermal energy collected, it is transported, stored, and utilized by means used in conventional energy systems and covered by the codes. Pipes, ducts, valves, storage tanks, controls, wiring, storage batteries, etc., are covered in the codes, but their use in a photovoltaic-thermal system may be novel. Use of materials, equipment, and methods not covered by the codes requires demonstration that the new technology is equivalent to that specified in the codes in strength, fire resistance, durability, quality, effectiveness, and safety. The first step toward meeting these six criteria for solar systems is the establishment of certification programs. At present, two organizations, the Air Conditioning and Refrigeration Institute and the Solar Rating and Certification Corporation (SRCC) are establishing solar certification programs (ref. VII-6).

The SRCC plans to publish a directory of certified solar equipment in 1982. Collectors will be rated based on Standards 93-77 and 96-80 of the American Society of Heating, Refrigeration, and Air Conditioning Engineers. Two certification programs, however, may complicate approval of solar applications. A building official unfamiliar with solar technology may find differences between the certification programs sufficient reason to question an entire system. He may require testing

of components, at the applicant's expense, by approved testing facilities (chosen by the official) using approved methods (again chosen by the official when not specified in the codes). The lack of specification or performance standards gives the building official discretionary powers which can easily delay permit approval and increase the expense of a solar system, or actually prevent an application.

The solar industry has not reported any particular code impediments, but there have not been a large number of commercial or industrial applications. As more systems are built, the overlap of traditional jobs involved in solar applications (roofers, electricians, plumbers, glazers, etc.,) may lead to labor unions using strict code enforcement as a tool while settling disputes. This problem can be overcome on a particular job by thoughtful negotiation with all unions involved before construction begins, and with careful specification of construction responsibilities. If solar construction has already become a sensitive issue in a unionized location, solar applications may have to wait until the jurisdictions have been established.

The building codes may represent a specific problem to commercial and industrial solar retrofit applications. There can be retroactive application of current standards to older buildings in retrofit situations. The costs of meeting current standards will have to be included in any analysis of the total cost of a solar system. In particular, current fire safety standards may include automatic sprinkler systems. A commerical solar retrofit using a flammable heat transfer fluid could require an upgraded sprinkler system. Roof-mounted retrofits may be rejected under the Standard Building Code because an existing building cannot be increased in height unless the entire structure is altered to meet the code under the Uniform Building Code, because there is a twelve-foot height restriction, or under the Basic Building Code because glass or plastic panels may be interpreted as being similar to skylights, which must be wire impregnated and not more than 48 inches in any dimension. Local building ordinances may also contain height limitations.

In addition to building codes, compliance with the National Electric Code will be an overriding concern during both design and installation of photovoltaic systems, although the code does not directly address photovoltaic panels. Sections covering photovoltaic systems are being developed, and are expected to be included in the 1984 version of the National Electric Code. Areas of special concern during design include lightning protection, ground fault interrupters, isolation of all live electrical parts, and grounding of the inverter, power conditioning equipment, and all exposed metal parts (ref. VII-7). Since live parts operating at 50V or more shall be guarded against contact during installation, and photovoltaic panels can be active during daylight installation periods, special installation requirements will have to be developed.

A general review of municipal-level building codes is not possible given the variations that exist. It will be necessary to review local ordinances before designing any site-specific solar application.

3. Liability and Insurance

Designers of PV-T systems, manufacturers of system components, retailers of components, and contractors who install the systems, are required to use reasonable care in design, manufacturing, testing, and distribution of their products. They are required to incorporate available safety devices into their products and to provide adequate warnings of hazards associated with their products. They are also required to furnish adequate installation and instructions for use of their product. If injury to a person or damage to property results from the installation or use of their product, they may be held liable. The theories of product liability that may be applied to solar systems are:

(1) strict liability
(2) express warranty
(3) implied warranty
(4) negligence
(5) misrepresentation

The current lack of standards and codes for solar components and systems and the limited experience with operating systems, makes it difficult to determine what is reasonable, available, and adequate. This general lack of experience and certainty affects the cost and availability of product liability insurance. Coverage is available as part of the comprehensive general liability policies held by businesses. The cost of that coverage is currently based on an estimate of risk derived from similar products and ultimately, on the carrier's judgment. Insurance costs will be adjusted to reflect actual risk as experience is gained.

It should be noted that some states currently require product warranties for solar components used if solar systems are to qualify for tax incentives and rebates. A recent study of solar components warranties found them to be in violation of applicable federal law and, in some cases, subjecting manufacturers to excessive liability (ref. VII-8). This type of problem may unfavorably affect insurance rates in the near future.

Professional liability insurance, like product liability insurance, will be affected by the untried nature of PV-T systems. Since no increase in professional liability insurance has been experienced by professionals involved in the design of solar thermal systems, it is reasonable to assume that an undue burden will not be placed on those designing PV-T systems. If, however, these systems present problems, rates will rise.

The owner/operator of a PV-T system is also liable for property damage and personal injury that might be caused by their system. In this area, there are differences between the way industrial and commercial systems will be handled. Many industrial plants currently generate a portion of the electricity they use. Commercial buildings, as a rule, do not, although some hospitals do have emergency generators. Insurance companies can draw upon a related experience and existing data in determining rates for industrial PV-T systems. The only area which might cause concern is the utility interface. The possibility exists for injury to utility line workers when the utility owner is down and the

photovoltaic system continues to feed into the grid. Insurance for commercial applications may be more complicated.

Commercial buildings are usually accessible to a larger number of people who would legally be classified as invitees (persons invited onto the property, including customers to retail stores and service establishments, students and teachers in schools, patients and medical professionals in hospitals, office workers and their clients in office buildings, etc.). An owner must warn invitees of any dangerous conditions and take positive actions to protect invitees from injury. Commerical establishments, in general, have less experience than industrial facilities in isolating and monitoring hazardous substances and equipment. The public ownership of many commercial buildings being considered for photovoltaic applications is another complicating issue. Liability insurance will probably be available as an extension of existing coverage. The carrier is likely to review safety features of the system and to investigate fully the utility interface. If experience shows liability to be high, a rider to the basic policy may be used in the future.

Both commercial and industrial systems will also require insurance against loss. Well-engineered systems with approved electrical and structural components should be insurable at rates comparable to building insurance. Stand-alone systems with no utility back-up would require insurance against downtime, which may be more difficult to obtain. The long-term effects of corrosion on industrial systems may affect insurance rates in the future.

B. ECONOMIC ISSUES

1. Tax Incentives

Tax incentives for solar energy outlays are constantly changing. Federal tax credits have not changed in the last year, but are currently being questioned in public statements concerning the Federal budget. Of the 13 Western states, seven modified their 1980 solar use

incentives in 1981. Each state has its own solar legislation. Local incentives, such as favorable industrial bond treatment, must be considered on a site-specific basis. In determining how tax incentives will influence the cost of a PV-T system, time and site must be considered.

At least one firm, Solar Energy Products, Inc., has found current tax laws to offer tax write-offs as high as 93 percent, and typically 81 percent. Their analysis of applicable tax laws showed that a corporation in the 50 percent marginal income tax bracket is entitled to depreciation allowances and credits which equal deductions equivalent to $40,714 on the purchase of a $50,000 solar system, and 81 percent effective write-off in the first year. Their data indicate that solar energy systems are a good tax shelter and a cost effective business investment (ref. VII-9).

Clearly, tax incentives will strongly influence the actual cost of PV-T systems, but there are other factors to be considered. Not all industries are in need of tax shelters and the variable nature of the legislation may mean that the effective write-off is reduced between the decision to design a system and its construction.

2. Investment Criteria

There has been little incentive for an industrial plant manager or commercial business manager to invest in a PV-T system, even when it could be shown that a solar system was competitive with conventional systems on a life-cycle basis. The availability of investment capital and the high cost of capital are major concerns to industry and commerce. Investments must meet stringent pay-back criteria, often of 3 to 5 years or less (ref. VII-10). Solar technologies require high front-end investments, and benefits are only apparent when life-cycle cost accounting techniques are used, rather than the usual industrial practice of required payback period.

Plant managers and business executives are accustomed to purchasing energy on an annual basis with minimal front-end investment costs. Methods of financing solar systems which provide a market

mechanism to make this possible, may side-step the payback criteria hurdle. A study of financing options showed that both conventional leasing and solar management company/limited partnership arrangements have advantages (ref. VII-11). Leasing does not require a large initial capital investment by the system user. The lessor has investment tax credits and accelerated depreciation benefits which may be passed on to the lessee in the form of low rents, while the lessee's payments are directly tax deductible. Solar management company/limited partnership agreements (currently used to finance commercial buildings and other large construction projects) have similar advantages to leasing in that the user is not responsible for purchasing equipment. The user pays only for delivered energy, which is a tax deductible expense. This type of arrangement will require some government assistance to attract equity investors. Legislation would be necessary to exempt investments in industrial or commercial solar systems from the at-risk provision in present U.S. tax law, but a precedent has been established in the current exemption for real estate investments.

Other legal actions could favorably influence solar economics. Conventional fuel sources, particularly coal, natural gas, and heavy fuel oil, are often still inexpensive enough to render solar energy noncompetitive even on a life-cycle cost basis. The cost of fossil fuel and purchased electricity is tax deductible as a business operating expense. Similar amounts of energy from an onsite PV-T system or from the conservation efforts likely to accompany solar installations are not. Establishing solar-derived energy on equal tax terms with conventional fuels would improve the economic comparisons.

3. Prototype Nature of Photovoltaic Systems

PV-T systems are new, and lending institutions have no history on which to base risk evaluations. The system's depreciation value, resale value, salvage value, and useful life, are all important considerations and all will be difficult to quantify. For example, if the technology is sound, the resale value may be higher than initial costs, but a component failure or a corrosive environment may greatly reduce useful

life. Each PV-T system is likely to be a unique investment risk for a lending institution. The conservative nature of lending practices may lead to stringent terms.

C. UTILITY INTERFACE

The utility interface has been given the status of a separate institutional issue. It represents an area of considerable economic importance with unsettled legal questions and definite need for further technical development. Financial considerations of PV-T energy systems usually depend upon selling excess generated electricity to a public utility. The Public Utilities Regulatory Policies Act (PURPA) requires electric utilities to interconnect with independent producers, and to purchase power generated by the independent producer at the highest rate which does not discriminate against its current customers. This act is believed by many to guarantee a market for excess electricity generated on weekends and holidays when a commercial or industrial facility will not use its full photovoltaic potential.

A recent Supreme Court decision upheld the constitutionality of the PURPA, challenged in a Mississippi State court one year ago. Principal to the decision for renewable energy interests was the unanimous support of the controversial Section 210, which mandates utilities to interconnect and pay reasonable "avoided-cost" rates for electricity produced by small, independent power producers.

Problems with utility interface are not uniform nationwide. Some utilities have encouraged independent power generation and have cooperated in a very positive manner with commercial and industrial PV-T facilities. Part of the utilities' reluctance to interface with independent power generators may be attributed to unresolved technical issues. There has been a limited amount of effort devoted to understanding and resolving the technical issues of widespread photovoltaic integration and even less effort devoted to understanding the ways in which photovoltaic systems will interact with other distributed

generation devices, such as windmills. The major areas of concern identified in a recent comprehensive review of distributed photovoltaic systems were (ref. VII-12):

1. Protection

To minimize damage and risk of injury and to ensure reliability of service, guidelines for overvoltage, overcurrent, and over- and underfrequency protection of the power conditioning subunit and the utility need to be estabilished. Some guidelines on protection requirements for dispersed independent generators have been formulated by individual utilities, but these guidelines are general and may not be sufficient if multiple generators interconnect with the utility.

2. Stability

Initial studies with individual photovoltaic systems indicate source stability (ability to maintain synchronous operation after a disturbance) problems. The impact of multiple photovoltaic interconnections on bulk system stability can be predicted using existing techniques, but this has not yet been done.

3. System Unbalance

Single-phase photovoltaic systems may accentuate unbalances in system voltage and current. Allowable voltage unbalance is approximately 2 percent. The procedures to calculate unbalances are available, but the necessary inputs such as phase and line voltages, currents and impedance are difficult to obtain.

4. Voltage Regulation

Utility systems must maintain proper voltage within a narrow band. Photovoltaic systems connected to the utility can interfere with voltage regulation by changing the flow of reactive power. There is not a standard definition of reactive power under non-sinusoidal conditions. Changes to utility distribution systems will have to be made if proper voltage cannot be maintained after photovoltaic interconnections are made. The cost of any changes would probably be passed on to the photovoltaic system owner.

5. Harmonics

Utility systems must also operate within a limited band of fundamental frequency for voltage and current. Any harmonics present can adversely affect system operation and its loads. Photovoltaic systems will produce harmonics in both current and voltage due to the DC/AC conversion process.

6. Employee Safety

Proper guidelines need to be developed to cover installation of photovoltaic arrays (modifications to the National Electrical Code) and operation of the systems to protect owners and utility personnel. Of particular concern is the ability of line-commutated inverters to feed a utility system during a utility outage.

7. Metering

Meters must be modified since they are inaccurate under non-sinusoidal conditions. A cost/benefit analysis of alternatives should be performed.

8. System Planning

The preceding concerns indicate that independent photovoltaic generation will have both economic and technical impacts on utilities. The rapid power fluctuations caused by solar transients will complicate maintenance of system continuity if there are multiple interconnections. Planning for photovoltaic systems must preceed design of future distribution systems.

These issues should be considered in assessing the true cost of a PV-T system which is interfaced with a utility.

D. HEALTH AND SAFETY

PV-T systems share many safety problems with conventional thermal and electrical systems used in industrial and commercial situations. Some aspects are unique to solar energy systems and must be recognized and dealt with during design, and subsequently, during operation. In particular, when the sun is shining, a photovoltaic system is on and generating electricity. A solar system should be designed, built, and

operated to prevent the creation of hazards from the solar system which are greater than the hazards without the system. The safety problems which may be unique to a PV-T system are in the areas of fire safety, physical hazards, component toxicity and disposal, overtemperature and overpressure protection, product contamination, and vandalism.

1. Fire Safety

The heat transfer fluids used in solar systems are often flammable or produce flammable products upon decomposition. Nonflammable fluids such as water or water-glycol mixtures are preferable for use in PV-T systems from a fire safety standpoint. If flammable transfer fluids are used, it is advisable to use them below their flash points, although the ability to pump at low temperatures, or vapor pressure characteristics, may be important considerations in choosing a heat transfer fluid for a particular application. The flammability and flame-spread characteristics of insulating materials used, particularly in conjunction with the selected heat transfer fluid, need to be analyzed. Insulation that wicks heat tansfer fluids may result in large soaked areas which are readily oxidized. In retrofit applications, materials near the system, such as roofing, should be analyzed to see if aging has affected their flammability. Intense irradiance can create a fire hazard zone. Such zones must be kept free of combustibles. The flammability of dry vegetation can present problems to ground-mounted systems.

Beyond the use of flammable materials in or near PV-T systems, the system may increase fire hazards by limiting access to other structures or by serving as a lightning path. These factors can be eliminated during design. Roofs of commercial buildings, land adjacent to schools, and the parking lots of hospitals, are often important features in existing fire safety plans. Existing emergency plans should be reviewed during design of any retrofit, and modified before construction begins. Well-grounded lightning protection is a must.

The provision for fire safety equipment will reduce damage if a fire occurs. A total kill switch which stow the collectors, breaks the circuit, and shuts down fluid flow is necessary. This will reduce the

supply of fuel if the transfer fluid is flammable and reduce heat in the entire system. Separate sprinkler systems or foam units may be advisable for some system components (steam generator, battery storage area). Proper fire extinguishers (dry chemical for oil-based transfer fluids) should be located at several accessible stations to contain small fires quickly. Berming ground-mounted systems and fluid storage tanks is recommended.

PV-T systems are new, therefore, new procedures should be established for fire prevention and control. Both employees and the local fire department should to be trained to use the available fire safety equipment. Regular employee drills will ensure that recently hired personnel are familiar with procedures. Accesibility of the system to fire equipment and egress paths for employees from all identified problem areas must be kept in mind during system installation and subsequent construction. Frequent inspection by fire prevention experts will help to identify and remedy potential problems. Periodic review of operating systems as the technology base expands, will identify generic problems if any occur.

2. Physical Hazards

The physical hazards specific to photovoltaic systems are hot surfaces and fluids, concentrated sunlight, breakable glazing, and electrical shocks. Collectors cannot be covered to prevent hot surfaces or to isolate glazing; therefore, protection against accidental burns and cuts must depend upon securing the entire system from unauthorized personnel, warning labels to increase vigilance of employees, and intensive employee education. Sunlight, either reflected off surfaces and glazing, or concentrated by reflectors or lenses, can cause annoyance and injury. The effects of glare from back panels and supports should be considered in design and placement of the array. Scalding by hot fluids can occur if there are leaks. This hazard is aggravated by large amounts of piping. Continuous monitoring, the ability to isolate sections, and remote control to stow collectors and drain affected piping should minimize the physical hazards for leaks. Electrical shocks are minimized by

proper drainage under the collector field, isolation of the system from untrained personnel, and adequate maintenance to reduce the possibility of component failure. Underground conduits could provide additional safety for ground-mounted systems.

Physical hazards may also result from the structural design of the system. Wind loads must be carefully considered in design and during operation to reduce the hazard from parts blowing free and/or debris damaging an operating system. Automatic stow at critical windspeeds may be necessary. Static loads such as snow must also be considered to prevent breakage or overstressing of components. Early morning operations may demand extra caution if snow or ice build-up can fall from heating roof-mounted collectors onto passers-by.

Hazards associated with the maintenance of photovoltaic systems can be reduced by following OSHA safety and health standards with respect to working surfaces, ladders, personal protective equipment, etc. Protective clothing, first aid stations, showers, and eyewash units, should be provided for the solar system. These facilities may not be found in a commercial building and may be too far from the system access point in an industrial setting. There are no specific OSHA standards directed toward the use of solar systems. Lock-out switches, which prevent operation of trackers, and circulating pumps during maintenance, further protect workers. The protection of utility line workers must be considered in design of the utility interface.

3. Component Toxicity and Disposal

Heat transfer fluids are generally toxic. Even water may contain rust inhibitors or biocides. The exact formulation of the heat transfer fluid should be known. Its toxicity should be quantified in terms of ingestion, skin contact, inhalation (both vapor and decomposition products), and eye contact. Any change in the fluid during use (biological degradation, corrosion products, etc.,) should be recognized. This information, and first-aid instructions should be readily available in case of an emergency. Posting information with the local poison control center is advisable. In commercial applications, storage of heat

transfer fluid should be carefully planned to avoid possible public contact. Disposal of the heat transfer fluid should be planned in advance and in compliance with local and federal toxic waste regulations. Ethylene glycol has a useful life of less than 2 years in most applications. Flushing several systems at the same time into a single treatment system could lead to interruption of normal biological treatment activities. Insulation, or other materials which have become contaminated with a toxic fluid should be disposed of in compliance with toxic waste regulations.

Storage batteries, which might be considered to balance electrical loads, contain toxic components. Battery maintenance and disposal is not unique to photovoltaic systems and should be handled according to established procedures.

4. Overtemperature and Overpressure Protection

Unlike conventional systems, PV-T collectors are on whenever the sun shines and electricity and heat are generated constantly. Stagnation caused by system breakdown, flow blockage and flow imbalance, can lead to development of excessive temperatures in the thermal parts of the system during periods of high irradiation. Excessive temperatures can degrade the heat transfer fluid, damage mechanical and electrical components, lead to outgassing from hot piping and insulation, cause ruptures from increased pressure, and increase the fire hazard. Return of flow after maintenance or breakdown can cause thermal shock damage.

To avoid overpressure, pressure relief valves should be installed in every piping section that can be isolated in any way. Discharge from the valves should be safely collected to avoid damaging other materials or equipment. To avoid overtemperature, emergency stow operations should be automatic and as fail-safe as possible. Specific provision may have to be made to monitor systems during industrial shutdowns, commercial holidays, and following storms.

Two types of failure of the coolant system may occur: 1) loss of flow in which the coolant stagnates in the receiver tube and 2) a break in the coolant line such that coolant drains out of the receiver.

The receiver temperature for E-Systems line focus Fresnel collector is shown versus time for each of these failures in figure VII-1. Calculations were also made for an operational failure and a disabled array. For an operational failure the cells are in focus, the coolant system malfunctions, and the collectors cease tracking but fail to stow so that the beam walks off the cells. For a disabled array, the cells are initially at ambient temperature because the collectors are not tracking. In this case, the beam focuses on the cells and walks off due to the sun's motion.

In the event of loss of flow but continual tracking, the stagnation temperature may reach 466°C (870°F), as shown in figure VII-2. These figures were supplied through the courtesy of E-Systems, Inc. and are published here with their permission.

5. Contamination of Product

Product contamination can occur directly through spillage or leakage of heat transfer fluids into processing, manufacturing, or storage areas; or indirectly, through carryover of fluids from incomplete clean-up or vaporization. Failure of the system, particularly in food processing industrial applications, can result in product contamination because proper process temperatures were not achieved. Physical, chemical, and biological contamination are possible also. Contamination can affect palatability and wholesomeness of food, can soil or degrade nonfood items, such as textiles, and can cause spoilage in both industrial and commercial environments.

Area contamination can occur from leaks in work areas or from venting heat transfer fluid fumes or components outgassing. Odors, eye irritation, and general respiratory discomfort can result in cessation of activities in an affected area until the source of contamination is located and clean-up completed.

Double separation through double-walled heat exchangers, plate-type heat exchangers, and heat exchangers in series, is recommended for food processing applications. Periodic tests for leakage into the intermediate fluid should be performed. Water supply contamination must

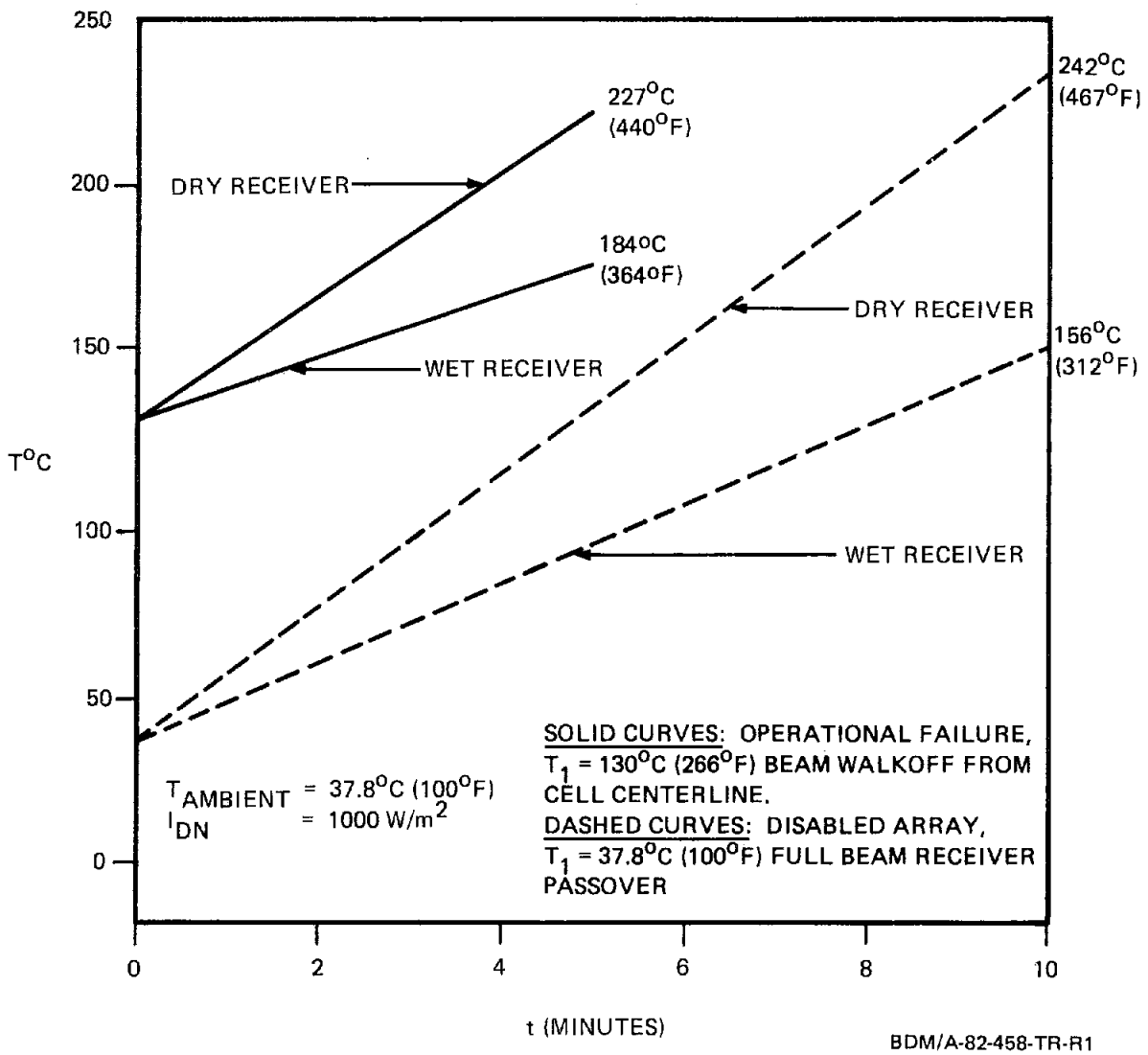

Figure VII-1. PV-T Receiver Heat-Up Curves for Two Types of Failure

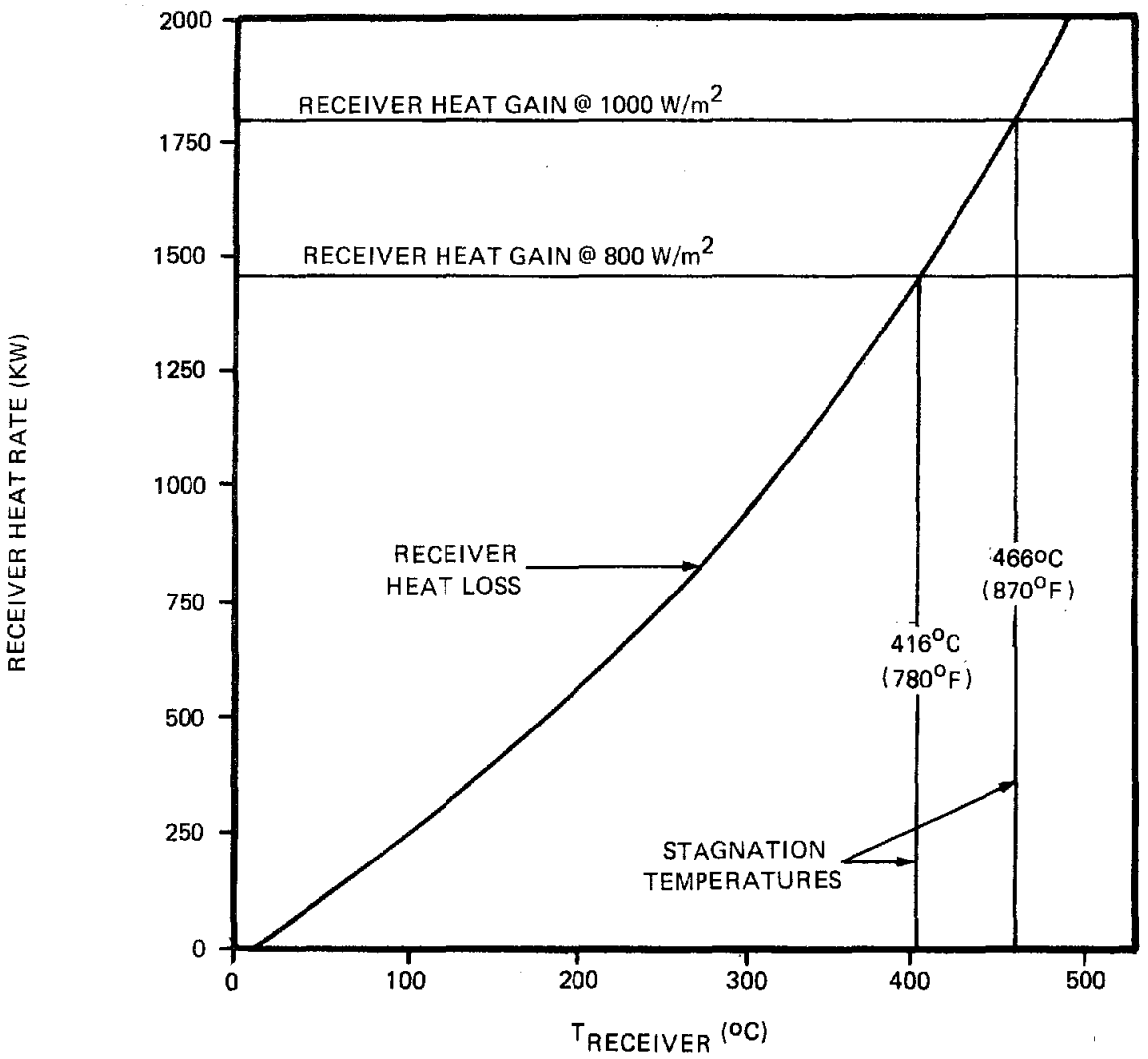

ASSUMPTIONS:

- 21.1°C (70°F) AMBIENT
- NO ELECTRICAL COLLECTION
- HEAT LOSS AT HIGH TEMPERATURES EXTRAPOLATED FROM LOW-TEMPERATURE MEASUREMENTS USING:

$$Q_{LOSS} = UA\,(T-T_o) + \sigma \epsilon A\,(T^4 - T_o^4)$$

- HEAT GAIN BASED ON MEASUREMENTS)

BDM/A-82-458-TR-R1

Figure VII-2. PV-T Receiver Stagnation Temperatures

be rigorously controlled through back flow preventors in systems using water make-up. Commercial facilities should be cautious in the locating of air conditioning intakes near solar systems.

6. Vandalism

The general public will be attracted to PV-T arrays because the technology is novel. This will be a greater problem with commercial systems than with industrial applications since industrial sites often have well-developed security systems. Access to roof-mounted arrays should be limited and fencing should adequately isolate ground-mounted systems from curious individuals. Public education and demonstrations may offset vandalism of publicly-owned systems. To date, vandalism has not been a major problem with solar systems.

E. ENVIRONMENTAL

Environmental issues, in general, are not unique for PV-T systems. Some jurisdictions now require that solar energy options be considered when new construction is being environmentally assessed. Land use for ground-mounted systems probably has the largest impact. Certain circumstances might require the preparation of comprehensive environmental impact assessments, including public controversy concerning the use of a PV-T system in a publicly-owned commercial building, large systems designed to serve several facilities and to operate as a central power station, and siting of a particular system where aesthetics are questioned (a PV-T system for the White House). The magnitude and significance of generic environmental issues are dependent on the technical design, site-specific location, surrounding environment and operating characteristics of the system. Several environmental issues, such as hazardous substance disposal, have been covered in other sections of the chapter. Only issues not previously discussed will be mentioned here.

1. Land Use

Land use must be considered in siting of an array. Site-specific land use factors include latitude, longitude, elevation, topographic features, existing structures and land use patterns, and meteorological data. These factors determine available insolation. Proposed site developments will influence system life from both shadowing and pollution; this must be considered in initial design. The amount of land available (or roof space) is more likely to determine system size than the reverse, and array design and process energy requirements determine land required for siting. Widespread use of solar systems may lead to decentralized growth in some areas or place undue burdens on available services in others, but these land and use affects must await greater employment of the technology.

2. Microclimate Effects

Any construction activities can have adverse effects on the local environment through vegetation removal, loss of wildlife habitat, erosion of cleared land, stream silting and blowing dust. Ground-mounted systems have greater potential for damaging the environment. Once construction is completed, a new microclimate will have been developed. Ground-mounted systems may increase local runoff, attract reptiles seeking warmth and shelter, require regular vegetation control, and may change the actual climate (temperature, humidity, insolation) near them. Roof-mounted systems generate fewer effects, since the building supporting them produced the major changes. Roof-mounted systems may provide bird habitats too, and can increase the temperature in the air space around them.

The microclimate or immediate environment around the collectors should also be considered during siting of a solar system. Industrial microclimates can be very corrosive. Emmissions of sulfate, nitrates, and other acid-forming compounds is common. Siting near process vents is a questionable practice. A recent study of solar industrial process heat systems found a correlation between accumulation of deposits (including dust, protein, and sugars) and proximity to vents (ref. VII-13).

Industrial pollution, clay soils dusts, low precipitation, and thermal cycling, all seem to contribute to persistent soiling of collector surfaces. Commercial environments may not be much better. Automobile pollution, local light industry, pigeons, construction dust and spray from air conditioning cooling towers can rapidly obscure a collector. Regular cleaning of collectors may create its own soil and water pollution problems. In arid regions, regular cleaning will certainly increase problems with vegetation control.

3. Electro-Magnetic Interference

One area of potential environmental sensitivity and public safety (especially with photovoltaic systems located near airports), is interference with electronic devices used in communications and navigation systems. The source of electromagnetic interference (EMI) is solid state power converters, which convert direct current (DC) power generated by the photovoltaic system to alternating current (AC) power. Proper photovoltaic system design may mitigate this problem by encapuslating the power converter device. Power inverters should conform to EMI standards specified in Military Standard (MIL-STD) 461-A entitled "Electromagnetic Interference Characteristics, Requirements for Equipment, 9 February 1971" and MIL-STD-462 entitled "Electromagnetic Interference Characterisits, Measurement of 9 February 1971".

4. Aesthetics

A high-technology image is usually not out of place in an industrial setting. Commercial applications may, however, encounter resistance to the appearance of PV-T collectors arrays. There is no easy answer to aesthetic disapproval. Elicting public opinion early in the decision making process is essential to the smooth application of new technologies. Acceptance of new concepts is usually gradual. Pushing a visually unacceptable system may lead to expensive vandalism after the project is completed and operating.

REFERENCES

VII-1. Phillips, J. D., 1975, Assessment of a Single Family Residence Solar Heating System in a Suburban Development Setting, p. 92., In Solar Heated Residence Annual Research Report., NSF-RA-N75078.

VII-2. Dubin, F. S., 1975, Analysis of Energy Usage on Long Island from 1975 to 1995: The Opportunities to Reduce Peak Electrical Demands and Energy Consumption by Energy Conservation, Solar Energy, Wind Energy and Total Energy Systems. Suffolk County Department of Environmental Control, New York.

VII-3. Dean, N. L., et. al, 1981, Solar Energy and the Law, p. 26-1. In J. F. Kreider and F. Kreith, Solar Energy Handbook, McGraw-Hill.

VII-4. Eisenstadt, M. M. and A. E. Utton, 1976, Solar Rights and Their Effect on Solar Heating and Cooling, Natural Resources Journal, 16:368.

VII-5. Watlkins, G. A., et. al., 1980, Photovoltaic Institutional Issues Study, Battelle-Columbus, SAND79-7954, Sandia National Laboratories.

VII-6. Curry, R., 1981, Solar Can't Afford Two Certification Programs, Solar Engineering, 6(12):2.

VII-7. Gupta, Y. P. and S. K. Young, 1981, Design Handbook for Photovoltaic Power Systems, Science Applications, Inc., SAND80-7147/a, Sandia National Laboratories.

VII-8. Eisenstadt, M., 1981, Performance Warranties for Residential and Light Commercial Photovoltaic System, SAND81-7008, Sandia National Laboratories.

VII-9. Adams, M. R., 1981, Tax Study Enhances Prospects for Commercial Solar Sales, Solar Age, 6(6):14-15.

VII-10. Hooker, D. W., et. al., 1980, Industrial Process Heat Case Studies, SERI/TR-733-323, Solar Energy Research Institute.

VII-11. Dickinson, W. C., 1980, The Role of Financing in the Marketability of Capital Intensive Solar Technologies for Industry, p 41-46, In Solar Industrial Process Heat Conference Proceedings, 1980, SERI.CP-632-952, Solar Energy Research Institute.

VII-12. Hassan, M. and J. Klwin., 1981, Distributed Photovoltaic System: Utility Interface Issues and Their Present Status, Jet Propulsion Laboratory, DOE/ET-20356-3, (Jet Propulsion Laboratory Publication 81-89).

VII-13. Randall, D. E. and V. L. Morris, 1981, Initial Experience and Preliminary Results, Solar-Collector Materials Exposure to the IPH Site Environment, McDonnel Douglas Astronautics Company, SAND81-0290, Sandia National Laboratories.

DISTRIBUTION LIST:

Acurex Corporation (1)
Attn: George Sutton
Bob Spencer
Dariush Rafinejad
485 Clyde Avenue
Mountain View, CA 94042

Arco Solar, Inc. (1)
Attn: Ray Kosanke
Library
P. O. Box 4400
Woodland Hills, CA 91365

Arizona State University
Attn: Charles Backus
College of Engineering
Tempe, AZ 85281

Battelle
Attn: Don Carmichael
505 King Avenue
Columbus, OH 43201

The BDM Corporation (3)
Attn: Bill Schwinkendorf
1801 Randolph Road SE
Albuquerque, NM 87111

Black & Veatch
Attn: Sheldon L. Levy
P. O. Box 8405
Kansas City, MO 64114

U. S. Dept. of Energy
Div. of PV Energy Technologies
Attn: R. Annan
A. Krantz
M. Prince
L. Herwig
A. Scolaro
1000 Independence Ave. SW
Washington, DC 20585

EPRI (2)
Attn: Roger Taylor
Ed DeMeo
P. O. Box 10412
Palo Alto, CA 94303

ENTECH, Inc.
Attn: Mark O'Neill
A. J. McDanal
P. O. Box 612246
DFW Airport, TX 75261

Intersol Power Corporation
Attn: John Sanders
Sid Broadbent
11901 West Cedar
Lakewood, CO 80228

Jacobs Engineering
Attn: Bob Martin
251 South Lake Ave.
Pasadena, CA 91101

Jet Propulsion Lab (3)
Attn: K. Shimada
R. Ferber
Solar Data Center
MS 502/414
4800 Oak Grove Drive
Pasadena, CA 91109

Martin Marietta
Attn: R. Hein
P. O. Box 179
Denver, CO 80201

Oak Ridge National Lab
Attn: Steve Kaplan
P. O. Box X
Oak Ridge, TN 37830

SERI, Library (2)
1536 Cole Blvd., Bldg. #4
Golden, CO 80401

SOLAVOLT
Attn: Ray Kendall
P. O. Box 2934
Phoenix, AZ 85062

Southern Cal Edison
Attn: Spencer Carlisle
2244 Walnut Grove Ave.
Rosemead, CA 91770

Spectrolab
Attn: Steve Olah
12500 Gladstone Avenue
Sylmar, CA 91342

United Energy Technologies
Attn: John Mackay
420 Lincoln Center Dr.
Foster City, CA 94404

Varian & Associates (1)
Attn: N. Kaminar
611 Hansen Way K-219
Palo Alto, CA 94303

6223 G. Jones
6223 M. Thomas
6224 D. Arvizu (10)
3141 C. M. Ostrander (5)
3151 W. L. Garner (3)
3154-3 C. H. Dalin (25)
For DOE/TIC
(Unlimited Release)
8424 M. A. Pound